REPORT DOCUMENTATION PAGE

Form Approved
OMB No. 0704-0188

1. AGENCY USE ONLY *(Leave blank)*

2. REPORT DATE

3. REPORT TYPE AND DATES COVERED
Proceedings 17-20 May 1994

4. TITLE AND SUBTITLE
Second USAF Aging Aircraft Conference

5. FUNDING NUMBERS

6. AUTHOR(S)
Dr. C. I. Chang, Editor

7. PERFORMING ORGANIZATION NAME(S) AND ADDRESS(ES)
Oklahoma City Air Logistics Center (AFMC)
3001 Staff Dr.
Tinker AFB, OK 73145-3019

8. PERFORMING ORGANIZATION REPORT NUMBER

9. SPONSORING/MONITORING AGENCY NAME(S) AND ADDRESS(ES)
Air Force Office of Scientific Research

10. SPONSORING/MONITORING AGENCY REPORT NUMBER
AFOSR-TR- 94 0756

11. SUPPLEMENTARY NOTES

12a. DISTRIBUTION/AVAILABILITY STATEMENT
APPROVED FOR PUBLIC RELEASE:
DISTRIBUTION IS UNLIMITED

12b. DISTRIBUTION CODE
A

13. ABSTRACT *(Maximum 200 words)*

The Air Force Office of Scientific Research gathered together representatives of universities funded under the University Research Institutes to present results of their Aging Aircraft research conducted over the preceding year. The purpose was to provide a forum for Technical Interchange and provide AFOSR an opportunity for the research community to interact with the applied engineering community and gain insight into the day to day problems experienced on Aging Aircraft. Technical presentations by personnal from HQ AFMC/EN Wright Labs, ASC, the five Air Logistics Centers, FAA and NASA were delivered on various topics including, corrosion, corrosion fatique, multi-site damage and advanced non-destructive evaluation methods. Approximately 160 people attended the conference.

14. SUBJECT TERMS
Aging Aircraft, Corrosion, Corrosion Fatique Crack Propagation

15. NUMBER OF PAGES
244

16. PRICE CODE

17. SECURITY CLASSIFICATION OF REPORT	18. SECURITY CLASSIFICATION OF THIS PAGE	19. SECURITY CLASSIFICATION OF ABSTRACT	20. LIMITATION OF ABSTRACT
UNCLASSIFIED	UNCLASSIFIED	UNCLASSIFIED	UNCLASSIFIED

GENERAL INSTRUCTIONS FOR COMPLETING SF 298

The Report Documentation Page (RDP) is used in announcing and cataloging reports. It is important that this information be consistent with the rest of the report, particularly the cover and title page. Instructions for filling in each block of the form follow It is important to ***stay within the lines*** to meet ***optical scanning requirements***.

Block 1. Agency Use Only *(Leave blank)*.

Block 2. Report Date. Full publication date including day, month, and year, if available (e.g. 1 Jan 88). Must cite at least the year.

Block 3. Type of Report and Dates Covered. State whether report is interim, final, etc. If applicable, enter inclusive report dates (e.g. 10 Jun 87 - 30 Jun 88).

Block 4. Title and Subtitle. A title is taken from the part of the report that provides the most meaningful and complete information. When a report is prepared in more than one volume, repeat the primary title, add volume number, and include subtitle for the specific volume. On classified documents enter the title classification in parentheses.

Block 5. Funding Numbers. To include contract and grant numbers; may include program element number(s), project number(s), task number(s), and work unit number(s). Use the following labels:

C -	Contract	PR -	Project
G -	Grant	TA -	Task
PE -	Program Element	WU -	Work Unit Accession No.

Block 6. Author(s). Name(s) of person(s) responsible for writing the report, performing the research, or credited with the content of the report. If editor or compiler, this should follow the name(s).

Block 7. Performing Organization Name(s) and Address(es). Self-explanatory.

Block 8. Performing Organization Report Number. Enter the unique alphanumeric report number(s) assigned by the organization performing the report.

Block 9. Sponsoring/Monitoring Agency Name(s) and Address(es). Self-explanatory.

Block 10. Sponsoring/Monitoring Agency Report Number. *(If known)*

Block 11. Supplementary Notes. Enter information not included elsewhere such as: Prepared in cooperation with...; Trans. of...; To be published in.... When a report is revised, include a statement whether the new report supersedes or supplements the older report.

Block 12a. Distribution/Availability Statement. Denotes public availability or limitations. Cite any availability to the public. Enter additional limitations or special markings in all capitals (e.g. NOFORN, REL, ITAR).

- **DOD** - See DoDD 5230.24, "Distribution Statements on Technical Documents."
- **DOE** - See authorities.
- **NASA** - See Handbook NHB 2200.2.
- **NTIS** - Leave blank.

Block 12b. Distribution Code.

- **DOD** - Leave blank.
- **DOE** - Enter DOE distribution categories from the Standard Distribution for Unclassified Scientific and Technical Reports.
- **NASA** - Leave blank.
- **NTIS** - Leave blank.

Block 13. Abstract. Include a brief *(Maximum 200 words)* factual summary of the most significant information contained in the report.

Block 14. Subject Terms. Keywords or phrases identifying major subjects in the report.

Block 15. Number of Pages. Enter the total number of pages.

Block 16. Price Code. Enter appropriate price code *(NTIS only)*.

Blocks 17. - 19. Security Classifications. Self-explanatory. Enter U.S. Security Classification in accordance with U.S. Security Regulations (i.e., UNCLASSIFIED). If form contains classified information, stamp classification on the top and bottom of the page.

Block 20. Limitation of Abstract. This block must be completed to assign a limitation to the abstract. Enter either UL (unlimited) or SAR (same as report). An entry in this block is necessary if the abstract is to be limited. If blank, the abstract is assumed to be unlimited.

Air Force Office of Scientific Research
2nd Annual Conference of Aging Aircraft
Minutes

Hosted by
Oklahoma City Air Logistics Center
at
Rose State College
Del City, Oklahoma
May 1994

Prior to the First Aging Aircraft Conference, the Air Force Office of Scientific Research (AFOSR) issued several University Research Initiative (URI) grants to various universities to study issues associated with aging aircraft. The papers presented in this document represent the first year's work for those investigations.

The initial presentations are from government agencies discussing current aging aircraft initiatives underway. They include papers from AFOSR, all of the Air Force Air Logistics Centers, Wright Laboratory, Air Force Material Command, Aeronautical systems Center, FAA and NASA. Later technical papers from the participating universities cover research into materials degradation, corrosion and corrosion fatigue, multi-site damage and non-destructive inspection methods. Two of the technical presentations given at the conference are not represented in this document. They are the presentations from Professor Regis Pelloux of MIT and Mr. Robert Smith of the Defence Research Agency of the United Kingdom. We apologize for the omissions, but were unable to obtain copies of these papers. If you are interested in more information concerning any of these topics, please contact me at (202) 767-4987.

The conference was hosted by the Oklahoma City Air Logistics Center, Tinker AFB, Oklahoma. OC-ALC maintains the largest number of oldest aircraft in the Air Force, which provided the opportunity for participants to see first hand where their research will be applied. We would like to thank all those from OC-ALC, ARINC Research Corporation, and Rose State College who gave their time and effort to make this conference a success.

C. I Chang

C.I. CHANG
Director of Aerospace
and Materials Sciences

TABLE OF CONTENTS

TABLE OF CONTENTS (continued)

AF OFFICE OF SCIENTIFIC RESEARCH

AGING AIRCRAFT CONFERENCE

17-19 May 1994

Oklahoma City OK

Briefed by: Dr Jim C.I. Chang, Director

Aerospace and Engineering Sciences

AFOSR/NA

110 Duncan Avenue, Suite B-115

Bolling AFB DC 20332-0001

(202) 767-4987

AGING AIRCRAFT
OUTLINE

- Problem/Challenge
- Air Force Program
- AFOSR Program
- User Examples vs. S&T Technology Issues
- AFOSR Research With Potential Application
- Conclusion

AIR FORCE AGING AIRCRAFT PROBLEM/CHALLENGE

PROBLEM/CHALLENGE

- No Funds For Replacement Aircraft
  - C/KC-135 — Must operate to 2040
  - B-52 — Must operate to 2030
  - E-3 — Indefinite
- C/KC-135 Structural Fatigue Life Adequate to 2040
  - Effects of Corrosion Not Considered
- Corrosion Increases as Aircraft Age
- Structural Degradation Due to Corrosion Will Limit C/KC-135 Life to Less Than 2040

Air Force Aging Aircraft

ACTIVE DUTY FLEET	AGE IN YEARS 0-6	7-12	13-18	18-24	24+	AVG
A-10		180	42			11.2
B-52					148	31.4
C-9				32	3	21.5
KC-10	12	47				7.7
C-130	30	9	51	77	167	21.9
C-135					479	30.9
C-141					241	26.1
F-15	241	249	194	4		8.3
F-16	744	102	20			3.7
F-111			12	188	32	21.5
T-37				77	427	29.8
T-38				177	508	26.1

Source: Air Force Magazine, May 1993

C-141 GROUNDING

"USAF AIR MOBILITY Command Chief, Gen. Ronald R. Fogleman, has grounded 45 C-141s and limited another 116 of the transport aircraft from any in-flight re-fueling. The new limitations follow a May order limiting all C-141s to 74% of their normal load capacity. All 249 C-141Bs will undergo inspectins to determine the severity of 'weep hole cracking' before being cleared for less restricted flight, being repaired or being retired."

Source: Aviation Week, 16 Aug 93

AIR FORCE AGING AIRCRAFT PROGRAM

AIR FORCE AGING AIRCRAFT PROGRAM

- AFOSR Sponsored Multi-site Damage Symposium at WR-ALC 18-20 February 1992 - AF, FAA, NASA

- AFOSR Initiatives Addressing Aging Aircraft Issues - MURI/URIP/Core
    - "Material Degradation and Fatigue in Aerospace Structures" - $3.75M/Year
        - Four Years at 10 Universities
    - "Detection and Prevention of Corrosion in Aging Aircraft" - $1.0M/Year
        - Three Years at 8 Universities
    - Individual PI Programs - $0.5M/Year
        - Three Universities

- First Aging Aircraft Conference Held 27-28 April 1993, Georgia Tech, Atlanta GA
    - AFOSR Funded Academic Institutions, WL, ASC, AFMC/EN, FAA and NASA

AIR FORCE AGING AIRCRAFT PROGRAM (CONTINUED)

- Technology/Program Integration
    - Full Participation of Technology Producers (Universities, WL) and Technology Users (ASC, AFMC/EN, ALCs)

- Technical/Program Management
    - Aging Aircraft Steering Group (AFOSR/NA, WL/CD and AFMC/EN)
    - Four Working Groups
        - NDE
        - Material Damage Behavior/Fatigue
        - Corrosion
        - Structural Integrity Assessment and Life Extension Methodology

- Second Air Force Aging Aircraft Conference scheduled 17-19 May 1994 at OC-ALC, Full AF Participation Plus FAA and NASA

AIR FORCE AGING AIRCRAFT PROGRAM (CONTINUED)

- SAB Summer Study 94 on Mission Support and Enhancement for Foreseeable Aircraft Force Structures
- Coordination Outside Air Force
  - FAA Headquarters, Jeff Lewis
  - FAA Technical Center, Chris Seher
  - NASA Headquarters, Phil Bogert
  - NASA Langley, Charles Harris, Joe Heyman
  - FAA Long Beach, Tom Swift
- USAF/ST - 6.2/6.3 Investment
- USAF/XR - 6.4 Tech Insertion, Post Production Weapon Systems R&D program
- Joint Third Air Force Aging Aircraft/Air Force Aircraft Structural Integrity Conference November 1995

AIR FORCE AGING AIRCRAFT STEERING GROUP MEMBERS

- AGING AIRCRAFT STEERING GROUP MEMBERS
  - Mr Les Smithers - WL/CD
  - Mr Otha Davenport - HQ AFMC/EN
  - Dr Jim C. I. Chang - AFOSR/NA
- ADVISOR
  - Dr Jack Lincoln - ASC: Structures

WORKING GROUP MEMBERSHIPS

- Air Force
  - Program, Expertise (?)
  - AFMC/EN Plus Local Management Decision
- Other S&T Participation
  - Working Group Coordinator's Decision

STRUCTURAL INTEGRITY ASSESSMENT AND LIFE EXTENSION METHODOLOGY DEVELOPMENT WORKING GROUP MEMBERS

- Mr James L. Rudd (WL/FIB) - Coordinator
- Dr Spencer Wu (AFOSR/NA) - Coordinator
- Mr Bill Sutherland (SM-ALC/LAFFE) - ALC Leader
- Mr Dan Register (WL-ALC/TIEDD)
- Mr Randy Jansen (WR-ALC/TIEDD)
- Mr Dave Ratzer (SA-ALC/LADD)
- Mr Ralph Garcia (SA-ALC/LADD)
- Mr Antonio Gonzalez (SA-ALC/LADE)
- Mr Neil Phelps (OO-ALC/LAAS)
- Mr Albert Arrieta (OC-ALC/TIESM)

NONDESTRUCTIVE EVALUATION (NDE) WORKING GROUP MEMBERS

- Dr Walter Jones (AFOSR/NA) - Coordinator
- Mr Tobey Cordell (WL/MLBT) - Coordinator
- Mr Don Hazen (WR-ALC/TIEDM) - ALC Leader
- Dr Harold Weinstock (AFOSR/NE)
- Mr Albert Rogel (SM-ALC/TIEE)
- Mr Bryan Sanbongi (SM-ALC/TIELD)
- Mr Thomas Secunda (SA-ALC/TIELM)
- Mr Dave Ratzer (SA-ALC/LADD)
- Mr Ralph Garcia (SA-ALC/LADD)
- Mr David Campbell (OC-ALC/LAPPI)

MATERIAL DAMAGE BEHAVIOR WORKING GROUP MEMBERS

- Capt Chuck Ward (AFOSR/NC) - Coordinator
- Mr Clay Harmsworth (WL/MLSE) - Coordinator
- Mr Ralph Garcia (SA-ALC/LADD) - ALC Leader
- Mr James Rudd (WL/FIB)
- Dr John Botsis (AFOSR/NA)
- Dr Walter Jones (AFOSR/NA)
- Mr Tom Yentzer (WR-ALC/TIEDM)
- Mr John Meininger (SM-ALC/TIELC)
- Mr Dave Ratzer (SA-ALC/LADD)
- Mr David Tanner (OC-ALC/TIESM)

CORROSION WORKING GROUP MEMBERS

- Maj Tom Erstfeld (AFOSR/NC) - Coordinator
- Mr Gary Stevenson (WL/MLSA) - Coordinator
- Mr Donald Nieser (OC-ALC/LACRA) - ALC Leader
- Mr Dick Kinzie (WR-ALC/TIEDM)
- Mr Dan Register (WR-ALC/TIEDD)
- Mr Dan Durham (SM-ALC/TIEE)
- Mr Dave Ratzer (SA-ALC/LADD)
- Mr Ralph Garcia (SA-ALC/LADD)
- Mr Johnathon Pok (SA-ALC/TIELM)
- Mr Dennis Flynn (SA-ALC/TIELP)
- Lt Deric Kraxberger (OC-ALC/TIETR)

AFOSR AGING AIRCRAFT PROGRAM

MATERIALS DEGRADATION AND FATIGUE IN AEROSPACE STRUCTURES

FY 1993 University Research Initiative

MASSACHUSETTS INSTITUTE OF TECHNOLOGY (**Regis Pelloux**) - **"Environmental Degradation and Fatigue in Aircraft Structural Materials"**

PURDUE UNIVERSITY (**Skip Grandt**) - **"Materials Degradation and Fatigue in Aerospace Structures"**

UNIVERSITY OF CALIFORNIA, LOS ANGELES (**Ajit Mal**) - **"Characterization of Materials Degradation Due to Corrosion and Fatigue in Aerospace Structures"**

UNIVERSITY OF ILLINOIS (**Jiri Jonas**) - **"Materials Degradation and Fatigue Under Extreme Conditions"**

MATERIALS DEGRADATION AND FATIGUE IN AEROSPACE STRUCTURES

(Continued)

VANDERBILT AND NORTHWESTERN UNIVERSITIES (**John Wikswo/ Jan Achenbach**) - **"Advanced Instrumentation and Measurements for Early NDE of Damage and Defects in Aging Aircraft"**

DETECTION AND PREVENTION OF CORROSION IN AGING AIRCRAFT STRUCTURES

FY 1993 URI RESEARCH INITIATIVE PROGRAM

IOWA STATE UNIVERSITY (James Rose) - "Nondestructive Detection and Characterization of Corrosion in Aircraft"

LEHIGH UNIVERSITY (Robert Wei) - "Corrosion and Fatigue of Aluminum Alloys: Chemistry, Micromechanics and Reliability"

SUNY AT STONY BROOK (Fu-Pen Chiang) - "NDE of Corrosion and Fatigue by Laser Speckle Sensor and Laser Moire"

UNIVERSITY OF CHICAGO (Stephen Sibener) - "Scanning Tunneling Microscopy Studies of the Morphology and Kinetic Pathways for Corrosion Reactions of Stresses in Materials"

UNIVERSITY OF CONNECTICUT (Wolodymyr Madych) - "Experimental and Theoretical Aspects of Corrosion Detection and Prevention"

DETECTION AND PREVENTION OF CORROSION IN AGING AIRCRAFT STRUCTURES

(Continued)

IOWA STATE UNIVERSITY (James Rose) - "Nondestructive Detection and Characterization of Corrosion in Aircraft"

UNIVERSITY OF DELAWARE (Fadil Santosa) - "NDE of Corrosion-Damaged Structures"

VANDERBILT UNIVERSITY (George Hahn) - "Fretting Corrosion in Airframe Riveted and Pinned Connections"

WAYNE STATE UNIVERSITY (Robert Thomas) - "Thermal Wave Imaging for NDE of Hidden Corrosion in Aircraft Components"

AIR FORCE AGING AIRCRAFT PROGRAM
TASKING
STEERING GROUP AND WORKING GROUPS

- <u>Purpose/Function</u>
  - Assure mission capability of Aging Aircraft Fleet
    - Reliability Assurance - Existing and Improved
    - Life Extension
  - Assure Effective Communication Between Technology Developers and Technology Users
    - Working Groups - Within/Across
    - Working Group Coordinator Role - Central Clearing House
  - Develop/Coordinate 6.1, 6.2, and 6.3a S&T Efforts
    - Steering Group and Working Groups
    - Roadmaps

AIR FORCE AGING AIRCRAFT PROGRAM
TASKING
STEERING GROUP AND WORKING GROUPS
(Continued)

- <u>Programmatic</u>
  - Steering Group/Working Group Meetings
  - Activity Coordination
  - Problem Identification/Tech Program Development
  - Subgroup Semi-annual Report

NDE

OC-ALC EXAMPLE

LAP JOINT INSPECTION AREAS

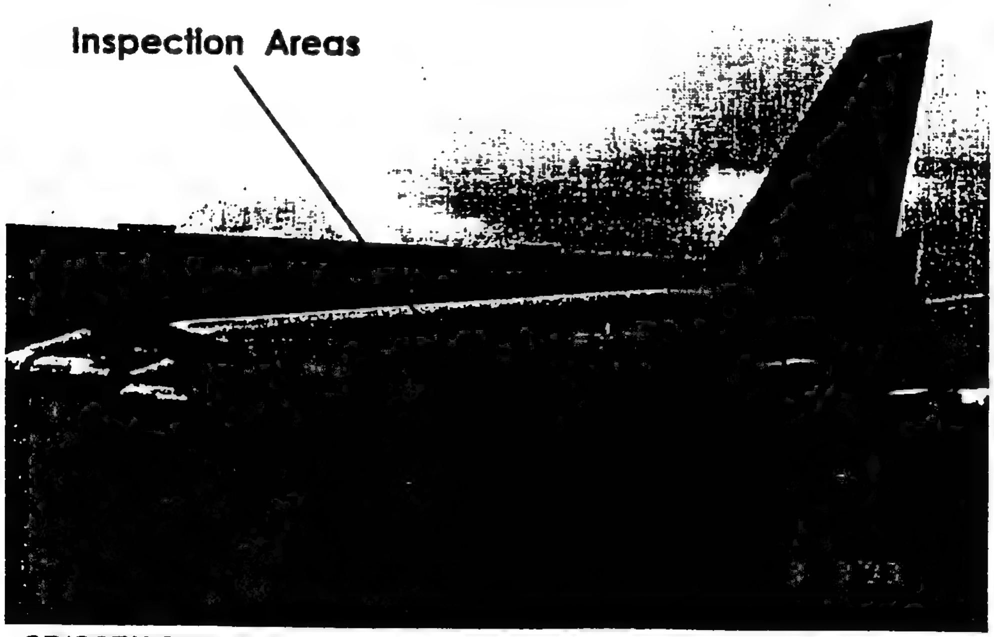

SD/OSE/AO/09-10-93

NON DESTRUCTIVE EVALUATION (NDE) S&T ISSUES

- **Explanations to Performance/Consistency Rendered by Different NDE Techniques**
    - **Understanding**
    - **Fundamental Mechanisms for Detection - UT/Wave Length**
    - **Test Specimen Geometry**
    - **Human Interface**
- **Differentiation Between 6.1, 6.2 and 6.3A Issues**
- **NDE Working Group**

STRUCTURAL INTEGRITY

OC-ALC EXAMPLE (ROUND ROBIN TEST)

OC-ALC STRUCTURAL INTEGRITY TESTING

- **Specimens From 30+ Year Old C/KC-135 Aircraft With and Without Possible Corrosion**
  - **Fuselage Lap Joints**
  - **Upper Wing Skins**
- **Fractographic and Corrosion Quantification After Testing and Invasive Disassembly**
- **Lab-to-Lab Standard and Preliminary Tests Completed**
- **Testing from Nov 93 to Jun 94**

CORROSION AN._AGING AIRCRAFT

ROUND ROBIN TESTING

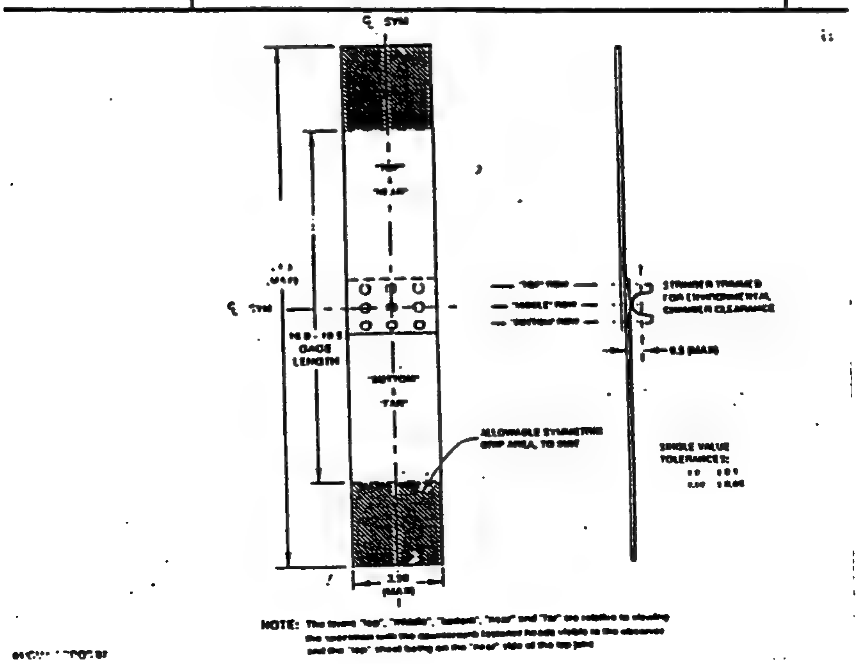

STRUCTURAL INTEGRITY
S&T ISSUES

- **Physical Parameters for Specimen Quantification Before the Test - Service Life, Baseline Materials, NDE Measurement, etc.**
- **Materials/Structures Parameters Measurement From/During the Test**
- **Proper Post Test Interpretation Which Leads to Physics-Based Aircraft Structural Life Prediction and Integrity Assessment**
- **Work Across the Working Groups**

SELECTED USER EXAMPLES
vs
SCIENCE & TECHNOLOGY ISSUES

AFOSR RESEARCH
With
POTENTIAL APPLICATION TO AGING AIRCRAFT

- NDE
  - Speckle Sensor - Chiang, SUNY (AFOSR-URIP)
  - Superconduction (SQUID) - Wikswo, Vanderbilt (AFOSR-Core)
- Material Damage Behavior
  - Functionally-Graded Materials - Erdogen, Lehigh (AFOSR-Core)
- Corrosion and Fatigue
  - Pit Corrosion - Wei, Lehigh (AFOSR-URIP/FAA)
- Structural Assessment and Life Extension Methodology
  - Multi-Site Damage - Atluri, Georgia Tech (AFOSR-Core/FAA)

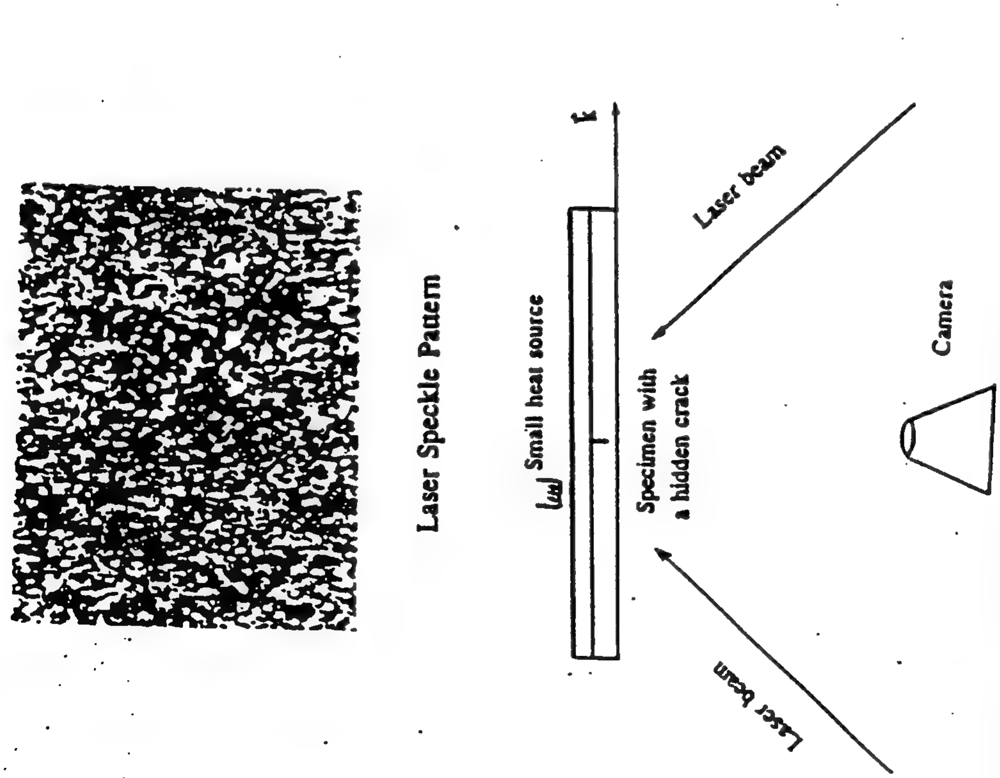

Field Eq: $\bar{u} \cdot \bar{k} = \lambda (2n+1)/2$; λ: wave length, n: fringe order, $\bar{u}$: generic displacement vector in specimen plane, $\bar{k}$: sensitivity vector.

Optical system of Laser Speckle Pattern to detect hidden corrosion

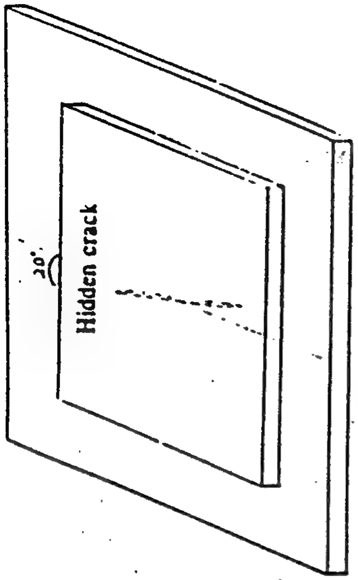

Schematic of the specimen with a hidden crack

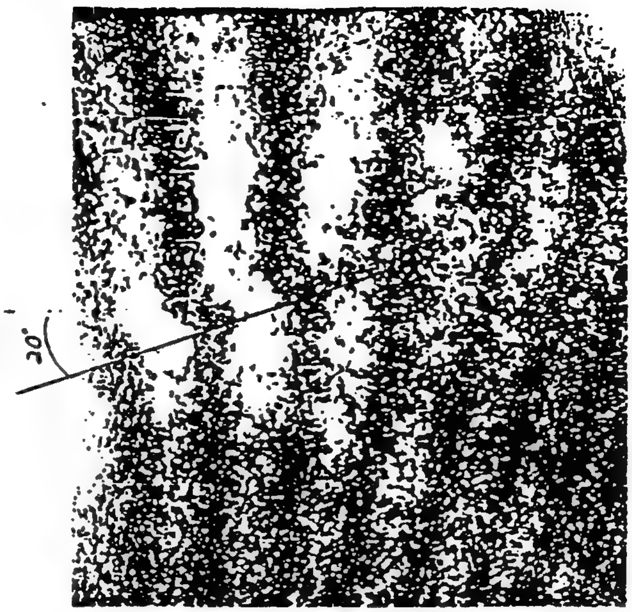

Hidden defects are revealed as sudden slope change of fringes upon small temperature variation of the structure

CONCLUSION

- **Aging aircraft is a very important Air Force issue**
- **S&T community is ready to face this challenge**
- **There are 6.1, 6.2 and 6.3A issues**
- **AF-wide program coordination established**
  - **6.1, 6.2, 6.3A**
  - **Technology User ⟷ Technology Developer**
- **Continue outside Air Force coordination - FAA, NASA and Navy**
- **Substantial 6.1 investment from AFOSR**
- **Community expectation vs. reality of 6.1 basic research**

Aging Aircraft Conference
17 May 1994

RESEARCH & DEVELOPMENT FOR POST PRODUCTION AIR VEHICLES

Otha Davenport
HQ AFMC/EN
(513) 257-7886

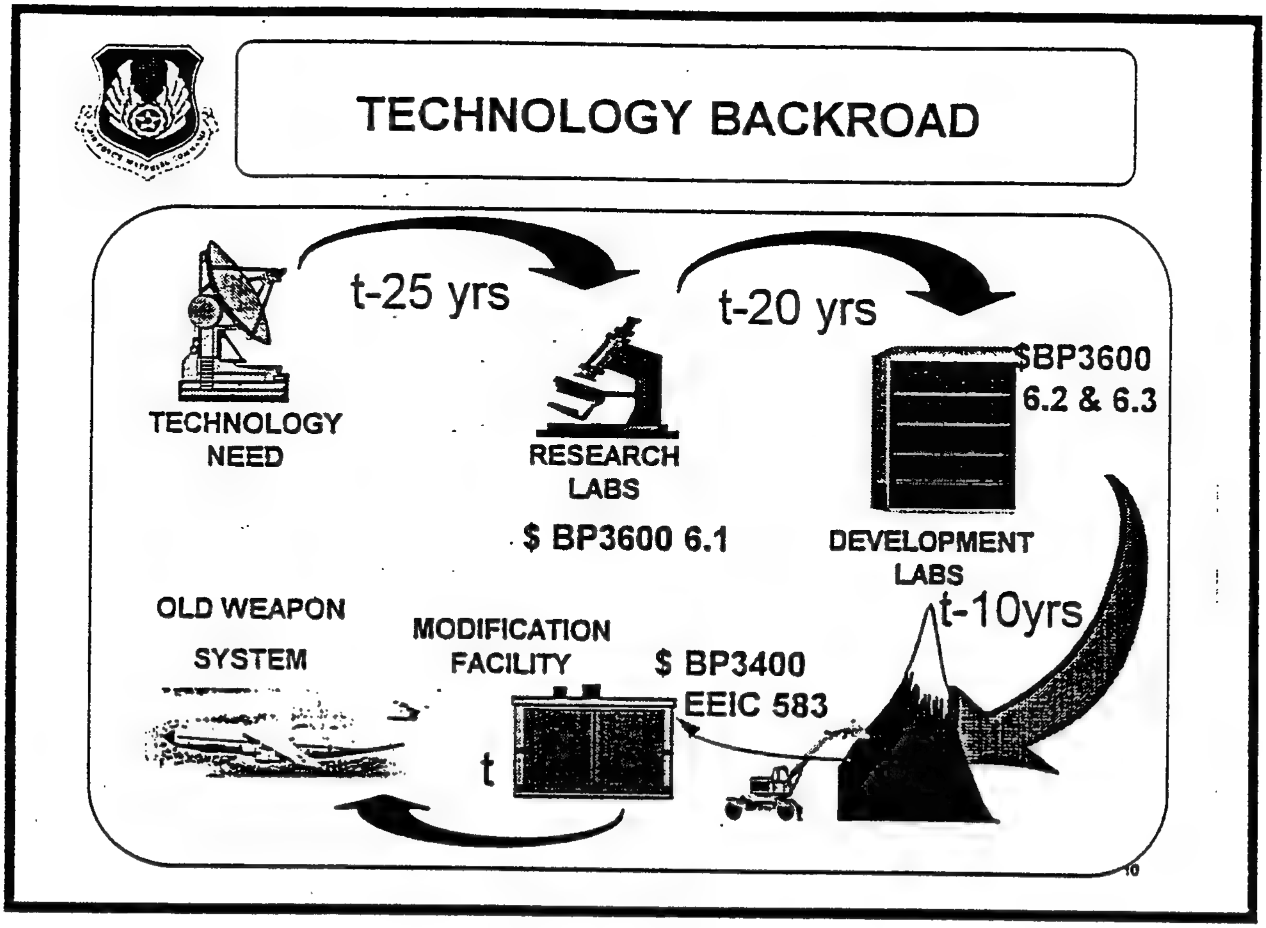
TECHNOLOGY BACKROAD
t-25 yrs
t-20 yrs
TECHNOLOGY NEED
RESEARCH LABS
$ BP3600 6.1
$BP3600 6.2 & 6.3
DEVELOPMENT LABS
t-10yrs
OLD WEAPON SYSTEM
MODIFICATION FACILITY
$ BP3400 EEIC 583
t
10

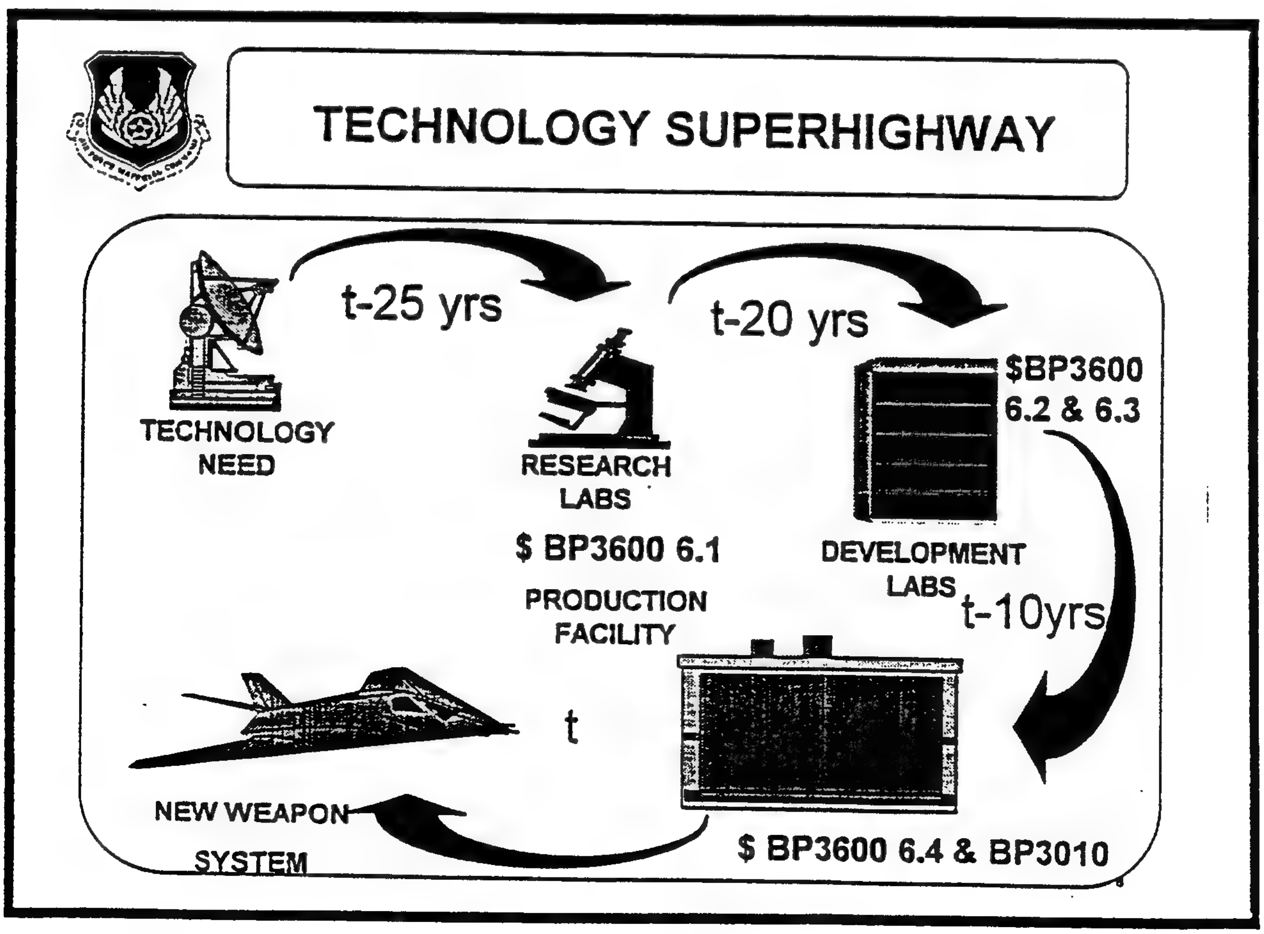
TECHNOLOGY SUPERHIGHWAY
t-25 yrs
t-20 yrs
TECHNOLOGY NEED
RESEARCH LABS
$ BP3600 6.1
$BP3600 6.2 & 6.3
DEVELOPMENT LABS
t-10yrs
PRODUCTION FACILITY
t
NEW WEAPON SYSTEM
$ BP3600 6.4 & BP3010

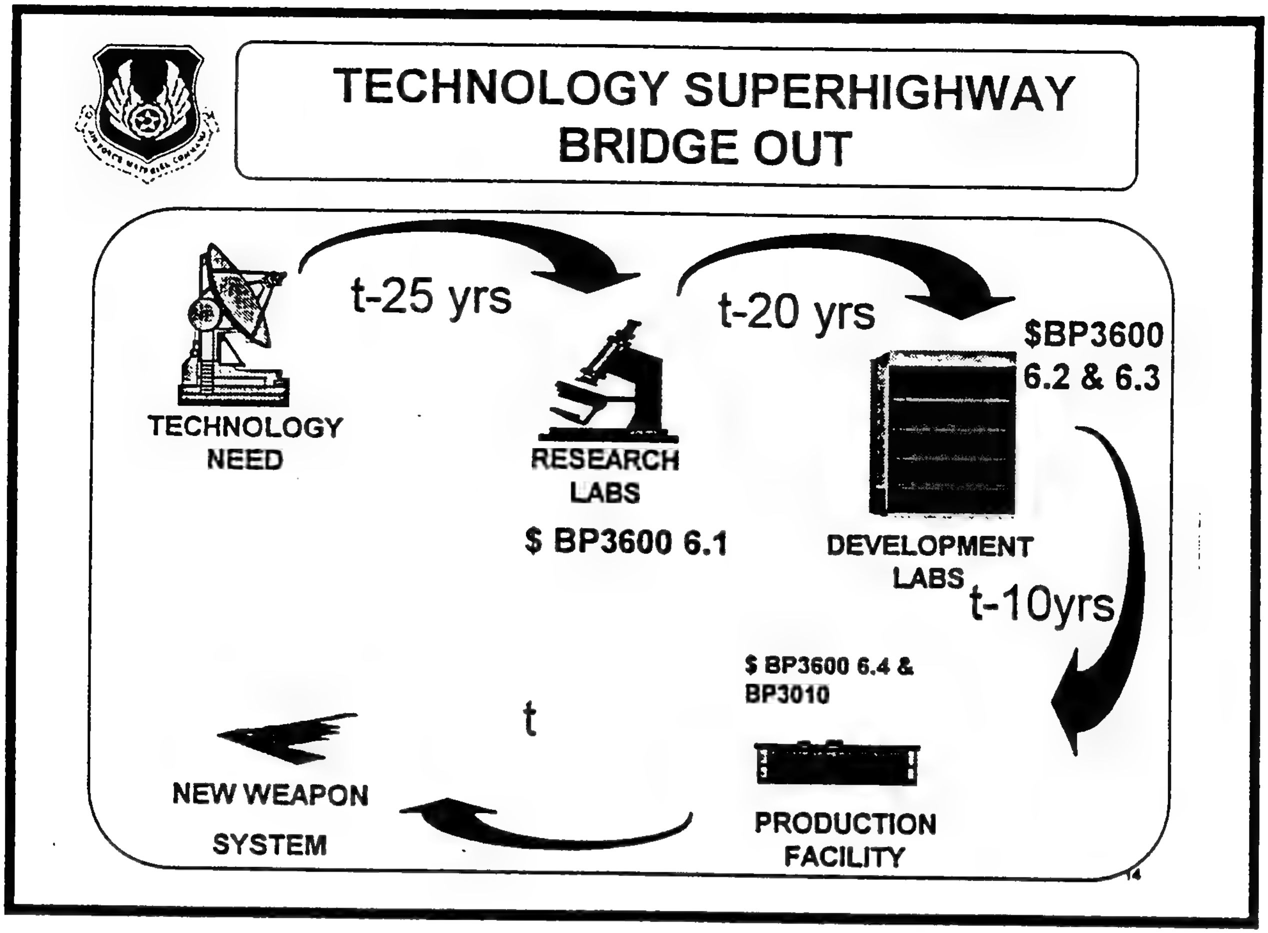
TECHNOLOGY SUPERHIGHWAY
BRIDGE OUT
t-25 yrs
t-20 yrs
TECHNOLOGY
NEED
RESEARCH
LABS
$ BP3600 6.1
$BP3600
6.2 & 6.3
DEVELOPMENT
LABS
t-10yrs
$ BP3600 6.4 &
BP3010
t
NEW WEAPON
SYSTEM
PRODUCTION
FACILITY
14

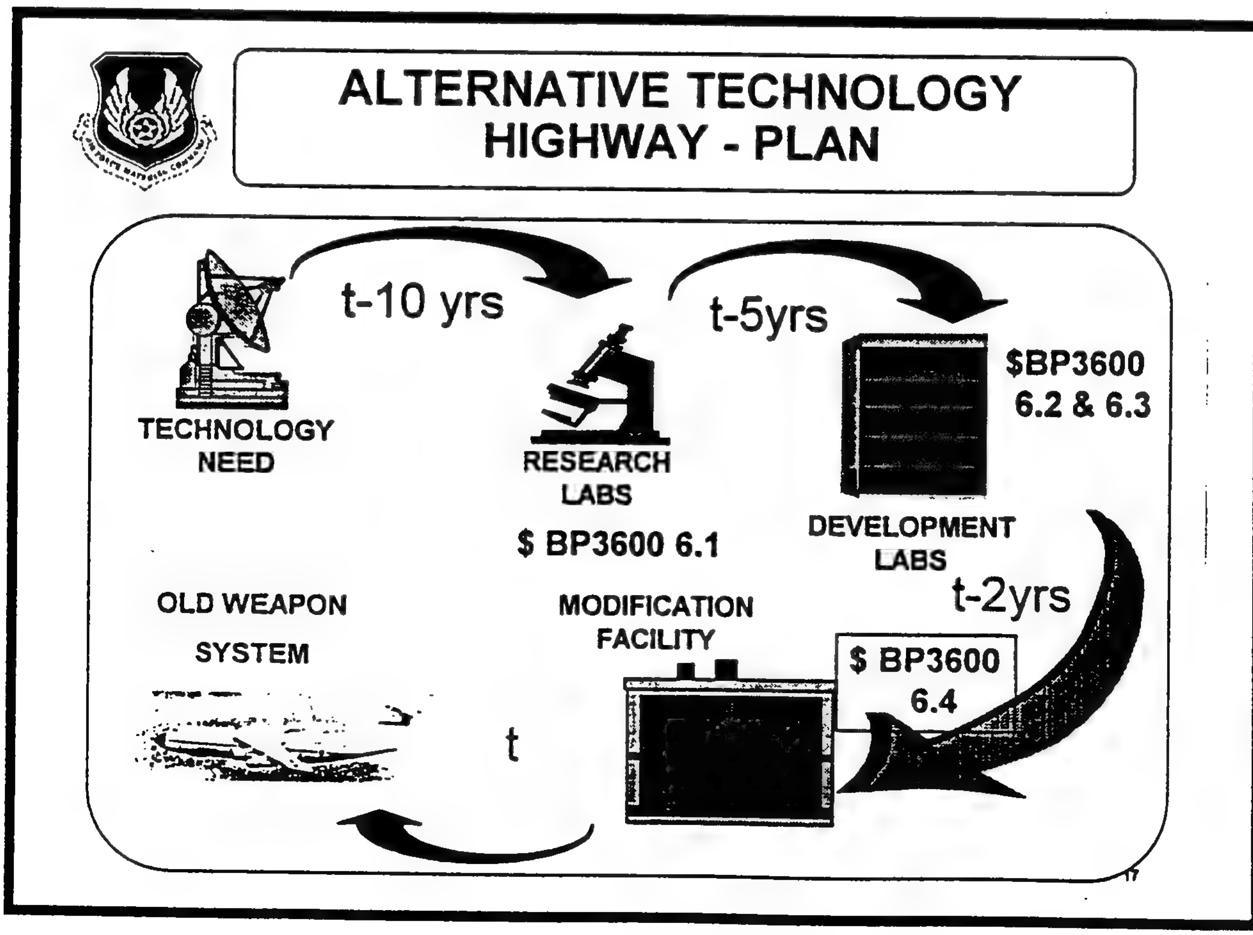
ALTERNATIVE TECHNOLOGY
HIGHWAY - PLAN
t-10 yrs
t-5yrs
TECHNOLOGY
NEED
RESEARCH
LABS
$ BP3600 6.1
$BP3600
6.2 & 6.3
DEVELOPMENT
LABS
t-2yrs
OLD WEAPON
SYSTEM
MODIFICATION
FACILITY
$ BP3600
6.4
t
17

USER NEED
THE KEY TO TECHNOLOGY USE

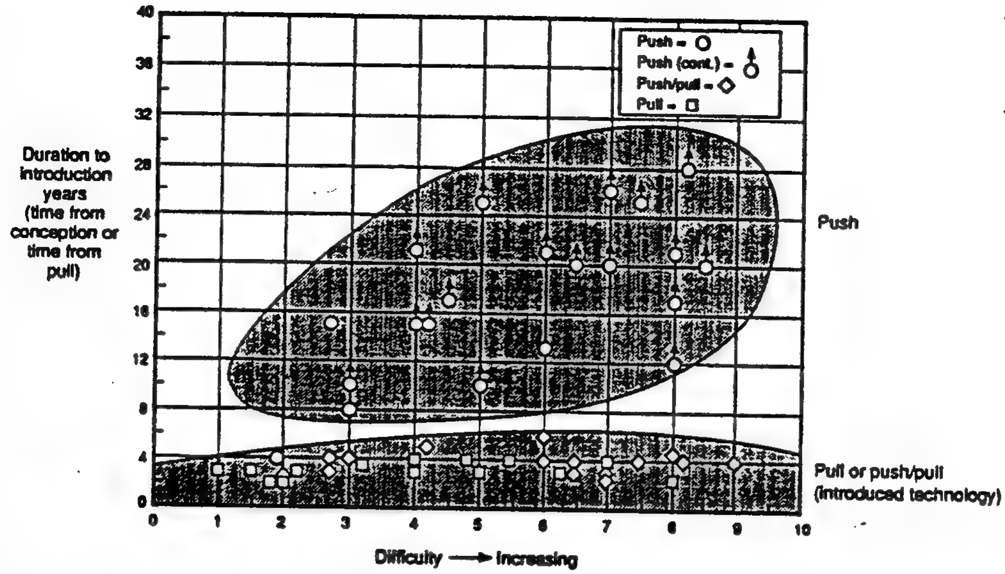

SOURCE: GENERAL ELECTRIC, SAE AEROSPACE ATLANTIC ,1992

AIR FORCE MATERIEL COMMAND

WRIGHT LABORATORY

AGING SYSTEMS CFIPT

O. LESTER SMITHERS, JR.
DEPUTY DIRECTOR
WRIGHT LABORATORY
WRIGHT-PATTERSON AFB, OHIO

THE NEW WRIGHT LABORATORY INTEGRATED PRODUCT TEAM PROCESS PHILOSOPHY

- **INFORMED CUSTOMERS/SUPPLIERS**
  - THE WARRIORS BECOME ADVOCATES OF CRITICAL TECHNOLOGY
- **TECHNOLOGY ORCHESTRATION**
  - WL QUARTERBACKS AIR VEHICLE TECHNOLOGY TEAM
- **CLEAR STRATEGIC FRAMEWORK:**
  - SYSTEM INTEGRATED TECHNOLOGIES
    - RESOURCE ALLOCATION
      - STRONG U.S. TECHNOLOGY BASE
- **EMPOWERMENT**
  - RIGHT PEOPLE/RIGHT JOBS

NEW WL IPT FRAMEWORK HOW IT WILL WORK

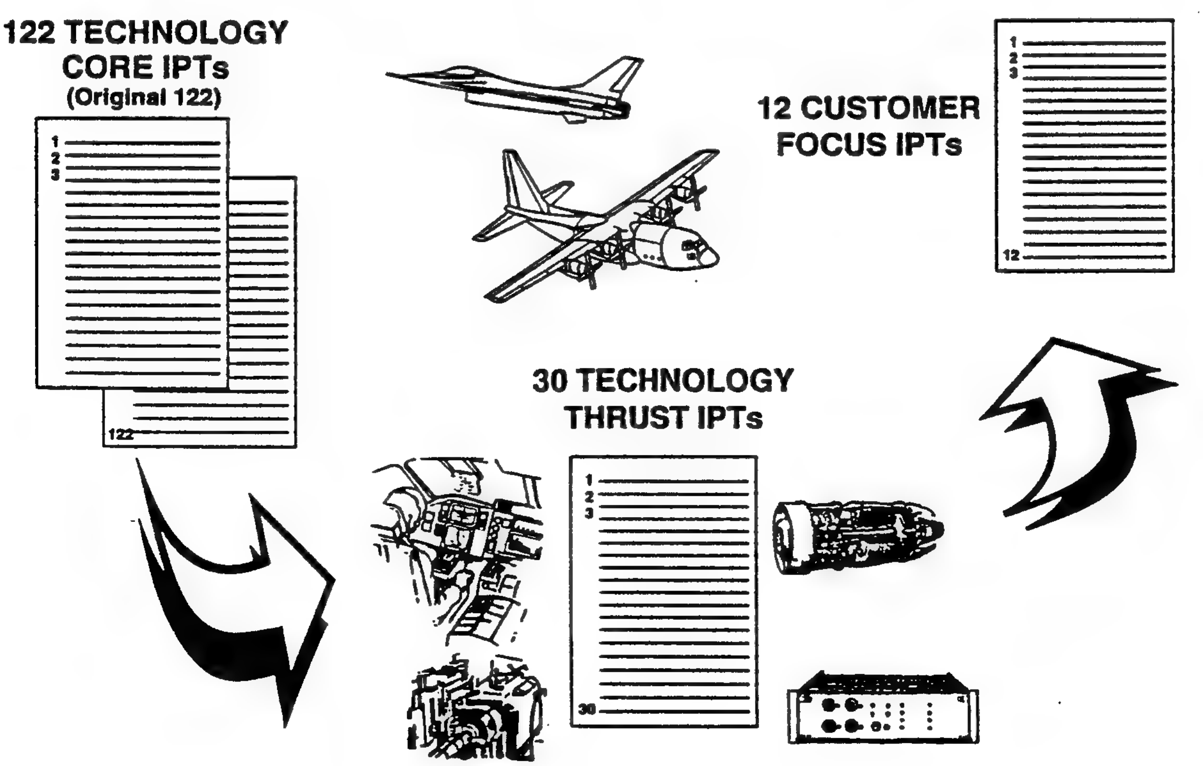

TECHNOLOGY THRUST IPTs

NAME

Avionics

1. Targeting & Attack Avionics
2. Electronic Warfare Technology
3. Systems Avionics
4. Electron Devices

Flight Vehicles

1. Aeromechanics
2. Structures
3. Control Science & Technology
4. Cockpit Integration
5. Vehicle Subsystems
6. Technology Integration/Flight Demonstration

Materials & Processes

1. Structures, Propulsion & Subsystems
2. Electronics, Optics & Survivability
3. Systems & Operational Support

NAME

Armament

1. Advanced Guidance
2. Weapons, Flight Mechanics
3. Ordnance
4. Instrumentation

Manufacturing Technology

1. Aircraft
2. Missiles & Munitions
3. C3I Mission Electronics
4. Space & Launch
5. Aerospace Sustainment
6. Manufacturing Systems
7. Advanced Manufacturing
8. Manufacturing 2005
9. Defense Production Act

Propulsion

1. Turbine Engine
2. Fuels & Lubrication
3. High Speed Propulsion
4. Aerospace Power

CUSTOMER FOCUSED IPTs

1. FIGHTERS
2. GLOBAL AIRLIFTERS / INTRA-THEATER TRANSPORT
3. BOMBERS
4. RECCE / INTEL
5. SPECIAL OPERATION FORCES
6. UNMANNED AIR VEHICLES
7. WEAPONS
8. SPACE SYSTEMS AND LAUNCH
9. AGING SYSTEMS AND ALC SUPPORT
10. T&E CENTER SUPPORT
11. POLLUTION PREVENTION
12. CORE TECHNOLOGIES

CFIPT

- WL team
- Focuses technology on products
- Works with TPIPTs (tech needs ⇄ military requirements)
- Translates technology needs → technology solutions
- Balances technologies
- Builds system oriented technology roadmaps (near, mid, far)
- Orchestrates resources to make it happen
- Members:
  WL Tech Thrust IPT members
- Partners: TPIPTs
- Leader:
  - Senior, experienced
  - Speaks both technology & systems
  - Reports directly to WL/CC/CD

TECH THRUST IPTs \ CUSTOMER FOCUS	FIGHTERS			GLOBAIRLIFT			BOMBE	
	INV	DEV	FUT	INV	DEV	FUT	INV	DEV
AVIONICS								
TARGETING & ATTACK AVIOINCS	X	X	X	X	X	X	X	X
ELECTRONIC WARFARE TECH	X	X	X	X	X	X	X	X
SYSTEM AVIOINCS	X	X	X	X	X	X	X	X
ELECTRONIC DEVICES	X	X	X	X	X	X		
FLIGHT VEHICLES								
AEROMECHANICS	X	X	X			X		X
STRUCTURES	X	X	X	X	X	X	X	X
CONTROL SCIENCE TECHNOLOGY	X	X	X	X	X	X	X	X
COCKPIT INTEGRATION	X	X	X	X	X	X	X	X
VEHICLE SUBSYSTEMS	X	X	X	X	X	X	X	X
TECH INTEGRATION/FLT DEMO	X	X	X				X	X
M & P FOR								
SUBSYSTEMS	X	X	X	X				
VIVABILITY	X	X	X					
	X	X	X					

OVERVIEW OF WL AGING SYSTEMS CFIPT

- **ESTABLISHED:** September 1993
- **PURPOSE:** Assure coordinated WL activities & leveraging the development & transition of technologies that support aging systems
- **VISION:** Extend lives & contain costs of aging weapon systems
- **PAYOFFS:**
  - Increased operational readiness ~ reduced repair downtime
  - Reduced maintenance & repair costs
  - Increased safe operating life (e.g., damage tolerance)

FLIGHT DYNAMICS DIRECTORATE

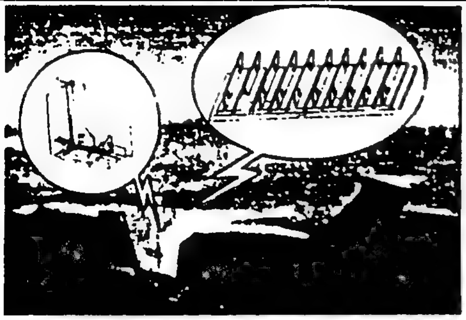
Widespread Fatigue Damage


Corrosion Fatigue

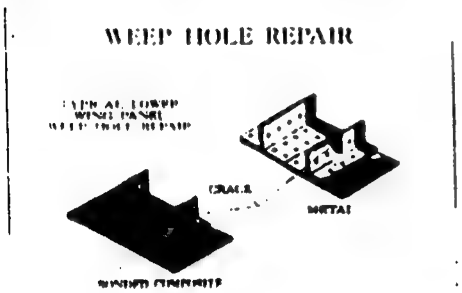

Repair Integrity

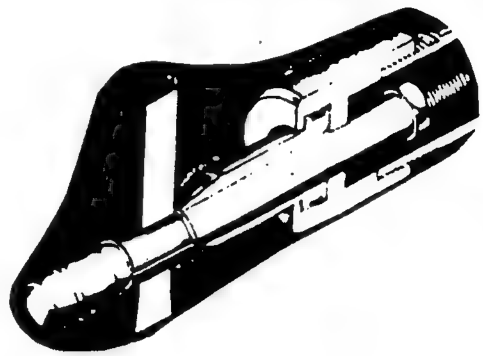
Life Enhancement

WRIGHT LABORATORY MATERIALS DIRECTORATE

NDE RESEARCH

SYSTEMS SUPPORT

CORROSION PROGRAMS

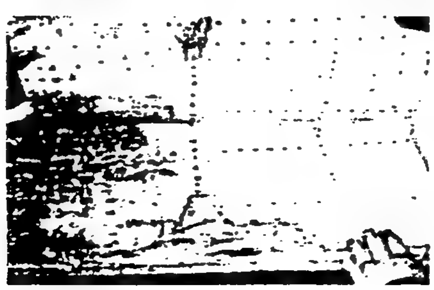

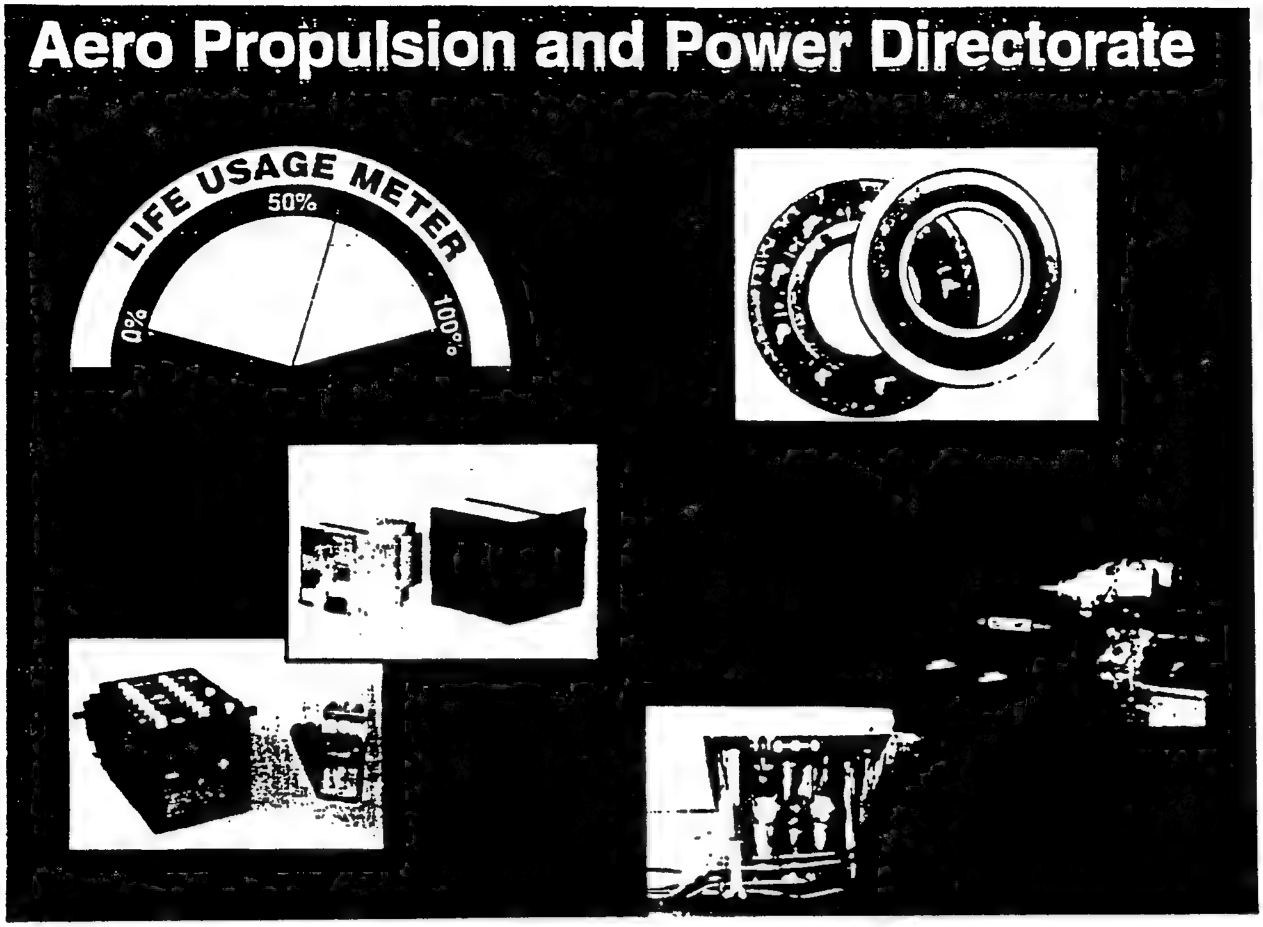

SOLID STATE ELECTRONICS DIRECTORATE

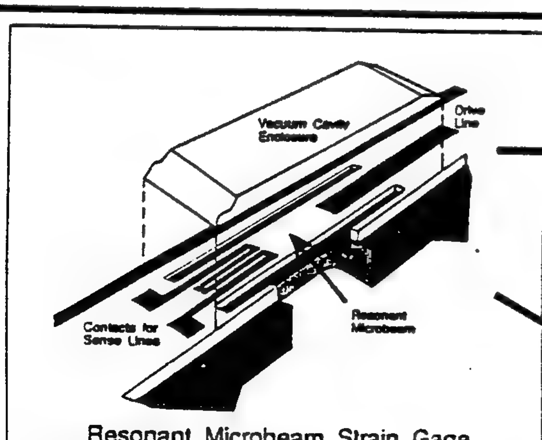

Resonant Microbeam Strain Gage

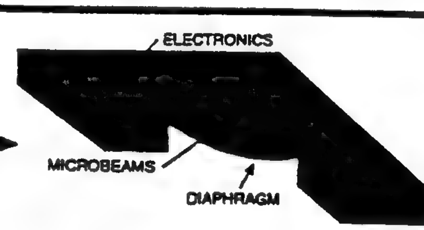

Pressure Sensor

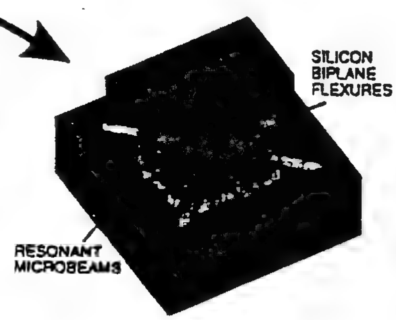

Accelerometer

OBJECTIVE

- DEVELOP SOLID STATE MICROSENSOR TECHNOLOGY FOR AIR FORCE SYSTEMS
- DEMONSTRATE
  - PRESSURE SENSOR
  - ACCELEROMETER
- PROVIDE CORE SENSOR TECHNOLOGY BASE APPLICABLE TO STRUCTURAL CRACK DETECTION

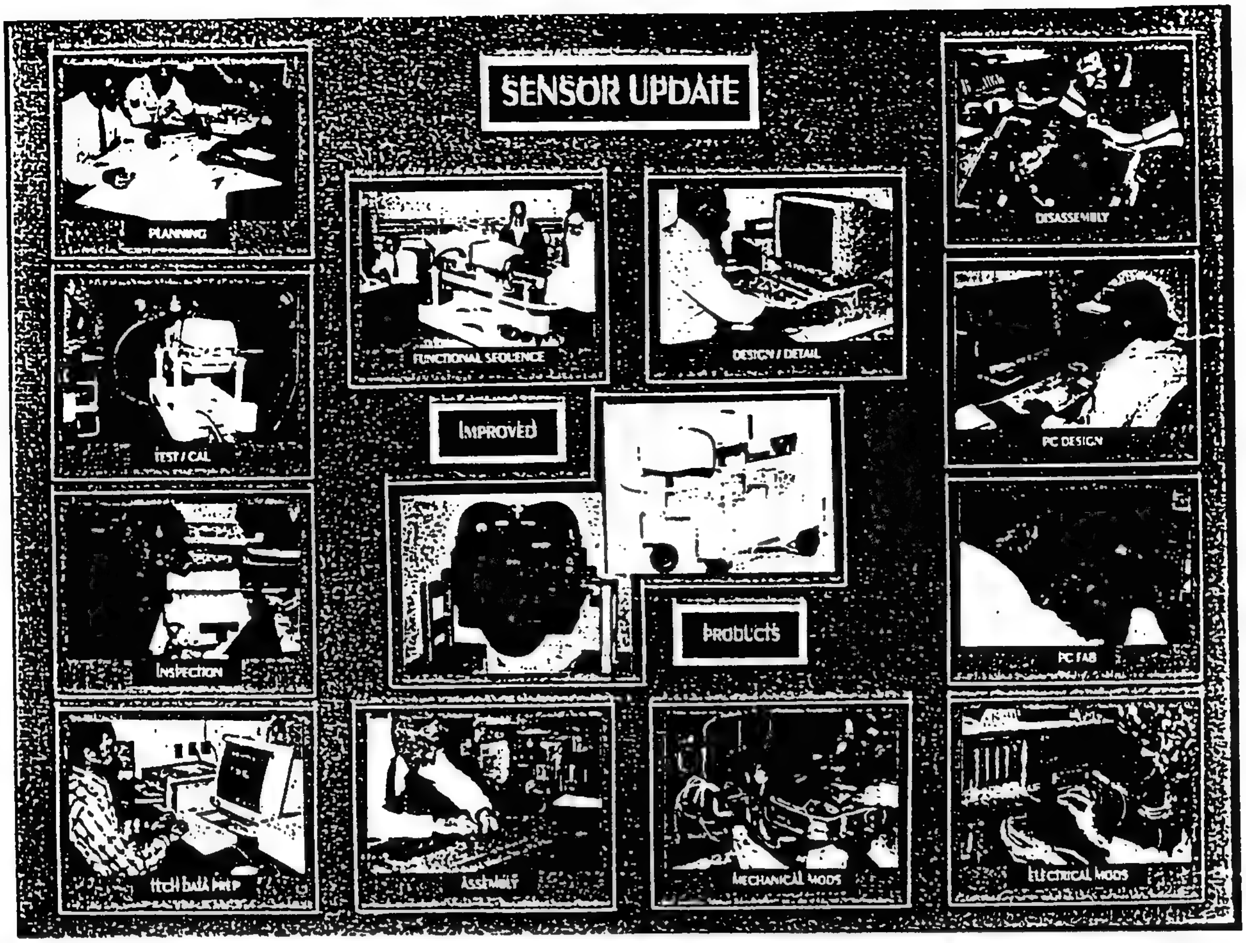

PLANS AND PROGRAMS DIRECTORATE

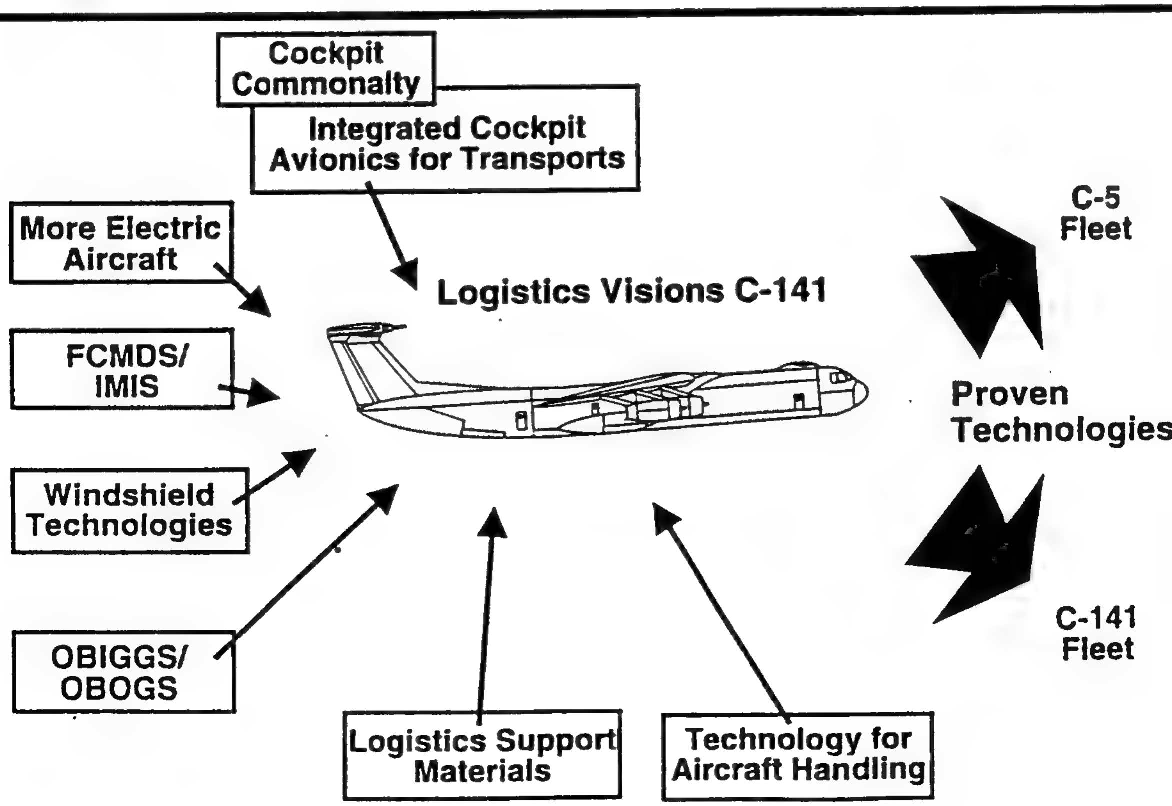

NASA AIRFRAME STRUCTURAL INTEGRITY PROGRAM

Program Overview and Recent Accomplishments

presented by

Dr. Charles E. Harris
Program Implementation Team Leader
Research and Technology Group
NASA Langley Research Center

at the

Air Force Workshop on Aging Aircraft Research

May 17, 1994
Oklahoma City (Tinker AFB), Oklahoma

NASA Airframe Structural Integrity Program

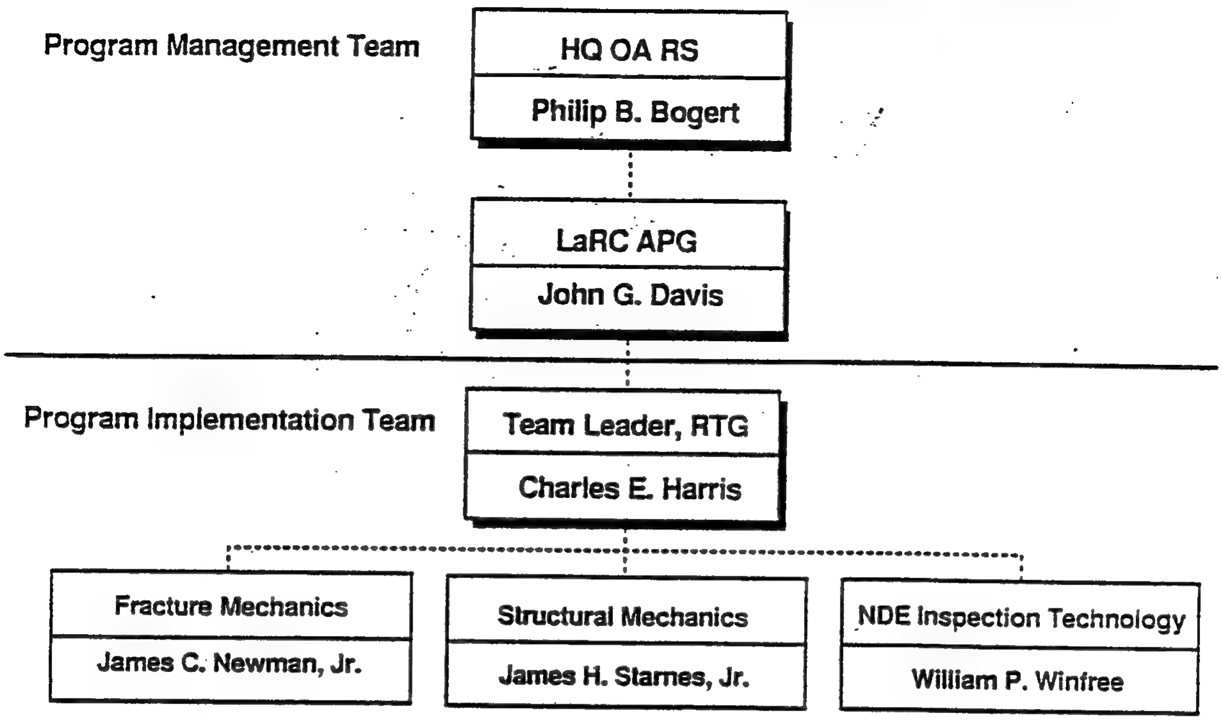

TECHNOLOGY REQUIREMENTS

Technology to reliably and economically inspect aging aircraft to detect:

- **Disbonds in fuselage splice joints and tear straps**
- **Fatigue cracks in riveted structure**
- **Airframe corrosion**

Damage tolerance analysis methodology for riveted structure to:

- **Establish inspection requirements**
- **Evaluate the need to repair damaged structure**
- **To conduct analyses of repaired structure**

Advanced quantitative technology to economically conduct structural audits of high time airplanes

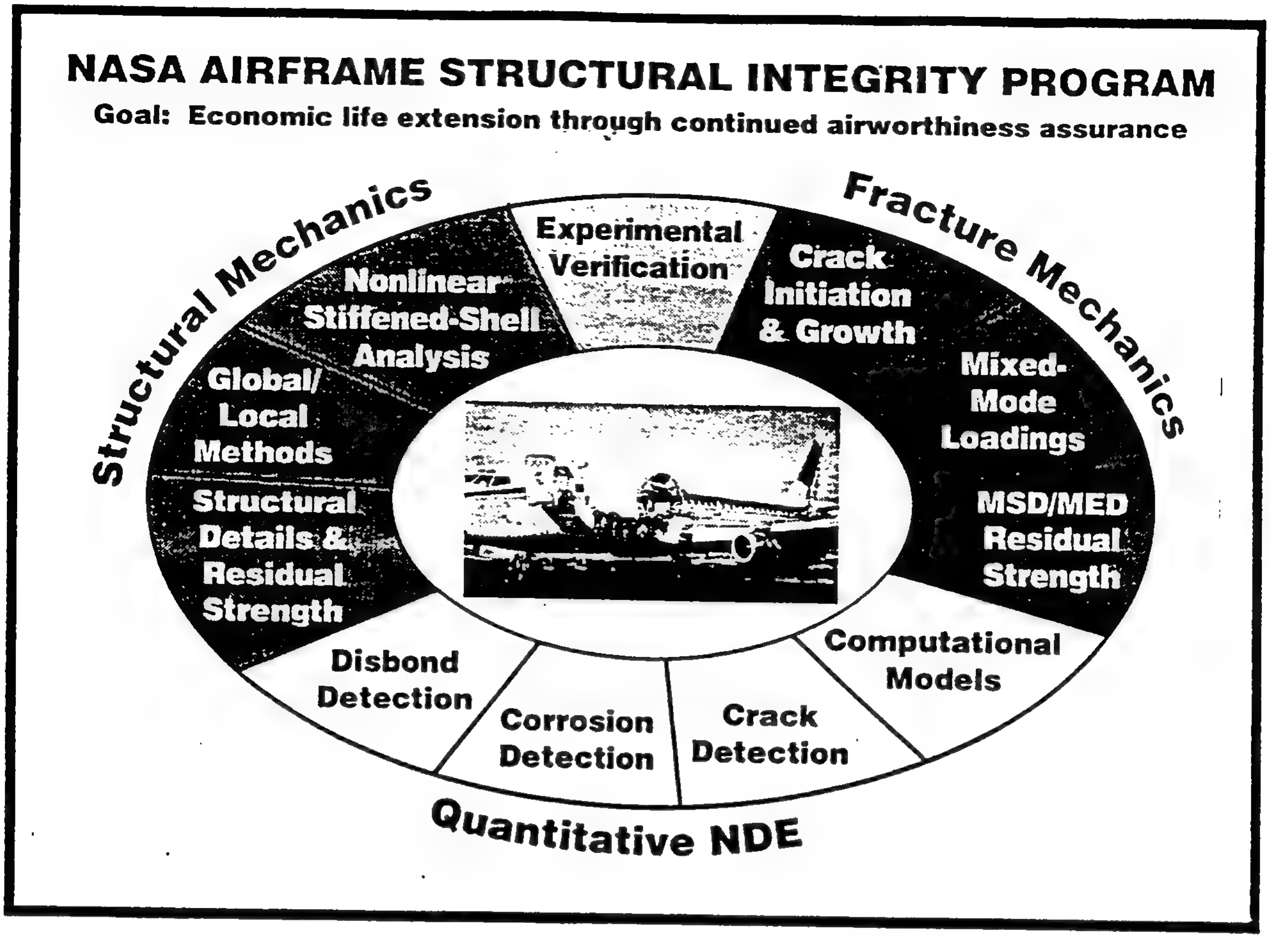
NASA AIRFRAME STRUCTURAL INTEGRITY PROGRAM
Goal: Economic life extension through continued airworthiness assurance
Structural Mechanics
Experimental Verification
Fracture Mechanics
Nonlinear Stiffened-Shell Analysis
Crack Initiation & Growth
Global/ Local Methods
Mixed-Mode Loadings
Structural Details & Residual Strength
MSD/MED Residual Strength
Disbond Detection
Corrosion Detection
Crack Detection
Computational Models
Quantitative NDE

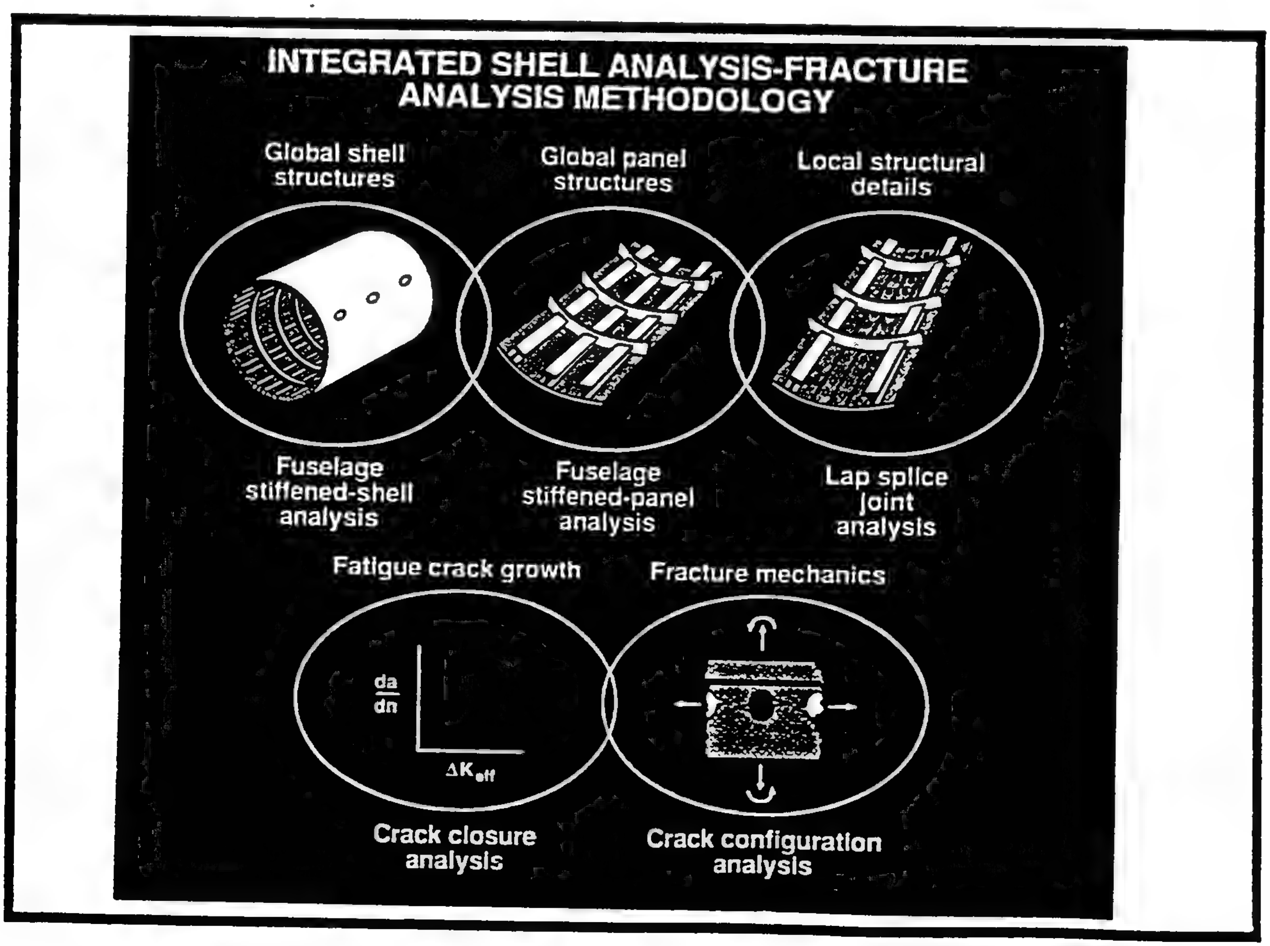
INTEGRATED SHELL ANALYSIS-FRACTURE ANALYSIS METHODOLOGY
Global shell structures
Global panel structures
Local structural details
Fuselage stiffened-shell analysis
Fuselage stiffened-panel analysis
Lap splice joint analysis
Fatigue crack growth
Fracture mechanics
da/dn
ΔK eff
Crack closure analysis
Crack configuration analysis

FRACTURE MECHANICS OF AIRCRAFT STRUCTURE

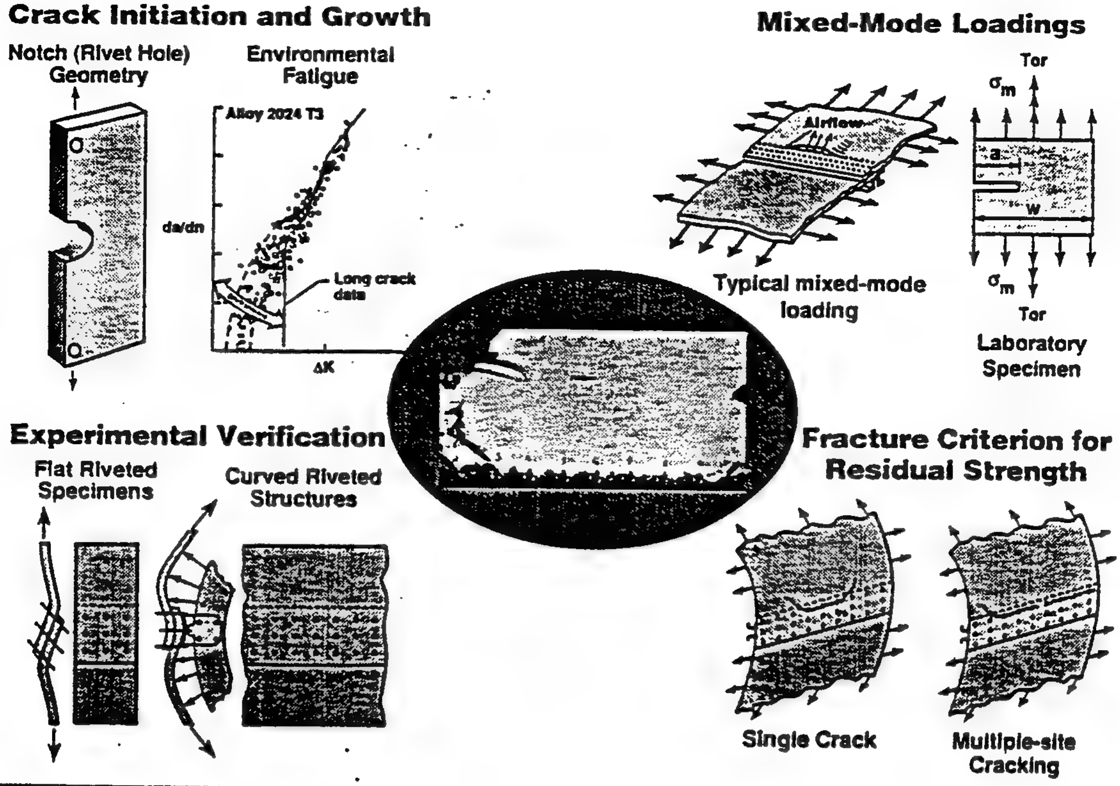

FRACTOGRAPHY OF WSFD IN STRUCTURAL FATIGUE TEST ARTICLE

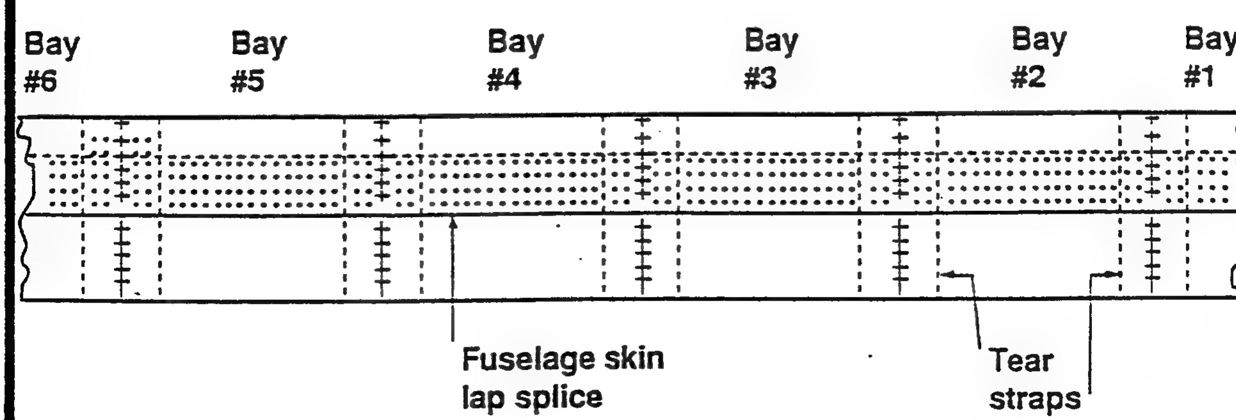

Fatigue Crack Growth Controlled by Closure Mechanism

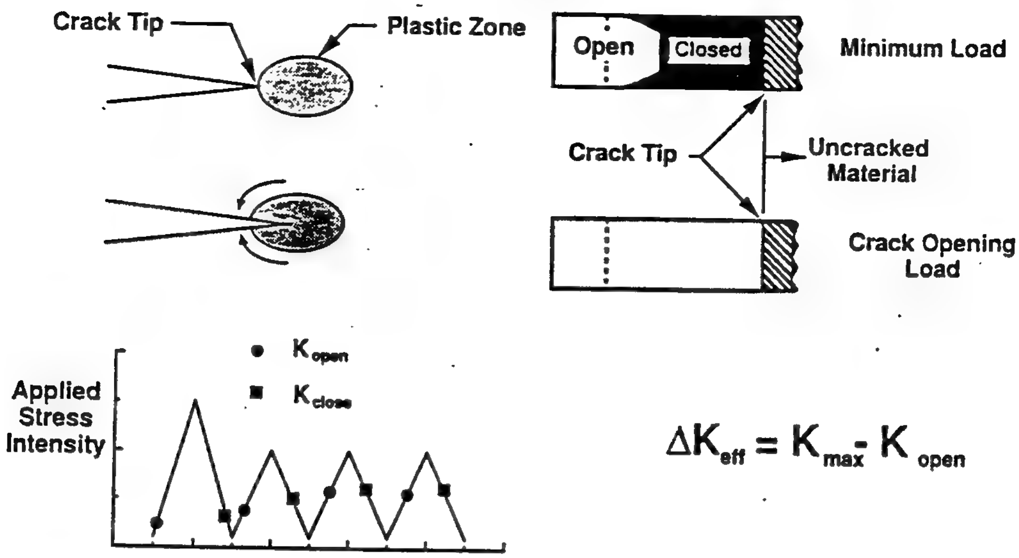

$$\Delta K_{eff} = K_{max} - K_{open}$$

WSFD Panel Bay #1

116

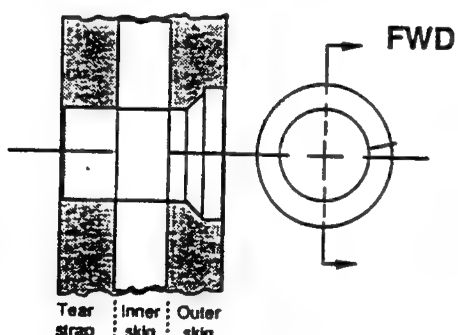

a)

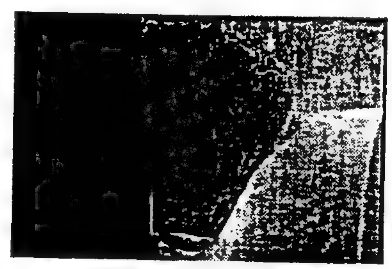

250 µm

b)

50 µm

c)

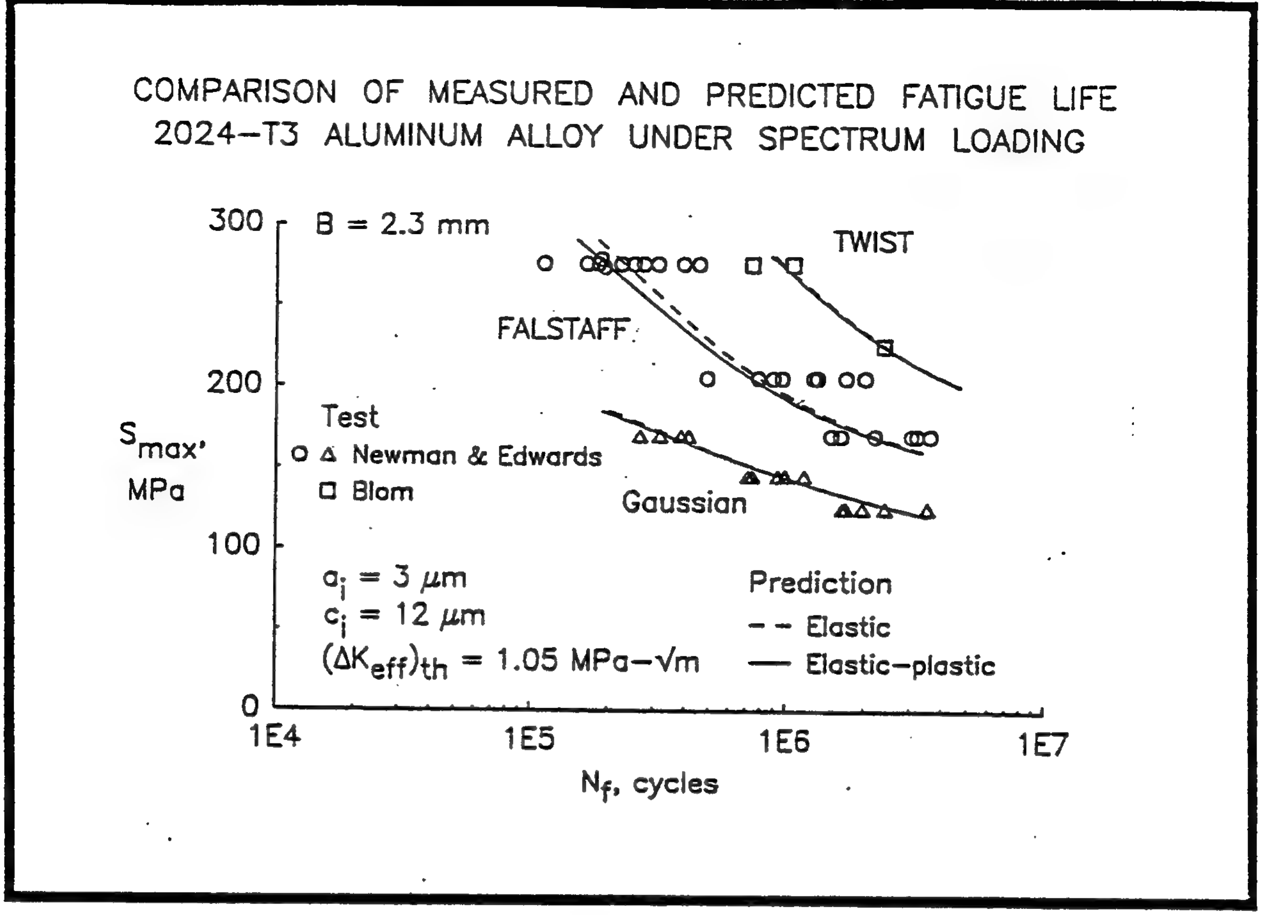

COMPARISON OF MEASURED AND PREDICTED FATIGUE LIFE
2024–T3 ALUMINUM ALLOY UNDER SPECTRUM LOADING
B = 2.3 mm
TWIST
FALSTAFF
Gaussian
Test
Newman & Edwards
Blom
a_i = 3 μm
c_i = 12 μm
$(\Delta K_{eff})_{th}$ = 1.05 MPa–√m
Prediction
Elastic
Elastic–plastic
S_{max}, MPa
N_f, cycles
300
200
100
0
1E4
1E5
1E6
1E7

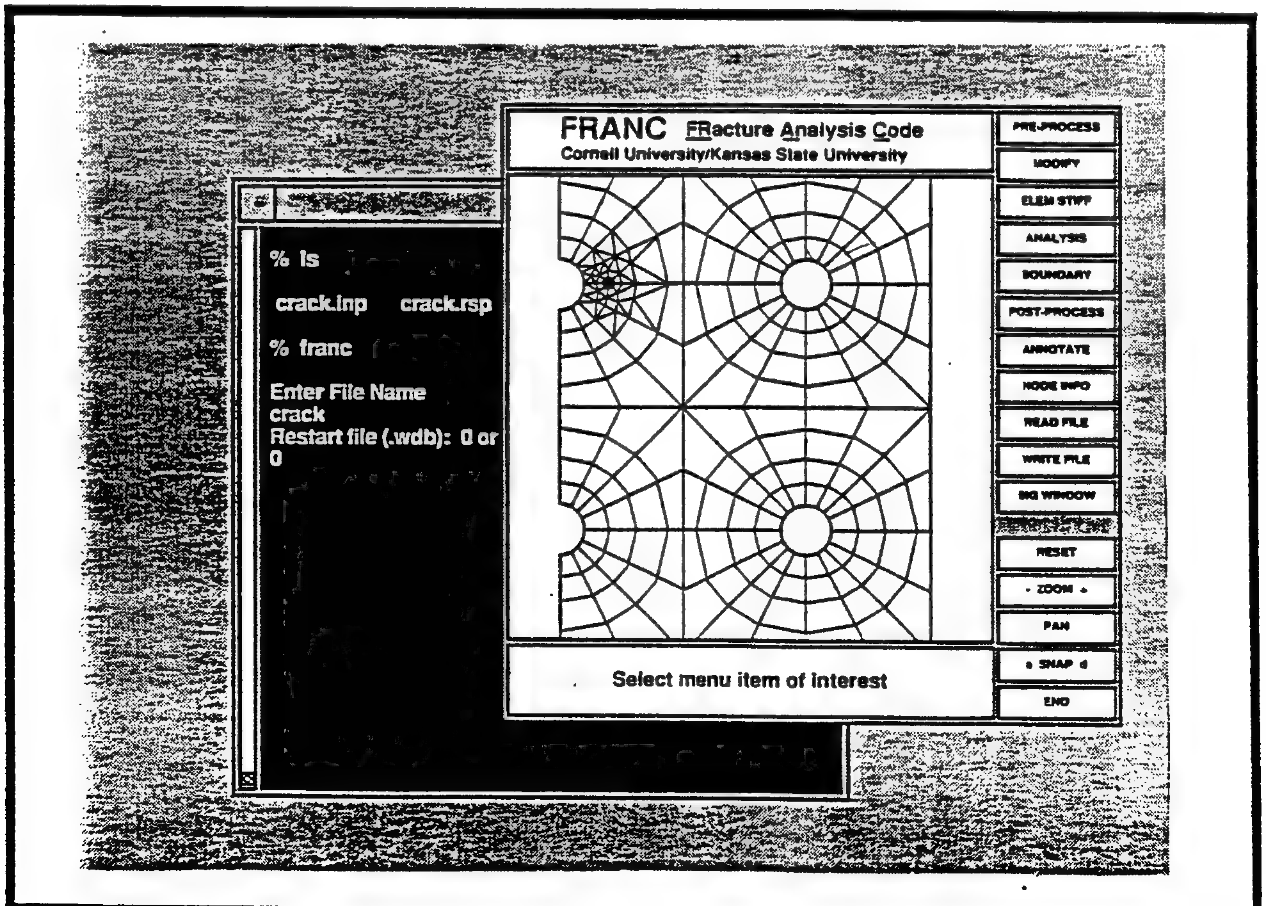

FRANC FRacture Analysis Code
Cornell University/Kansas State University
% ls
crack.inp crack.rsp
% franc
Enter File Name
crack
Restart file (.wdb): 0 or
0
PRE-PROCESS
MODIFY
ELEM STIFF
ANALYSIS
BOUNDARY
POST-PROCESS
ANNOTATE
NODE INFO
READ FILE
WRITE FILE
BIG WINDOW
RESET
- ZOOM +
PAN
SNAP
END
Select menu item of interest

FRACTURE MECHANICS OF CRACKS EXTENDING FROM RIVETS

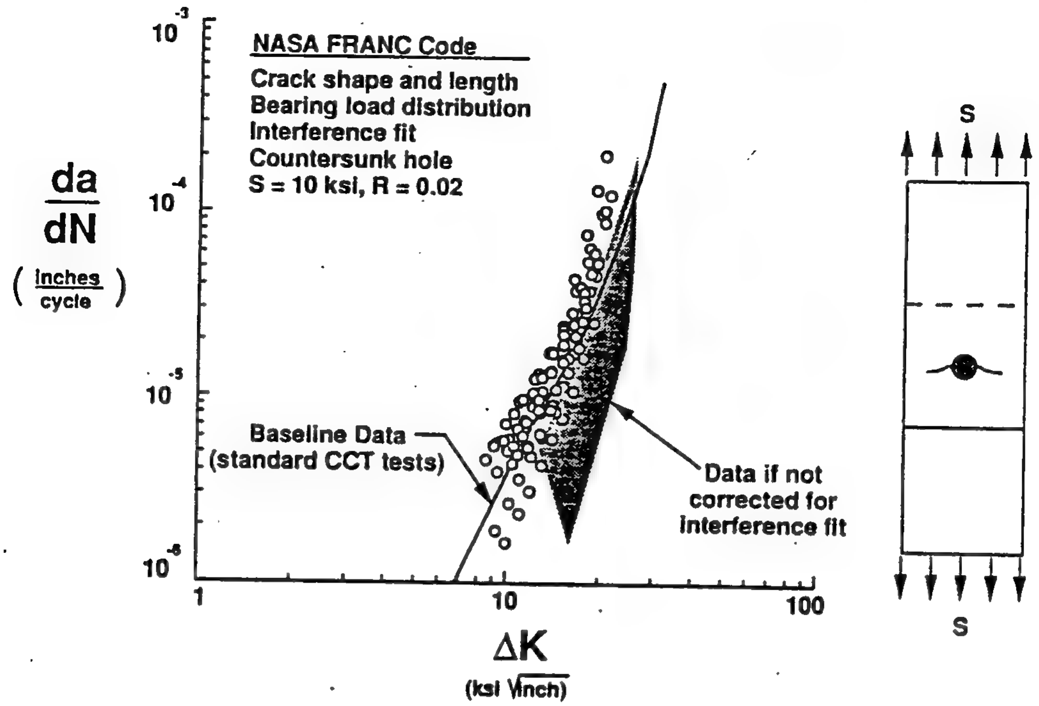

CRITICAL CRACK-TIP-OPENING ANGLE (CTOA) FRACTURE CRITERION

Experimental Verification Program

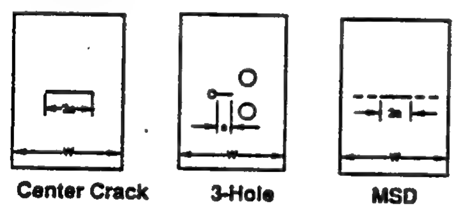

Video Image of CTOA Measurement

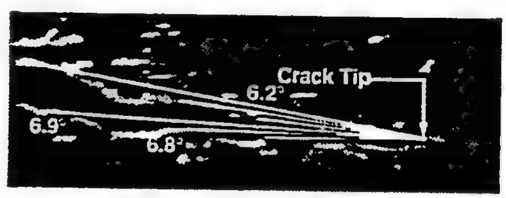

Measured CTOA as a Function of Crack Growth

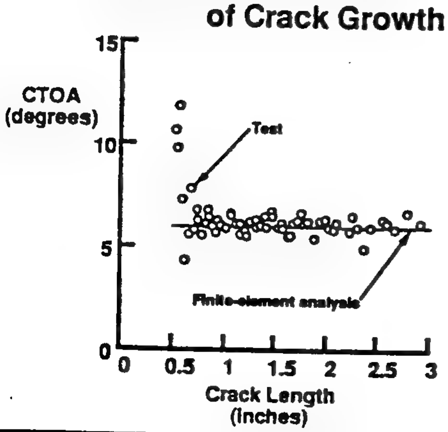

Predicted Stable Crack Growth

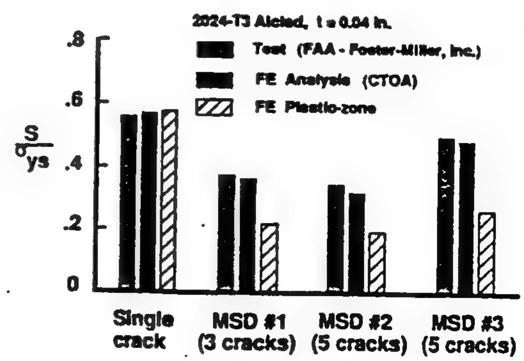

STRUCTURAL MECHANICS OF AIRCRAFT STRUCTURE

Nonlinear Stiffened-Shell Analysis (STAGS & FRANC3D)

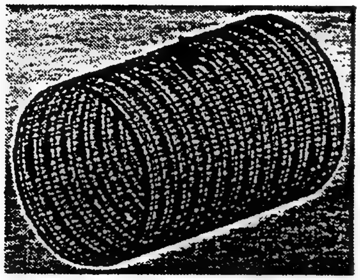

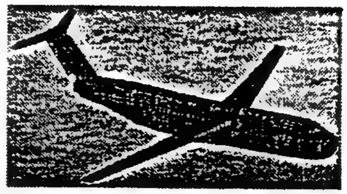

Global/Local Methods

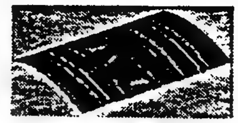

36 Bay local model

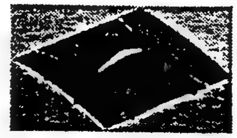

6 Bay local model

Experimental Verification

Pressure box

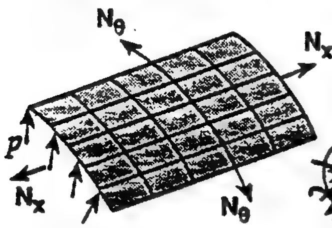

Stiffened cylinder

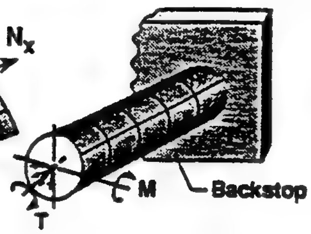

Structural Details & Residual Strength

Single Crack

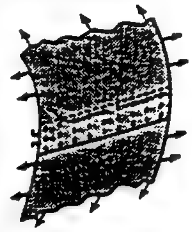

Multiple-site Cracking

Stiffened Aluminum Fuselage Shell with 20" Skin Crack

Pressure = 8.0 psi
Radius = 74 in.
Skin thickness = .036 in.

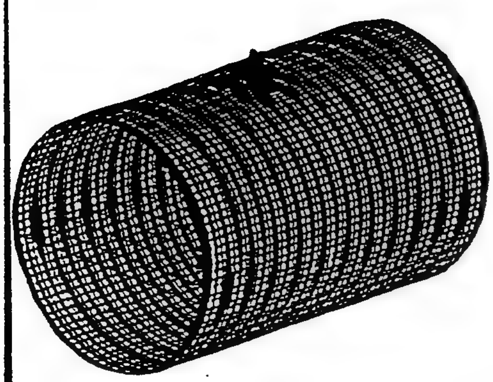

Global Model

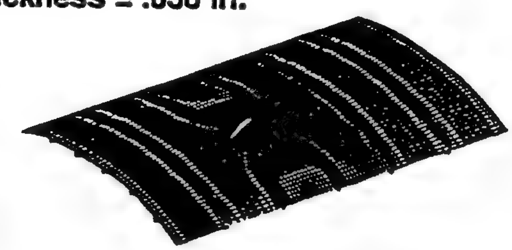

36 Bay Local Model

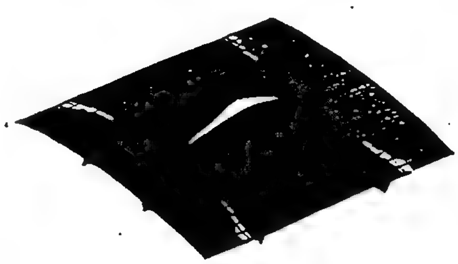

6 Bay Local Model

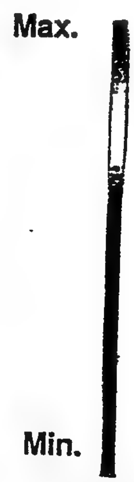

Resultant Hoop Stress

Stiffened Aluminium Fuselage Shell with a Skin Crack
2 x 3 Bay Model

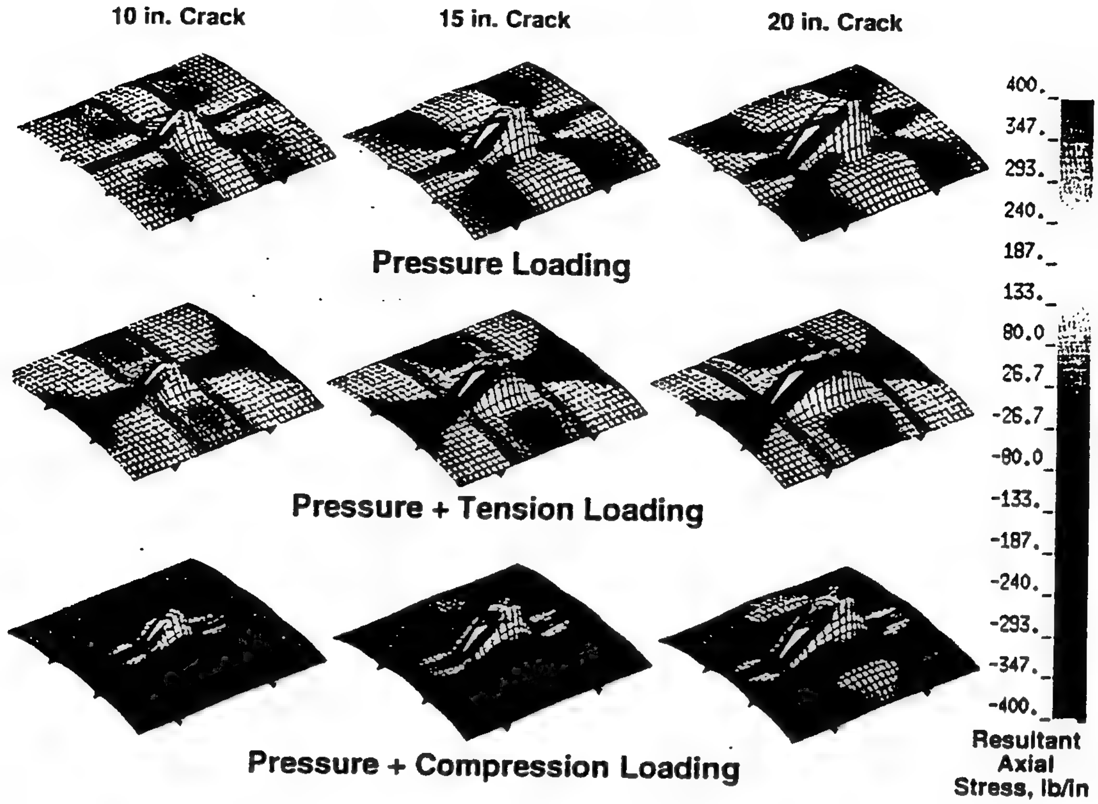

Crack Growth Model for Stiffened Aluminum Fuselage Shell with Skin Crack and Broken Frame

Pressure = 8.0 psi
Radius = 74 in.
Skin thickness = .036 in.

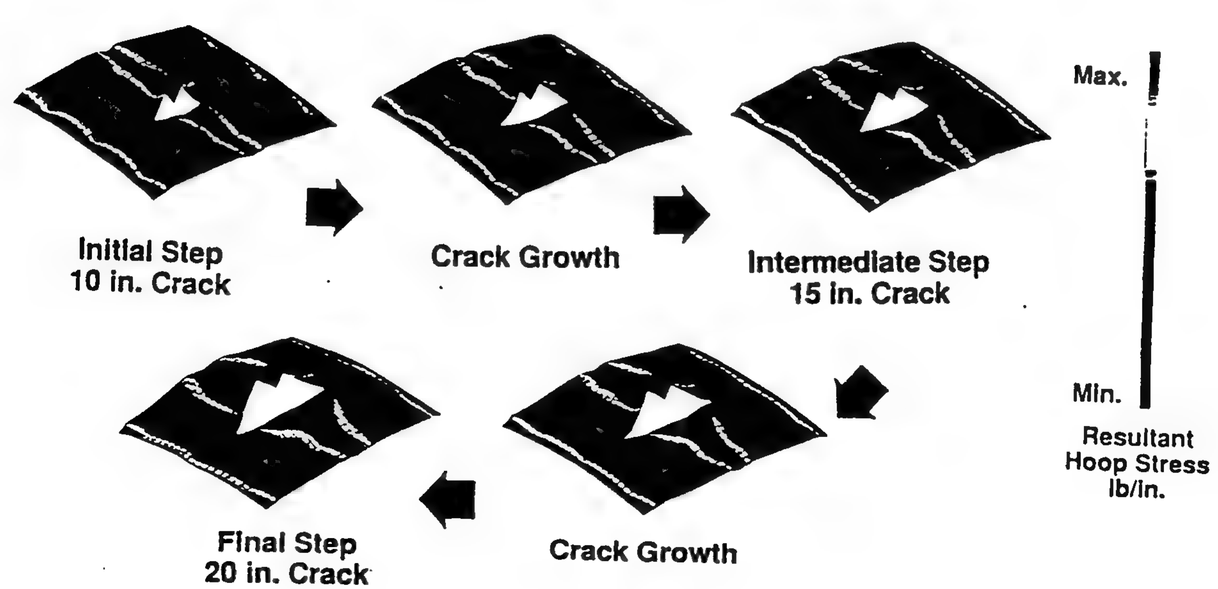

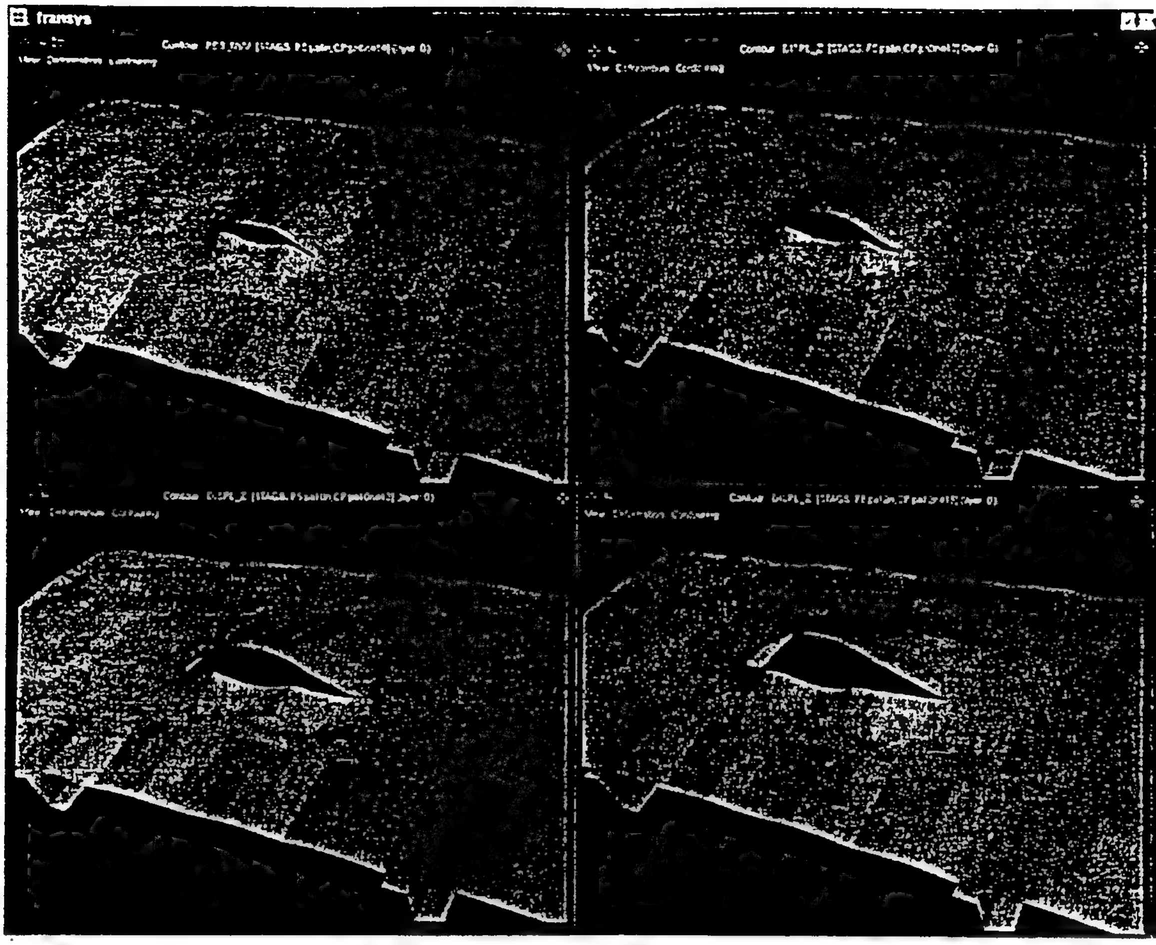

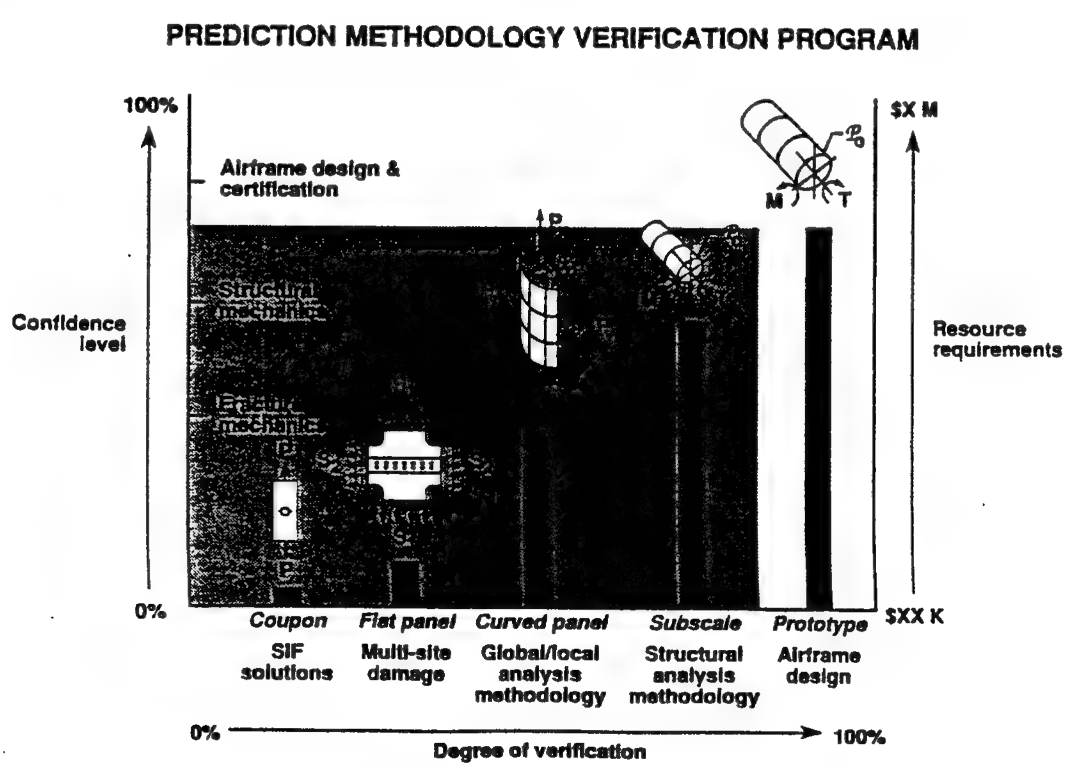

PREDICTION METHODOLOGY VERIFICATION PROGRAM
100%
0%
Airframe design & certification
Confidence level
$X M
$XX K
Resource requirements
Coupon
SIF solutions
Flat panel
Multi-site damage
Curved panel
Global/local analysis methodology
Subscale
Structural analysis methodology
Prototype
Airframe design
0%
100%
Degree of verification

PRESSURE-BOX STRUCTURAL TEST FIXTURE

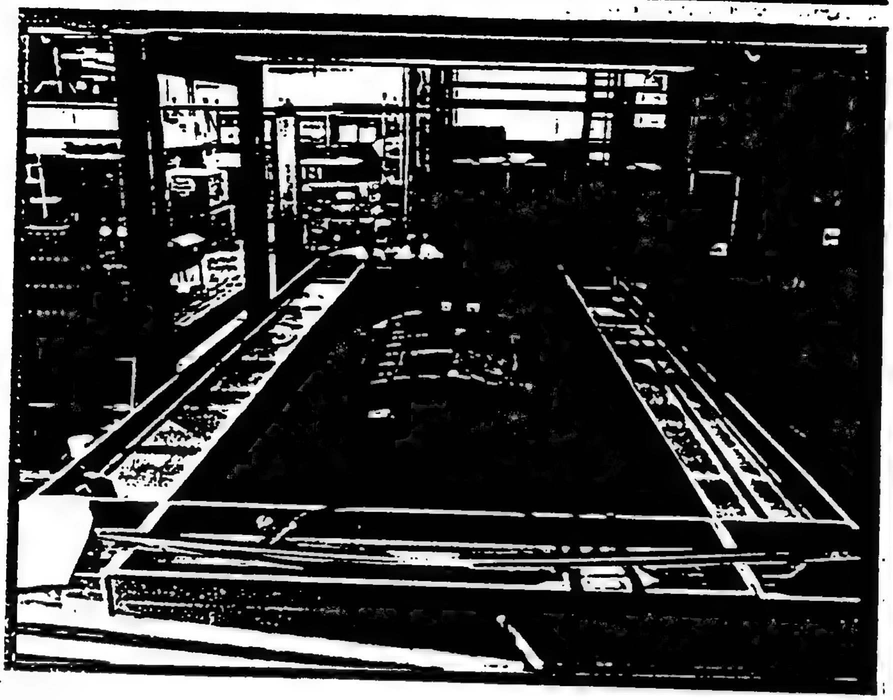

QUANTITATIVE NDE FOR AIRCRAFT STRUCTURES

Disbond Detection
(Ultrasonics, thermography, optics)

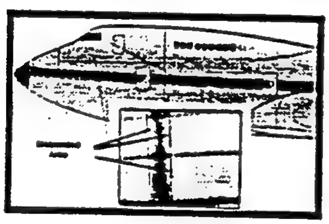

Corrosion Detection
(Ultrasonics, magnetics, thermography, radiography, optics)

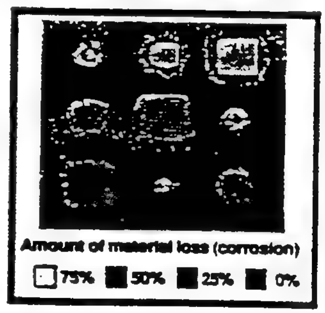

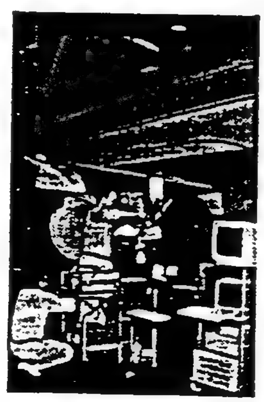

Computational Models

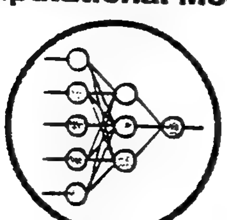

Trained
Artificial Neural Network

Crack Detection
(Ultrasonics, magnetics, thermography, optics)

MOI image of cracks at rivet

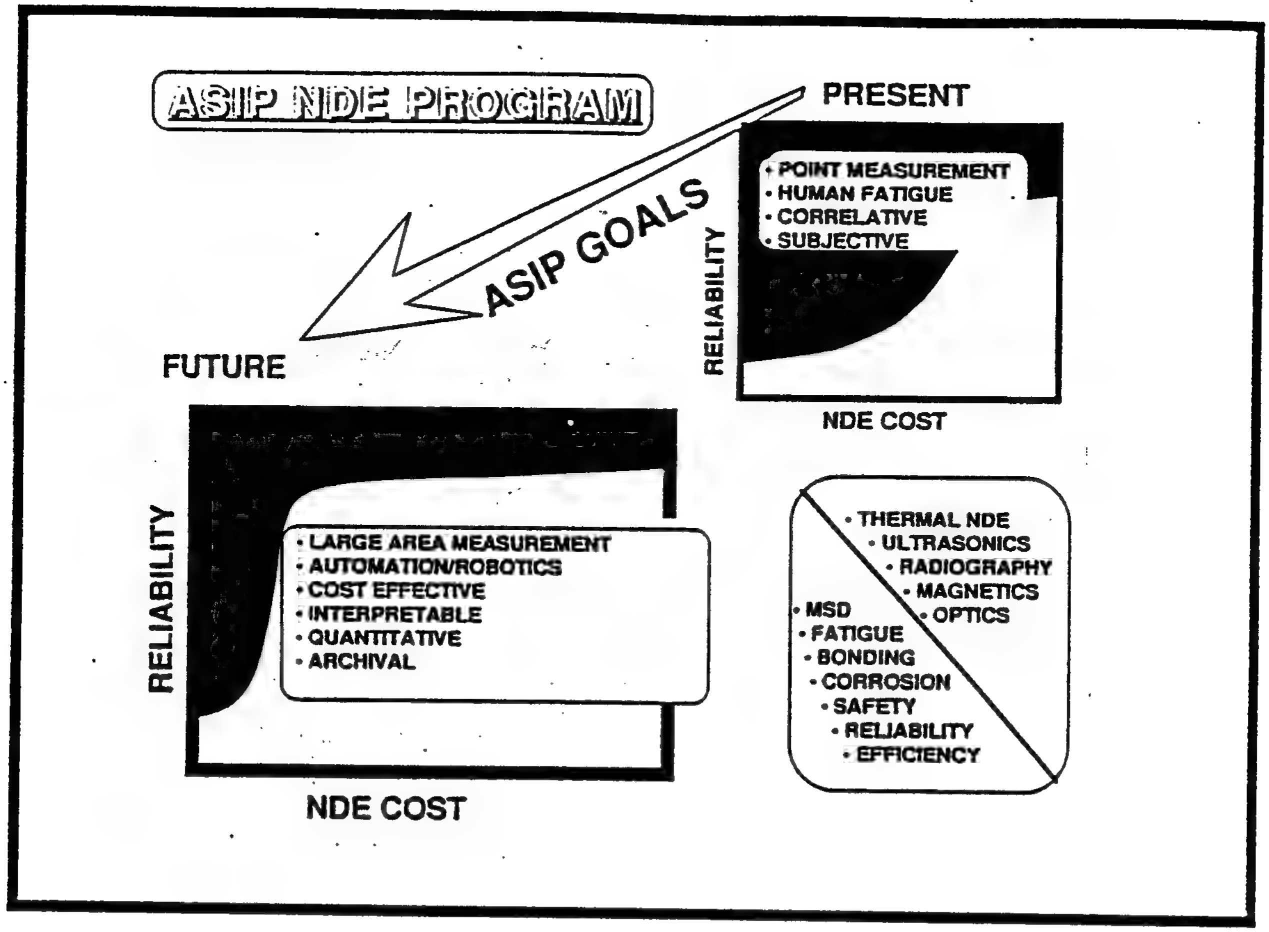
ASIP NDE PROGRAM
PRESENT
ASIP GOALS
FUTURE
• POINT MEASUREMENT
• HUMAN FATIGUE
• CORRELATIVE
• SUBJECTIVE
RELIABILITY
NDE COST
• LARGE AREA MEASUREMENT
• AUTOMATION/ROBOTICS
• COST EFFECTIVE
• INTERPRETABLE
• QUANTITATIVE
• ARCHIVAL
RELIABILITY
NDE COST
• THERMAL NDE
• ULTRASONICS
• RADIOGRAPHY
• MAGNETICS
• OPTICS
• MSD
• FATIGUE
• BONDING
• CORROSION
• SAFETY
• RELIABILITY
• EFFICIENCY

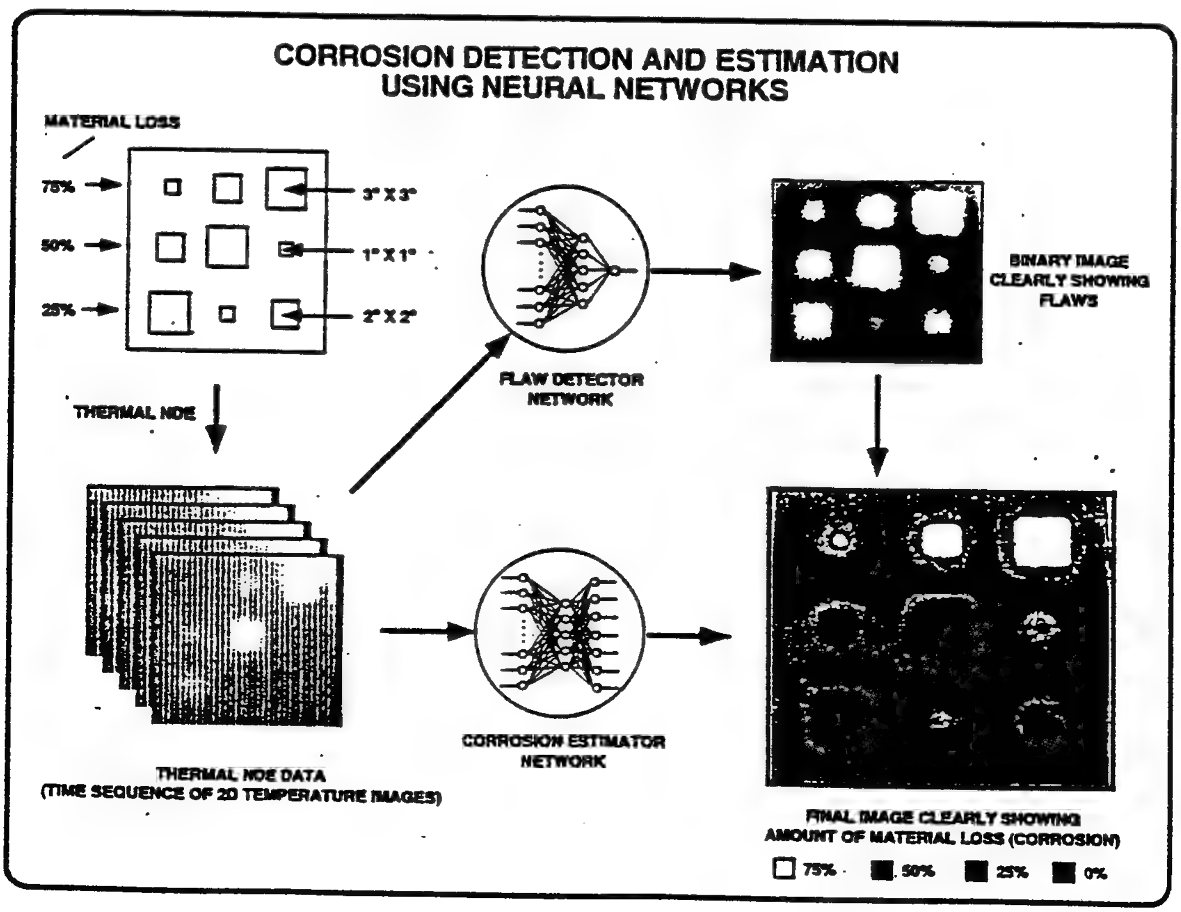
CORROSION DETECTION AND ESTIMATION
USING NEURAL NETWORKS
MATERIAL LOSS
75%
50%
25%
3" X 3"
1" X 1"
2" X 2"
THERMAL NDE
FLAW DETECTOR
NETWORK
BINARY IMAGE
CLEARLY SHOWING
FLAWS
THERMAL NDE DATA
(TIME SEQUENCE OF 2D TEMPERATURE IMAGES)
CORROSION ESTIMATOR
NETWORK
FINAL IMAGE CLEARLY SHOWING
AMOUNT OF MATERIAL LOSS (CORROSION)
75%
50%
25%
0%

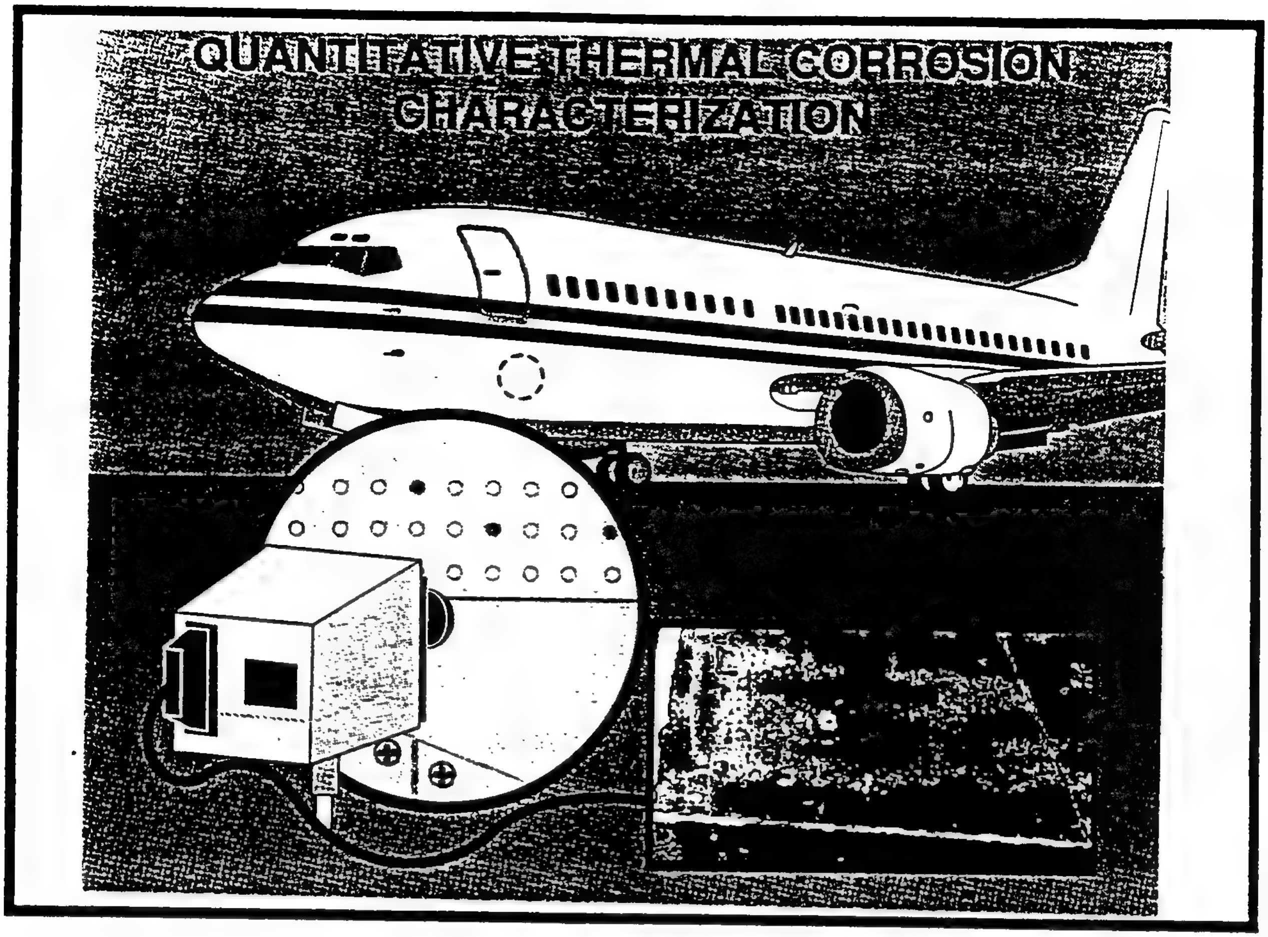
QUANTITATIVE THERMAL CORROSION
CHARACTERIZATION

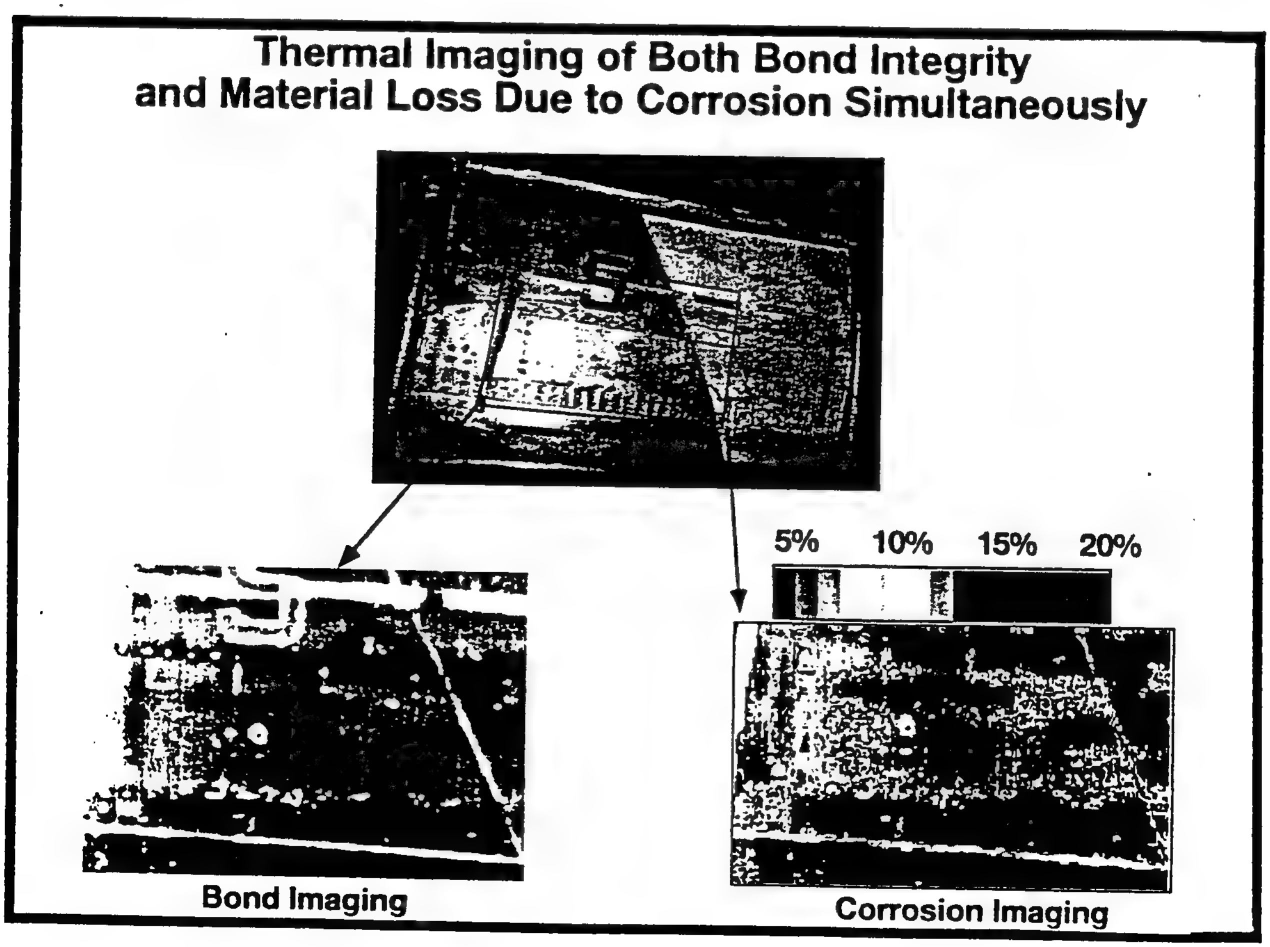
Thermal Imaging of Both Bond Integrity
and Material Loss Due to Corrosion Simultaneously
5%
10%
15%
20%
Bond Imaging
Corrosion Imaging

PORTABLE PC-BASED ULTRASONIC INSTRUMENT FOR DETECTION OF FLAWS

DEVELOPED AT NASA LANGLEY RESEARCH CENTER

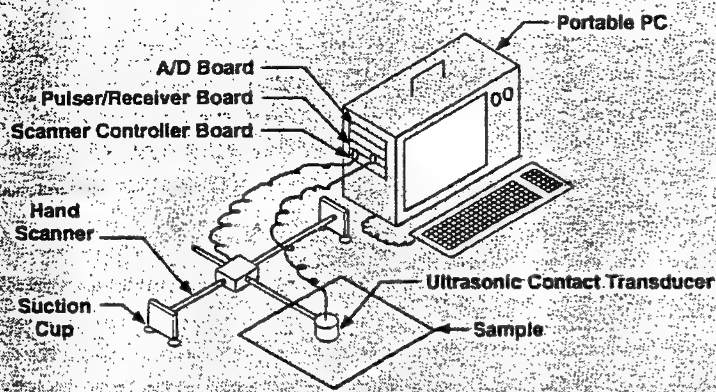

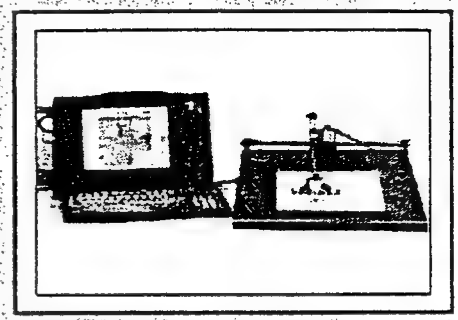

- INSTRUMENT CURRENTLY CONFIGURED FOR SIMULTANEOUS DETECTION OF DISBONDS AND CORROSION IN ADHESIVE JOINTS
- DISBOND DETECTION USING NEURAL NETWORKS
- QUANTIFICATION OF CORROSION THROUGH SPECTRAL ANALYSIS

COMPARISON BETWEEN MATERIAL LOSS OBTAINED ULTRASONICALLY AND MECHANICALLY MEASURED MATERIAL LOSS

SINGLE LAYER OF ALUMINUM, THICKNESS 1.0 mm WITH MILLED MATERIAL LOSS

TRANSDUCER CENTER FREQUENCY 3.5 MHz

NUMBER OF POINTS FOR FFT = 2048

SINGLE LAYER OF ALUMINUM, THICKNESS 1.6 MM WITH MILLED MATERIAL LOSS

TRANSDUCER CENTER FREQUENCY 2.25 MHZ

NUMBER OF POINTS FOR FFT = 256

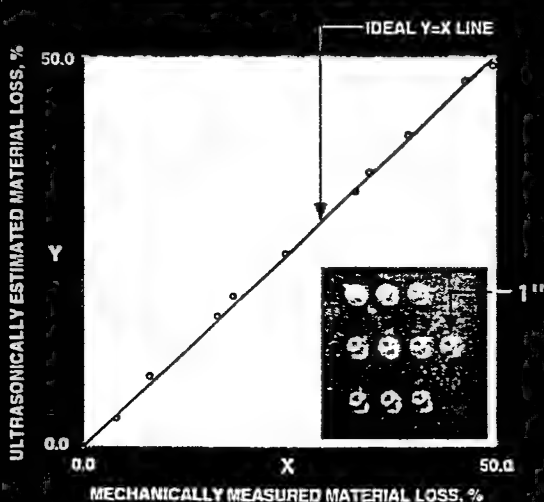

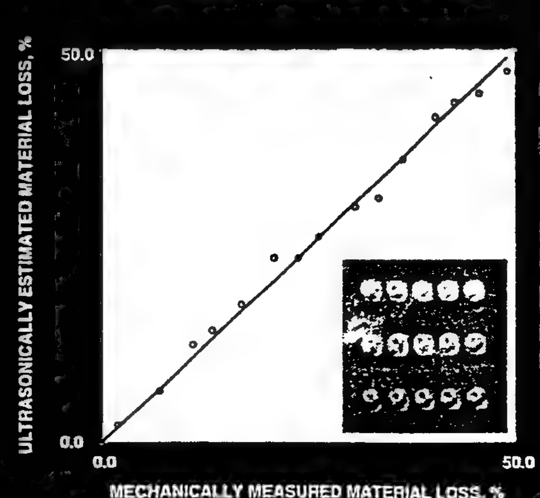

FIRST LAYER CORROSION SCAN OF BOEING 727 LAP JOINT

ULTRASONIC CONTACT SCAN (HAND-SCAN)

TRANSDUCER CENTER FREQUENCY 3.5 MHz
NOMINAL SKIN THICKNESS 1.16 MM

QUANTITIVE ESTIMATION OF CORROSION (MATERIAL THINNING)
THROUGH SPECTRAL ANALYSIS

NOTE

THE BRIGHT RED REGIONS ARE DUE TO THE PRESENCE OF RIVETS, WHICH RESULTS IN BAD CONTACT BETWEEN SPECIMEN AND TRANSDUCER

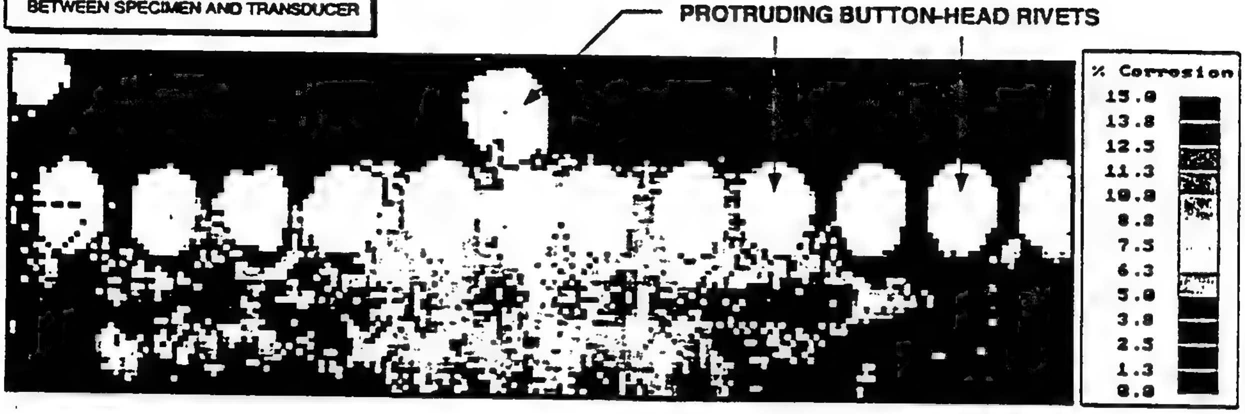

ULTRASONIC CONTACT SCAN OF AIRCRAFT PANEL

SIMULTANEOUS DETECTION OF DISBONDS AND TOP-LAYER CORROSION (MATERIAL THINNING)

TRANSDUCER CENTER FREQUENCY 2.25 MHZ

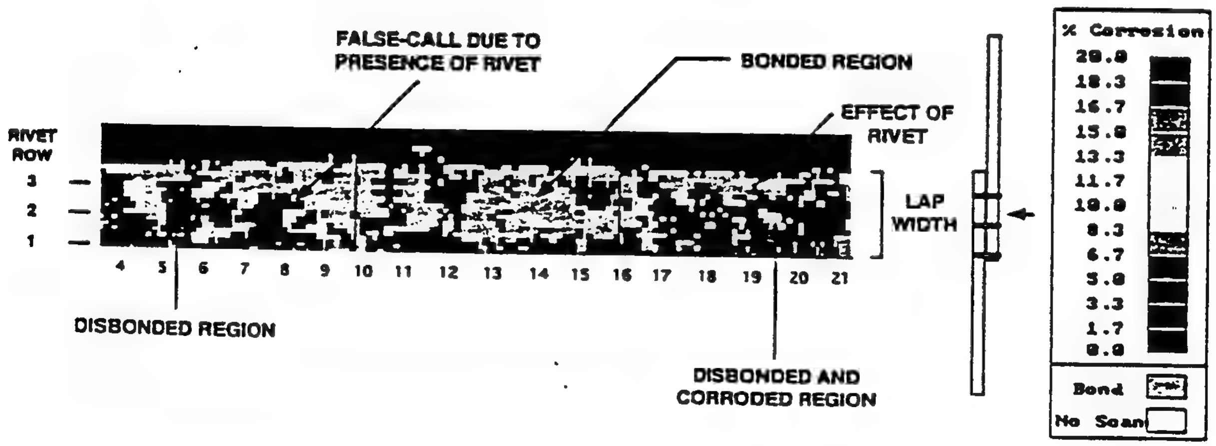

- DISBOND DETECTION USING A TRAINED NEURAL NETWORK
- CORROSION ESTIMATION THROUGH SPECTRAL ANALYSIS

SIMPSON PROBE

LaRC Develops Self-nulling Electromagnetic Probe

Hand held

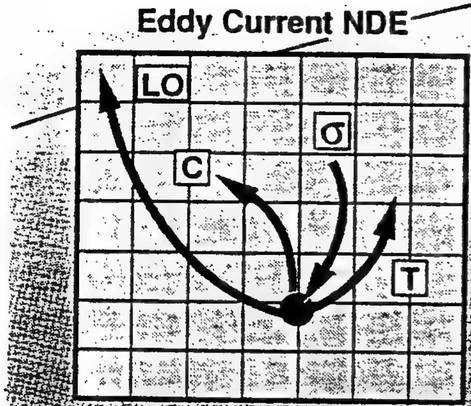

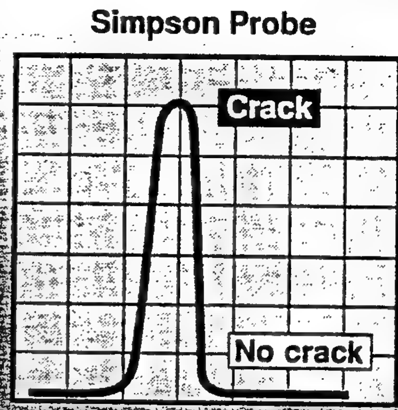

- Costly to Operate
- Difficult to interpret
- Requires High Levels of Training

- 100 X Cost Savings
- Simple to Operate
- Addresses Human Factors
- Industry Ready

FATIGUE CRACK DETECTION WITH SELF NULLING EDDY CURRENT PROBE

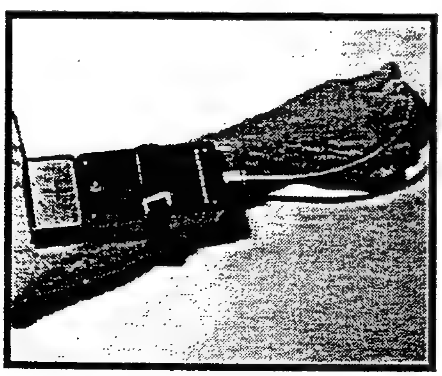

Probe response from unflawed sample

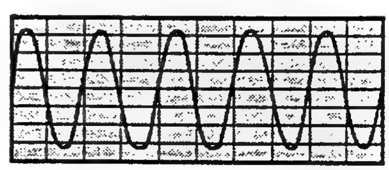

Probe response from fatigue crack

- Unambiguos flaw signature
- Insensitivity to lift-off and probe wobble
- Low cost for operator training and instrumentation requirements

C-Scan Image of a Boeing 727 Lap Splice Using the Simpson Probe

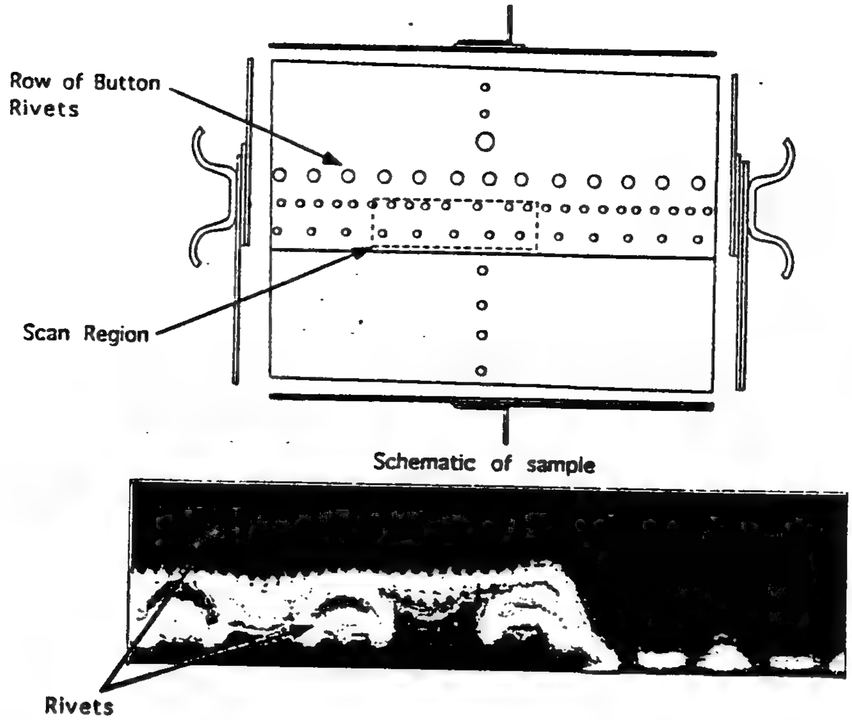

C-Scan Image of a lap splice sample obtained with the Simpson Probe operating at 2.5 kHz. Red, Yellow and dark green regions between the rivets correspond to a higher probe output and signify either material loss or an air gap between the layers.

CONCLUDING REMARKS

- The NASA Program was initiated in 1990.
- U. S. Government Strategic Plan (FAA, NASA, USAF)
- Cooperative programs with the U. S. OEM's and Airlines
- Significant technical accomplishments have occurred and technology has been transferred to industry

AERONAUTICAL SYSTEMS CENTER
AGING AIRCRAFT PROGRAMS

DR JOHN LINCOLN
ASC/ENFS
WRIGHT-PATTERSON AFB

ASCAA0594

AGING AIRCRAFT DEFINITION

- AN AGING AIRCRAFT CAN BE DEFINED AS ONE THAT REQUIRES A CHANGE TO THE MAINTENANCE PROGRAM OR OPERATING RESTRICTIONS BECAUSE OF
  - OPERATIONS BEYOND DESIGN LIFE
  - CORROSION
  - ONSET OF WIDESPREAD FATIGUE DAMAGE
  - REPAIRS

ASCAA0894

AERONAUTICAL SYSTEMS CENTER AGING AIRCRAFT PROGRAM

THE PROGRAM FOR AGING AIRCRAFT WITHIN THE AERONAUTICAL SYSTEMS CENTER IS TO ESTABLISH REQUIREMENTS THROUGH

- MIL-STD-1530A (ASIP)

AND

- AFGS-87221A (MIL-PRIME SPEC)

TO PRECLUDE AGING OR DELAY AGING EFFECTS THROUGHOUT THE AIRCRAFT'S LIFETIME

ASCAA0894

AGE OF USAF AIRCRAFT

AIRCRAFT	DEVELOPMENT INITIATED
T-37	1953
T-38	1956
F-111	1962
F-15	1970
F-16	1975
C-130	1951
C-141	1959
C-5A	1965
KC-135	1954
B-52G	1956
A-10	1974

ASCAA0594

ELEMENTS OF TASK I OF ASIP

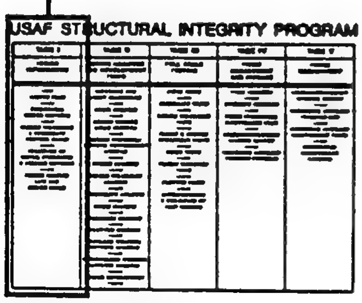

TASK I

DESIGN INFORMATION

- ASIP MASTER PLAN
- STRUCTURAL DESIGN CRITERIA
- DAMAGE TOLERANCE AND DURABILITY CONTROL PLANS
- SELECTION OF MATERIALS, PROCESSESS, AND JOINING METHODS
- DESIGN SERVICE LIFE AND DESIGN USAGE

OPERATIONAL USAGE
AN AGING AIRCRAFT ISSUE

- ESSENTIALLY ALL OF THE USAF AIRCRAFT ARE OPERATED MORE SEVERELY IN OPERATIONAL SERVICE THAN THE DESIGN USAGE

  EXAMPLES ARE

  F-15

  F-16

  A-10

  B-1B

  C-141

- THESE USAGE CHANGES ARE DERIVED FROM
  - INCREASE IN LOAD FACTOR EXCEEDANCES
  - INCREASE IN FUEL RESERVES
  - WEIGHT GROWTH

ASCAA0594

FUTURE ACTIONS
OPERATIONAL USAGE

- USE SIMULATORS IN DEM/VAL PHASE TO BETTER ESTIMATE LOAD FACTOR EXCEEDANCES
- USE LOAD LIMITERS ON LOW G AIRCRAFT
- WORK WITH USING COMMAND TO OBTAIN MORE REALISTIC FUEL RESERVE REQUIREMENTS
- ENSURE THAT THE DESIGN WEIGHT IS THE PROJECTED WEIGHT AT IOC
- PERFORM TRADE STUDY FOR PROVIDING ADDITIONAL LIFE MARGIN IN DESIGN TO ASSESS COST AND SCHEDULE IMPACT
- UPDATE FSMP (DADTA) AT LEAST EVERY FIVE YEARS
- PM UPDATE ASIP COSTS FOR AIRCRAFT LIFE YEARLY

ASCAA0594

CORROSION
AN AGING AIRCRAFT ISSUE

- MOST SIGNIFICANT COST BURDEN OF ANY STRUCTURALLY RELATED ITEM
  - COST ESTIMATED AT $700 MILLION/YEAR
- ADDITIONAL FUNDING NEEDED TO PROTECT SOME WEAPON SYSTEMS
  - EXAMPLES
    KC-135
    C-141
- ENVIRONMENTAL PROTECTION LAWS CAUSING SEARCH FOR NEW INHIBITORS
- NONDESTRUCTIVE EVALUATION MARGINAL
- NO PREDICTIVE CAPABILITY

ASCAA0894

FUTURE ACTIONS
CORROSION

- ESTABLISH ADVISORY COUNCIL FROM USA, USAF, USN, FAA, AND NASA TO ADVISE ON CORROSION PROBLEMS
  - ESTABLISH STANDARDS AND RESEARCH AND DEVELOPMENT INITIATIVES
- DEVELOP THE NONDESTRUCTIVE EVALUATION TOOLS TO DETERMINE EXTENT OF CORROSION
- ENFORCE THE POLICY THAT CORROSION DAMAGE WILL BE FIXED AND NOT BE ALLOWED TO JEOPARDIZE SAFE AND ECONOMICAL OPERATIONS
- PLACE EMPHASIS ON THE DEVELOPMENT OF NEW CORROSION PROTECTION SYSTEMS THAT ARE ENVIRONMENTALLY SAFE

ASCAA0894

ELEMENTS OF TASK II OF ASIP

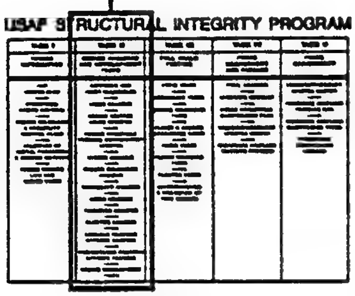

TASK II
DESIGN ANALYSES AND DEVELOPMENT TESTS
MATERIALS AND JOINT ALLOWABLES LOADS ANALYSIS DESIGN SERVICE LOADS SPECTRA DESIGN CHEMICAL/THERMAL ENVIRONMENT SPECTRA STRESS ANALYSIS DAMAGE TOLERANCE ANALYSIS DURABILITY ANALYSIS SONIC ANALYSIS VIBRATION ANALYSIS FLUTTER ANALYSIS NUCLEAR WEAPONS EFFECTS ANALYSIS NON-NUCLEAR WEAPONS EFFECTS ANALYSIS DESIGN DEVELOPMENT TESTS

EXTERNAL AND INTERNAL LOADS
AN AGING AIRCRAFT ISSUE

- EXTERNAL LOAD ERRORS HAVE SIGNIFICANTLY IMPACTED THE LIFE OF AIRCRAFT STRUCTURES - EXAMPLES ARE
  F-4
  A-7
- THE TECHNOLOGY TO ACCURATELY PREDICT BUFFET LOADS IS NOT AVAILABLE
- SIGNIFICANT VARIATIONS HAVE BEEN FOUND IN THE QUALITY OF FINITE ELEMENT ANALYSES
- THE STATE OF THE ART FOR DETERMINATION OF THERMAL LOADS IS NOT ADEQUATE

ASCAAG594

FUTURE ACTIONS
EXTERNAL AND INTERNAL LOADS

- EMPHASIZE THE USE OF COMPUTATIONAL FLUID DYNAMICS FOR DETERMINATION OF BOTH STEADY STATE AND BUFFET LOADING
- EMPHASIZE USE OF MORE COMPREHENSIVE FLIGHT LOAD SURVEYS TO VALIDATE STEADY STATE AND BUFFET LOAD PREDICTIONS
  - INCREASE THE SCOPE OF FLIGHT LOAD SURVEYS FOR PROTOTYPE AIRCRAFT
- PROVIDE GUIDANCE IN THE MIL-PRIME SPECIFICATION ON THE USE OF EXPERIMENTAL APPROACH TO BE USED FOR VALIDATION OF THE INTERNAL LOADS IN MAJOR SUB-ASSEMBLY TESTING LEADING TO FULL-SCALE TESTING

ASCAA0894

ELEMENTS OF TASK III OF ASIP

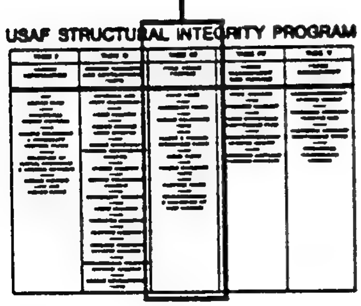

TASK III
FULL-SCALE TESTING
STATIC TESTS
DURABILITY TESTS
DAMAGE TOLERANCE TESTS
FLIGHT AND GROUND OPERATIONS TESTS
SONIC TESTS
FLIGHT VIBRATION TESTS
FLUTTER TESTS
INTERPRETATION AND EVALUATION OF TEST RESULTS

FULL SCALE TESTING
AN AGING AIRCRAFT ISSUE

- TIMELY START OF STATIC TESTING TO PERMIT EARLY AND ADEQUATE FLIGHT AND GROUND LOAD SURVEYS
- TIMELY START OF DURABILITY TESTING TO AVOID RETROFIT PROBLEMS
- ADEQUATE DURABILITY TESTING TO IDENTIFY ALL LOCATIONS THAT COULD BE DAMAGE TOLERANT CRITICAL
- APPROACH TO BE USED FOR DAMAGE TOLERANCE TESTING TO VALIDATE THE CRACK GROWTH PREDICTIONS

ABCAA0594

ELEMENTS OF TASK IV OF ASIP

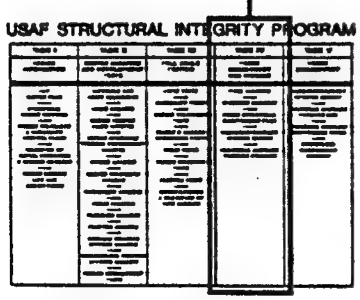

TASK IV
FORCE MANAGEMENT DATA PACKAGE
FINAL ANALYSES STRENGTH SUMMARY FORCE STRUCTURAL MAINTENANCE PLAN LOADS/ENVIRONMENT SPECTRA SURVEY INDIVIDUAL AIRCRAFT TRACKING PROGRAM

ELEMENTS OF TASK V OF ASIP

USAF STRUCTURAL INTEGRITY PROGRAM

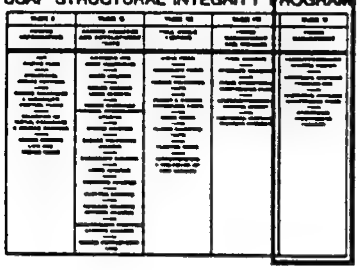

TASK V
FORCE MANAGEMENT
LOADS/ENVIRONMENT SPECTRA SURVEY
INDIVIDUAL AIRCRAFT TRACKING PROGRAM
INDIVIDUAL AIRPLANE MAINTENANCE TIMES
STRUCTURAL MAINTENANCE RECORDS

WIDESPREAD FATIGUE DAMAGE DEFINITIONS (DETERMINISTIC AND PROBABILISTIC)

- ONSET OF WIDESPREAD FATIGUE DAMAGE IN A STRUCTURE IS CHARACTERIZED BY THE SIMULTANEOUS PRESENCE OF CRACKS AT MULTIPLE STRUCTURAL DETAILS WHICH ARE OF SUFFICIENT SIZE AND DENSITY WHEREBY THE STRUCTURE WILL NO LONGER MEET ITS DAMAGE TOLERANCE REQUIREMENT (E.G., MAINTAINING RESIDUAL STRENGTH REQUIREMENT AFTER PARTIAL STRUCTURAL FAILURE)
- THE ONSET OF WIDESPREAD FATIGUE DAMAGE IS THAT POINT IN THE OPERATIONAL LIFE OF AN AIRCRAFT WHEN THE DAMAGE TOLERANCE OR FAIL SAFE CAPABILITY OF THE STRUCTURE HAS BEEN DEGRADED SUCH THAT THE PROBABILITY OF FAILURE OF THE INTACT STRUCTURE OR THE STRUCTURE WITH A PARTIAL FAILURE HAS BEEN INCREASED ABOVE AN ACCEPTABLE THRESHOLD

ASCAA0594

WIDESPREAD FATIGUE DAMAGE (WFD) TYPES OF DAMAGE

- MULTIPLE ELEMENT DAMAGE
  - EXAMPLES (PROBABILISTIC METHODS)
    - KC-135 WING
    - C-5A WING
    - C-141 FUSELAGE AND WING
    - T-38 FUSELAGE AND WING
  - APPROACH IS ESTABLISHED
- MULTIPLE SITE DAMAGE
  - EXAMPLES
    - BOEING 727 AND 737 FUSELAGES
  - APPROACH IS MATHEMATICALLY SIMILAR TO THE MULTIPLE ELEMENT DAMAGE PROBLEM
    - CRACK ARREST STRUCTURAL INTEGRITY IS THE FOCAL POINT OF THE ANALYSIS

ASCAA0594

WIDESPREAD FATIGUE DAMAGE (WFD) AN AGING AIRCRAFT ISSUE

- THREAT ASSESSMENT FOR PARTIAL FAILURE
  - POTENTIAL SOURCES OF DAMAGE TO THE STRUCTURE
    - ENGINE DISINTEGRATION
    - ACCIDENTAL DAMAGE
    - BATTLE DAMAGE
    - FATIGUE DAMAGE
- DETERMINATION OF ANALYSIS INPUTS
  - CRACK DISTRIBUTION FUNCTION
  - APPLIED STRESS DISTRIBUTION FUNCTION
  - FAILURE CRITERIA
- NONDESTRUCTIVE EVALUATION METHODS FOR CRACKING THAT WOULD CONSTITUTE WFD

ASCAA0594

FUTURE ACTIONS
WIDESPREAD FATIGUE DAMAGE (WFD)

- ESTIMATE THE THREAT OF PARTIAL DAMAGE
  - EXAMINE EXISTING DATA BASES
  - CONDUCT FIELD SURVEYS FOR DAMAGE
- EXAMINE ALTERNATIVES FOR INITIAL CRACK DISTRIBUTIONS
- USE DETERMINISTIC AND PROBABILISTIC METHODS FOR ESTABLISHING ESTIMATE OF THE TIME OF ONSET OF WFD

RECOGNIZE THAT THIS IS ONLY AN ESTIMATE !!

- ESTABLISH THE NONDESTRUCTIVE EVALUATION CAPABILITY FOR (SMALL CRACKS) TO VALIDATE EXISTENCE OF WFD

ASCAA0594

REPAIRS
AN AGING AIRCRAFT ISSUE

- MANY REPAIRS ON USAF AIRCRAFT ARE NOT DESIGNED BASED ON DAMAGE TOLERANCE
  - TRACKING OF REPAIRS OFTEN NOT ACCOMPLISHED
  - CONFIGURATION CONTROL OF REPAIRS IS ALSO A PROBLEM
- DEFINITION OF EXTERNAL AND INTERNAL LOADS A PROBLEM FOR OFF-THE-SHELF AIRCRAFT
  - CONTRACT FOR MODIFICATIONS OFTEN NOT WITH ORIGINAL EQUIPMENT MANUFACTURER
- BATTLE DAMAGE REPAIR CRITERIA
  - NO UNIVERSAL AGREEMENT WITHIN USAF

ASCAA0594

FUTURE ACTIONS
REPAIRS

- DEVELOP METHODOLOGY FOR ESTABLISHING EXTERNAL AND INTERNAL LOADS FOR USE IN THE DESIGN OF REPAIRS
- DEVELOP GUIDELINES FOR USE IN DEPOTS FOR DESIGN OF DAMAGE TOLERANCE REPAIRS
- ENFORCE THE POLICY THAT REPAIRS WILL BE BASED ON DAMAGE TOLERANCE PRINCIPLES
- ADOPT NEW GUIDANCE ON THE DESIGN OF BATTLE DAMAGE REPAIRS FOR USE IN THE FIELD

ASCAA0594

OFF THE SHELF AIRCRAFT
AN AGING AIRCRAFT ISSUE

- CERTIFICATION BASIS FOR OTS AIRCRAFT OFTEN INCOMPATIBLE WITH THE ASIP
- DIFFICULT TO ESTABLISH THE EXTENT OF HIDDEN CORROSION
- SOME AIRCRAFT MAY BE IN A STATE OF WIDESPREAD FATIGUE DAMAGE WHEN PURCHASED BY THE AIR FORCE
- THE EXTERNAL AND INTERNAL LOADS MAY NOT BE AVAILABLE TO THE CONTRACTOR MAKING THE REPAIRS AND MODIFICATIONS
- AIR FORCE MISSION MAY BE SIGNIFICANTLY DIFFERENT THAN DESIGN MISSION

ASCAA0594

OFF THE SHELF AIRCRAFT FUTURE ACTIONS

- BASIS FOR STRUCTURAL QUALIFICATION OF OTS AIRCRAFT WILL BE THE AIR FORCE STRUCTURAL INTEGRITY PROGRAM
- USE EMERGING NDE TECHNOLOGY FOR ASSESSING THE EXTENT OF HIDDEN CORROSION
- PERFORM TEARDOWN INSPECTIONS AND ANALYSES AS APPROPRIATE TO DETERMINE THE TIME OF ONSET OF WFD
- DEVELOP THE EXTERNAL AND INTERNAL LOADS TECHNOLOGY THAT WOULD BE SUITABLE FOR MAKING DAMAGE TOLERANT REPAIRS AND MODIFICATIONS

ASCAA0594

CONCLUSIONS

- ASIP HAS BEEN SUCCESSFUL IN REDUCTION OF SAFETY OF FLIGHT PROBLEMS FOR OPERATIONAL AIRCRAFT
- SOME CHANGES ARE NECESSARY TO ENSURE THAT NEW WEAPON SYSTEMS ARE BEING DESIGNED TO ACCOMMODATE NEW TECHNOLOGY AND LESSONS LEARNED FROM THE PAST
- SOME CHANGES ARE NECESSARY TO ENSURE THAT AGING WEAPON SYSTEMS ARE BEING MAINTAINED IN THE MOST ECONOMICAL MANNER

ASCAA0594

OVERVIEW OF WRIGHT LABORATORY MATERIALS DIRECTORATE SYSTEMS SUPPORT PROGRAMS

Thomas D. Cooper
Chief, Systems Support Division
Materials Directorate
Wright Laboratory
17 May 94

WRIGHT LABORATORY
MATERIALS DIRECTORATE

OUTLINE

- Overview of the Materials Directorate, Wright Laboratory
- Technical Program
- Special Emphasis Areas (SEAs)
- Support for Aging Aircraft
  - NDE
  - Corrosion Control/Protective Coatings
  - Composite Supportability
  - Composite Repair of Metals Structures
  - Sealants
  - Failure Analysis
- Conclusions

WRIGHT LABORATORY
MATERIALS DIRECTORATE

MISSION

Plan and execute the USAF program for materials and processes in the areas of basic research, exploratory development, and advanced development. Provide systems support to Air Force product centers, logistics centers, and operating commands to solve system related problems and to transfer expertise in the areas of materials and processes.

WRIGHT LABORATORY
MATERIALS DIRECTORATE

ML ORGANIZATION

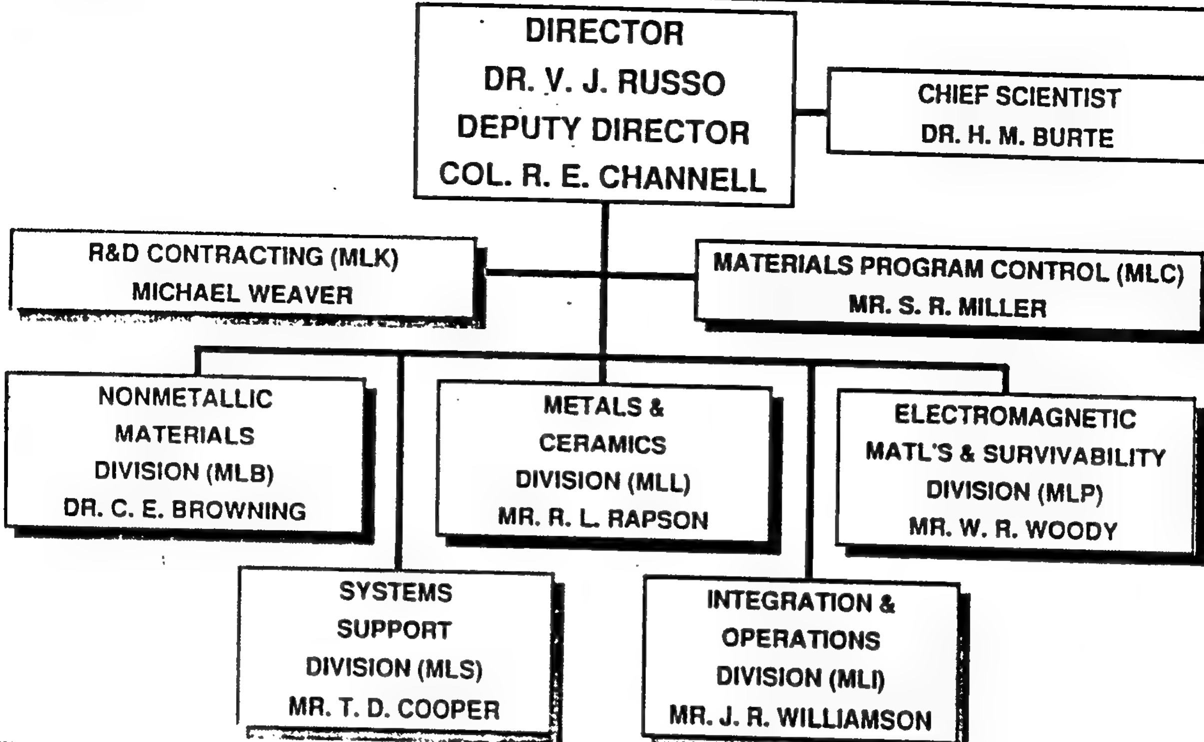

WRIGHT LABORATORY
MATERIALS DIRECTORATE

MATERIALS DIRECTORATE FACILITY

- 386,000 Square Feet
- >$100,000,000 Brick and Mortar Built in Mid '80s
- >$125,000,000 Equipment Replacement Value
- Designed Specifically for Materials and Processes R&D

WRIGHT LABORATORY
MATERIALS DIRECTORATE

TECHNOLOGY AREA FUNDING FOR FY94

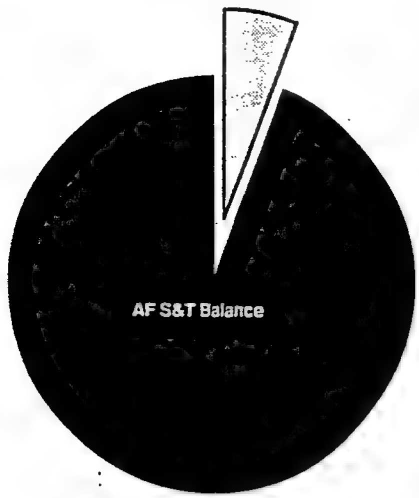

ESTIMATED AF S&T FUNDS:

$1457.0M

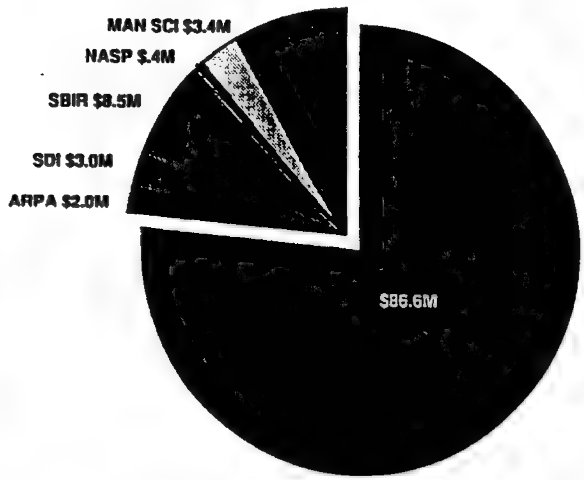

ESTIMATED TOTAL TECH AREA FUNDS:

$113.3M: TOTAL FUNDING

WRIGHT LABORATORY
MATERIALS DIRECTORATE

STRATEGIC EMPHASIS AREAS
(in alphabetical order)

- Aging Systems
- Dual Use
- Pollution Prevention
- Processing
- Space

WRIGHT LABORATORY
MATERIALS DIRECTORATE

SUPPORT FOR AGING AIRCRAFT

- NDE (To be Presented by Tobey Cordell)
- Corrosion Control/Protective Coatings
- Composites Supportability
- Composite Repair of Metal Structures
- Sealants
- Failure Analysis

CORROSION CONTROL WL/MLS SUPPORT

- CORROSION PREVENTION ADVISORY BOARDS
- CONSULTATIONS, EVALUATIONS, AND PROBLEM SOLVING
- INPUT TO AF WIDE CORROSION SUMMARY
- MAINTENANCE
  - OPERATIONAL COMMAND CORROSION SURVEYS
  - UPDATE TECHNICAL ORDERS, SPECIFICATIONS, STANDARDS
- CORROSION DATA BASE ON EMERGING MATERIALS/ PROCESSES
  - STRUCTURAL MATERIALS
  - COMMERCIAL PRODUCTS AND PROCESSES
  - HAZARDOUS MATERIALS SUBSTITUTIONS

WL/MLSA ON-GOING CORROSION CONTROL ACTIVITIES

ENVIRONMENTAL, HEALTH, SAFETY RELATED

- COATINGS
  - LOW VOC POLYURETHANE TOPCOATS
  - LOW VOC, CHROMATE FREE PRIMER
  - ELECTROCOAT PRIMER
  - POWDER TOPCOAT
  - LOW VOC FUEL TANK COATING
- SURFACE PRETREATMENTS
  - ALUMINUM
  - MAGNESIUM

WRIGHT LABORATORY
MATERIALS DIRECTORATE

GOALS/SUBGOALS FOR WL'S PAINT/COATING TEAM

GOALS

- Develop List of Potential Projects
- Develop S&T Strategy for Coating Systems

SUBGOALS

- Define Future Enviro Compliance Requirements
- Establish Min Coating Performance Standards
- Examine Alternative Surface Protection Methodologies
- Quantify Impact of New Methodologies on Structural Integrity, IR Signature, Etc.
- Examine Why Paint/Depaint

WRIGHT LABORATORY
MATERIALS DIRECTORATE

ROADMAP DEVELOPMENT PROCESS

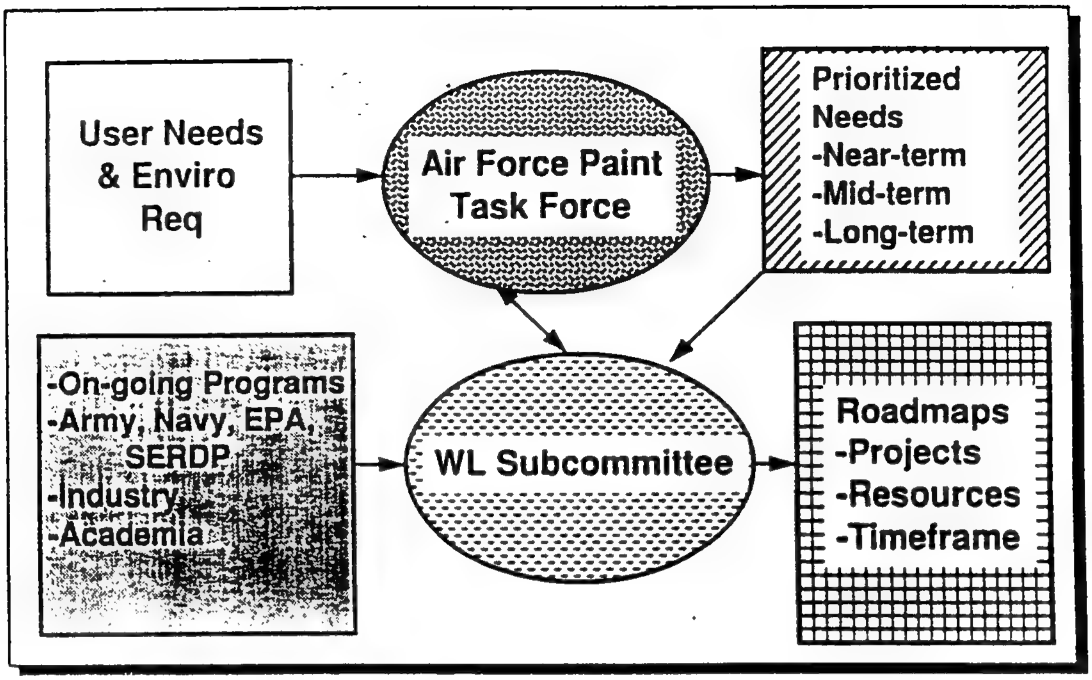

WL PAINT STRATEGY ROADMAP OVERVIEW

NEAR TERM (2-5 YEARS)
- Low VOC
- Minimum Chromate
- Improved Formulations
- Lower IR Reflectance

NEAR TERM EFFORTS
- Refine Existing Primers/ Topcoats
  - Adhesion, Flexibility, Appearance

MID-TERM (5-10 YEARS)
- Low/No VOC
- No Chromate
- Low IR
- Lasts from PDM to PDM

LONG-TERM (+10 YEARS)
- No VOC
- No Chromate
- Low IR
- Lasts Life of System

WL/PAINT COATING WORKSHOP
- Refined Roadmaps
- Defined Possible Projects
  - Coating Application
  - Removal
  - Corrosion Control

WRIGHT LABORATORY
MATERIALS DIRECTORATE

TECHNOLOGY THRUST INTEGRATED PRODUCT TEAMS

TTIPT 1: Materials and Processes for Structures, Propulsion and Subsystems
- Subthrust 1.A: Carbon-Carbon & Thermal Protection
- Subthrust 1.B: Nonmetallic Structural Materials
- Subthrust 1.C: Nonstructural Materials
- Subthrust 1.D: Metallic Materials
- Subthrust 1.E: Ceramics & Very High Temp Materials

TTIPT 2: Materials and Processes for Electronics, Optics and Survivability
- Subthrust 2.A: Electronic and Optical Materials
- Subthrust 2.B: Survivable Materials

TTIPT 3: Materials and Processes for Systems and Operational Support
- Subthrust 3.A: Nondestructive Evaluation
- Subthrust 3.B: Systems Support

COMPOSITES SUPPORTABILITY GOALS

- IMPROVE SUPPORTABILITY OF EXISTING COMPOSITE MATERIALS
- IMPROVE SUPPORTABILITY OF FUTURE COMPOSITE MATERIALS
- REDUCE SUPPORT COST OF AGING AIRCRAFT
- DEVELOP ABDR CAPABILITY OF COMPOSITES

COMPOSITES SUPPORTABILITY
EXISTING COMPOSITE MATERIALS

TECHNOLOGY DEVELOPMENT

- HEAT DAMAGE OF COMPOSITES
- HOT BONDER DEVELOPMENT/TRANSITION
- LOW TEMPERATURE CURING RESINS/ADHESIVES
- REPAIR MATERIALS EVALUATION

COMPOSITES SUPPORTABILITY
HEAT DAMAGE OF COMPOSITES

OVERALL AIR FORCE PROGRAM OBJECTIVES

- TO DEVELOP A FUNDAMENTAL UNDERSTANDING OF THE EFFECTS OF OVER HEAT DAMAGE (NOT DESIGNED FOR) ON COMPOSITE MATERIALS FOR MILITARY AIRCRAFT STRUCTURE

- TO DEVELOP AN OPERATOR'S ASSESSMENT GUIDE WHICH CAN ASSIST IN THE EVALUATION OF HEAT DAMAGE IN COMPOSITE MATERIALS

TECHNOLOG[illegible]

Standardized Hot Bonded Repair System Improves Maintenance of Composites

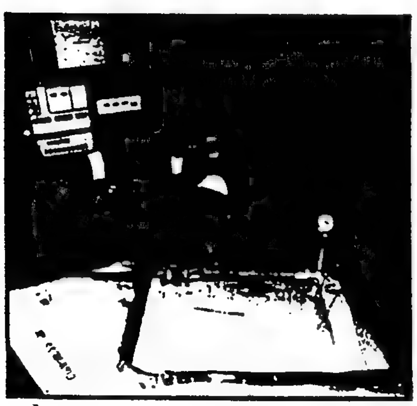

NEED: Eliminate the inconsistent application of hot bonded repair systems used by the Air Force.

APPROACH: Government and industry composite repair experts teamed together to evaluate hot bonded repair systems and develop standard specifications for use throughout the Air Force.

APPLICATION: Standardized hot bonded repair specifications are now used by the Air Force for composite structure repairs.

Reduces training, maintenance, and system reliability problems.

Expected to save $6 million over a 10-year period.

COMPOSITES SUPPORTABILITY
HOT BONDER DEVELOPMENT

- SPECIFICATION DEVELOPED FOR AIR FORCE
- ONE YEAR FIELD EVALUATION
- TRANSITIONED TO SA-ALC
- SA-ALC CONTRACT AWARDED
  - ML PROVIDING TECHNICAL INPUT
  - PDR @ ML ON JAN 94
  - FOLLOW-UP @ SA-ALC ON MAR 94

COMPOSITES SUPPORTABILITY
REDUCE COST OF SUPPORTING AGING SYSTEMS

- TODAY'S AGING SYSTEMS ARE OF METAL CONSTRUCTION
- COMPOSITES PLAY A LARGE AGING SYSTEMS ROLE
  - REPAIR/ENHANCEMENT WITH COMPOSITE "PATCHES"
  - SUBSTITUTION FOR CURRENT METAL PARTS
- PROBLEMS WILL INCREASE AS FLEET CONTINUES TO AGE

COMPOSITES SUPPORTABILITY
DIRECT SYSTEMS SUPPORT CUSTOMERS

- SA-ALC
  - T-38 FORMER AND INLET
  - C-5 FORWARD RAMP

- OC-ALC
  - B-52 UPPER WING SKIN
    - MLSE SILANE TECHNOLOGY
  - KC-135 BEAM CAP AND WING REPAIRS
  - B-1B 25^0 LONGERON
    - SIGNIFICANT MLSE MATERIALS/PROCESSES INPUT

- SM-ALC
  - LOW VOC ADHESIVE PRIMER QUALIFICATION FOR F-111 AND A-10

COMPOSITES SUPPORTABILITY
DIRECT SYSTEMS SUPPORT CUSTOMERS

- OO-ALC
  - F-16 FUEL VENT HOLE AND SPEED BRAKE
    - MLSE SILANE AND M&P TECHNOLOGY
  - F-4
    - POTENTIAL FOR USE OF MLSE SILANE TECHNOLOGY

- WR-ALC
  - C-141 WEEP HOLE REPAIR
    - MLSE SILANE AND M&P TECHNOLOGY
  - GENERIC "HAVE PATCH WILL TRAVEL" EFFORT
  - C-141 ALUMINUM/KEVLAR TRAILING EDGE

WRIGHT LABORATORY
MATERIALS DIRECTORATE

TECHNOLOGY TRANSITION

Composite Patch Repair Process To Speed Aircraft Maintenance, Save Millions

ACHIEVEMENT

- Demonstrated permanently bonded composite patches to repair aircraft metal skin and structure

BENEFITS

- Saves $20 thousand for each F-16 requiring repairs
- Reduces aircraft ground time and can be performed in the field
- Reduces metal panel and skin replacement
- Permanent repair

WRIGHT LABORATORY
MATERIALS DIRECTORATE

TECHNOLOGY TRANSITION

Improved Composite Patch Repair Process Speeds Return Of Grounded C-141 Aircraft To Operational Status

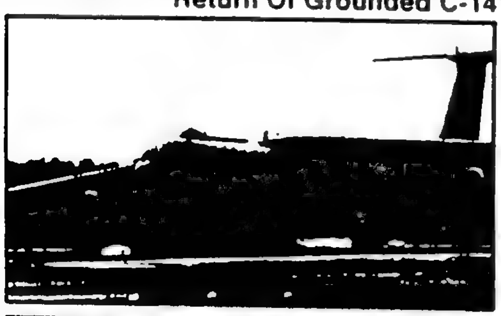

ACHIEVEMENT

- Developed composite patch process to repair C-141 wing weep hole cracks and transitioned it to WR-ALC

BENEFITS

- Avoided extensive downtime and cost for numerous aircraft, since no other repair was available
- WR-ALC now using the process on all C-141s needing similar repair
- Procedure can be adapted to other forms of damage and other aircraft

F-15 FUEL LEAKS

PROBLEM

- CONUS IS CONVERTING FROM JP-4 FUEL TO JP-8
- CALIFORNIA AND NEVADA CONVERTED OCT 93
- F-15'S AT NELLIS AFB WERE SEVERELY AFFECTED BY THE CHANGE
- IN FEBRUARY 37 OF 39 AIRCRAFT WERE GROUNDED FOR FUEL LEAKS
- RED FLAG EXERCISES WERE SEVERELY HANDICAPPED
- F-15 WEAPONS SCHOOL HAD TO CANCEL CLASSES FOR THE FIRST TIME IN 30 YEARS

F-15 FUEL LEAKS

CAUSE

- JP-8 EVAPORATES SLOWER THAN JP-4
- JP-8 CAUSES THE SEALS AND SEALANT TO SHRINK
- EXCESSIVE GUN PRESSURES WERE USED TO INJECT SEALANT
- SEALANT NOT ABLE TO BRIDGE GAPS IN FAYING SURFACES

F-15 FUEL LEAKS

BACKGROUND WORK

- IN 1986 F-15 FUEL LEAKS WERE EXPERIECED WITH JP-5
- AN IN-HOUSE EFFORT WAS ESTABLISHED TO DETERMINE THE CAUSE
- WORK WAS DONE BY A SEALANT MANUFACTURER TO DEVELOP TWO NEW SEALANTS
- THESE SEALANTS WERE TESTED IN-HOUSE

F-15 FUEL LEAKS

SHORT TERM SOLUTION

- USE NEW SEALANTS THAT WERE PREVIOUSLY DEVELOPED
- DIFFERENT SEALANT APPLICATION TECHNIQUES WERE USED
- RE-EVALUATE LEAK CRITERIA IN DRY BAYS
- BY END OF FEBRUARY, ONLY ONE AIRCRAFT WAS GROUNDED

LONG TERM SOLUTION

- A DEPOT PROGRAM IS BEING DEVELOPED TO REPAIR THE BLOWN CHANNELS
- WORK WITH DEPOT ENGINEERS TO SPECIFY THE SELANTS USED AND THE APPLICATION PROCESS

MISSION

PROVIDE FAILURE ANALYSIS/TECHNICAL CONSULTATION ON STRUCTURAL AND ELECTRONIC SYSTEMS, SUBSYSTEMS, AND COMPONENTS ON A QUICK REACTION BASIS TO PRIMARILY AIR FORCE BUT WHEN REQUESTED TO ALL DOD AND OTHER CUSTOMERS

...HNOLOGY TRANSITION

Fuel Probe Failure Analysis Prevents Possible Grounding of T-37 Aircraft Fleet

NEED: Eliminate potential safety hazard caused by improperly functioning fuel probes on T-37 aircraft.

APPROACH: ML analysis of failed fuel probes revealed a materials degradation process between the fuel probes' silver plated wiring and residual sulfur in jet fuel.

Recommended improved fuel probe design and new maintenance procedures.

APPLICATION: Using ML recommendations, San Antonio ALC engineers effectively managed the fuel probe problem without having to ground the aircraft.

WRIGHT LABORATORY
MATERIALS DIRECTORATE

CONCLUSIONS

- Materials and Processes Technology is Critical for Extending Life of Aging Aircraft
- WL/ML has a Broad Ranging Program Addressing These Problems
- Transitioning Technology to ALCs, Operating Commands has High Priority
- More Research and Development Required to Provide Needed Technology

AIR FORCE NDE R&D:

FOCUS ON THE CUSTOMER

TOBEY CORDELL
NDE BRANCH CHIEF
WRIGHT LABORATORY
MATERIALS DIRECTORATE
513-255-9802

NDE R&D Goals

- Reduce operations and maintenance costs of AF weapons systems via enhanced NDI/E technology
  - Improve existing and develop new technologies for detection of potential failure-causing defects
  - Provide novel nondestructive materials and process characterization / evaluation methodologies
- Ensure rapid NDI/E technology transition to ALC customers via effective coordinated use of 6.3 advanced development
- Create customer satisfaction via involving customers aggressively in the program selection and decision-making processes

REORGANIZED AIR FORCE

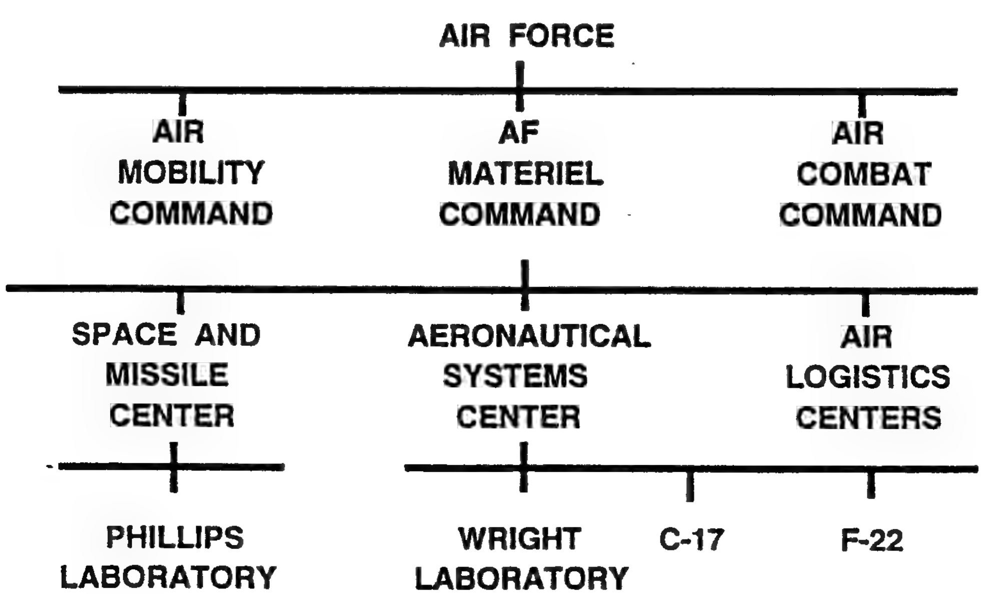

AIR FORCE MATERIEL COMMAND

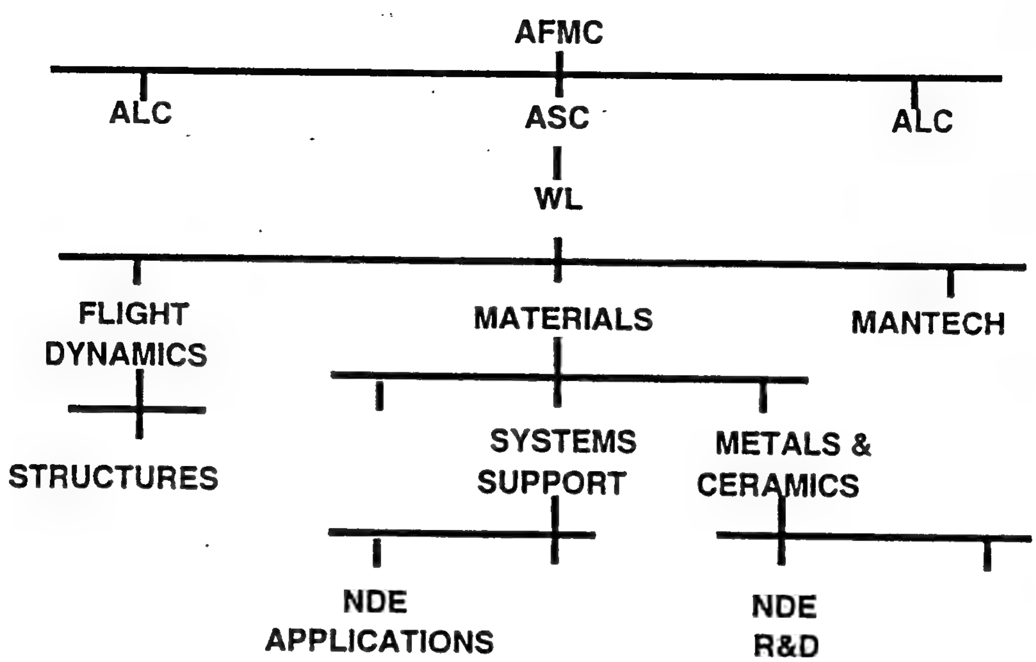

CHANGING AF WEAPON SYSTEM POSTURE

- **ENHANCE MANAGEMENT OF CURRENT SYSTEMS**
  - Airframes (C-141, C-5, C-130, F-16, F-15)
  - Engines (F100 RFC, F110 ENSIP)
  - **INCREASED focus on SLEP with ASIP / ENSIP**

- **NEW SYSTEMS ACQUISITION DECELERATING**
  - C-17 - 40 AIRCRAFT
  - B-2- SMALL FLEET(20) - NOT AT DEPOT
  - F-22 - IOC DELAYED TO ?

- **INCREASING LOW OBSERVABLES REQUIREMENTS**
  - F-117 / F-16 / B-1B / SOF / ACM / B-2 / F-22 / OTHERS
  - SIGNATURE SUPPORTABILITY PROBLEMS

Air Force Aging Aircraft

ACTIVE DUTY FLEET	0-6	7-12	13-18	18-24	24+	AVG
	AGE IN YEARS					
A-10		180	42			11.2
B-52					148	31.4
C-9				32	3	21.5
KC-10	12	47				7.7
C-130	30	9	51	77	167	21.9
C-135					479	30.9
C-141					241	26.1
F-15	241	249	194	4		8.3
F-16	744	102	20			3.7
F-111			12	188	32	21.5
T-37				77	427	29.8
T-38				177	508	26.1

Source: Air Force Magazine, May 1993

FOCAL AREA 4 TEAM MEMBERS / CHANGES

MLLP

T. CORDELL	FOCAL POINT
M. BLODGETT	X-RAY, ULTRASONIC TECHNOLOGY
C. BUYNAK	COMPUTED TOMOGRAPHY, UT
C. FIEDLER	OPTICS, LASER-GENERATED UT
G. JABLUNOVSKY	EDDY CURRENT, LO, AGING
R. KENT	OPTICAL METROLOGY
L. MANN	IMAGE ENHANCEMENT AND ANALYSIS
T. MORAN	WUD LEADER
C. VICKERS	ASC, UT

MLSA

- G. HARDY
- J. BRAUSCH

MLSS

J. SIERON	ALC SUPPORT

MLIM

S. RUEGGSEGER	PROCESS PLANNING

FIB

- C. PAUL
- J. BURNS

NAVY

V. AGARWALA	JDL RELIANCE

FOCAL AREA 4 CUSTOMER INVOLVEMENT

ASC
- EN J. LINCOLN, A/C STRUCTURES
- SM S. VUKELICH, ENGINES

MANTECH
- D. BREWER, REPTECH
- T. SWIGART, NDI
- S. RICKLES, ENGINES

WRIGHT LABORATORY
- XPN, J. POTTER, LO APPLICATIONS
- XPT, C. KROPAS, MOBILITY TPIPT
- XPT, J. KUZNIAR

SM-ALC
- A. ROGEL
- D. FROOM , D. BAILEY

WR-ALC
- D. HAZEN
- N. WOODWARD

SA-ALC
- G. BURKHARDT, R. GARCIA
- R. PAGLIA (AF NDI)
- M. PAULK

OO-ALC
- J. HOUSEKEEPER
- A. McCARTY

OC-ALC
- C. MOORE, J. WHITTAKER
- D. NIESER (KC-135)

Slide 8

USAF NDI IPT

AF NDI Program Office (SA-ALC / LDN)
- R. PAGLIA
- CAPT C GUYER
- M. PAULK
- K. CORREALE
- CMS S. PALUMBO
- SMS D. LOCKE

HQ AFMC
- SMS G. MONGELLI

WL
- TOBEY CORDELL
- CAPT G. JABLUNOVSKY

SUBSYSTEMS SPO (ASC / SM)

SM-ALC, A. ROGEL
WR-ALC, D. HAZEN
SA-ALC, G. BURKHARDT,
OO-ALC, J. HOUSEKEEPER
OC-ALC, C. MOORE

ACC, CMS J. MILLER

AMC, MS B. SCHMIDT

ANG, T. NAGY

AF Res, MS D. WILSON

Slide 9

LOGISTICS NEEDS (RANK ORDERED)

- LN 79004 AIRCRAFT BATTLE DAMAGE REPAIR TECHNOLOGY
- **LN 79003 DETECTION OF HIDDEN AND INACCESSABLE CORROSION**
- LN 91006 UNIVERSAL AVIONICS MODULE
- **LN 84039 RAPID NDI FOR ADVANCED COMPOSITES WITH COMPLEX SHAPES, VARIABLE DENSITIES**
- **LN 88030 NDI TECHNIQUES FOR CRACK DETECTION IN SECOND LAYER STRUCTURE**
- LN 80181 DAMAGE TOLERANCE FOR ADVANCED COMPOSITES
- LN 91049 RELIABLE FASTENING SYSTEMS
- **LN 90077 NDI TECHNIQUE TO RELIABLY DETECT SMALL FATIGUE CRACKS**

AIRFRAME LIFE MANAGEMENT ISSUES

CRACK DETECTION

- NDI CITED AS CRITICAL AT AF ASIP CONF
- TACTICAL FIGHTER LIFE EXTENSION ISSUES
- TRANSPORT DURABILITY

CORROSION DETECTION

- C/KC-135 CONVERSION TO C/KC-135R
- CORROSION IS LIFE-LIMITING

ASIP CONFERENCE -TACTICAL FIGHTERS

F - 16

BULKHEAD / FUEL SHELF CRACKING

SIGNIFICANT INCREASE IN SEVERITY OF USAGE

SAFETY LIMITS REDUCED

- **INSPECTION INTERVALS REDUCED**

LESSONS LEARNED

- **POOR HOLE QUALITY IN BULKHEAD HOLES**
- **INITIAL CRACKS ALL STARTED NEXT TO HOLES**

FATIGUE LIFE EXTENSION VIA COLD-EXPANSION OF HOLES

F -15

LOWER WING SPAR CRACKING

CURRENTLY INACCESSIBLE

- NECESSITATES REMOVAL OF UPPER WING COVER

Slide 12

ASIP - EXTENDED SERVICE LIFE TRANSPORTS

C-141

WING SPLICE - STATION 405

MSD - FATIGUE CRACKING AT MULTIPLE SITES

CURRENT FORCE AVERAGE 34,000 HRS

DECISION: CONTINUE WITH RELIABLE INSPECTIONS AND REPAIR

INSPECTION DECREASES PROBABILITY OF FAILURE TENFOLD

C-130

WING DURABILITY

'86 & ON - 2 TO 3 TIMES AS SEVERE USAGE

3 MAJOR CENTER WING REVISIONS

5 MAJOR OUTER WING REVISIONS

NEW STRUCTURAL TESTS

SIGNIFICANT CRACKS DETECTED VIA NDI

SEVERAL REPAIR APPROACHES INCLUDE COMPOSITES

NDI TECHNIQUES BEING DEVELOPED AS REQUIRED

Slide 13

APPROACH to Corrosion Detection

- ALCs evaluating current equipment to detect >10% material loss

  - ML transitioning near-term technologies for < 10% material loss

  - ML developing NEW TECHNOLOGIES for NASCENT corrosion DETECTION and corrosion DISCRIMINATION

CORROSION DETECTION / CHARACTERIZATION

- COOPERATIVE EFFORT WITH NAVAL AIR WARFARE CENTER
- DEVELOPMENT OF CORROSION SPECIFIC SENSORS
  - THIN FILM GALVANIC SENSORS
  - CORROSION SENSITIVE COATINGS
  - APPLICATION HAS SOME LIMITIATIONS
- LEVERAGING FUNDS 3 YRS
- CUSTOMER = OC-ALC / INSTALLING ON KC-135

FY93 NEW START PRDA

- NOVEL NDE METHODS FOR CORROSION DETECTION
  - IDENTIFY/ASSESS FEASIBILITY OF NOVEL CORROSION DETECTION AND CHARACTERIZATION METHODS
  - PRDA ALLOWS SELECTION OF MULTIPLE APPROACHES
- PAYOFF: REDUCED OPERATIONAL MAINTENANCE COSTS THROUGH EARLY DETECTION AND TRACKING OF CORROSION

HIGH RES RTR ADV DEVELOPMENT

OBJECTIVE: DEVELOP PROTOTYPE REAL-TIME RADIOGRAPHIC IMAGING SYSTEM WHICH DEMONSTRATES VIABILITY AND CAPABILITY TO REPLACE IN-FIELD FILM TECHNIQUES

CONTRACTOR: LOCKHEED MISSILES AND SPACE CO. (F33615-91-C-5623)

APPROACH: 6.3 PROGRAM BASED ON 6.2 DEVELOPMENTS

TASK I - BUILD AND EVALUATE CORE SYSTEM

TASK II - BUILD AND EVALUATE BRASS BOARD SYSTEM

TASK III - BUILD AND EVALUATE PROTOTYPE

HIGH RES RTR ADV DEVELOPMENT

GOALS

- REPLACE FILM → LOWER COST, FASTER, INCR DYNAMIC RANGE
- ELIMINATE HAZARDOUS WASTE (NO PROCESSING CHEMICALS)
- PROVIDE DIGITAL DATA ANALYSIS / ARCHIV ING

PERFORMANCE OBJECTIVES

PARAMETER	CURRENT	TASK I EXPECTED	TARGET
SPATIAL RESOLUTION	10 (lp/mm)	10	20
CONTRAST SENSITIVITY	1%	.3%	.1%
DYNAMIC RANGE	3000	3500	>3000
IMAGE ACQUISITION TIME	10 (Seconds)	5	1
FIELD OF VIEW (Inches)	2 x 2	4 x 4	4 x 4

NDE, A FULL SPECTRUM TECHNOLOGY

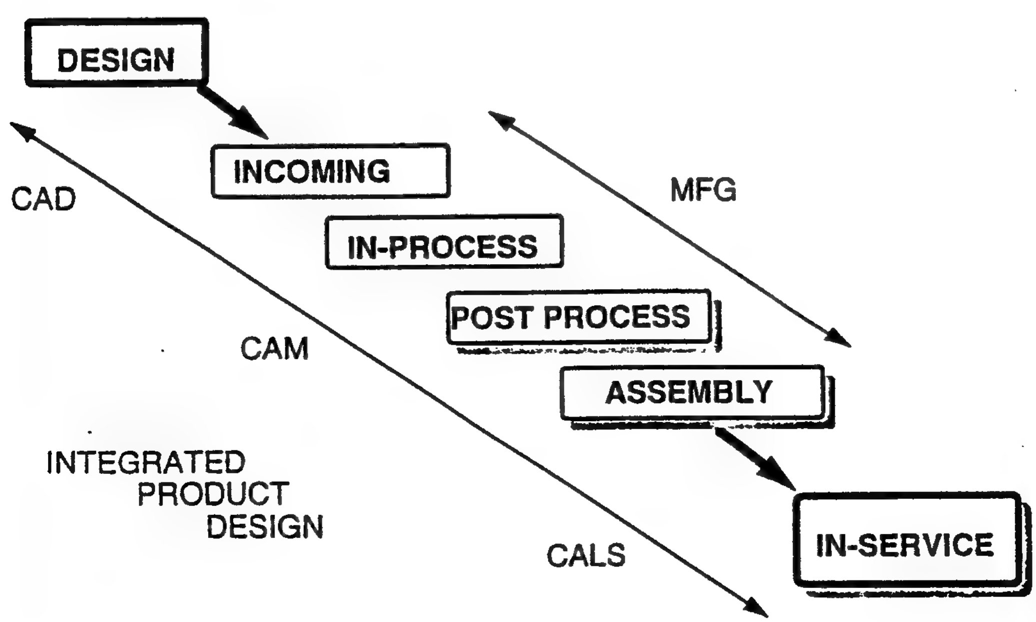

WRIGHT LABORATORY
FLIGHT DYNAMICS DIRECTORATE
STRUCTURES PROGRAMS

James L. Rudd
Deputy Chief, Structures Division

Presented at Second Air Force Aging Aircraft Conference
Oklahoma City Air Logistics Center
Tinker AFB, OK
17 - 19 May 1994

5-4-87hg

OUTLINE

- Background on importance of structural life enhancement
- Description of structural life enhancement research
  - Aging aircraft
  - Structural integrity of composites
  - Dynamics & loads
- Payoffs
- Summary

WL AGING AIRCRAFT BACKGROUND

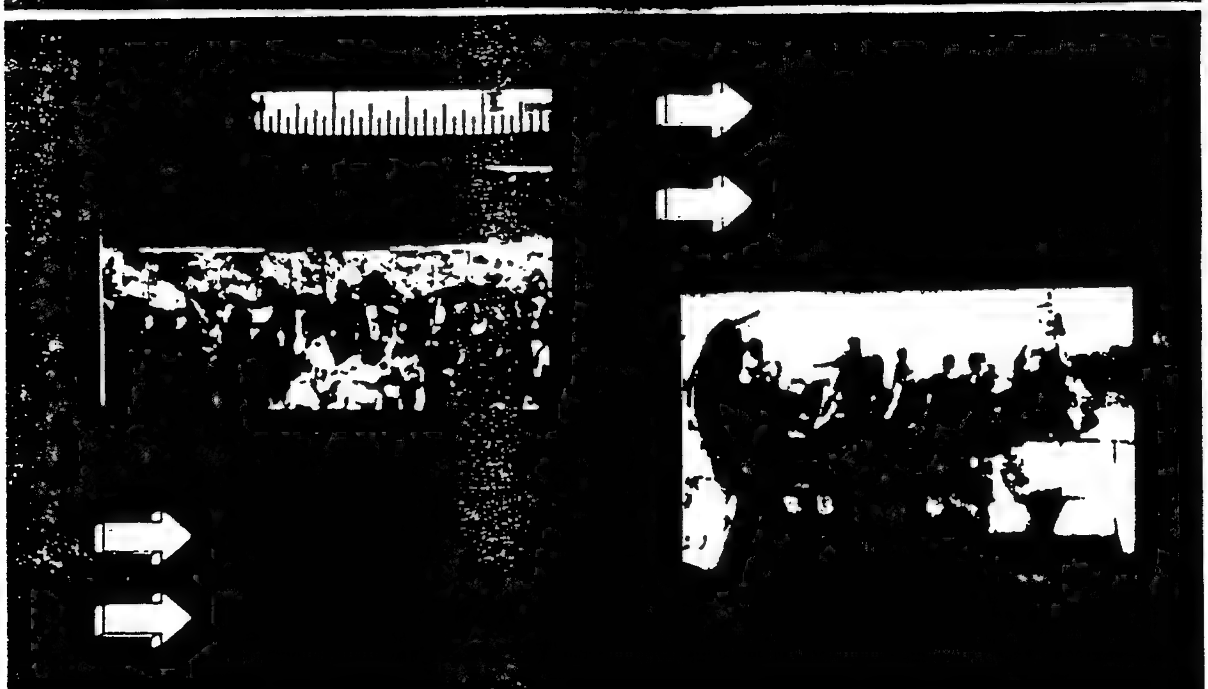

AIR FORCE AGING AIRCRAFT
(AS OF 30 SEP 92)

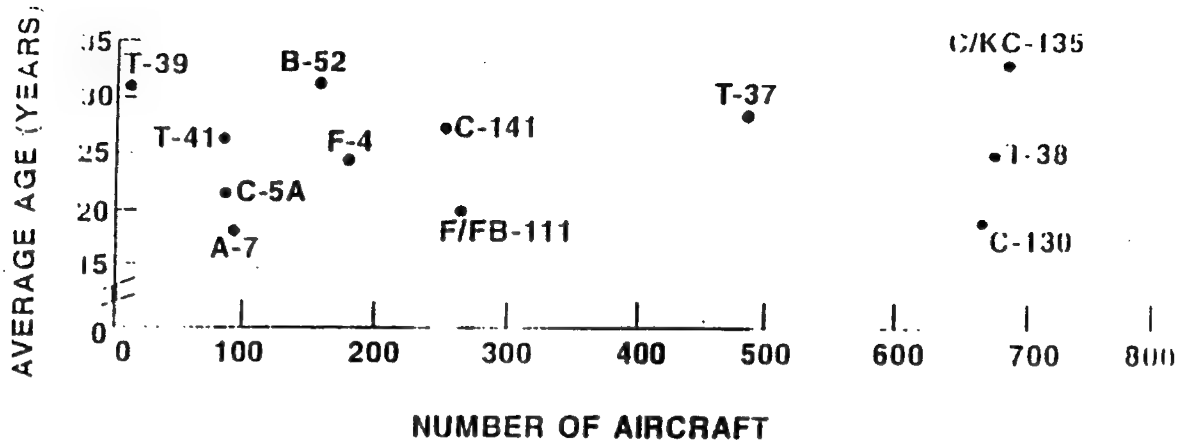

AGING AIRCRAFT

<u>TECHNOLOGY FOCUS AREAS</u>

- **Damage/ Life/ Risk Assessment**
  - **WFD/ MSD/ MED**
  - **Corrosion/ Fatigue**
- **Repairs & Life Enhancement Techniques**
  - **Repair Integrity Analysis & Airworthiness Verification**
  - **Life Enhancement Techniques**

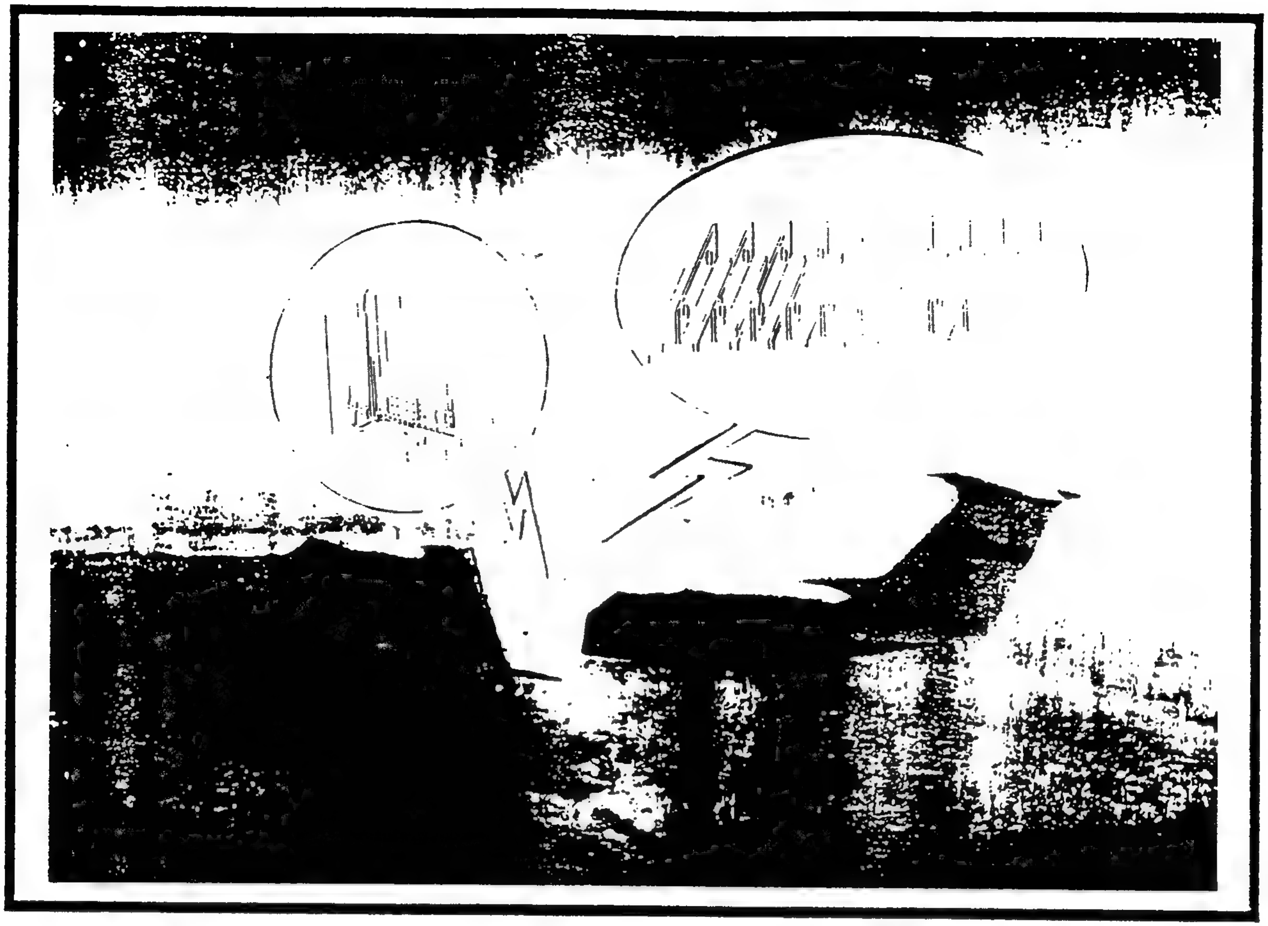

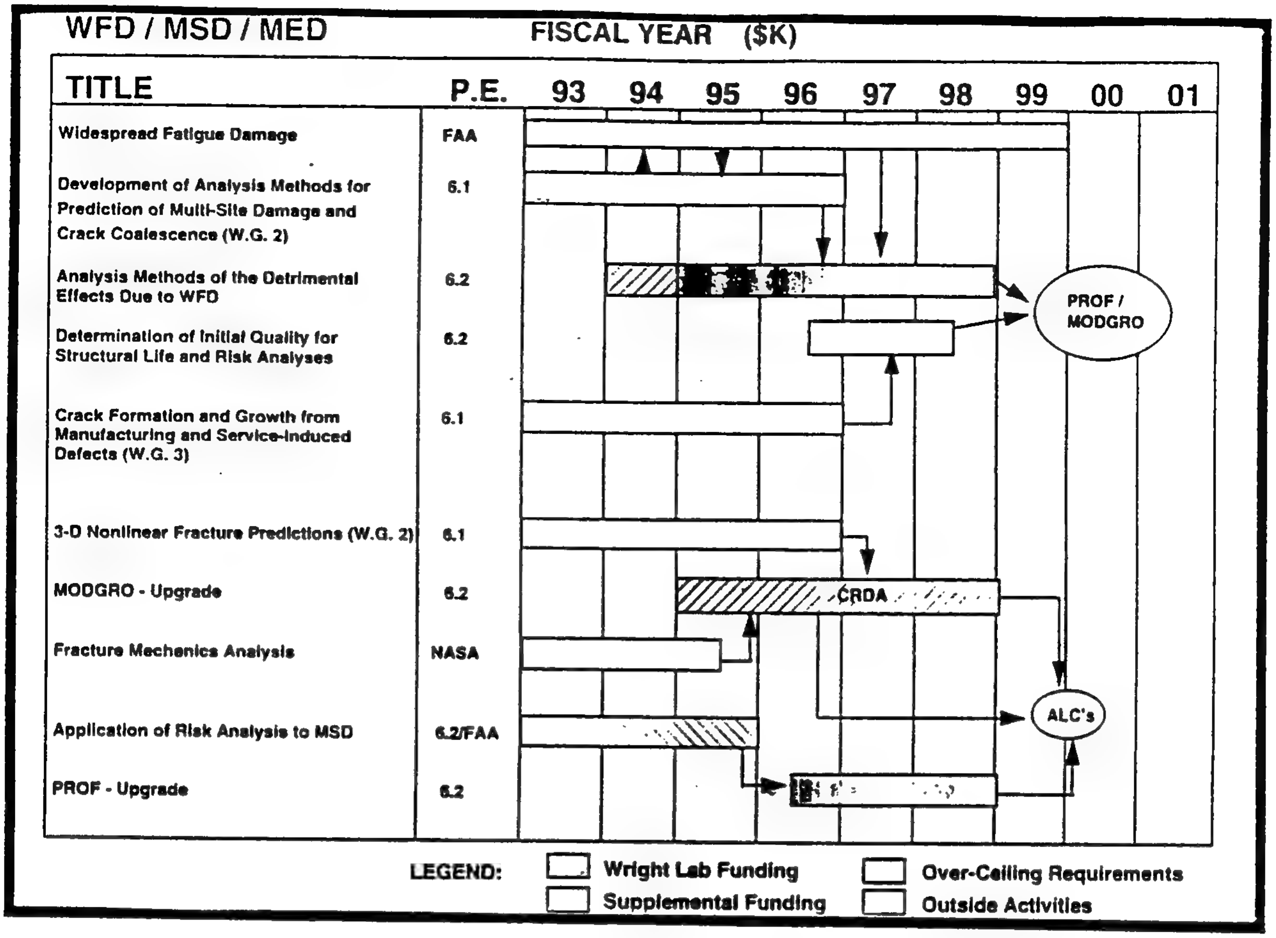
WFD / MSD / MED
FISCAL YEAR ($K)
TITLE
P.E.
93
94
95
96
97
98
99
00
01
Widespread Fatigue Damage
FAA
Development of Analysis Methods for Prediction of Multi-Site Damage and Crack Coalescence (W.G. 2)
6.1
Analysis Methods of the Detrimental Effects Due to WFD
6.2
Determination of Initial Quality for Structural Life and Risk Analyses
6.2
Crack Formation and Growth from Manufacturing and Service-Induced Defects (W.G. 3)
6.1
3-D Nonlinear Fracture Predictions (W.G. 2)
6.1
MODGRO - Upgrade
6.2
CRDA
Fracture Mechanics Analysis
NASA
Application of Risk Analysis to MSD
6.2/FAA
PROF - Upgrade
6.2
PROF / MODGRO
ALC's
LEGEND:
Wright Lab Funding
Supplemental Funding
Over-Ceiling Requirements
Outside Activities

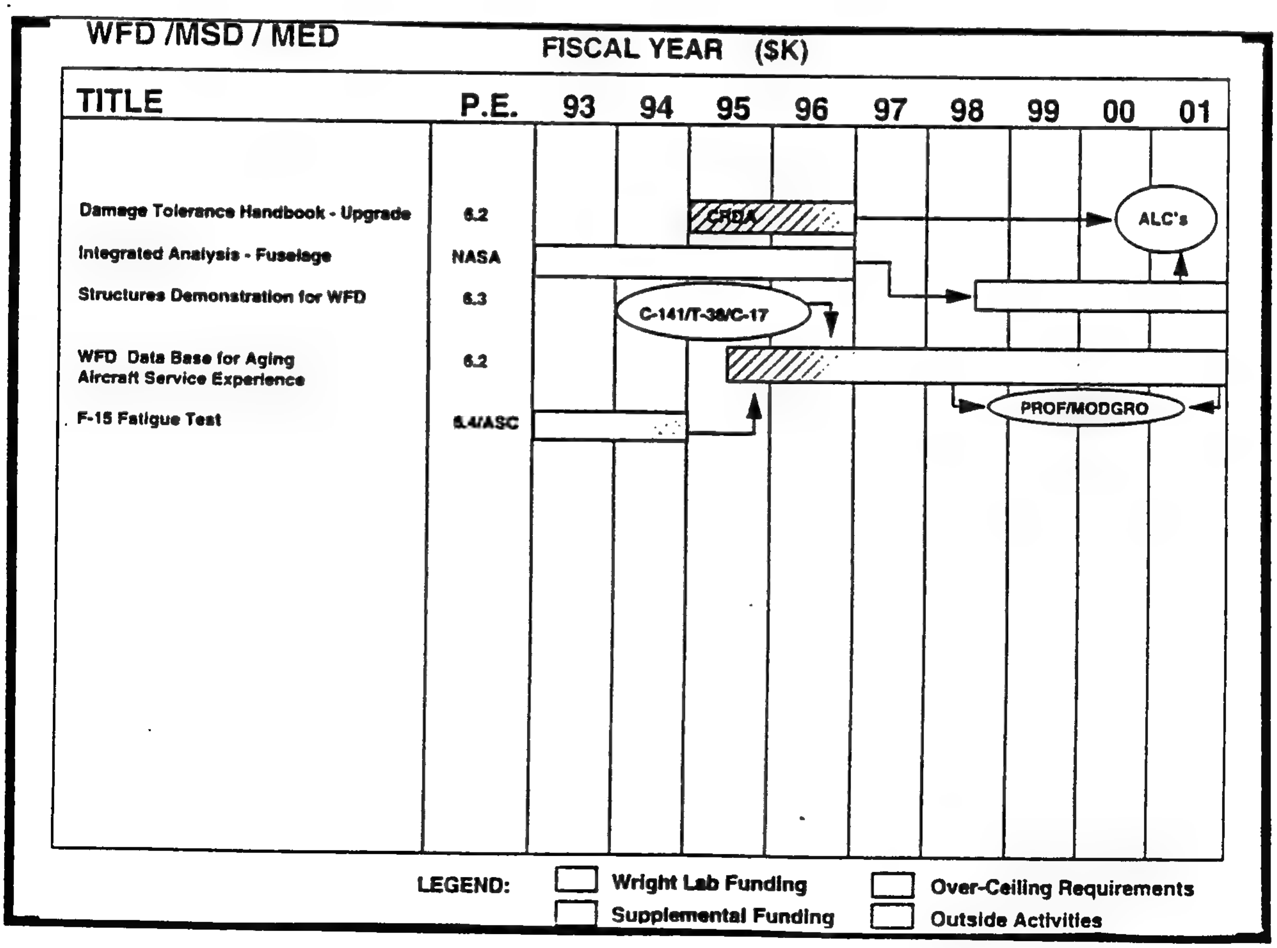
WFD /MSD / MED
FISCAL YEAR ($K)
TITLE
P.E.
93
94
95
96
97
98
99
00
01
Damage Tolerance Handbook - Upgrade
6.2
CRDA
Integrated Analysis - Fuselage
NASA
Structures Demonstration for WFD
6.3
C-141/T-38/C-17
WFD Data Base for Aging Aircraft Service Experience
6.2
F-15 Fatigue Test
6.4/ASC
ALC's
PROF/MODGRO
LEGEND:
Wright Lab Funding
Supplemental Funding
Over-Ceiling Requirements
Outside Activities

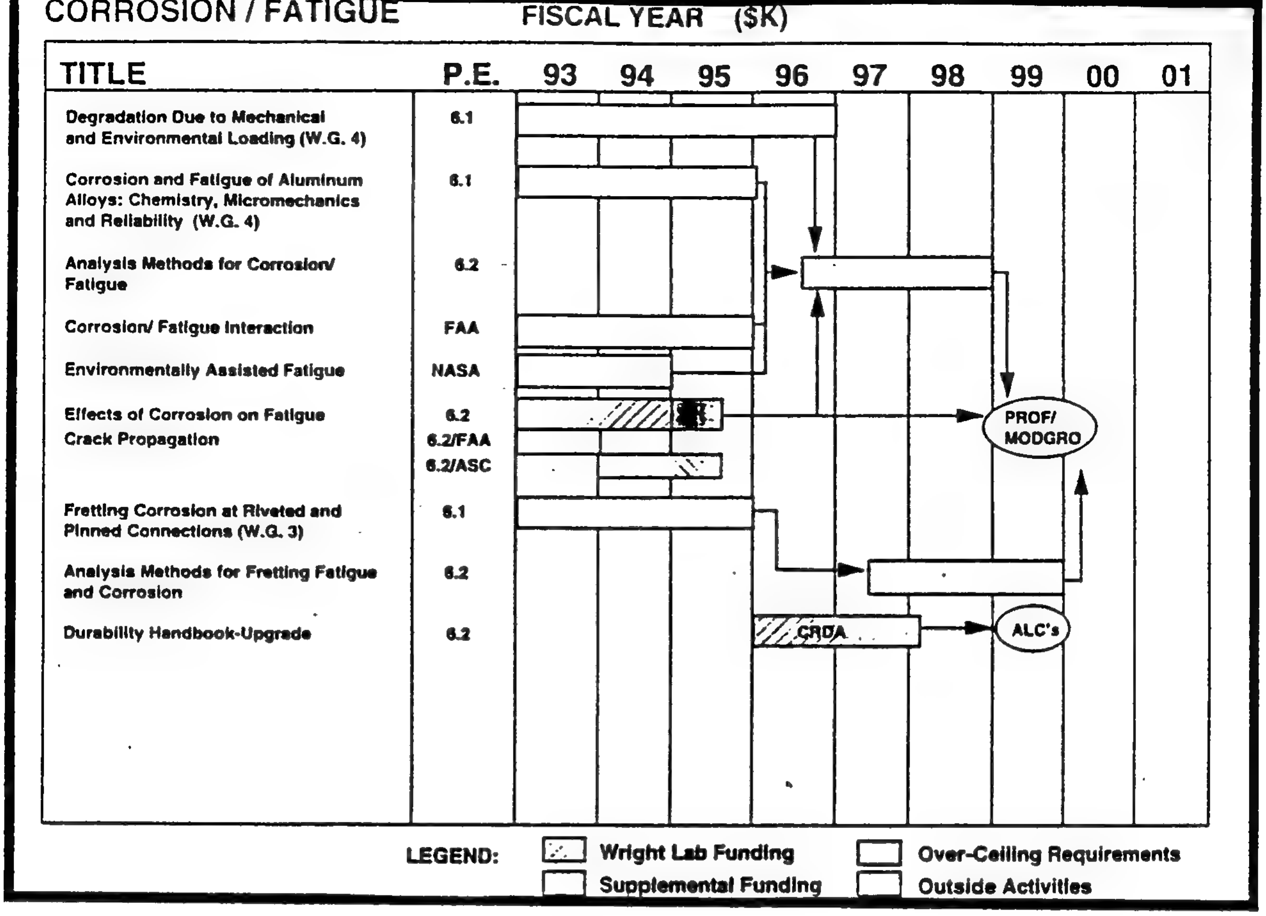
CORROSION / FATIGUE
FISCAL YEAR ($K)
TITLE
P.E.
93
94
95
96
97
98
99
00
01
Degradation Due to Mechanical and Environmental Loading (W.G. 4)
6.1
Corrosion and Fatigue of Aluminum Alloys: Chemistry, Micromechanics and Reliability (W.G. 4)
6.1
Analysis Methods for Corrosion/ Fatigue
6.2
Corrosion/ Fatigue Interaction
FAA
Environmentally Assisted Fatigue
NASA
Effects of Corrosion on Fatigue Crack Propagation
6.2
6.2/FAA
6.2/ASC
PROF/ MODGRO
Fretting Corrosion at Riveted and Pinned Connections (W.G. 3)
6.1
Analysis Methods for Fretting Fatigue and Corrosion
6.2
Durability Handbook-Upgrade
6.2
CRDA
ALC's
LEGEND:
Wright Lab Funding
Supplemental Funding
Over-Ceiling Requirements
Outside Activities

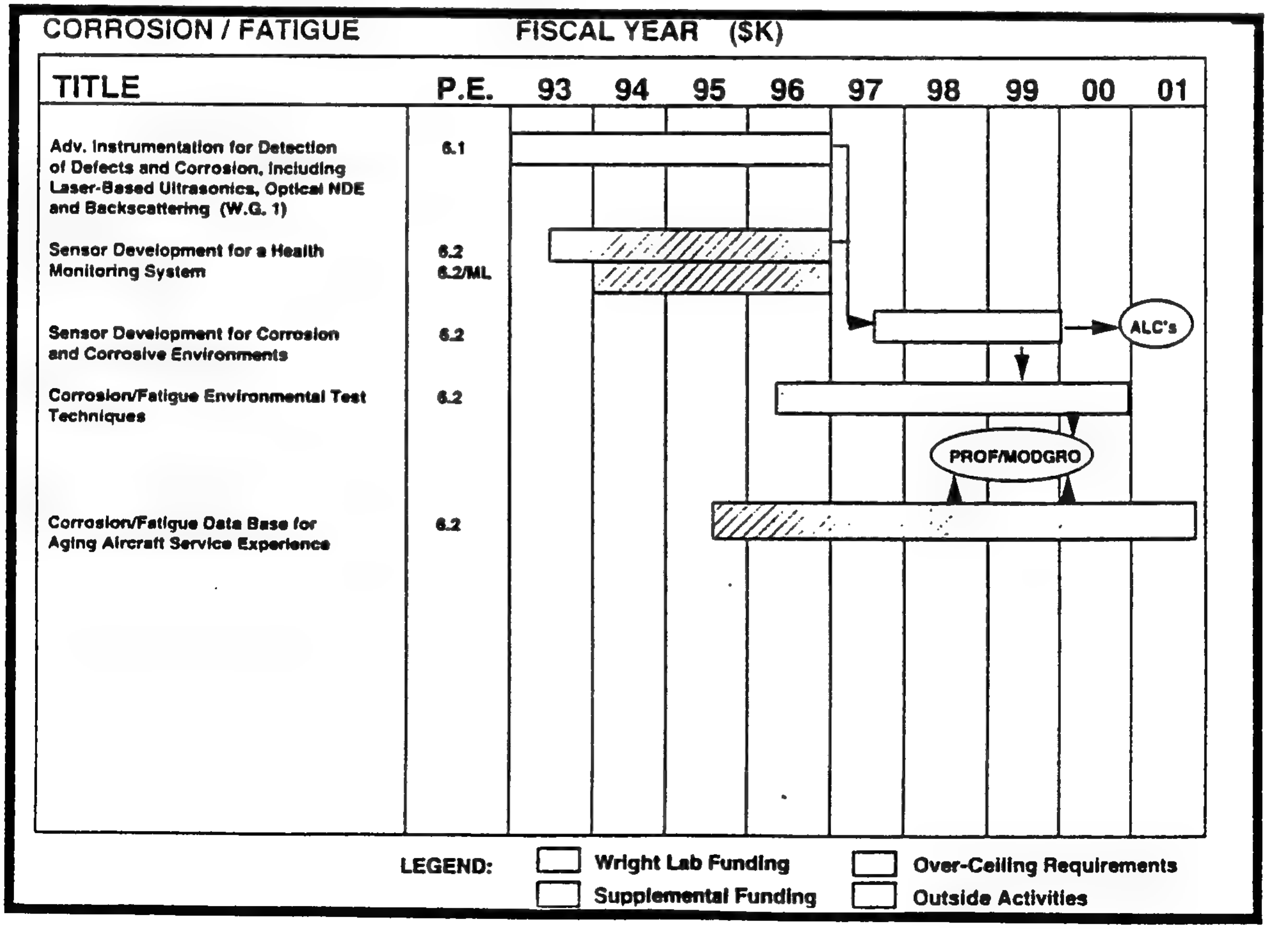
CORROSION / FATIGUE
FISCAL YEAR ($K)
TITLE
P.E.
93
94
95
96
97
98
99
00
01
Adv. Instrumentation for Detection of Defects and Corrosion, Including Laser-Based Ultrasonics, Optical NDE and Backscattering (W.G. 1)
6.1
Sensor Development for a Health Monitoring System
6.2
6.2/ML
Sensor Development for Corrosion and Corrosive Environments
6.2
ALC's
Corrosion/Fatigue Environmental Test Techniques
6.2
PROF/MODGRO
Corrosion/Fatigue Data Base for Aging Aircraft Service Experience
6.2
LEGEND:
Wright Lab Funding
Supplemental Funding
Over-Ceiling Requirements
Outside Activities

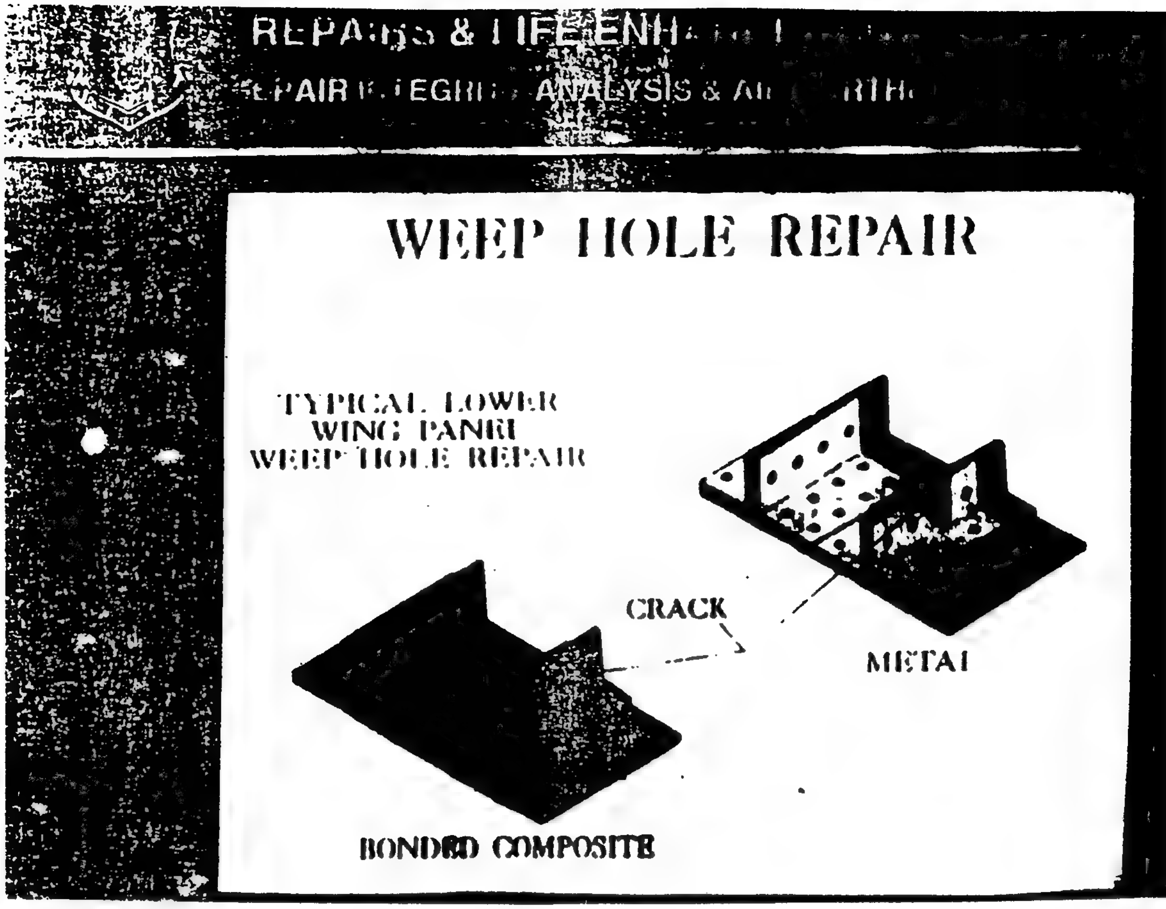

REPAIR INTEGRITY ANALYSIS
AND AIRWORTHINESS VERIFICATION FISCAL YEAR ($K)

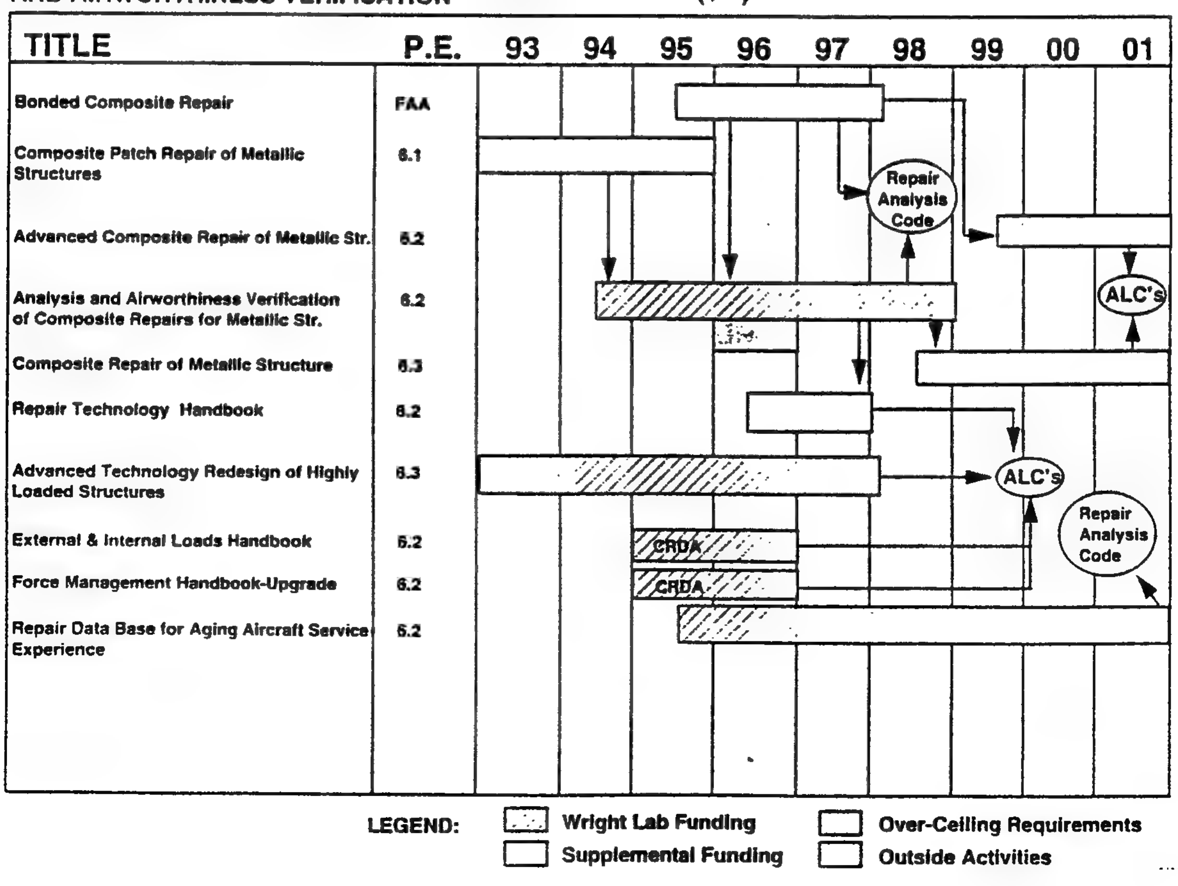

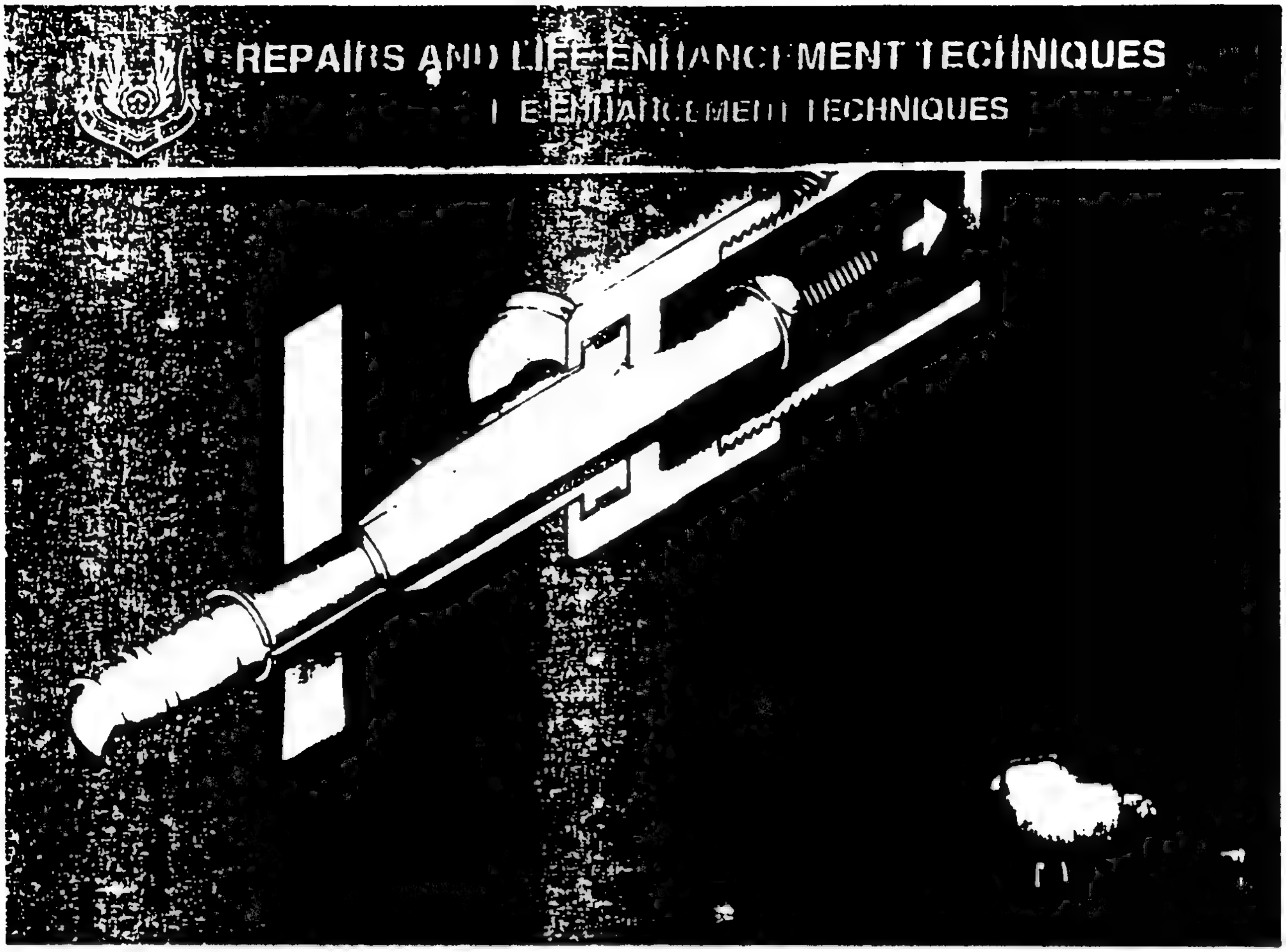

LIFE ENHANCEMENT TECHNIQUES

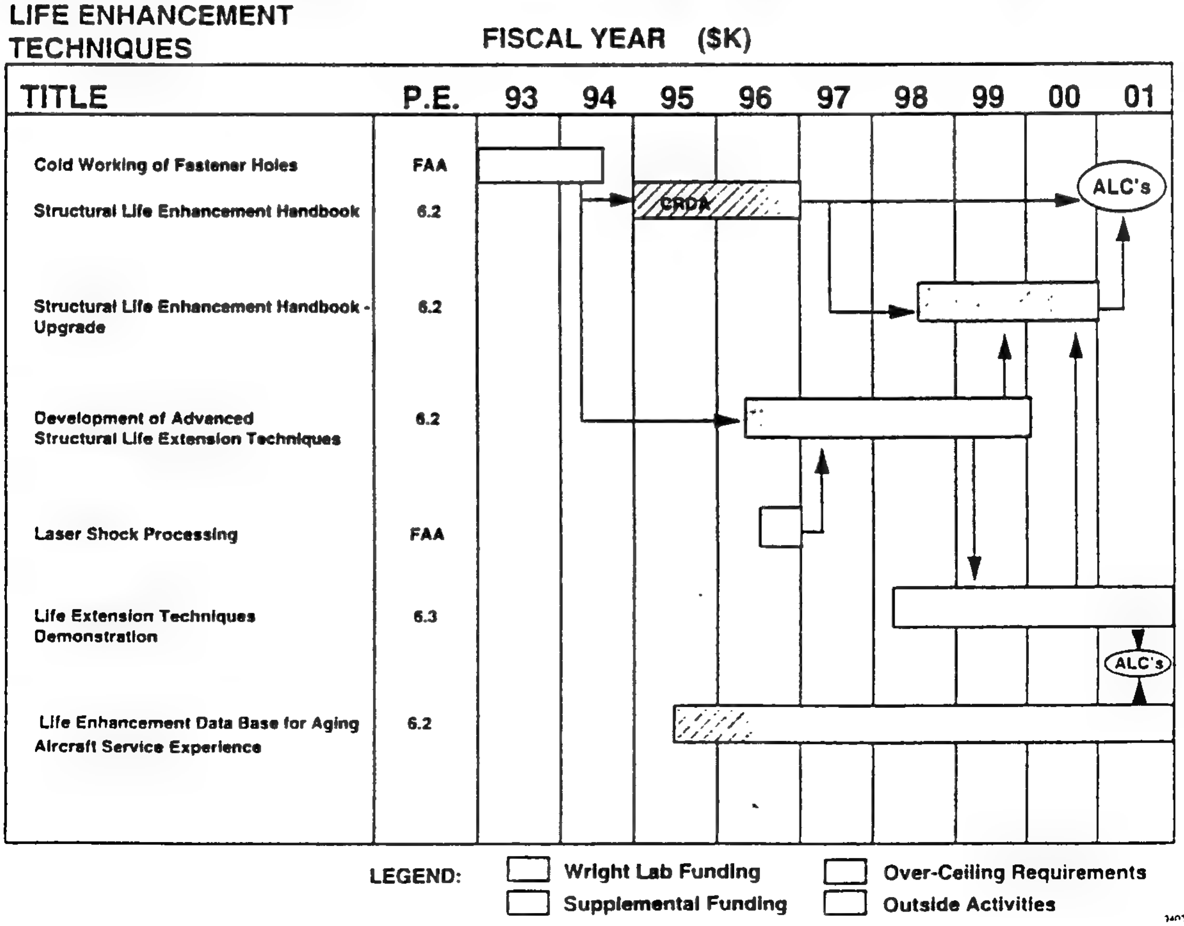

STRUCTURAL INTEGRITY OF COMPOSITES

TENSION PRELOADED IMPACT

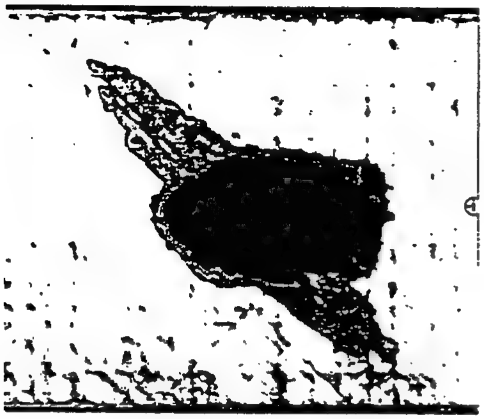

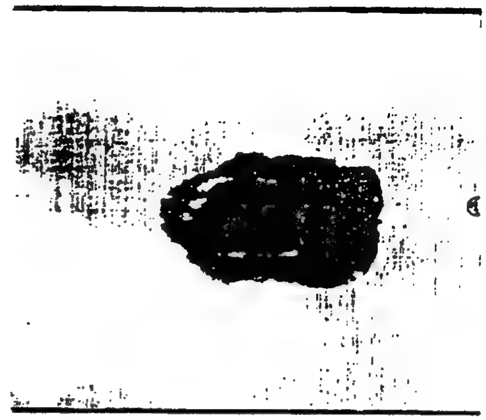

25 PERCENT PRELOAD

STRUCTURAL INTEGRITY OF COMPOSITES

FISCAL YEAR ($K)

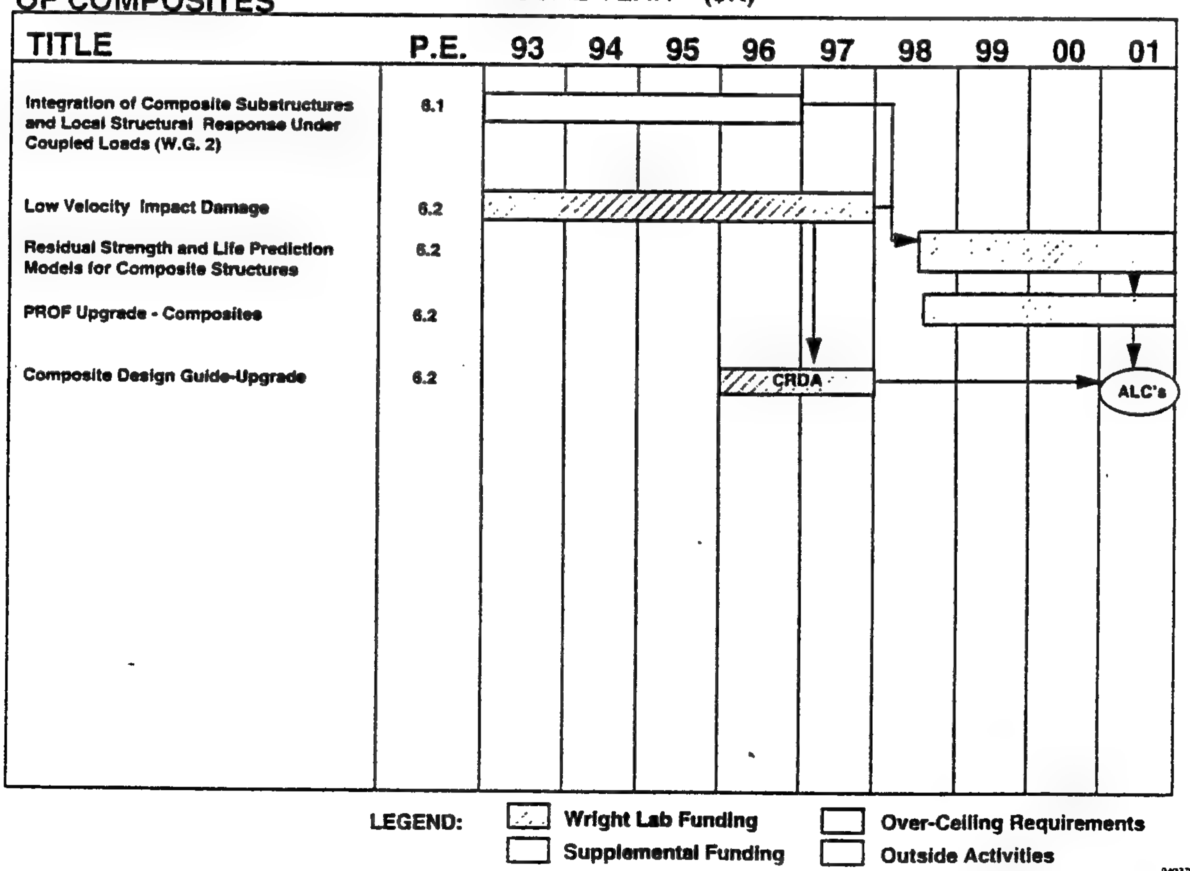

94037C

DYNAMICS & LOADS

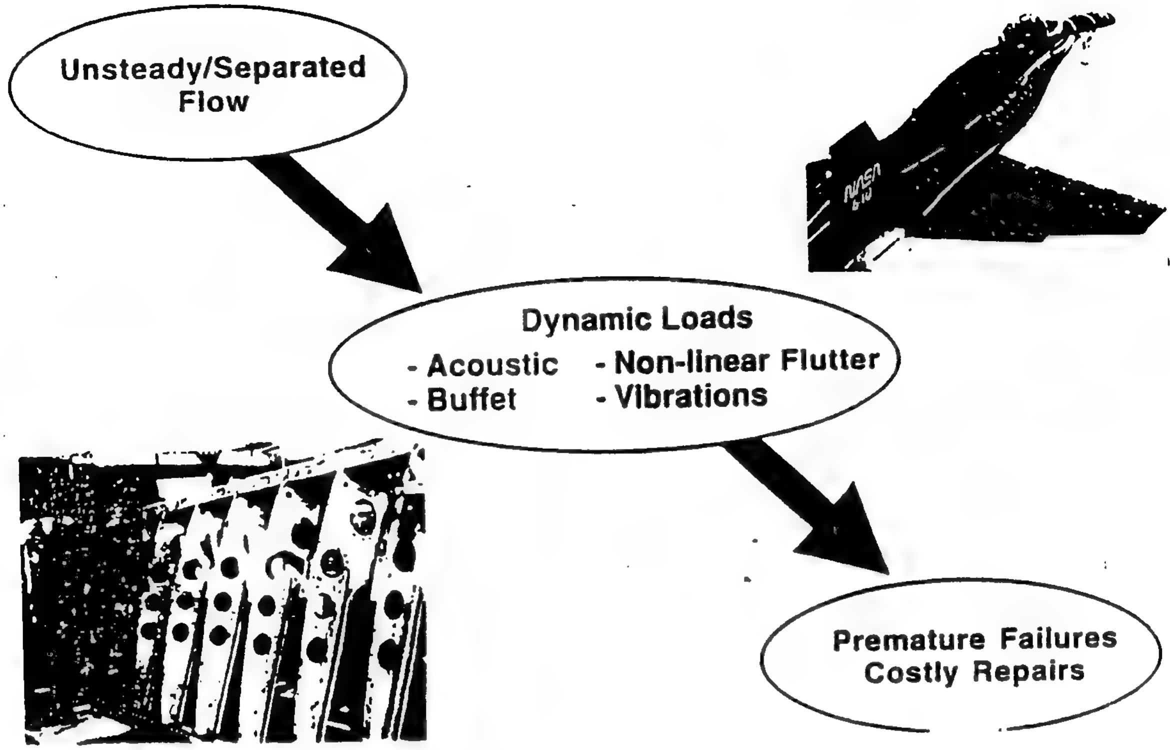

DYNAMICS & LOADS FISCAL YEAR ($K)

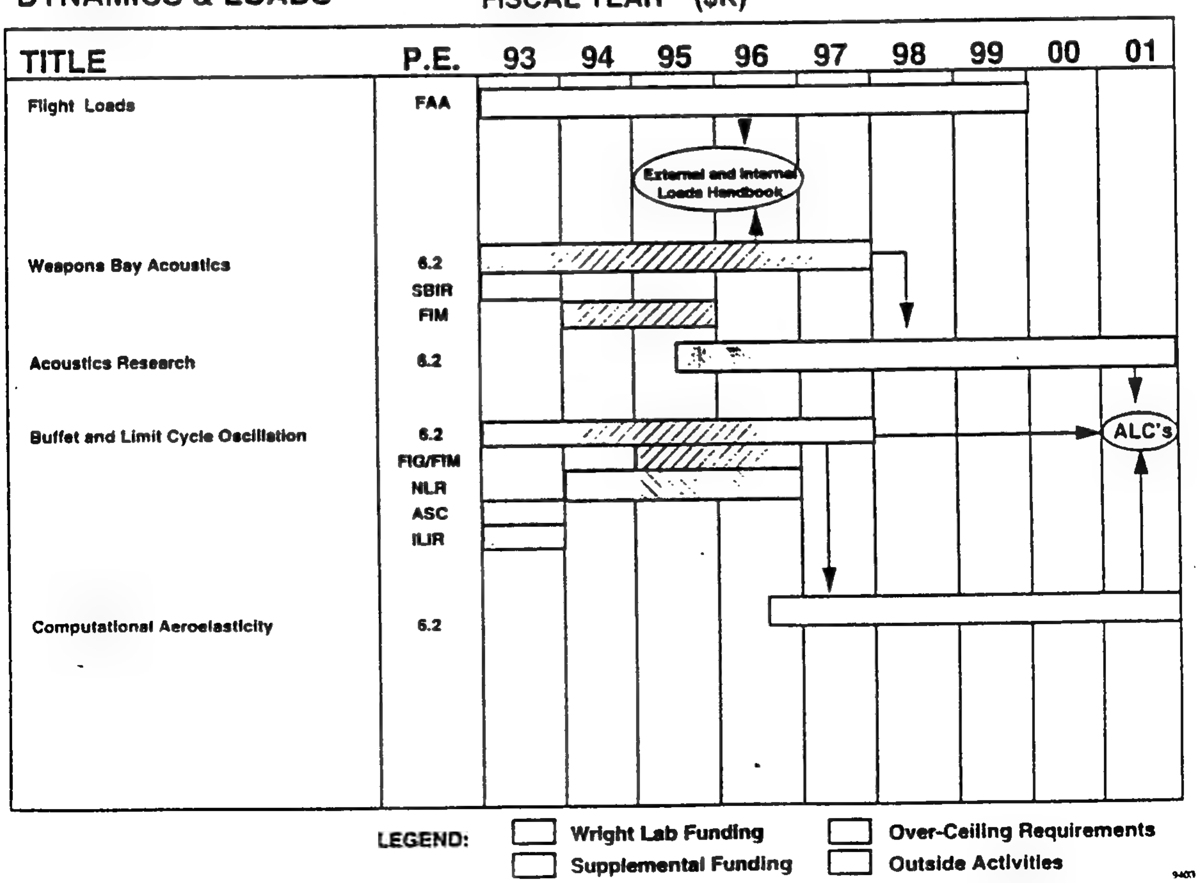

STRUCTURAL LIFE ENHANCEMENT PAYOFFS

Increased Structural Safety

Want to prevent an AF Aloha

Reduced Acquisition Costs

Extend structural life
Delay replacement of fleet

Reduced Operational Costs

Early detection/repair vs. late detection/replace

Bonus: Increase Operational Readiness

SUMMARY

- Increase in importance of structural life enhancement research
  - Limited number of new weapon systems
  - Aging aircraft must remain in service much longer than anticipated
  - Must insure structural integrity of aging aircraft
- WL research plan developed that addresses structural life enhancement issues
  - Aging aircraft
  - Structural integrity of composites
  - Dynamics & loads

The National Aging Aircraft Research Program

Federal Aviation Administration Technical Center (FAATC)
Atlantic City International Airport
New Jersey

Dick Johnson

ACD/DJ5/001/94.5

FAA Aging Aircraft Program

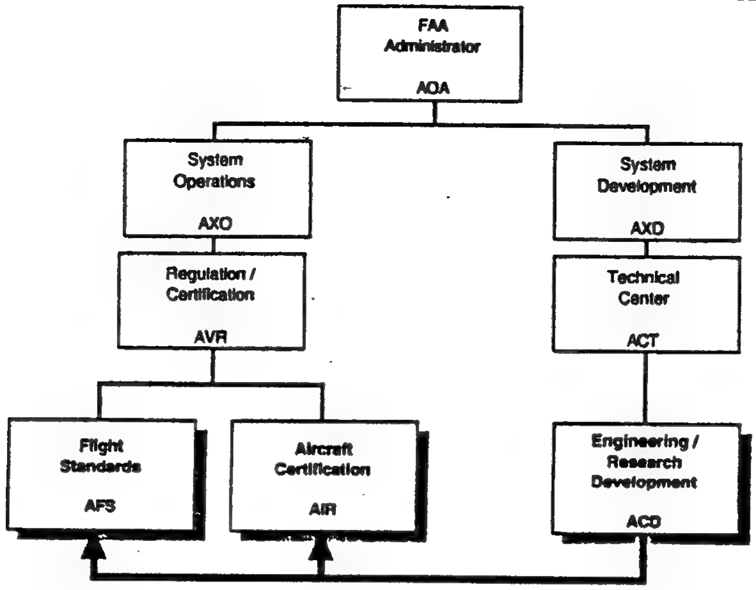

Overview

- Background
- Issues
- Goals
- Program Plan
- Objectives / Tasks
- Accomplishments

Background

June 1988	International Aging Airplane Conference (1)
November 1988	Aviation Safety Research Act / Research Initiation
May 1989	FAA Research Program Plan
October 1990	Center for Aviation Systems Reliability
July 1992	Non-Destructive Inspection (NDI) Validation Center
October 1993	Center for Computational Modeling of Aircraft Structures
October 1993	FAA Research Program Plan Update
June 1995	International Aging Airplane Conference (6) — (Planned)

Aviation Safety Research Act of 1988

Directs FAA to:

- **Develop Technologies and Conduct Data Analysis for Predicting the Effects of Aircraft Design, Maintenance, Testing, Wear, and Fatigue on the Life of Aircraft and Air Safety**

- **Develop Methods of Analyzing and Imposing Aircraft Maintenance Technology and Practices, Including NDI of Aircraft Structures**

Issues

- Increased Frequency of Cracking in Uniformly Stressed Areas Leading to Multi-Site Damage that Causes Large Cracks to Form More Rapidly Than Is Acceptable from a Damage Tolerance and Detection Viewpoint
- Increased Frequency of Cracking in Isolated Regions of the Structure Coupled with a High Probability that These Cracks Will Be Undetected during Periodic Inspections
- The Acceleration of Fatigue by Corrosion
- The Effects of Multiple Repairs

Basic Questions

- How Long Can Structural Life Be Extended?
- Is the Current System Adequate?
  (Techniques, Methodologies, and Analyses Used In Design, Manufacture, Maintenance, and Inspection)
- What System Is Appropriate for the Future?

U.S. Transport / Commercial Airplane Fleets

	Large Transport FAR 25	Commuter FAR 23 / 25
No. Airplanes	5084	1144
No. Airplane Types	17	32
No. Manufacturers	5	18
No. Operators	11	117

Percent of Wide-Body Aircraft Over 20 Years Old in the U.S. Fleet as of Year-End 1993

Model	Total	> 20 Years	% > 20 Years
B-747	215	117	54.4
B-767	180	0	0
DC-10/MD11	315	93	29.5
L-1011	18	0	0
A-300	63	0	0
Total Wide-Body	791	210	26.5

Source: Boeing World Jet Airplane Inventory, Year-End 1993

Percent of Standard Aircraft Over 20 Years Old in the U.S. Fleet as of Year-End 1993

Model	Total	> 20 Years	% > 20 Years
B-707	133	65	48.9
B-720	3	3	100
B-727	1182	593	50.2
B-737	1012	151	14.9
B-757	369	0	0
DC-8	216	216	100
DC-9/MD80	1157	421	36.4
L-1011 STD Body	96	24	25.0
CONV 880	16	16	100
CONV 990	1	1	100
A-310	30	0	0
A-320	78	0	0
Total Standard Body	**4293**	**1490**	**34.7**

Source: Boeing World Jet Airplane Inventory, Year-End 1993

Percent of Wide-Body and Standard Aircraft Over 20 Years Old in the U.S. Fleet as of Year-End 1993

Type	Total	> 20 Years	% > 20 Years
Wide-Body	791	210	26.5
Standard Body	4293	1490	34.7
Total Fleet	**5084**	**1700**	**33.4**

Source: Boeing World Jet Airplane Inventory, Year-End 1993

Program Goals

- Develop Technology for Service Life Assessment and Extension for Metallic Structures
- Develop New and Enhance Existing Maintenance, Repair and Inspection Techniques
- Integrate and Modernize FAA Information Systems and Databases
- Develop Improved Design and Manufacturing Procedures for Future Fleet

National Aging Aircraft Research Program Plan

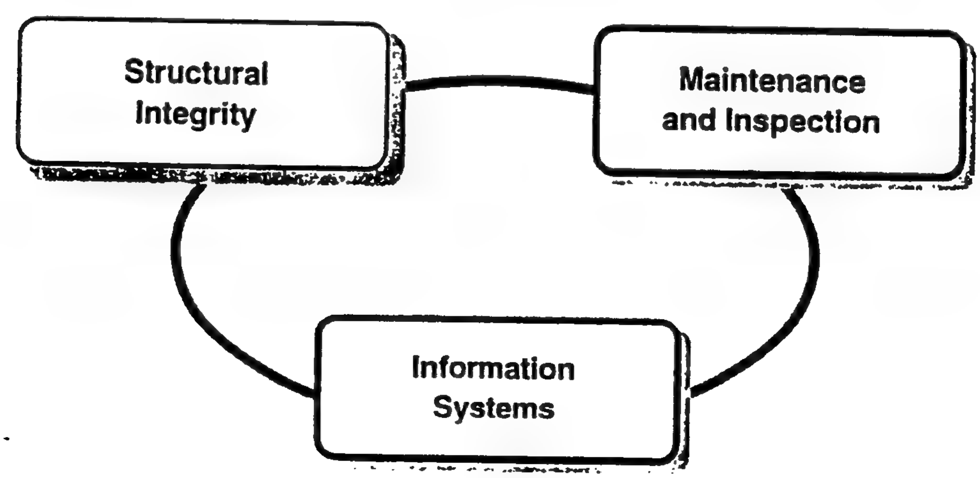

Structural Integrity Objectives

- A "Quick Response" Test Methodology
- Database and Models of Crack Growth, Corrosion, and MSD
- Analytical Approach for Inspection Interval Determination

Structural Integrity Research Tasks

Project	Tasks	Completion
Commuter Structures	Develop Practical Analysis Techniques	1999
Corrosion and Fatigue	Quantify Fatigue and Corrosion Interaction	1996
Engine Life Prediction	Develop Crack Growth Based Inspection Requirement	1999
Widespread Fatigue Damage	Develop Methods to Predict WFD Onset	1998
Repair Effects	Develop User Friendly Repair Assessment Tool	2000
Flight Loads	Collect Usage Data for Analysis and Design	1997

Schematic of Typical Structural Integrity Effort

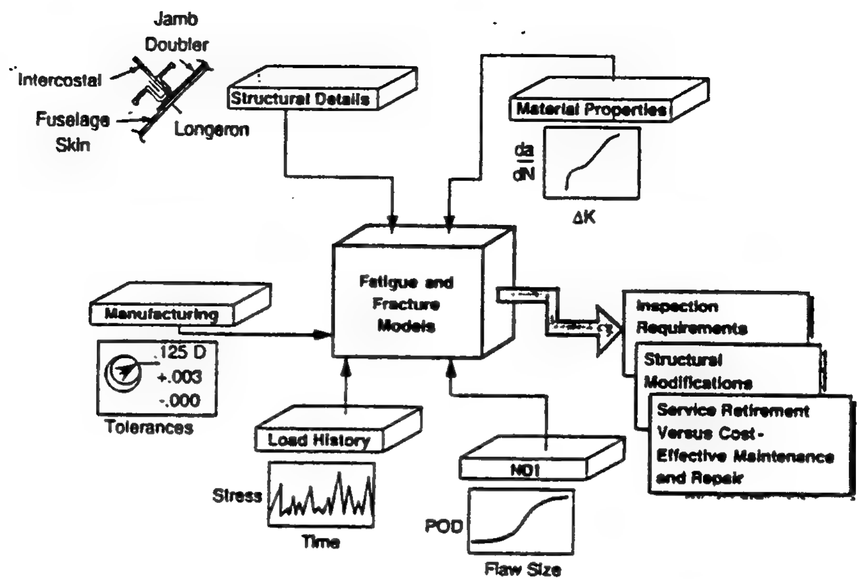

Maintenance (and Repair) Objectives

- Fatigue and Fracture Mechanics Compatible Airframe Repairs
- Uniformity of Repairs and Maintenance
- Understanding of New Composite Repair Technology
- Corrosion Control and Protection

Maintenance and Repair Research Tasks

Project	Tasks	Completion
Repair Procedure Development	Develop New In-Service Repair Guidelines	2000
Alternate Repair Strategies	Establish Applicability of Bonded Composite Repair	1999
Corrosion Protection Procedure Development	Develop New Corrosion Control Guidelines	1998
Job Task Analysis	Develop Basis for AMT Curriculum	1998
Proficiency and Equipment Standards	Establish Limits for Airframe / Engine Repair Facilities	1997

NDI Objectives

- **Reliable Crack Detection**
- **Broad Area Crack NDI**
- **Corrosion Detection**
- **Bond Quality Measurement**
- **Consistent, Quality Inspector Performance**

NDI Technology Development Process

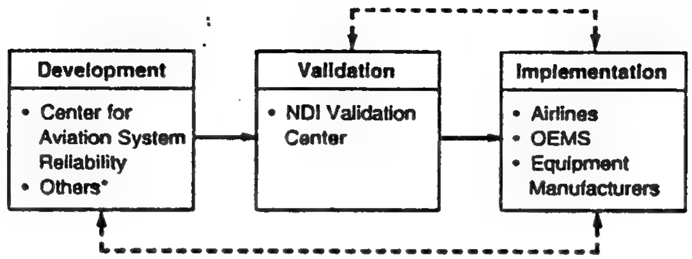

* Industry / Government / Academia

Inspection Research Tasks

Project	Tasks	Completion
NDI Training	Provide FAA NDI Training	1996
Techniques for Flaw Detection	Develop Reliable, Cost-Effective Methods	1997
Robotics	Develop Automated Inspection System	1996
Validation Center	Validate Inspection Procedures and Equipment	1998
Engine Parts	Develop Reliable Cost-Effective Methods	1997
Visual Inspection	Develop Basis for Technique and Aids	1995
NDI Reliability	Determine System Reliability (POD) and Effect	1997

Information System Objectives

- Provide Timely Distribution of Safety Critical Information
- Assist Aviation Safety Inspectors in Identifying Problem Areas
- Provide Comprehensive Risk Assessment Decision Support Capability

Information System Research Tasks

Project	Tasks	Completion
Safety Performance Analysis System (SPAS)	Develop Automated Safety Information Collection System	1996
Safety Information Network	Demonstrate Integrated FAA / Industry Network	2000

Major Accomplishments

• Corrosion Control for Airplanes	September 1991
• Generation of Spectra and Stress Histories for Fatigue and Damage Tolerance Analysis of Fuselage Repairs	October 1991
• General Aviation Airplane Flight Loads Data Analysis and Collection Program	December 1991
• Current NDI Methods for Aging Aircraft	June 1992
• Inspection of Fabricated Fuselage Panels Using Electronic Shearography	July 1992
• Shearographic Inspection of a Boeing 737	July 1992
• Actuarial Trending / Component Reliability Study and Engine Case NDI Development for JT9D, CF6, and PT6 Turbine Aircraft Engines	August 1992

Major Accomplishments
(Continued)

• Damage Tolerance Assessment Handbook	October 1992
• Reliability Assessment at Airline Inspection Facilities, Volume I: *A Generic Protocol for Inspection Reliability Experiments*	March 1993
• Reliability Assessment at Airline Inspection Facilities, Volume II: *Protocol for an Eddy Current Inspection Reliability Experiment*	May 1993
• Emerging NDI Methods for Aging Aircraft	June 1993
• Reliability Assessment at Airline Inspection Facilities, Volume III: *Results of an Eddy Current Inspection Reliability Experiment*	November 1993
• Visual Inspection for Aircraft	December 1994

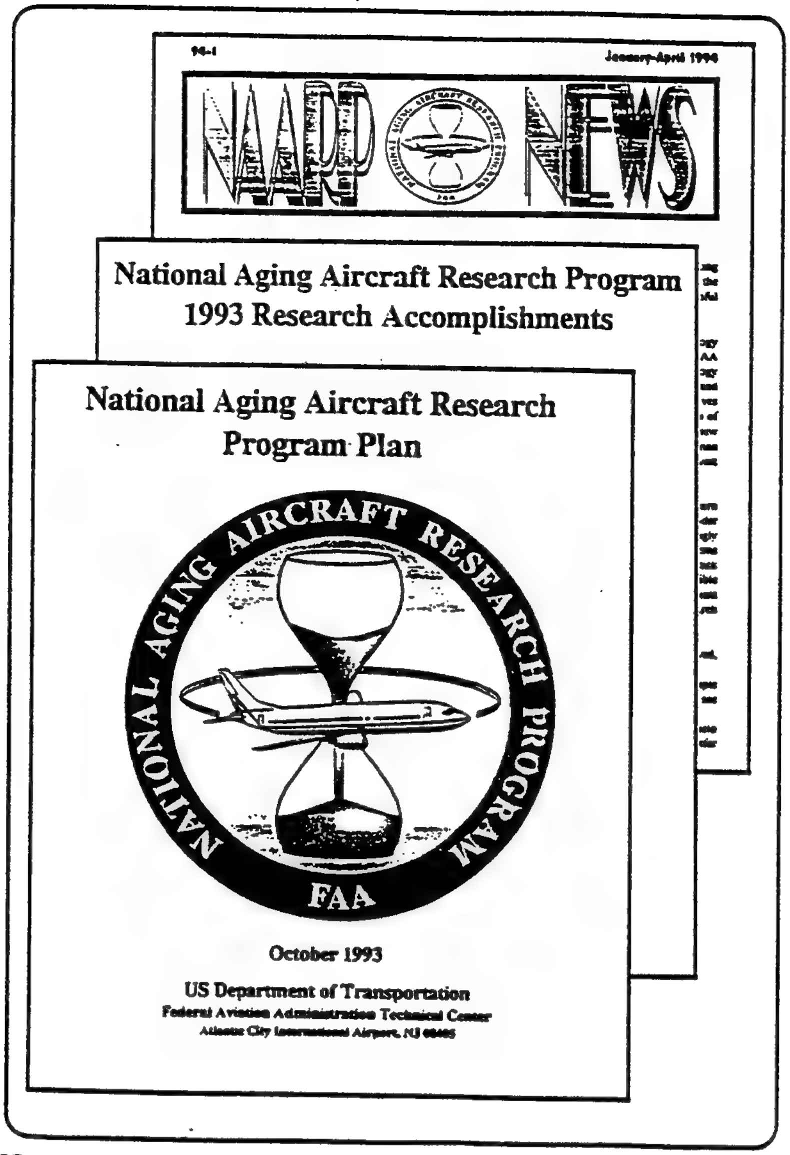

Dick Johnson
FAA Technical Center

Telephone: 609 485–4280

Fax: 609 485–4569

AIR FORCE LOGISTICS CENTER
PROGRAMS IN AGING AIRCRAFT

WR-ALC AGING AIRCRAFT
STRUCTURES & CORROSION PROGRAMS

WILLIAM R. ELLIOTT
WR-ALC/TIED
(912) 926-9835, DSN 468-9835
FAX (912) 926-1743

Like old age in people...
Old age in aircraft is accelerated by:

1) Increase in severe usage;
2) Increase in gross weight;
3) Improper or inadequate maintenance;
4) Inadequate protection systems; and,
5) Presence of widespread fatigue damage.

OVERVIEW

AIR FORCE LOGISTICS CENTER
PROGRAMS IN AGING AIRCRAFT

- ACTIVITIES
  - STRUCTURES
    - C-141
    - C-130
    - F-15
    - SOF
  - CORROSION
- ISSUES
- CONCERNS
- SUMMARY

ACTIVITIES
Structures

AIR FORCE LOGISTICS CENTER
PROGRAMS IN AGING AIRCRAFT

- C-141

	Man Hrs Per Repair	No Aircraft Affected	Total No Of Repairs	Total Man Hrs
•• WS 405 Chordwise Splice Repair	1500	244	488	732,000
•• Chordwise/Spanwise @ WS 405	2000	90	180	360,000
•• Center Wing Box Replacement	10,000	118	118	1,180,000
•• Coral Weep Repair				
••• Weep Hole Boron Patch Repair	100	133	500	50,000
••• Lower Wing Panel Replacement	2000	48	91	182,000
••• Ream/Coldwork Weep Hole	0.15	244	336,000	50,400
•• FS 998 MLG Hub Frame Replacement	1500	244	488	732,000
			TOTAL	3,286,400

ACTIVITIES
Structures

AIR FORCE LOGISTICS CENTER
PROGRAMS IN AGING AIRCRAFT

- C-130

	Man Hrs Per Repair	No Aircraft Affected	Total No Of Repairs	Total Man Hrs
•• Center Wing Box Replacement On Special Operations Aircraft	8000	52	52	416,000

- •• Outer and Center Wing Durability Test
  - ••• 5-Year Test at Lockheed Ontario (Now Complete)
  - ••• AMC C-130E Test Spectrum (Severity of 2.0)
  - ••• Center Wing Demonstrated 45,000 SFH; Outer Wing Demonstrated 3 Lifetimes
- •• 5-Year Fuselage Durability Test Planned To Begin FY96

ACTIVITIES
Structures

AIR FORCE LOGISTICS CENTER
PROGRAMS IN AGING AIRCRAFT

- F-15
  - Fatigue Test
    - A/B Proof of Design
    - A/B/C/D Economical Life
    - F-15E
  - Flight Profile Structural Impact
    - High AOA
    - High G
    - High Q
  - Honey Comb
  - Advanced Materials
  - Field Problems

ACTIVITIES
Structures

AIR FORCE LOGISTICS CENTER
PROGRAMS IN AGING AIRCRAFT

- Special Operations Forces
  - Heavyweight MH-53J Pave Low III
    - ☞ Modifications
    - ☞ Gross Weight Increase
    - Logistics Plan
    - ACE/OCM Program
  - HH/MH-60G Pave Hawk
    - ☞ Modifications To UH-60s
      - Converts 10 Existing UH-60s
      - Procures 93 Additional UH-60s
    - ☞ Gross Weight Increase And FWD CG Envelope Expansion
    - ASIP

ACTIVITIES
Corrosion

AIR FORCE LOGISTICS CENTER
PROGRAMS IN AGING AIRCRAFT

- Air Force Corrosion Program Office
  - ☞ Job 1: Prevent, Detect, And Control Corrosion & Minimize Impact Of Corrosion On Air Force Systems
  - Job 2: Extend Service Life Of Air Force Systems
  - Corrosion Costs Air Force $1+ Billion Annually
    - Aging Aircraft Are A Major Cost Driver
  - 90% Of Toxic & Hazardous Materials Result From Corrosion Prevention & Control Efforts
  - Responsibilities Include (Among Many Others):
    - Coordination of Corrosion Prevention Advisory Boards
    - Majcom Surveys

ACTIVITIES
Corrosion

AIR FORCE LOGISTICS CENTER
PROGRAMS IN AGING AIRCRAFT

- The Air Force Corrosion Program
  - Identified Detection Of Hidden Corrosion As A Technology Void
    - Number 1 Logistics Need Since 1992
    - Identified As WR-ALC Number 3 Priority In Early 1994
  - Never Funded
- Joint NASA And WR-ALC Hidden Corrosion Detection Initiative
  - NASA Demonstrated Thermal Wave Enhanced Thermography To WR-ALC - Nov 93
  - WR-ALC Purchased Hardware In Mar 94

ISSUES

AIR FORCE LOGISTICS CENTER
PROGRAMS IN AGING AIRCRAFT

- Technical Issues
  - Most Technical Issues Already Identified By FAA, NASA, & Air Force
    - ☞ Resolutions Needed
    - Joint Agency Agreements To Work On Technical Issues
  - Generally Long Term In Nature
    - ☞ Conflict With Schedules/Costs
  - No Coherent Air Force R&D For Aging Aircraft
    - APPN 3600 6.1, 6.2, & 6.3 Funds
    - APPN 3600 6.4 (Applied Development) Funds

ISSUES

AIR FORCE LOGISTICS CENTER
PROGRAMS IN AGING AIRCRAFT

- Organizational Issues
  - Warrants General Officer Steering
  - Requires Technical Advisory Oversight
  - No Specific Air Force Organizational Structure For Generic Aging Aircraft Issues
    - Coordination Across Program Office Disciplines
      - ☞ Corrosion ☞ NDI ☞ ABDR ☞ Advanced Composites
    - DoD Regulations Prevent COD Engineers At ALCs From Working Non-Operations Projects, i.e., Joint Agency Contracts

ISSUES

AIR FORCE LOGISTICS CENTER
PROGRAMS IN AGING AIRCRAFT

- Funding Issues
  - Long Term Issues Require More Than 1-Year Funds
    - ☛ ASIP Traditionally 1-Year Funded
  - Congressional Support of FAA Aging Aircraft R&D

Year	FAA Budgeted	Congressional Supplement	Total
FY91	$6.049M	$6.4M	$12.449M
FY92	$13.225M	$1.5M	$14.725M
FY93	$20.638M	$0M	$20.638M
FY94	$24.033M	$3.5M	$27.533M
FY95	$22.089M	-------	$22.089M

  - NASA Aging Aircraft R&D ☛ FY91-FY98: $45.8M
  - No Separate Air Force Funding For Aging Aircraft R&D Or Applied Development
    - HQ AFMC/EN's New Start Initiative - POM Submittal FY98

CONCERNS

AIR FORCE LOGISTICS CENTER
PROGRAMS IN AGING AIRCRAFT

- Extending Aircraft Service Life, Increasing Gross Weight, And/Or Flying Aircraft More Severely Exact A Toll On Aging.
- There Are Generic Aging Aircraft Issues Needing R&D Resolutions.
- Can A Fewer Number Of ALCs Continue To Do More Without More Funds To Address Aging Aircraft?

SUMMARY

AIR FORCE LOGISTICS CENTER
PROGRAMS IN AGING AIRCRAFT

- WR-ALC Is Very Active In Aging Aircraft Issues
  - All Our Aircraft Are In That Category
- Technical Issues Generally Identified
  - ☞ Resolutions Needed
- Air Force Should Fund Aging Aircraft R&D And Applied Development
- Funds Are Needed ASAP

ENGINE STRUCTURAL INTEGRITY PROGRAM (ENSIP)

RALPH GARCIA
SA-ALC/LADD
KELLY AFB, TX

OVERVIEW

HISTORICAL

ENSIP

- » MISSION USAGE
- » DAMAGE TOLERANCE
- » NDE

SUMMARY

HISTORICAL PERSPECTIVE

1946 - EARLY TURBINE ENGINES HAD 25 HOURS LIFE

1952 - UP TO 160 HOURS LIFE

PRE 1969 - ENGINE SPECIFICATIONS WERE DEFICIENT IN THE STRUCTURAL DURABILITY AREA

- LIFE REQUIREMENTS
- DUTY CYCLE
- ANALYSIS
- TESTING - NOT MISSION RELATED

HISTORICAL PERSPECTIVE (cont)

IMPROVED CRITERIA APPLIED IN 1969 TO F101 AND TF34 PROGRAM

1973 - SPECIFICATION UPDATED

1976 - SCIENTIFIC ADVISORY BOARD (SAB) REVIEW

1978 - ENSIP DEVELOPED

1979 - DADTA ON F100 ENGINE

1984 - ENSIP MIL-STD-1783 PUBLISHED

SAB ASSESSMENT

...WE NEED TO APPLY A SYSTEM OF DISCIPLINE TO OUR DEVELOPMENT PROCEDURES

...AIR FORCE SHOULD DEFINE AN AGGRESSIVE PROGRAM FOR ENGINE MECHANICAL AND STRUCTURAL INTEGRITY AND DURABILITY. .....THIS PROGRAM SHOULD BE REQUIRED BY REGULATION

...DURABILITY AND DAMAGE TOLERANCE ASSESSMENTS (DADTA) SHOULD BE PERFORMED ON FLEET ENGINES ANALOGOUS TO THOSE BEING PERFORMED ON SEVERAL WEAPON SYSTEM AIRFRAMES

ENSIP

WHAT IS IT?

IT IS AN ORGANIZED AND DISCIPLINED APPROACH TO THE STRUCTURAL DESIGN, ANALYSIS, QUALIFICATION,PRODUCTION, AND LIFE MANAGEMENT OF GAS TURBINE ENGINES

ENSIP

GOALS:

» ENSURE ENGINE STRUCTURAL SAFETY

» REDUCED LIFE CYCLE COSTS

» INCREASED SERVICE READINESS

TYPICAL FAILURE MODES

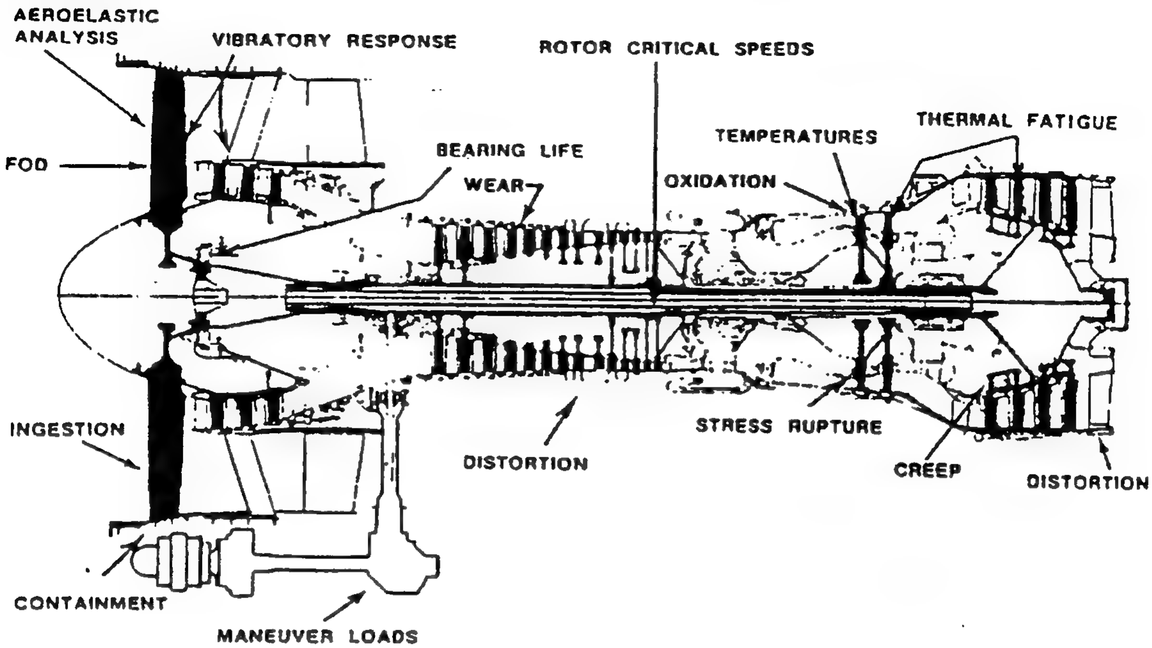

ENSIP

THE TWO BASIC CRITERIA FOR ENGINES ARE:

DURABILITY - ABILITY TO RESIST CRACKING, CORROSION, DETERIORATION, AND WEAR FOR A SPECIFIED TIME PERIOD

DAMAGE TOLERANCE - ABILITY TO RESIST FAILURE DUE TO THE PRESENCE OF FLAWS, CRACKS OR OTHER DAMAGE FOR A SPECIFIED TIME PERIOD

HOW IT'S DONE

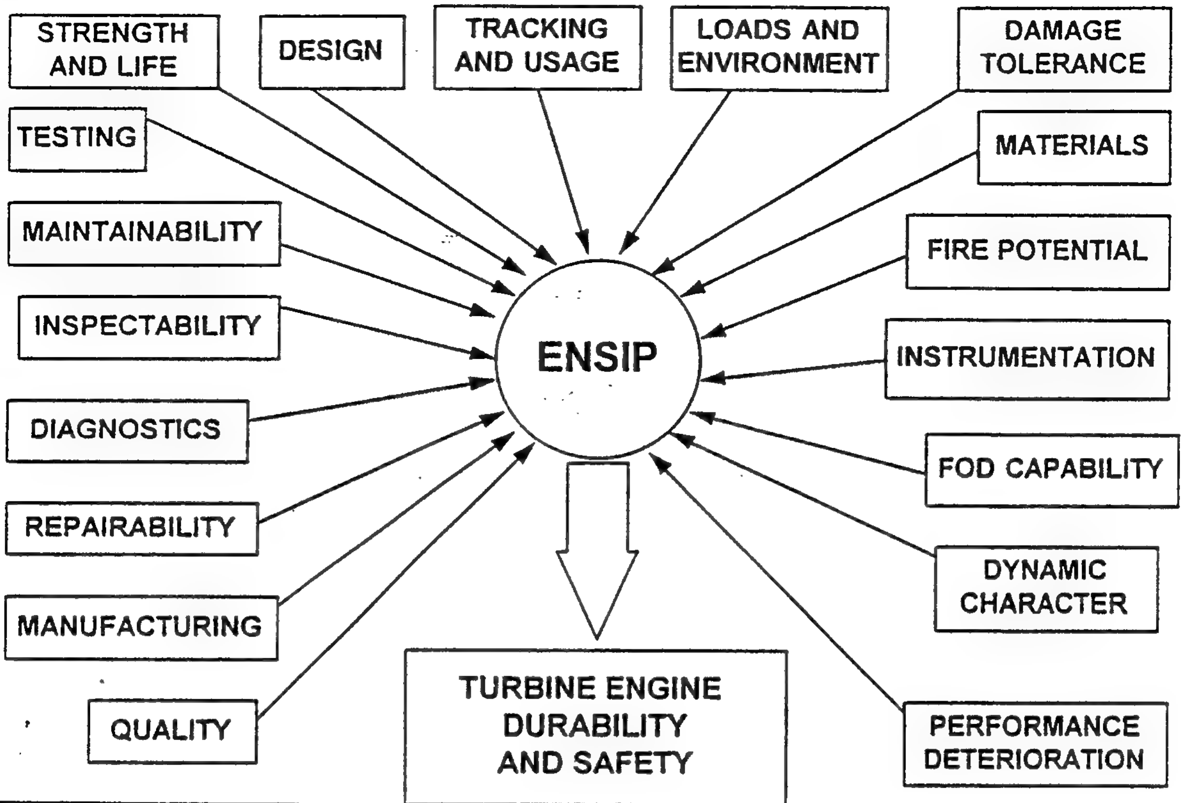

ENSIP TASKS

TASK I	TASK II	TASK III	TASK IV	TASK V
DESIGN INFORMATION	DESIGN ANAL. COMPNT. & MAT. CHARAC.	COMPONENT & CORE ENG. TESTING	GROUND & FLIGHT ENG. TESTS	PROD. QUAL. CONTROL & ENG. LIFE MGT.
• ENSIP MASTER PLAN • DESIGN SERV. LIFE & USAGE REQUIREMENTS • DESIGN CRITERIA	• DESIGN DUTY CYCLE • MAT'LS AND PROCESSES DESIGN DATA CHARACTERIZED • STRUCTURAL/ THERMAL ANALYSIS • MFG. AND QUALITY CONTROL	• STRENGTH TESTING • DAMAGE TOLERANCE TESTS • DURABILITY TESTS • THERMAL SURVEY • VIBRATORY STRAIN & FLUTTER BOUNDARY SURVEY	• ENVIR. VERIF. TESTING • (AMT) TEST SPEC. DERIV • DURABILITY TESTS (AMT) • DAMAGE TOL. TESTS • FLIGHT TEST STRAIN SURVEY • UPDATED DURA. & DAM. TOL. CONTROL PLAN • PERFRM. DETERIOR. STRUC. IMPACT ASSESSMENT • CRITCL. PART UPDATE	• PROD. ENG. ANALYSIS • STRUC. SAFETY & DURAB. SUM. • ENG. STRUC. MAINT. PLAN • INDIV. ENG. TRACKING • LEAD THE FORCE PROG. (USAGE) • DURA. & DAM. TOL. CONTROL PLAN IMPL. • TECHNICAL ORDER UPDATE

MISSION USAGE

DEFINES DUTY CYCLE

» DESCRIPTION OF ENGINE USAGE IN THE AIRCRAFT

DEFINES ACCELERATED MISSION TEST (AMT)

» REALISTIC DURABILITY TEST OF ENGINE

» RETAINS DAMAGING CYCLES AND HOT TIME

THROTTLE TRANSIENTS DRIVE MECHANICAL AND THERMAL STRESSES

» CHANGES IN RPM, TEMPERATURE GRADIENTS

MISSION USAGE
(cont)

TYPICAL MISSION

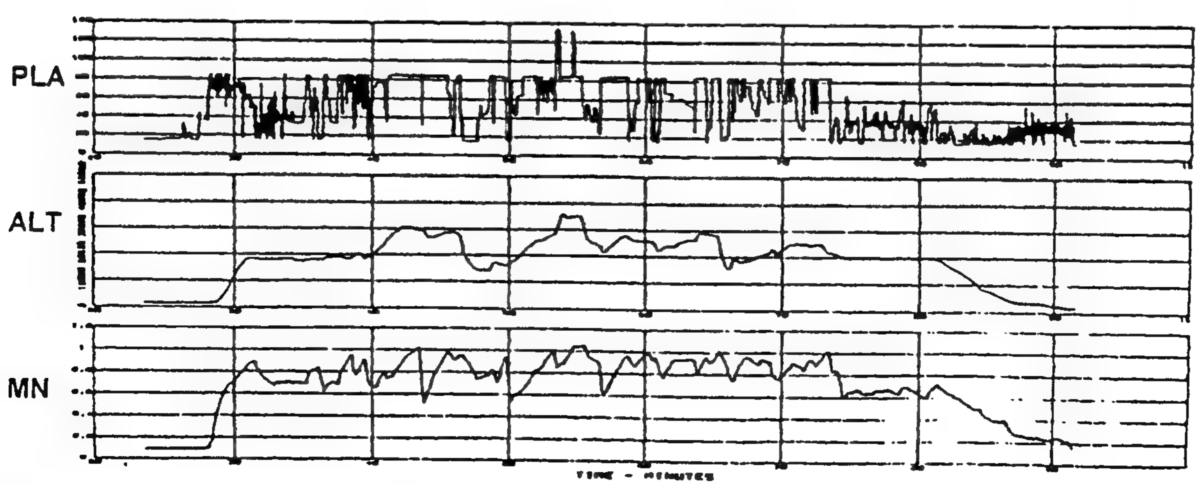

MISSION USAGE
(cont)

USED TO DETERMINE STRESSES

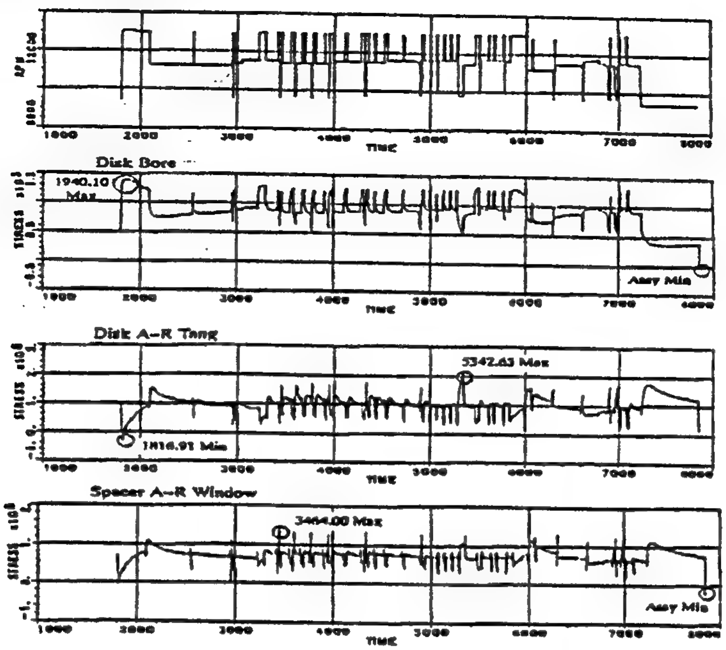

MISSION USAGE
(cont)

LARGE STRESS VARIATION OVER SMALL TIME PERIOD

Spacer A—R Window

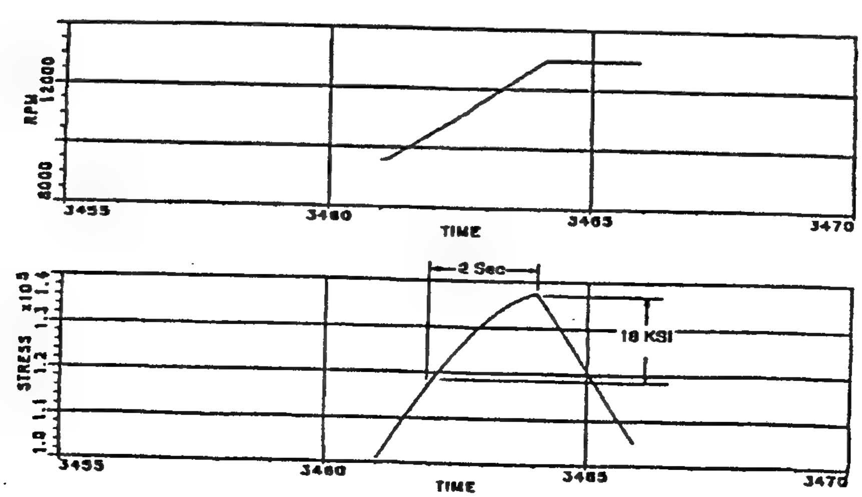

DAMAGE TOLERANCE

USED FOR FRACTURE CRITICAL COMPONENTS

» FAILURE OF COMPONENT CAN RESULT IN LOSS OF AIRCRAFT

» e.g., FAN DISK, TURBINE BLADE IN A SINGLE ENGINE AIRCRAFT

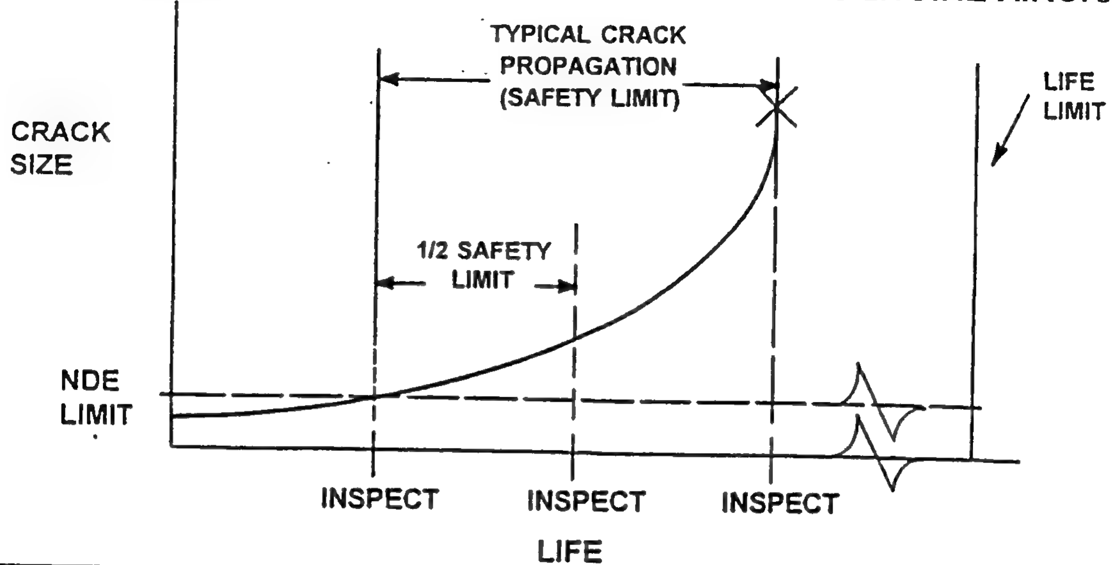

BENEFITS OF DAMAGE TOLERANCE

PRIMARY

» ENHANCED SAFETY

» OPTIONAL LIFE EXTENSION

» INCREASED READINESS

» LOWER OWNERSHIP COSTS

SECONDARY

» DRIVES NDE CAPABILITY IMPROVEMENTS

» DRIVES MATERIAL DAMAGE TOLERANCE IMPROVEMENTS

» REQUIRES INTEGRATED DESIGN (MFG, NDI, DESIGNERS, etc)

» ENHANCED PART QUALITY

BOTTOM LINE:

» DEFINES INTELLIGENT/COST EFFECTIVE WAY TO INSPECT

DAMAGE TOLERANCE EXPERIENCE

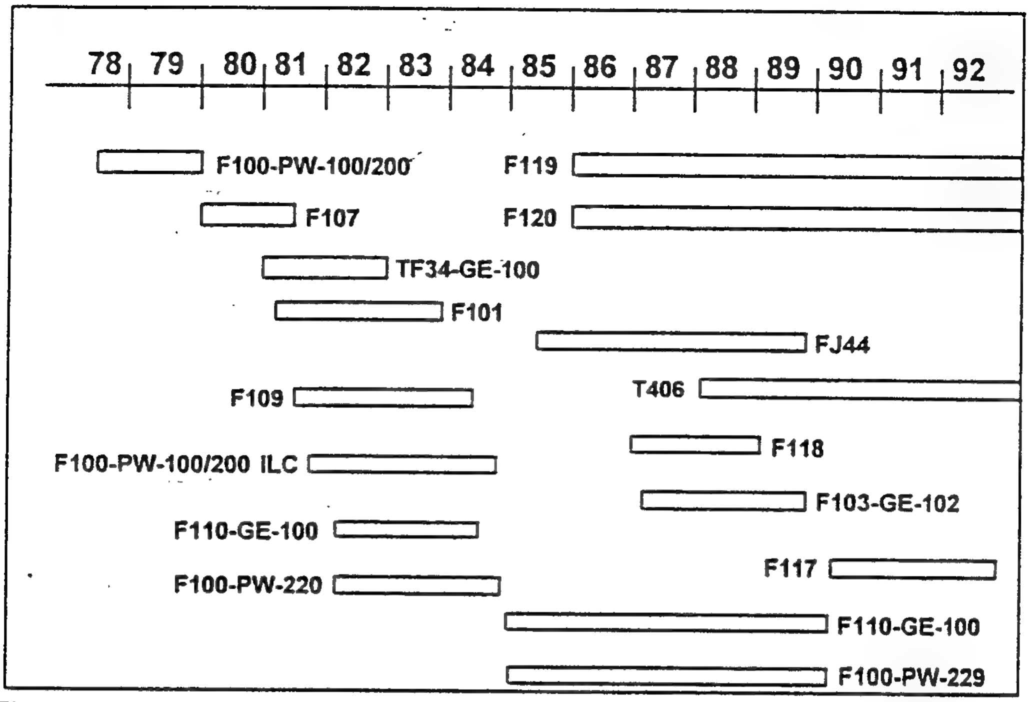

LOWER OWNERSHIP COSTS EXAMPLE

ENSIP DESIGNED F100-PW-220 VS F100-PW-100

COSTS

INCREASE - $7,600/ENGINE

MATERIAL

MAT'L CHARACTERIZATION

INCREASED ANALYSIS

MACHINING

INSPECTION

DECREASE - $320,000/ENGINE

REDUCED MAINTENANCE

PARTS SAVINGS

ELIMINATE SHOP VISIT

SAVINGS = 40

WEIGHT INCREASE < 1%

OPTIONAL LIFE EXTENSION

RETIREMENT FOR CAUSE (RFC)

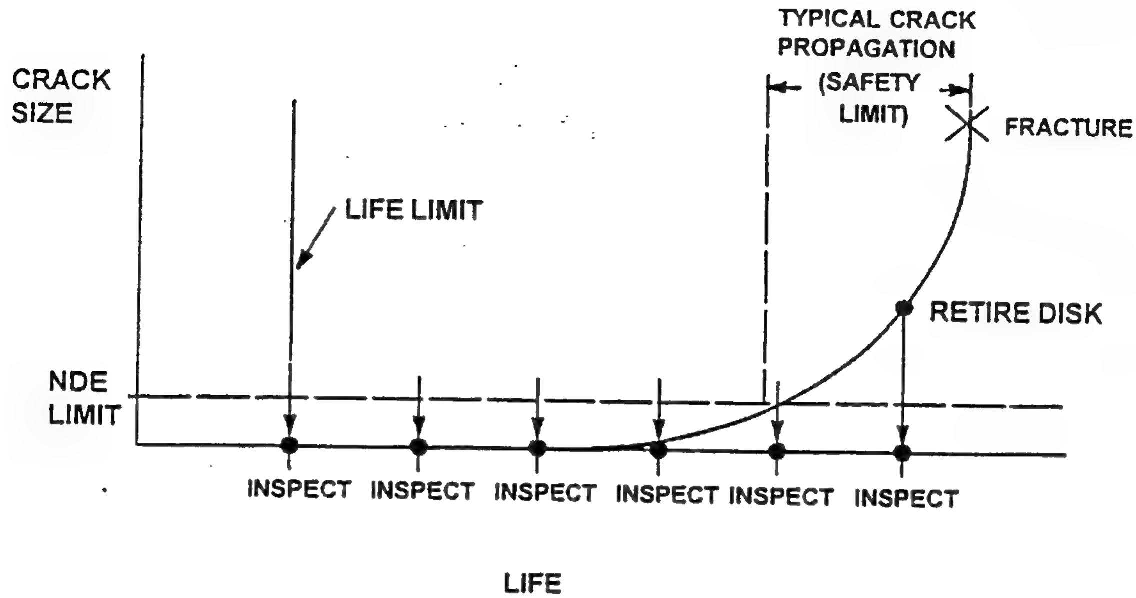

NDI CAPABILITY ENHANCEMENTS

EDDY CURRENT INSPECTION CAPABILITY IMPROVEMENT

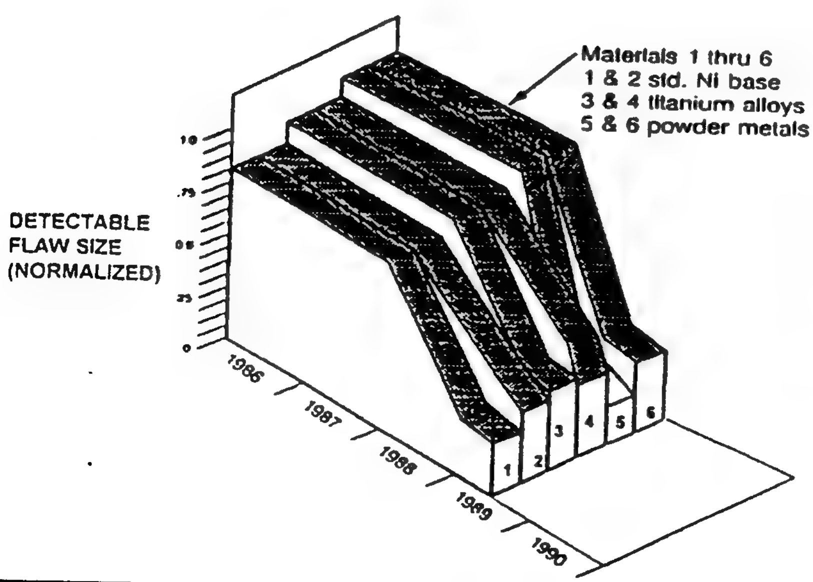

EDDY CURRENT INSPECTION CAPABILITY

PROBABILITY OF DETECTION FOR BOLTHOLES

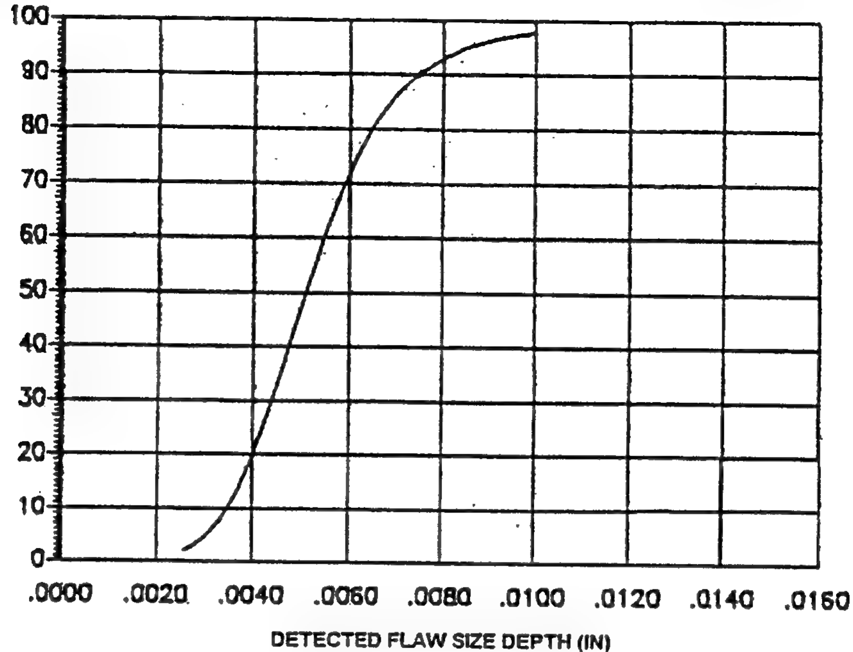

ENSIP

IN SUMMARY

ENSIP HAS BEEN APPLIED ON USAF ENGINES SINCE 1978

IT IS A TOTAL ENGINE STRUCTURAL PROGRAM

- REQUIREMENTS
- TESTS AND ANALYSIS
- LIFE MANAGEMENT

HAS PROVEN IT'S VALUE WITH INCREASES IN

- SAFETY
- RELIABILITY
- LIFE CYCLE SAVINGS

OC-ALC AGING AIRCRAFT DISASSEMBLY AND HIDDEN CORROSION DETECTION PROGRAM

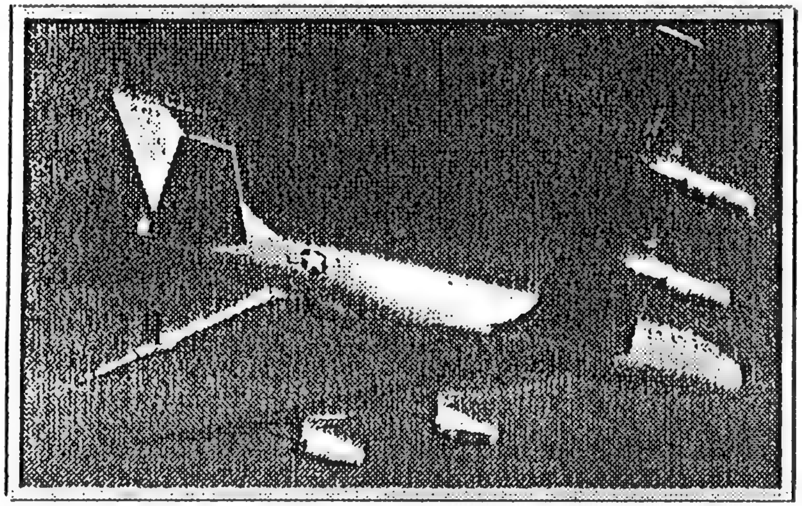

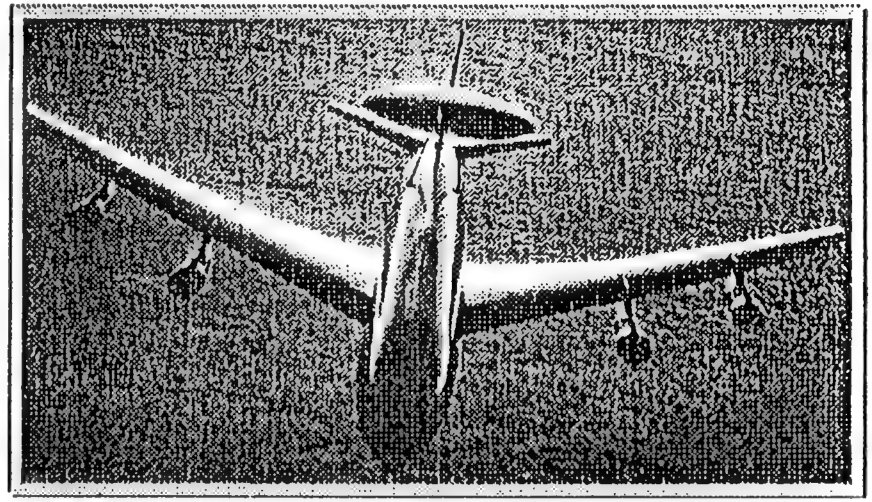

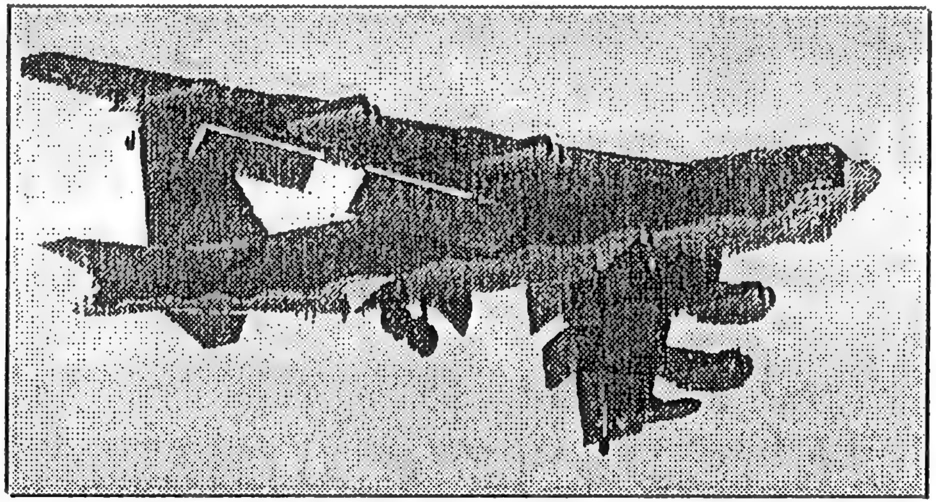

Donald E. Nieser, P.E
OC-ALC/LACRA
Tinker AFB, OK 73145
DSN 336-3832 - (405)736-3832

PURPOSE

- EXPLAIN THE C/KC-135 AGING AIRCRAFT DISASSEMBLY AND HIDDEN CORROSION DETECTION PROGRAM AND SHOW WHY CONTINUED USAF ENGINEERING INVESTMENT IS IMPERATIVE
- TO SHOW THAT THE "IMPROVED REFUELING SYSTEMS", NDI PROGRAM OFFICE AND SUSTAINING ENGINEERING FUNDING SOURCES ARE PROVIDING THE ONLY FOCUSED PROACTIVE AND INTEGRATED RESPONSE TO C/KC-135 AGING AIRCRAFT CORROSION PROBLEMS
- SHOW THAT FAILURE COMPREHEND AND ADDRESS THE ISSUES ASSOCIATED WITH FLYING THE C/KC-135 NEARLY 80 YEARS SUBJECTS DOD AIR REFUELING AND SPECIAL MISSIONS TO INCREASED RISKS, COST AND REDUCED AVAILABILITY

BACKGROUND

- UP TO NOW AIRCRAFT CORROSION HAS ONLY BEEN AN ECONOMIC PROBLEM FOR THE USAF
  - USAF SPENDS ~ $800 MILLION/YEAR
  - USAF SPENDS ~ $100 MILLION/YEAR ON C/KC-135 CORROSION
- CORROSION INDUCED MATERIAL DEGRADATION IS INCIDEOUS AND TIME DEPENDENT
- THE OCCURRENCES OF C/KC-135 ARE ON THE INCREASE
- EFFECTS OF CORROSION ON STRUCTURAL INTEGRITY NOT FULLY UNDERSTOOD

BACKGROUND

- CORROSION IS AN ECONOMIC AND SAFETY CONCERN FOR AIRLINES
- FAR EASTERN AIR B-737 EXPERIENCED EXPLOSIVE DECOMPRESSION AND FATAL IN-FLIGHT BREAKUP (AUG 81) DUE TO EXTENSIVE CORROSION DAMAGE
- ALOHA B-737 HAD SEVERE CORROSION BETWEEN FUSELAGE LAP JOINTS, TEAR STRAPS AND ADHESIVE BONDING (APR 88)
  - CORROSION INDUCED MATERIAL DEGRADATION CAUSED PREMATURE WIDE SPREAD FATIGUE CRACKING
  - CONCENTRATION ON MULTI-SITE FATIGUE DAMAGE (MSD) HAS DIVERTED ATTENTION FROM CORROSION

COMMERCIAL FLEET PROGRAM

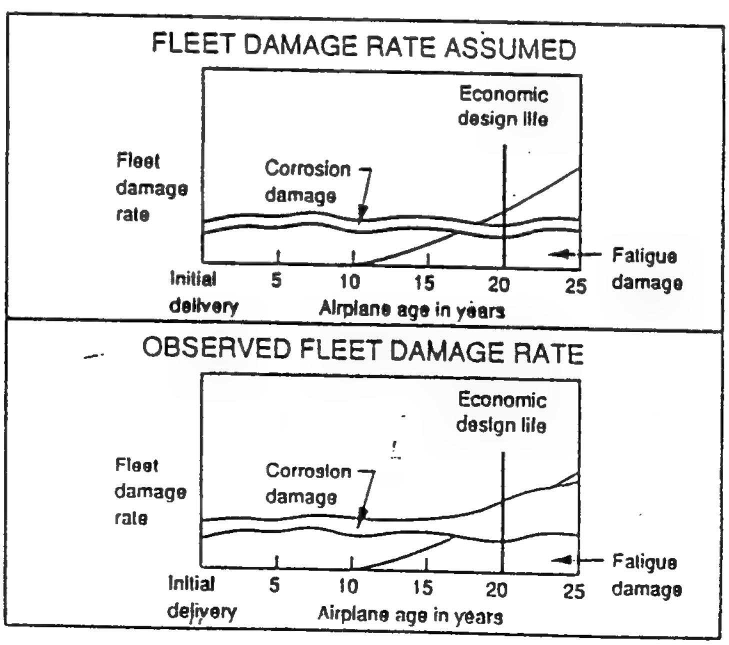

BOEING

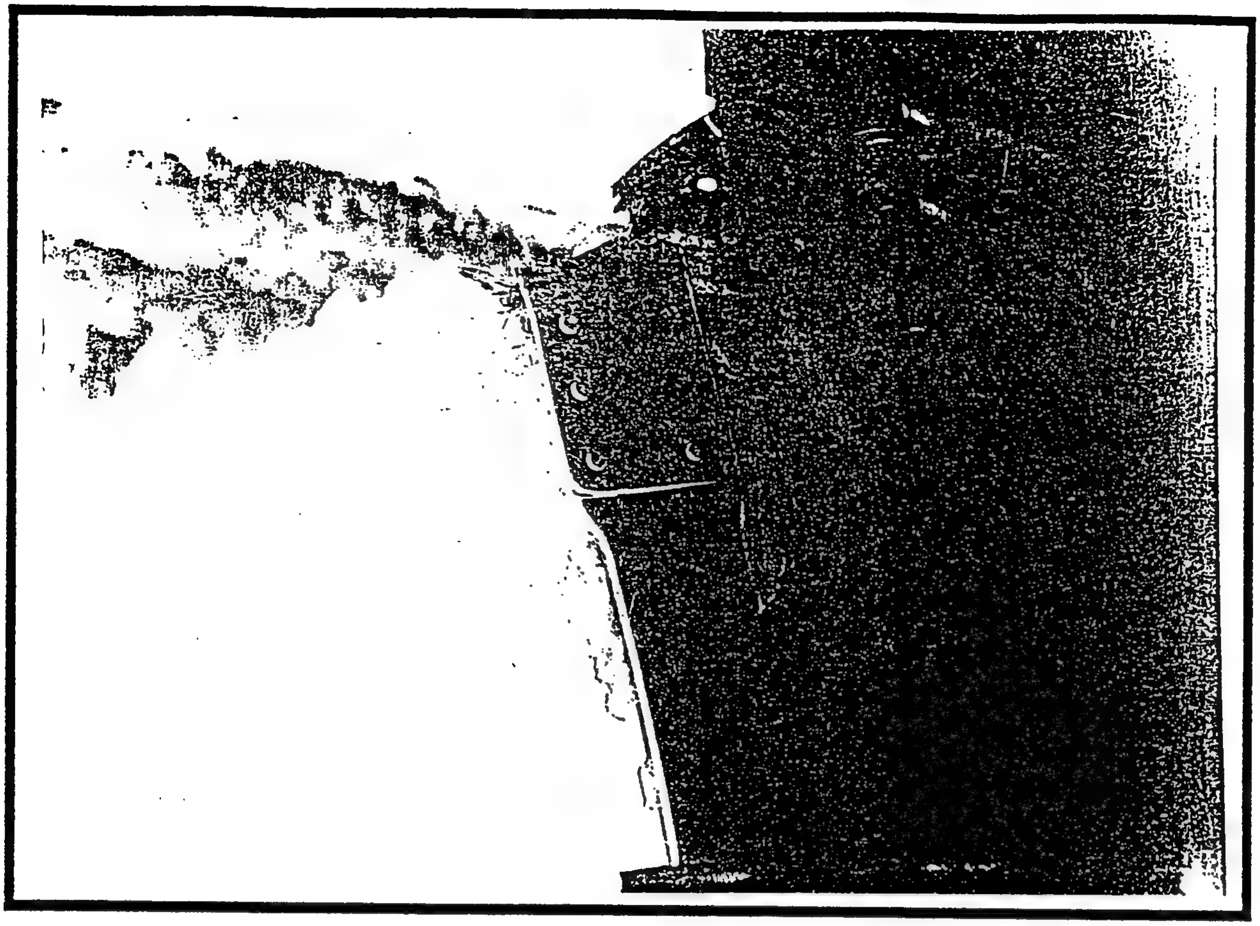

CHALLENGE

- PROJECTED DOD BUDGET REDUCTIONS FORCE LIFE EXTENSION OF EXISTING AIRCRAFT
  - 60 TO 80 YEARS
- AIRCRAFT DESIGNED FOR FINITE LIFE
  - DID NOT CONSIDER EFFECTS OF CORROSION
- NEW SET OF TECHNICAL PROBLEMS (AGING AIRCRAFT)
  - WIDE SPREAD CORROSION DAMAGE
  - WIDE SPREAD FATIGUE DAMAGE; MULTI-SITE DAMAGE
  - MATERIAL LOSS DUE TO CORROSION
  - INTERGRANULAR CORROSION ATTACK
  - EMBRITTLEMENT, FRETTING

OC-ALC CHALLENGES

- NO FUNDS FOR REPLACEMENT AIRCRAFT
  - C/KC-135 MUST OPERATE TO 2040
  - B-52 MUST OPERATE TO 2030
  - E-3 E-3 INDEFINITE
- CORROSION INCREASES AS AIRCRAFT AGE
- DEGRADATION OF STRUCTURAL INTEGRITY UNKNOWN OR UNQUANTIFIED AT CURRENT STATE-OF-THE-ART

C/KC-135 MISSION NEED

- CORROSION PROBLEMS AND COMBINED EFFECTS OF CORROSION AND FATIGUE MUST BE SOLVED TO MAINTAIN AIRWORTHINESS TO 2040
  - AS AIRCRAFT AGE CORROSION PROBLEMS WILL BECOME MORE SIGNIFICANT CAUSING SUBSEQUENT INCREASES IN MAINTAIN EXPENDITURES AND DOWN TIME
  - INCREASED RISKS OF AIRCRAFT LOSSES DUE TO CORROSION INDUCED STRUCTURAL FAILURES
- BEST ENGINEERING JUDGEMENT IS THAT UNLESS CORROSION IS FOUND FIXED AND/OR ELIMINATED, CORROSION WILL REDUCE STRUCTURAL LIFE TO LESS THAN 2040
- THEREFORE A PROTECTIVE PLAN WAS IMPLEMENTED TO ADDRESS CORROSION ISSUES BEFORE ANY AIRCRAFT ARE LOST DUE TO CORROSION INDUCED CATASTROPHIC STRUCTURAL FAILURES

LAP JOINT

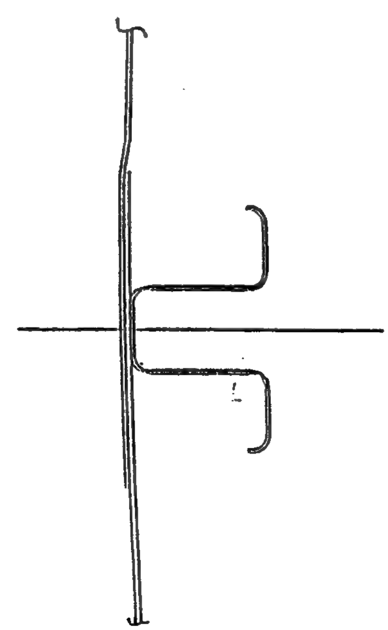

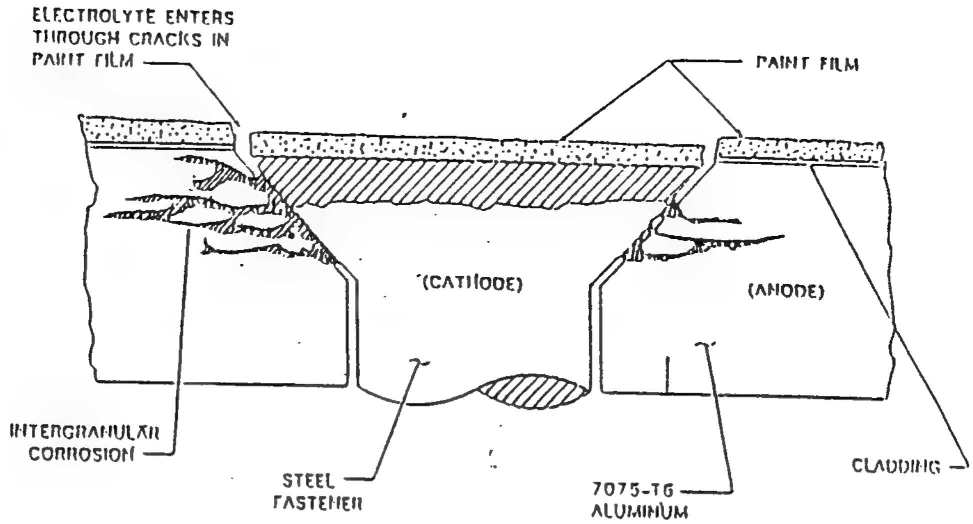

Intergranular Corrosion of 7075-T6 Aluminum Adjacent to Steel Fastener

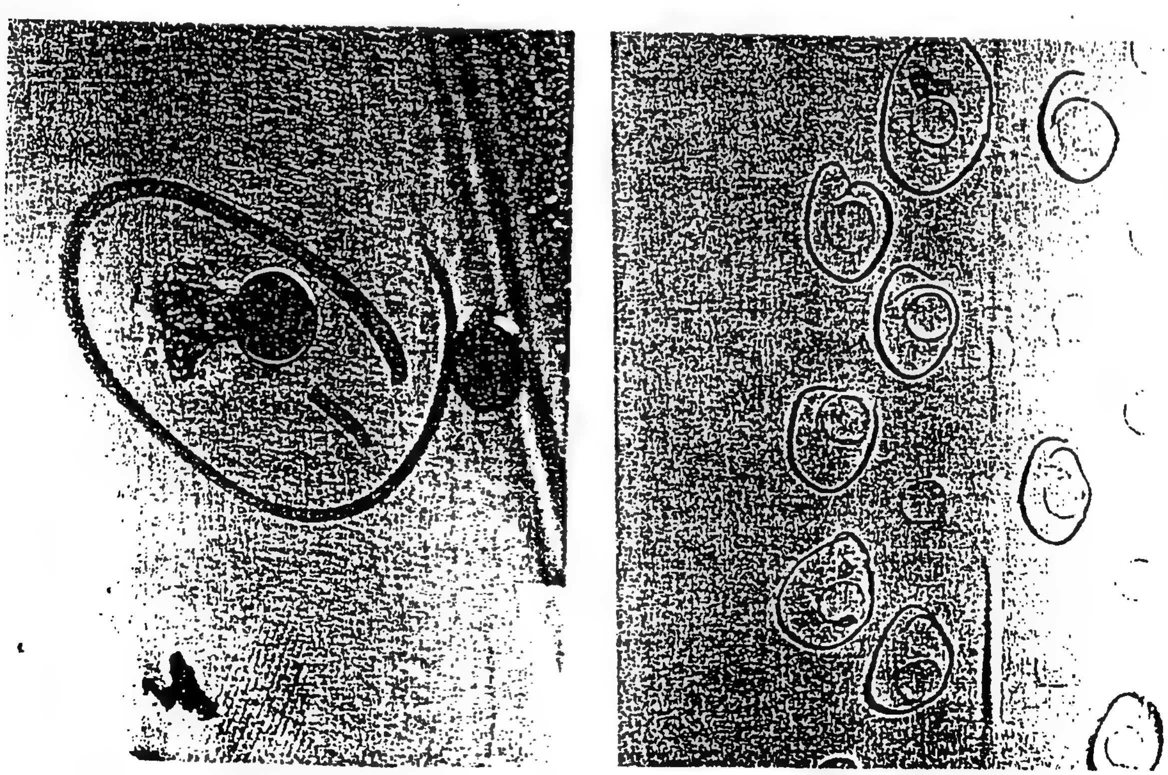

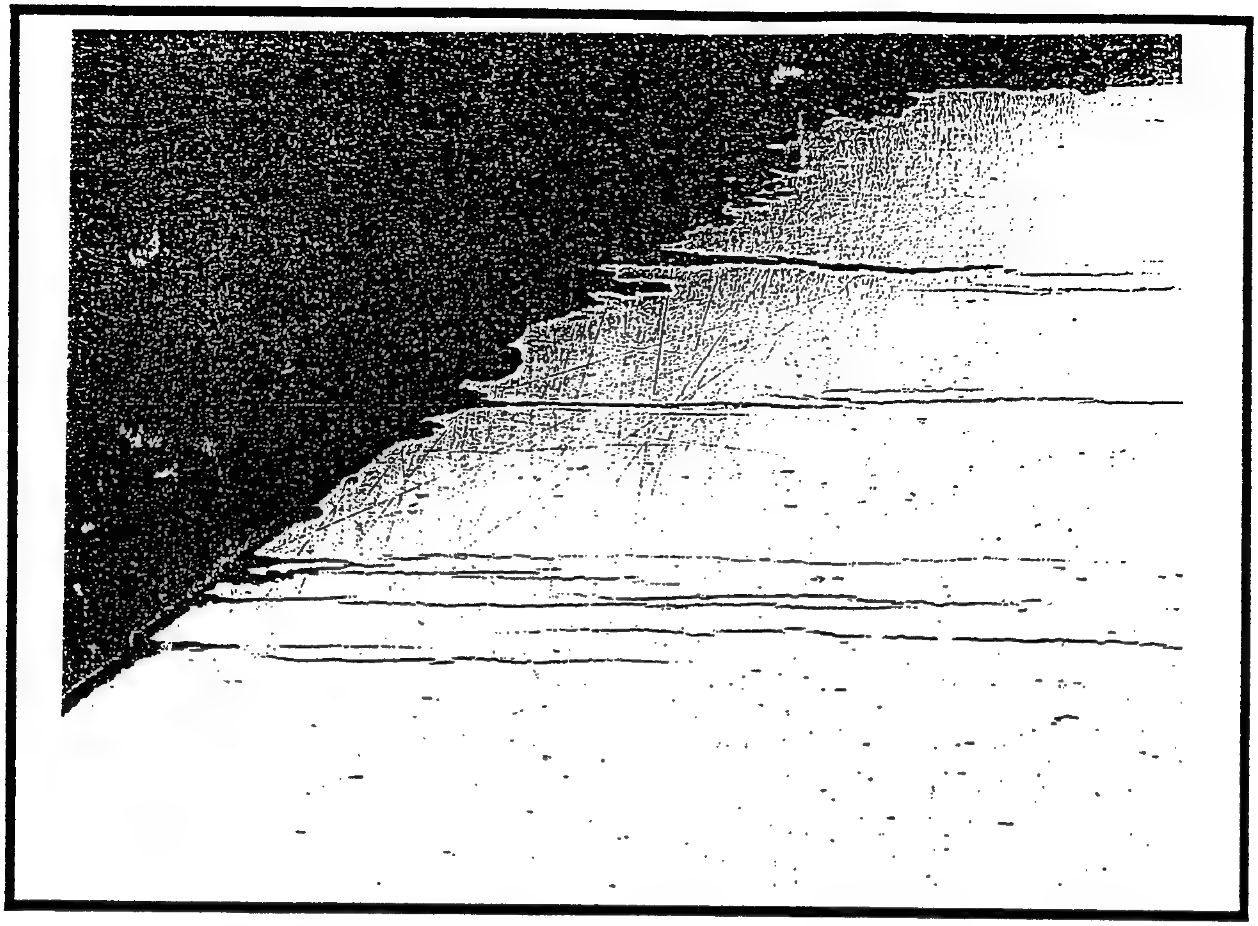

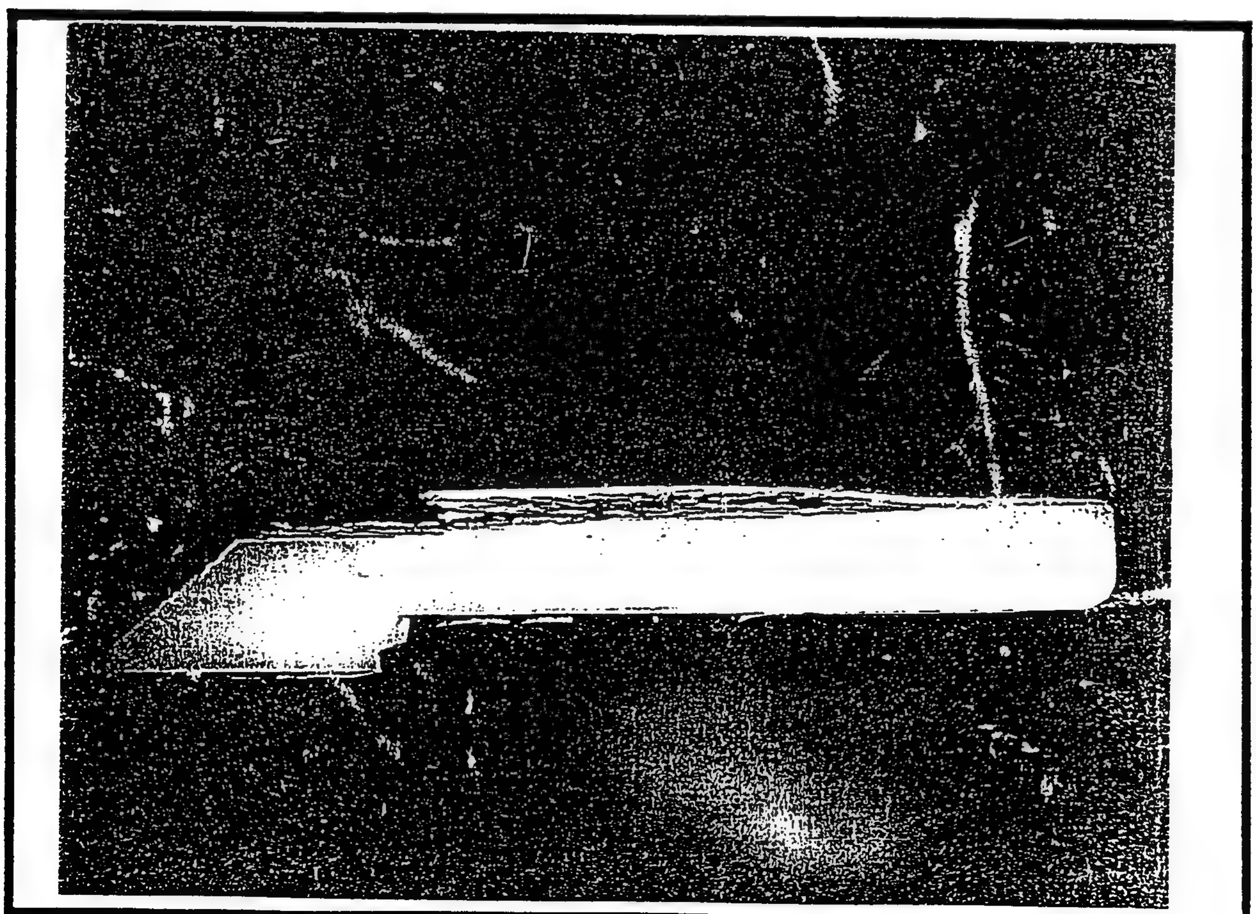

PROGRAM PLAN

- REVIEW EXISTING AGING AIRCRAFT CORROSION AND FATIGUE INFORMATION
- IDENTIFY PROGRAM ELEMENTS THAT NEED TO BE ADDRESSED
- FIND AND FUND AUTHORITIES/EXPERTS FOR EACH ELEMENT
- INTEGRATE OUTPUT DATA FROM EACH ELEMENT
- ESTIMATE FATIGUE/ECONOMIC LIFE OF C/KC-135 AIRCRAFT WITH EFFECTS OF CORROSION INCLUDED
- DEVELOP PLANS AND IDENTIFY MODIFICATIONS/MAINTENANCE TO ENSURE CONTINUED AIRWORTHINESS TO THE YEAR 2040

MAJOR PROGRAM ELEMENTS

- AIRCRAFT DISASSEMBLY/CORROSION/DOCUMENTATION
- NDI/NDT DEVELOPMENT/IMPLEMENTATION
- CORROSION DOCUMENTATION/DATA BASE DEVELOPMENT
- CORROSION/STRUCTURAL INTEGRITY TESTING
- CORROSION QUANTIFICATION TESTING AND ANALYSIS
- CORROSION PREDICTION MODELING
- CORROSION GROWTH RATE TESTING
- C/KC-135 SERVICE LIFE PREDICTION AND EXTENSION PLAN

OC-ALC AGING AIRCRAFT PROGRAM

PROGRAM ELEMENT SUMMARY

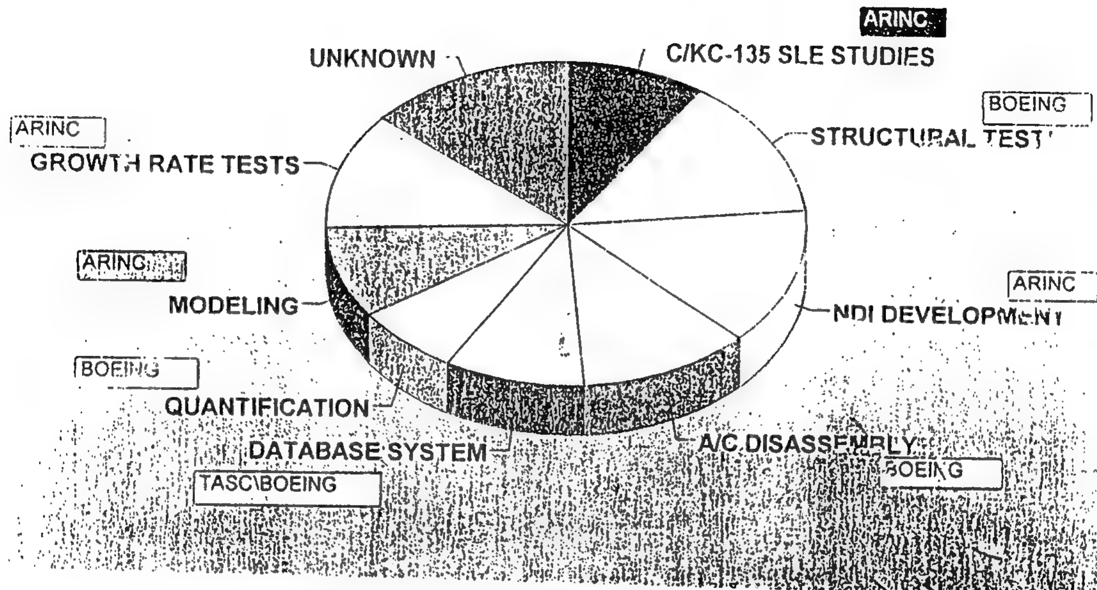

SCHEDULE

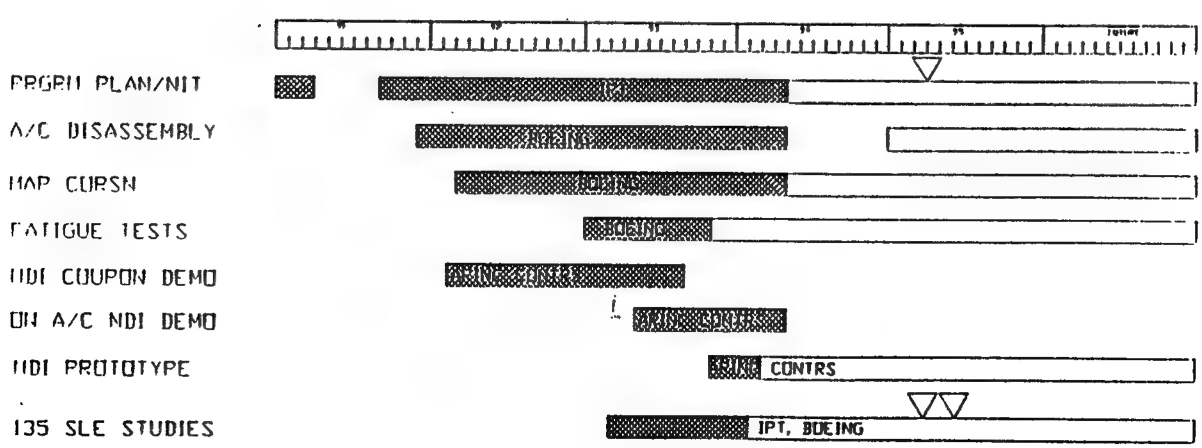

OUR TEAM

- C/KC-135 ENGINEERING - PROGRAM MANAGEMENT

  - B-52, E-3, B-1 JOINT EFFORT NDI STUDIES

  - TIE - TECHNOLOGY & INDUSTRIAL SUPPORT

- AFMC AND ASC TANKER PROGRAMS - FUNDING
- WRIGHT LABS, ASC, NAVY, FAA, NASA - TECHNICAL CONSULTANTS
- AMARC - AIRCRAFT CUTTING/SECTION REMOVAL
- BOEING WICHITA - DISASSEMBLY/ANALYSIS
- ARINC CORP - NDI-NDT TESTING/ANALYSIS
- METRO TECH - NDI DEMOS FACILITIES

AIRCRAFT DISASSEMBLY/CORROSION/FATIGUE DOCUMENTATION/MAPPING

- IDENTIFIED AND CUT FIRST C/KC-135 (EC-135H 61-0291) RETIRED INTO 300 SECTIONS ALSO SECTIONS FROM B-52 AND B-707 AIRCRAFT
- APPROXIMATELY 200 SECTIONS INVASIVELY DISASSEMBLED AND CORROSION DOCUMENTED
- LIGHT TO MODERATE CORROSION IN MANY HIDDEN AND INACCESSIBLE AREAS
- SEVERE CORROSION BETWEEN STEEL MAIN LANDING GEAR TRUNNION AND TOP SURFACE OF BOTTOM WING SKIN (REPLACED 1978 ECP405)
- SEVERE CORROSION BETWEEN WING SKIN AND SPAR CAPS

CORROSION DETECTION NDI OBJECTIVES

- LOCATE COMMERCIAL OFF-THE-SHELF NDI EQUIPMENT
  - STATE-OF-THE-ART
  - WIDE AREA RAPID SCAN AND PRECISION/FINITE
- SATISFY IMMEDIATE CRITICAL CORROSION DETECTION NEEDS
  - LAP SEAM/DOUBLERS
  - WING SKIN FASTENER AREAS
- PROTOTYPE SELECTED EQUIPMENT FOR DEPOT IMPLEMENTATION
  - C/KC-135/B-52/E-3

CORROSION NDI DEVELOPMENT MILESTONES

- INDUSTRY SURVEY (JUNE 92)
- EQUIPMENT/VENDOR DEMONSTRATION ON AIRCRAFT SAMPLE COUPONS (SEPT 92)
  - INVASIVE DISASSEMBLY OF COUPONS (JAN 93)
  - QUANTIFICATION OF ACTUAL CORROSION (FEB 93)
  - COMPARATIVE ANALYSIS OF VENDOR RESULTS VS ACTUAL CORROSION (MAR 93)
- ON-AIRCRAFT DEMONSTRATION OF NDI EQUIPMENT IN OVERHAUL ENVIRONMENT (JUNE 93)
- SELECTION OF PROTOTYPE CORROSION NDI EQUIPMENT (FY 94)

CORROSION QUANTIFICATION BY WRIGHT LABS

- TOPOGRAPHIC RADIOSCOPY (TR)
- RADIOGRAPHED EACH CORRODED SURFACE
- PERFORMED A DENSITY SCAN OF RADIOGRAPHIC IMAGES
- CREATED COMPUTER ENHANCED COLOR IMAGE OF DENSITY VARIATIONS
- OVERLAY TWO SHEETS REPRESENT CORROSION BETWEEN LAYERS

COUPON DEMONSTRATION REVIEW

- Held at Metro-Tech Aviation Career Center, Oklahoma City, Oklahoma Jun-Sept. 92.
  - Twelve Test Coupons
    - Six lap joint/six wing panel
    - Two baseline coupons per problem set
  - Boeing 727 Lap Joint
- Participation
  - Vendors Involved: 32
  - Vendors Participating & Providing Data: 15
  - Non-Vendor Representatives
- Technologies Represented: Eddy Current, Ultrasonics, Radiography, Thermal Image, D-Sight, Shearography, and Acoustic Emission

COUPON 39
EDDY CURRENT RESULTS

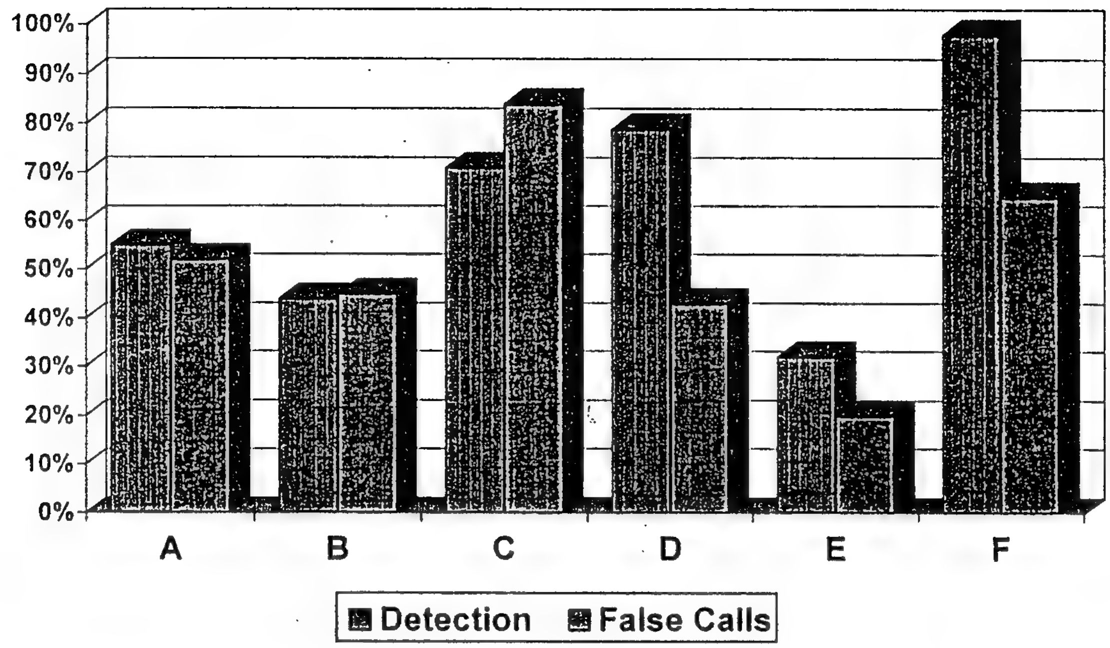

ON-AIRCRAFT DEMONSTRATION REVIEW

- Held at OC-ALC May 10 to May 26, 1993
- On Aircraft #2671
  - Four Vendors Inspected Lap Joints Using The Following NDI Technologies:
    - Eddy Current
    - Enhanced Visual
    - Thermal Imaging
  - Seven Vendors Inspected Wing Skin Fastener Countersinks Using The Following NDI Technologies:
    - Eddy Current
    - Ultrasonic
    - Magneto Optic
    - Enhanced Visual
    - Thermal Imaging

AREA 1 VENDOR IMAGE COMPARISON

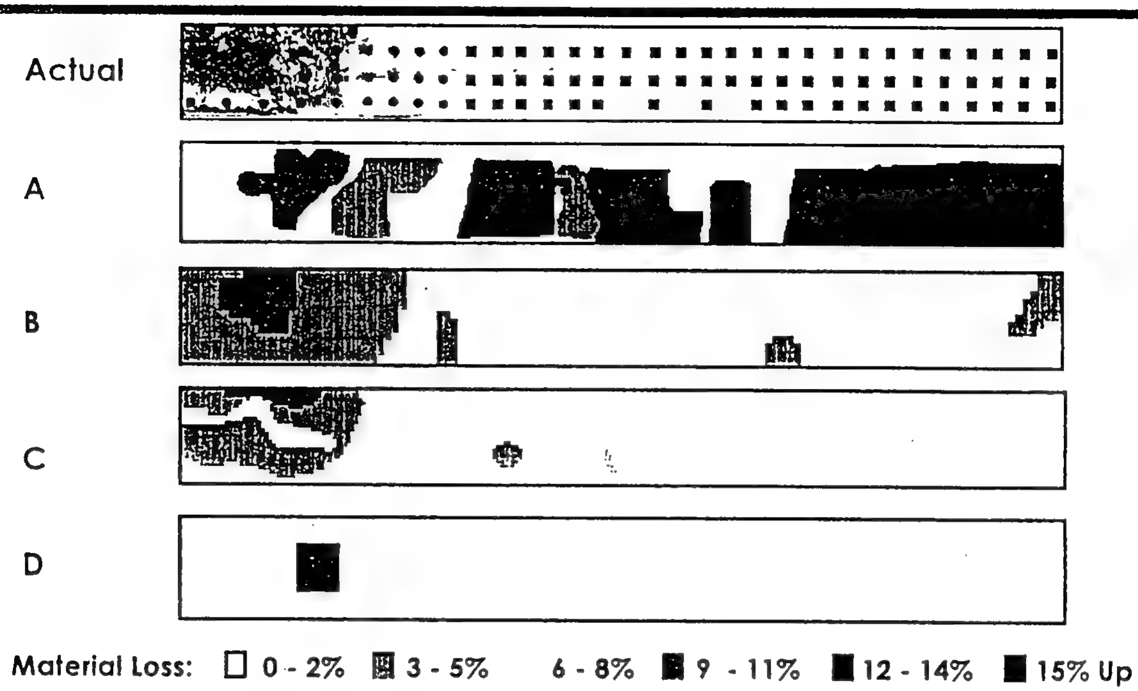

FASTENER COUNTERSINK INSPECTION AREA

- Selected area on KC-135 upper wing containing 95 fasteners
- Criteria for selection:
  - Variety of fastener sizes and thicknesses
  - Know corrosion problem areas

FASTENER COUNTERSINK RESULTS

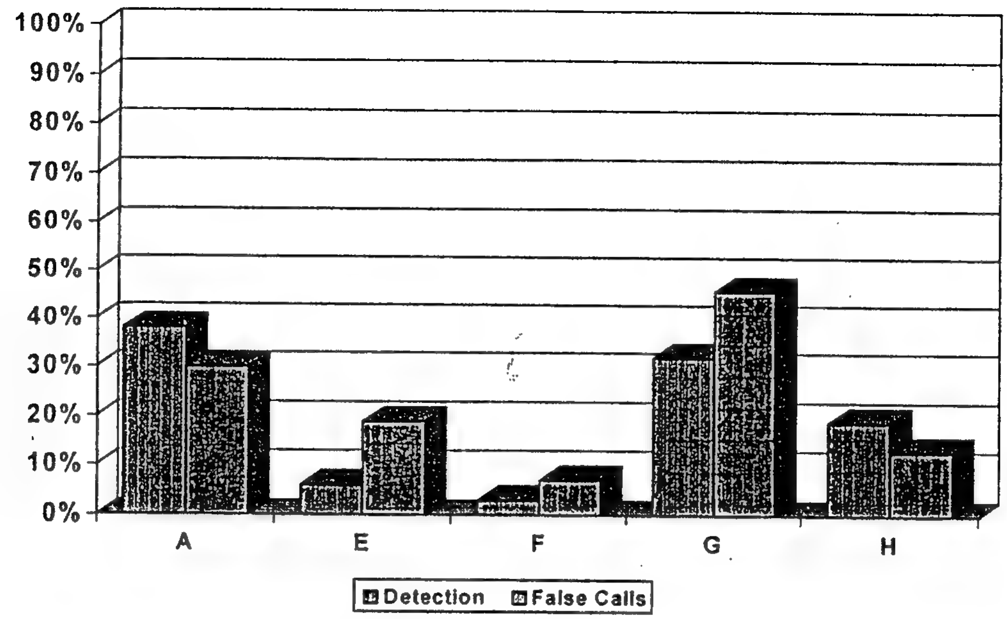

STRUCTURAL INTEGRITY TESTING

- ASSESS EFFECTS OF CORROSION ON STRUCTURAL INTEGRITY
- SPECIMENS FROM 30+ YEAR OLD C/KC-135 AIRCRAFT WITH AND WITHOUT POSSIBLE CORROSION AND LAB GROWN SEVERE CORROSION
  - FUSELAGE LAP JOINTS (2024-T3,-T4 AND 7075-T6)
  - UPPER WING SKINS (7178-T6)
- STRESS VS CYCLES TO FAILURE FATIGUE TESTS
- CRACK PROPAGATION FATIGUE TESTS
- RESIDUAL STRENGTH FATIGUE TESTS

STRUCTURAL INTEGRITY TESTING (CONT.)

- FRACTOGRAPHIC ANALYSIS AND CORROSION QUANTIFICATION AFTER TESTING AND INVASIVE DISASSEMBLY
- LAB-TO-LAB STANDARD AND PRELIMINARY TESTS COMPLETED
- TESTING FY 94 - FY 95

STRUCTURAL INTEGRITY TESTING

<u>ROUND ROBBIN TEST LABS</u>

- BOEING - WICHITA KANSAS
- ALCOA RESEARCH CENTER PENNSYLVANIA
- NAVAL AIR WARFARE CENTER (NAWC) PENNSYLVANIA
- WRIGHT LABS (WL/FIBE) WRIGHT PATTERSON AFB OHIO
- UNIVERSITY OF UTAH
- OC-ALC/TIE TINKER AFB OKLAHOMA

CORROSION AND AGING AIRCRAFT

ROUND ROBIN TESTING

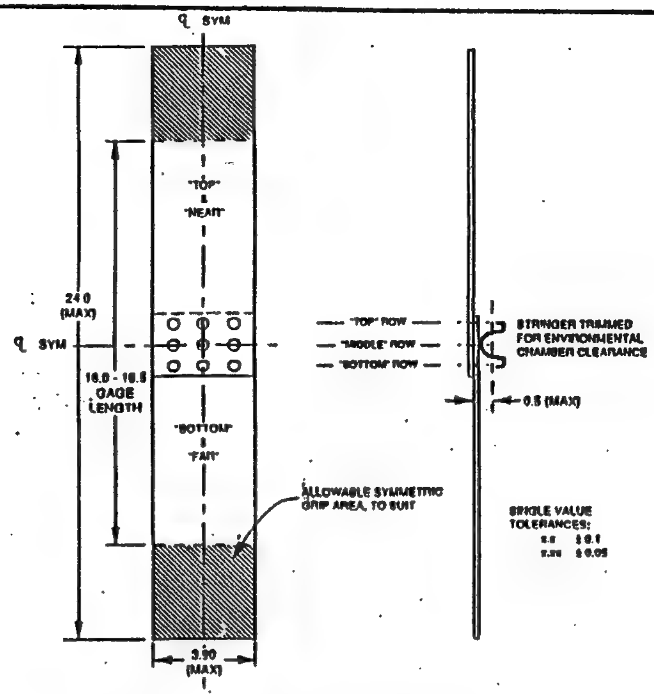

NOTE: The terms "top", "middle", "bottom", "near" and "far" are relative to viewing the specimen with the countersunk fastener heads visible to the observer and the "top" sheet being on the "near" side of the lap joint.

01/GM/CORROS 07

C/KC-135 FUSELAGE LAP JOINT COUPON (TYPICAL)

C/KC-135 UPPER WING SKIN SPECIMEN (TYPICAL)

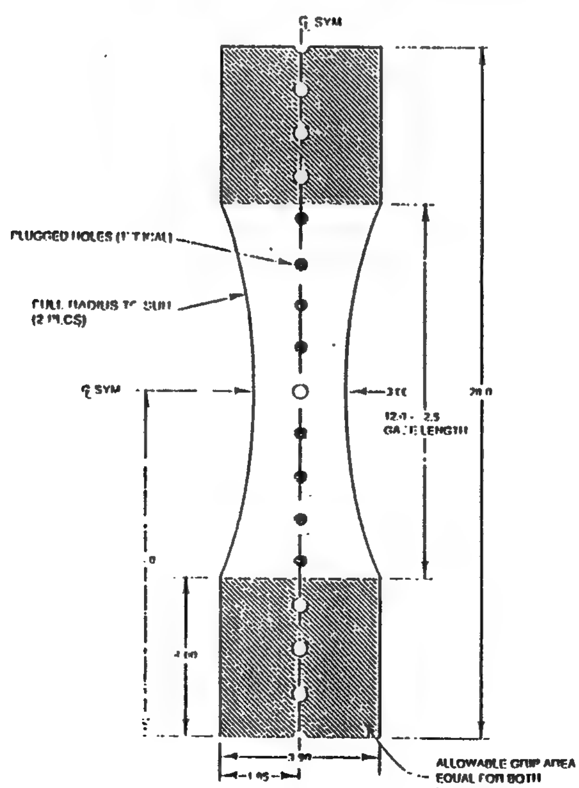

CORROSION INFORMATION SYSTEM

- DEVELOP COMPUTERIZED DOCUMENTATION SYSTEM FOR STORAGE, RETRIEVAL AND MANIPULATION OF CORROSION DATA
- DEFINE SYSTEM FUNCTIONAL DESCRIPTION
  - CORROSION DATA FORMAT
  - SOFTWARE REQUIREMENTS
  - INTERFACE REQUIREMENTS
- DEMONSTRATION/PROTOTYPE 3rd QTR FY94

CORROSION GROWTH RATE TESTING AND ANALYSIS

- DETERMINE CORROSION GROWTH RATES AS A FUNCTION OF MATERIAL, ENVIRONMENT AND OTHER VARIABLES
- PLACE C/KC-135 AIRCRAFT SECTIONS AT SEVERE CORROSION STATIONS AROUND THE WORLD
  - PERIODICALLY DISASSEMBLE PORTIONS AND QUANTIFY CORROSION
  - INSTALL CORROSION SENSOR/DETECTOR
- INITIAL PLACEMENT AT JEDDAH AND RIYADH, SAUDI ARABIA DEC 93
- OTHER LOCATIONS OR METHODOLOGIES (TBD)

CORROSION PREDICTION MODELING

- DEVELOP EMPIRICAL/MATHEMATICAL RELATIONSHIPS
  - EXISTING DATA
  - PROGRAM GENERATED TEST DATA
  - PROBABILISTIC APPROACH
- PLAN AND TEAM MEMBERS TO BE IDENTIFIED JAN - FEB 94

C/KC-135 SERVICE LIFE PREDICTION AND EXTENSION STUDIES

- DETERMINE STRUCTURAL LIFE WITH EFFECTS OF CORROSION INCLUDED
- UPDATE STRUCTURAL INTEGRITY PROGRAM
- CONDUCT FAILURE MODES AND EFFECTS ANALYSIS/RISK ANALYSIS
- DEVELOP PLANS AND IDENTIFY MODIFICATIONS/MAINTENANCE ACTIONS TO ENSURE CONTINUED AIRWORTHINESS TO THE YEAR 2040
- CONDUCT COST BENEFIT/BREAK EVEN ANALYSIS OF MODIFICATIONS/MAINTENANCE VS. NEW AIRCRAFT/ACQUISITION
- PRELIMINARY LIFE PREDICTION AND PLAN 2nd QTR FY95

C/KC-135 LIFE EXTENSION

SYSTEMS APPROACH

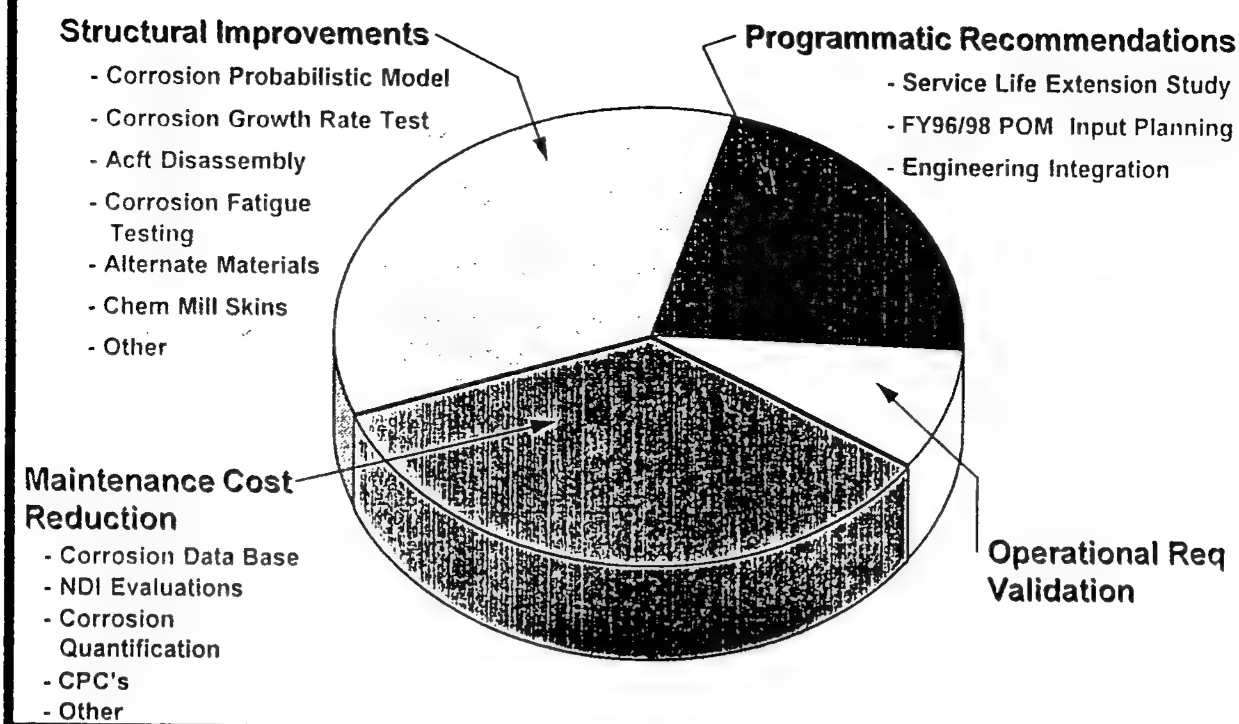

USAF C/KC-135 ENGINEERING INVESTMENT ESSENTIAL FOR 21ST CENTURY OPERATIONS

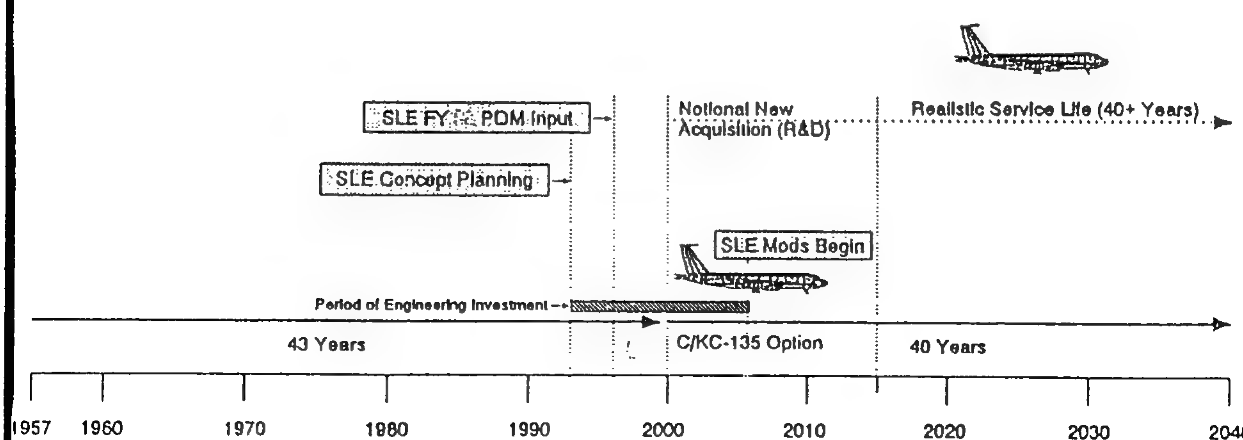

FUTURE INITIATIVES 1995 - 2000

- EXPAND NDI EQUIPMENT DEVELOPMENT
  - CORROSION AROUND, WING SKIN FASTENERS, BETWEEN WING SKIN AND SPARS
  - ADDRESS INTERGRANULAR/EXFOLIATION AND STRESS CORROSION/CRACKING
- IMPLEMENT CORROSION DETECTION EQUIPMENT AT ALL C/KC-135 PDM SITES
- INVESTIGATE ROBOTIC OPERATED CORROSION DETECTION NDI EQUIPMENT
- EXTEND STRUCTURAL INTEGRITY TESTING AND ANALYSIS
  - FULL SCALE TESTING OF FUSELAGE SECTIONS
  - FULL SCALE FATIGUE TESTING OF CORRODED WING SKIN

FUTURE INITIATIVES 1995 - 2000

- PREPARE C/KC-135 SLEP POM INPUTS

CONCERNS

- LACK OF SCIENTIFIC KNOWLEDGE OF AGING AIRCRAFT CORROSION AND ITS EFFECTS ON STRUCTURAL INTEGRITY
- NO CONCENTRATED EFFORTS TO SOLVE THESE PROBLEMS
- THEREFORE OUR PROGRAM HAS HAD TO ADDRESS AREAS THAT SHOULD BE COVERED BY THE LABS
- ASKED TO DEVELOP STRATEGIC PLANS AND MOA/MOU BETWEEN OC-ALC AND NASA, FAA AND THE NAVY TO FORMALIZE OUR WORKING LEVEL COOPERATIVE/COMPLIMENTARY EFFORTS
- THE SCIENTIFIC COMMUNITY, NASA, FAA & NAVY RECOGNIZE THE SIGNIFICANCE OF THE OC-ALC AGING AIRCRAFT CORROSION PROGRAM

RECOMMENDATIONS

- ESTABLISH A USAF AGING AIRCRAFT COORDINATING ORGANIZATION, PROGRAM OFFICE, OR CENTER OF EXCELLENCE
- EXPAND AND ENLARGE AGING AIRCRAFT CORROSION R&D AT WRIGHT LABS, AFOSR AND THE NAVY
- ESTABLISH AND STAFF A CORROSION TECHNICAL ORGANIZATION AT WRIGHT LABS (ML OR FI)
- ESTABLISH AN OFFICE OR ORGANIZATION TO COORDINATE AGING AIRCRAFT EFFORTS BETWEEN ALL GOVERNMENT AGENCIES, USAF, NAVY, FAA, AND NASA

CONCLUSIONS

- BUSINESS "AS USUAL" WILL NOT ENSURE THE CONTINUED, COST EFFECTIVE AVAILABILITY OF AGING C/KC-135 AIRCRAFT
- CONSIDERABLE INFORMATION IS NEEDED TO ESTABLISH C/KC-135 AGING AIRCRAFT INITIATIVES THAT CAN BE IMPLEMENTED THROUGH AIR FORCE MAINTENANCE AND PROCUREMENT PROGRAMS — UPFRONT INVESTMENT IS CRITICAL

SCIENTIFIC EFFORTS NEEDED

- NDI EQUIPMENT FOR DETECTING INTERGRANULAR CORROSION AROUND WING SKIN FASTENERS
- CORROSION QUANTIFICATION
- CORROSION GROWTH RATES
- EFFECTS OF CORROSION ON:
  - FATIGUE STRENGTH
  - RESIDUAL STRENGTH
  - STATIC STRENGTH
- PROBABILISTIC MODELING OF CORROSION

WORLDWIDE AGING AIRCRAFT PROBLEM

- OC-ALC CORROSION PROGRAM
  - PROVIDE BASELINE/SOLUTIONS TO OTHER USAF AGING AIRCRAFT
- USAF CORROSION PROBLEMS
  - PARTS OF LARGER DOD AND WORLDWIDE AGING AIRCRAFT/CORROSION PROBLEMS
- COORDINATION WITH OTHER AGENCIES
  - OTHER ALC'S
  - USAF LABS
  - NAVY
  - FAA - AIRLINES
  - NASA
  - ACADEMIA

AFMC

Name Neal Phelps

Title - Aerospace Engineer

- Hill AFB Representative for Aging Aircraft
  - Member of Structural Integrity Assessment and Life Extension Methodology Working Group

Company - F-16 Structures Team @ Hill AFB, UT

Current Assignment - Lead Engineer for Durability and Damage Tolerance Analysis (DADTA)

Past Experience - Navy P-3 Orion, Air Force C-130, OV-10, F-4, F-16

LASER SHOCK PROCESS

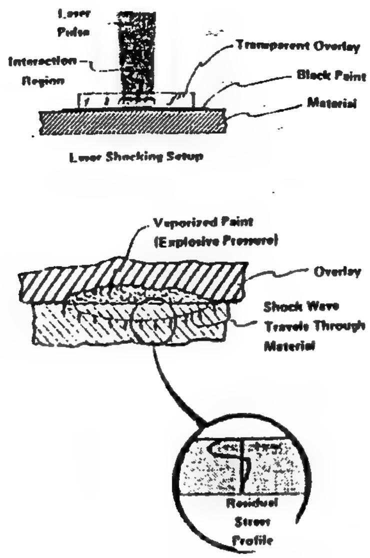

PROPERTY IMPROVEMENTS

- *Fatigue life*
- *Fatigue strength*
- *Fretting fatigue resistance*
- *Surface hardness*
- *Thin section strength*
- *Relieve residual weld stresses*

AFMC

INCREASE IN FATIGUE LIFE

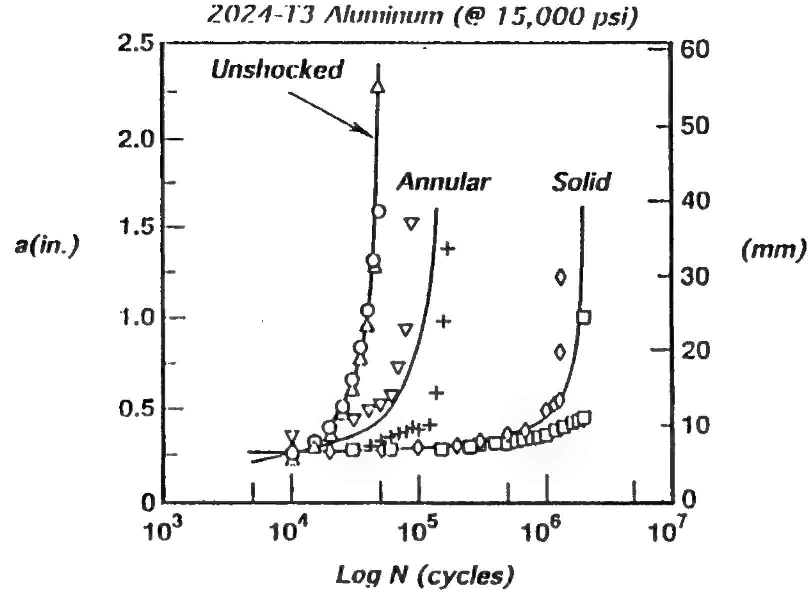

OO-ALC/LAAS F-16 STRUCTURES

AFMC

Increased Fatigue Strength

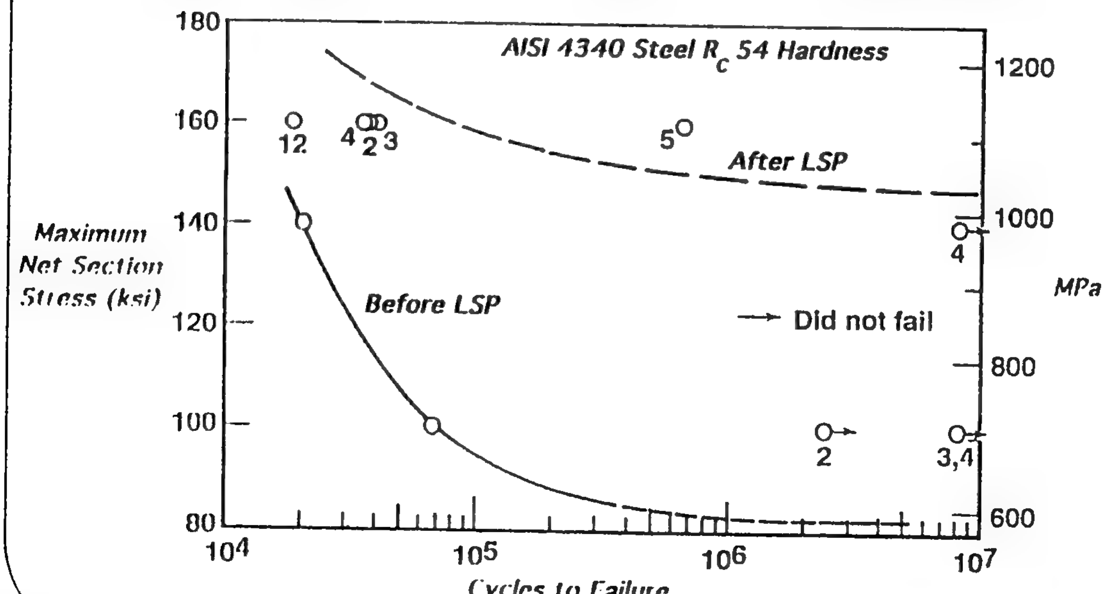

OO-ALC/LAAS F-16 STRUCTURES

RESIDUAL STRESS PROFILES

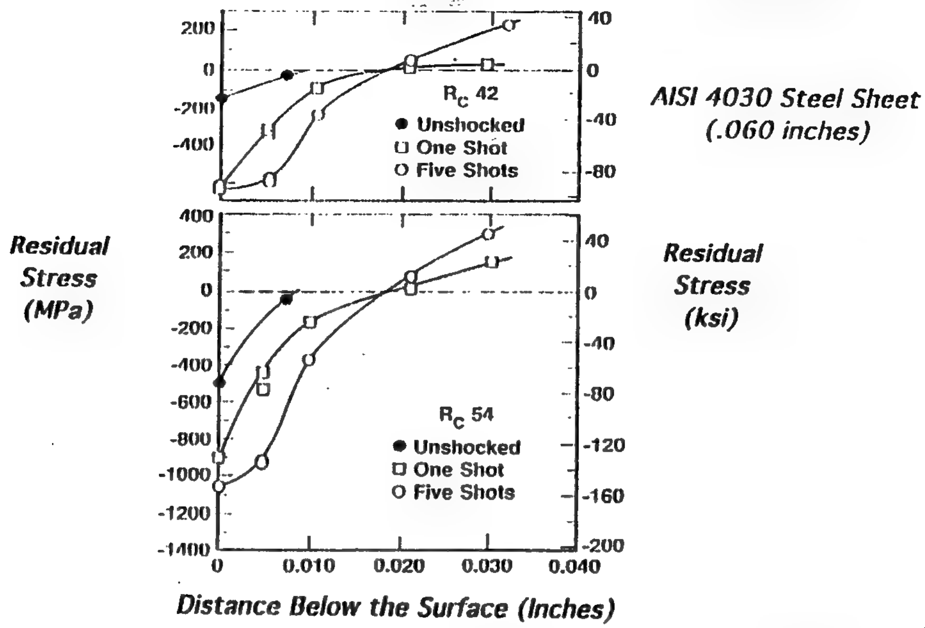

OO-ALC/LAAS F-16 STRUCTURES

LSP Slows Growth of Existing Cracks

2024-T351 Aluminum (@ 15,000 psi)

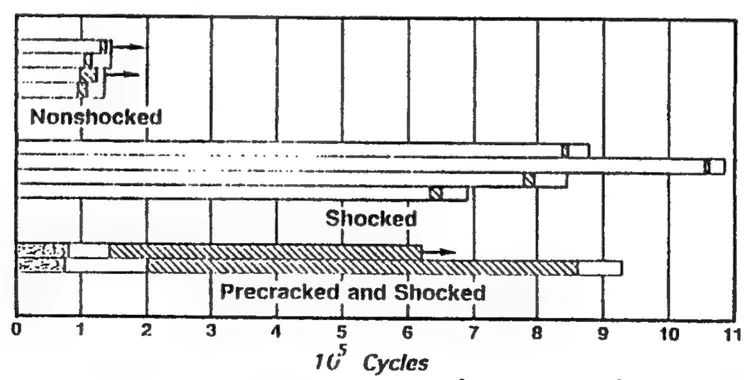

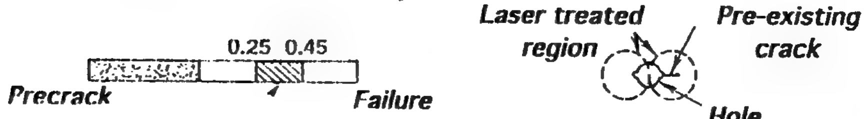

Cycles for crack growth to given length

Laser Shock Pattern

OO-ALC/LAAS F-16 STRUCTURES

RELIEVE RESIDUAL WELD STRESSES

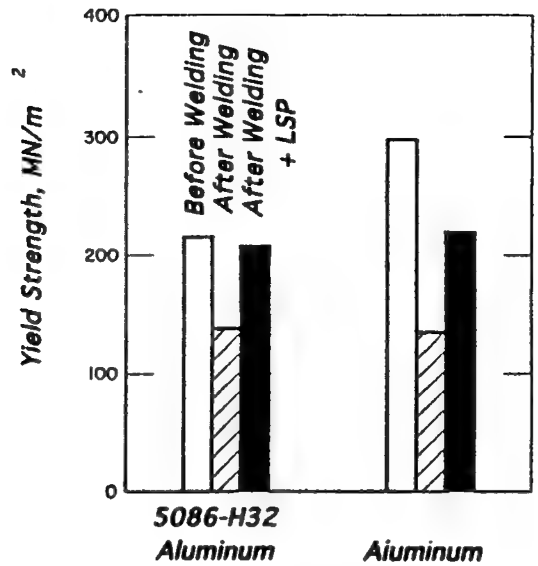

OO-ALC/LAAS F-16 STRUCTURES

Steering Rod Treatment

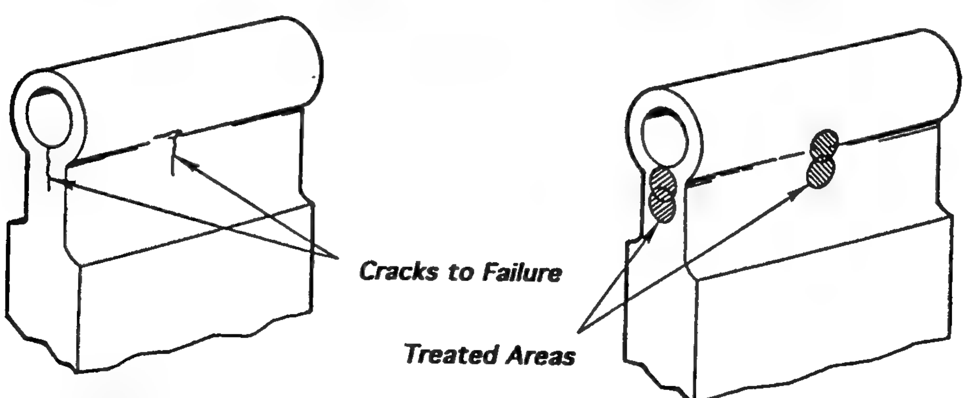

Untreated

33,000 Cycles to Failure

LSP Treated

92,000 Cycles to Failure

OO-ALC/LAAS F-16 STRUCTURES

AFMC

F-16 GUN PORT BOLTS

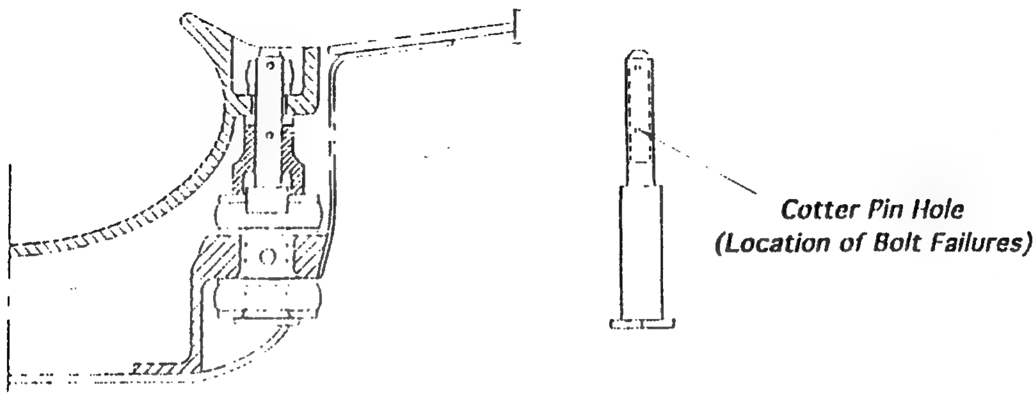

OO-ALC/LAAS F-16 STRUCTURES

AFMC

FATIGUE TESTS RESULTS F-16 GUN PORT BOLTS

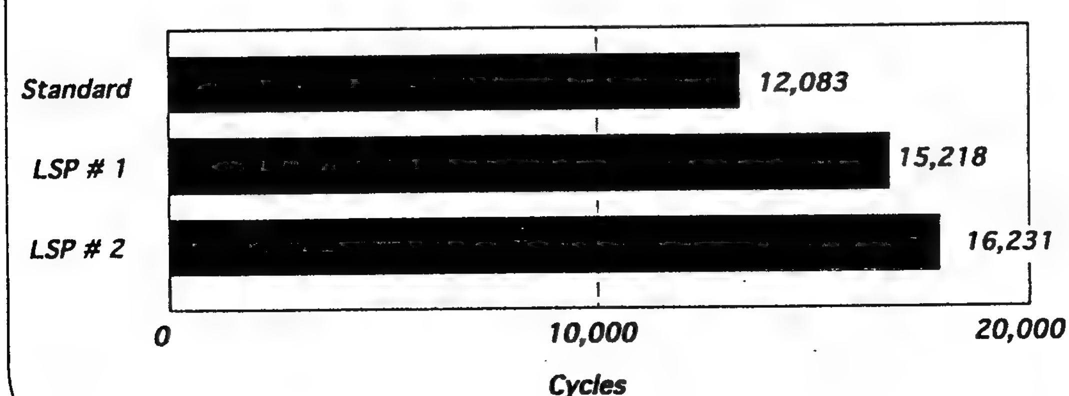

OO-ALC/LAAS F-16 STRUCTURES

AEMS

Advanced

Emissions

Monitoring

System

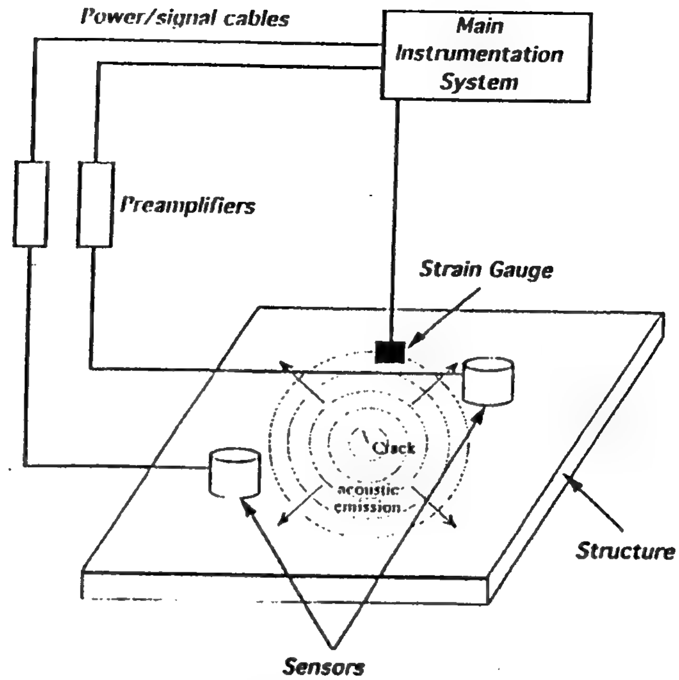

OO-ALC/LAAS F-16 STRUCTURES

Comparison of Acoustic Emission Results with 44 Defects Detected by Eddy Current (Canadair 31 Aug 90)

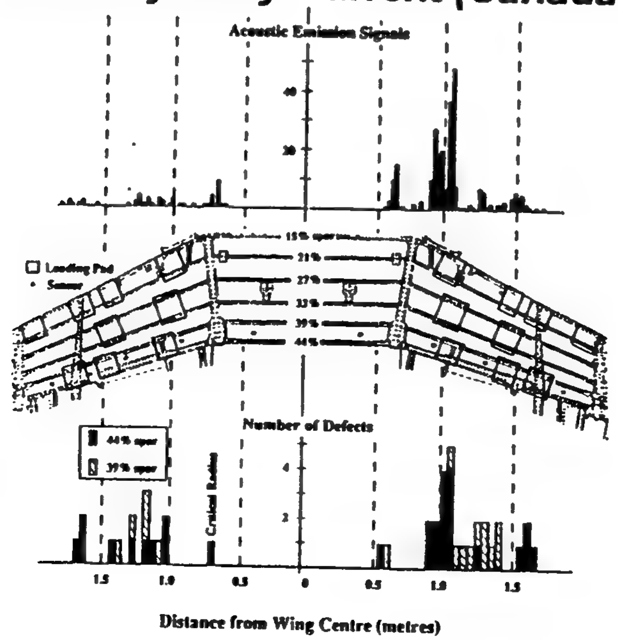

OO-ALC/LAAS F-16 STRUCTURES

AFMC

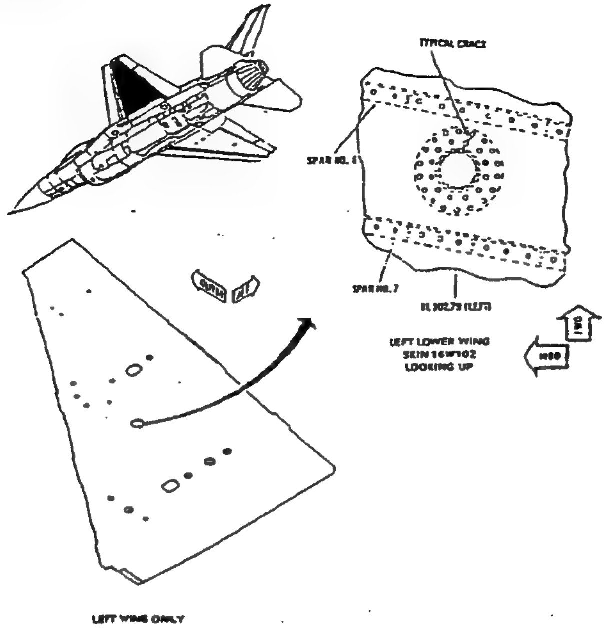

AFMC

BORON/EPOXY FOR FUEL VENT HOLE

BORON/EPOXY TAPE
350 DEG CURE

NOTES:

1. *Plies to drop in symmetric pairs as shown in section X.*
2. *.25 " min between ply drops in all directions.*
3. *Thickness of section X not to scale.*

PLY#	L	THETA
18	.0052	+45
17	.0052	-45
16	.0052	0
15	.0052	0
14	.0052	0
13	.0052	0
12	.0052	0
11	.0052	0
10	.0052	0
09	.0052	0
08	.0052	0
07	.0052	0
06	.0052	0
05	.0052	0
04	.0052	0
03	.0052	0
02	.0052	-45
01	.0052	+45

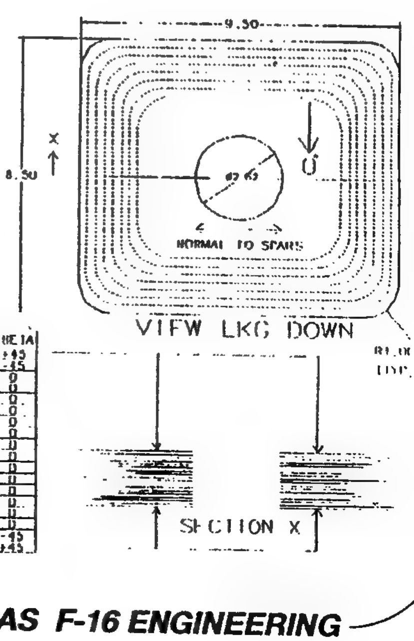

OO-ALC/LAAS F-16 ENGINEERING

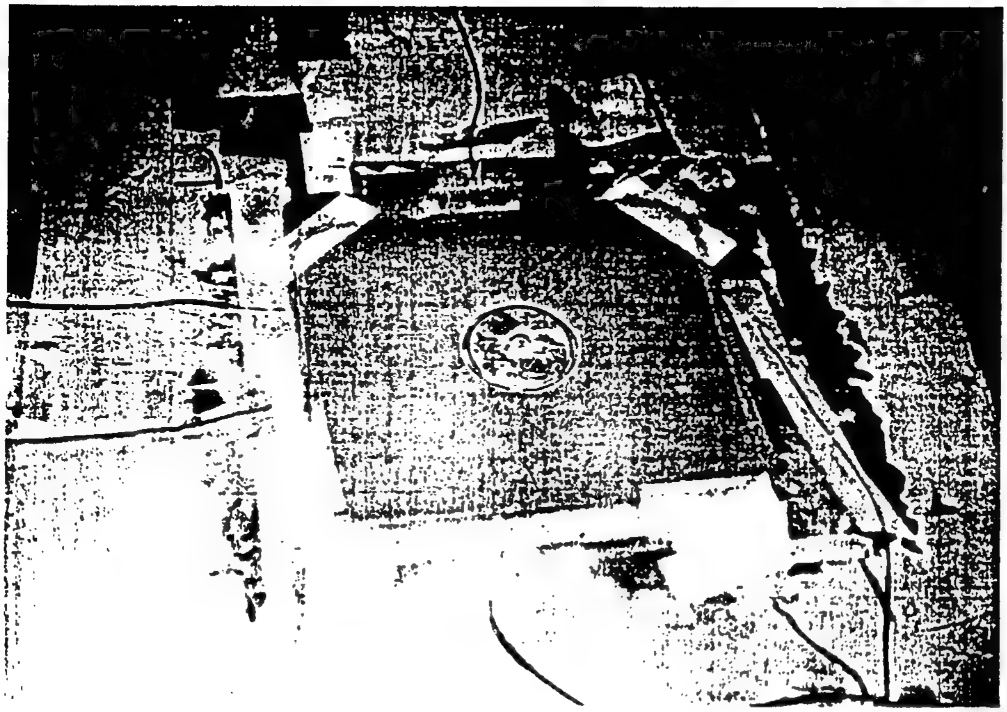

Fatigue Lives of Riveted Repair
(Effect of patch selection)

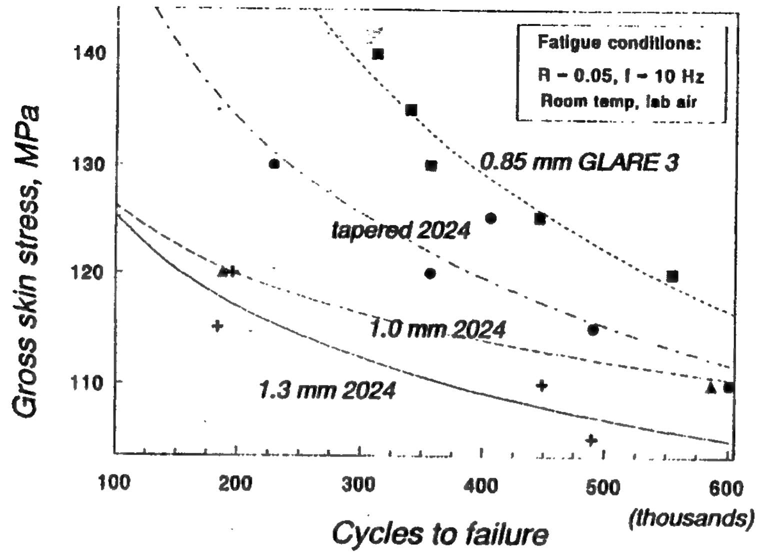

OO-ALC/LAAS F-16 STRUCTURES

Maximum Adhesive Shear Strain
(over crack location)

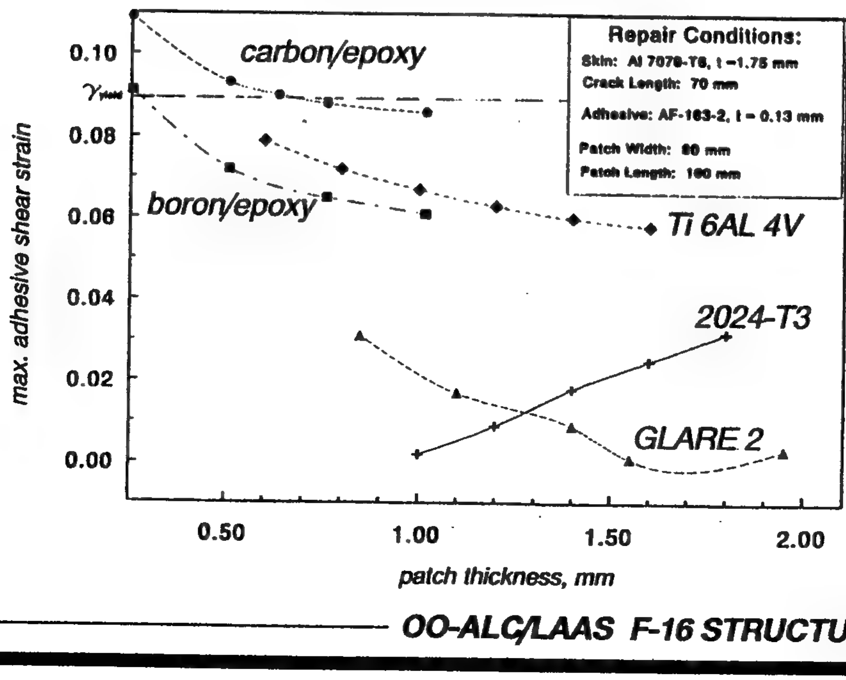

OO-ALC/LAAS F-16 STRUCTURES

AFMC

Crack Patching Effectiveness

(Reduction of K, no thermal effects)

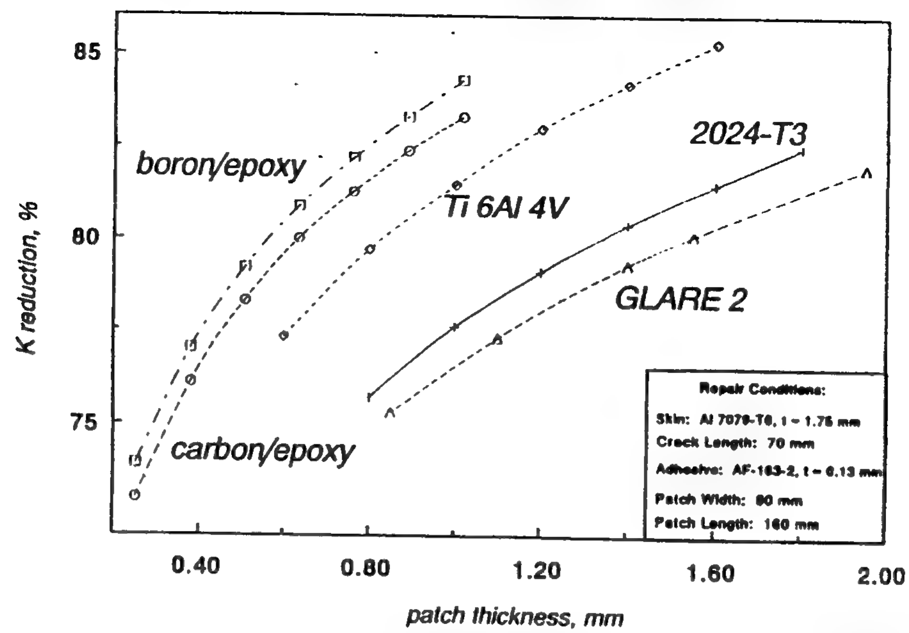

OO-ALC/LAAS F-16 STRUCTURES

AFMC

Crack Patching Effectiveness

(Reduction of K, thermal effects included)

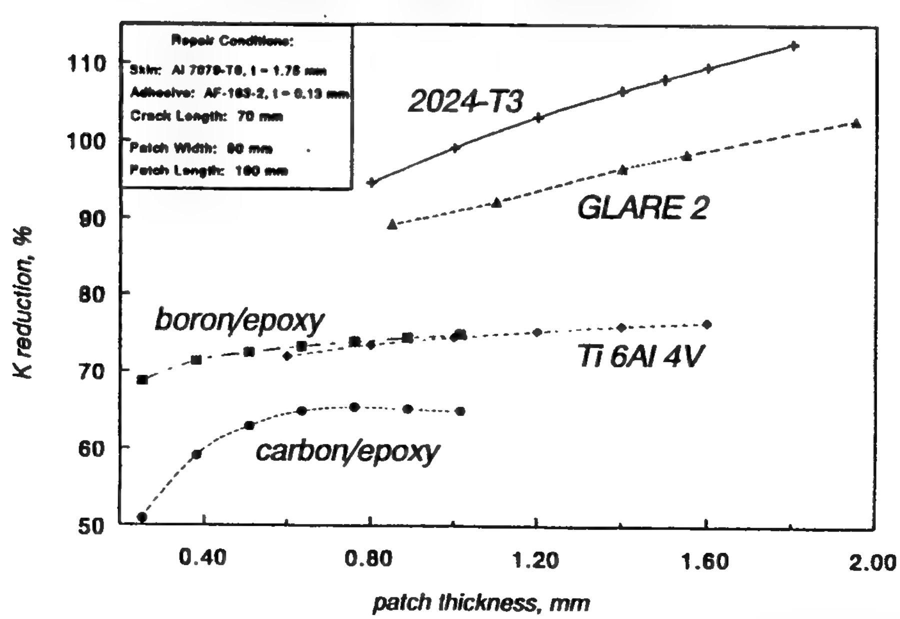

OO-ALC/LAAS F-16 STRUCTURES

F-111

STRUCTURAL INTEGRITY REVIEW

AIR FORCE AGING AIRCRAFT CONFERENCE

17 MAY 94

BILL J. SUTHERLAND

SACRAMENTO AIR LOGISTICS CENTER / LAFFE

DSN 633-4224

SM-ALC - AGING AIRCRAFT WORKING GROUP MEMBERS

- NON DESTRUCTIVE EVALUATION

  ALBERT ROGEL, TIEE, DSN 633-3147
  SM-ALC NDI MANAGER

  DON BAILEY, TIELD, DSN 633-5476
  MATERIALS ENGINEERING TECHNICIAN

- STRUCTURAL INTEGRITY ASSESSMENT AND LIFE EXTENSION METHODOLOGY DEVELOPMENT

  BILL SUTHERLAND, LAFTE, DSN 633-4224,
  CHIEF, F-111 / A-10 STRUCTURAL ENGINEERING

- MATERIAL BEHAVIOR

  JOHN MEHRINGER, TIELC, DSN 633-2451
  MATERIALS ENGINEER

- CORROSION

  DAN DUNHAM, TIEE, DSN 633-3147
  SM-ALC CORROSION MANAGER

F-111 ASIP REVIEW SUMMARY

AIRCRAFT HISTORY / STATUS

EF-111A STRUCTURAL INTEGRITY ROADMAP

F-111 STRUCTURAL PROBLEM CATEGORIES

F-111 INVENTORY SUMMARY — 1 MAY 1994

MODEL	NUMBER OF AIRCRAFT				
	PRODUCED	ATTRITED	RETIRED	CONVERTED	IN-SERVICE
F-111A PRE-PRODUCTION	30	5	25	0	0
F-111A PRODUCTION	129	39	43	46 (42 EF-111A) (4 F-111C)	1
EF-111A (42 CONVERTED FROM F-111A)	0	2	0	0	40
F-111D	96	18	78	0	0
F-111E	94	17	51	0	26
F-111F	106	25	0	0	81
FB-111A	76	14	26	36 (F-111G)	0
F-111G (36 CONVERTED FROM FB-111A)	0	0	21	15 (F-111C)	0
F-111C RAAF (+4 CONVERTED FROM F-111A / +15 CONVERTED FROM F-111G)	24	7	0	0	36
TOTALS	555	127	244	N/A	184

F-111 OPERATIONAL HISTORY

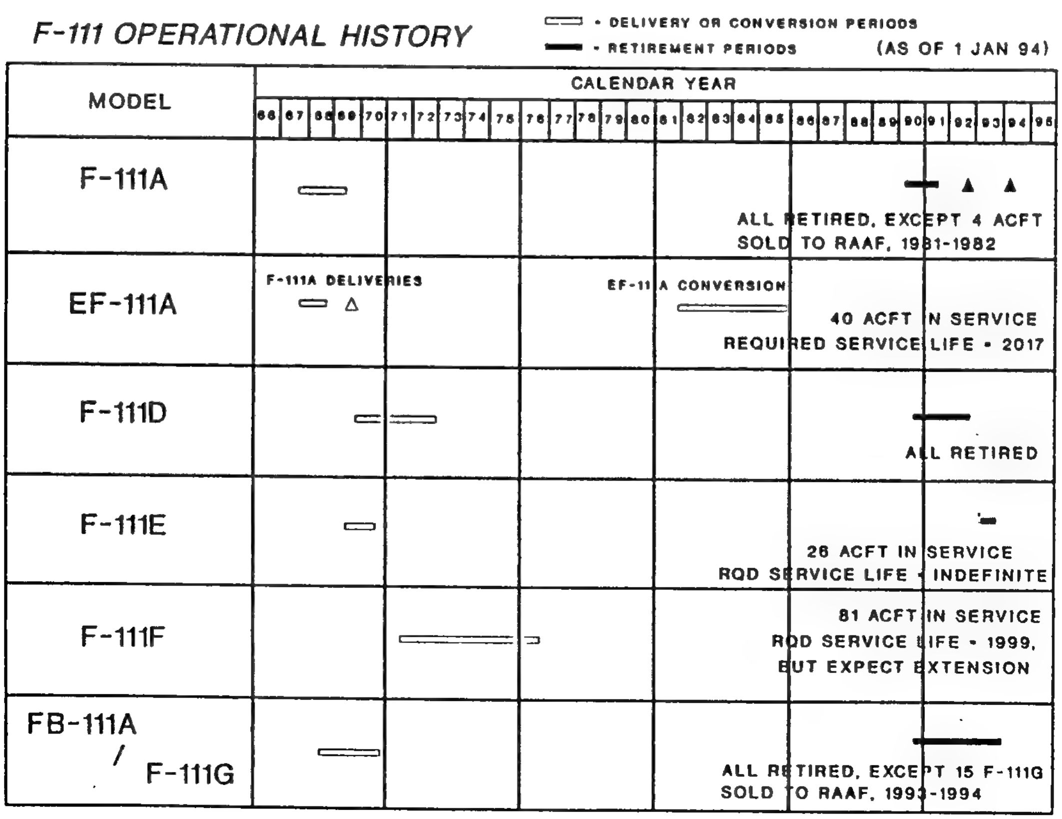

F-111 FLIGHT TIME SUMMARY - 11 JAN 94

	FLIGHT HOURS		
MDS	HIGH	AVERAGE	LOW
EF-111A	6541	5417	4264
F-111E	6101	5320	2067
F-111F	5889	5058	2351

EF-111A FLIGHT HOUR PROJECTIONS
BY CALENDAR YEAR @ 300 HOURS PER YEAR

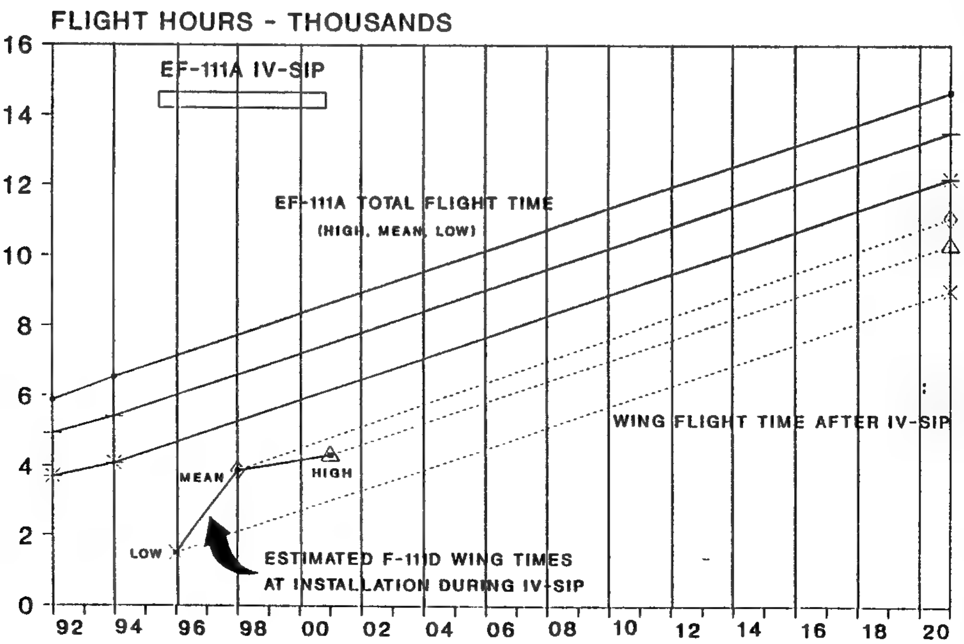

EF-111A STRUCTURAL INTEGRITY ROADMAP (SM-ALC/LAFFE/MAR94)

ACTIVITIES	CALENDAR YEAR 91 92 93 94 95 96 97 98 99 00 01 02 03 04 05 06 07 08 09 10 11 12 13 14 15 16 17 18 19 20
PROGRAMMED DEPOT MAINTENANCE (PDM)	RECURRING REQUIREMENT - INSPECTION INTERVAL = 1500 HOURS
COLD TEMPERATURE PROOF TESTING	III-SIP IV-SIP V-SIP VI-SIP
NACELLE FORMER REPAIR	ONE-TIME TCTO • PDM
CARRY THRU BOX / INLET INTERFERENCE REWORK	ONE-TIME PDM TASK
BOLT HOLE COLD WORK MODIFICATION	ONE-TIME TCTO • PDM
STANDARD FLIGHT DATA RECORDER MOD (SFDR)	MODIFICATION INSTALLED • PDM
F-111D WING SWAP	ONE-TIME TCTO • IV-SIP
HIGH TIME F-111A TEARDOWN INSPECTION	ONE-TIME ENGINEERING TASK - TO BE SCHEDULED SHOULD BE DONE BY THE YEAR 2000.

F/FB-111 STRUCTURAL ARRANGEMENT

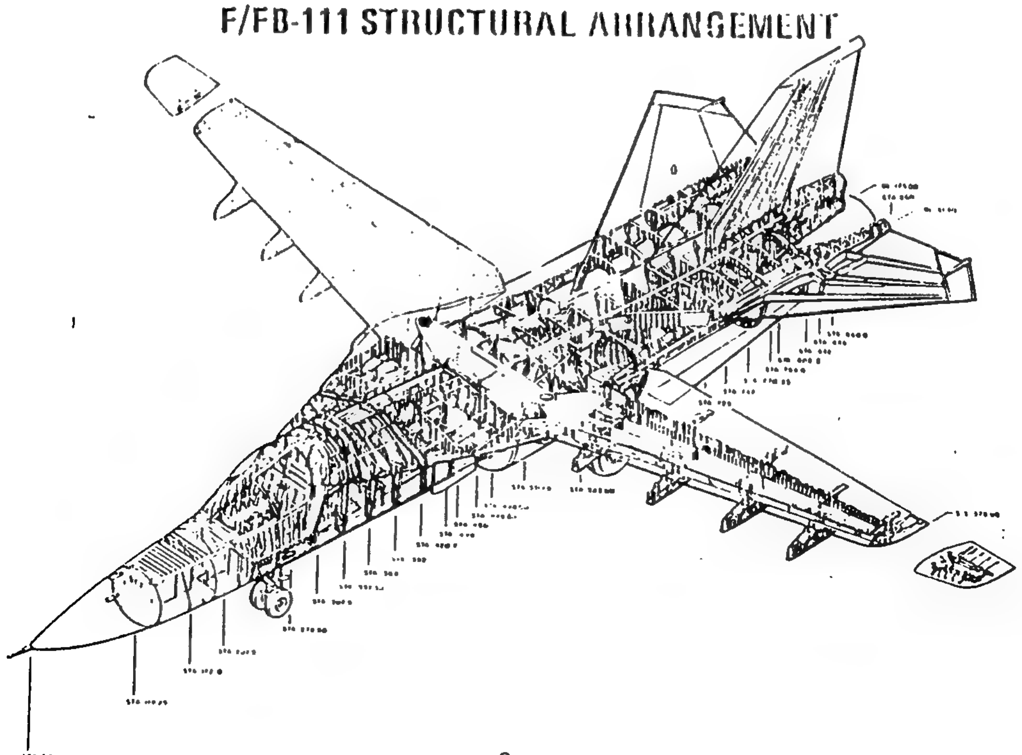

F-111 STRUCTURAL PROBLEM CATEGORIES

CATEGORY	CHARACTERISTICS	GENERAL SOLUTIONS
STRESS-CORROSION CRACKING	7079-T6 ALUMINUM PLATE IN FORWARD FUSELAGE FRAMES, LONGERONS, BULKHEADS, & MISCELLANEOUS FITTINGS	PDM INSPECTION & REPAIR HAMPERED BY IMPROVEMENTS IN TANK SEALING PROCESS SOME COMPONENT REPLACEMENTS (MLG CENTRAL TRUNNION) (UPPER TUNNEL TRUSSES)
BONDED STRUCTURE DELAMINATION AND CORROSION	1960s BONDING TECHNOLOGY UNPRIMED SKINS BARE CORE	FIELD & DEPOT INSPECTION AND REPAIR DESIGN CHANGES IN REPAIR AND NEW MANUFACTURING CORROSION TREATED CORE PHOSPHORIC ACID ANODIZE ADHESION PROMOTING PRIMERS
D6AC STEEL FATIGUE CRACKING	HIGH STRENGTH LOW TOUGHNESS VERY SMALL CRITICAL CRACK SIZES CRITICAL AREAS ON BOTH TENSION AND COMPRESSION SIDES	PDM INSPECTIONS / REWORK: MAGNETIC RUBBER - EVERY CYCLE PROOF TEST - EVERY 2ND CYCLE MECHANICAL REMOVAL OF CRACKS RECONFIGURE GEOMETRY OF CRITICAL AREAS COLD WORK OF UPPER LONGERON HOLES AND SOME HOLES IN WING CARRY THRU BOX

PDM / ASIP NDI PROGRAM

(EF-111A BASELINE)

WING CARRY THRU BOX

★UPPER PLATE NO-LOAD BOLT HOLES
▽★UPPER PLATE SEALANT INJECTION HOLES
★LOWER PLATE FORWARD CORNER
LOWER PLATE LUG
OUTBOARD BULKHEAD HOLES
OUTBOARD BULKHEAD UPPER AFT CORNER
★FORWARD POSTS
▽LOWER PLATE STIFFENERS

WING PIVOT FITTING/WING BOX

▽★UPPER PLATE STIFFENER RUNOUTS
★UPPER PLATE FUEL VENT HOLES
LOWER PLATE LUG
SHEAR LUG
★SHEAR RING
LOWER WING SKIN • INBOARD PYLON
★WELD ZONE REPAIRS

FS 770 HORIZ STAB SUPPORT STRUCTURE

★PIVOT SHAFT RELIEF HOLE
▽★PIVOT SHAFT RELIEF HOLE (EXPANDED AREA)
★PIVOT SHAFT CLEVIS HOLES
▽★PIVOT SHAFT TOOLING HOLE
★CENTER BULKHEAD LOWER LUGS

FS496 NACELLE FORMER

POST-FLANGE INTERSECTION
★TIE LINK LUGS
★UPPER FLANGES
★LOWER TAB
★SPIKE ISLAND TAB

MLG SUPPORT STRUCTURE

SHOCK STRUT SUPPORT, 12B10521
DRAG BRACE SUPPORT, 12B10502
LOWER LONGERON, 12B10571
RETRACT ACTUATOR BRACKET
UPLOCK HOOK

FUSELAGE (GENERAL)

★NACELLE TIE LINK
★12B4802 INTERCOSTAL
★12B4811 CENTER LONGERON
★OVERWING LONGERON, FS 532 & FS 560
★FORWARD FUSELAGE FRAMES
★UPPER GLOVE ROUTING TUNNEL
★COWL BEAM LUGS
★CREW MODULE FLOOR TRUSSES
SPEED BRAKE ACTUATOR BRACKET
FS 449 LONGERON SPLICE

LEGEND:
★ - CRACKS BEING FOUND BY NDI
▽ - PROBLEM DISCOVERED BY PROOF TEST

(AS OF 1 OCT 93)

Materials Degradation and Fatigue in Aerospace Structures

A. F. Grandt, Jr.
School of Aeronautics and Astronautics
Purdue University

Air Force Aging Aircraft Conference
May 17-19, 1994
Tinker AFB

Purdue University Research Team

- School of Aeronautics & Astronautics
  - A. F. Grandt (PI)
  - T. N. Farris
  - C. T. Sun
- School of Mechanical Engineering
  - B. M. Hillberry
- School of Materials Engineering
  - E. P. Kvam
- School of Statistics
  - G. P. McCabe

Purdue Structural Integrity Program

Aging Aircraft -- Key Issues

- An older aircraft may contain prior service induced damage
  - fatigue
  - corrosion
  - fretting
  - accidental damage
- When does such damage compromise safety or limit economic operation?
  - How does discrete site damage form/grow?
  - How does multiple-site damage limit safety?
  - How may damage be detected?
  - How may damage be repaired?

Purdue Structural Integrity Program

Overview of Aging Aircraft Issues

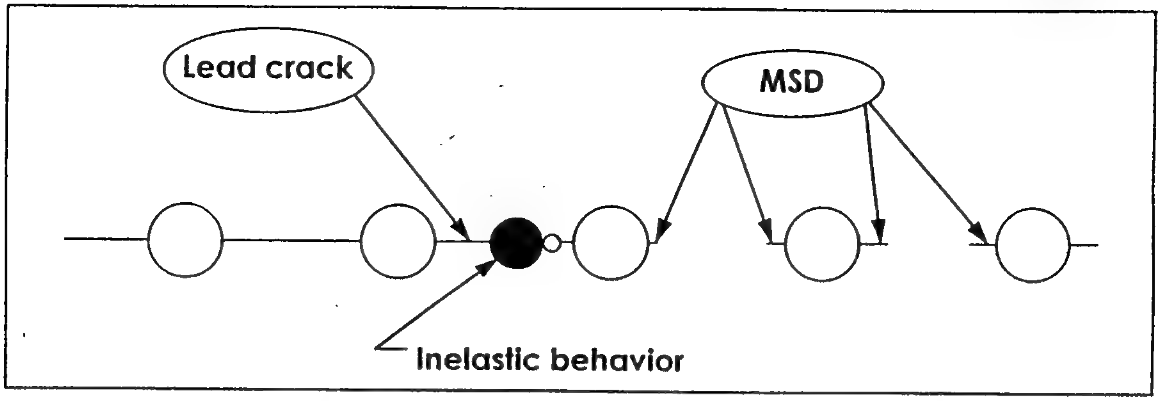

- How does service induced damage effect life of an older aircraft ?
- How does corrosion, fretting, fatigue form?
- How does it grow, coalesce?
- When does it compromise safety?
- How can it be delayed/repaired?

- Spectrum loading
- Environmental attack
- Inelastic behavior
- Complex structure
- Prior service/repair
- Unknown conditions

Purdue Structural Integrity Program

Overview of Current Projects

- MSD
  - Residual strength
  - Fatigue life
  - Parametric study
  - Probabilistic analysis
- Corrosion/fatigue
  - LEFM quantification of corrosion
  - da/dN in retired a/c
  - Breaking load characterization of corrosion
  - Crack initiation from pits
- Tribology/Fretting
- Composite patching

Purdue Structural Integrity Program

Lead Crack Residual Strength

- Airplanes are designed to safely contain large cracks from unexpected damage sources (e.g. engine burst)

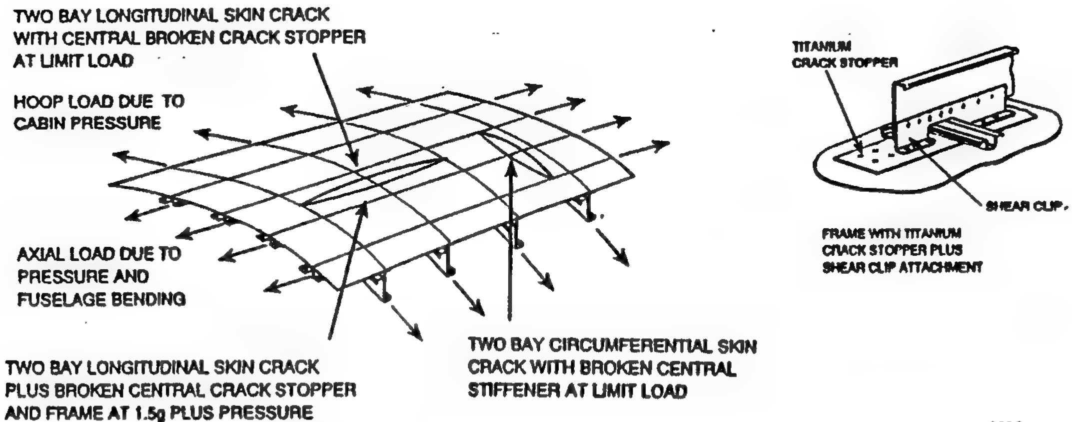

FUSELAGE DAMAGE SIZES USED FOR LARGE DAMAGE SUBSTANTIATION

(From Swift)

Effect of MSD on Residual Strength

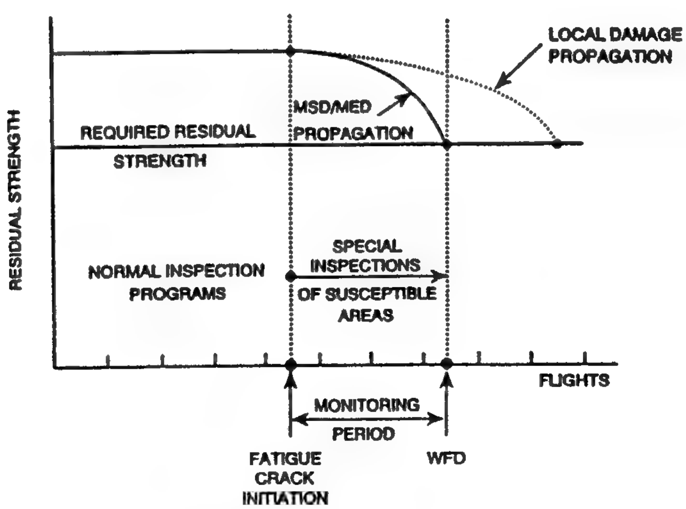

FIGURE 1 RESIDUAL STRENGTH CAPABILITY AND RESULTING INSPECTION ACTIONS

(From Swift)

Decrease in Residual Strength due to MSD

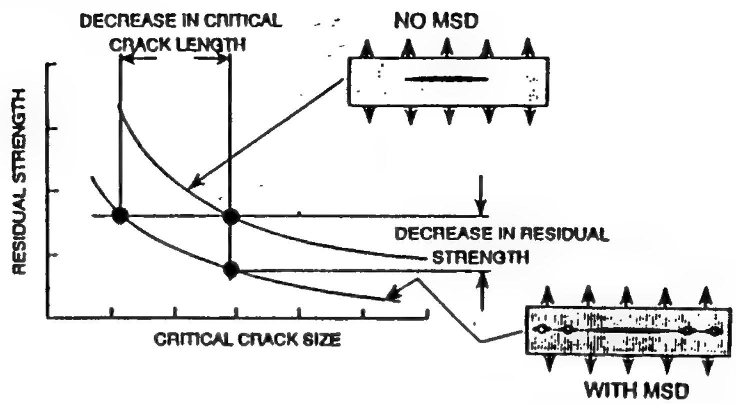

EFFECT OF MSD ON CRITICAL CRACK SIZE AND RESIDUAL STRENGTH

(From Swift)

Influence of MSD on 3.2 inch lead crack specimens

Lead crack = 3.2 inch
6 holes with MSD
avg MSD crack = a*

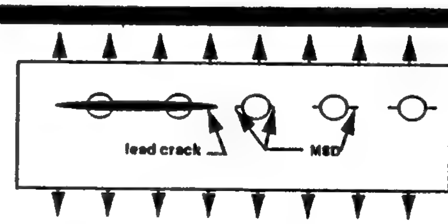

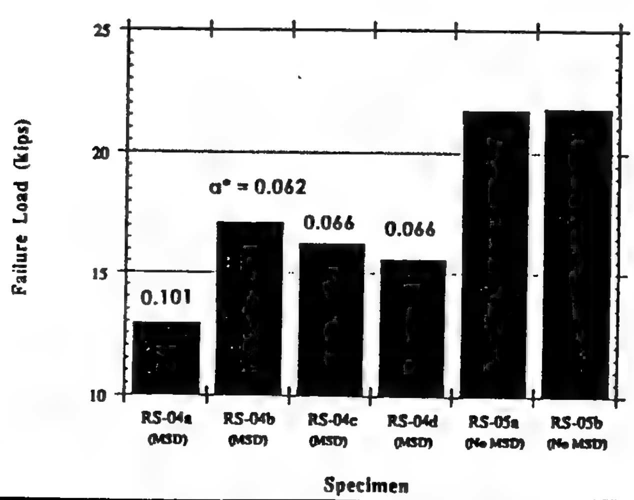

Residual Strength Criteria

- $K_{apparent}$
  - fails when critical stress intensity factor reached
- Net Section Yield
  - fails when net section stress reaches yield
- Ligament Yield (Swift)
  - ligament fails when crack tip plastic zones touch

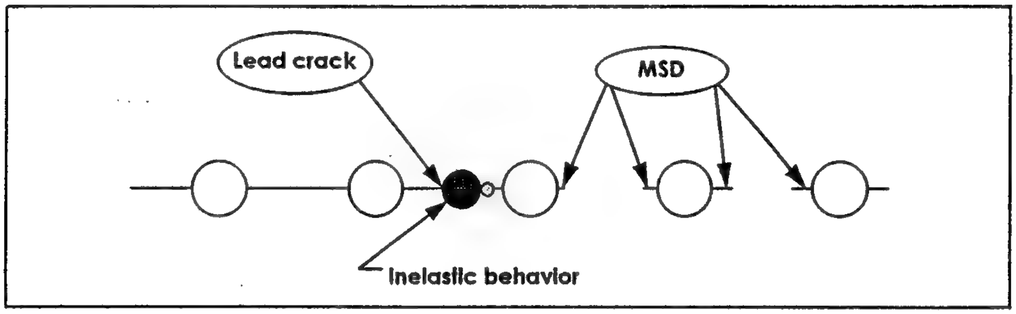

Comparison of Various Failure Criteria with Measured Loads

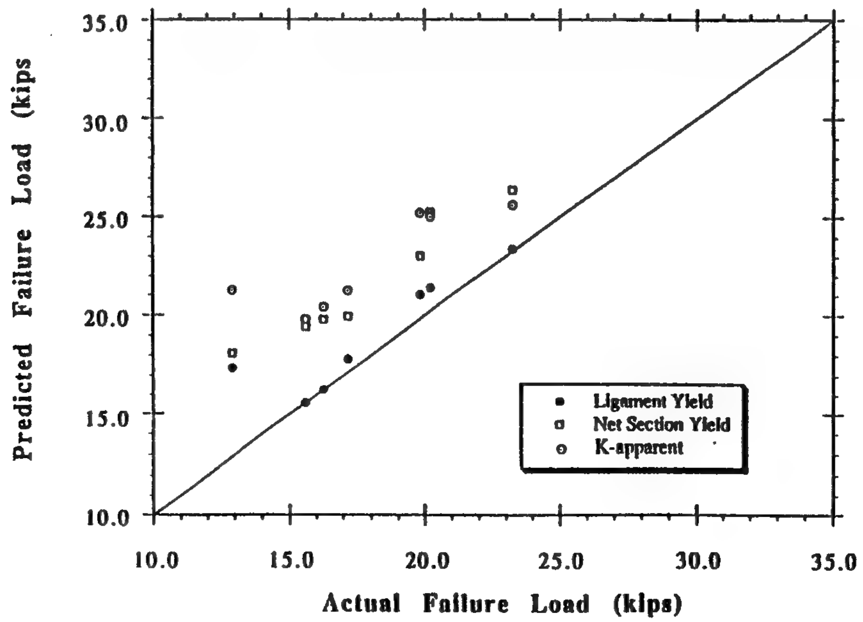

MSD Fatigue Crack Growth

Objectives:

- Develop computer algorithm to predict fatigue life of panels with MSD
  - MSD crack growth/interaction
  - crack initiation at holes without MSD
  - total panel life and individual crack growth
- Evaluate algorithm with experiments on panels with open holes
- Extend analysis to more realistic structural configurations
  - stiffened structure
  - load transfer through fastened joints

Effect of MSD on Lead Crack Life

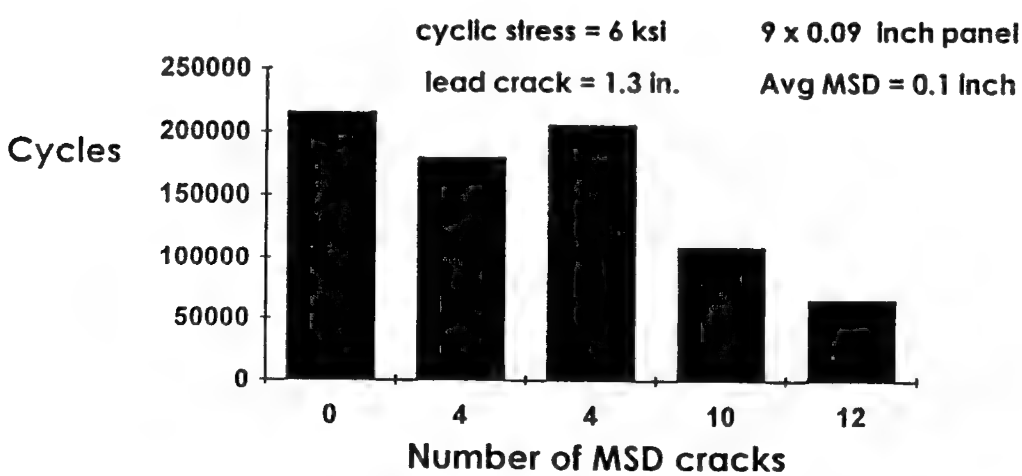

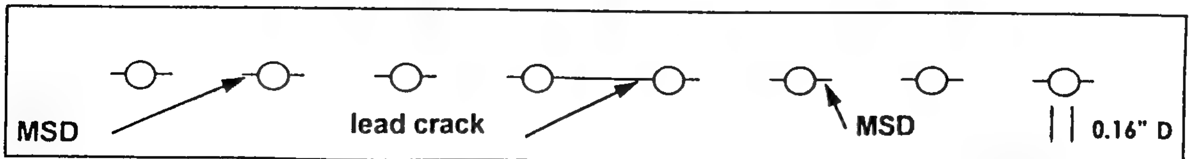

Purdue Structural Integrity Program

MSD CONFIGURATIONS

- 'Lead Crack' in Center. MSD at all holes.

$2a_{Lead}$ = 1.29", 1.38" and 3.40". Typical $a_{msd} \approx 0.15$".

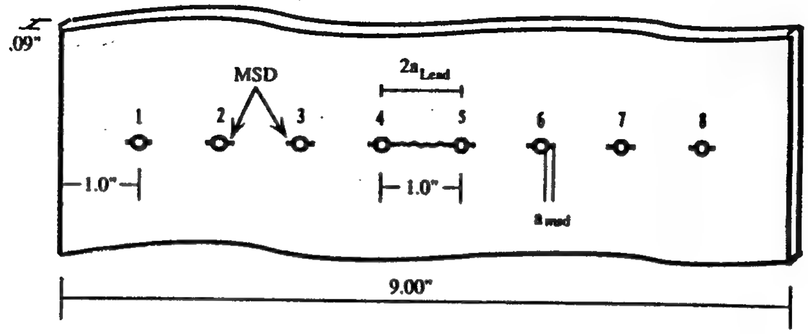

United States Coast Guard
Aeronautical Engineering

Purdue University
Aeronautical & Aerospace Engineering

ALGORITHM

- Calculate the Stress Intensity Factor (ΔK) at each crack tip.
- Compute each crack's growth rate (da/dN).
- Determine the number of cycles (ΔN) to grow the smallest crack a specified amount (Δ):

$$\Delta N = (\Delta) / (da/dN)$$

- Calculate crack growth (Δa) of all other cracks:

$$\Delta a = (\Delta N) * (da/dN)$$

- Iterate until panel "fails".

United States Coast Guard
Aeronautical Engineering

Purdue University
Aeronautical & Aerospace Engineering

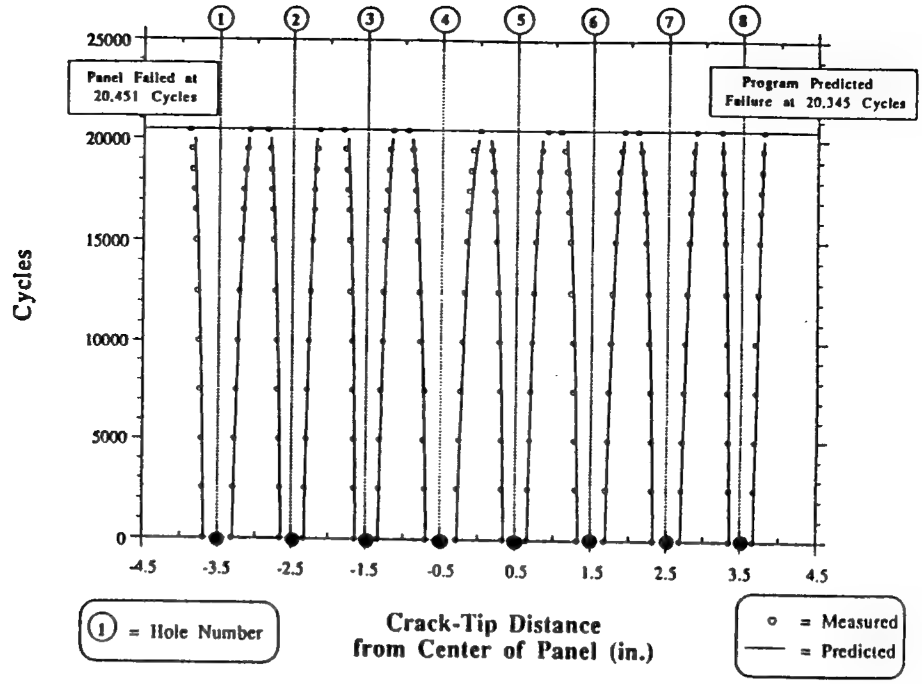

Figure 4-12 Crack Propagation Diagram for MSD04.

MSD07 -- Crack Propagation

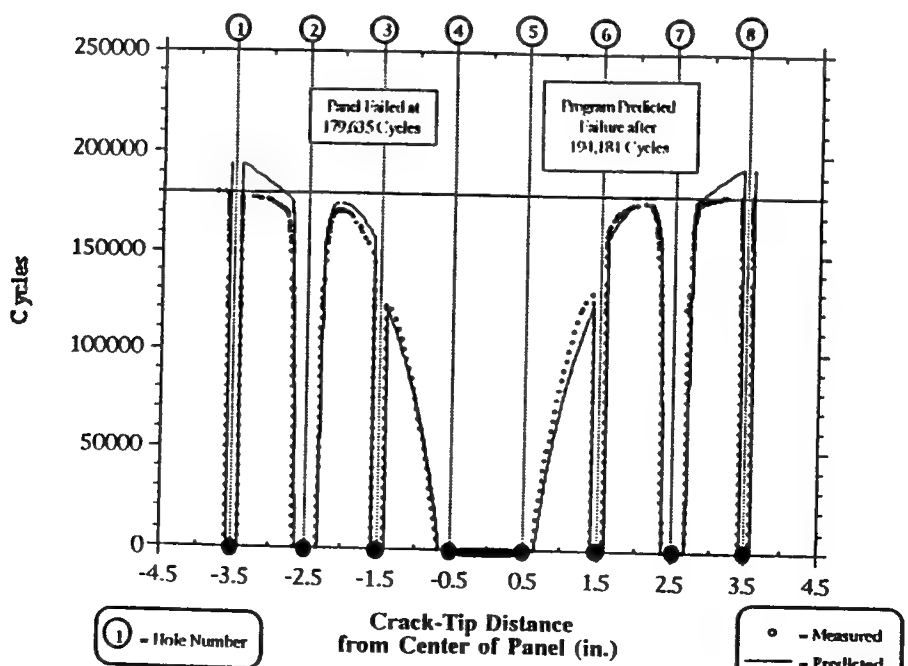

Probabilistic MSD Model

- Objective: Incorporate probabilistic aspects to deterministic model for MSD fatigue life
- Variables:
  - initial crack sizes (eifs distributions)
  - fatigue crack growth properties (use Hillberry, Ostergaard fit of Virkler 2024-T3 data)

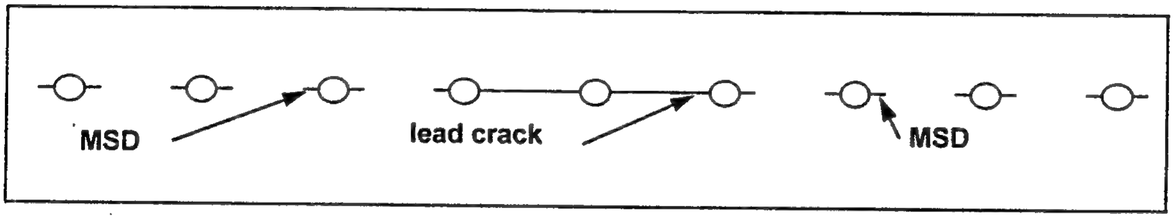

SUMMARY OF PREDICTED FATIGUE LIVES WITH TEST RESULTS

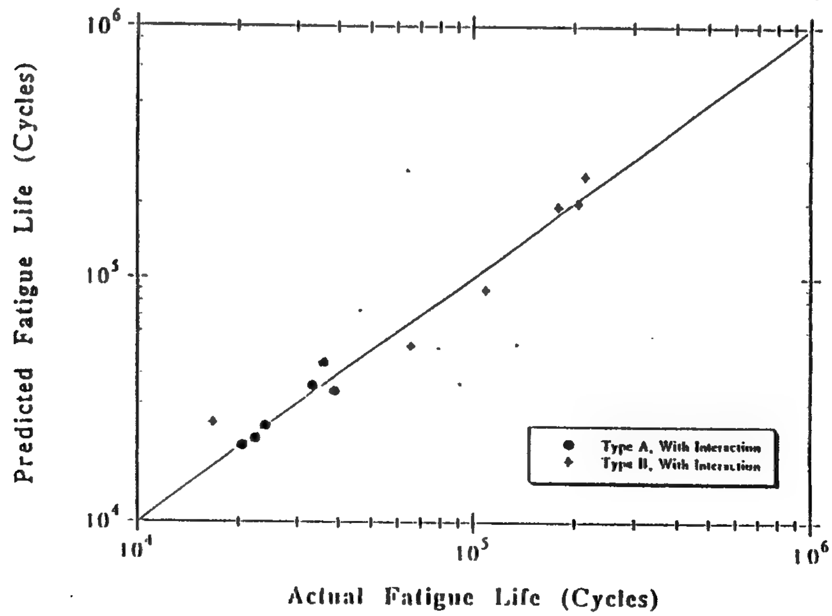

Probability damage model combinations

Crack Size Variability	Material Variability: mean	Material Variability: variable each panel	Material Variability: variable each hole
mean		CASE 1 $\bar{C} \bullet \tilde{M}_p$	
variable (sym) each hole	CASE 2 $\tilde{C}_i \bullet \bar{M}$	CASE 4 $\tilde{C}_i \bullet \tilde{M}_p$	CASE 6 $\tilde{C}_i \bullet \tilde{M}_h$
variable (unsym) each hole	CASE 3 $\tilde{C}_{ij} \bullet \bar{M}$	CASE 5 $\tilde{C}_{ij} \bullet \tilde{M}_p$	

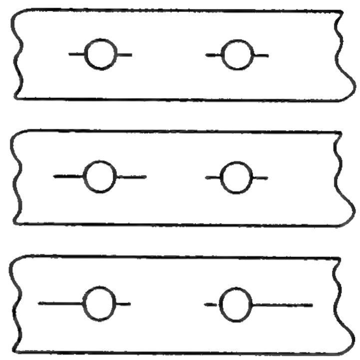

Remaining life to failure

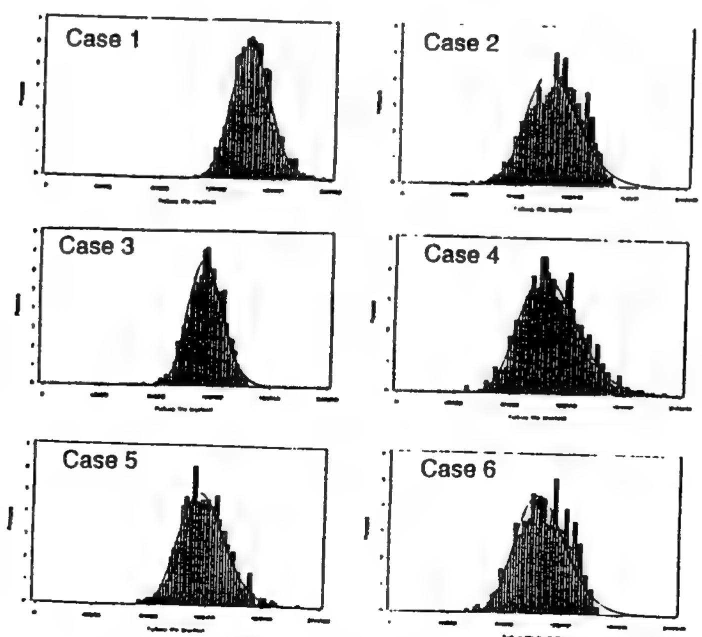

Probabilistic MSD Analysis

Applications:

- Determine when MSD develops
  - EIFS analysis for crack "Initiation"
- Determine degradation in lead crack residual strength as MSD develops

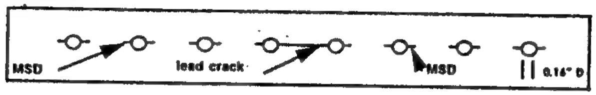

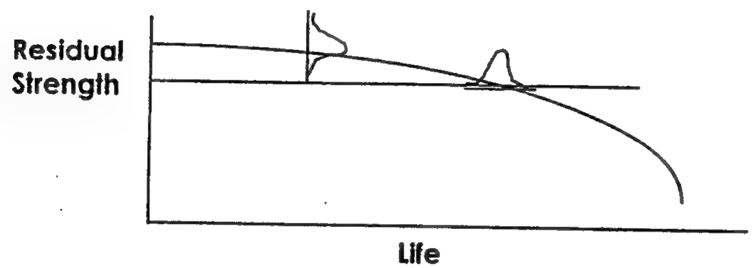

Purdue Structural Integrity Program

Representation of Corrosion Damage

Thickness Reduction (Global Damage)

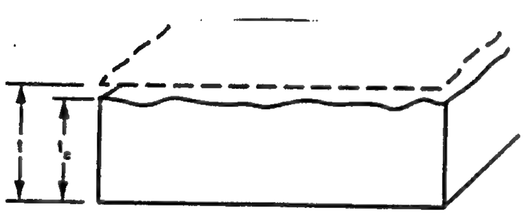

Widespread surface corrosion resulting in thickness reduction

t = Original thickness listed on part drawing

t_c = Corroded thickness (average)

⇓

increase stress

Stress Concentration (Local Damage)

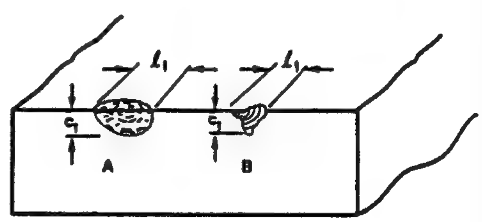

Stress concentration resulting from localized corrosion attack

A. Integranular attack

B. Corrosion pit

c_1 = Depth of penetration from the surface

ℓ_1 = Surface dimension

⇓

initial crack

Application of Fracture Mechanics

- Quantify existing corrosion state w.r.t. remaining life criteria:

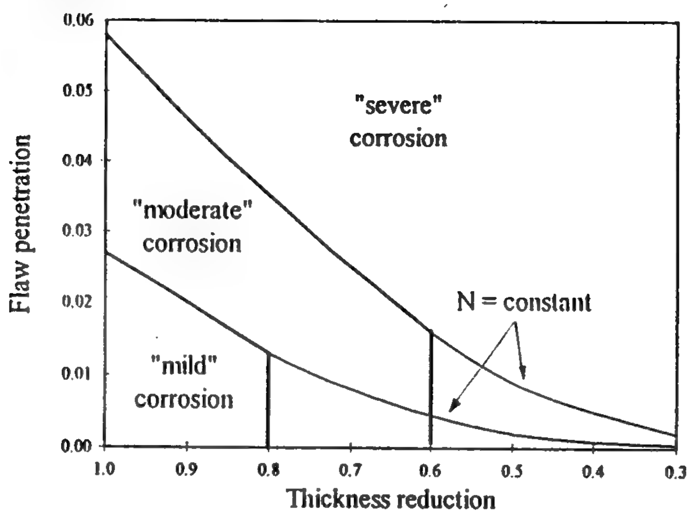

Fix
- geometry
- stress

- Structural evaluation tool ➡handbook format

Multi-site Damage Panel

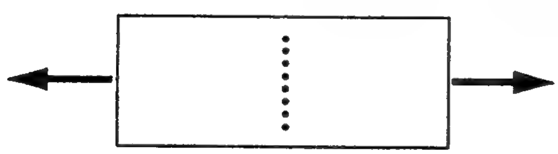

8 holes
all holes with sym. cracks
all cracks equal length

Refs: Neussl
Moukawsher

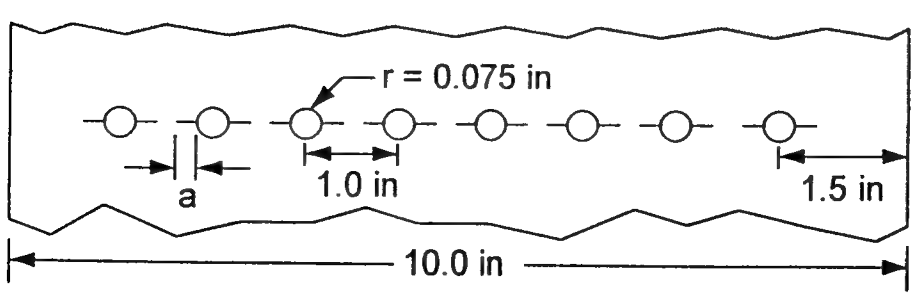

MSD Panel Results

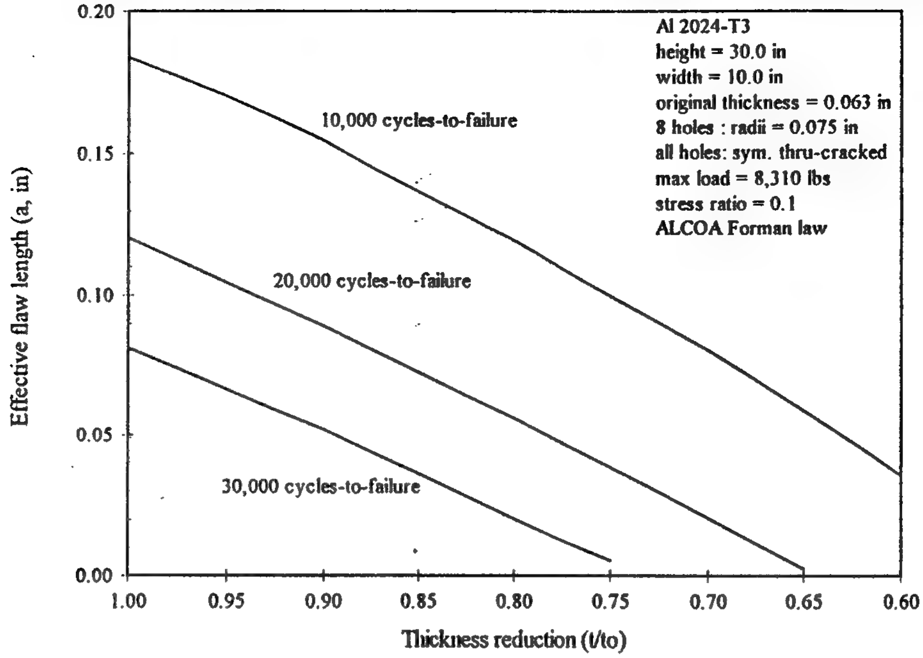

Planned Test Program

- Artificial corrosion method
  - Alternate Immersion (ASTM G-44)
  - Vary exposure to produce degrees of damage
- Material
  - Al 2024-T3
- Cyclic loading
  - constant amplitude (after corrosion)--various stress levels
  - variable amplitude?
- Specimen geometries
  - rectangular strips
  - notched strips (holes)
  - other? ~ lap-joint

Aged Material Response

- **Objective:**
  - Determine if cyclic and static properties of "aged" materials differ from design allowables
- **Approach:**
  - Measure stress-strain, S-N, and fatigue crack growth in retired aircraft material
    - » (7075-T6, 2024-T3, 2024-T4, 7178-T6)
  - Determine whether prior service degraded properties below MIL-HDBK 5 allowables

Aged Material Response

- **Status:**
  - Have 1 KC-135 fuselage lap joint panel (7075-T6 clad)
  - Preliminary da/dN tests in progress
  - Measure da/dN via compliance
  - Need panels with various degrees of corrosion

Crack Measurements: Compliance vs Optical

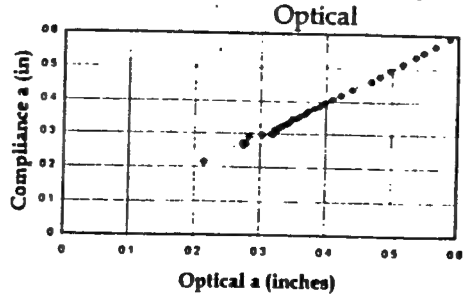

Damage Development due to Fretting Fatigue

- Objective:
  - determine fretting fatigue crack formation and growth mechanisms in aircraft joints
- Approach:
  - measure effect of contact pressure, size and tangential force on initiation of fretting fatigue
  - employ 3-d Boundary Element Analysis to calculate stress intensity factors and predict da/dN
  - employ 3-d finite element analysis to characterize fretting zones in joints
  - relate fretting fatigue to initiation of MSD in structure

Composite Patch Repair of Cracked Metallic Structures

- Objective: Study basic issues that control effectiveness of composite patch repair of metal structures
- Approach:
  - model stress intensity factor reduction with finite element models
  - study bending issues
  - examine patch stiffness, thickness, and geometry
  - unidirectional versus laminate layups
  - type of composite used for patch
  - adhesive/surface treatment issues
  - adhesive properties and thickness

Summary

- Interdisciplinary research program began 1 July 93
  - 6 faculty/4 departments
- Focus on:
  - crack formation (fretting, corrosion, EIFS)
  - crack growth/interaction (MSD)
  - residual strength
  - failure prevention/repair
- Presentations
  - USAF SAB
  - AIAA SDM - 2 papers
  - NASA/FAA Aging Aircraft Conf -3 papers
- Campus impact
  - faculty team
  - industrial collaborations
  - laboratory developments
  - courses

MECHANICS OF WIDE-SPREAD FATIGUE DAMAGE AND LIFE- EXTENSION METHODOLIES

Satya N. Atluri

Institute Professor & Regents' Professor of Engineering

Georgia Institute of Technology

Presented at the

Oklahoma City Air-Logistics Center

17 May 1994

Research Funded By
The Air Force Office of Scientific Research
(Dr. James Chang)

ANALYSIS OF PATCHED CRACKS

SHEET WITH REPAIRED CRACK

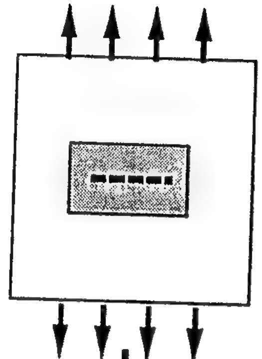

COMPUTE PATCH STRESS BY FEM USING

$$K_a = \frac{A_a}{\left(\frac{t_a}{G_a} + \frac{3\,t_s}{8\,G_s} + \frac{3\,t_p}{8\,G_p} \right)}$$

TO MODEL ADHESIVELY BONDED PATCH

SHEET WITH PATCH STRESSES APPLIED

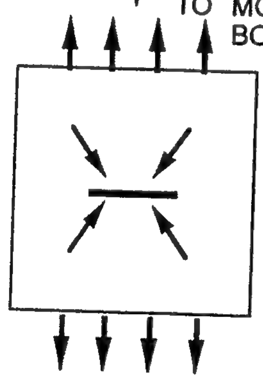

HEATER BLANKET METHOD

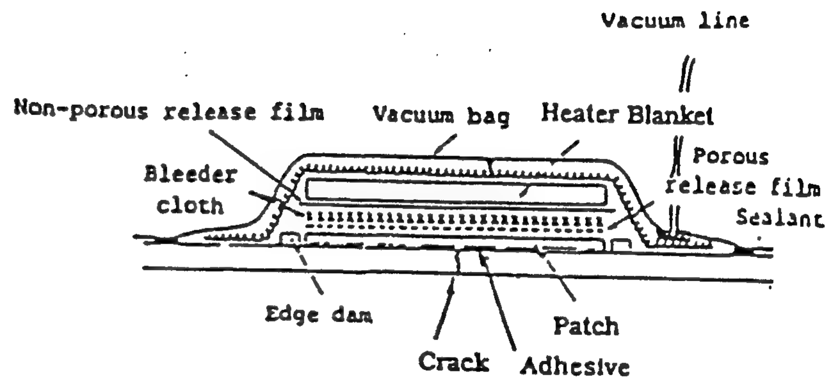

HEATER BLANKET METHOD FOR REPAIR APPLICATION USING VACUUM BAG FOR IN-SITU CO-CURE

ANALYSIS RESULTS

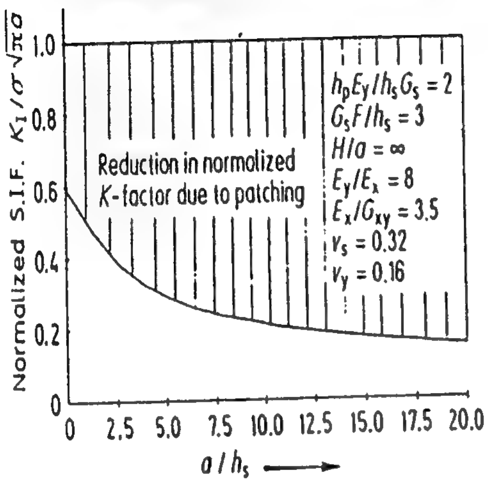

REDUCTION IN NORMALIZED K FACTOR

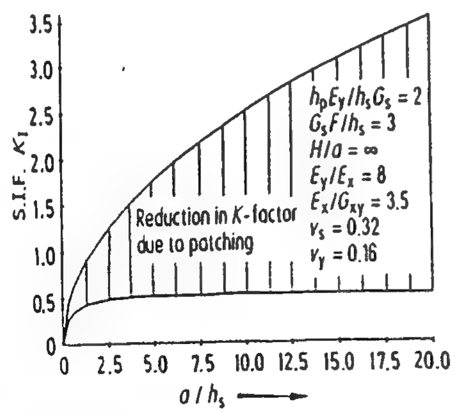

REDUCTION IN ACTUAL K FACTOR

GEORGIA TECH

ALGORITHM FOR REPAIR ANALYSIS

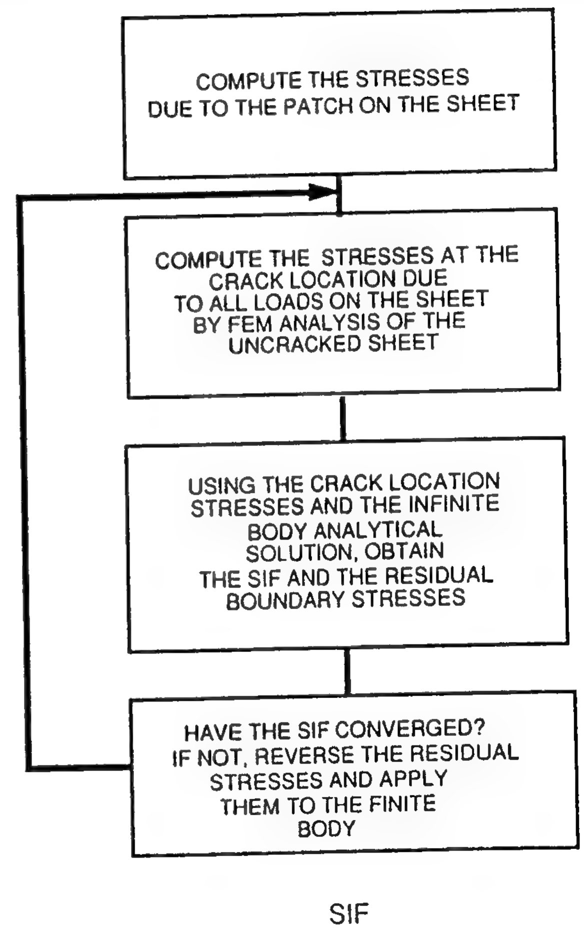

TYPICAL PROPERTIES OF UNIDIRECTIONAL COMPOSITES

PROPERTY	Graphite/ Epoxy (V_f = 60%)	Boron/ Epoxy (V_f = 50%)	Glass/ Epoxy (V_f = 45%)	Aramid/ Epoxy (V_f = 60%)
Strength, GPa				
longitudinal				
tensile	1.1	1.3	1.1	1.4
compressive	0.7	2.5	0.6	0.2
transverse				
tensile	0.02	0.06	0.03	0.01
compressive	0.13	0.20	0.12	0.05
Modulus, GPa				
longitudinal	130	200	40	80
transverse	7	19	8	6
shear	6	6	4	2
Shear Strength, GPa	0.06	0.07	0.07	0.03
Poisson's ratio, ν_{12}	0.28	0.23	0.26	0.34

ANALYSIS RESULTS

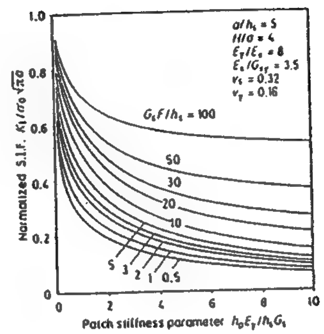

Reduction in SIF Vs Patch Stiffness

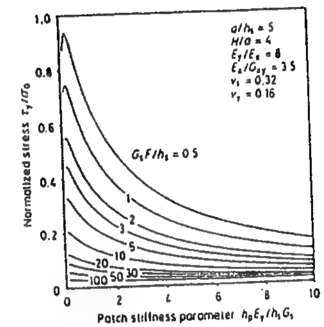

Patch Shear Stress at x=0 y=0 Vs Patch Stiffness

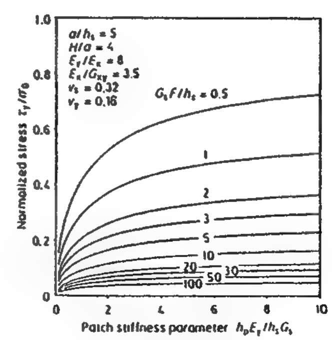

Patch Shear Stress at x=0,y=H Vs Patch Stiffness

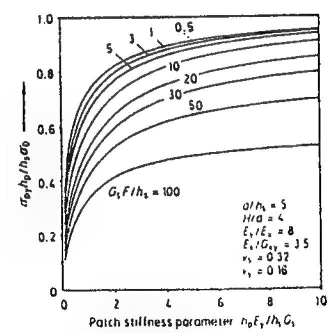

Patch Normal Stress at x=0,y=0 Vs Patch Stiffness

COMPARISON WITH EXPERIMENTS

CRACK LENGTH Vs NUMBER OF CYCLES

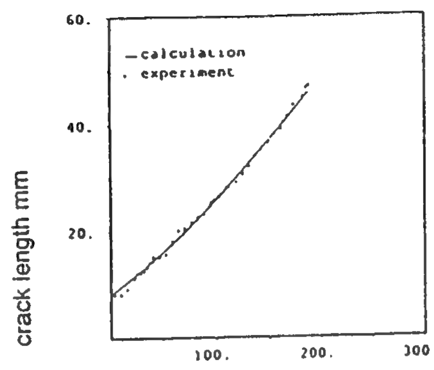

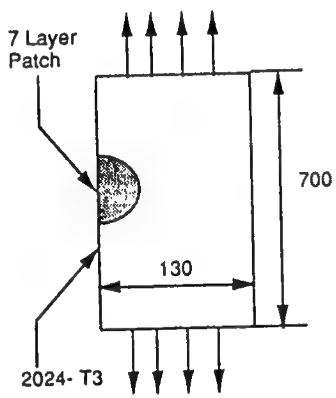

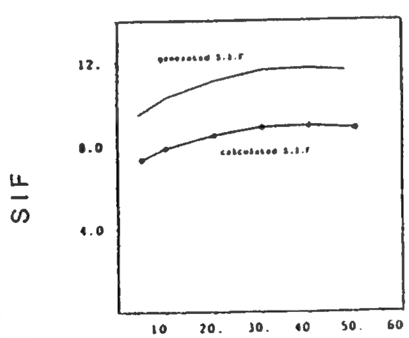

DIRECTLY INFERRED SIF Vs INFERRED FROM FATIGUE DATA

ANALYSIS RESULTS - HOLE CRACK

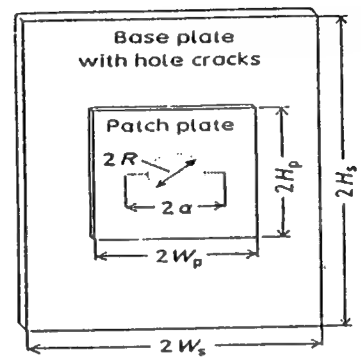

MODEL

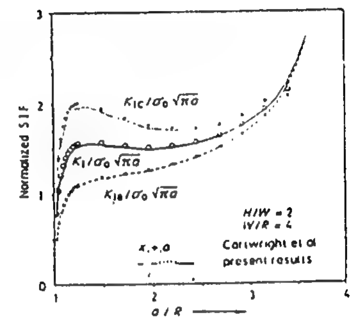

VARIATION OF SIF - UNREPAIRED

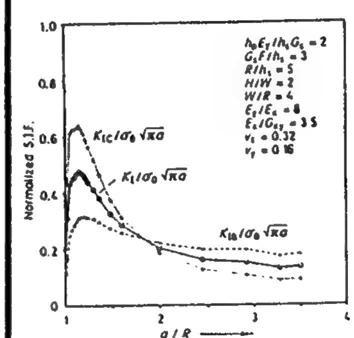

VARIATION OF SIF - REPAIRED

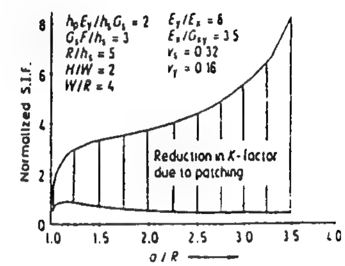

REDUCTION IN SIF

VARIATION OFSHEAR STRESS

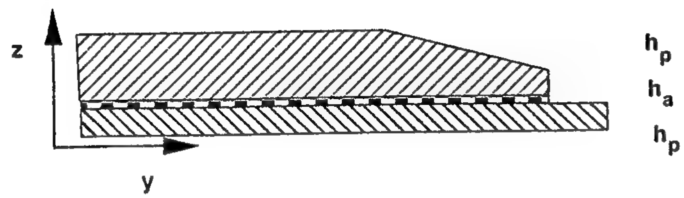

$E_s = 71{,}000$ MPa $\gamma_s = 0.32$ $G_{xy} = 7240$ MPa

$E_{xp} = 25400$ MPa $E_{yp} = 208000$ MPa $G_a = 965$ MPa

$h_a = 0.1$ mm $h_p = 0.889$ mm $h_s = 10$ mm $\nu_y = 0.168$

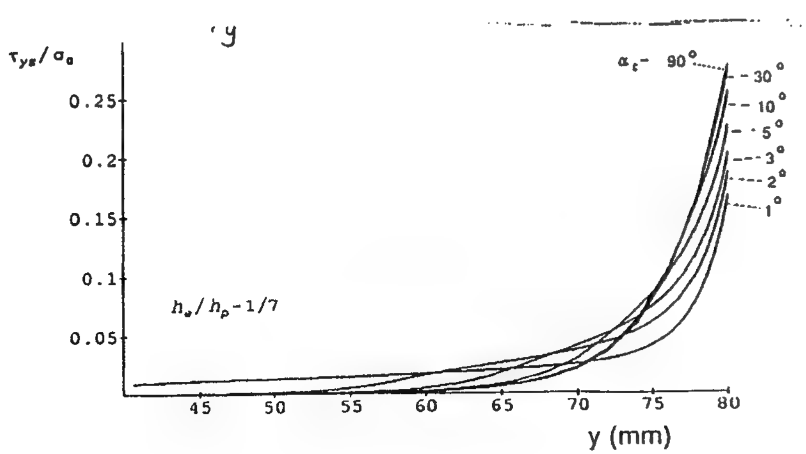

COMPARISON WITH EXPERIMENTS

COMPARISON OF CALCULATED FATIGUE CRACK GROWTH HISTORY.

- CALCULATED SIF ADJUSTED FOR POSSIBLE DISBONDING

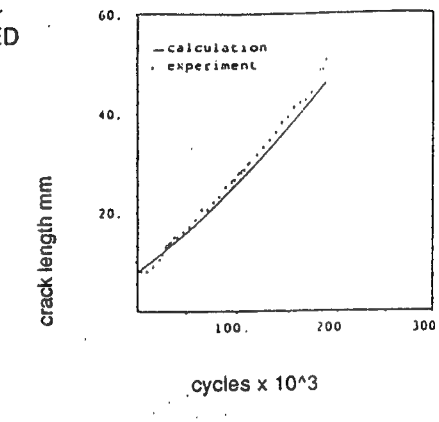

Expt. 2

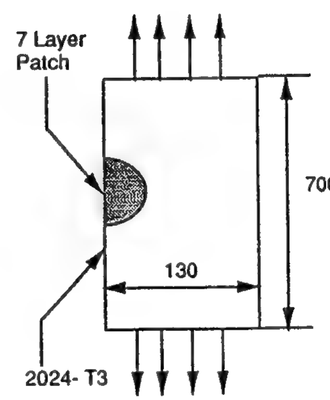

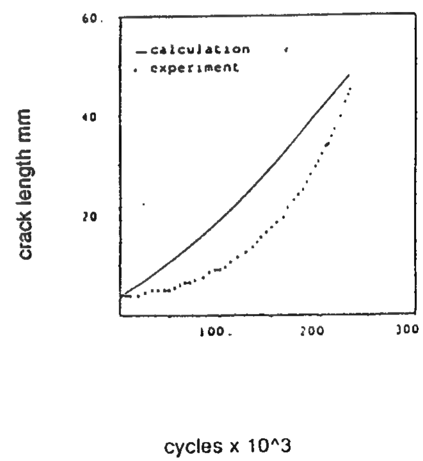

Explt 3.

VARIATION OF SHEAR STRESS

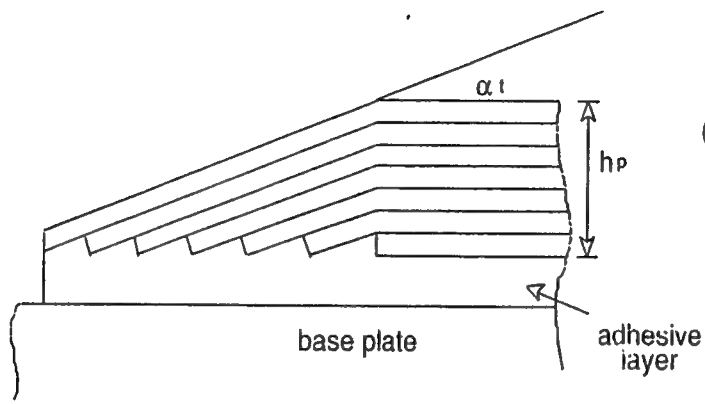

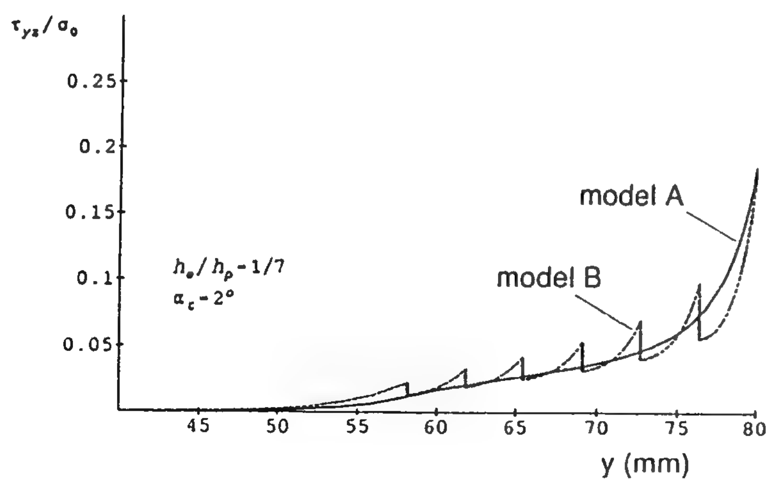

model A
(used in previous examples)

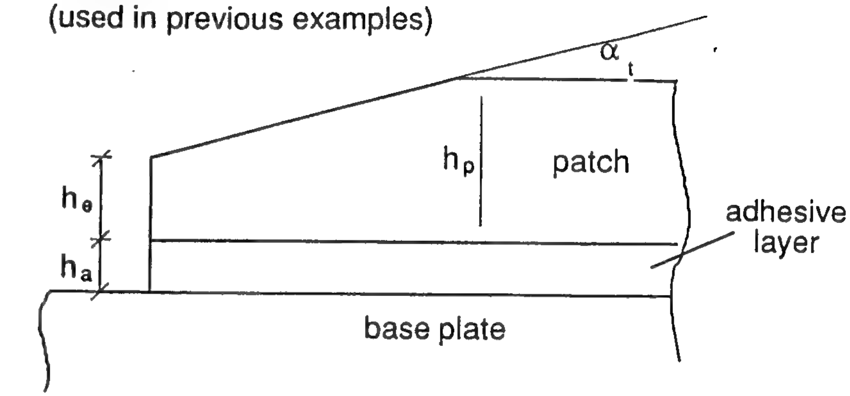

model B
(more realistic model)

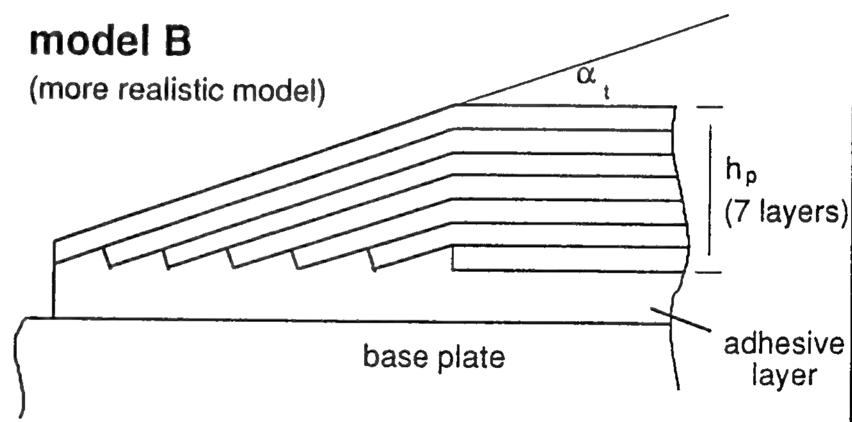

Adhesive layer thickness is changing with y coordinate

VARIATION OF NORMALIZED SIF

VARIATION OF NORMALIZED SIF AS A FUNCTION OF b_d/a. b_d IS THE MINOR AXIS OF AN ELLIPTICAL DEBONDING REGION.

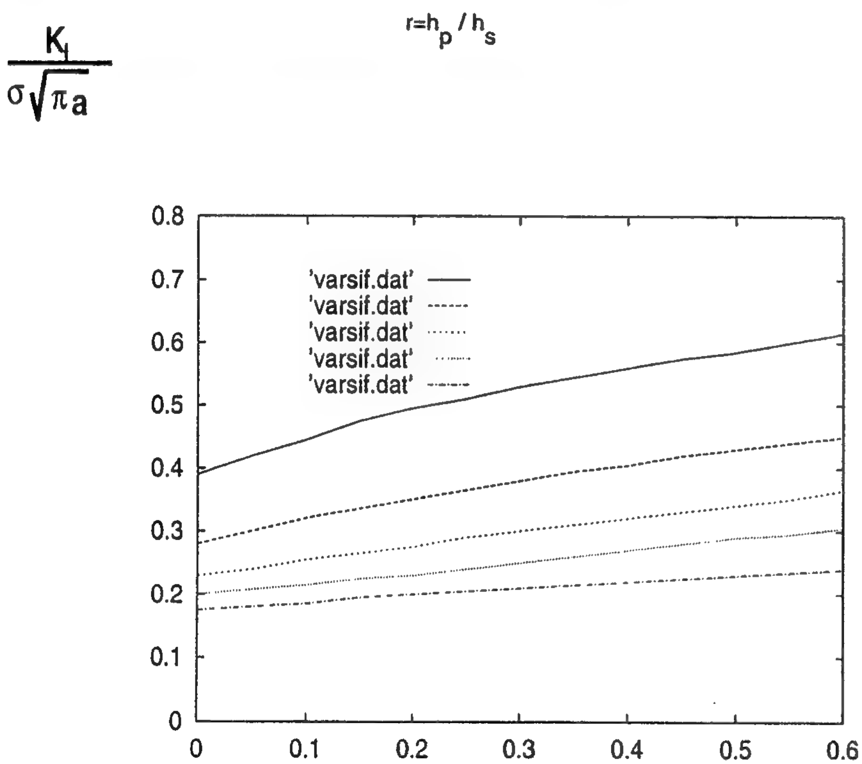

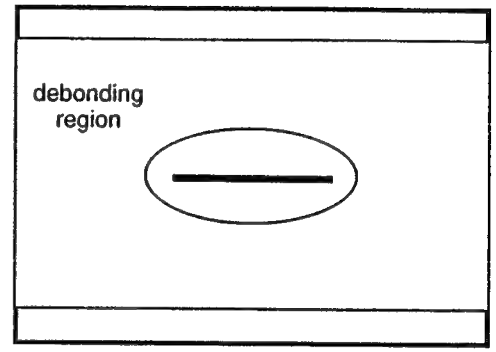

Debonding Region

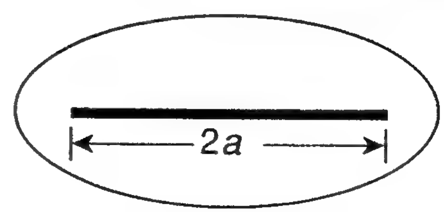

GEORGIA TECH

VARIATION OF SIF

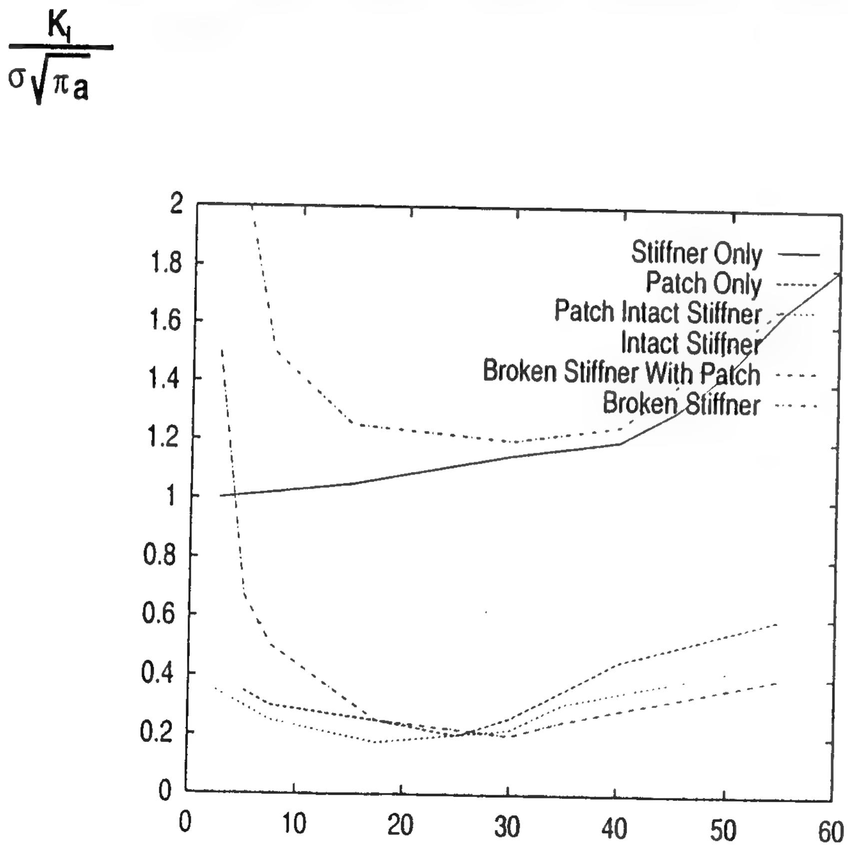

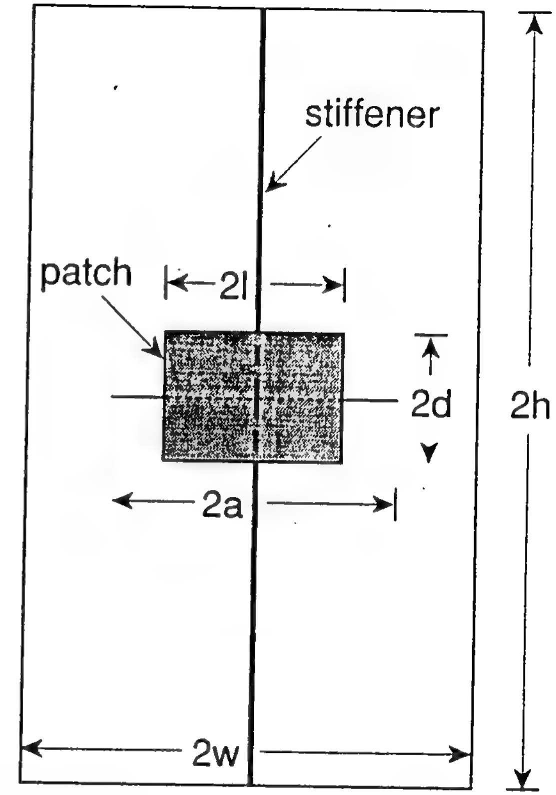

Patched and Stiffened Center Cracked Sheet

GEORGIA TECH

FATIGUE CRACK GROWTH METHODOLOGY

CALCULATE STRESS INTENSITY FACTORS AS A FUNCTION OF CRACK SIZE AND SHAPE WITH SAFEFLAW3D

VARIABLE AMPLITUDE LOAD DATA

↓

CALCULATE CRACK GROWTH CYCLE BY CYCLE UNDER SPECTRUM LOADING WITH NASA FLAGRO

↓

CRACK GROWTH RESULTS

Figure 1

REPAIR ANALYSIS - 3D

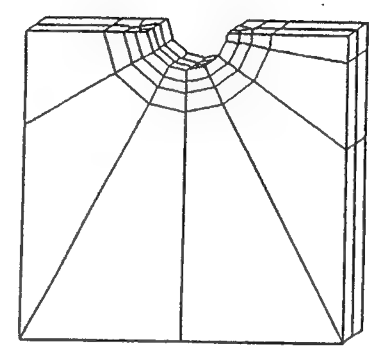

FEM MESH FOR BASE PLATE

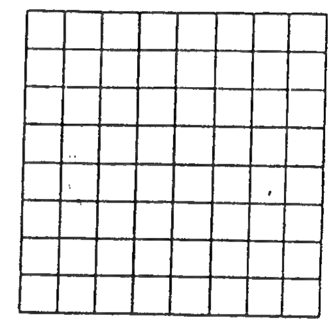

FEM MESH FOR PATCH PLATE

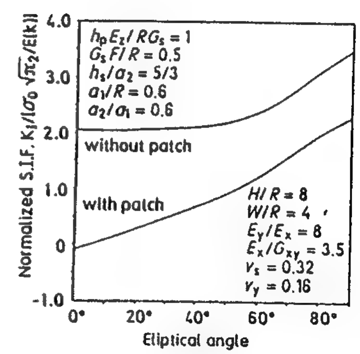

VARIATION OF SIF WITH AND WITHOUT PATCHING

GEORGIA TECH

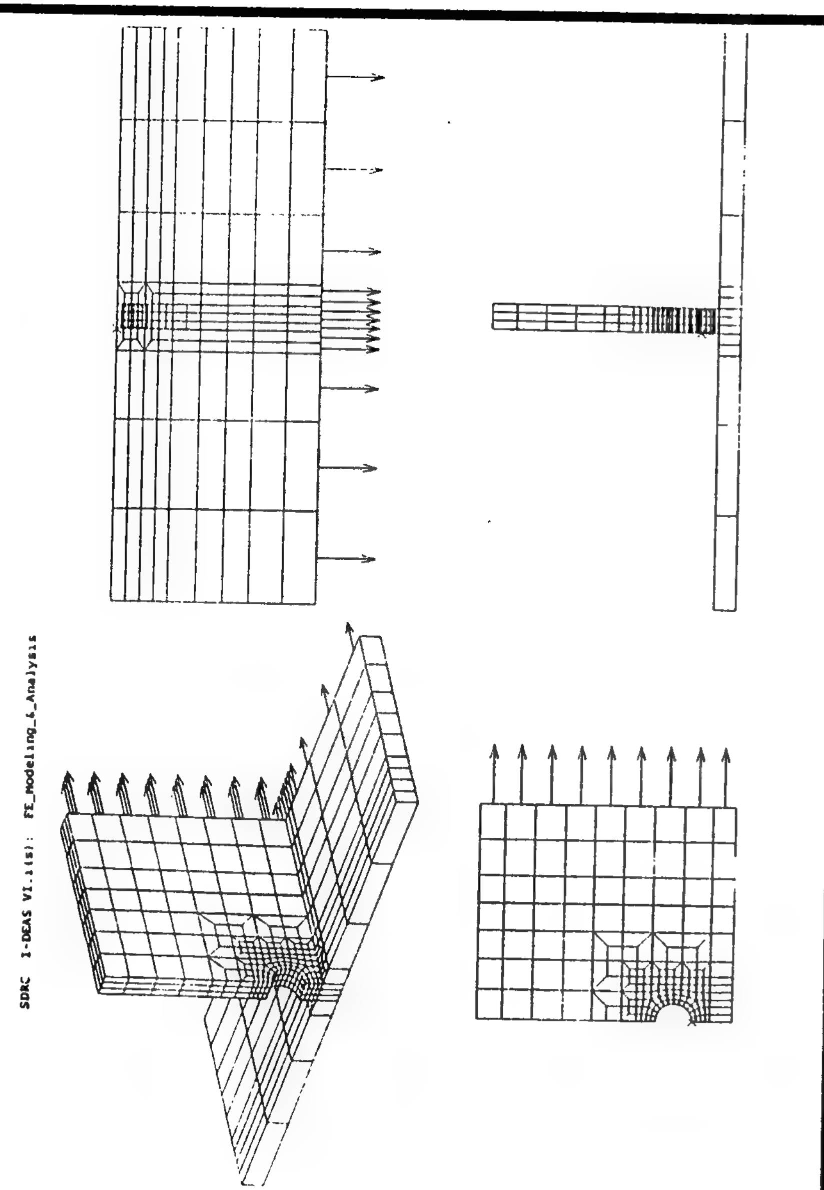

Figure 3

C-141B WEEP HOLE GEOMETRY AND MATERIAL PARAMETERS

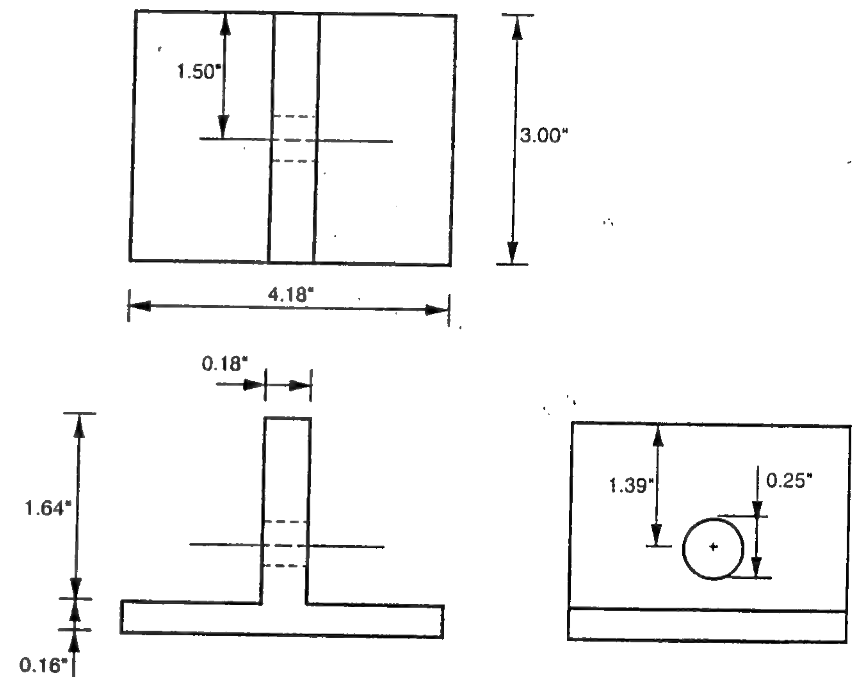

Material: AL 7075-T651
Young's Modulus: 10.3E+06
Shear Modulus: 3.9E+06
Poisson's Ratio: 0.33

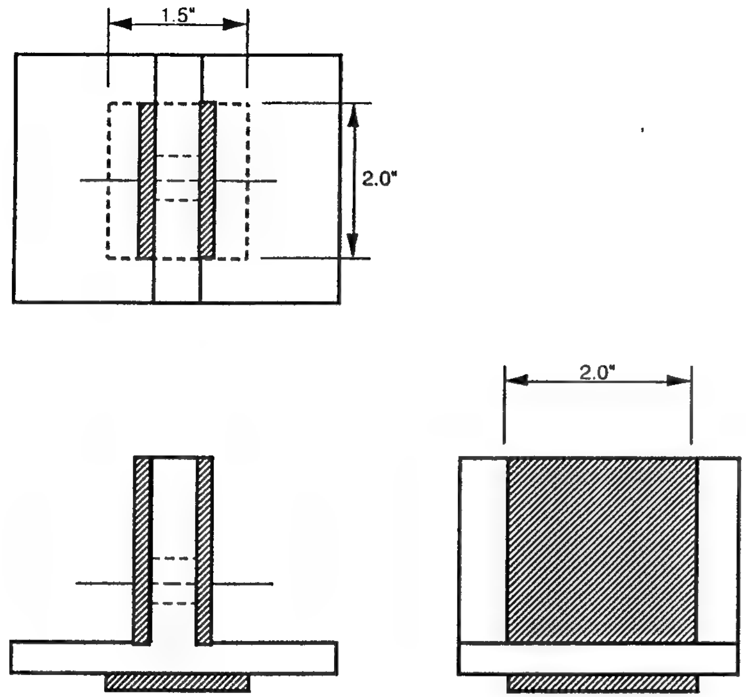

Material: Boron-Epoxy
Thickness: 0.04"
E_x: 30.2E+06 psi
E_y: 3.69E+06 psi
G_{xy}: 1.05E+06 psi
G_{xz}: 1.05E+06 psi
G_{yz}: 0.716E+06 psi
υ_{xy}: 0.1677

Material: Adhesive
Thickness: 0.004"
Young's Modulus: 0.31E+06 psi
Shear Modulus: 0.105E+06 psi
Poisson's Ratio: 0.48

Figure 5

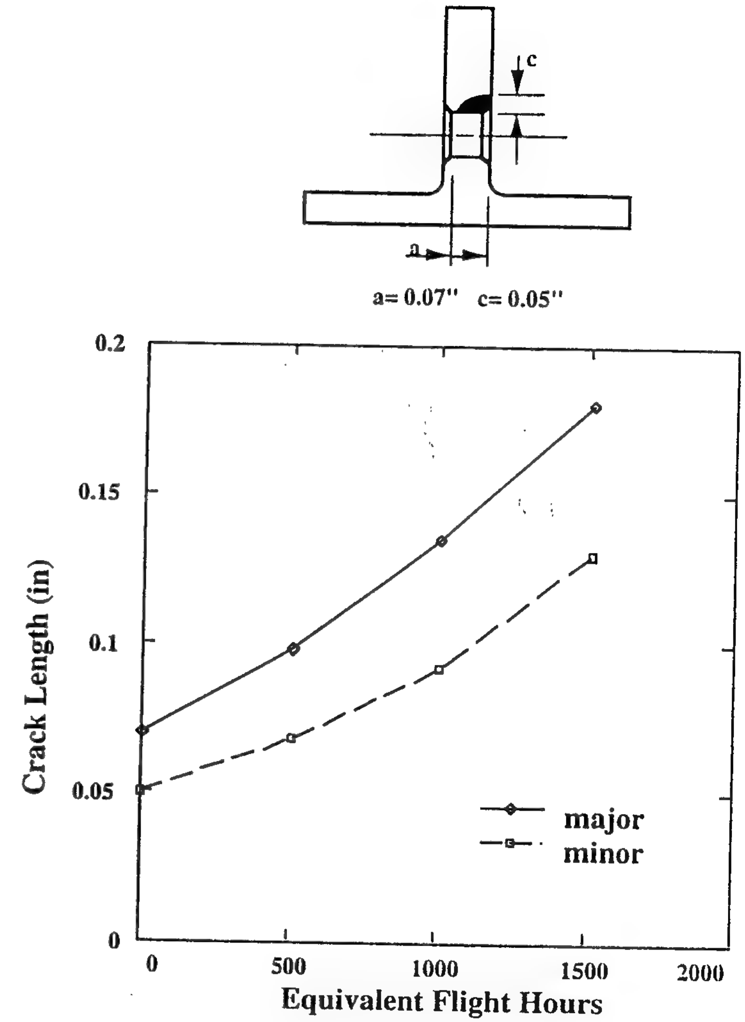

Figure 4

CASE 2

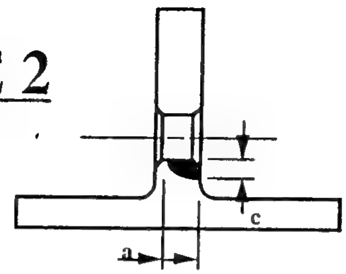

a= 0.10"   c= 0.08"

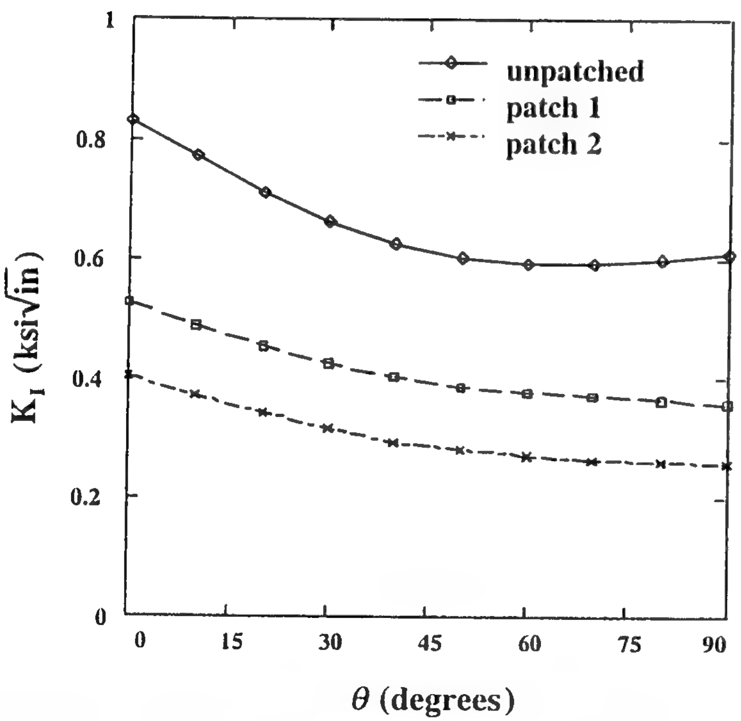

Figure 7

CASE 1

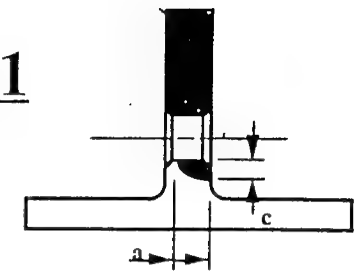

a= 0.10"   c= 0.08"

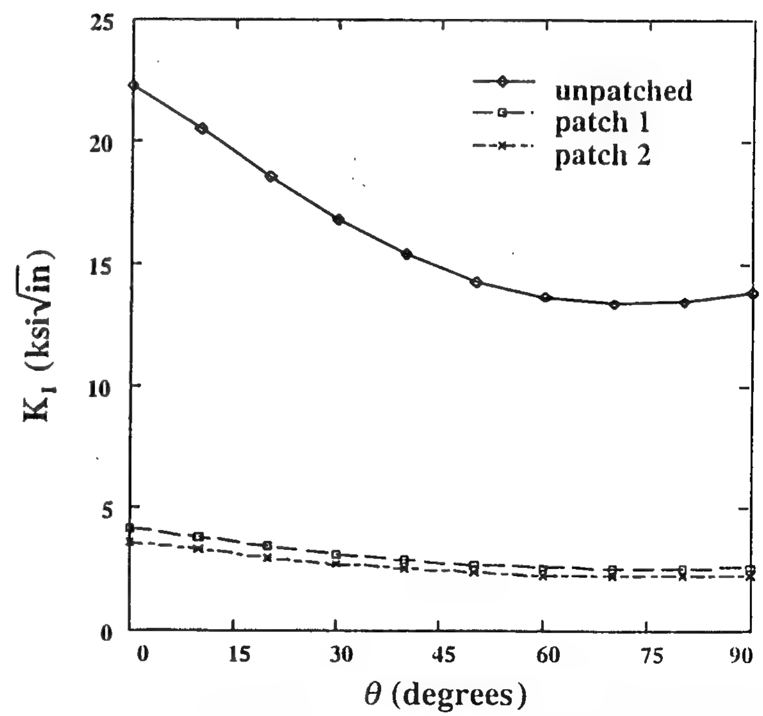

Figure 6

CASE 4: Upper Crack

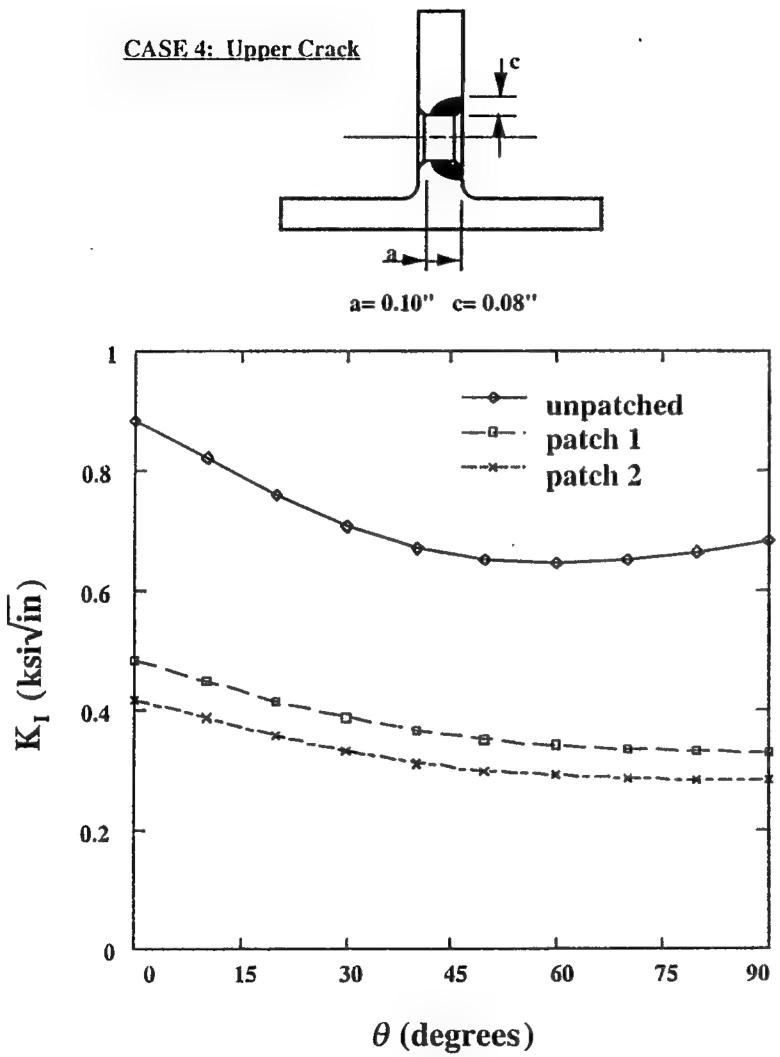

Figure 9

CASE 3

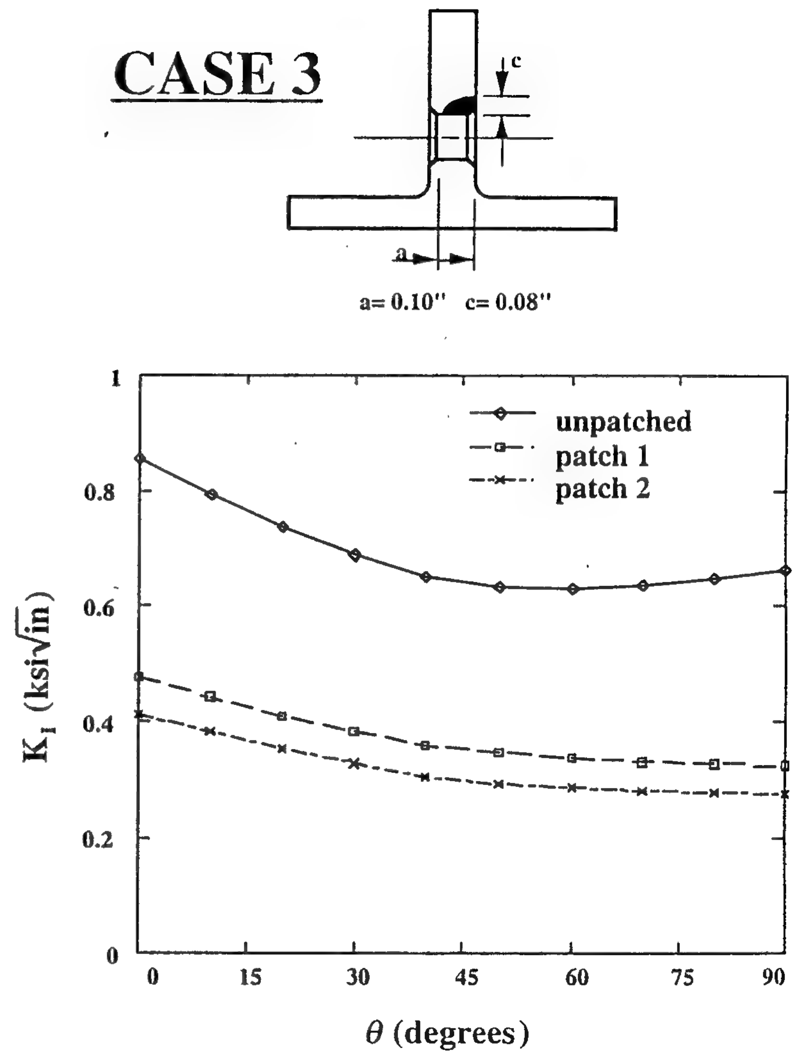

Figure 8

CASE 4: Lower Crack

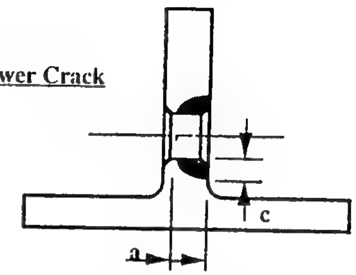

a= 0.10"   c= 0.08"

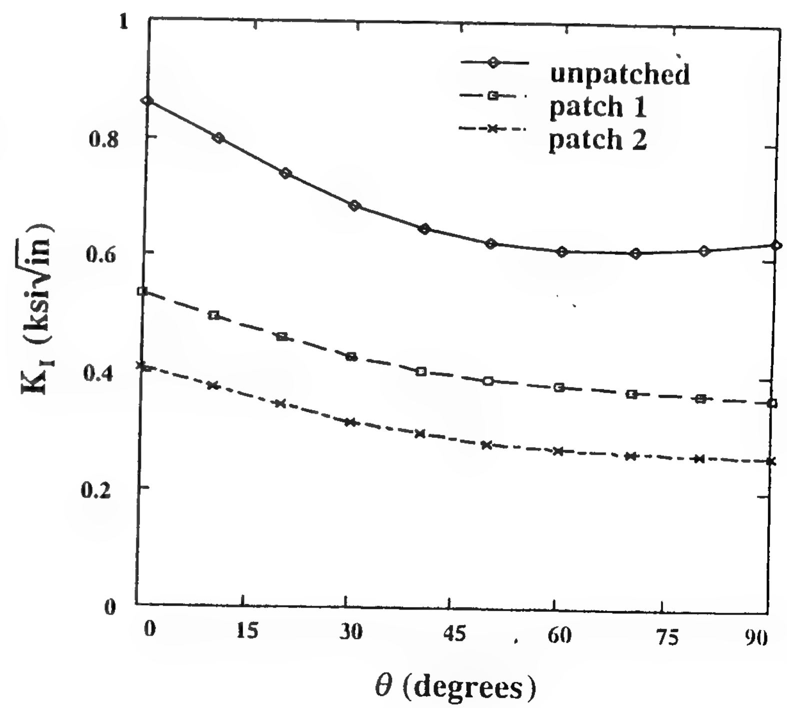

Figure 10

Second Air Force Aging Aircraft Conference
Oklahoma City, OK -- 17-19 May 1994

CORROSION AND FATIGUE OF ALUMINUM ALLOYS: CHEMISTRY, MICROMECHANICS AND RELIABILITY

ROBERT P. WEI
Department of Mechanical Engineering and Mechanics
& Zettlemoyer Center for Surface Studies
LEHIGH UNIVERSITY
Bethlehem, PA 18015

TABLE OF CONTENTS

ANALYSES AND DETECTION OF FRETTING CORROSION
IN AIRFRAME RIVETED AND PINNED CONNECTIONS
(F49620-93-1-0488)

ABSTRACT

This project is assessing the contribution of fretting to the corrosive deterioration of riveted and pinned connections of aging Air Force airframes. Finite element calculations are being performed to evaluate the mechanical parameters, including the contact pressure and cyclic slip amplitude, that govern the fretting process. A piezoelectric fretting wear machine has been designed and constructed that can reproduce the fretting conditions in connections. The machine will be used to perform systematic measurements of fretting corrosion of aluminum alloys in contact with either aluminum or steel. In addition, tests of simple, riveted connections under severe fretting and corrosion conditions are being performed. These samples will be used to evaluate NDE procedures for the early detection of corrosion in connections.

1. INTRODUCTION

1.1 Background

Corrosion of riveted connections and splices of aging Air Force airframes is a pervasive problem. According to R. Kinzie and D. Hazen of the AF Warner Robins ALC, the corrosion damage of riveted connections is frequently extensive. It can produce exfoliation, visible swelling of the rivet surroundings and even the extrusion of the rivet, and frequently requires repair work. Yet the presence of the corrosion can remain hidden to the eye by the exterior paint. When corroded joints are repaired, all of the surrounding metal affected by corrosion must be removed to prevent rapid recurrence. Fretting, by exposing clean metal surfaces and metal wear fragments can accelerate corrosion, but relatively little is known about either the fretting conditions generated in connections or the contribution of fretting to corrosion damage.

The tribological conditions favoring fretting wear are large values of the specific wear rate, the contact pressure and the

TABLE 1. DEPENDENCE OF THE DEPTH OF THE FRETTING DAMAGE (WEAR PLUS CORROSION) ON THE SPECIFIC WEAR/CORROSION RATE FOR CONDITIONS ENCOUNTERED IN AIRFRAME CONNECTIONS*

Specific Wear Rate m^3/Nm	10^{-15}	10^{-14}	10^{-13}	10^{-12}
Depth of Damage, μm				
For $\delta = 10\ \mu m$	0.4	4.0	40	400
For $\delta = 30\ \mu m$	1.2	12	120	1200

* Estimated using Equation 1 in footnote on p. 4 and $N = 5 \cdot 10^4$ cycles and a contact pressure $p = 400$ MPa.

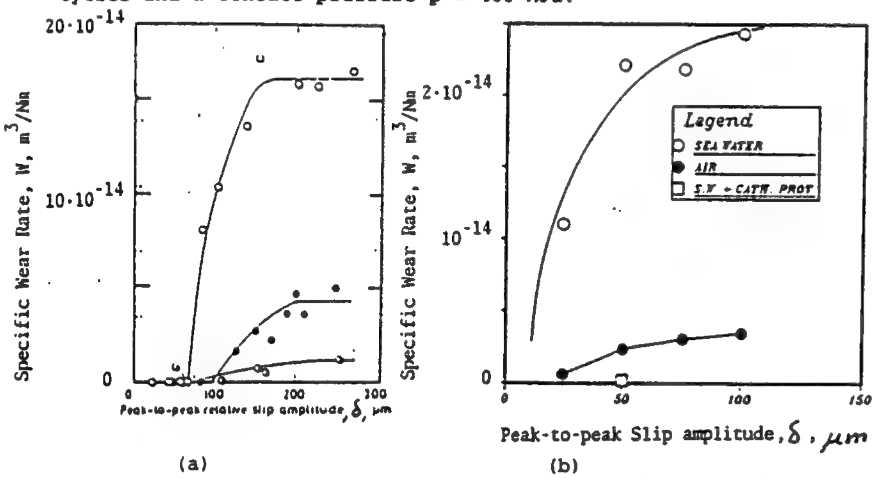

Figure 1. Influence of corrosive conditions on the specific wear rates produced by fretting with different slip amplitudes: (a) Age hardened AL-Zn-Mg alloy in contact with itself: o-in wet air, •-dry air and ⊙-dry argon. after Goto, Ashida and Endo (3) and (b) 0.64% C steel in contact with itself: O-in sea water, ●-air and □-in sea water with cathodic protection after Pearson and Waterhouse (4).

amplitude[1]. The specific fretting wear rate, W, chages radically with the amount of slip, increasing from $W = 10^{-16}$ m^3/Nm to $W = 5 \cdot 10^{-14}$ m^3/Nm or by about 500-fold in the range $\sim 10\ \mu m < \delta < \sim 100\ \mu m$ (1,2). There is a synergistic relation between corrosion and the fretting wear of aluminum in contact with aluminum and steel against steel (3,4), and this is also likely to be the case for steel against aluminum. Goto, Ashida and Endo (3) have conducted a systematic study of environmental effects on the fretting wear behavior of an age hardened Al-Zn-Mg alloy in contact with itself. Their findings are reproduced in Figure 1a. Consistent with expectations, the material loss rate (wear plus corrosion) increased by a factor of about 4.5x when fretting proceeded in the presence of wet air. According to Table 1, a measured wear rate of $W = 1.5 \cdot 10^{-13}$ m^3/Nm, for aluminum fretting against aluminum in wet air, could convert an ~100 μm-deep layer of metal on either side of the fretting interface to corrosion product provided the slip amplitude $\delta > 50\ \mu m$. Studies by Pearson and Waterhouse (4) summarized in Figure 1b show similar, 3-fold increase in the material loss rate when the fretting of steel proceeds in seawater as opposed to air. In this case, the electrochemical nature of the fretting corrosion is demonstrated by the large reductions in the loss rate realized by cathodic protection. No information is available on the material loss attending the fretting contact of steel against aluminum.

The actual values of pressure and slip amplitude are not known for pinned and riveted connections. These parameters depend on such features as: (i) the interference between the hole and the fastener, and (ii) the lateral support derived from clamping and

---

[1]Fretting wear can be expressed in terms of the average depth of the fretting damage (wear scar), y:

$$y = 2N\ (W/\mu)\ F_1. \qquad (1)$$

where N is the number of fretting cycles, W is the specific wear rate of the system, μ is the coefficient of friction and $F_1 = p\mu\delta$ is the fretting wear parameter, p is the contact pressure, and δ is the per cycle, peak to peak slip amplitude. The specific wear rate W, is a property of all the materials in the system, and in the case of fretting, may also depend on δ and p.

adhesive bonds that reduce the forces acting on the bore (1). The relevant coefficient of friction and coatings that separate the contacting surfaces and inhibit corrosion also play a crucial role.

1.2 Objectives

This research initiation project has 2 general objectives. One is to assess the contribution of fretting to the corrosive deterioration of the riveted and pinned connections of aging Air Force airframes. To accomplish this, some of the analytical and experimental capabilities which would also be needed to pursue the control of fretting corrosion will be developed. These include analytical procedures for evaluating the mechanical fretting contact conditions, short duration tribolgical test methods for characterizing the long term fretting corrosion of airframe materials and coatings, and promising NDE concepts for detecting fretting corrosion in connections. Should the importance of fretting corrosion be confirmed, the present research will provide the foundations for a follow-on project on the control and detection of fretting corrosion.

1.3 Summary of Progress

Research began on September 1, 1993 and is currently in its 9th month. The study includes 6 tasks:

Task 1. Survey of Fretting in Airframe Connections.

The objective of this task is to identify airframe connections that have been particularly susceptible to corrosion damage. Though scheduled, work on this task has not yet begun.

Task 2. Continuum and Finite Element Modelling.

This task calls for continuum and finite element calculations of the mechanical parameters that govern fretting wear such as the contact pressure and slip amplitudes for 3 types of fretting elements: (i) airframe connections (ii) the tribological testing devices to be assembled as part of Task 3. and (iii) the model connections to be tested as part of Task 4. An idealized, 2-dimensional, pinned connection subject to cyclic loading has been analyzed. The results of this work are described more fully in Section 2.1 and in reference (5). The calculations define the fretting conditions in the connection which will be studied by Task 3.2. Work on a 2-dimensional model of a lap joint has been initiated. This will be followed by anayses of 3 dimensional model during the second year of the project.

Task 3. Tribolgical and Corrosion Measurements.

3.1 **Tribological Testing Devices.** The objective of this task is to acquire a tribometer capable of subjecting laboratory samples to the slip amplitudes and contact pressure conditions existing in connections. Such a device has been designed and built and is described in Section 2.2. The tribometer is currently undergoing calibration.

3.2 **Characterization of Fretting Corrosion.** Systematic studies of the fretting corrosion of aluminum against steel and aluminum against aluminum will begin as soon as the calibration work is completed. This work will draw on the fretting conditions already defined by Task 2.

3.3 **Accelerated Fretting Corrosion.** The last part of this task will seek procedures for accelerating corrosion to simulate long term service with short duration fretting. Anodic dissolution will be promoted with an imposed EMF. Initial efforts are described in Section 2.3.

Task 4. Material and Component Testing.

A limited number of simple, riveted connections will be tested with the aim of accomplishing the following:

(i) Test the reliability of the contact mechanics modelling of Task 2.
(ii) Evaluate the contribution of fretting to long term corrosion.
(iii) Calibration of the laboratory tests.
(iv) Generate model connections with different and well characterized amounts of corrosion for the NDE studies of Task 6.

This work has been begun and preliminary results are reported in the Section 2.3. The task also called for measurements of the cyclic, plastic constitutive relations of the sheet and rivet

materials needed for finite element modelling of Task 2. This work is being accomplished as part of a separate Air Force Project.

Task 5. <u>Metallographic Studies</u>.

This task provides for metallographic studies using optical and SEM of the tribometer samples and the fretted connections. Preliminary results are presented in Section 2.2.2.

Task 6. <u>Evaluation of Advanced NDI Procedures</u>

The objective of this task is to examine corroded connections prepared as part of Task 4 using SQUID AC-current and magnetic susceptibility imaging techniques developed by Prof. Wikswo and his associates at Vanderbilt University. The same corroded connections will be examined using ultrasonics, X-ray backscattering and ESPI by Prof. Achenbach and his associates at Northwestern University. The ability of these techniques to detect the corrosion will be evaluated. This work is scheduled to for the 3rd year of the project.

To summarize, work is underway on 4 of the 6 tasks and, with the exception of Task 1, is on schedule.

2. RESULTS

2.1 <u>Continuum and Finite Element Modelling (Task 2)</u>

2.1.1 Finite Element Models

A finite element model of an idealized, 2 dimensional, pinned connection in which the pin axis remains normal to the sheet has been devised. This model offers lower bound estimates of the slip amplitudes because: (i) it is less compliant than real connections where the pin or rivet shears or bends and (ii) it does not experience out-of-plane, slip displacements accompanying the shearing and bending of the fastener. The dimensions of the sheet and hole are shown in Figure 1a; the finite element model is shown in Figure 1b. The mesh has 4933 nodes, about 1400 elements and is more refined in the area adjoining the interface where most of the deformation is concentrated. The length of the sheet is 5.5 times its width so that the effect of far-field loading on the hole-sheet interface may be examined. In addition to fixing the pin at its center, the long sides of the sheet were constrained in the x-direction, in keeping with the conditions found within in a wide panel with many pins with a repeat distance of S = 30.6 mm (see Figure 2). The pin was modeled as purely elastic, consistent with the absence of plastic deformation except at its constrained center. The sheet was considered to be in plane stress; the pin was treated as if in plane strain.

The calculations were performed for a AA7075-T6 aluminum alloy sheet and its cyclic stress-strain response was approximated by isotropic hardening behavior with the following properties: elastic modulus, E = 70 GPa; yield strength, σ_0 = 531 MPa and plastic modulus (slope), M = 0.70 GPa, consistent with experimental measurements. The calculations were performed for an aluminum pin (E = 70.00 GPa) and a steel pin (E = 207 GPa), three pin diameters designed to produce 0%, 1% and 2% interference, and two values of the coefficient of friction at the pin-sheet interface: μ = 0.2 and μ = 0.5. A cyclically varying nominal stress was applied at the top surface of the sheet, with a peak value of 125 MPa to a minimum of 13 MPa (stress ratio R = 0.1). No plastic deformation was obtained after the first load-unload cycle.

Work has also begun on a 2-dimensional model of a lap joint with a "continuous" or smeared out rivet. This model is illustrated in Figure 3. It can account for lateral support derived from clamping and provides access to the out-of-plane slip displacements.

2.1.2. Results of Calculations

Figures 4 - 6 show the variations with angular location, θ, of the contact pressure, the slip, and the fretting wear parameter F_1. In all cases, the location θ = 0° corresponds with 3 o'clock; θ = ± 180° with 9 o'clock, with negative values in the 3d and 4th quadrants (see Figure 1). Results are presented for the aluminum pin, 2 coefficients of friction and the different amounts of interference. Results for the steel pin are essentially the same. While plastic deformation is observed during the first loading cycle, no plastic deformation, either forward or reversed, occurred during the unload cycle. This means that the values obtained after the first load cycle and first unload cycle, and those after subsequent load and unload cycles are the same.

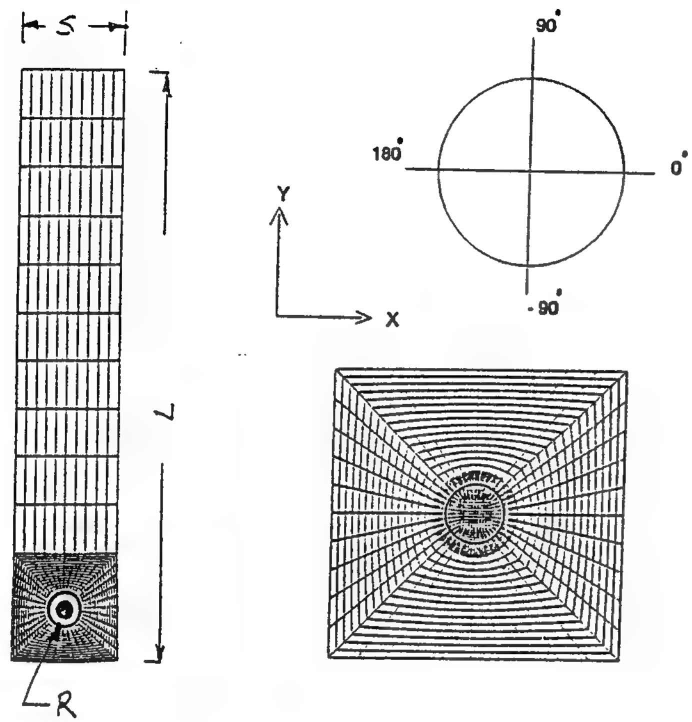

(a) (b)

Figure 2. Finite element model of the pinned connection: (a) dimensions of the repetitive element, and (b) refined mesh for pin and region around hole (the dark circle identifies the location of the pin-sheet interface) and (c) example of a deformed mesh in the vicinity of the pin-hole interface ($\mu = 0.2$) showing relative slip displacements at the pin-hole interface. The dimensions of the sheet are: S = 30.6 mm, L = 168.3 mm, R = 3.06 mm and t (thickness) = 1.53 mm.

Figure 4 illustrates that relatively high contact pressures between p = 450 MPa and 550 MPa are associated with the interference fit. A peak contact pressure of about p = 560 MPa is produced by the σ = 125 MPa nominal stress at $\theta = -90°$ for $\mu = 0.5$ in the absence of interference; this drops to zero at $\theta = 0°$ and $\theta = \pm 180°$. The 2 small peaks near $\theta = -60°$ and $\theta = 120°$, which are absent when $\mu = 0.2$, are reminiscent of the slip-stick solutions for rolling and sliding contact (6). The interference and friction coefficient exert a relatively modest effect on the peak contact pressure in the fully loaded state, but do alter the angular positions where contact pressure is lost. Figure 5a describes the absolute slip displacements and Figure 5b the slip amplitude, δ (the difference between the load and unload value of the local slip displacements). The δ-values are maximum in the first and second quadrants where the contact pressure is zero, and $\delta = 0$ at the $\theta = -90°$ location where the pressure is maximum. The slip values are in the range, $2\ \mu m < \delta < 5 \mu m$ at locations obtained at locations where contact pressures exceed p > 300 MPa. Both interference and the coefficient of friction have a large, inverse effect on the slip amplitude.

The net effect of these variations on the angular variation of F_1 is illustrated in Figures 6. The peak values are very sensitive to small amounts of interference, i.e., less than 1%, but relatively insensitive to the friction coefficient interference value when $0.2 < \mu < 0.5$ and 1% < interference < 2%. The peak values of F_1, their angular positions and corresponding values of contact pressure and slip are described in Figure 7 and in Table 2.

2.1.3 Discussion of Finite Element Calculations

The peak value of the fretting wear parameter in the absence of interference is about $F_1 = 3{\cdot}10^3$ Pam at angular positions corresponding with about 3 o'clock and 6 o'clock. Since this value is associated with relatively small slip amplitudes: $2\ \mu m < \delta < 25\ \mu m$, the specific fretting wear rate for aluminum even under corrosive conditions is likely to be $W = 10^{-14}$ m^3/Nm (7) or smaller. This implies that fretting can remove $y \leq 6\ \mu m$ of metal from the pin body and sheet bore after N = 50,000 stress cycles in the absence of interference; $y \leq 1 \mu m$ with 1% interference. In other words, the contribution of fretting corrosion is negligable in this case because the amount of slip is relatively small.

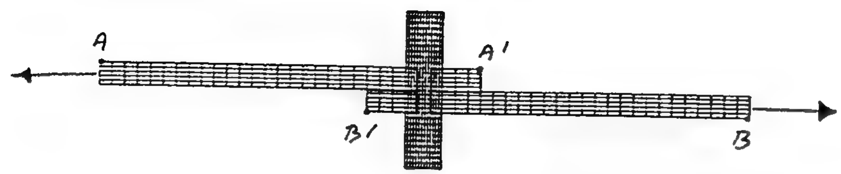

Figure 3. Finite element mesh of a 2-dimensional, out-of-plane model of a lap joint. The x-direction displacements of points A' and B' are equated to those of points A and B, respectively.

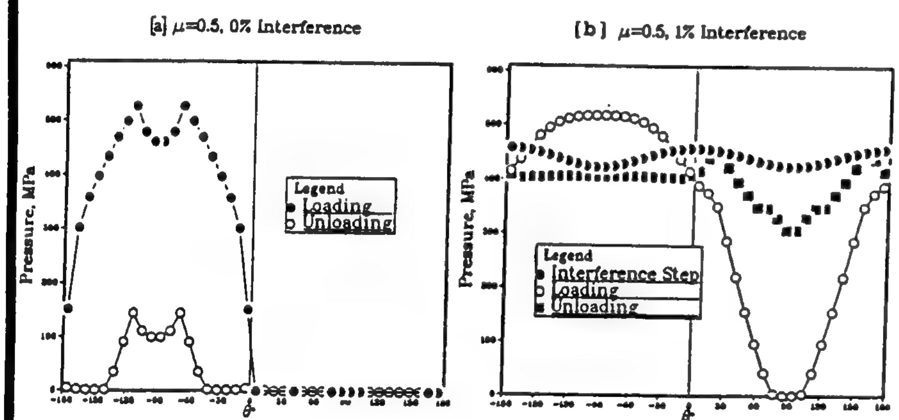

Figure 4. The variation of the contact pressure with angular position about the pinned hole with the cyclic stress applied and partially released for the aluminum pin: (a) μ = 0.5 and 0% interference, (b) μ = 0.5 and 1% interference.

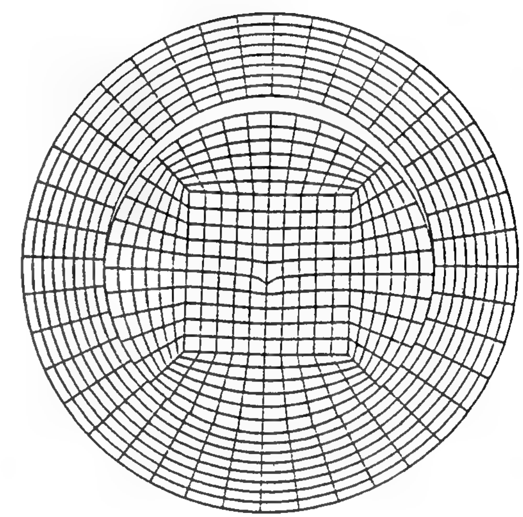

(c)

Figure 2 (Cont'd). (c) Example of a deformed mesh in the vicinity of the pin-hole interface (μ = 0.2) showing the relative slip displacements at the pin-hole interface.

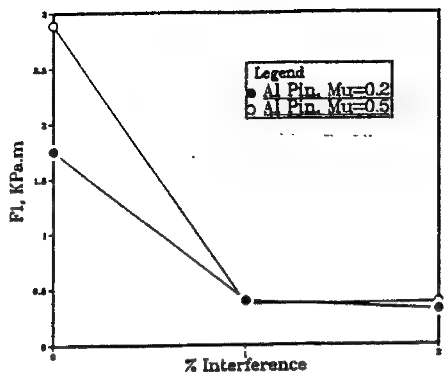

Figure 7. Variation of the fretting parameter F_1 with interference and friction coefficient.

Table 2. THE PEAK VALUES OF THE FRETTING WEAR PARAMETER, F_1, THEIR ANGULAR POSITIONS AND THE CORRESPONDING VALUES OF THE CONTACT PRESSURE AND SLIP AMPLITUDE

Pin Material, % Interference	μ	Peak F1, KPa.m	θ Range, Degrees	$\delta,\mu m$	p, MPa
Al, 0%	0.2	1.75	-13.1	24.8	336.1
Al, 1%	0.2	0.40	13.7	4.8	416.7
Al, 2%	0.2	0.32	4.6	2.9	536.3
Al, 0%	0.5	2.89	-13.3	19.7	301.5
Al, 1%	0.5	0.37	13.6	2.0	376.3
Al, 2%	0.5	0.38	31.5	1.86	403.6

*The stresses in the sheet adjacent and normal to the hole remain compressive for the 2% interference cases and hence F_2 does not have any meaning.
δ- slip amplitude, p-contact pressure, θ-angular position, and μ-coefficient of friction

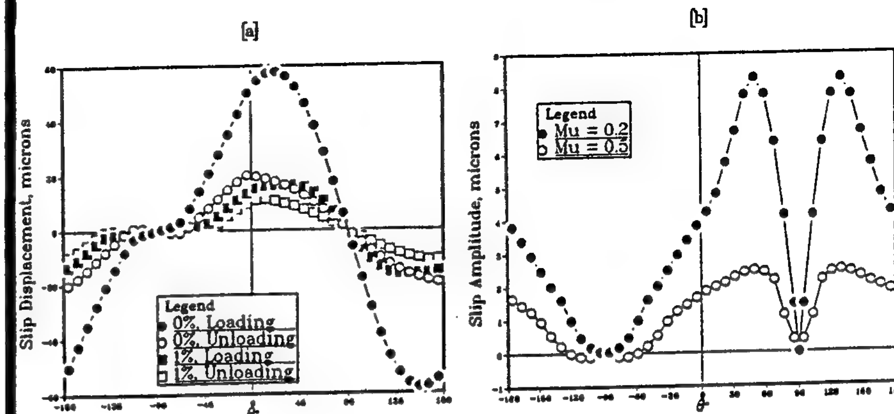

Figure 5. The variation of the slip with angular position about the pinned hole with the cyclic stress applied and partially released for the aluminum pin and 1% interference: (a) slip displacements and (b) slip amplitude (the differences between the on load and partially loaded slip displacements).

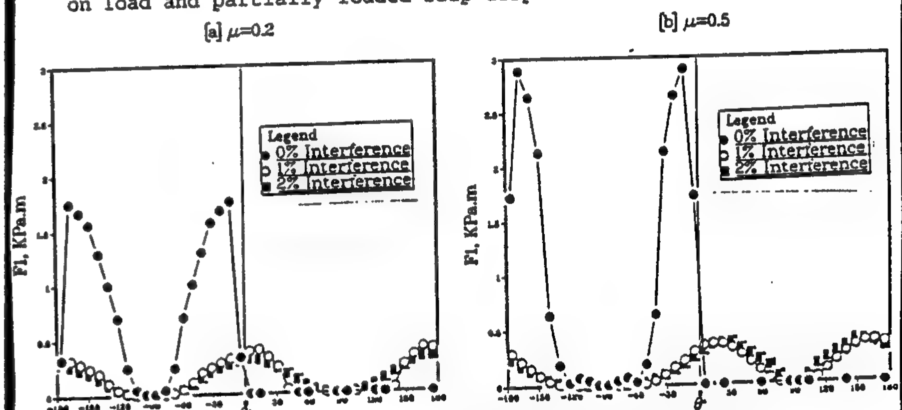

Figure 6. The variation of the fretting wear parameter, F_1 with angular position about the pinned hole with the cyclic stress applied and partially released for the aluminum pin and with 1% and 2% interference and different coefficients of friction: (a) μ = 0.2 and (b) μ = 0.5.

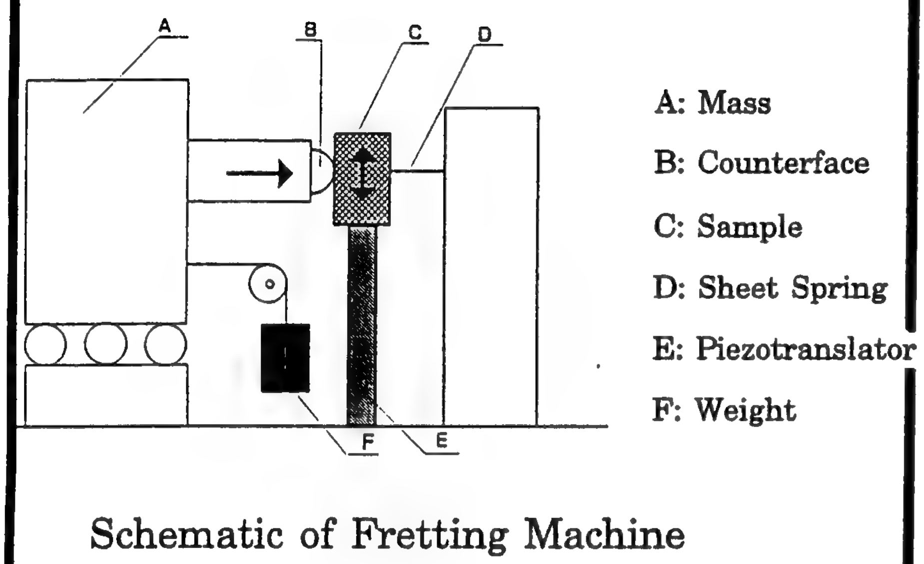

Figure 8. Schematic of the Piezoelectric Fretting Wear Machine.

However, real riveted lap joints are likely to be more compliant than the idealized configuration examined here, with the fasteners experiencing shear and bending which produce out-of-plane as well as in-plane displacements. At the same time, such connections can derive support from lateral forces. The sudies of the 2-dimensional model of a lap joint with a "continuous" rivet, mentioned in Section 2.1.1, will shed more light on these issues.

2.2 Tribolgical and Corrosion Measurements (Task 3)

2.2.1 Design and Operation of a Piezoelectric Fretting Wear Machine.

A unique fretting wear machine has been constructed which will facilitate the measurements of Task 3. The machine utilizes a stacked, piezoelectric actuator which moves the specimen thru very small and controllable slip amplitudes relative to a fixed contacting surface. A schematic drawing of the machine is shown in Figure 8; Photographs of the actual unit are given in Figure 9. The machine, as designed, will fit in an available bell jar which can be evacuated to 10^{-6} Torr and can also accommodate corrosive media at the contacting interface.

In this machine, the contacting surfaces consist of a flat plate which is moved by the piezoelectric actuator against either a hardened 1.5 in.-diameter steel hemisphere or a cylindrical aluminum counterface. The normal force between the contacting surfaces is provided by the weight, W, shown in Figure 8. In the actual unit, the force is applied by 2 weights acting through 2 levers, one in front and one in the rear (see Figure 9) with a mechanical advantage of ~9x. The calibration curve in Figure 10 was obtained by applying known weights and measuring the normal force generated on a Chatillon force gage normal to the mass, A, shown in Figure 8.

Slip Amplitude Control. The micropositioning and controlling unit consists of 2 components: one piezoelectric (PZT) translator with a strain gage sensor (SGS) and one piezoelectric controller. These 2 components work in a closed loop mode which is called Expansion Control (EC) Mode. In the EC mode, the PZT expands in a known range of amplitude which is preset by the operator at the beginning of an experiment. The piezoelectric controller then

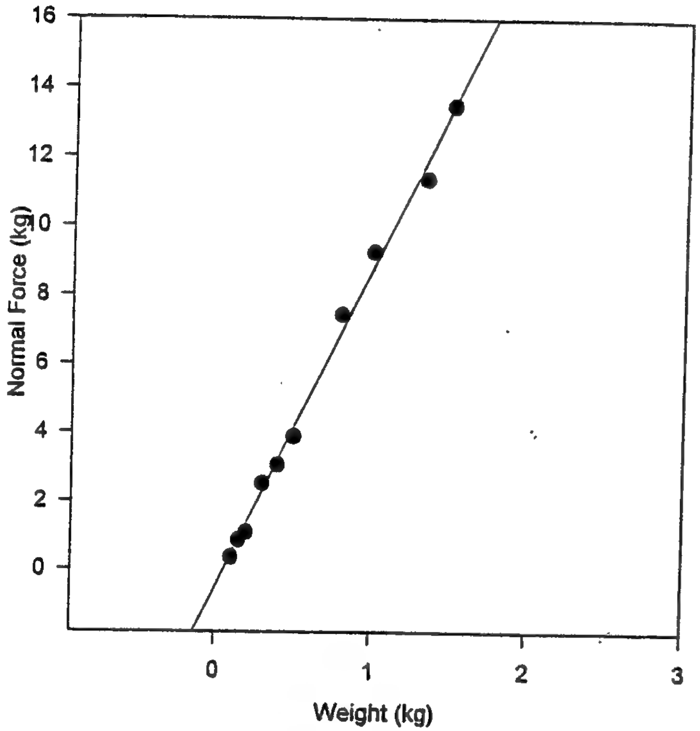

Figure 10. Calibration curve relating the applied load, W, to the normal force exerted on the sample.

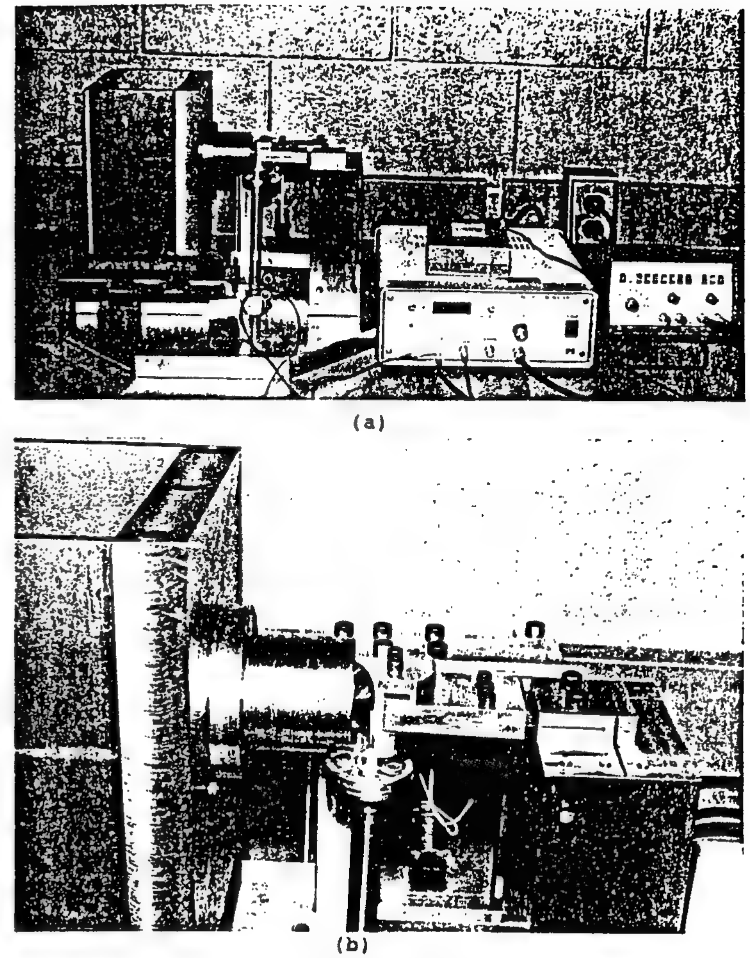

Figure 9. Photographs of the Piezoelectric Fretting Wear Machine: (a) overall view showing machine and elecronic controler and fucntion generator, and (b) close-up view of specimen and hardened steel ball counterface. The loading lever and linkage in the front of the unit (which is identical to the one visible in the rear) has been removed to obtain a clearer view of the sample holder and counterface.

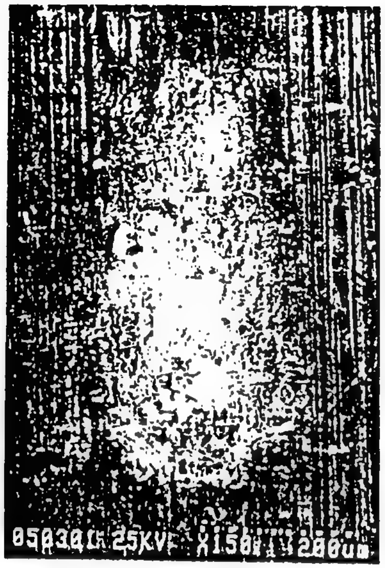

(a)

(b)

(c)

Figure 11. Scanning electron micrographs of fretted region on an aluminum alloy surface caused by 8600 cycles at a Hertzian pressure, p_0 = 276 MPa, and slip amplitude δ = 12 μm: (a) low magnification view showing the entire wear scar, (b) higher magnification view of center of fretted area, (c) same region at still higher magnification showing debris and fracture of the surface which is delaminating, and fragments to enter the system as wear.

regulates the expansion amplitude of the PZT consistent with the preset value using the feedback by the strain gauge sensor. While it is expected that the amplitude would be affected by hysteresis and possible drift movement of the PZT and also by the changing frictional forces, these phenomena are automatically compensated by the piezoelectric controller. The actual expansion of the PZT is determined by the sensor signal to achieve the control input supplied to the PZT. Thus the PZT amplitude will be constantly adjusted until the desired amplitude is reached. In the EC mode, the actual slip amplitude is always constant within the range of accuracy. The maximum and minimum values of expansion can be obtained continuously, or at any time, during the experiment. The slip amplitude is simply the maximum expansion minus the minimum expansion. The maximum slip amplitude of this fretting machine is 120 microns and the minimum slip amplitude is approximately 0.2 microns.

Friction Force Measurement. While the friction force can not be measured directly, it is closely related to the input voltage to the PZT when the unit is under amplitude control. Therefore, the larger the friction force, the higher the voltage supplied to the PZT must be to maintain constant amplitude. On this basis, a simple but indirect measurement of the friction force is being developed. Essentially, the friction force is obtained from conversion of the input voltge signal into a force signal. Three steps are involved:

(i) The relation between force and input voltage will be calibrated for different slip amplitudes.

(ii) The input voltage, which reflects changes in the force with changes in the friction coefficient, will be recorded continuously.

(iii) The time variation of the friction force combined with the normal force will define the friction coefficient at any point in the fretting experiment.

2.2.2 Preliminary Fretting Experiments

To prove the piezoeletric fretting wear machine design concept, a preliminary fretting experiment on 7075-T6 aluminum

alloy in fretting contact with the 1.5 in.-diameter, hardened steel ball was carried out. The sample was subjected to N = 8600 fretting cycles at a frequency of ~1 Hz with a force, W = 0.2 kg (which produces a peak Hertzian contact pressure p_o = 276 MPa) and a slip amplitude, δ = 12 μm. The wear scar observed in the scanning electron microscope is shown in Figure 11 at various magnifications[2]. Figure 11d is especially interesting, showing a portion of the heavily worked surface which is in the process of delaminating and fracturing. This portion of the surface will then enter the system as loose wear debris.

2.3 Material and Component Testing (Task 4)

2.3.1 Preliminary Accelerated Corrosion Fretting Test of a Riveted Connection

A preliminary experiment examining the feasibility of accelerated fretting corrosion tests of riveted connections was performed. The connection, was fabricated from 0.060 in.-thick, 7075-T6 aluminum sheet with countersunk steel fasteners installed "dry" (without a coating), and is illstrated in Figure 12. The fasteners were installed by Textron Aerostructures. The tests were performed with only the bottom row of the 2 rows of 3 rivets immersed in 4% NaCl solution and an applied emf making the sample anodic as shown schematically in Figure 13. The exterior surfaces of the sheet and fasteners in contact with the solution were protected by a coating of Microstop. However, the coating was removed around the fasteners to give the solution access to the fastener-sheet interfaces at the hole bore. The sample was subjected to cyclic loading at a frequence of 0.2 Hz with a peak nominal stress of 75 MPa and stress ratio, R = 0.1.

The sample failed along the top row of rivets (which were not immersed in the saline solution) after 14,208 load cycles. So far, one of the countersunk fastener installations that was exposed to anodic disssolution has been examined under the microscope. As shown in Figure 14a, significant corrosion can be

---

[2]The wear scar is longer than 12 μm because the test was interrupted several times and the test sample removed for observation and not returned to its exact original postion.

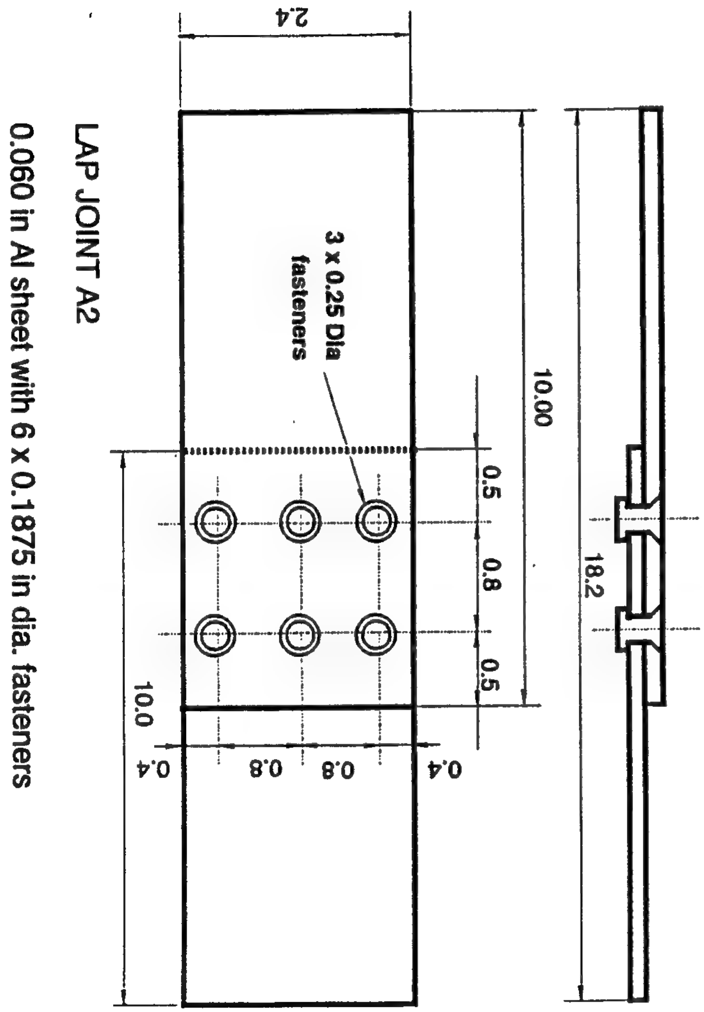

Figure 12. Dimensions of riveted sample

(a)

(b)

Figure 14. SEM micrographs of the corroded fastener hole bore: (a) countersunk regions and (b) exfoliation-type crack below countersink.

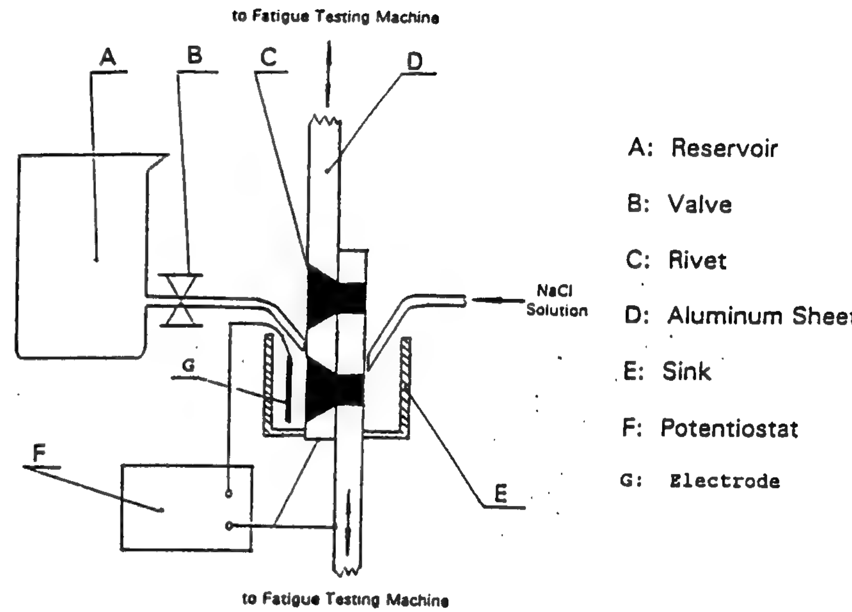

Figure 13. Schematic of riveted sample fretting corrosion test.

observed in the 7075-T6 sheet along the countersunk surface. Several delamination or possibly exfoliation type cracks were observed in this region (see Figure 14 b). The other portions of the bore appeared bright with no signs of either fretting wear or corrosion.

No general conclusions can be drawn from this isolated test, However, the test promises to porvide useful insights to fretting and corrosion in connections, especially when coupled with the calculations of the mechanical fretting parameters demostrated in Section 2.1 and the systematic fretting corrosion measurments made possible by the piezoelectric fretting wear machine.

3. FUTURE WORK

The following activities activies are planned for the remainder of 1994:

(i) The survey of fretting and corrosion in airframe connection will be undertaken.

(ii) The finite element analyses will be extended to the 2-dimensional, out-of-plane model of a lap joint and work on a 3-dimensional model of a lap joint will be initiated.

(iii) Systematic measurements of fretting wear and corrosion will be performed for 7075-T6/steel and 7075-T6/7075-T6 combinations for the contact pressures and slips generated in connections.

(iv) Accelerated corrosion fretting tests will be performed on riveted samples with the aim of simulating severe corrosion and generating samples for evaluating NDE procedures. Metallographic studies will be performed on these samples.

4. CONCLUSIONS

(i) Finite element analyses of an idealized, pinned connection have been performed to evaluate the mechanical parameters that govern fretting wear and fretting corrosion. The calculations reveal that a nominal cyclic tensile stress range of 112 MPa (R = 0.1) generates peak contact pressures in the vicinity of p = 500 MPa to 600 MPa at the pin-bore interface. The slip amplitude is about 20 μm to and 2 μm for 0% and 1% to 2% interference for friction coefficients in the range 0.2 to 0.5. The peak values of the fretting wear factor, 0.3 kPam < F_1 < 3 kPam together with the relatively small slip amplitudes are consistent with the absence of significant corrosion fretting damage in aluminum alloy connections.

(ii) A Piezoelectric Fretting Wear Machine has been designed, constructed, and demonstrated which will make it possible to make systematic measurements of fretting wear and corrosion with convenient laboratory samples for the contact pressures and slip amplitudes generated in pinned and riveted connections.

(iii) A procedure for testing simple, riveted connections under conditions designed to promote accelerated fretting wear and corrosion has been demonstrated.

(iv) With the exception of Task 1, a survey of fretting damage in airframe connections, the research of this project is on schedule.

ACKNOWLEDGEMENTS

The authors wish to thank Messrs J. Veciana and T. Warrion of Textron Aerostructures for supervising the fastener installations.

REFERENCES

1. Waterhouse, R. B. "Avoidance of Fretting Fatigue Failures" Fretting Fatigue, pp. 221-240. Ed.R. B. Waterhouse, Applied Science Publishers LTD, (ISBN 0-85334-932-0) london, 1981.

2 Vingsbo, O., and S. Soderberg, "On Fretting Maps", Wear, Vol. 126, 1988, pp. 131-147.

3. Goto, H., Ashida, M. and K. Endo, "The Influence of Oxygen and Water Vapor on the Friction and Wear of an Aluminum Alloy Under fretting Conditions", Wear, Vol. 116, 1987, pp 141-155.

4. Pearson, B. R. and R. B. Waterhouse, "The Fretting Wear of Steel Ropes in Sea Water -- Effect of Cathodic Protection", Wear of Materials, 1985, K. C. Ludema, Ed. ASME.

5. Iyer, K., Hahn, G.T., Bastias, P.C. and C. A. Rubin, "Analysis of Fretting Conditions in Pinned Connections", Submitted to Wear.

6. J. J. Kalker, "Review of Wheel-Rail Rolling Contact Theories", The General Problem of Rolling Contact, New York, N.Y., pp 77-83.

D44/A:AFPRORPT
D44/A:AFPRORP3
C:AFPRORPT

Progress Report

for

ANALYSES AND DETECTION OF FRETTING CORROSION IN AIRFRAME RIVETED AND PINNED CONNECTIONS (F49620-93-1-0488)

by

K. Iyer*, M. Xue*, R. Kasinadhuni*
P. C. Bastias**, C. A. Rubin***, J. J. Wert*** and G. T. Hahn***

Department of Mechanical Engineering
Box 1592, Station B
Vanderbilt University
Nashville, TN 37235

Prepared for Presentation at the

WORKSHOP ON AGING AIRCRAFT RESEARCH
Oklahoma City (Tinker AFB) Oklahoma

May 17-19, 1994

* Graduate Research Assistant, **Research Assistant Professor and *** Professor, Department of Mechanical Engineering.
Phone: (615)322-3594, FAX (615)343-6687

SPONSORSHIP

"Corrosion and Fatigue of Aluminum Alloys: Chemistry, Micromechanics and Reliability"
Air Force Office of Scientific Research
AFOSR Grant F49620-93-1-0426
(University Research Initiative)
Robert P. Wei and D. Gary Harlow, Co-PI
01 July 1993 to 30 June 1996

"Corrosion and Corrosion Fatigue of Airframe Materials"
Federal Aviation Administration
FAA Grant 92-G-0006
(Aging Airplane Program)
Robert P. Wei, PI
15 June 1992 to 14 June 1995

OBJECTIVES

- ☐ To develop quantitative mechanistic understanding of the processes of localized corrosion and corrosion fatigue crack initiation and growth in high strength aluminum alloys used in aircraft construction

- ☐ Based on this understanding, develop mechanistically based probability models that can aid in life prediction and assessment of reliability

CONCEPTUAL FRAMEWORK

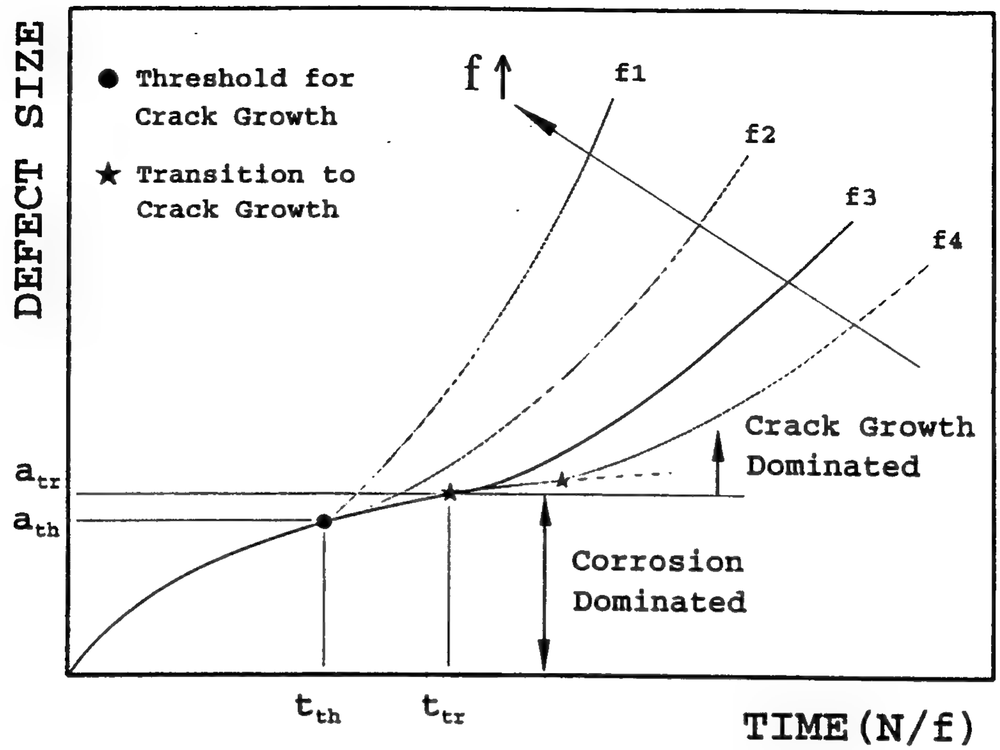

UNIT PROCESSES OF CORROSION AND CORROSION FATIGUE CRACK GROWTH

- ☐ Local corrosion damage (pit nucleation and growth) -- mechanisms and kinetics
- ☐ Transition from pitting to fatigue crack growth (crack initiation)
- ☐ Early stages of corrosion fatigue crack growth (short-crack regime)
- ☐ Corrosion fatigue crack growth

UNIT PROCESSES & MODELING FRAMEWORK

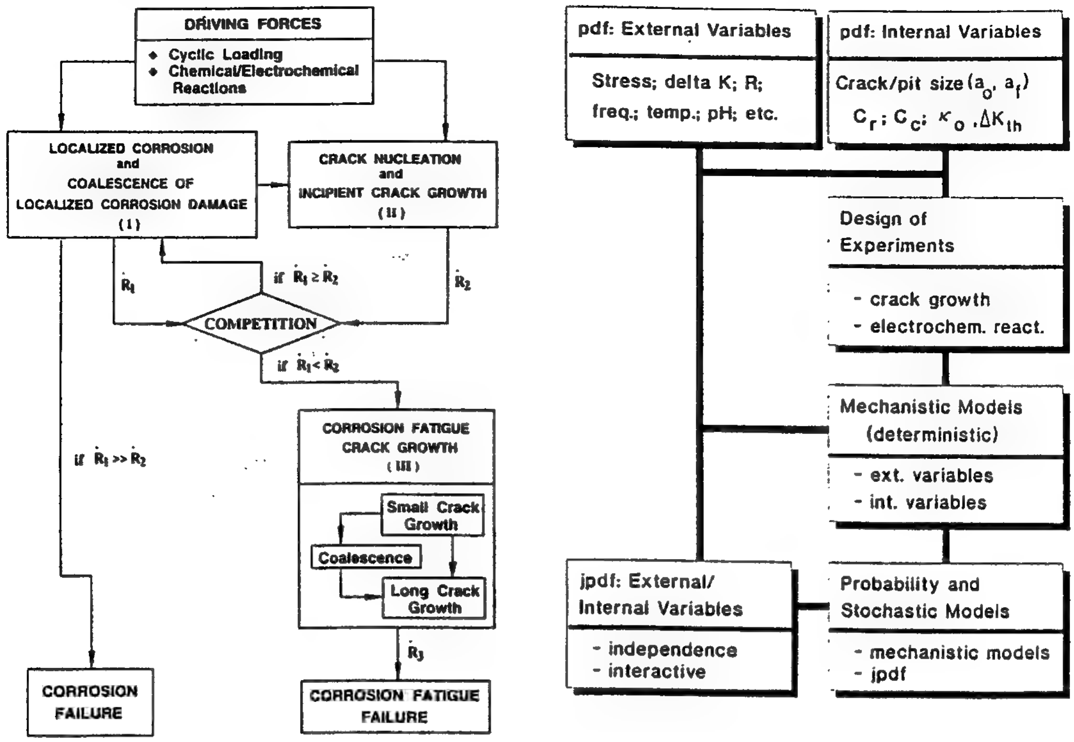

NEED FOR MECHANISTICALLY BASED APPROACH TO LIFE PREDICTION

- ☐ Identification of damage mechanism
- ☐ Identification of key (*random*) variables
- ☐ Fundamentally based functional dependence on key variables -- *viz.* mechanistically based models (minimize uncertainty associated with statistically based parametric models)
- ☐ Optimum utilization of limited experimental data
- ☐ Rational basis for interpolation and extrapolation

NEED FOR MECHANISTICALLY BASED APPROACH TO LIFE PREDICTION

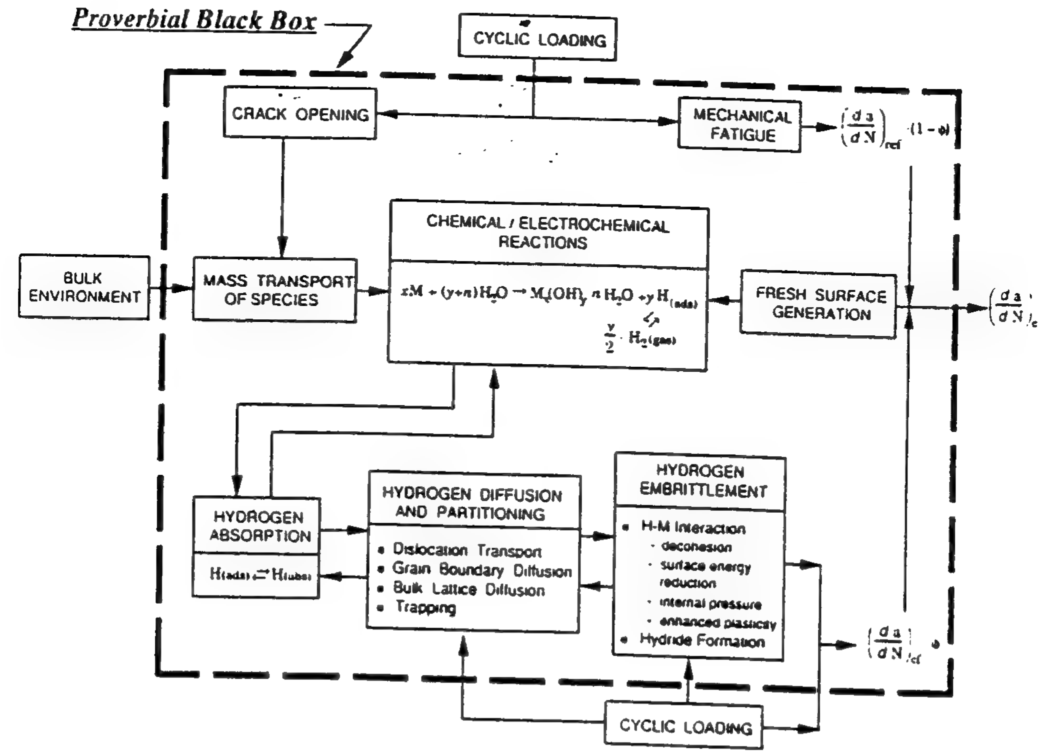

PRINCIPAL ISSUES TO BE ADDRESSED

- Identification and verification of key internal and external random variables that control each of the unit processes, and determination of the stochastic nature of each process
- Quantification of the probability distribution function (including time variance) of each of the key variables
- Development of quantitative understanding of the rate controlling step and mechanism for each damage process, and formulation of a mechanistic (*deterministic*) model for each that describes the functional dependence on the key variables
- Integration of mechanistic models and probability distribution functions, and formulation of mechanistically based probability models for life prediction and reliability assessment

CHEMISTRY FOR SIMULATED CREVICE

(2024-T3 Aluminum Alloy)

- Crevice geometry (cell volume: 10 mℓ; crevice height: 0.27 mm, non-crevice-to-crevice area ratio: 2:1); bulk solution (0.05, 0.5, 2.0M NaCl; $[O_2] \approx 7$ ppm; pH $\approx$ 6; T $\approx$ 20°C; flow $\approx$ 2.5 mℓ/min.)

- Solution pH inside crevice depends mildly on $[Cl^-]$; pH increases at first (more alkaline) and then becomes acidic with time, stabilized at about 4.5

- Corrosion potential inside crevice depends on $[Cl^-]$, tending to be more noble (cathodic) at the higher concentrations (-540, -610, and -650 mV *versus* Ag/AgCl for 0.05, 0.5, and 2.0M NaCl solutions, respectively)

LOCALIZED CORROSION IN 2024/7075 ALLOYS

- Localized corrosion (*pitting*) in both alloys are associated with *constituent particles*; about 3,000 particles/mm^2 ($>1\ \mu m^2$)

- Two types of particles identified: Type A (*anodic*) and Type C (*cathodic*) with respect to the matrix; Type A dissolves, Type C induces trenching in adjacent matrix

2024:	Type A (Al,Cu,Mg)	Type C (Al,Cu,Fe,Mn)
7075:	Type A (Al,Cu,Mg,Zn)	Type C (Al,Cu,Fe,Cr,Mn,Zn)

- Pitting strongly temperature and pH dependent

- Pitting very complex and appears to involve 3-D interactions with constituent particles; kinetics and distribution needed

- Corrosion sensitivity appears to be orientation dependent; being *more severe in the thickness orientation*

LOCALIZED CORROSION IN 7075-T6 ALUMINUM ALLOY

0.5M NaCl @ RT (Free Corrosion, pH 6) -- 3 h

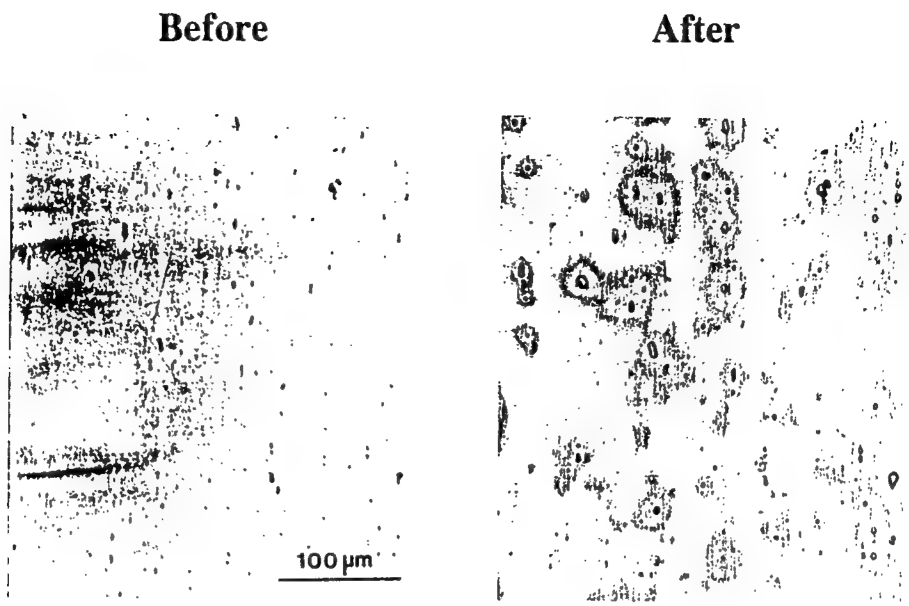

CONSTITUENT PARTICLES IN 7075-T6 ALLOY

Typical Size Distribution in Weibull Format

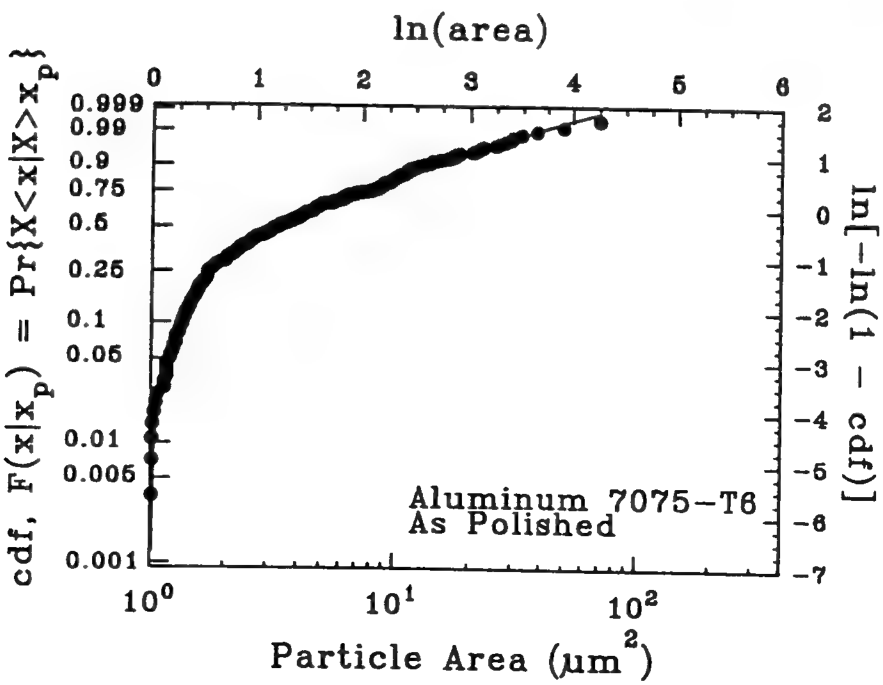

EDX RESULTS FOR SELECTED PARTICLES IN 7075-T6 *BEFORE* AND *AFTER* CORROSION (0.5M NaCl @ 80°C, 3 h)

Type A

Particle Type	Corrosion Testing	K_α Intensity (counts)						
		Mg	Cr	Mn	Fe	Cu	Zn	Al
A1	before	TR*	ND*	ND	ND	8510	759	1027
	after	TR	ND	ND	ND	7828	654	837
A2	before	313	ND	ND	ND	8326	718	1761
	after	240	ND	ND	ND	6841	591	1571
A3	before	N/A	N/A	N/A	N/A	N/A	N/A	N/A
	after	ND	ND	ND	ND	6221	536	1548
A4	before	N/A	N/A	N/A	N/A	N/A	N/A	N/A
	after	ND	ND	ND	ND	8756	650	287

* ND: not detected   * N/A: not available   * TR: trace

EDX RESULTS FOR SELECTED PARTICLES IN 7075-T6 *BEFORE* AND *AFTER* CORROSION (0.5M NaCl @ 80°C, 3 h)

Type C

Particle Type	Corrosion Testing	K_α Intensity (counts)						
		Mg	Cr	Mn	Fe	Cu	Zn	Al
C1	before	ND*	383	531	6899	1479	407	2021
	after	ND	435	610	7530	1454	399	2892
C2	before	ND	381	509	6256	3053	417	1343
	after	ND	408	501	5201	3606	384	1468
C3	before	ND	903	804	6826	1401	428	4320
	after	ND	794	802	6846	1716	424	4512
C4	before	ND	464	599	8072	1506	462	3571
	after	ND	460	681	7793	1337	453	2628

* ND: not detected

ELEMENTAL MAPS FOR 7075-T6 (Thickness)

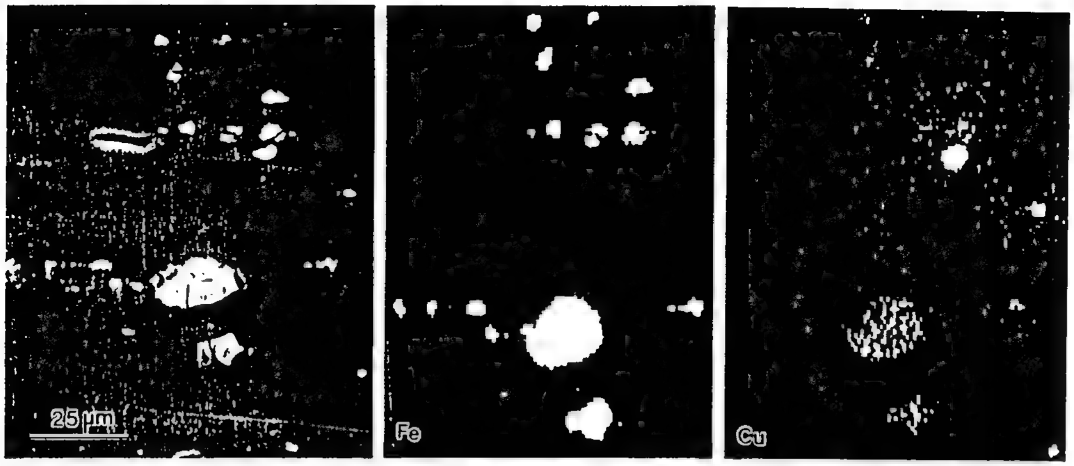

LOCALIZED CORROSION AT CONSTITUENT PARTICLES IN 7075-T6 ALUMINUM ALLOY

0.5M NaCl @ RT (Free Corrosion, pH 6) -- 42 h

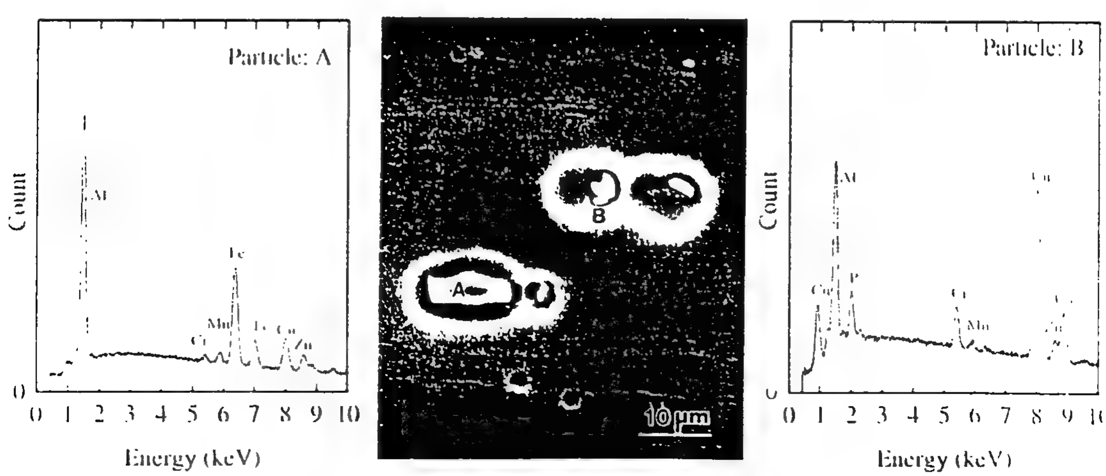

LOCALIZED CORROSION AT CONSTITUENT PARTICLES IN 7075-T6 ALUMINUM ALLOY

0.5M NaCl @ 65°C (Free Corrosion, pH 6) -- 10 h

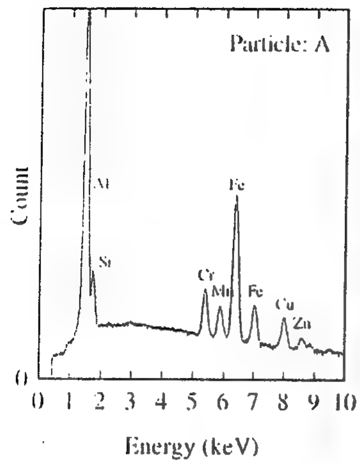

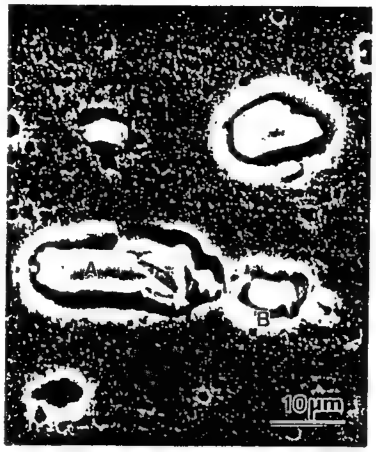

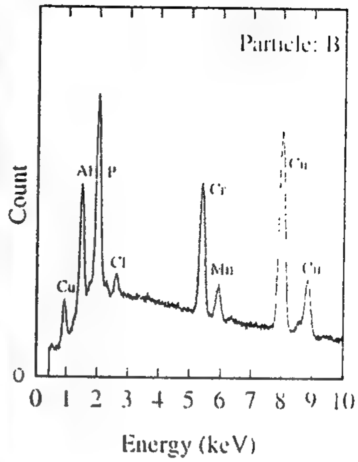

GROWTH AND COALESCENCE OF PITS

0.5M NaCl @ 65°C (Free Corrosion, pH 6) -- 10 h (7075-T6)

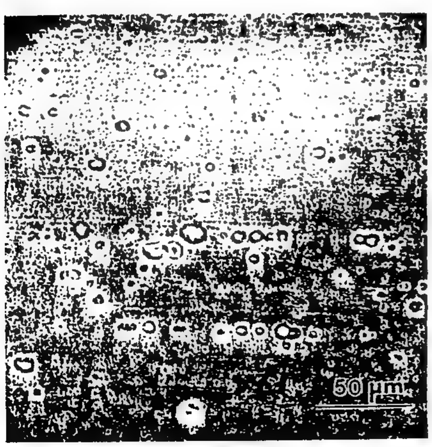

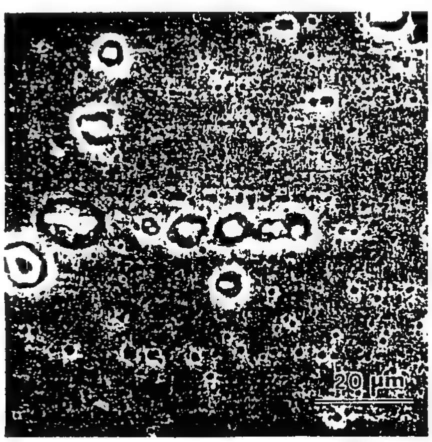

LOCALIZED CORROSION IN 2024-T3

0.5M NaCl @ RT (Free Corrosion, pH 6) -- 3 days

A01F36-614,5,6

CRACK NUCLEATION AND EARLY GROWTH

- Crack nucleates from areas of severe local corrosion (*pits*)

- Failure by-and-large results from a *single* nucleation site (formed by pitting corrosion from a cluster of Type A particles); dominant flaw model appears to be appropriate

- Pit-to-crack transition size appears to depend on frequency, being larger at lower frequencies (*competition*) -- addition to transition criterion needed; suggest

  $\Delta K \geq \Delta K_{th}$ and $(da/dt)_{crack} \geq (da/dt)_{pit}$

- Transition ΔK: about 2.5 $MPa\sqrt{m}$ at 5-20 Hz to about 5 $MPa\sqrt{m}$ at 0.1 Hz for applied σ_{max} = 320 MPa (@ open hole)

- Extent of (post crack growth) pitting of the fracture surface also depended on frequency (reflecting the duration of exposure), further confirms the competition between corrosion and corrosion fatigue crack growth

CRACK INITIATION AND EARLY GROWTH

0.5M NaCl @ RT (Free Corrosion, pH 6)

$(\sigma_{max})_{hole}$ = 320 MPa, R = 0.1, f = 0.5 Hz (43.3 h)

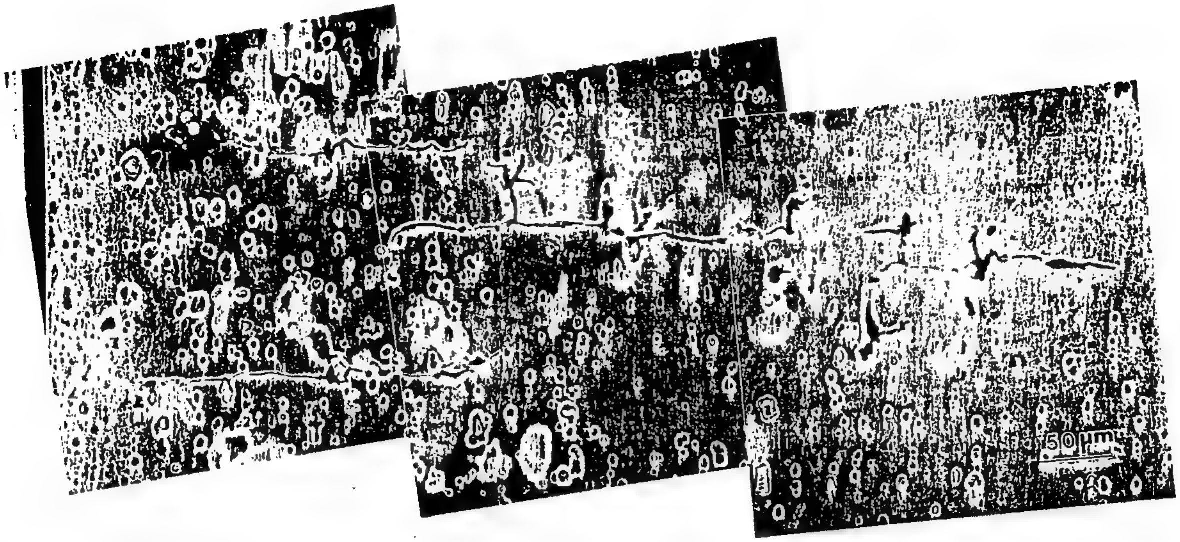

Multiple Initiation Adjacent to Main Crack

A01F51-129,30,31

CRACK INITIATION AND EARLY GROWTH

0.5M NaCl @ RT (Free Corrosion, pH 6)

$(\sigma_{max})_{hole}$ = 320 MPa, R = 0.1, f = 10 Hz (2.2 h)

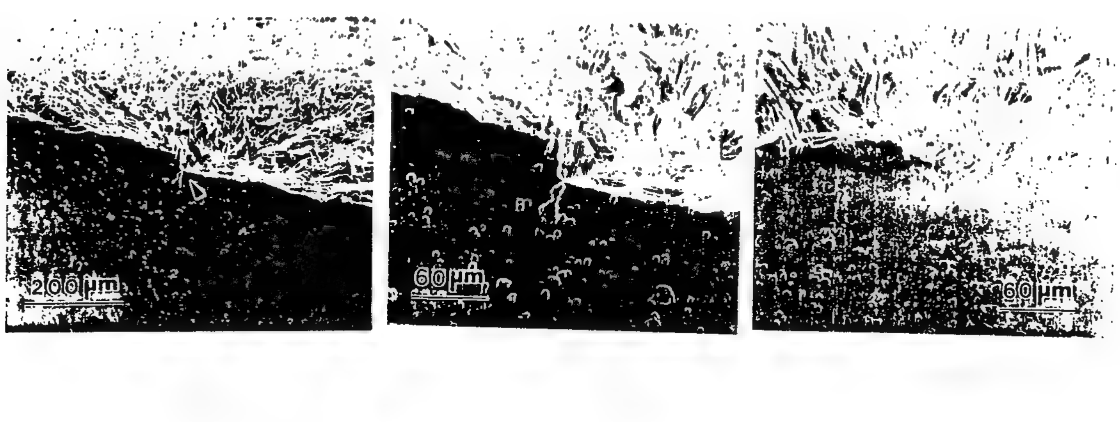

A01F14-401,2,3

CRACK INITIATION AND EARLY GROWTH

0.5M NaCl @ RT (Free Corrosion, pH 6)

$(\sigma_{max})_{hole}$ = 320 MPa, R = 0.1, f = 10 Hz (2.2 h)

Sub-surface Corrosion Damage

A01F14-405.6

CRACK INITIATION AND EARLY GROWTH

0.5M NaCl @ RT (Free Corrosion, pH 6)

$(\sigma_{max})_{hole}$ = 320 MPa, R = 0.1, f = 0.1 Hz (160 h)

Initiation Site A

A01F20-007,14,18

TRANSITION FROM PITTING TO FCG

Effect of Frequency (0.5M NaCl @ RT, σ_{max}=320MPa, R=0.1)

Sample No.	Frequency [Hz]	N_i [cycles] / t_i [hrs]	N_f [cycles] / t_f [hrs]	(Pit Size)* 2c x a [μm]	(ΔK) @ surface [MPa√m]
A01F29	20	*not available*	58,629 / 0.81	50 x 80	2.83
A01F14	10	29,700 / 0.83	78,745 / 2.19	45 x 35	2.27
A01F05	5	23,970 / 1.33	59,381 / 3.3	45 x 60	2.60
A01F39	5	27,470 / 1.53	64,800 / 3.6	40 x 60	2.50
A01F51	0.5	39,830 / 22.13	77,875 / 43.26	75 x 200	3.65
A01F08	0.5	41,138 / 22.85	*not available*	67 x 150	3.41
A01F20	0.1	18,635 / 51.76	57,809 / 160.58	100 x 250	4.20
A01F36†	5	8,000 / 0.44	67,392 / 3.74	100 x 150	3.96

* 2c = maximum width of the pit;
a = maximum depth of the pit.

† Three day pre-exposure to NaCl solution prior to corrosion fatigue testing.

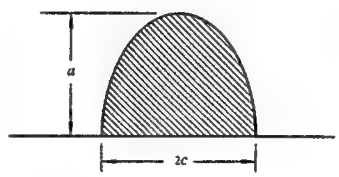

A PROBABILITY MODEL FOR PITTING AND FATIGUE CRACK GROWTH

A Dominant Flaw Model for Pitting and Corrosion Fatigue

(After Y. Kondo, 1989; Kondo and Wei, 1989)

- Pitting corrosion (constant volumetric rate; coalescence of particle induced pits)
- Transition from pit (hemispherical) to crack (semi-circular) based on fatigue crack growth threshold (need to incorporate frequency dependence and effect of chemically short crack)
- Further transition from semi-circular crack at open-hole to through-thickness crack

A PROBABILITY MODEL FOR PITTING AND FATIGUE CRACK GROWTH

(continued)

- Constant stress amplitude fatigue crack growth using a power-law relationship @ 2 and 10 cycles per day (spectrum loads are being incorporated)
- Models were assumed to capture some of the key mechanistic features, and provide reasonable "predictions" of response
- The model incorporated initial defect size, corrosion rate, fatigue crack growth rate coefficient, and fatigue crack growth threshold (ΔK_{th}) as random variables, and permitted examinations of the contribution of each of these variable to the distribution in life.

A PROBABILITY MODEL FOR PITTING AND FATIGUE CRACK GROWTH

Pitting Corrosion and Crack Initiation

$$\frac{dV}{dt} = 2\pi a^2 \frac{da}{dt} = \frac{MI_{P_o}}{nF\rho} \exp\left[-\frac{\Delta H}{RT}\right]$$

$$t_{ci} = \frac{2\pi nF\rho}{3MI_{P_o}}\left(a_{ci}^3 - a_o^3\right)\exp\left[\frac{\Delta H}{RT}\right]$$

$$\Delta K_{th} = \frac{2.2}{\pi} K_t \Delta\sigma \sqrt{\pi a_{ci}} \quad \Rightarrow \quad a_{ci} = \pi\left(\frac{\Delta K_{th}}{2.2 K_t \Delta\sigma}\right)^2$$

A PROBABILITY MODEL FOR PITTING AND FATIGUE CRACK GROWTH

Corrosion Fatigue Crack Growth

$$(da/dN)_c = C_c(\Delta K)^{n_c}$$

$$\Delta K_s = \frac{2.2}{\pi} K_t \Delta\sigma\sqrt{\pi a}; \quad \Delta K_{tc} = F_{tc}\left(\frac{a}{r_o}\right)\Delta\sigma\sqrt{\pi a}$$

$$F_{tc}\left(a/r_o\right) = \frac{0.865}{\left(a/r_o\right)+0.324} + 0.681$$

A PROBABILITY MODEL FOR PITTING AND FATIGUE CRACK GROWTH

Time-to-Failure

$$t_f = t_{ci} + t_{tc} + t_{cg}$$

$$K_t = 2.6; \quad r_o = 3mm; \quad a_f = 3mm; \quad n_c = 3$$

$$t_f = \frac{6.064\times 10^{10}}{I_{P_o}\exp\left[-\frac{\Delta H}{RT}\right]}\left(8.853\times 10^{-4}\left[\frac{\Delta K_{th}}{\Delta\sigma}\right]^6 - a_o^3\right)$$

$$+\frac{\dfrac{0.192\Delta\sigma}{\Delta K_{th}} - 0.751}{\nu C_c(\Delta\sigma)^3}$$

rvs: $a_o, C_c, I_{P_o}, \Delta K_{th}$; *parameters:* $\nu, \Delta\sigma, T$

A PROBABILITY MODEL FOR PITTING AND FATIGUE CRACK GROWTH

Cumulative Distribution Function for t_f

t_f is a function of the *rvs*: $a_o, C_c, I_{P_o}, \Delta K_{th}$.

Its *cdf* is found via the multi-dimensional change of variables theorem for Φ: $\mathbf{B} \rightarrow \mathbf{N}$, where the components of **B** and **N** are

$$B_1 = C_c; B_2 = I_{P_o}; B_3 = \Delta K_{th}; B_4 = a_o$$

$$N_1 = t_f; N_2 = B_2; N_3 = B_3; N_4 = B_4.$$

The inverse Φ^{-1} and the Jacobian J can be found explicitly.

$$F_{t_f}(t) = \int_0^t \int_0^\infty \int_0^\infty \int_0^\infty |J| \, f_{\mathbf{B}}(\Phi^{-1}(\mathbf{n})) \, dn_4 dn_3 dn_2 dn_1$$

A PROBABILITY MODEL FOR PITTING AND FATIGUE CRACK GROWTH

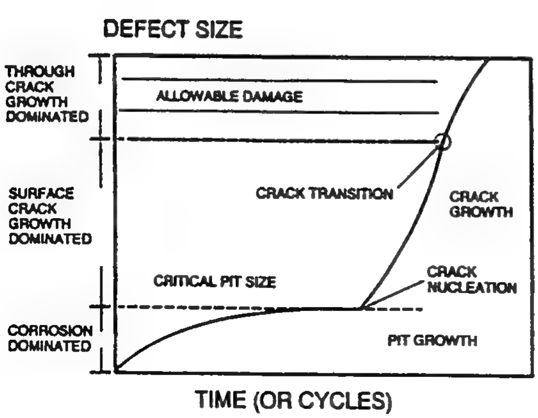

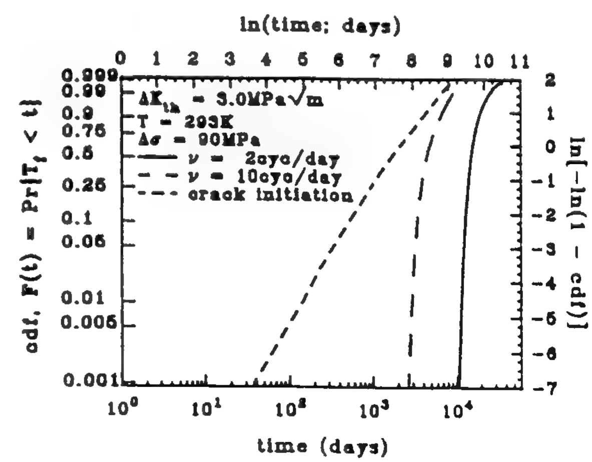

A PROBABILITY MODEL FOR PITTING AND FATIGUE CRACK GROWTH

Influences of Stress Level and Temperature

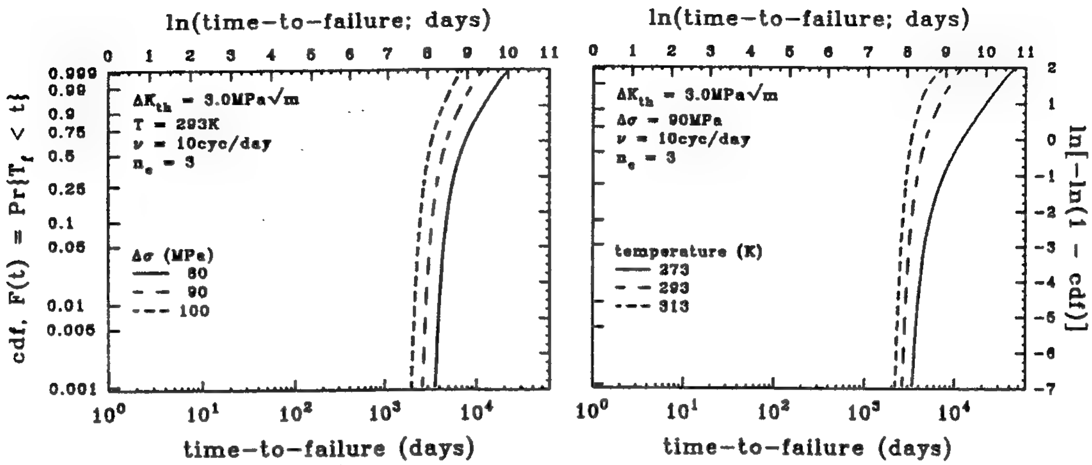

A PROBABILITY MODEL FOR PITTING AND FATIGUE CRACK GROWTH

Contribution of Individual Randon Variables

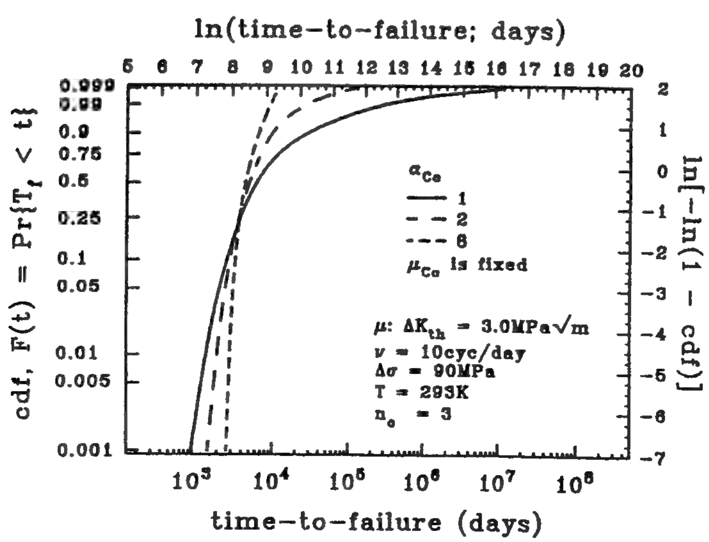

SUMMARY

- *Pitting* in aluminum alloys is associated with *constituent particles*
- Cracks nucleate from areas of severe local corrosion (i.e., *pits* formed from clusters of particles)
- Failure by-and-large results from a *single* nucleation site; dominant flaw model appears to be appropriate
- Pit-to-crack transition size depends on frequency (and stress level), being larger at lower frequencies (*competition*) -- transition criteria:

$$\Delta K \geq \Delta K_{th} \quad \text{and} \quad (da/dt)_{crack} \geq (da/dt)_{pit}$$

- Development of mechanistic and stochastic models to incorporate 2 and 3 dimensional aspects of pit coalescence and frequency dependent transition (crack nucleation) criteria, along with an appropriate model for corrosion fatigue crack growth

Introduction

Background:

Surface cracks under rolling contact loadings grow faster in the presence of lubricants.

Issues:

- Role of hydraulic pressure in crack propagation.
- Solid-Viscous fluid interaction.
- Properties of lubricants.

AFOSR/URI

University of Illinois at
Urbana-Champaign

Materials Degradation and Fatigue Under Extreme Condition

Objectives:

- Develop a mathematical model to predict crack growth rate.
- Identify important parameters which controll the surface crack growth.

Approach:

Fracture Mechanics

\+ Fluid Mechanics

\+ Chemistry.

AFOSR/URI

University of Illinois at
Urbana-Champaign

Materials Degradation and Fatigue Under Extreme Condition

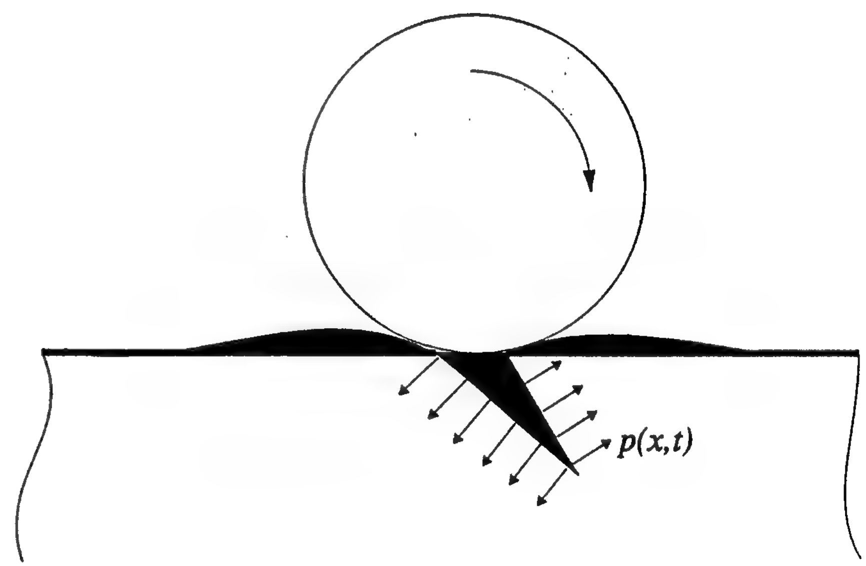

FIG.1 Surface crack with hydraulic pressure

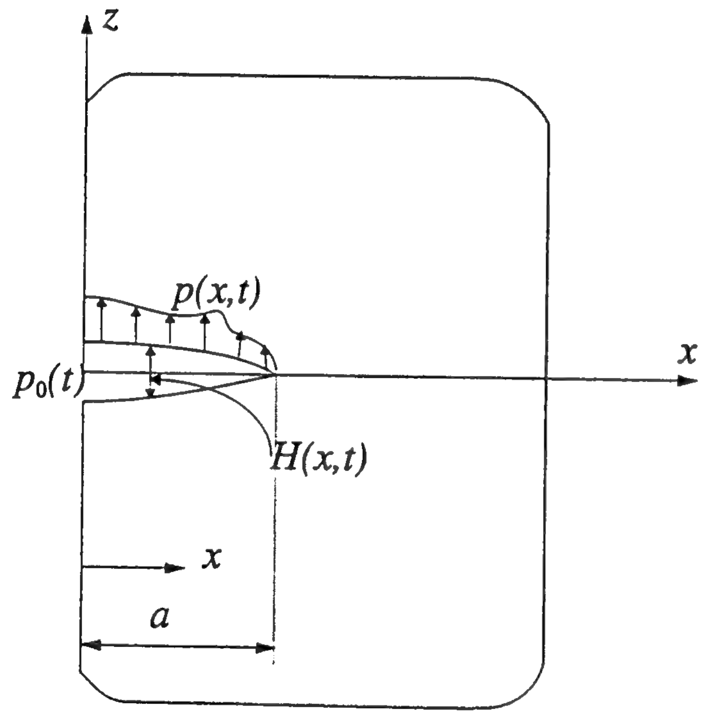

FIG.2 Idealized model

Idealized Model

- Plane strain deformation with a surface crack normal to the surface.
- Linear elastic solid (Young's modulus E).
- Pressure at crack mouth $p_0(t)$ prescribed.
- Linear viscous, incompressible fluid (viscosity μ).

Basic Assumption:

Local pressure depends only on local displacement as,

$$p = k_\beta H^\beta$$

where k_β, β are constants.

Governing equation:

$$H - \frac{\beta k_\beta}{12\mu} \frac{\partial}{\partial x}\left(H^{2+\beta} \frac{\partial H}{\partial x} \right) = 0$$

AFOSR/URI
University of Illinois at
Urbana-Champaign

Materials Degradation and Fatigue Under Extreme Condition

Fluid equations

$$\begin{cases} \dfrac{\partial p}{\partial z} = 0 \\ \dfrac{\partial p}{\partial x} = \mu \dfrac{\partial^2 u}{\partial z^2} \\ \dfrac{\partial u}{\partial x} + \dfrac{\partial w}{\partial z} = 0 \end{cases}$$

where u, w are velocity components of fluid.

Crack tip stress intensity under pressure

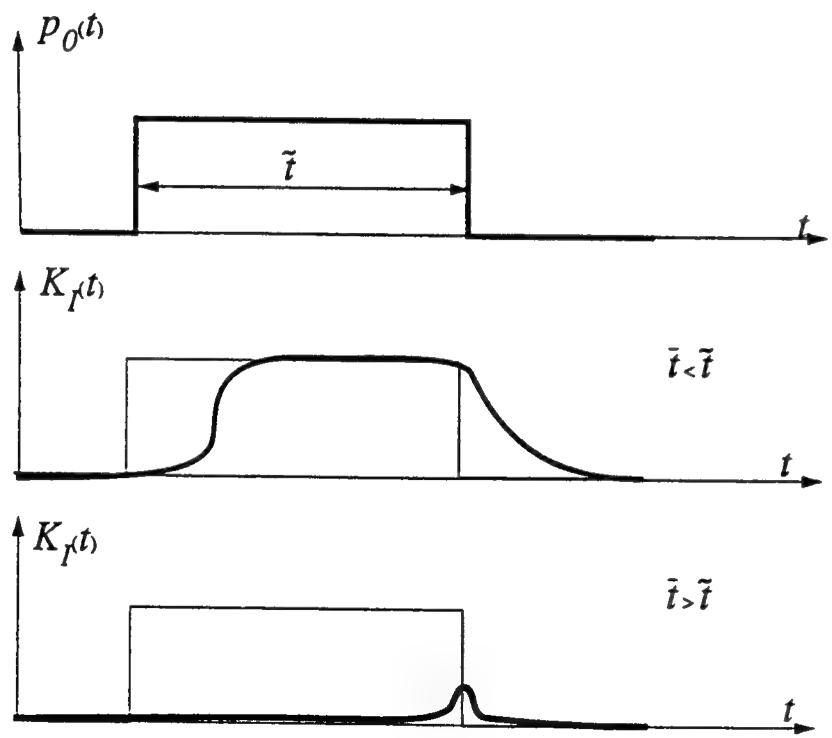

FIG.7 Response of crack to hydraulic pressure

Characteristic penetration time

$$\hat{t} = \frac{\mu}{E'}\left(\frac{a}{\hat{H}}\right)^3 F_T(\beta, BC)$$

where $F_T(\beta, BC)$ is a coefficient dependent on β, boundary condition and loading.

Surface Rheometer

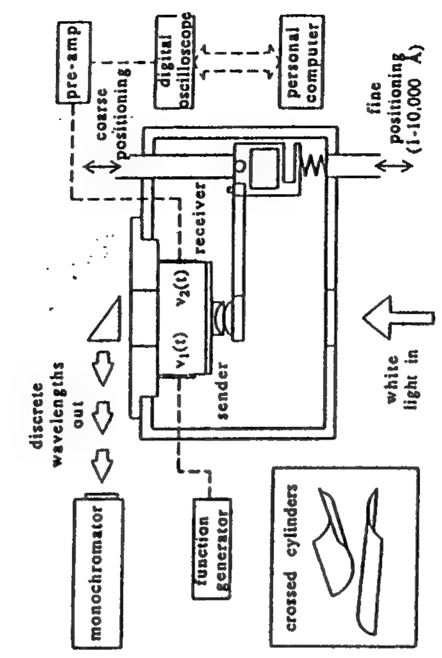

Figure 6. Surface rheometer designed by Van Alsten.

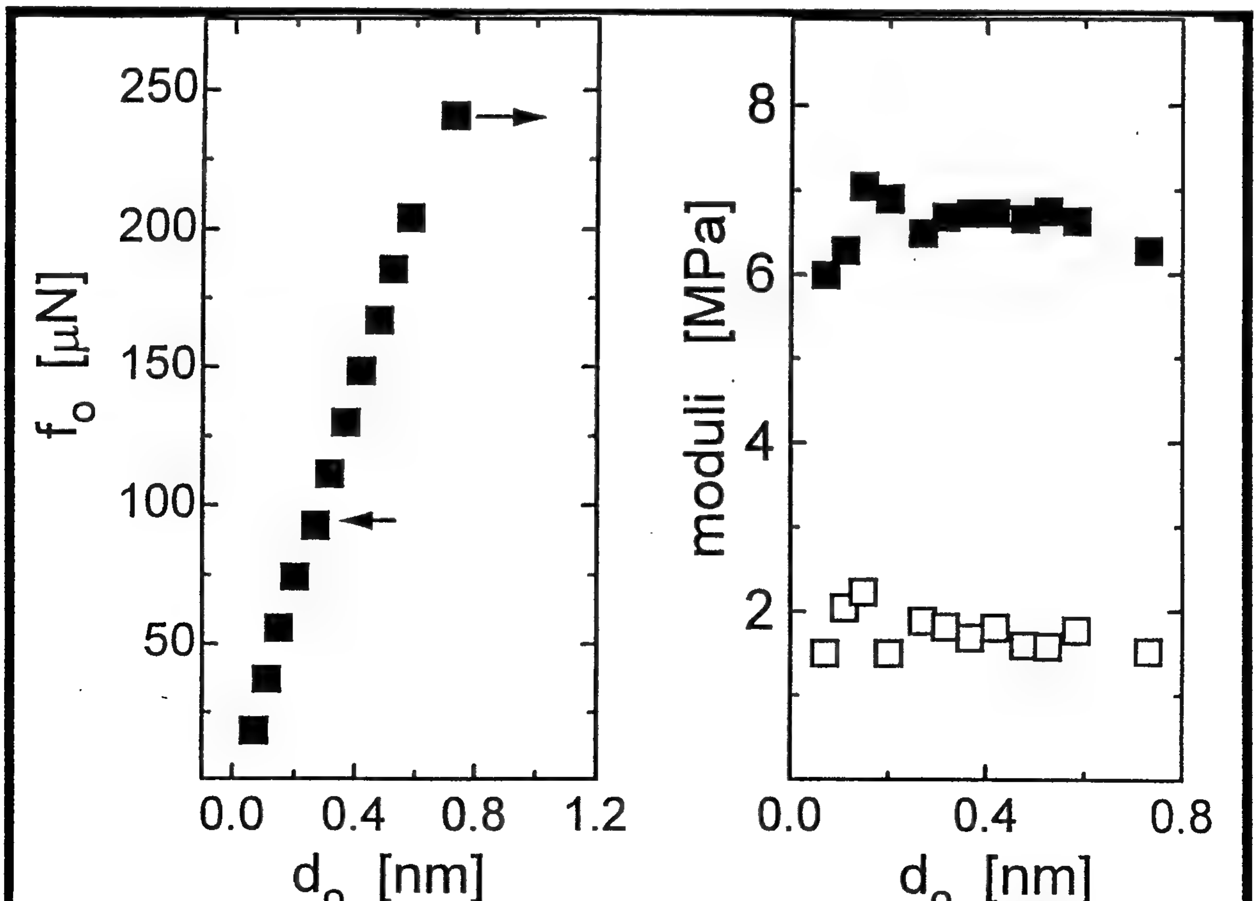

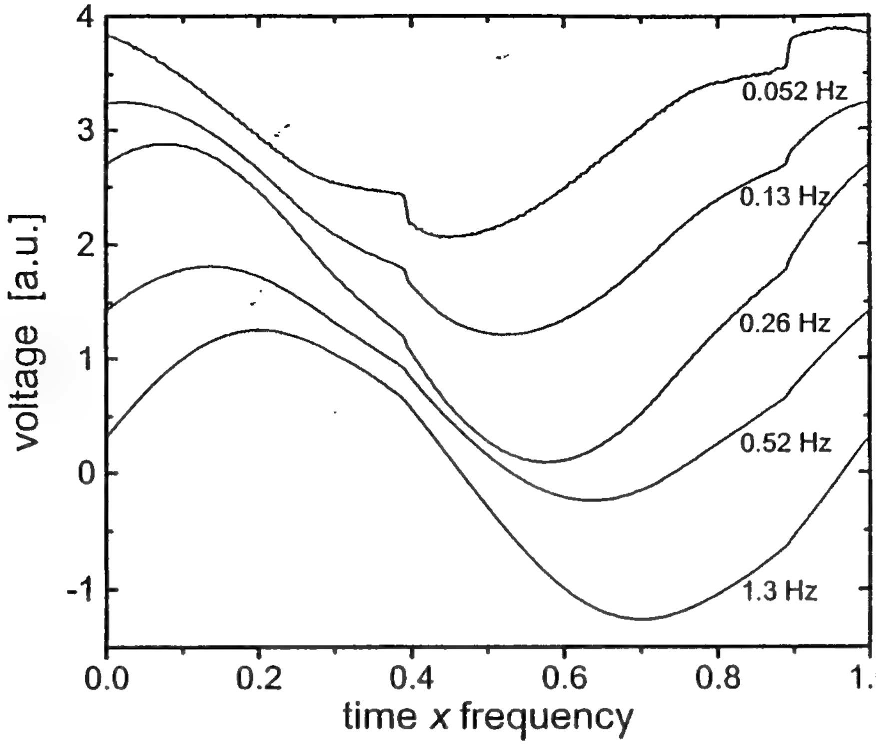

voltage [a.u.]
time x frequency
0.052 Hz
0.13 Hz
0.26 Hz
0.52 Hz
1.3 Hz

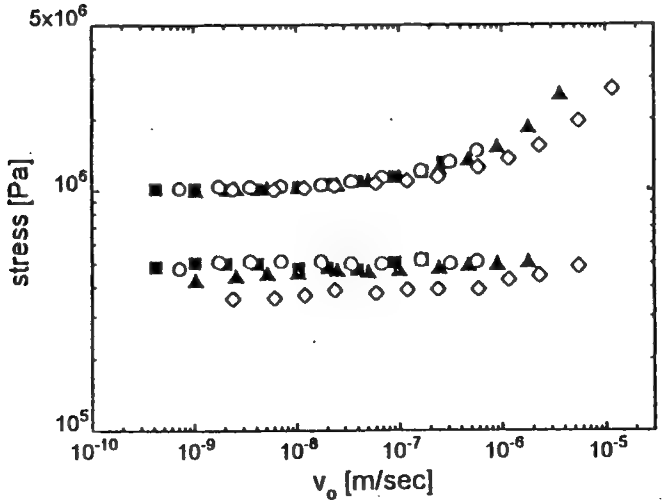

stress [Pa]
v_o [m/sec]
5x10^6
10^6
10^5

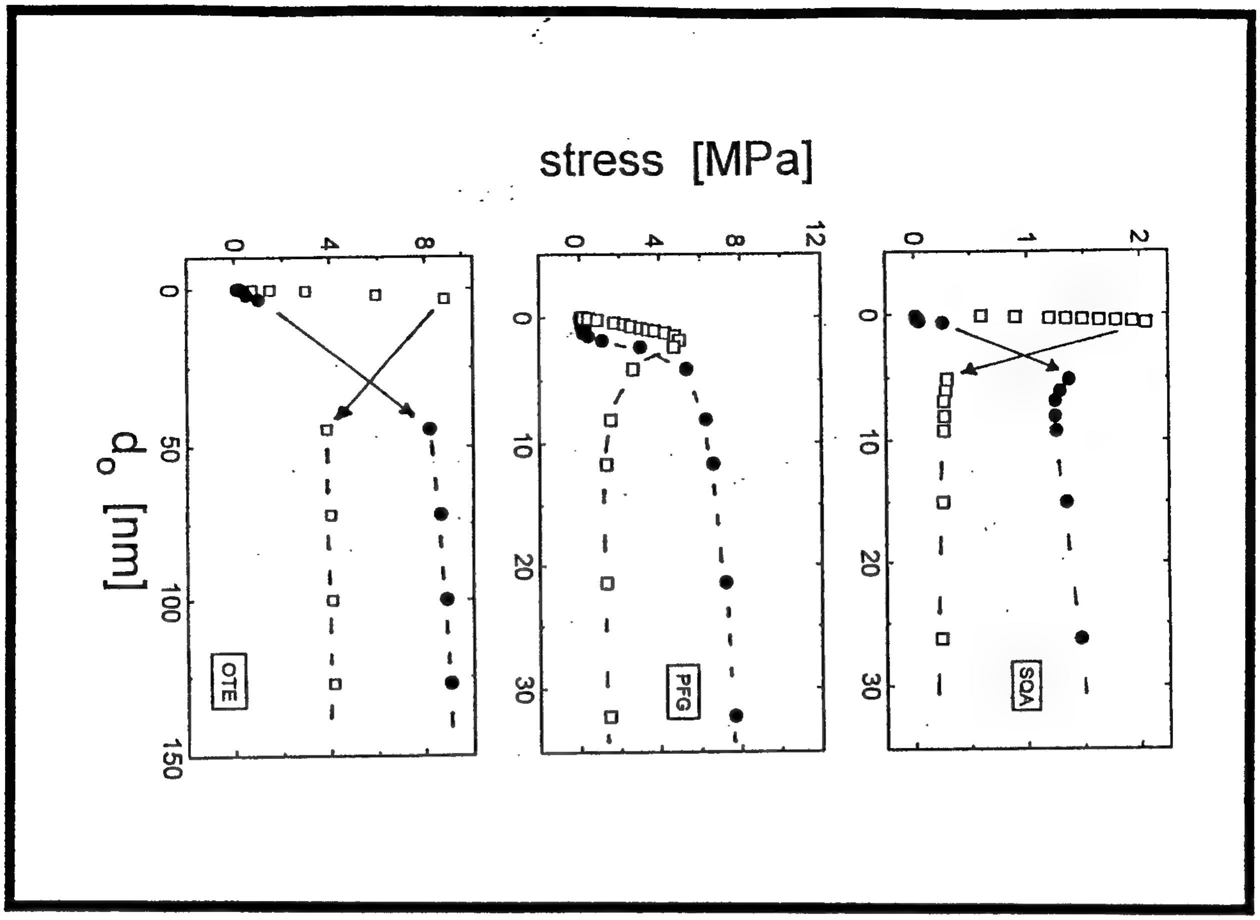
stress [MPa]
d_o [nm]
SQA
PFG
OTE
0
1
2
4
8
12
10
20
30
50
100
150

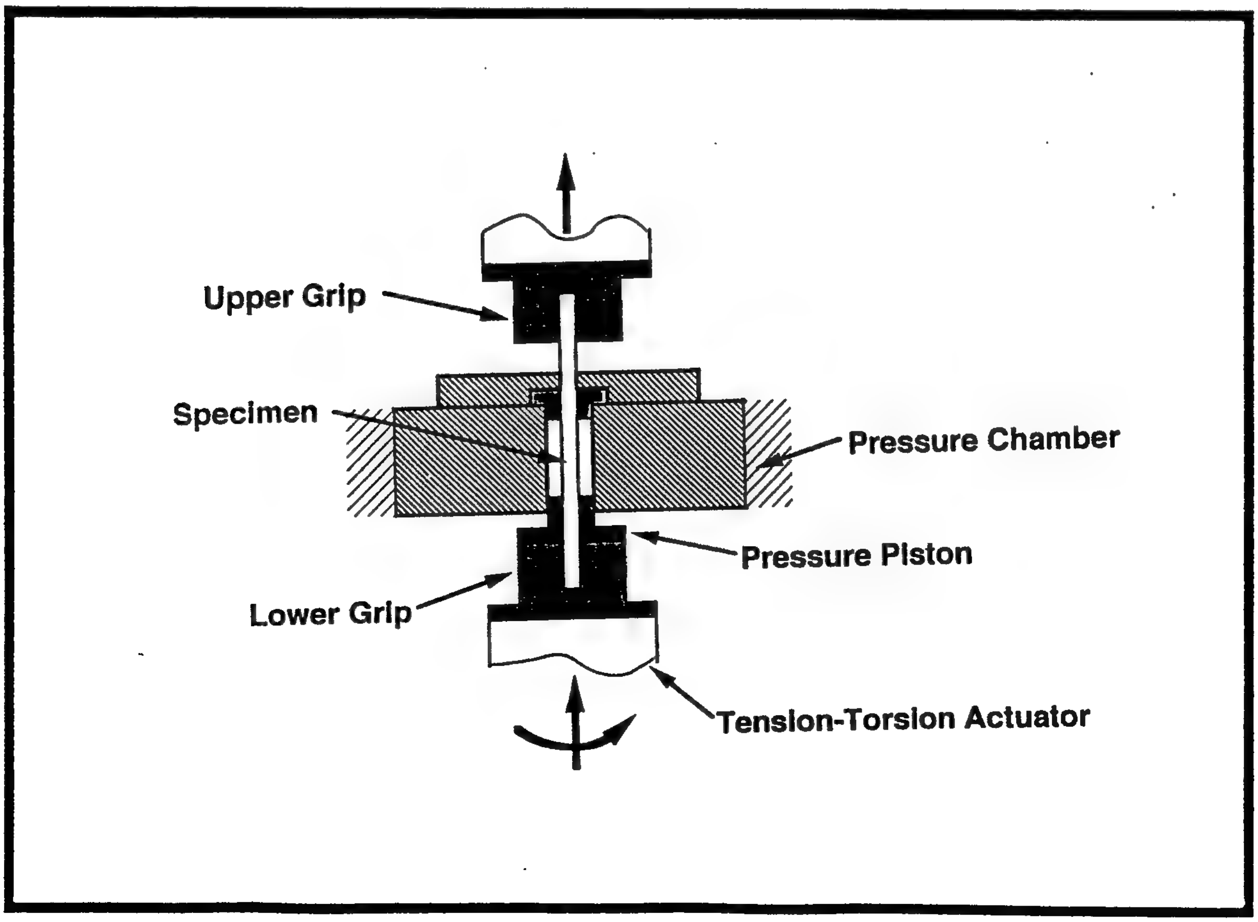
Upper Grip
Specimen
Pressure Chamber
Pressure Piston
Lower Grip
Tension-Torsion Actuator

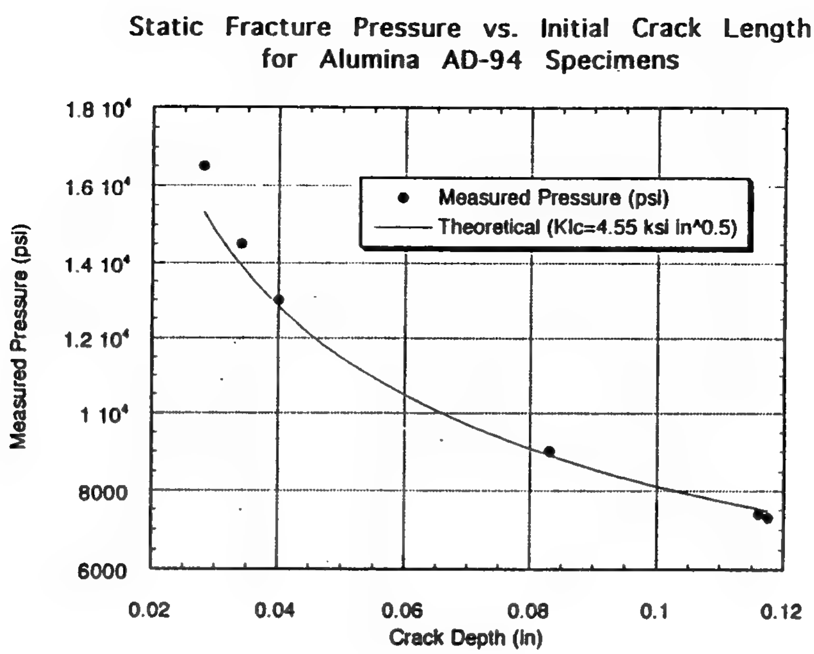

Static Fracture Pressure vs. Initial Crack Length
for Alumina AD-94 Specimens
Measured Pressure (psi)
Theoretical (KIc=4.55 ksi in^0.5)
1.8 10⁴
1.6 10⁴
1.4 10⁴
1.2 10⁴
1 10⁴
8000
6000
Measured Pressure (psi)
0.02
0.04
0.06
0.08
0.1
0.12
Crack Depth (in)

Initial Stages of Metallic Oxidation

Professor Steven J. Sibener

James Franck Institute and
Department of Chemistry
The University of Chicago
5640 South Ellis Avenue
Chicago, IL 60637

Today's Topics

- Electron Stimulated Oxidation of Metallic Interfaces: Ni(111) at Low Temperatures
  - Synergistic Effects Due to Electron Irradiation
- Initial Stages of Oxidation for a Stepped Metallic Surface: Ni(977)
  - Step Doubling/Undoubling Due to Oxygen Adsorption
- Atomic Force and Scanning Tunneling Microscopy Studies of Metallic Oxidation
  - Real Space Imaging of Corrosion Events
  - Future: Stress Effects in Metallic Corrosion

Schematic View of the Combined Molecular Beam/Inelastic Electron Scattering Apparatus

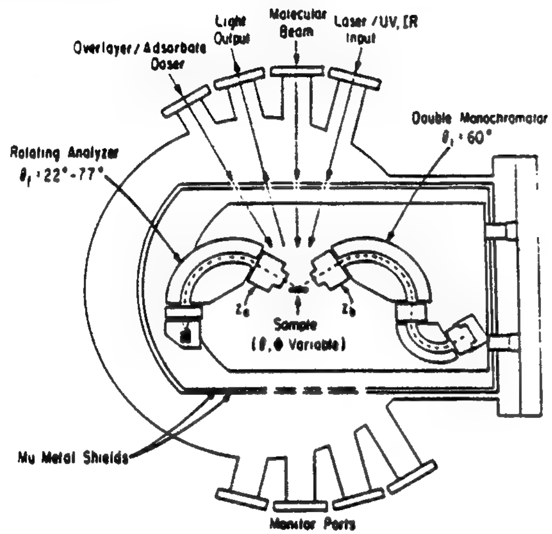

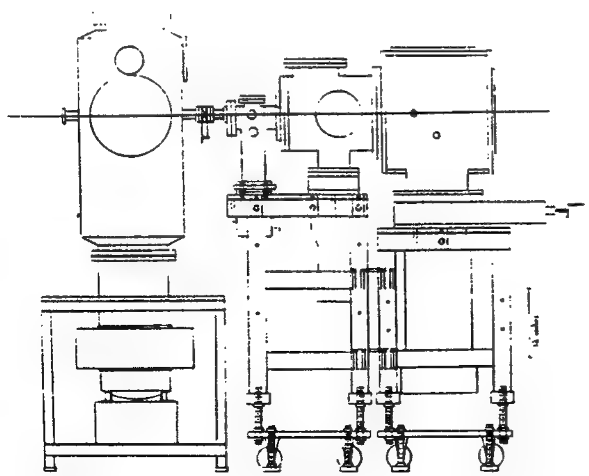

Electron Stimulated Oxidation of Metallic Interfaces: Ni(111) at Low Temperatures

<u>Question</u>: Can the oxidation/corrosion behavior of metallic interfaces be modified by the presence of electrons, and, if so:

- Can electrons influence the rate of interface oxidation?
- Can oxidation be stimulated to occur in regimes where such chemistry does not normally occur?
- Must oxidant and electrons simultaneously strike the target surface to stimulate oxidation, or may the substrate be sequentially exposed to oxygen and electrons?
- What is the cross section (i.e., probability) for such synergistic effects for electrons of various energies?
- Can we develop a theoretical model to explain such effects?

<u>Strategy</u>: Start with a low temperature substrate to maximize the signature of such synergistic effects. Use a wide variety of surface science techniques to address the problem:

- Auger Spectroscopy for elemental analysis and identification of metallic oxidation state; Low Energy Electron Diffraction (LEED) for structural analysis; High Resolution Electron Energy Loss Spectroscopy (HREELS) for vibrational spectroscopy of the interface; Electron Guns for investigating electron energy/flux effects; Molecular Beams (including kinetic energy control) for mechanistic studies; Scanning Tunneling/Atomic Force Microscopy for atomic level imaging/surface morphology studies, etc...

Direct Evidence for Electron Stimulated Oxidation of Ni(111) at Low Temperature

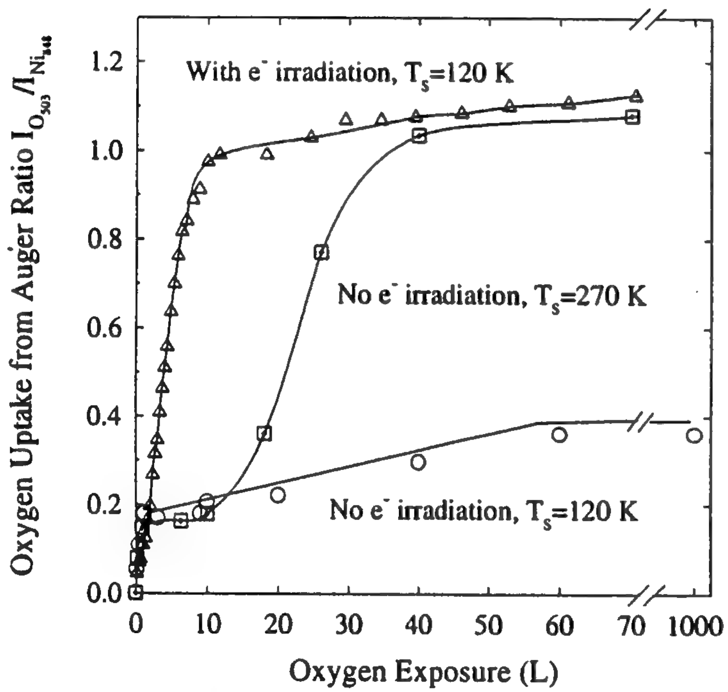

Conclusion: Synergistic Effects Involving Electrons Lead to Enhanced Interface Oxidation at Low Temperature

Various Stages of Ni(111) Interface Oxidation (Without Presence of Electrons)

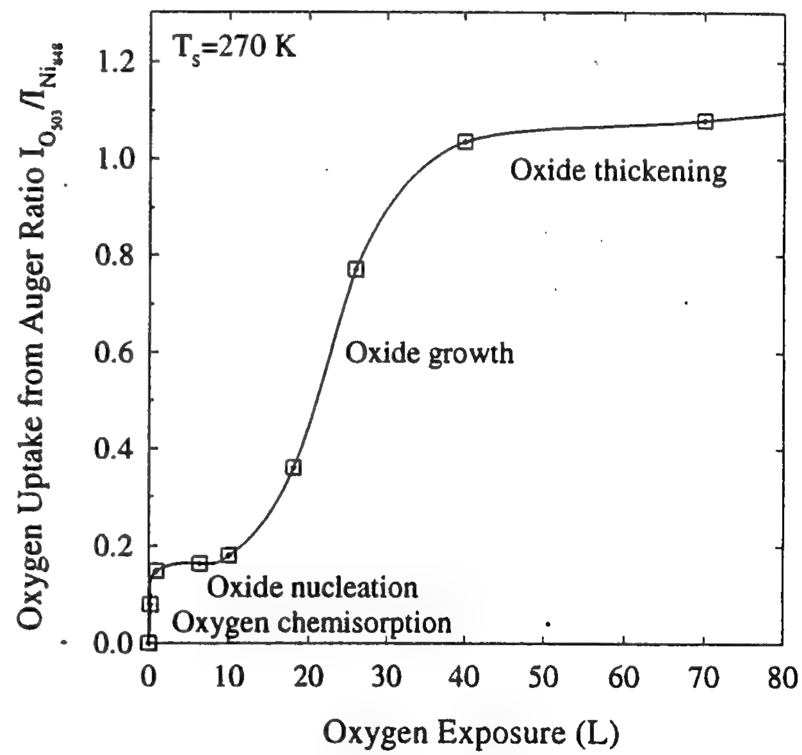

Electron Stimulated Oxidation Can Occur Under Two Very Different Irradiation Procedures:

- o Electron and Oxygen Exposure Occurring Simultaneously
- o Electron and Oxygen Exposure Occurring Alternately

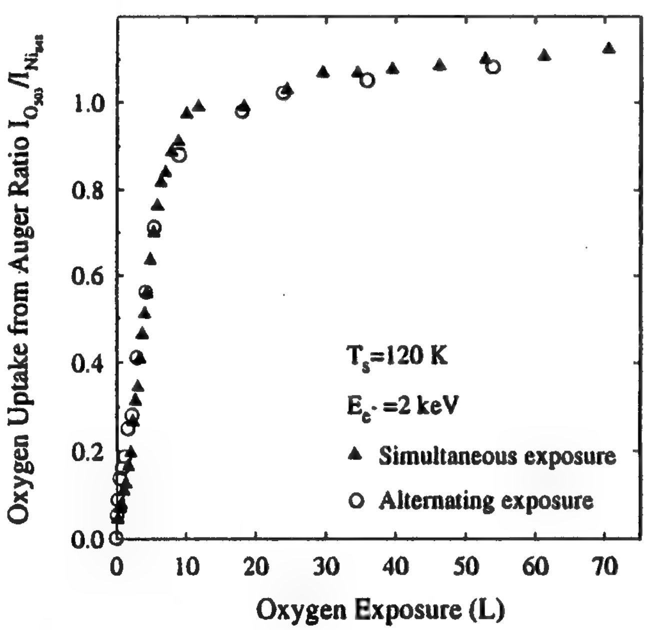

Conclusion: Electron Irradiation Creates Oxide Nucleation Centers Which are Relatively Stable

Surface Vibrational Spectra Can Differentiate Between Interfaces in Various Stages of Oxidation

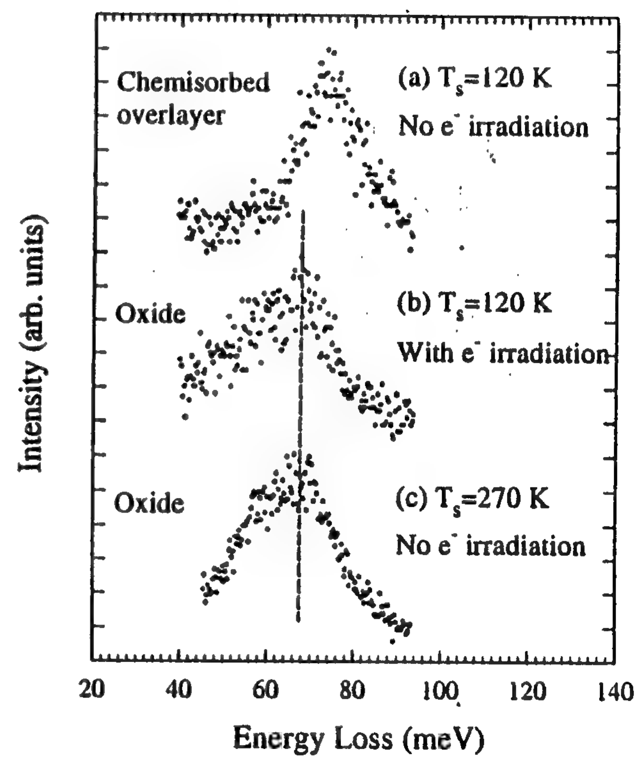

Conclusion: Electron Irradiation at Low Temperatures Can Stimulate the Formation of Nickel Oxide

Cross Sections for Electron Stimulated Oxidation Can Be Extracted From Modeling of the Data

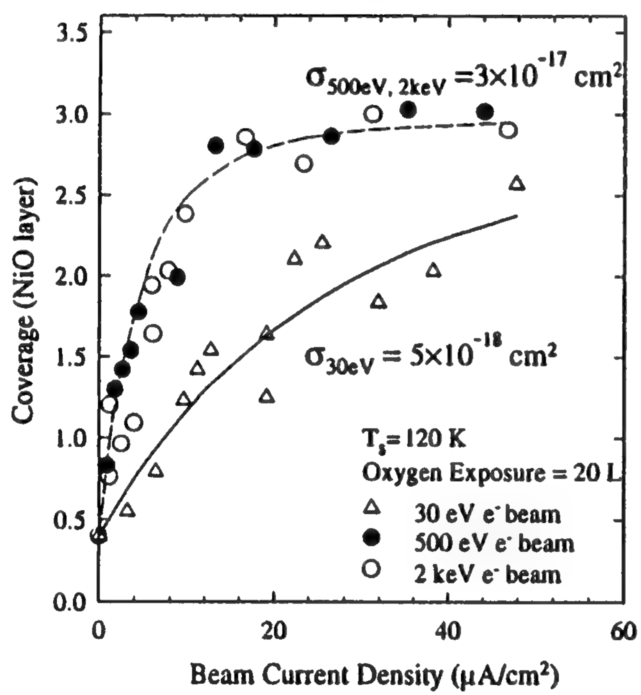

Conclusion: Cross Section Varies as a Function of Incident Electron Energy

Theoretical Model

Number (N) of nucleation centers created:

$$\frac{N}{N_0} = 1 - \exp\left(-\frac{i\sigma t}{e}\right)$$

N_0 --- saturation number of nucleation centers
i --- electron beam current density
t --- is electron exposure time
e --- unit electron charge
σ --- cross section

Oxide growth:

$$\frac{d\theta}{dt} = k(\theta_s - \theta)\frac{N}{N_0}$$

θ --- oxygen coverage
θ_S --- saturation coverage,
k --- rate constant

$$\theta = \theta_s - (\theta_s - \theta_c)\exp\left(-k\left(t_o + \frac{e}{i\sigma}\exp\left(-\frac{i\sigma t_o}{e}\right) - \frac{e}{i\sigma}\right)\right)$$

Summary

Primary Finding: Synergistic effects involving electrons can significantly modify the oxidation/corrosion behavior of nickel.

Future : Continue to explore the mechanism which accounts for this effect. Extension to other materials, oxidants, and temperature regimes.

Related Work

- How does the incident kinetic energy of the oxygen beam influence the rate and extent of metallic oxidation/corrosion?
- Does oxidation/corrosion behavior depend strongly on the chemical composition of the oxidant?
- How does *stress* factor into our atomic-level view of oxidation/corrosion?

Comparison of Model Predictions and Oxygen Uptake Data for Electron Stimulated Oxidation of Ni(111) Using Constant Electron Flux Densities

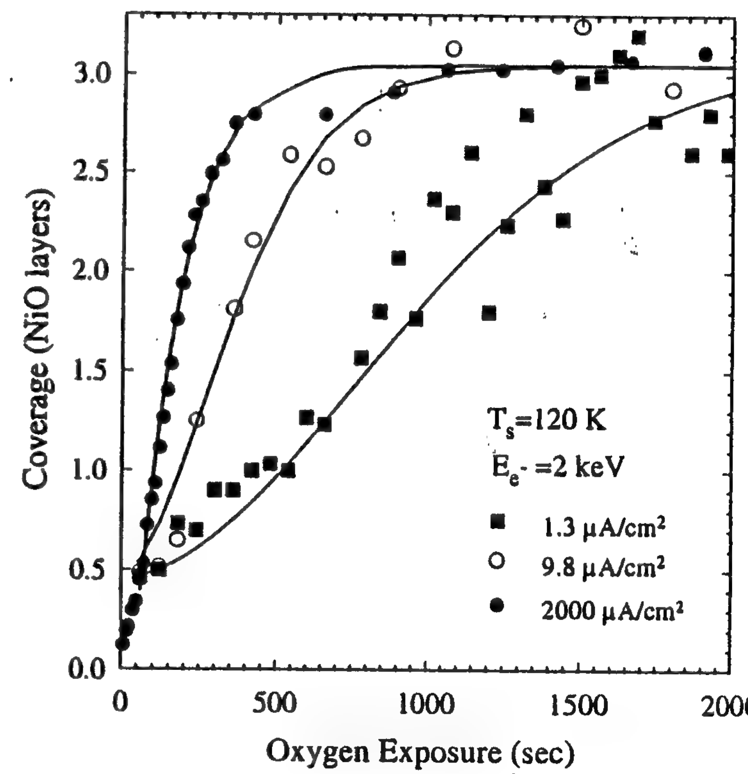

Conclusion: Theoretical Model Successfully Accounts for the Experimental Data

What are the initial stages of oxidation for a stepped metallic surface?

- Ni(977): Model system for corrosion studies
- Structural and Vibrational Properties Characterized with Low Energy Neutral He Scattering
- Observation of Step Doubling and Un-Doubling
  - Kinetics
  - Diffusion Coefficients for Ni during Oxidation
  - Mechanism of Step Coalescence
- How do the forces present at stepped surfaces differ from those at smooth surfaces and the bulk?
  - New Localized Modes
  - Concepts: Surface Stress and Surface Softening

SCHEMATIC DIAGRAM OF THE HIGH RESOLUTION NEUTRAL PARTICLE SCATTERING APPARATUS

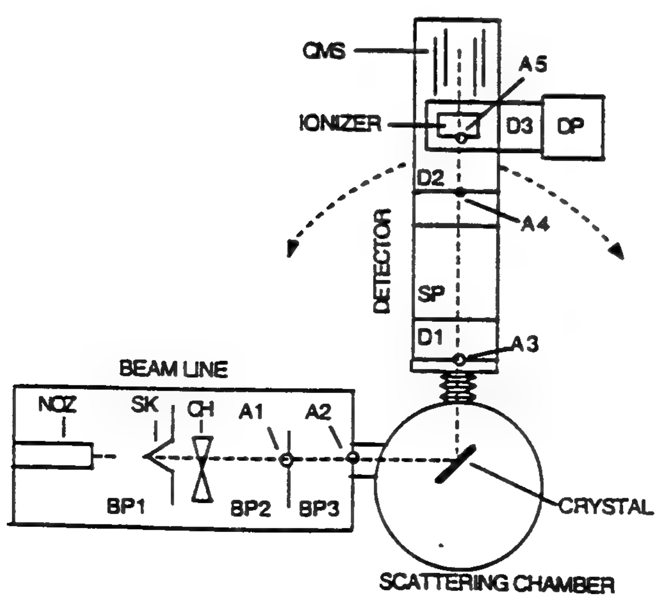

SCHEMATIC DIAGRAM OF NI(977) SURFACE AND SCATTERING GEOMETRY ALONG ITS STEP DIRECTION

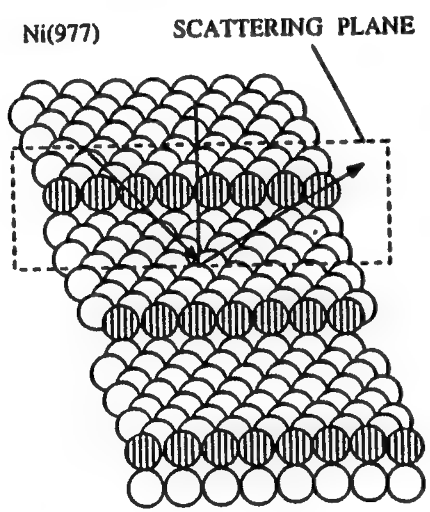

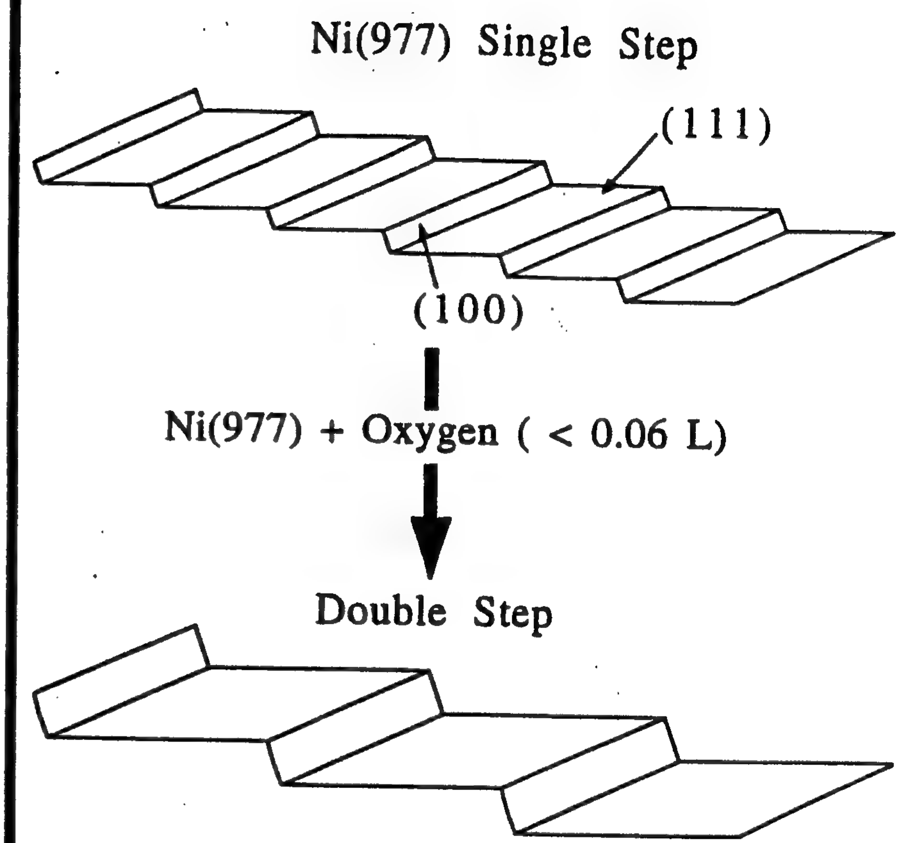

Step Doubling

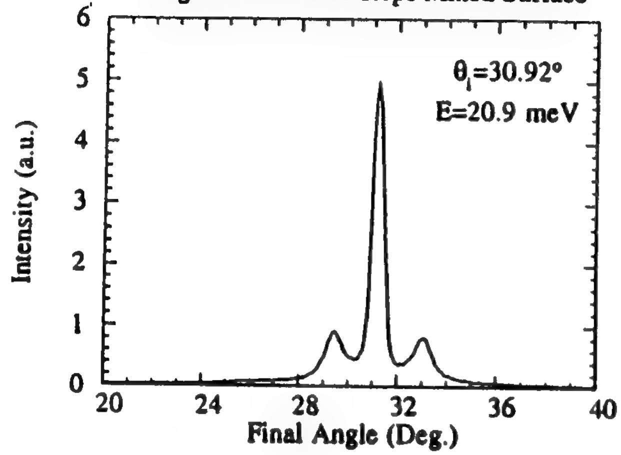

Experimental Diffractive Spectrum Due To
A Single And Double Steps Mixed Surface

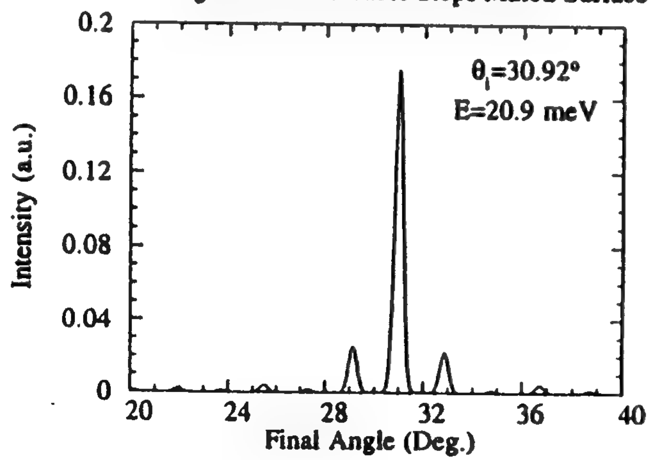

Calculated Diffractive Spectrum Due To
A 1/5 Single And 4/5 Double Steps Mixed Surface

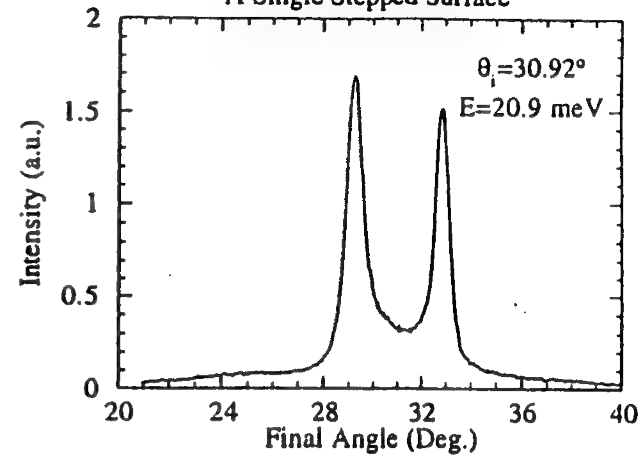

Experimental Diffractive Spectrum Due To
A Single Stepped Surface

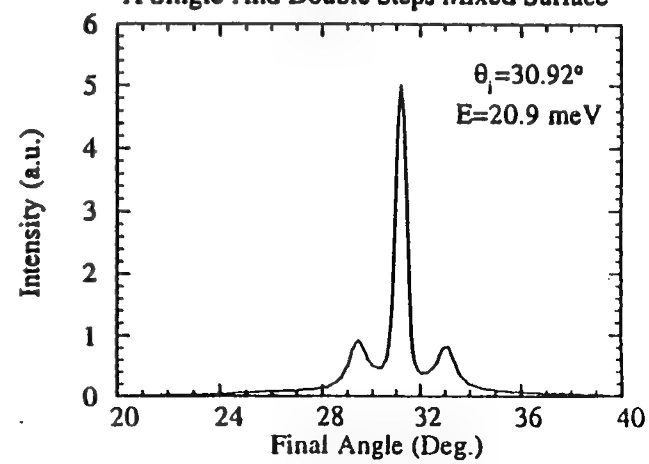

Experimental Diffractive Spectrum Due To
A Single And Double Steps Mixed Surface

Structural Evolution During Oxidation at Fixed Crystal Temperature (500K) Const. Dosing Rate of 5×10^{-10} torr O_2

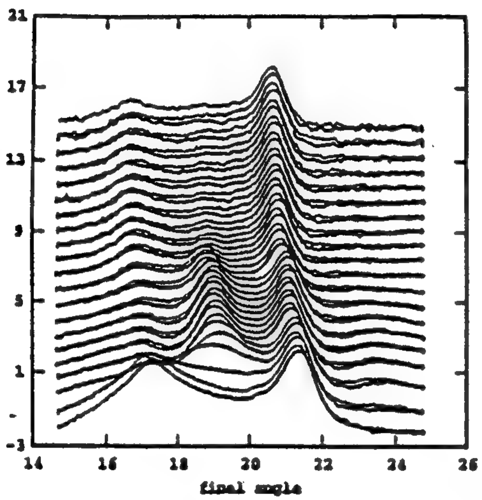

Expanded View

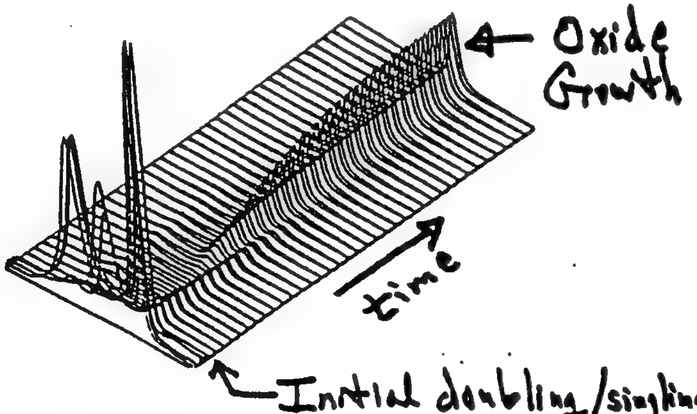

Structural Evolution of Ni(977) Surface Under Constant Oxygen Dosage Pressure of 4×10^{-10}

(Peak from step doubling/undoubling)

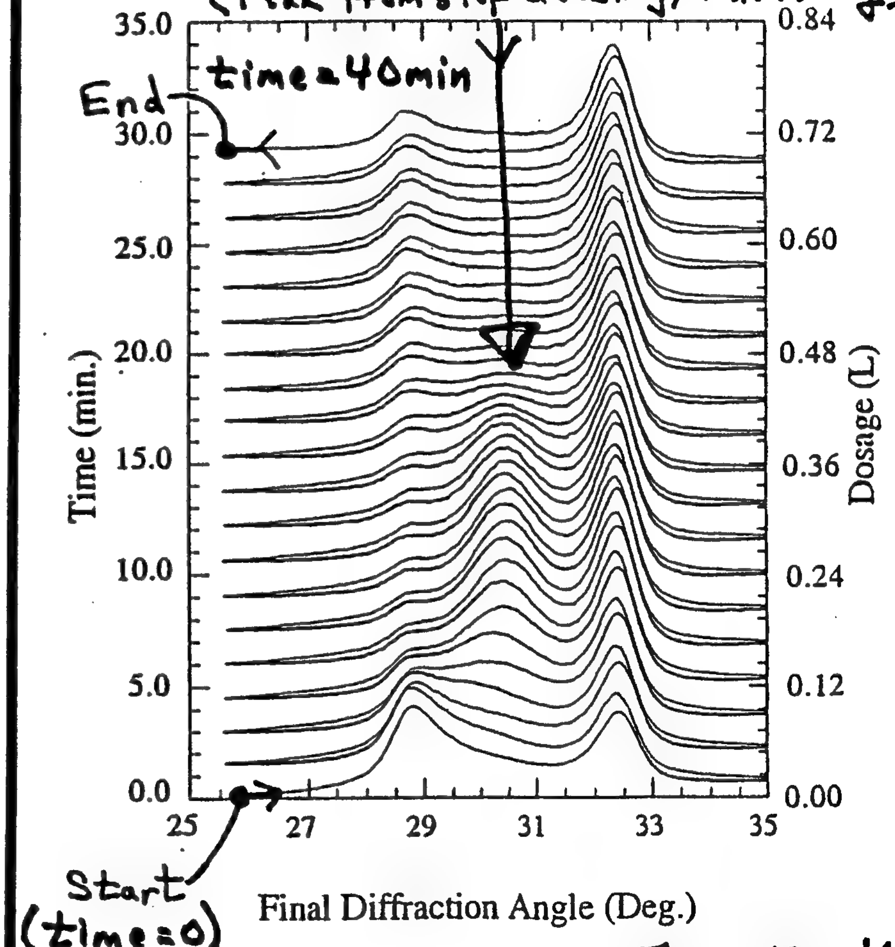

$T_{surf} = 500K$

Double Step Growth As A Function of Crystal Temperature At A Fixed Oxygen Coverage (0.018L)

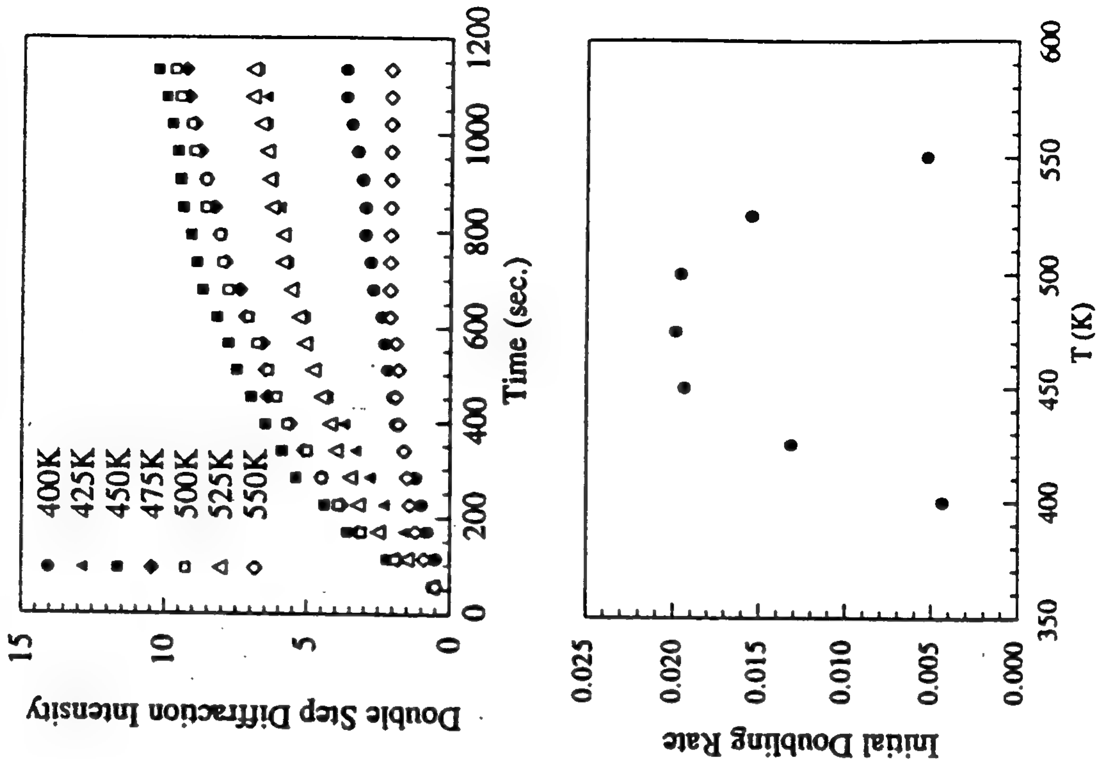

Temperature Range Over Which Step Doubling Occurs
(ca. 375 - 575K)

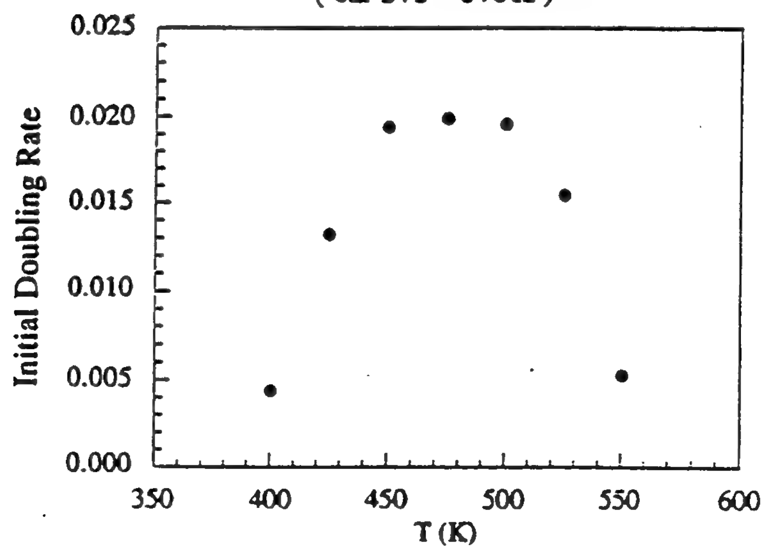

Key Technique:

We use out-of-phase condition for single stepped surface:

$$kh(\cos\theta_i + \cos\theta_f) = (2n+1)\pi,$$

and in-phase condition for double stepped surface:

$$k(2h)(\cos\theta_i + \cos\theta_f) = 2(2n+1)\pi = 2m\pi,$$

so that we can monitor the diffraction intensity due to double stepped surface only.

Helium Scattering From A Fully Double Stepped Surface (In-Phase: High Signal) And A Fully Single Stepped Surface (Out-of-Phase: Low Signal)

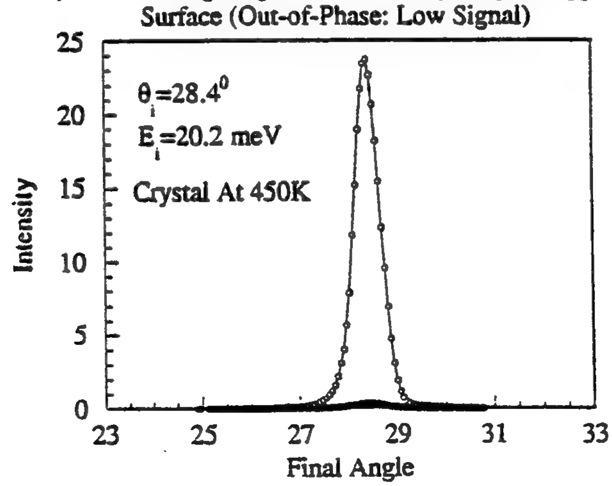

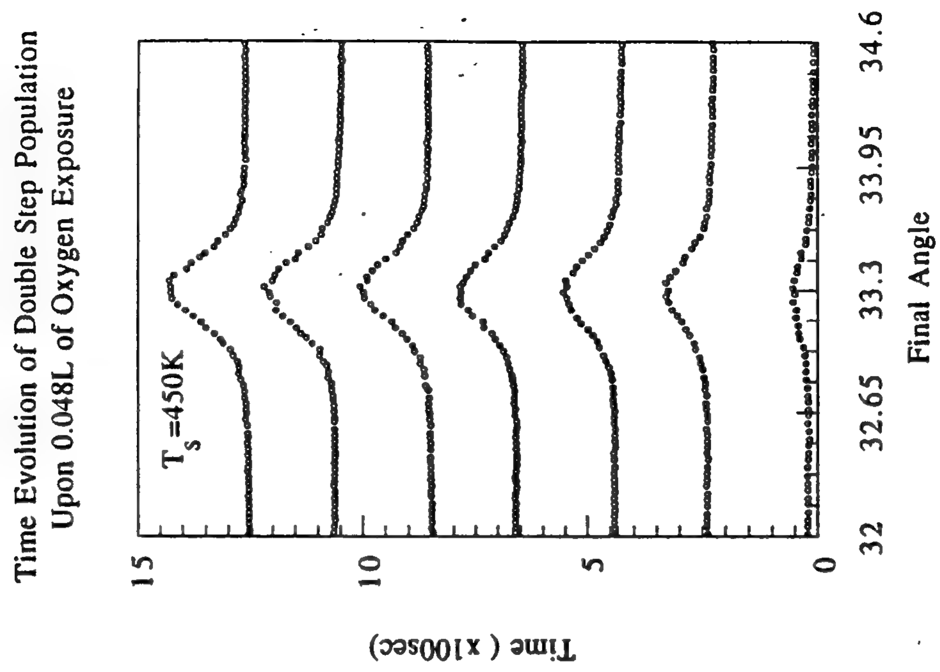

Kinetics of Step Doubling:

$S + S \longrightarrow D$, 2nd Order,

$$\frac{d[D]}{dt} = K\{1-[D]\}^2,$$

Assume $I_D \propto [D]$,

Then, $I_D(t) = I_0(1-\frac{1}{Kt+1})$

Arrhenius Analysis: Mobility information for surface Ni atoms with the presence of oxygen.

Under 0.018L of oxygen exposure:

$E_a = 0.74eV$, $A_0 = 5.2x10^5 S^{-1}$

Under 0.048L of oxygen exposure:

$E_a = 0.52eV$, $A_0 = 1.35x10^3 S^{-1}$

Oxygen coverage dependent, surfactant assisted.

Conceptual Views of Stepped Surfaces

Single Steps

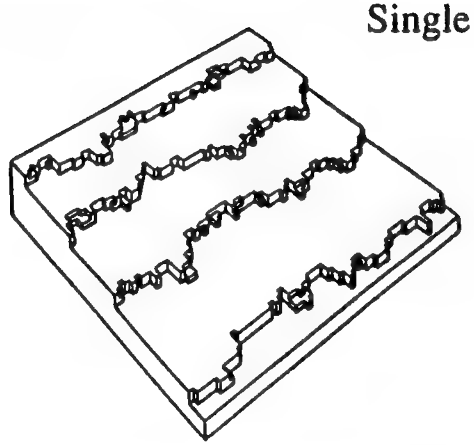

Mixed Single and Double Steps

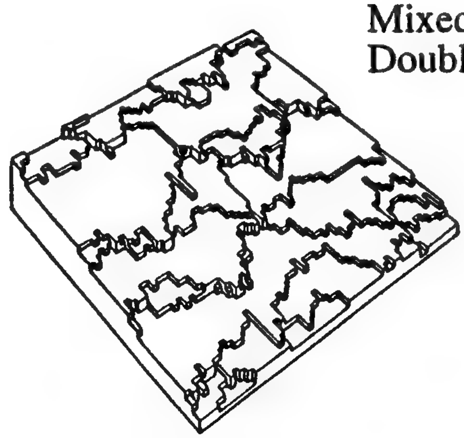

Step Doubling and 2^{nd} Order Kinetics Fits

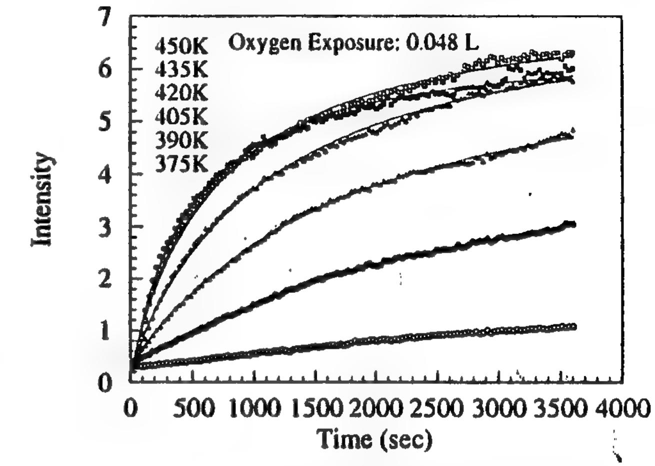

Arrhenius Analysis for Step Doubling Rate Due to Oxygen Exposure: Rate = $A_0 \exp(-E_a/k_B T)$

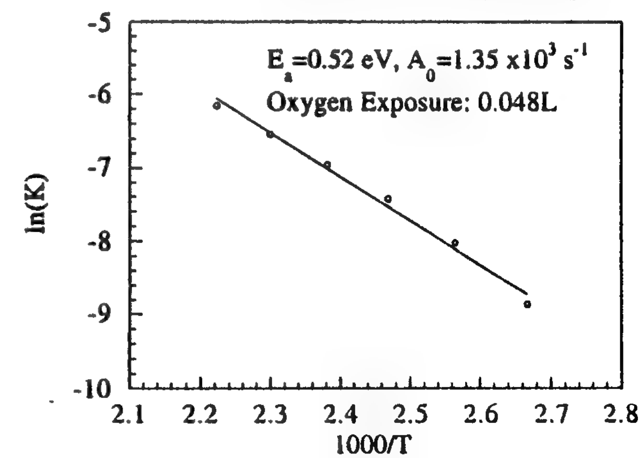

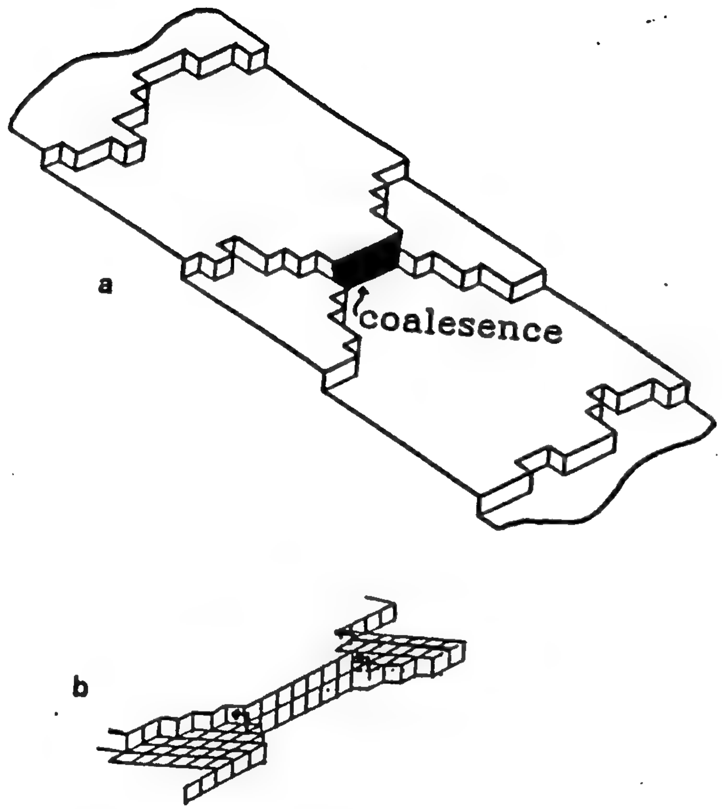

Step Coalescence

Ni(977) Oxidation

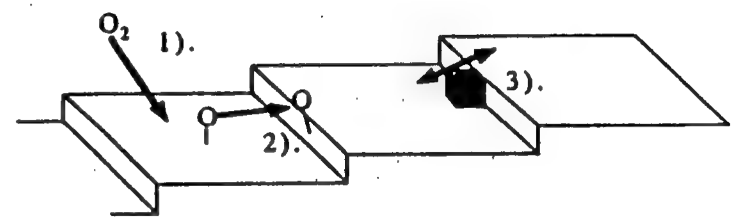

1). Adsorb Oxygen

2). Oxygen migrates to step edge

3). Steps coalesce

Figure 100. Diagram of the oxidation mechanism describing some of the kinetic steps that occur during the initial oxygen induced step doubling mechanism.

Surface Stress on Ni(111)
Via Surface Phonon Spectroscopy

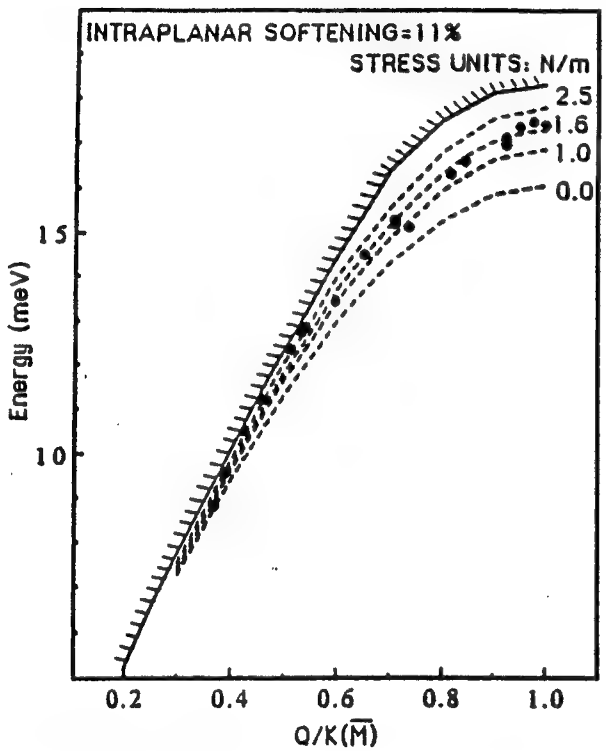

→ Stress plays a significant role on the atomic level (e.g., thin film stability)

STM and AFM Studies of the Morphology and Kinetic Pathways for Corrosion Reactions of Stressed Materials

- New atomic/mesoscopic level imaging program is getting underway
- These instruments will provide real space imaging data to complement and further leverage our other kinetic measurements
- Attempt to correlate surface morphology with reactivity: role of steps, kinks, grain boundaries
- Effect of local chemical environment on oxidation promotion or surface passivation
- Will ultimately examine the role that stress plays in atomic level kinetic processes relating to interface oxidation and corrosion -- We can assess the magnitude of surface stress on clean and adsorbate covered surfaces via surface phonon spectroscopy measurements and other methods. Can we develop a model of surface oxidation kinetics including stress effects?
- Imaging in air, electrochemical, and vacuum environments will be possible

ATOMIC FORCE MICROSCOPY IMAGE FOR POLISHED SAMPLE OF AIR OXIDIZED ALUMINUM

Wide field 3-D view 1.0 um x 1.0 um x 630 A

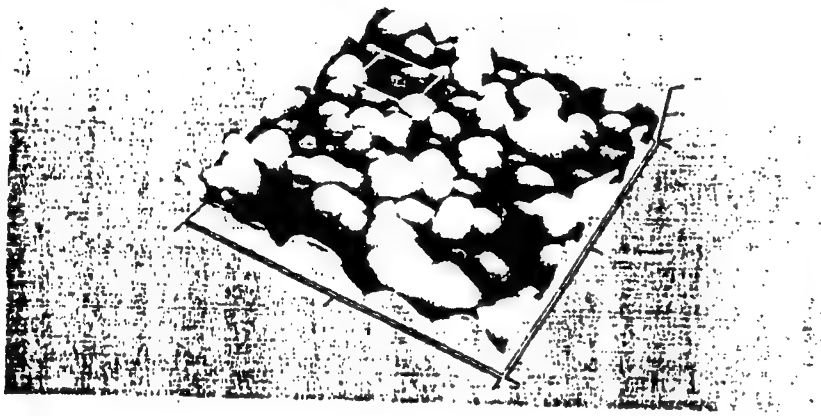

Small field 3-D view 0.2 um x 0.2 um x 380 A

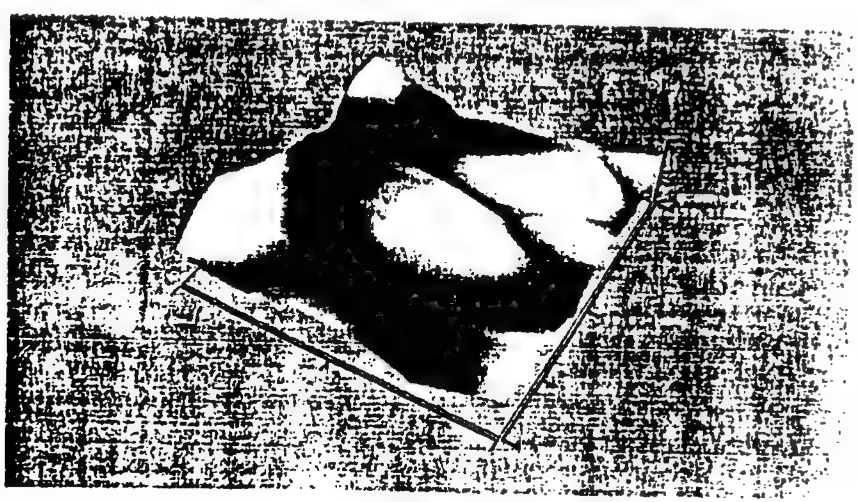

SCHEMATIC REPRESENTATION OF ATOMIC FORCE MICROSCOPY

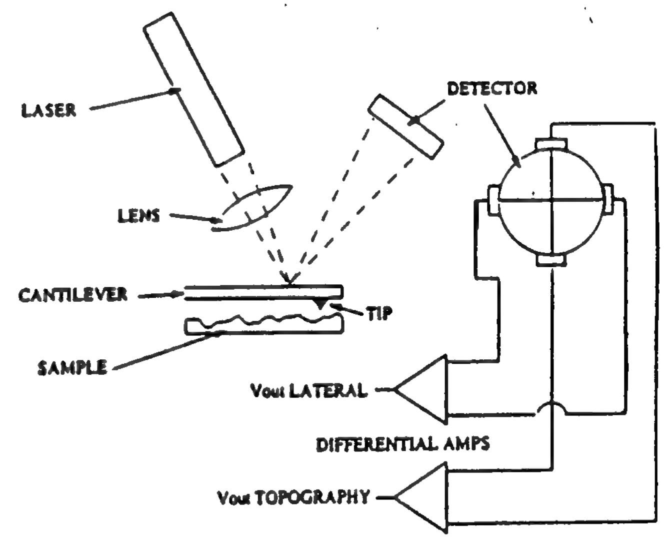

Summary & Take Home Lessons

- Many important issues must be explored with modern tools to improve our understanding of interface oxidation/corrosion at the atomic level

- The few topics we have already explored have all yielded major surprises and fresh insights

- Chemical Corrosion

- Electrochemical Corrosion

⇒ The Hope: An improved understanding of atomic level mechanisms may hold the key to improved methods of corrosion inhibition for real-world technical materials...

Cancer ←←←"Disease"→→→ Corrosion

Antioxidants ⇐ *Prevention* ⇒ Chemical Potential

MRI/Biopsy ⇐ *Detection* ⇒ NDE/Sectioning

Chemotherapy ⇐ *Treatment* ⇒ Replacement
Surgery... Refurbishment...

ATOMIC FORCE MICROSCOPY IMAGE FOR POLISHED SAMPLE OF AIR OXIDIZED ALUMINUM

Wide field 2-D view 1.0 um x 1.0 um x 630 Å

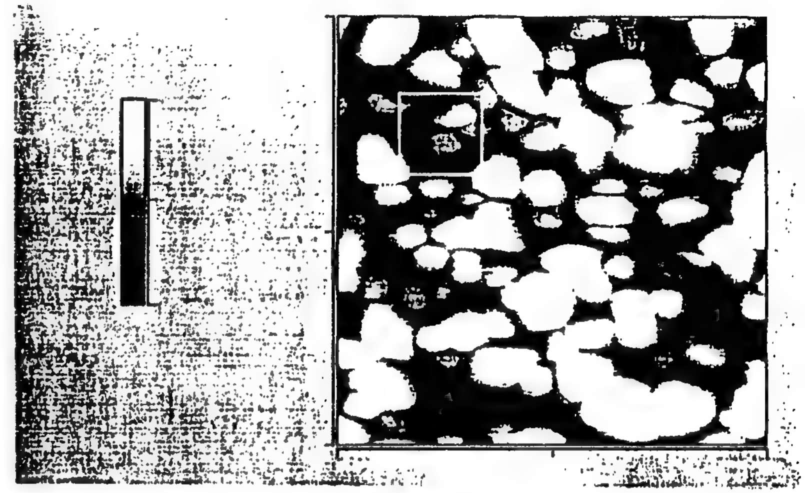

Small field 2-D view 0.2 um x 0.2 um x 380 Å

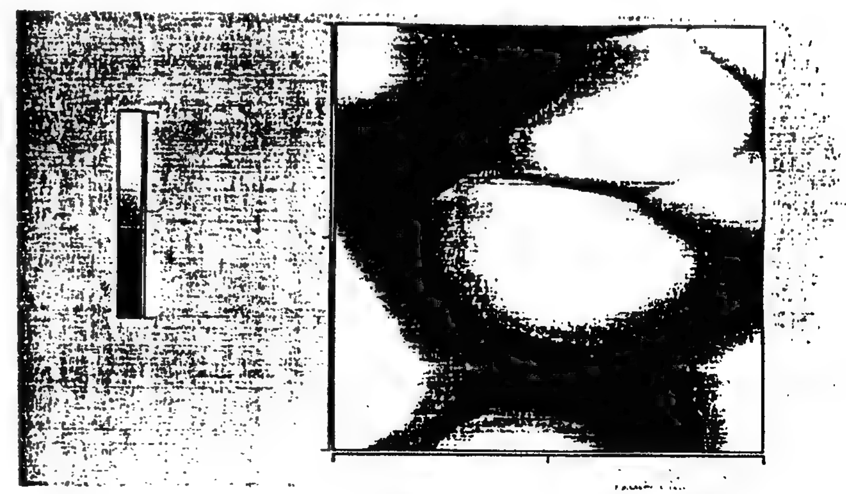

Acknowledgments

Electron Stimulated Oxidation of Ni
Wei Li
Michael Stirniman

Oxidation of Stepped Ni Surfaces
Daniel Gaspar
Suzanne King
Daniel Koleske
Licheng Niu

Surface Phonon Spectroscopy of Ni and O/Ni
Peter Knipp
Warren Menezes
Glenn Tisdale

Atomic Force/Scanning Tunneling Microscopy
Errol Sanchez

Financial Support
AFOSR, AFOSR/Corrosion URI, AASERT, and
Seed Funding from NSF-MRL at U. of Chicago

Experimental and theoretical aspects of corrosion detection.

University of Connecticut

P.I.– W. R. Madych, Mathematics
Co P.I.'s – O. Devereux, Metallurgy and G. Hernandez, Mathematics
Research Assistant – P. Su, Metallurgy

Theory (Hernandez)

We study the model for internal/external oxidation of an alloy composed of two metals A and B as detailed in Hagan, Polizzotti, and Luckman, Internal oxidation of binary alloys, *SIAM J. Appl. Math.* 45 (1985) , 956-971.. The basic assumption is that only metal B will react, i.e. only oxide of B, BO_q is formed, and that this oxide is protective, so A , B atoms and the oxygen O atoms can not diffuse through these oxide particles. Generally, oxide blocking is not accounted for in standard treatments of alloy oxidation.

Notation:

$$
\begin{aligned}
\Omega &= \text{element of volume } = \Omega_M \cup \Omega_Z \\
\Omega_Z &= \text{volume of all oxide particles} \\
\Omega_M &= \text{volume containing all } A, B, O \\
\epsilon &= \Omega_M / \Omega \\
a &= \text{concentration of } A \text{ in } \Omega_M \\
b &= \text{concentration of } B \text{ in } \Omega_M \\
c &= \text{concentration of } O \text{ in } \Omega_M \\
Z &= \text{concentration of } BO_q \text{ in } \Omega
\end{aligned}
$$

The equations which are used to describe the oxidation are as follows:

$$
\begin{aligned}
(\epsilon b)_t &= \nabla \cdot (E(kZ) d_1 \nabla b) - \nabla \cdot (\mathbf{v} \epsilon b) - \frac{\epsilon b c}{\eta} \\
(\epsilon c)_t &= \nabla \cdot (E d_0 \nabla c) - \nabla \cdot (\mathbf{v} \epsilon c) - \frac{q \epsilon b c}{\eta} \\
Z_t &= -\nabla \cdot (\mathbf{v} Z) + \frac{r}{\eta} \\
v_x &= (k-1) \frac{\epsilon b c}{\eta} \\
\epsilon + kZ &= 1
\end{aligned}
$$

and the initial-boundary conditions:

$$
\begin{aligned}
&v = 0 \ , \quad b_x = 0 \ , \quad c = c^*, \quad \text{at} \quad x = 0 \\
&b = b_0 \ , \quad c = 0 \ , \quad Z = 0 \quad \text{at} \quad t = 0. \\
&\qquad \epsilon(0, t) = \epsilon_0(t) \quad \text{for} \quad t > 0
\end{aligned}
$$

where the parameters E, d_0, d_1, η, q, and k are related to each other and the bulk velocity $\mathbf{v}$ and the variables ϵ, a, b, c, and Z in a known (hypothesised) way.

The goal is to

- Understand this system mathematically. i.e. existence. uniqueness: continuous dependence. numerical solutions.
- Determine whether it is useful in predicting failure. i.e. practical value, how well does it model reality.

Results to date:

Application of known mathematical techniques gives existence theory. Because system is hyperbolic/parabolic answers to other questions are still at a very preliminary state.

IMPEDANCE IMAGING FOR AIRFRAME CORROSION PREDICTION AND DETECTION

Prof. Owen F. Devereux
Pocheng Su

Department of Metallurgy
and
Institute of Materials Science
University of Connecticut

samples from — Naval Air Research Center, Penn.

Notes re

"Impedance Imaging for Airframe Corrosion Prediction and Detection"

Slide 1:

Slide 2:

All metallic corrosion is electrochemical in nature.

Electrochemistry describes the reactions between an electronic conductor (the metal, or electrode) and an ionic conductor (the electrolyte).

The corrosion reaction is Faradaic (proportional to the current passed) and resistive, but typically non-Ohmic (R_p).

The electrode surface has a non-homogeneous distribution of charges due to selective adsorption of ion - this creates capacitive behavior (C_p).

The electrolyte is an Ohmic conductor of ions (R_s).

Slide 3:

An RC circuit can be represented as a Nyquist (or Cole-Cole) plot of Z(imaginary) vs. Z(real) over a range of frequencies or . . .

Slide 4:

a Bode plot of Z(real and Z(imaginary) vs. frequency, typically on a log-log plot.

Slide 5:

The electrochemical system comprising the aircraft structure is complicated by the presence of dissimilar metals (a *Galvanic* cell) and a protective coating (either paint or a *chemical conversion coating*, e.g., chromate).

Slide 6:

Localized corrosion can occur if the protective coating is broken, and be manifested as crevice corrosion between mating components or between paint and component, or as intergranular corrosion.

Slide 7:

The mechanism of crevice corrosion is well established as a *differential oxygen cell*. General corrosion is a balance of anodic and cathodic reactions. Within a crevice the environment is oxygen deficient (oxygen has been consumed and can only be re-supplied by diffusion) and the anodic reaction dominates, making this region negative with respect to the exposed surface, which is then cathodic. Metal dissolution occurs within the crevice and the hydrolysis of metal cations to form a solid corrosion product further isolates the crevice environment.

Slide 8:

The mechanism of crevice corrosion is identical to that for pitting corrosion except that pitting is initiated by a breakdown in passivity, while crevice corrosion is initiated by geometric factors. Once started, they progress in the same manner.

Slide 9 and 10:

Our plan is to characterize various electrodes representative of both the normal and the corroded aircraft structure via *electrochemical impedance spectroscopy* (EIS), to model this behavior by an appropriate RC circuit, and to understand the electrochemical implications of the circuit (i.e., determine the physical interpretation of the various resistors, capacitors, and other elements). We will then propose a hand-held instrument suitable for field use that will determine such characteristic spectra for an in-service aircraft and assess the presence or absence of corrosion.

Slide 11:

This slide depicts a Nyquist plot, Z(imaginary) vs. Z(real), for a painted aluminum specimen for different times of immersion in 3% aqueous NaCl. The curves are comprised of two circular arcs, representing two (RC) elements in parallel. One of these elements, the small circle at the left (high frequency) represents reaction at the paint metal interface; the other, the large circle, represents the geometric capacitance of the paint film. The figure shows that the resistance of the paint film decreases with exposure time, indicating diffusion of water into the paint.

Slide 17:

The foregoing data are initial results, intended to give us experience with application of EIS (electrochemical impedance spectroscopy) to the aluminum/salt water system and to demonstrate that the EIS spectra are sensitive to changes in the surface.

We propose to:

A) Continue with a methodical "fingerprinting" of the electrochemical behavior of surfaces representing both intact and corroded airframe structures,

B) Continue to model our experimental observations with circuits that are consistent with electrochemical expectations, and

C) Devise specifications for the construction of a prototype field instrument.

Slides 18 & 19

Experimental Setup.

Slide 12:

The circuit corresponding to the painted aluminum electrode. This is identical to the circuit for the simple electrode, with a geometric capacitance and "pore" resistance forthefilm superposed on it.

Slide 13:

This set of plots is similar to the previous Nyquist plot except that the paint film displayed a blister. Note that the scale of the axes is appreciably different; the big circle in these figures corresponds to the small circle in the previous figure. This means that the effective resistance of the paint coating has decreased from meg ohms to kilo ohms and that the coating now offers very poor protection.

Slide 14:

This is a Nyquist plot for chromated aluminum in 3% NaCl. The chromating process entails immersion of the aluminum in a chromic acid bath; this oxidizes the aluminum surface (as does anodizing) and produces a protective aluminum oxide layer that contains some residual chromate ion. It is believed that if the coating is subsequently damaged, the chromate ion diffuses to the site of the damage and repassivates the surface. As in the case of the paint film this figure indicates that the resistance of the film diminishes upon prolonged exposure to salt water.

Slide 15:

This slide is similar to the preceding plot, but the markedly different behavior suggests that the coating is flawed. The looping of the impedance spectrum below the axis is characteristic of an inductive element. One cause of inductive-like behavior is a potential-dependent adsorption of a reactive species at the surface, in this case possibly the chromate ion.

Slide 16:

This circuit corresponds to the curve on the preceding slide. In effect, the flawed portion of the surface dominates the interfacial behavior, and an inductor replaces the interfacial capacitance.

ELECTROCHEMICAL IMPEDANCE SPECTROSCOPY

Metal / Electrolyte Interface behaves as RC Circuit

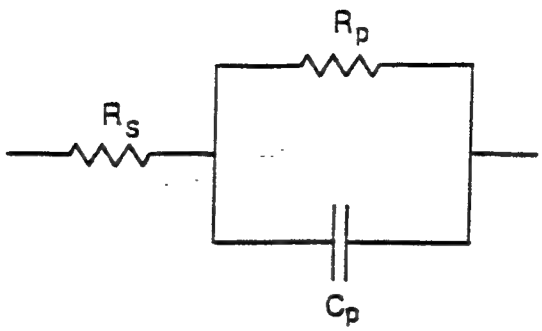

R_s: **Solution Resistance**

R_p: **Corrosion Resistance**

C_p: **Capacitance**

"Nyquist" plot for the circuit

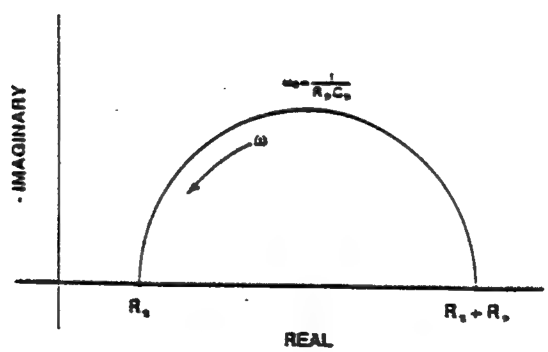

Real component of impedance vs. imaginary component
(Parametric in frequency)

ω : Angular frequency

Corresponding " Bode " plot
(log| z | vs. log frequency)

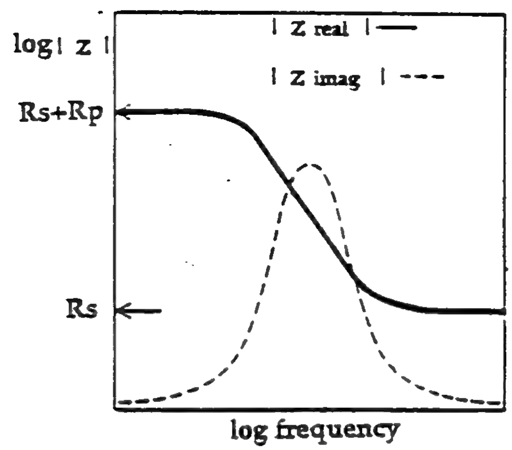

Real and imaginary components of impedance vs. frequency.

Paint Film Protected Aircraft Structure

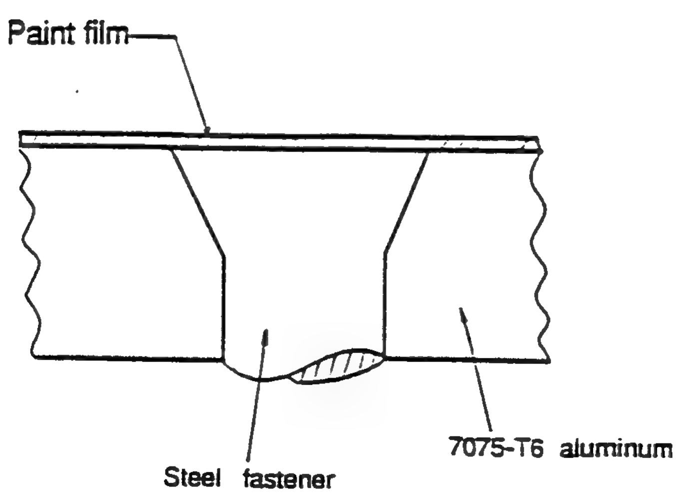

Localized Corrosion in Aircraft structure

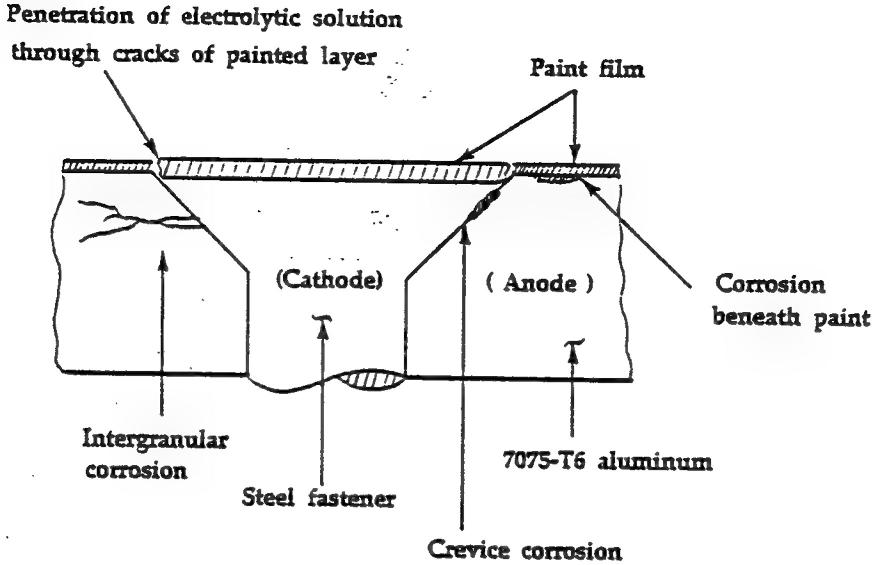

Crevice Corrosion at Fastened Joints

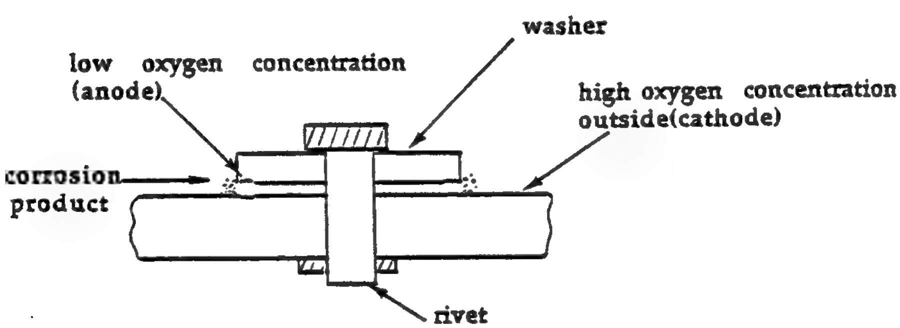

Cathodic reaction (at oxygen rich site)

$$1/2\,O_2 + H_2O + 2e^- \longrightarrow 2OH^-$$

Anodic reaction (at oxygen poor site)

$$M \longrightarrow M^{2+} + 2e^-$$

At mouth of crevice

$$M^{2+} + 2OH^- \longrightarrow M(OH)_2 \text{ (solid)}$$

Systematic Study

Bare Metal

Painted or Chromated Metal

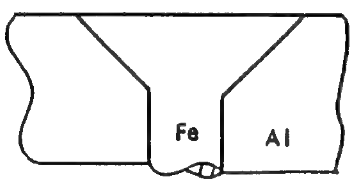

Galvanic couple

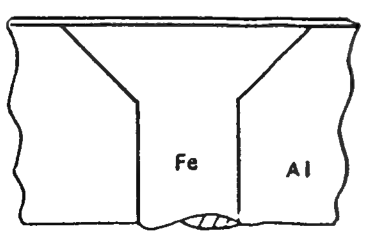

Protected galvanic couple

Autocatalytic Mechanism of Pit Growth and Crevice Corrosion

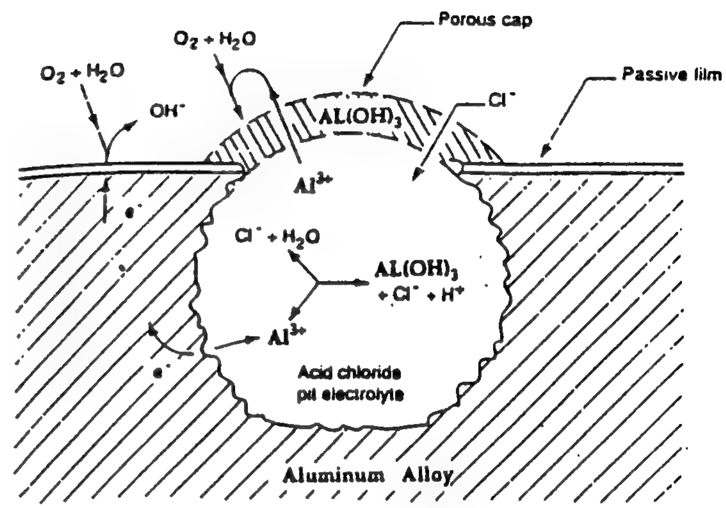

$$Al \longrightarrow Al^{3+} + 3e^-$$

$$Al^{3+} + 3H_2O + 3Cl^- \longrightarrow Al(OH)_{3(s)} + 3HCl$$

* Anodic dissolution of Al and hydrolysis of Al^{3+} produces hydrochloric acid that accelerates pit growth.

* Solid corrosion product traps HCl in pits.

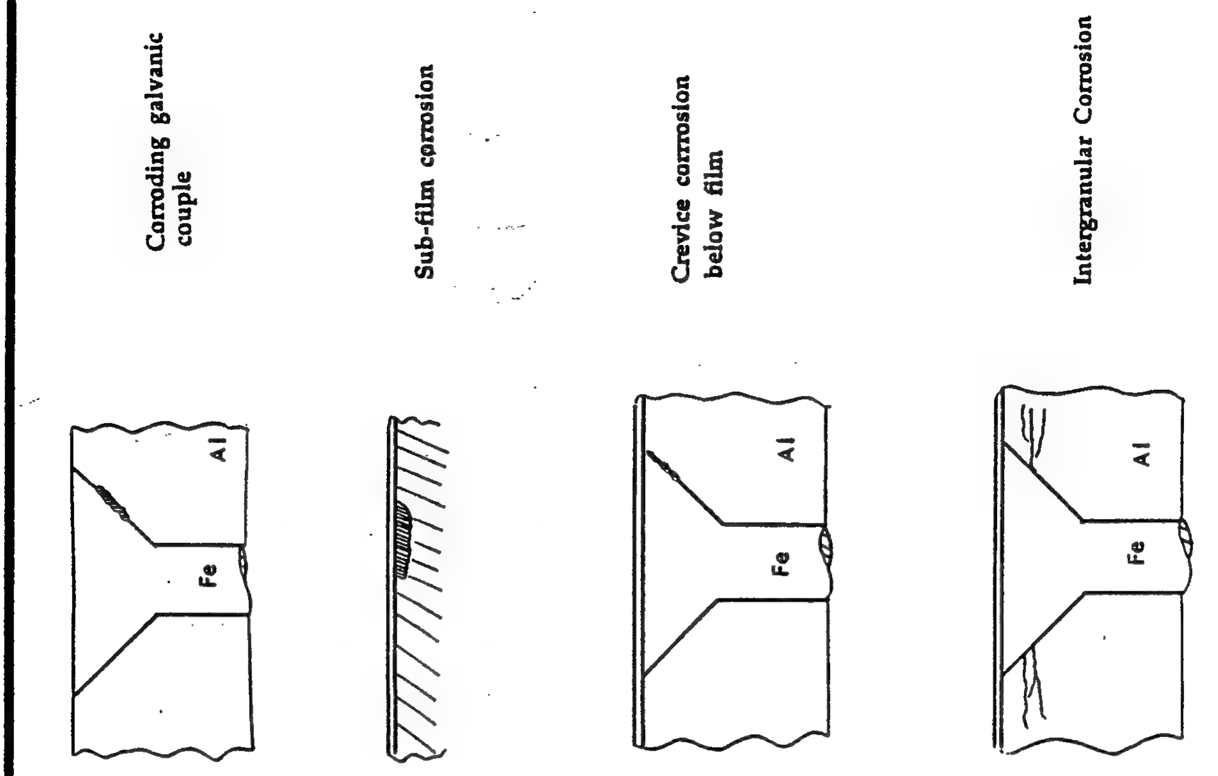

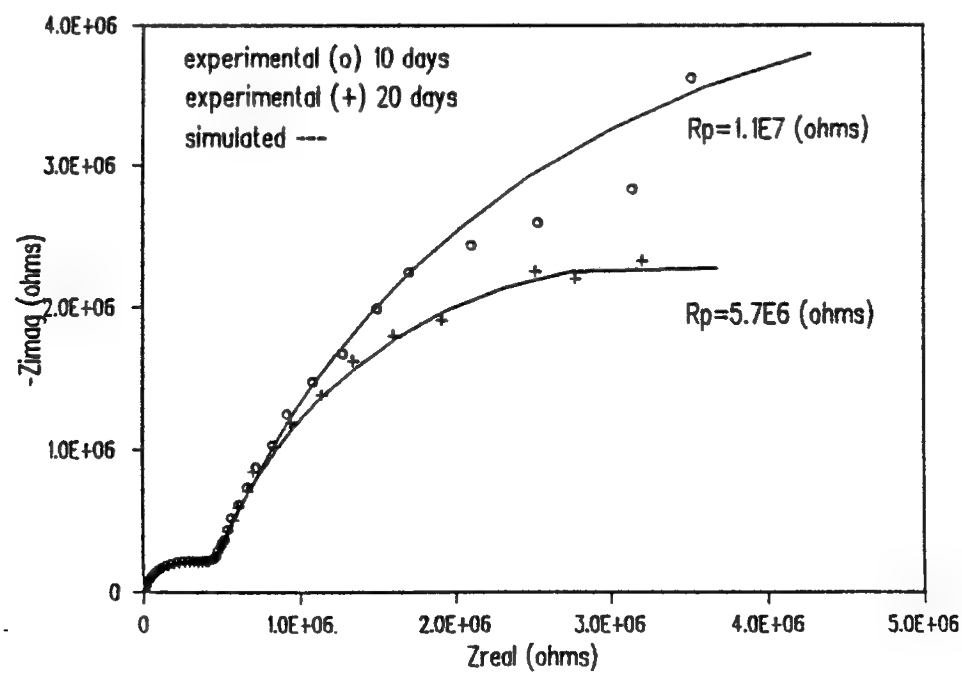

Impedance of painted 2024-T3 aluminum specimen in sea water — intact paint film.

Equivalent circuit for coated specimen

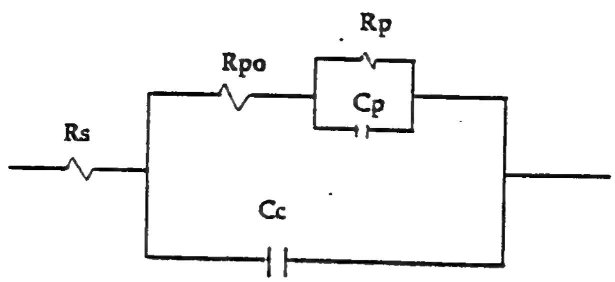

Rs : solution resistance

Rpo: pore resistance

Cc : coating capacitance

Cp : capacitance of corroding interface(double layer)

Rp : corrosion resistance

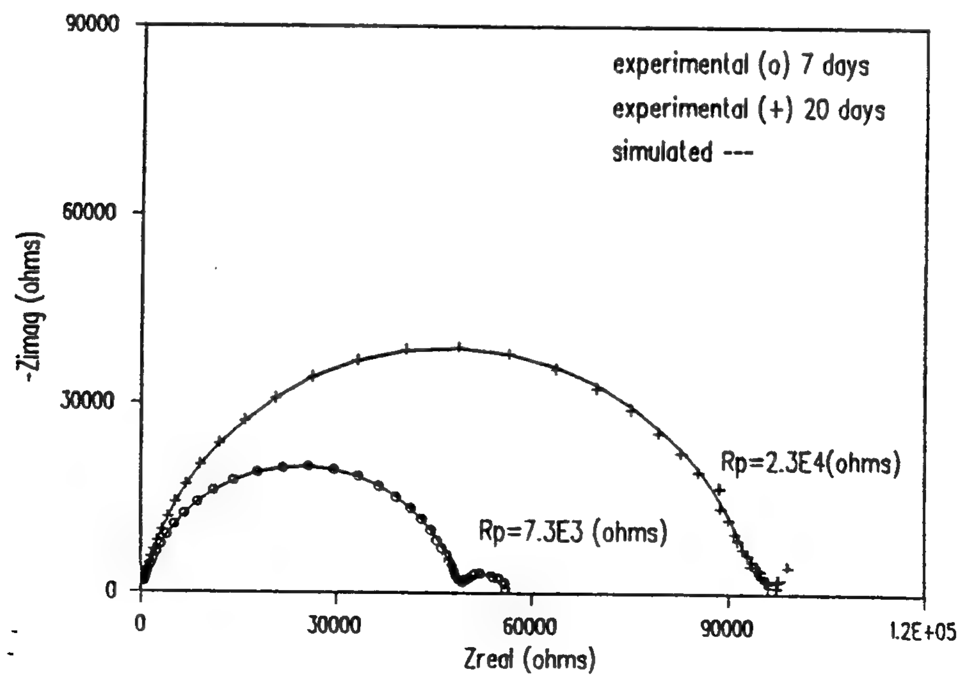

Impedance of painted 2024-T3 aluminum specimen in sea water — visible blister.

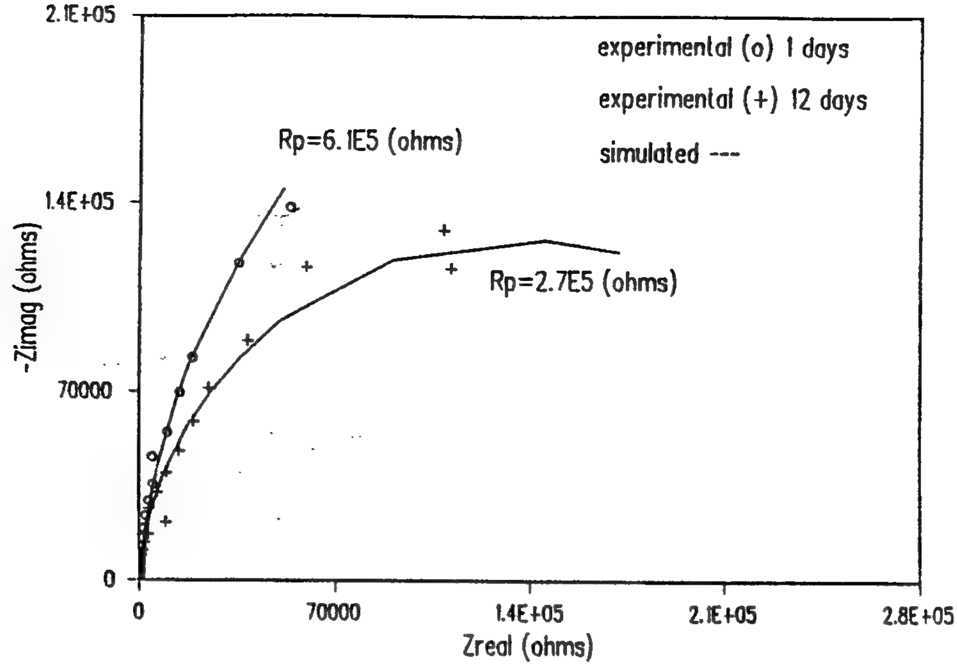

Impedance of chromated 7075-T6 aluminum in sea water.

IMPEDANCE SPECTROSCOPY

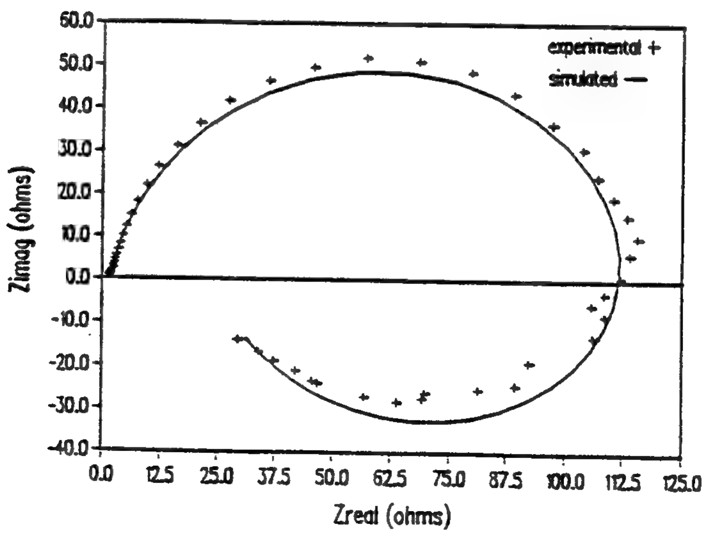

Chromated 7075-T6 in sea water with film defect showing inductive behavior.

Equivalent circuit for coated specimen

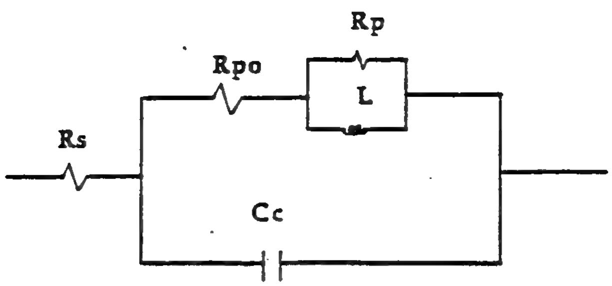

Rs : solution resistance

Rpo: pore resistance

Cc : coating capacitance

L : inductor associated with adsorption(chromate ?)

Rp : corrosion resistance

Project Objectives

1. " Fingerprint " various modes of corrosion via electrochemical impedance spectroscopy.

2. Understand " fingerprints " in terms of electrochemical fundamentals.

3. Develop field instrument to collect " fingerprints " from aircraft.

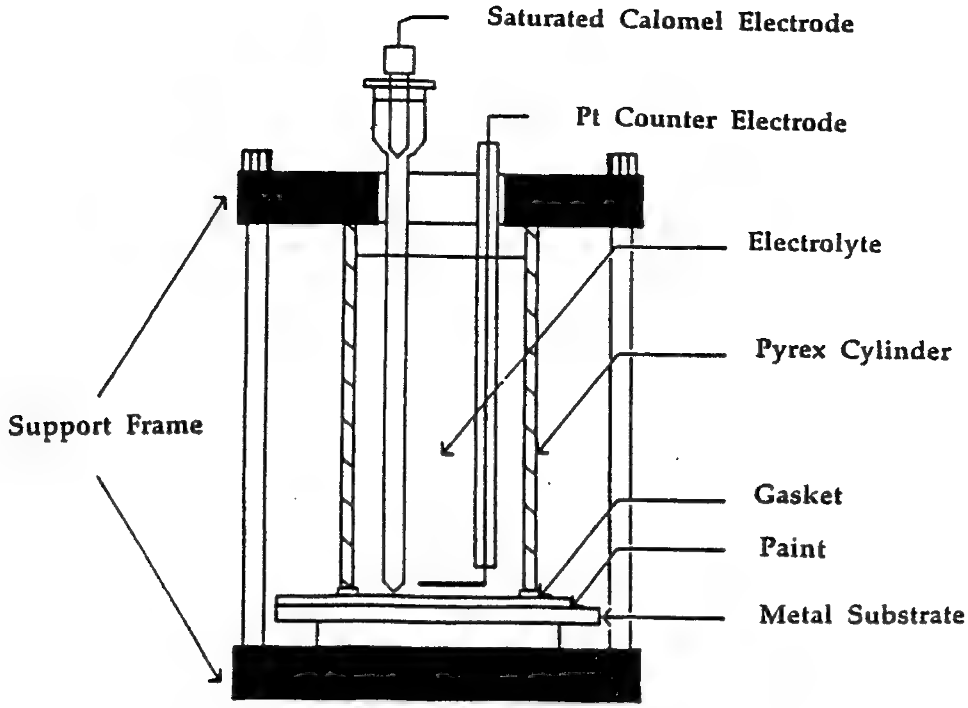

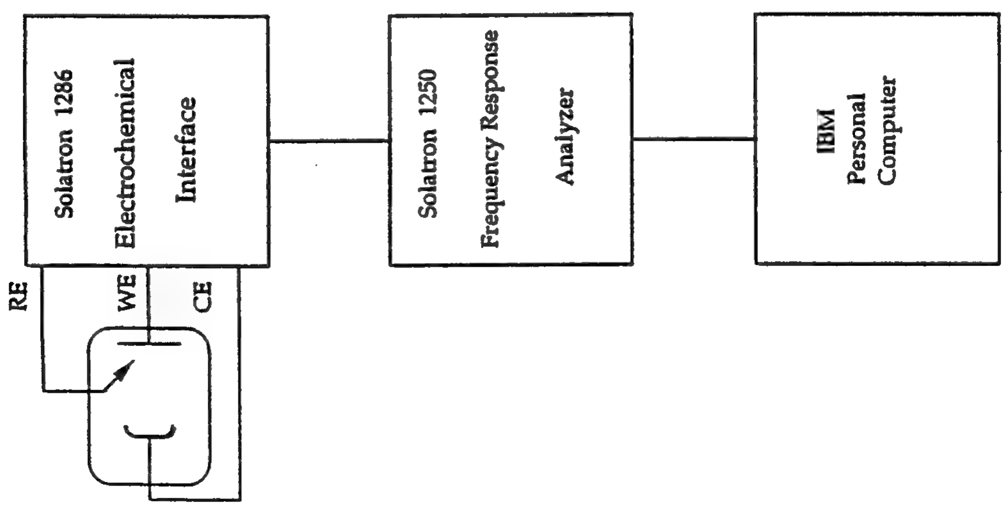

Schematic diagram of instrumentation set-up for AC impedance studies

Project title:

Nondestructive Evaluation of Corrosion-Damaged Structures

"Application of Electrical Impedance Tomography to Corrosion Monitoring"

Fadil Santosa
Mathematical Sciences
University of Delaware

Ian Hall
Material Science
University of Delaware

Michael Vogelius
Mathematics
Rutgers University

William Mayo
Mechanics and Material Science
Rutgers University

Peter Kaup and Henry Konstanty (Grad Students)
To be named (Postdoc)

Main Goals:

- To assess, through theoretical, computational and laboratory work, if Electrical Impedance Tomography can be used effectively as a Nondestructive Evaluation tool for corrosion management.
- To generate knowledge base for future development of realtime NDE tool for corrosion.
- To develop basic knowledge of corrosion phenomena in modern materials particularly those used in aircraft applications.

Practice problem: 2-dimensional model problem

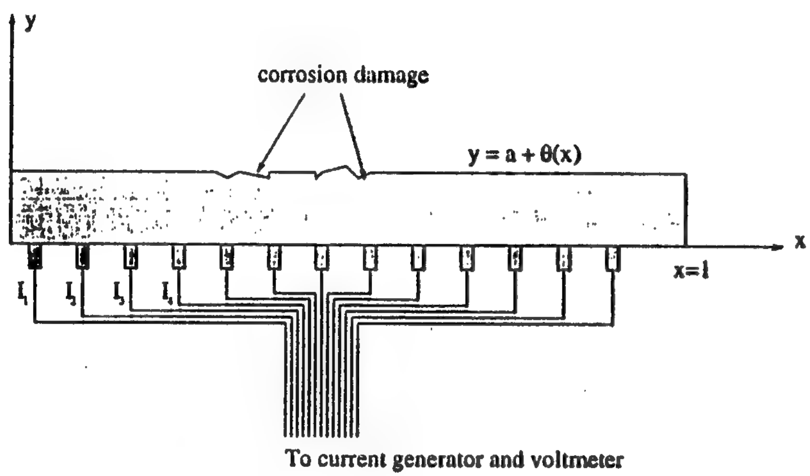

Damage: Model presence of pits and surface roughening by change in surface description.

Upper surface: $y = a + \theta(x)$; undamaged $\rightarrow \theta(x) \equiv 0$.

Data: Apply current $\{I_1, I_2, I_3 \cdots I_n\}$
measure voltages $\{V_1, V_2, V_3, \cdots, V_n\}$.

We can choose distribution of current as long as their sum is zero.

Problem: Determine $\theta(x)$ from current and voltages.

Why EIT?

- simple, portable device;
- fast accurate data aquisition possible, realtime imaging possible;
- mathematical modeling of physical phenomenon well understood, a large body of mathematical and practical knowledge developed in the last 15 years;
- resolution of images somewhat limited but amenable to image enhancement and can "see" through large contrasts in material properties.

Project tasks

The tasks outlined below are interrelated and requires collaboration from the personnel with different expertise.

1. Develop computational method for real time imaging corrosion from EIT data.
2. Build laboratory device for data collection from calibrated phantoms and real aircraft parts.
3. Develop basic understanding of corrosion in modern materials through experimental and theoretical investigation.
4. Develop damage models of corrosion whose characteristics can be detected by EIT; e.g., understand local changes in electrical properties of damaged material.

Mathematical problem:

$u(x, y)$ voltage potential generate by current distribution, satisfies

$$\nabla^2 u = 0 \quad \text{for} \quad 0 < x < 1, \quad 0 < y < a + \theta(x).$$

$$\frac{\partial u}{\partial x}(0, y) = \frac{\partial u}{\partial x}(1, y) = 0, \quad \frac{\partial u}{\partial y}(x, a + \theta(x)) = 0.$$

Input current idealized as

$$\frac{\partial u}{\partial y}(x, 0) = f(x)$$

Data idealized as

$$u(x, 0) = V(x).$$

Notation: $u_0(x, y)$ potential when $\theta(x) = 0$; $V_0(x) := u_0(x, 0)$.

Problem: Determine $\theta(x)$ from $V(x)$ given $f(x)$.

Some pertinent issues:

- What distribution of current, $f(x)$, is best?
- What is the smallest anomaly, represented by $\theta(x)$, that such a device can detect?
- How to find the anomaly from the data $V(x)$?

Best current:

The best $f(x)$ will depend on what $\theta(x)$ we are trying to find.

Optimization problem: Find $f(x)$ such that for a given known $\theta(x)$ such that $(V(x) - V_0(x))$ is as large as possible (say in RMS).

In absence of prior knowledge, we assume that we are trying to find a pit at the center of the plate.

Smallest object:

How large is $(V(x) - V_0(x))$ for different size anomaly?

Notch depth 0.005, width 0.125; plate 0.1 by 1.0.

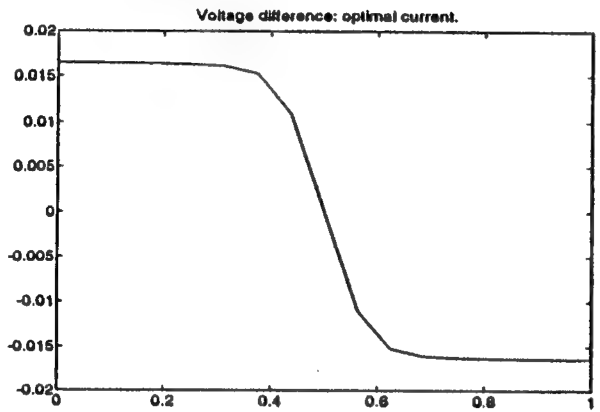

Notch depth 0.005, width 0.067; plate 0.1 by 1.0.

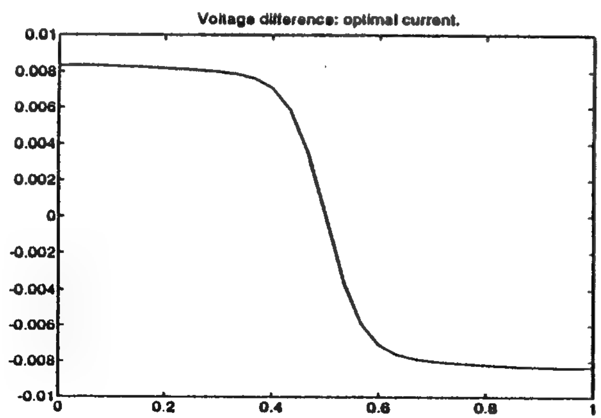

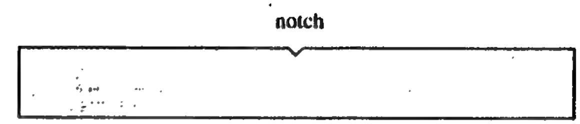

optimal current distibution

Current distribution $f(x)$ that produces the largest difference $(V(x) - V_0(x))$ when we assume that the boundary anomaly is a notch.

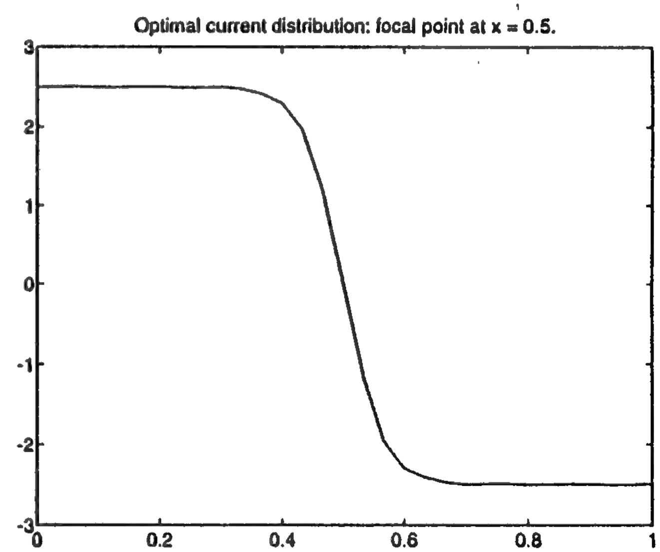

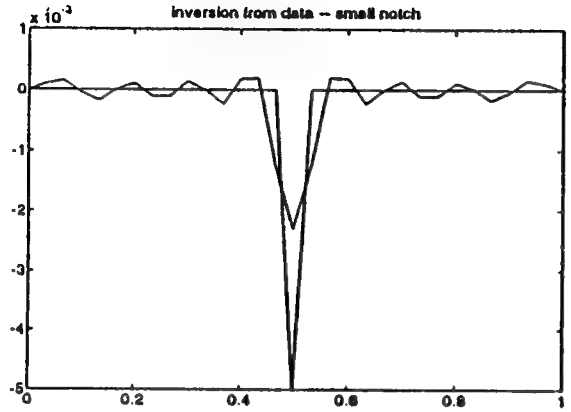

Rule of thumb: the signature of theta is found in the derivative of the data $V(x) - V_0(x)$. The smaller the plate thickness, the better the resolution.

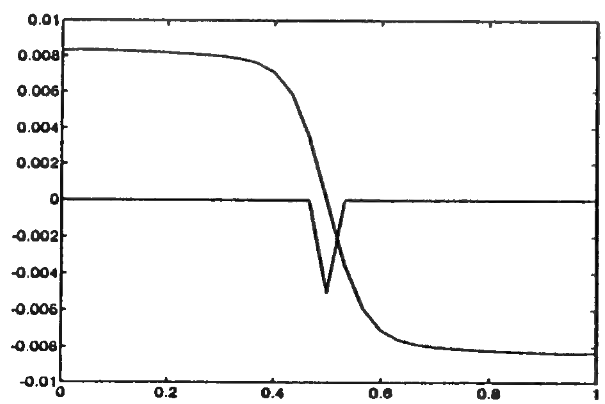

Need 3 digits of accuracy in voltage reading for detection; at least 4 digits for characterization of the notch.

Data inversion:

How to find $\theta(x)$ from $V(x)$ for a given $f(x)$.

We assume that $|\theta(x)| \ll a$ then θ satisfies integral equation:

$$(V(x) - V_0(x)) = \int_0^1 \theta(x') K(x', x)\, dx',$$

Where

$$K(x', x) = \sum_{n=1}^{\infty} \frac{\sin(n\pi x')\cos(n\pi x)}{\sinh(n\pi a)} F(x').$$

The function $F(x)$ depends on the current distribution $f(x)$.

First kind equation, expect instability, sensitivity to data.

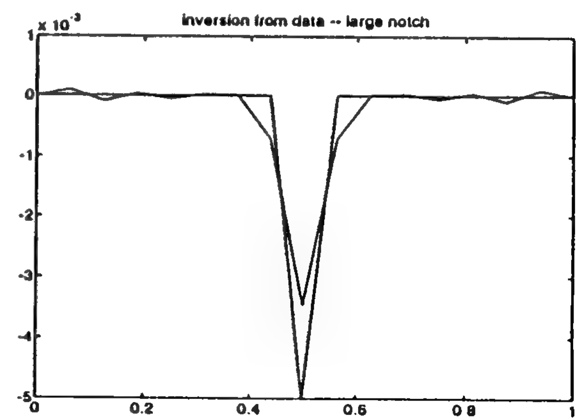

Immediate plans

- develop enhancement technique to handle limited resolution
- complete construction of laboratory equipment
- test method against laboratory data
- develop three dimensional version of the method and laboratory experiment

Other activities:

- Experimental investigation of corrosion in metal-matrix composites (Hall and student). Some data already generated.
- Experimental investigation of stress corrosion cracking (Mayo).

CHARACTERIZATION OF MATERIALS DEGRADATION DUE TO CORROSION AND FATIGUE IN AEROSPACE STRUCTURES

Principal Investigator:

Ajit K. Mal
Mechanical Aerospace and Nuclear Engineering

Co-Principal Investigators:

Jenn-Ming Yang
Material Science and Engineering

Ken Nobe
Chemical Engineering

University of California, Los Angeles

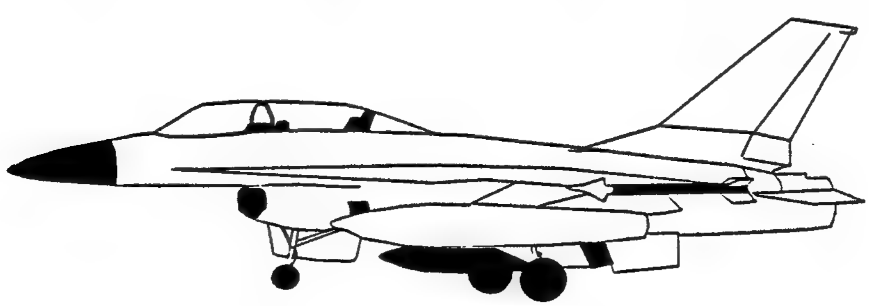

Project supported by the Air Force Office of Scientific Research (AFOSR) Under University Research Initiative (URI)

OVERVIEW OF RESEARCH

1. **Electrochemistry of Corrosion in Metals and Alloys**

- Conduct laboratory tests to determine the parameters that control the growth and dissolution of salt films at crack and pit sites in aluminum, titanium and their alloys.

2. **Degradation of Metal–Matrix Composites Under Fatigue Loads**

- Conduct laboratory tests and micromechanical modeling to develop a fundamental understanding of the relationship between damage accumulation and property degradation in SiC/Ti composites under fatigue loading.

3. **Nondestructive Evaluation of Materials Degradation**

- Develop ultrasonic techniques using immersion as well as contact type arrangements to detect and characterize hidden damage in structural components.

ELECTROCHEMISTRY OF CORROSION IN METALS AND THEIR ALLOYS

- Growth and breakdown of salt films on 2024T4 and 6061T5 aluminum and pure titanium in concentrated chloride media were studied in an effort to understand the electrochemistry of localized corrosion in these materials.

  Fig. 1a shows the experimental setup and Fig. 1b shows the details of the cell used.

  Figures 2, 3 and 4 show typical results for a 2024–T4 aluminum rotating disc electrode in 5M NaCl solution.

- Results indicate that the growth and dissolution of anodic films give rise to strong potential peaks. The dynamics of the process is chaotic at low current densities but becomes quasiperiodic with frequency of approximately 12 Hz at higher currents.

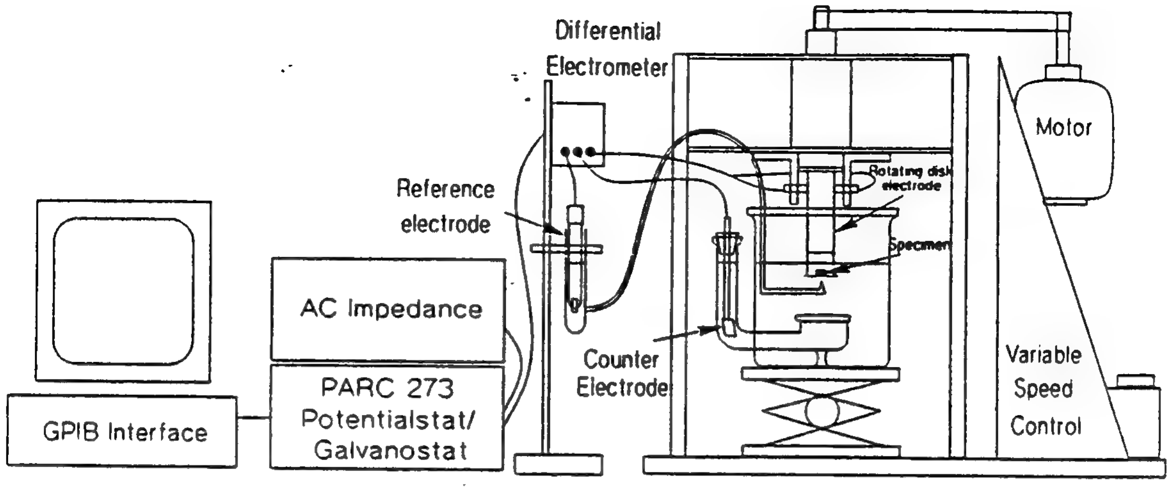

Fig. 1a. The general experimental setup used in the corrosion experiment

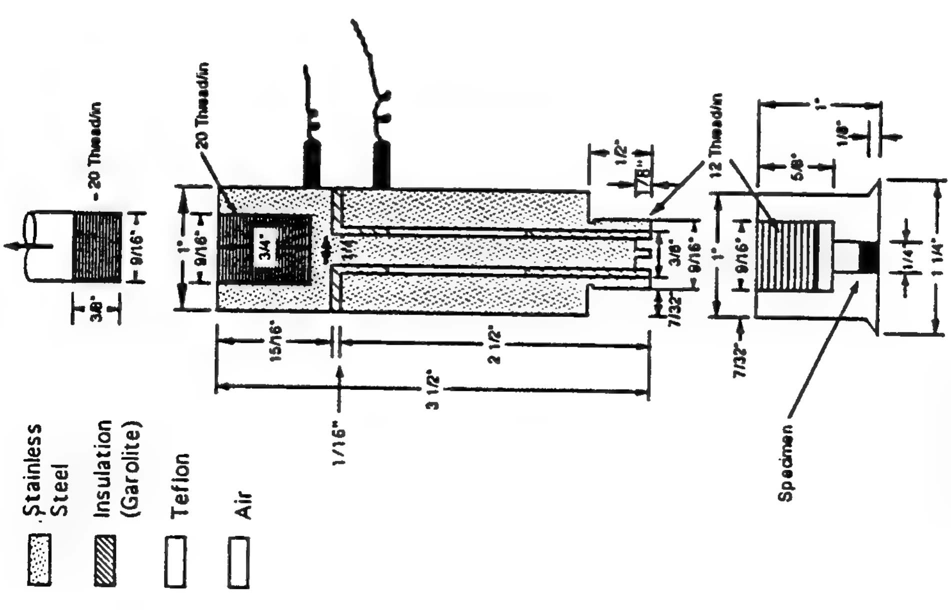

Fig. 1b. Details of the rotating disk electrode used in the corrosion experiment

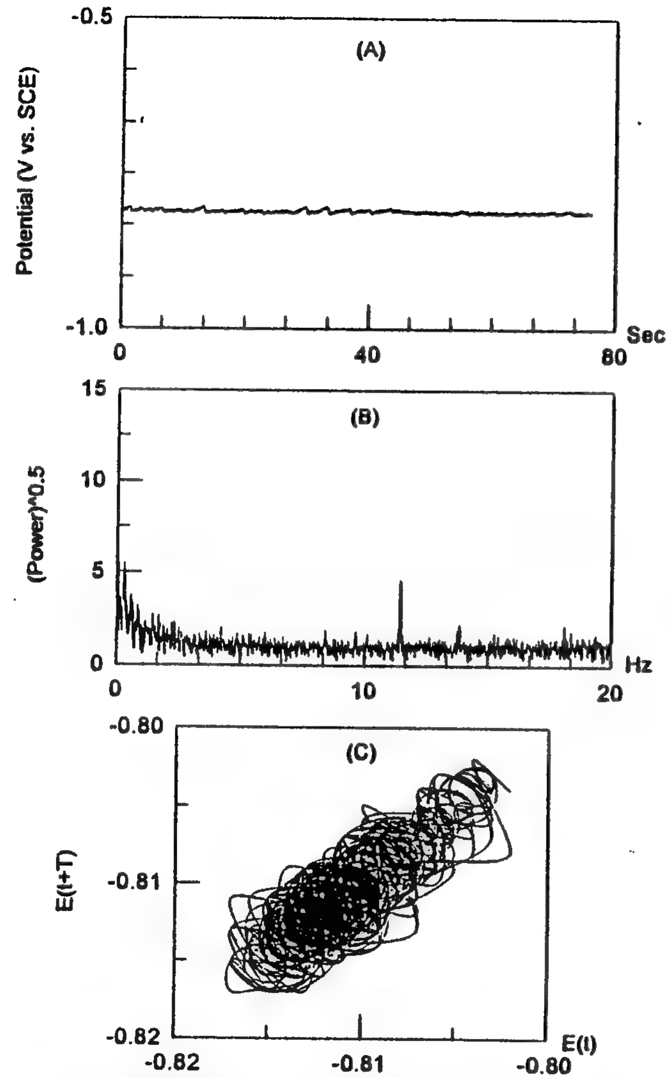

Fig 3. Aluminum in 5M NaCl with applied constant current 1 mA
(A) time series, (B) power spectra, (C) phase portrait.

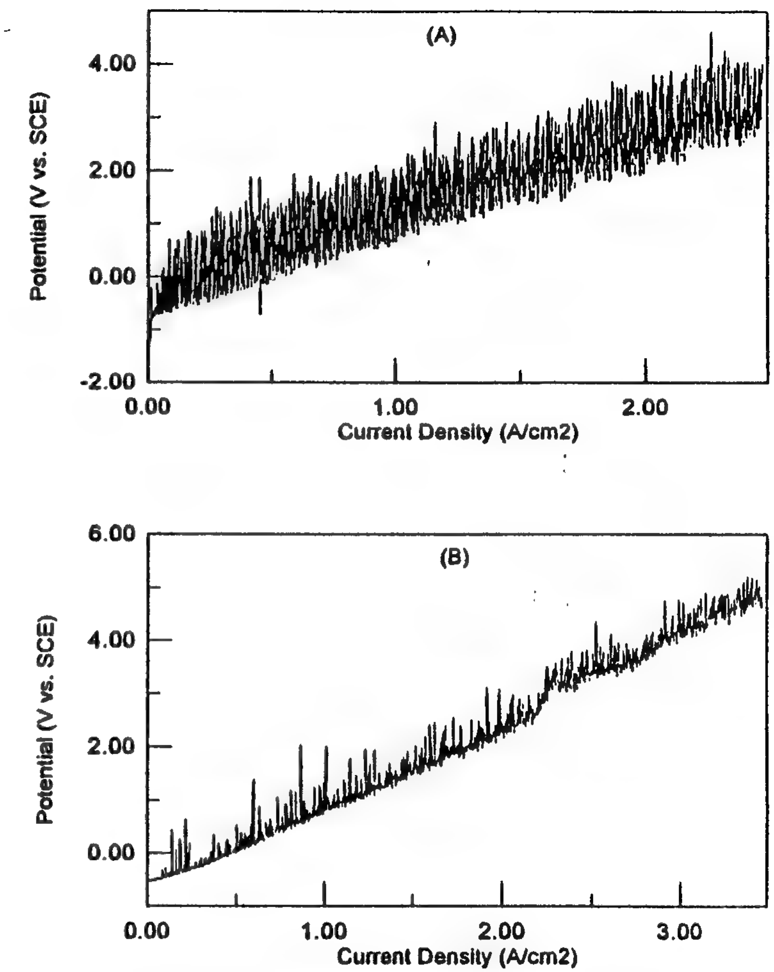

Fig. 2. Potential oscillations in 6061T5 aluminum in 5M NaCl and 500 rpm
with current sweep rate of (A) 10 mA/sec, (B) 50 mA/sec.

DEGRADATION OF SiC/Ti COMPOSITES UNDER FATIGUE LOADING

- Fatigue damage accumulation, failure modes and stiffness reduction in unidirectional SCS-6/Ti-15-3 composites were characterized through laboratory tests and micromechanical modeling.

- In unnotched unidirectional specimens the damage evolution is as follows (Fig. 5):

  An initial slow reduction of about 5% in stiffness due to interfacial debonding and/or cracking.

  A rapid drop in stiffness at approximately 10^4 to 10^5 cycles due to simultaneous cracking of interfaces and the matrix.

  Stiffness saturation at higher cycles with 70-75% of the original.

- Micromechanical modeling using a newly developed volume integral method (VIEM) was carried out; results are shown in Figs. 6, 7 and 8.

  Fig. 6. The maximum radial stress (σ_{rr}) occurs at $\theta = \theta^o$ (point A in Fig. 6) and it is about 166 MPa for $\sigma_o = 144$ MPa. The residual compressive stress in the matrix is about 138 MPa. Thus if debonding initiates at this stress level, then the interfacial tensile strength is about 30 MPa.

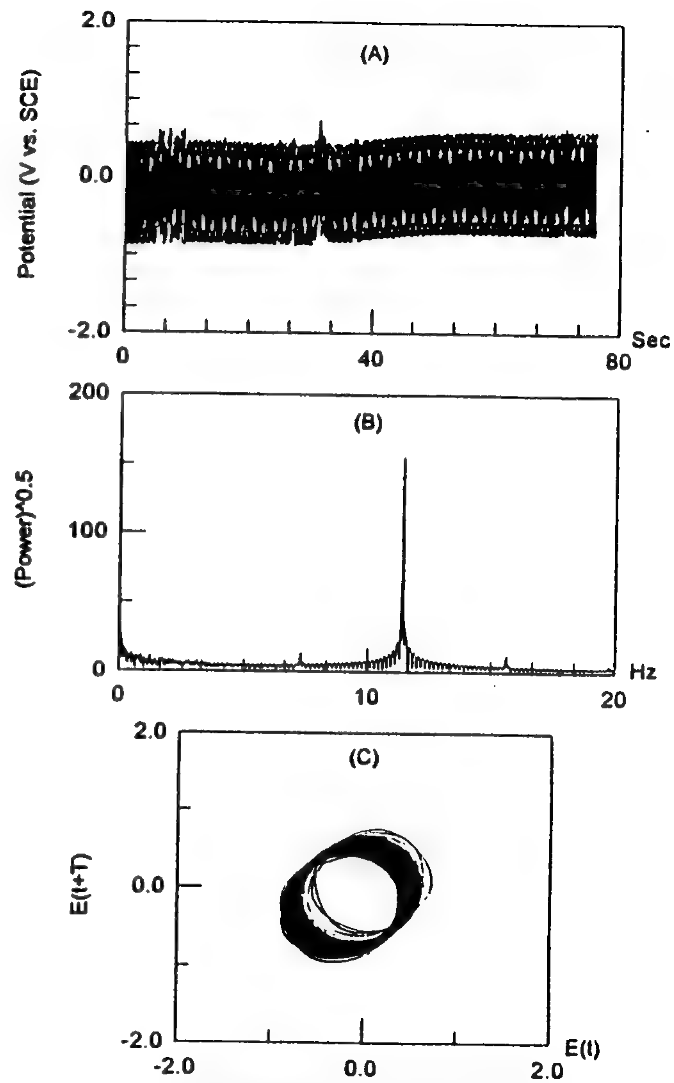

Fig. 4. Aluminum in 5M NaCl with applied constant current 40 mA (A) time series, (B) power spectra, (C) phase portrait.

Fig. 7. The maximum radial stress (σ_{rr}) at the edges of the debonds increases sharply as their length increases, indicating unstable behavior of the debond. Furthermore, if complete debonding occurs in the fiber, the maximum hoop stress ($\sigma_{\theta\theta}$) at $\theta = 90°$ (point B in Fig. 6) is approximately $3\sigma_o$. Thus at 332 MPa, material failure occurs due to matrix yielding (the yield stress of titanium is about 700 MPa) which begins at $\theta = 90°$ and propagates through the material.

Fig. 8. The effect of the fiber-matrix interphase is found to be significant. The transverse crack in the matrix may be initiated at lower loads if the interphase material is more compliant than the matrix. Thus, transverse cracks may be initiated in the carbon-rich reaction layer at $\theta = 90°$ at a lower load after complete debonding occurs in the fiber, especially when the fibers are close to each other. The stress intensity factor increases as the crack length increases indicating unstable behavior of the transverse cracks for all cases considered.

- In notched unidirectional and angle ply laminates damage consisted of interfacial debonding, fiber failure and plastic deformation of the matrix (Fig. 9).

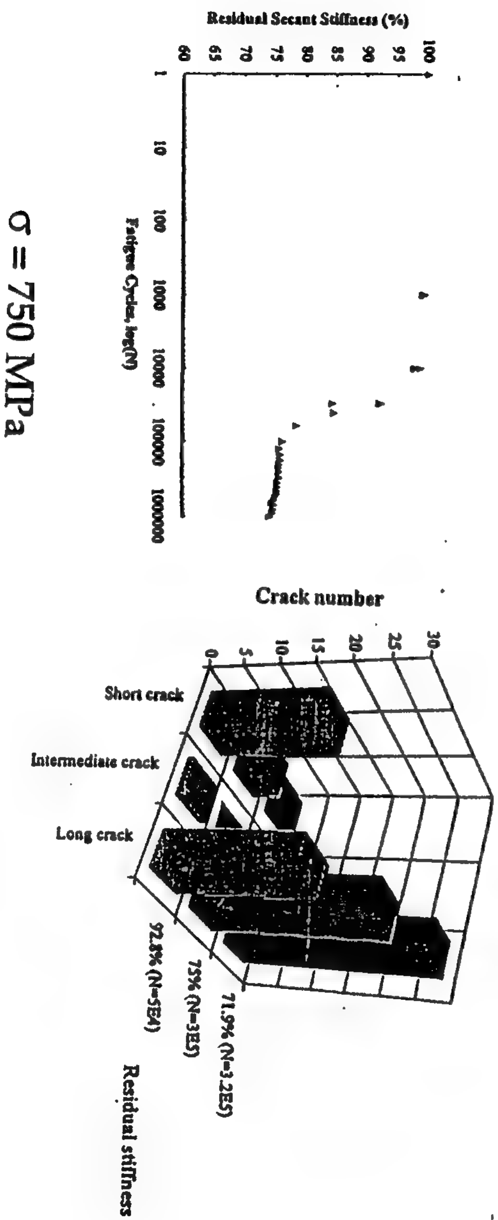

$\sigma = 750$ MPa

Fig. 5 Stiffness reduction of unidirectional SCS-6/Ti-15-3 composite

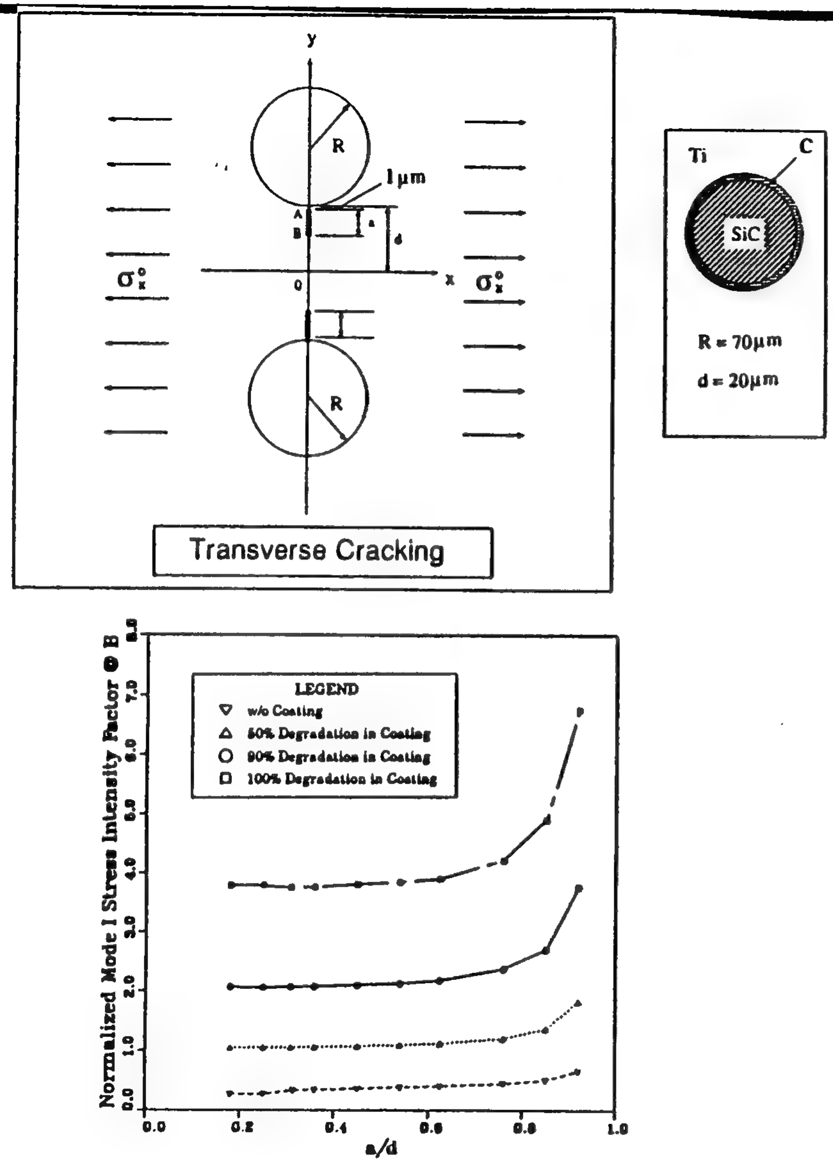

Fig. 8. Normalized mode I stress intensity factor for a pair of transverse cracks between two close fibers in an infinite matrix subjected to transverse tensile stress.

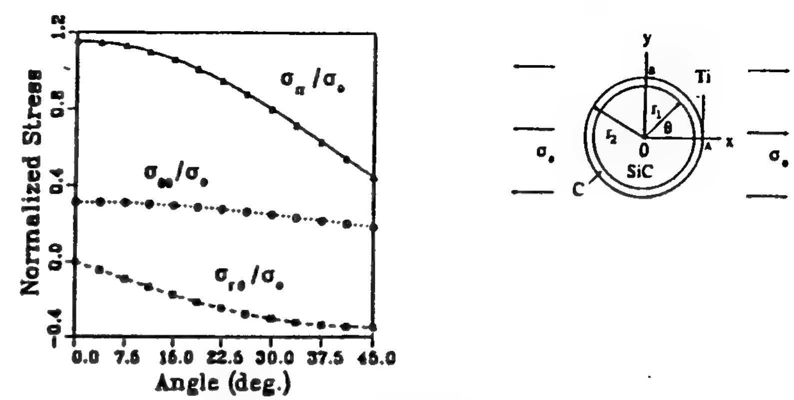

Fig. 6. Stresses at fiber matrix interface under remote tensile stress in absence of debonding.

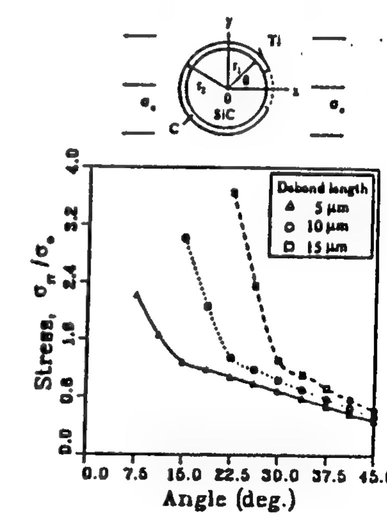

Fig. 7. Stresses at fiber matrix interface under remote tensile stress in presence of debonding.

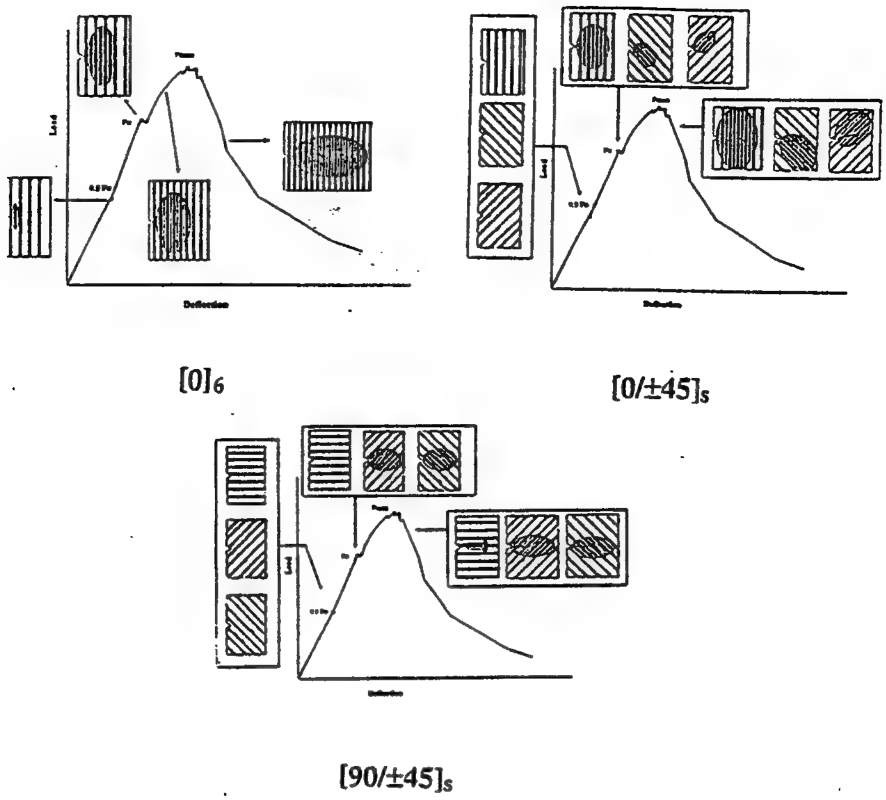

Fig. 9 Damage evolution near crack tip in SCS-6/Ti-15-3 composites

NONDESTRUCTIVE EVALUATION OF MATERIALS DEGRADATION

- Stiffness and thickness reduction in corroded aluminum and heat-damaged Gr/Ep composite panels were characterized based on the measurement and analysis of guided wave speeds using contact transducers.

- Characterization of hidden defects in aluminum lap joints was accomplished using contact ultrasonics.

- Source location was determined through measurement and analysis of waveforms from fatigue crack propagation events in notched aluminum specimens.

- Thermal degradation in adhesive joints and Gr/Ep composites was characterization from measurement and analysis of leaky Lamb waves.

- Characterization of stiffness and thickness reduction in corroded aluminum and heat-damaged Gr/Ep composite panels based on the measurement and analysis of guided wave speeds using contact transducers.

  Fig. 10 shows a typical source/receiver arrangement, the recorded waveforms and their frequency spectra for an aluminum plate of 1/8" (3.2 mm) thickness.

  The source is a 5–cycle, 200 kHz tone burst. The first two wave–arrivals are the extensional and flexural waves propagating across the array.

  The group velocity of each wave was calculated from the data; they are 5.2 mm/μs and 3.1 mm/μs, respectively. The shear wave speed in the material and the thickness of the panel are calculated from these two values.

  Reductions in shear wave speed and/or thickness from their standard values can be attributed to degradation.

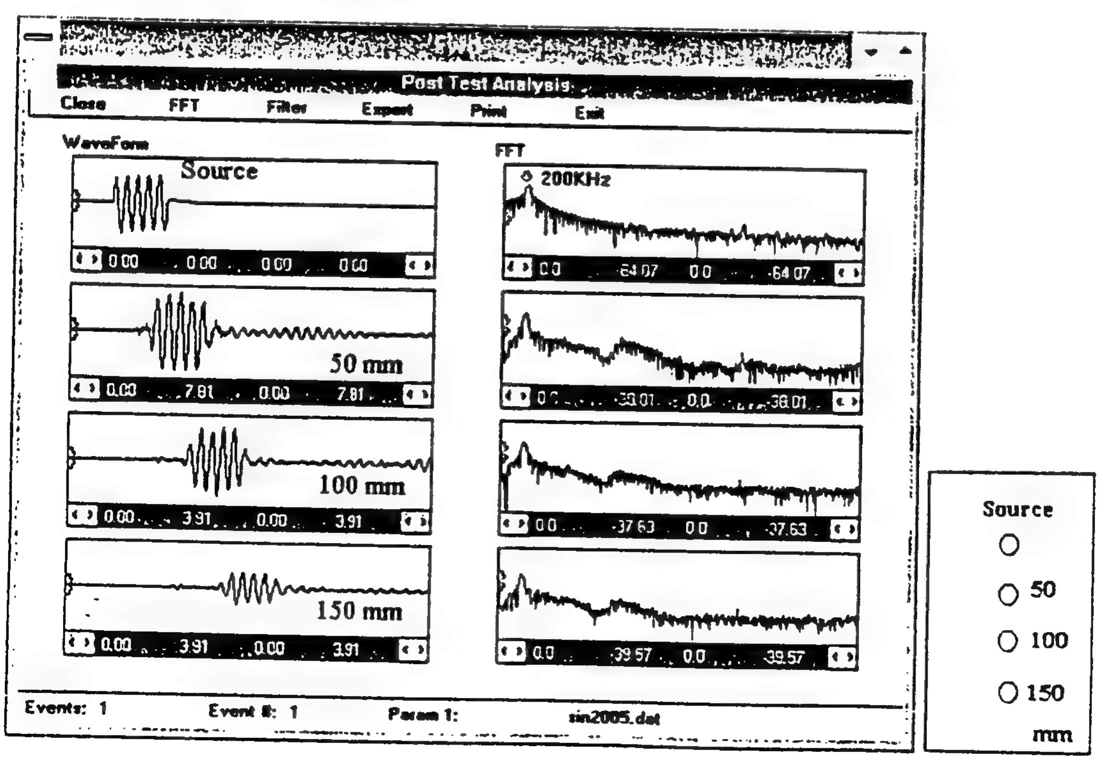

Fig. 10. Velocity measurement of guided waves using multiple receivers.

- Characterization of hidden defects in aluminum lap joints using contact ultrasonics.

  Figures 11 and 12 show the transducer arrangements and recorded waveforms in an undamaged and a damaged lap joint.

  The amplitudes of the waves recorded by the third receiver in the two specimens are significantly different.

  The reduction in the amplitude is caused by the hidden damage; the amount of reduction is a measure of the degree of damage.

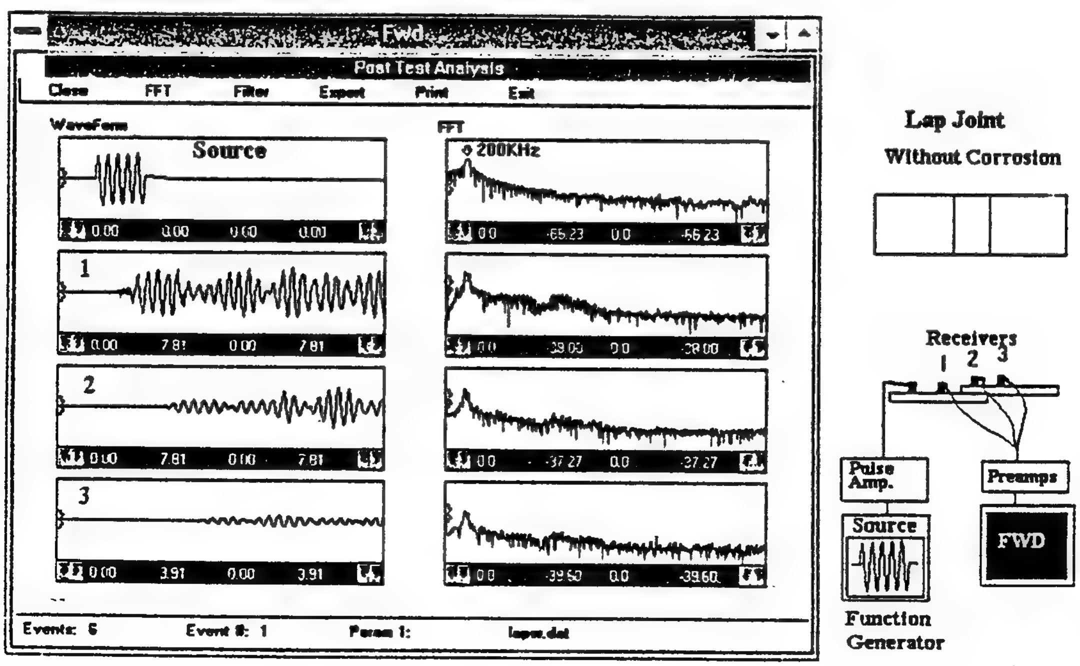

Fig. 11. Lap joint inspection using contact ultrasonics: no hidden corrosion.

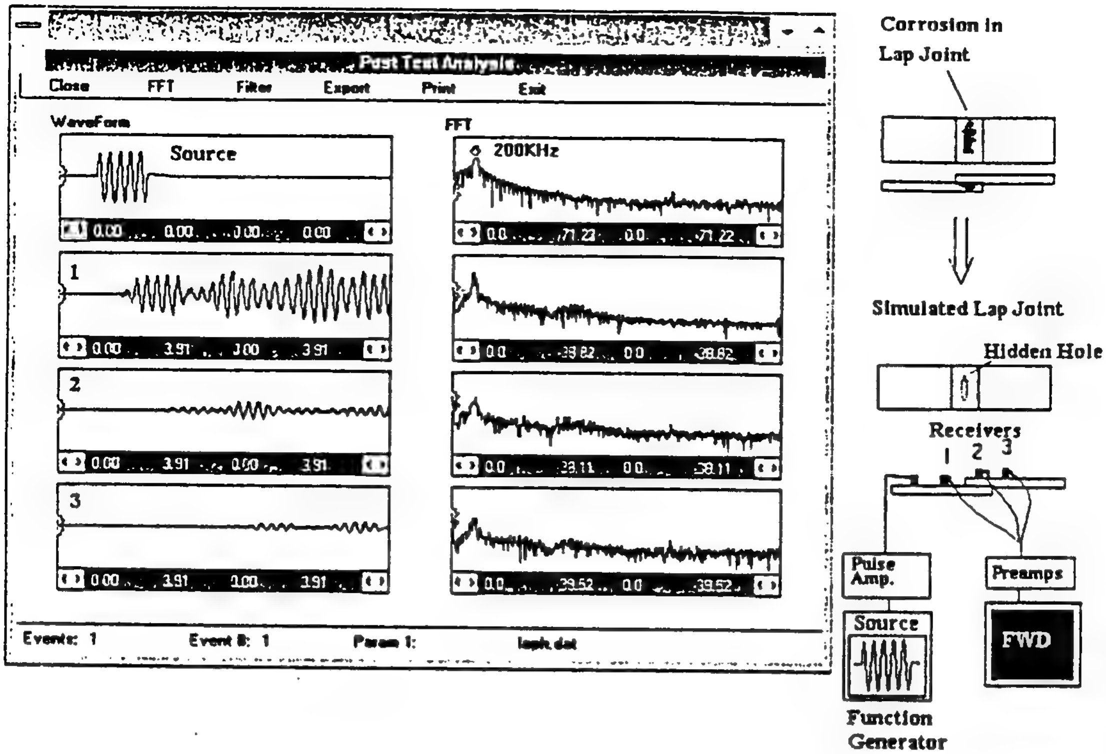

Fig. 12. Lap joint inspection using contact ultrasonics: joint with hidden corrosion.

- Source location and characterization from measurement and analysis of waveforms due to fatigue crack propagation events in aluminum specimens using the Fracture Wave Detector made by Digital Wave Corporation.

Fig. 13 shows a typical experimental arrangement using an array of four receivers and a simulated AE source (lead break). Also shown are the recorded waveforms which consist of extensional and flexural waves propagating across the array.

Spectral analysis of the waves leads to the determination of the source location.

Fig. 14 shows a fatigue test on a notched aluminum specimen. The Fracture Wave Detector was used to locate cracking events during the fatigue test at 2 Hz. A total of 432 events were located.

The waveforms recorded in a typical event are shown in the top left panel; the source is located through signal processing and spectral analysis of the flexural waves.

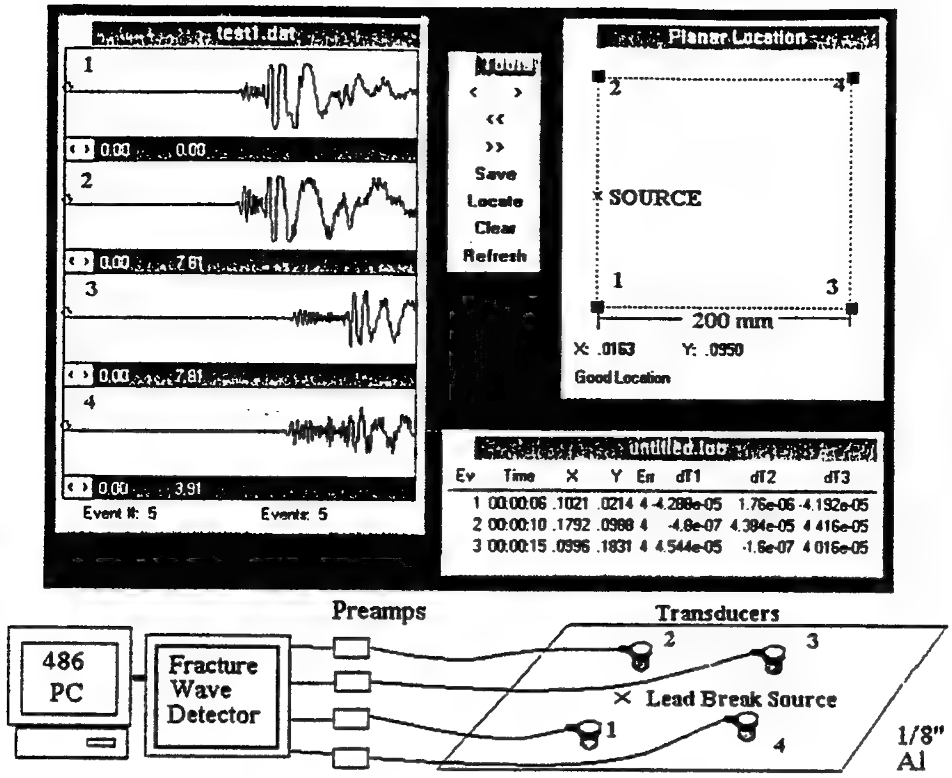

Fig. 13. Source location in 2D using Fracture Wave Detector made by Digital Wave Corporation.

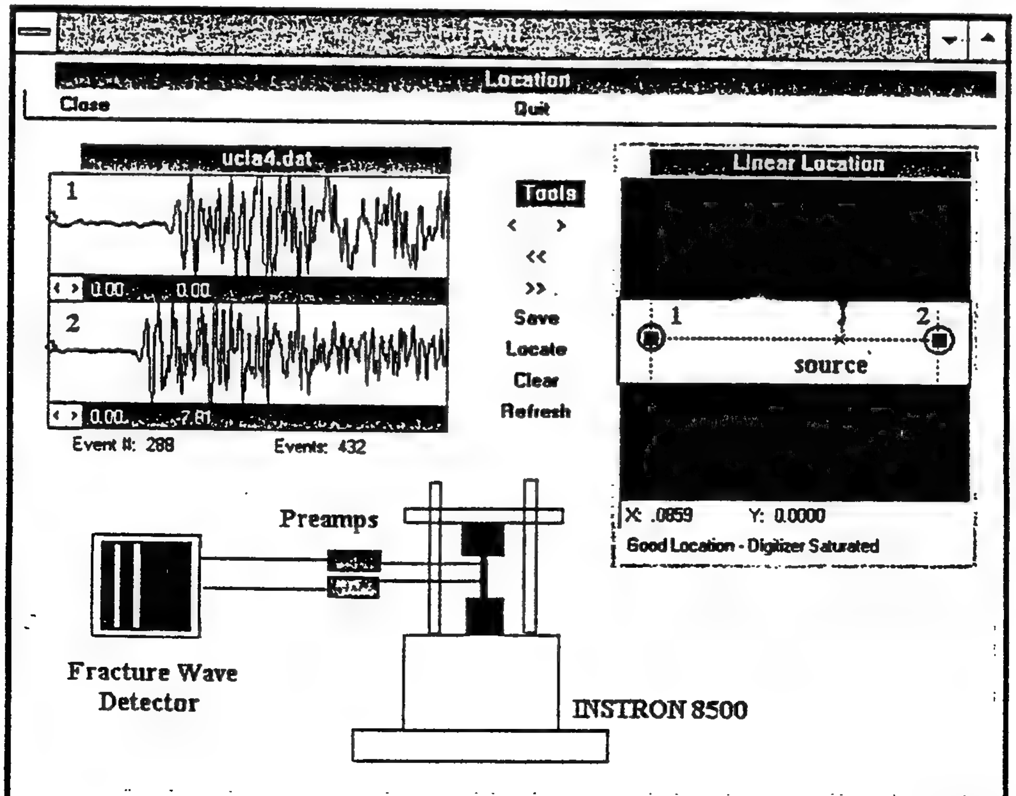

Fig. 14. Source location in fatigue test using Fracture Wave Detector made by Digital Wave Corporation.

- Characterization of thermal degradation in aluminum adhesive joints from the measurement and analysis of leaky Lamb waves.

  Fig. 15 shows the leaky Lamb wave setup; it is used to measure guided wave speeds in specimens immersed in water.

  Fig. 16 shows the Lamb wave dispersion curves in an area away from the bond before and after heat treatment. Clearly, there is no change in the properties here.

  Figure 17 shows the same for the bonded region; there is a significant shift downward in the dispersion curves, indicating reduction in overall stiffens.

  Figure 18 shows the change in the dispersion curves due to heat damage in a bonded titanium specimen.

  The data will be analyzed through modeling in an effort to quantify the damage.

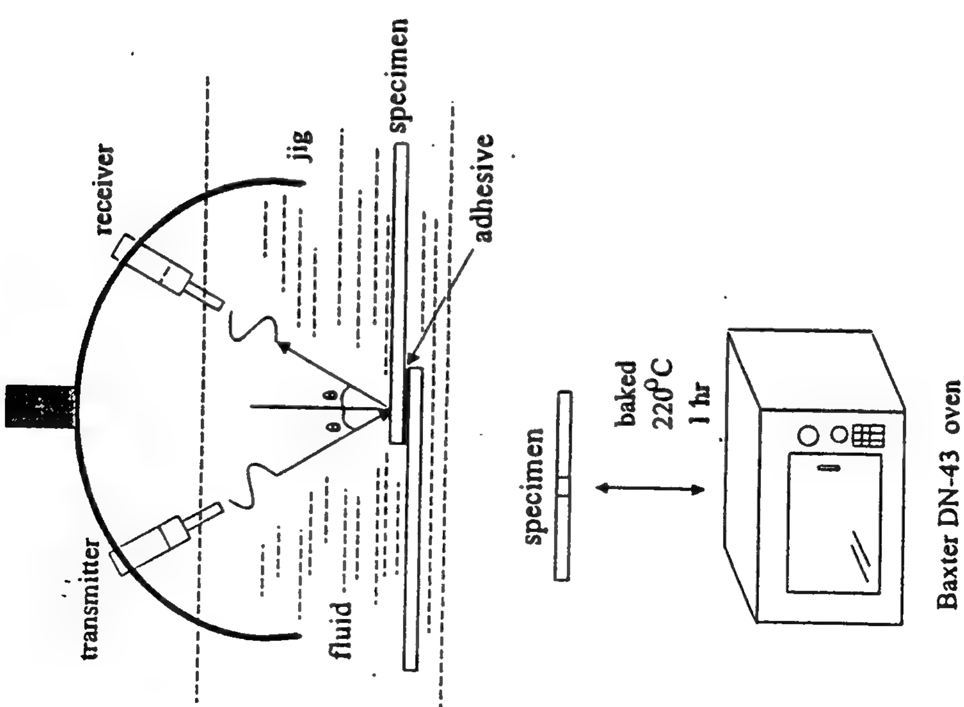

Fig 15 The leaky Lamb wave setup for inspection of heat damaged adhesive joints.

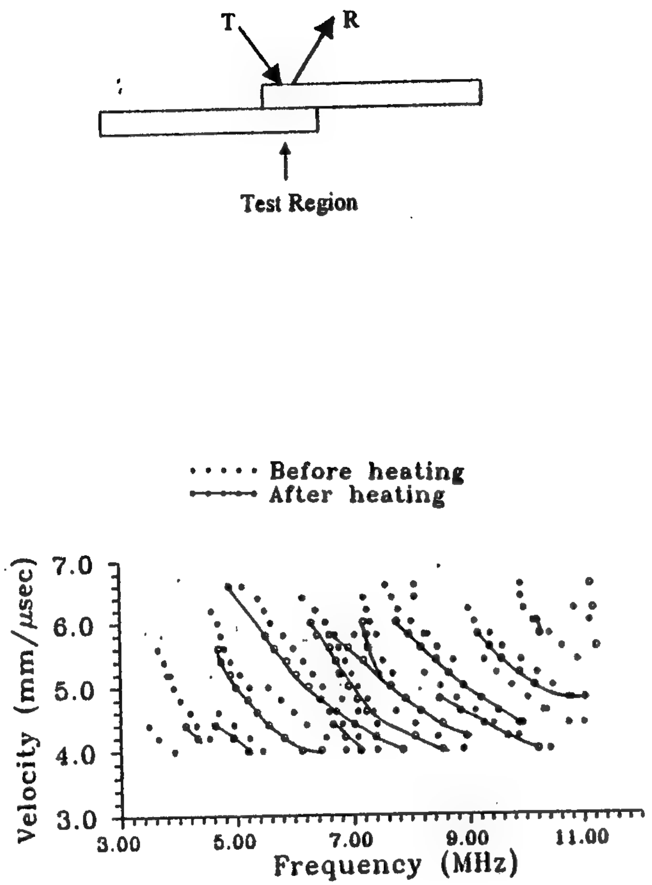

Fig. 17. Lamb wave dispersion curves for a bonded aluminum plate before and after heat damage.

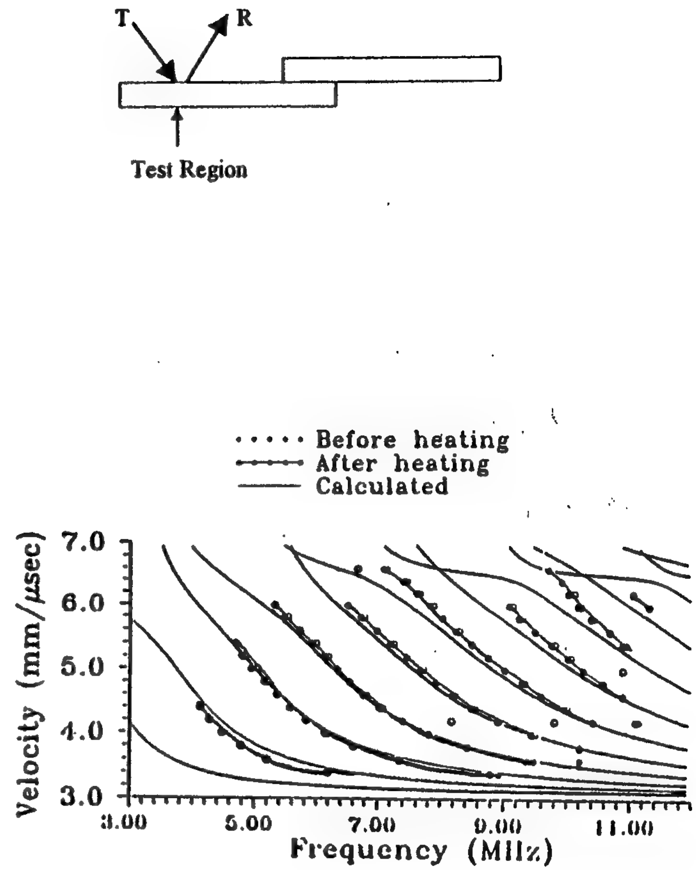

Fig. 16. Lamb wave dispersion curves for an aluminum plate of 1.5 mm thickness.

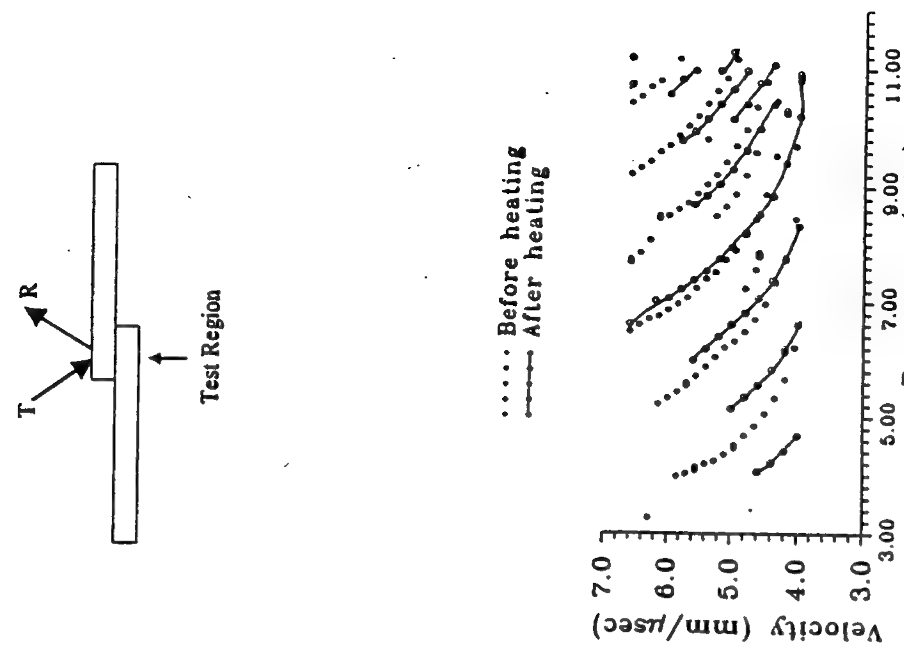

Fig 18. Lamb wave dispersion curves in bonded titanium before and after heat treatment

RESEARCH PLAN FOR NEXT YEAR

- Extend corrosion experiments to include simultaneous application of quasistatic and cyclic loading in aluminum specimens.
- Construct predictive models for crack initiation and extension from pit sites in corroded aluminum panels under static and fatigue loadings.
- Continue work on the characterization of fatigue–induced degradation in high temperature composites.
- Continue research on ultrasonic NDE using guided as well as bulk waves for quantitative characterization of: (a) hidden corrosion in real lap joints, (b) bond deterioration in adhesive joints, (c) heat damage in Gr/Ep composite panels and (d) the integrity of boron/epoxy repair patches in aluminum panels.

Advanced Instrumentation and Measurements for Early Nondestructive Evaluation of Damage and Defects in Aerostructures and Aging Aircraft

Vanderbilt University

John P. Wikswo, Co-PI
James A. Cadzow
Thomas A. Cruse
William F. Flanagan
George T. Hahn
Barry D. Lichter

Northwestern University

Jan D. Achenbach, Co-PI
Isaac M. Daniel
Shridar Krishnaswamy

AFOSR Contract F49620-93-1-0268

Techniques

SQUID magnetometers

- Injected current
- Eddy current
- Corrosion currents
- Magnetic susceptibility*

Ultrasonics

- Self-compensating ultrasonic bridge*
- Laser-based ultrasonics*
- Fiber-optic scanner
- Time reversal for focused excitation

Optical interferometry

- Electronic speckle techniques* – Real-time; full field; digital system
- Dynamic holographic techniques – Real-time; full-field; analog system using photorefractive crystals

Modeling

- Measurement models
- Image processing
- Inverse solutions

Basic Studies

Crack formation

Corrosion

* previously developed

Advanced Instrumentation and Measurements for Early Nondestructive Evaluation of Damage and Defects in Aerostructures and Aging Aircraft

Specific objectives

1. **Instrumentation development** – Wikswo and Achenbach
2. **NDE theory and techniques** – Wikswo and Achenbach
3. **Image processing** – Cadzow
4. **Damage detection in composite materials** – Daniel
5. **Fatigue damage** – Hahn
6. **Corrosion** – Lichter and Flanagan
7. **Evaluation of NDE capabilities** – Cruse
8. **Technology transfer** – Wikswo and Achenbach

Research Tasks

Task 1 NDE Instrumentation Development

- Existing instruments: MicroSQUID, imaging susceptometer, nanoSQUID
- High-sensitivity ELF eddy current system
- Digital SQUID (with Hypres, Inc)
- High-T_c systems
- Fiber-optic/laser ultrasonic technique to image cracks perpendicular to the scanning plane
- Real-time optical NDE systems using adaptive photorefractive crystals and synchronized stressing

VANDERBILT MAGNETIC IMAGING FACILITY

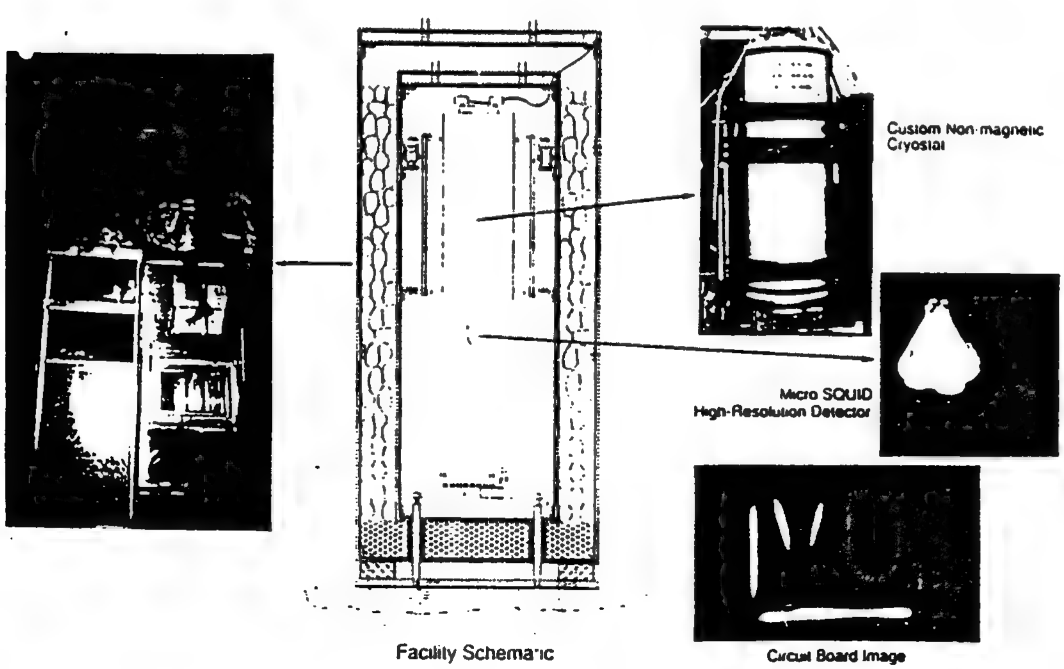

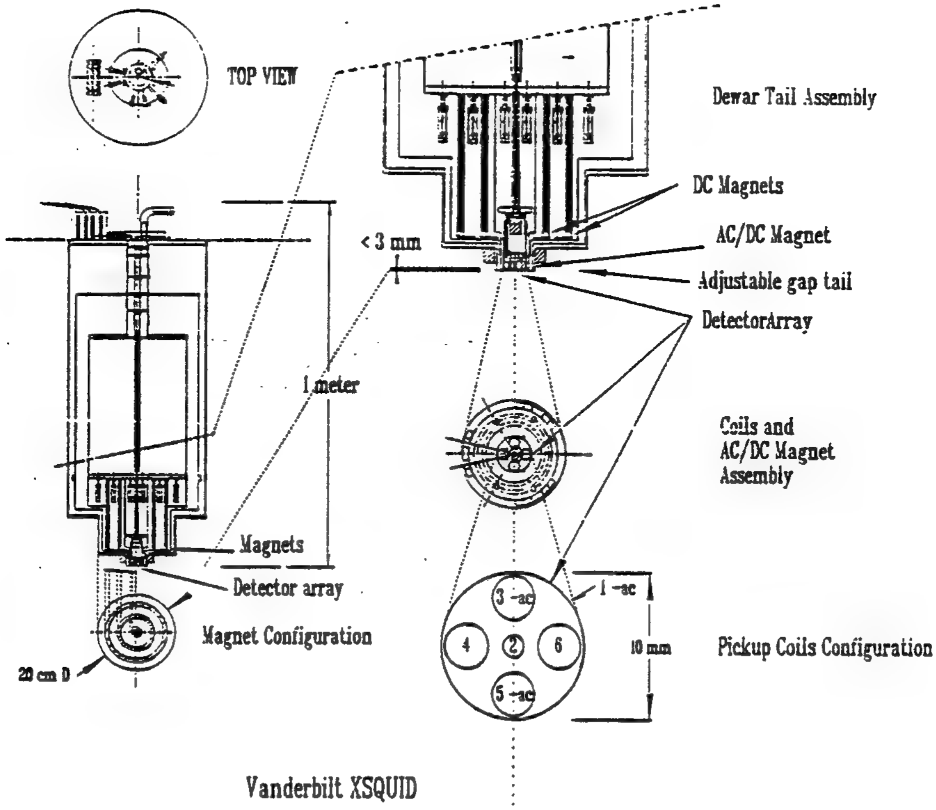

Vanderbilt XSQUID

SUSCEPTIBILITY IMAGES OF PLEXIGLASS

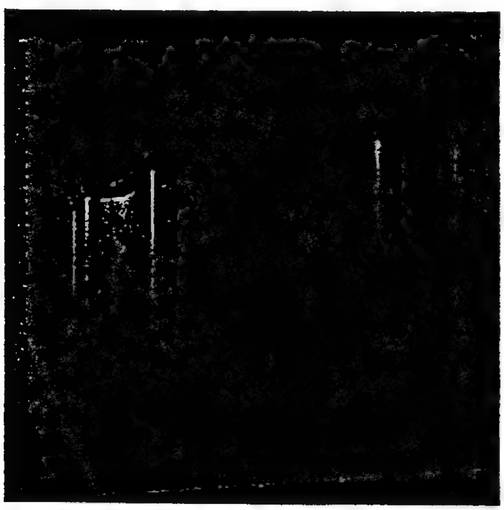

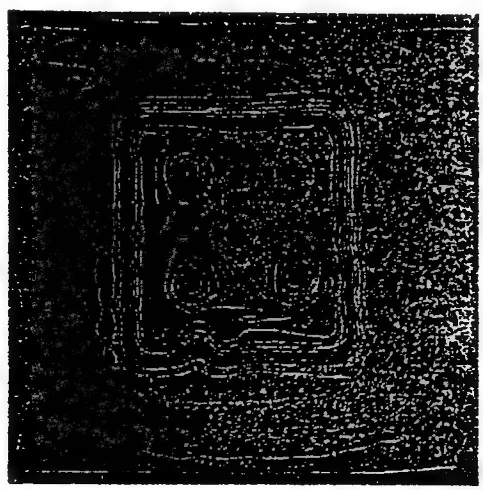

A 25.4 mm square sample of plexiglass containing five 1.8 mm diameter holes was magnetized in a 110 uT applied field and scanned at a distance of 2.0 mm. Images show the distribution of diamagnetic material.

MAGNETIC DECORATION OF SURFACE DEFECTS

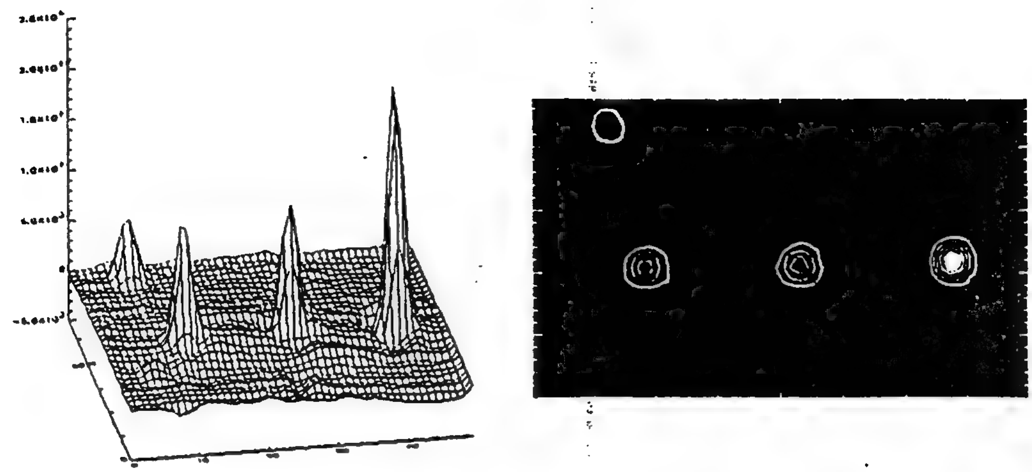

NDE test sample containing electric discharge machined rectangular slots with dimensions of ~100 um, surface decorated with paramagnetic microspheres. Magnetic field recorded 2.0 mm from sample with 174 uT applied field. Susceptibility images display location and size of surface defects.

AC-NULLING: CRACK BENEATH RIVET

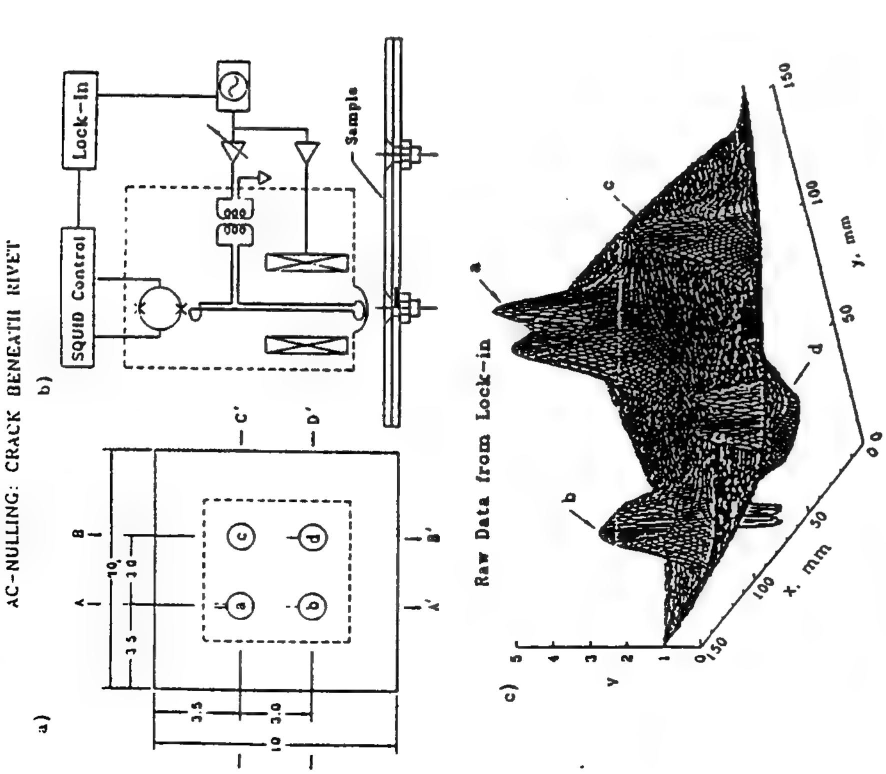

Figure 1-1. Ac-nulling images of the cracks beneath the rivets (a) The test sample is made of two plates of 7075-T6 aluminum bolted together by four 0.25 inch diameter aluminum flat head fasteners. Each panel is 10 × 10 in² and 0.125 inch thick. The crack defects beneath the surface a simulated by 0.25 inch long EDM slots beneath the fasteners. Adjacent to fastener *a* are 0.25 inch slots in both the top and bottom layers. Fastener *b* has a slot in the bottom layer and fastener *d* has a slot in the top layer. Fastener *c* is without slots and for reference only. The dashed line indicates the 6 × 6 in² mapping area. (b) Schematic of ac-nulling technique. The induced eddy currents flow in a circular pattern beneath the magnet. The currents are perturbed by both the fastener and the slot. (c) The raw data, free of any signal processing. The signal for fastener *c*, which is without cracks, is symmetrical. All three signals from the cracked fasteners are asymmetric.

Task 2 NDE Theory and Techniques

- SQUID measurements: Imaging of injected and ELF eddy currents
- Time reversal techniques for ultrasonic NDE methods
- Models for NDE measurements
  - Static model of spheroidal holes
  - Static, three-dimensional finite element model
  - Boundary element model
  - Eddy current models
  - Measurement models for ultrasonics

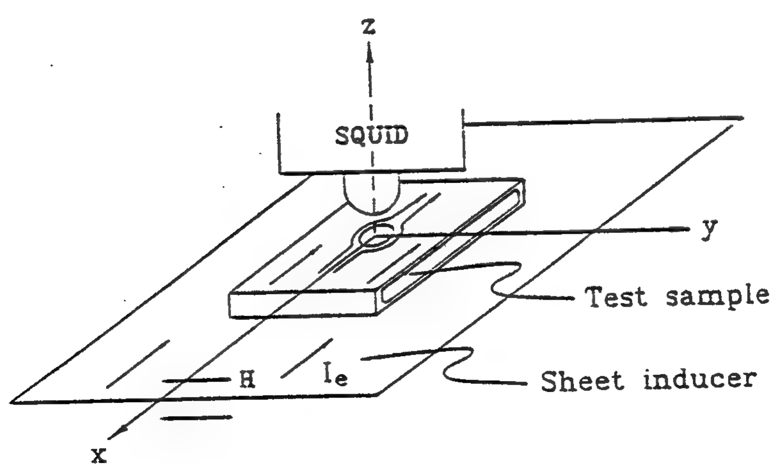

Aluminum plate with aluminum rivets
Induced current (f=144Hz) in transverse direction

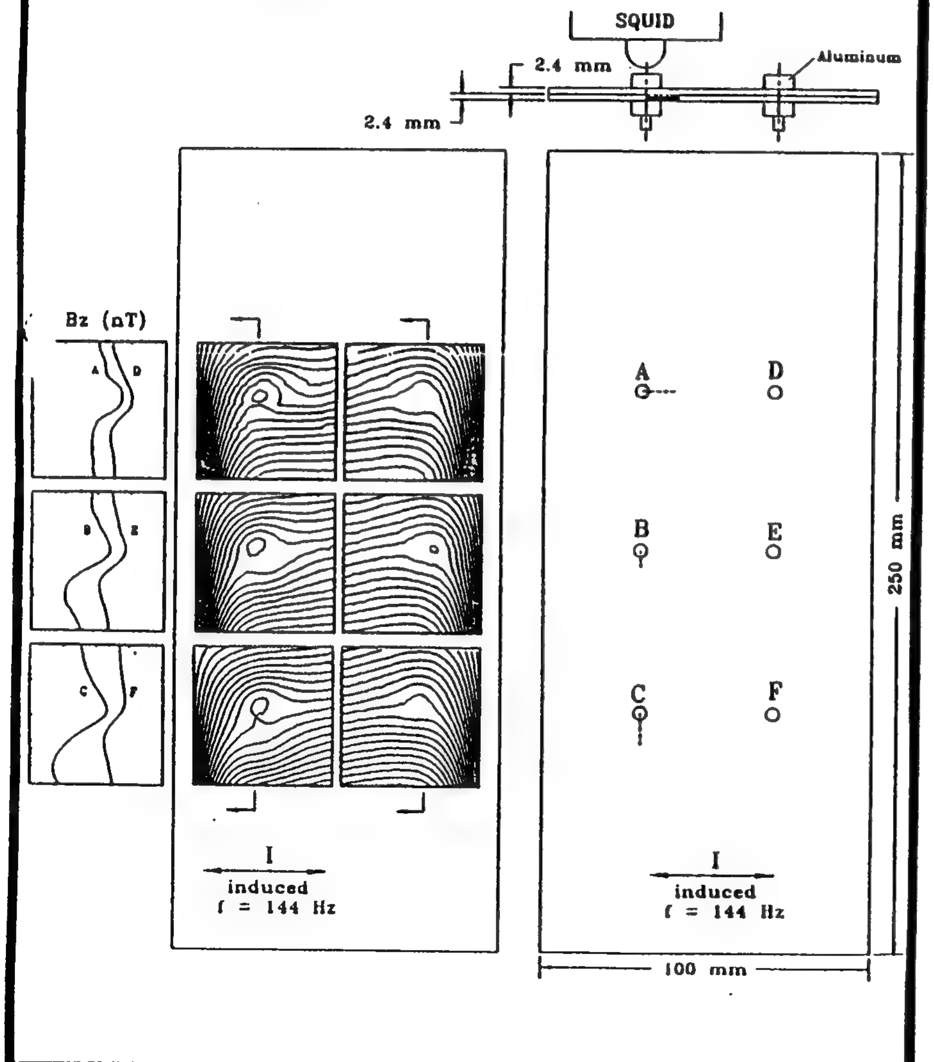

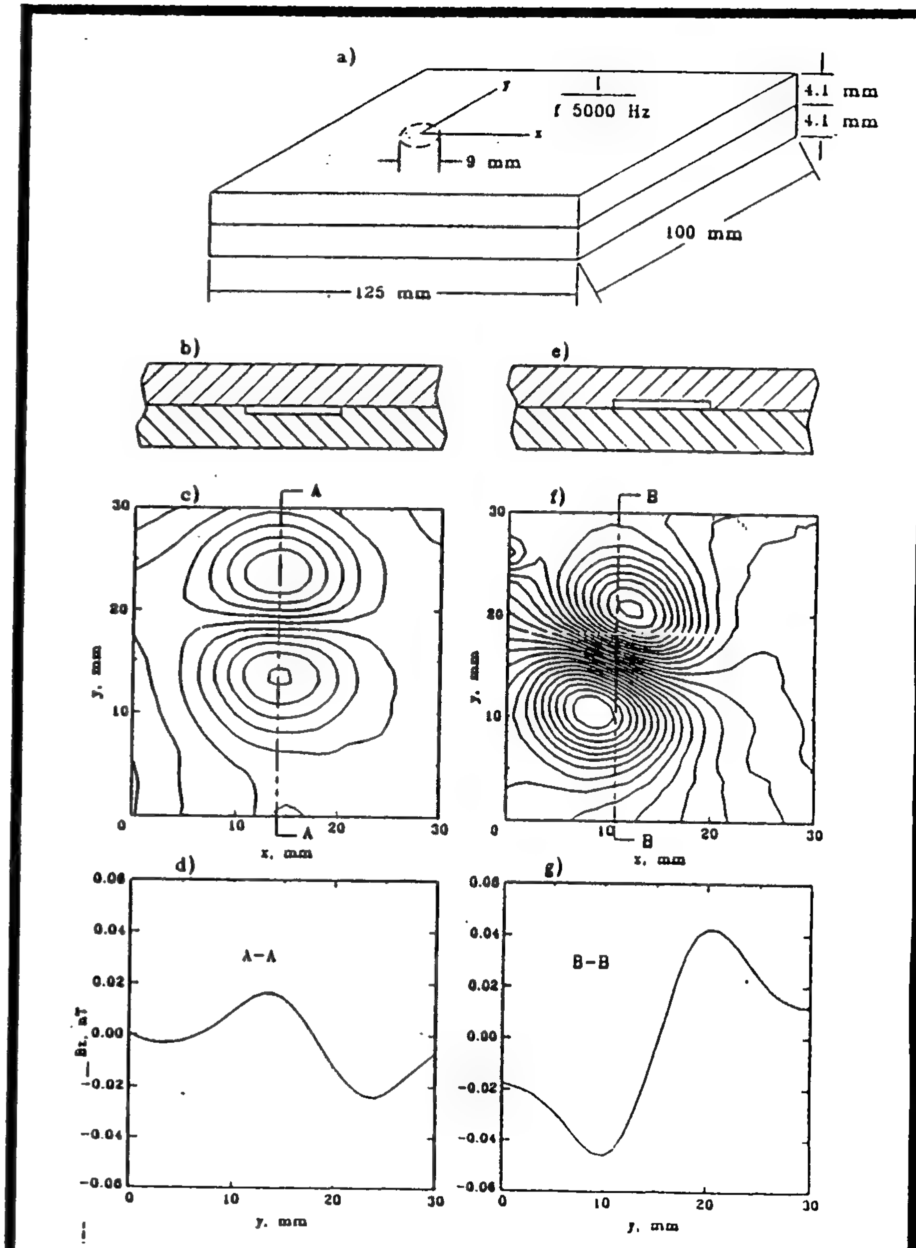

Coordinated Sample I
First and Second Layer Cracks

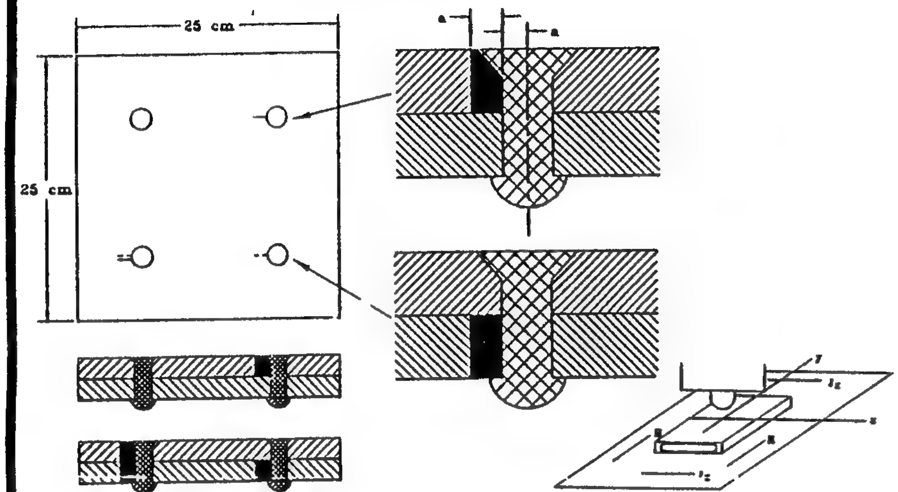

New techniques

- Ultrasonic fiber optic scanner (NU)
- SQUID ELF eddy current (VU)

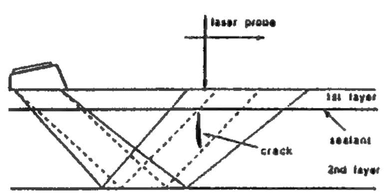

Existing techniques

- Self-compensating ultrasound bridge (NU)
- SQUID injected current (VU)
- Magneto-optical inspection (VU/Lockheed)

Measurements and measurement models

Quantitative comparison of techniques

- Variation of flaw dimensions, location, and orientation
- Probability of detection

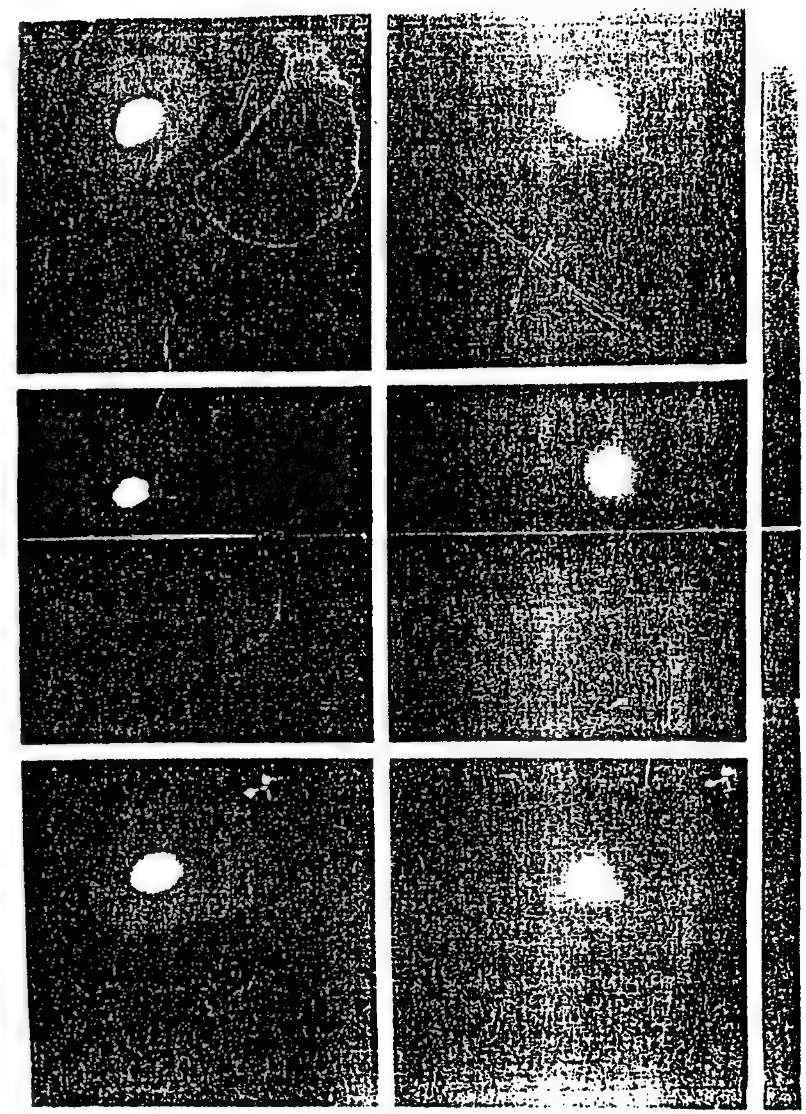

STRIPED INDUCER

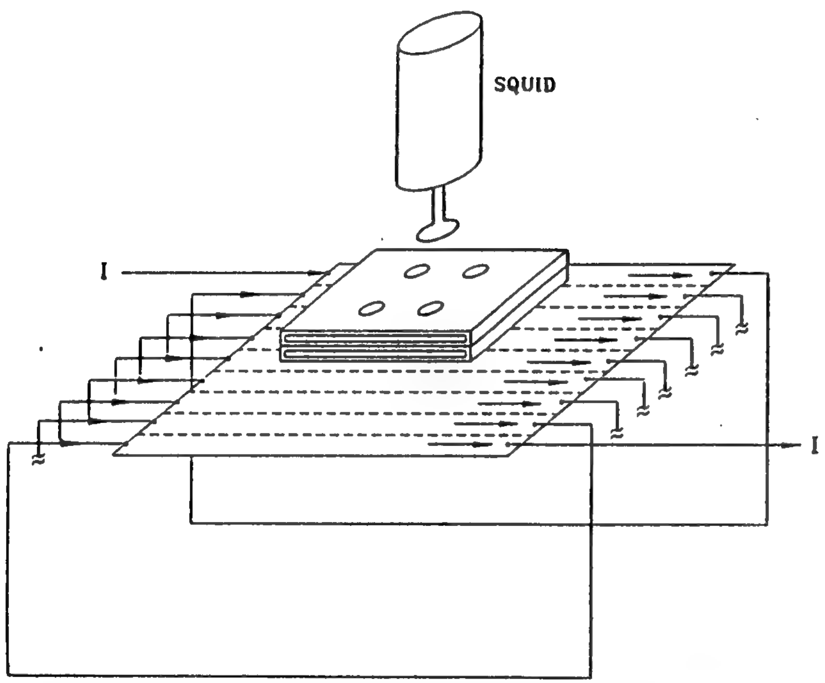

Figure 2-2. Striped sheet inducer. A 300 μm thick copper sheet, carrying a low frequency ac-current and located below the test sample, is used for inducing an eddy current inside the sample. The magnetic field above the sample surface due to the current distribution is measured by the SQUID magnetometer. The copper sheet has been divided into a set of 2 cm wide parallel strips which is serially connected with an ac-voltage source. Normally, the sheet inducer would be placed between the SQUID and the sample.

Coordinated Sample II
Hidden Corrosion

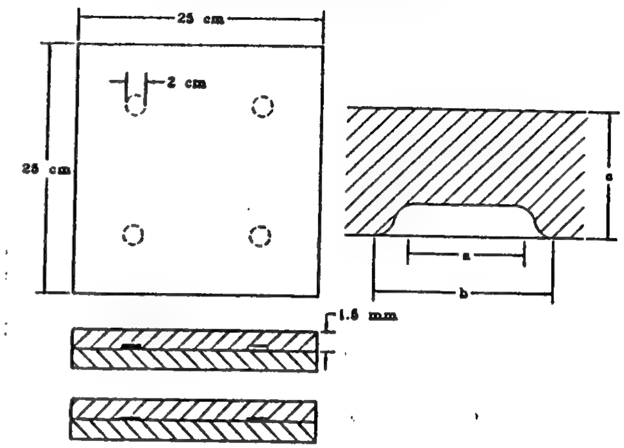

New techniques

- Ultrasonics (NU)
- Electronic speckle laser interferometry (NU)
- SQUID injected current (VU)
- SQUID ELF eddy current (VU)

Existing techniques

- X-ray back scattering (NU)
- SQUID susceptibility imaging (VU)
- Magneto-optical inspection (VU/Lockheed)

Measurements and measurement models

Quantitative comparison of techniques

- Variation of flaw dimensions and properties
- Probability of detection

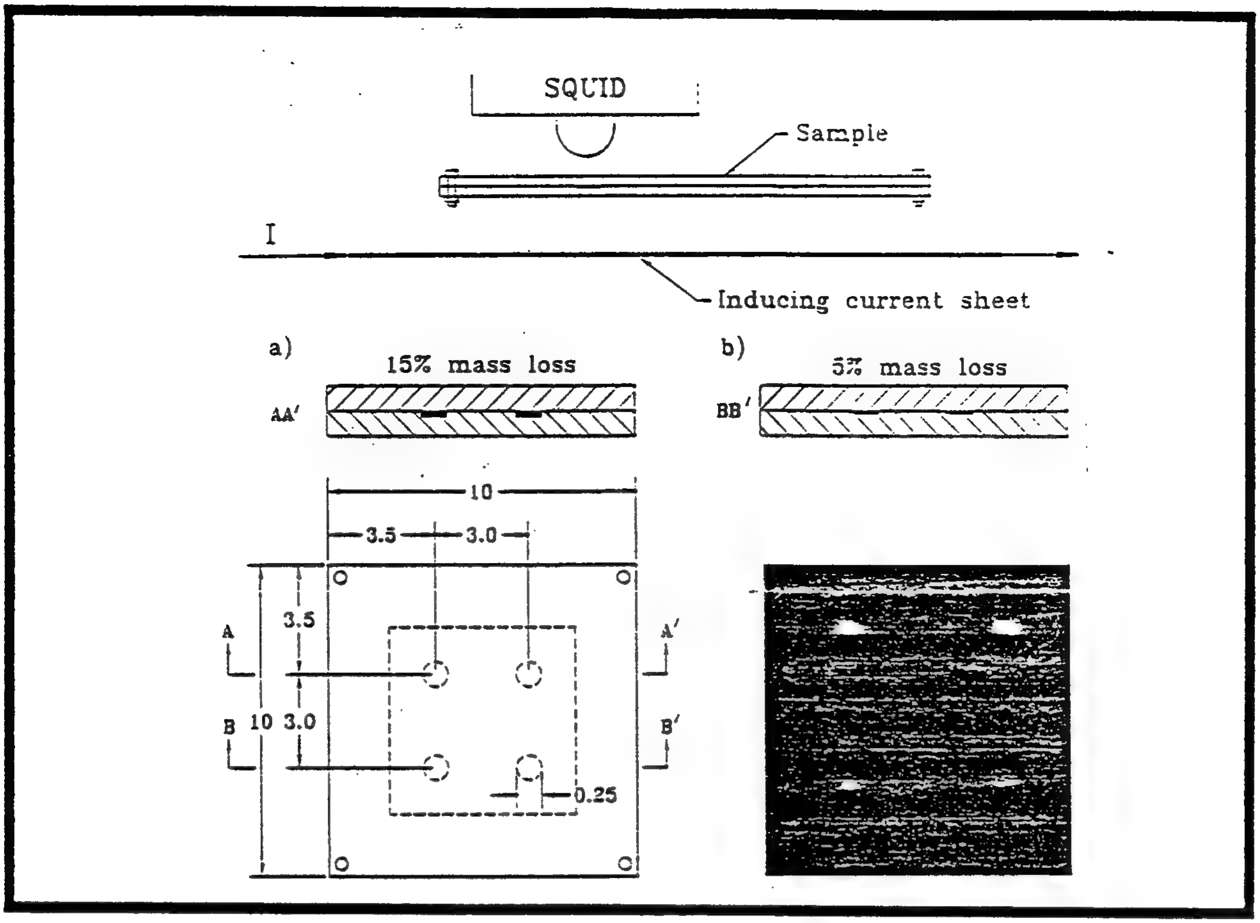

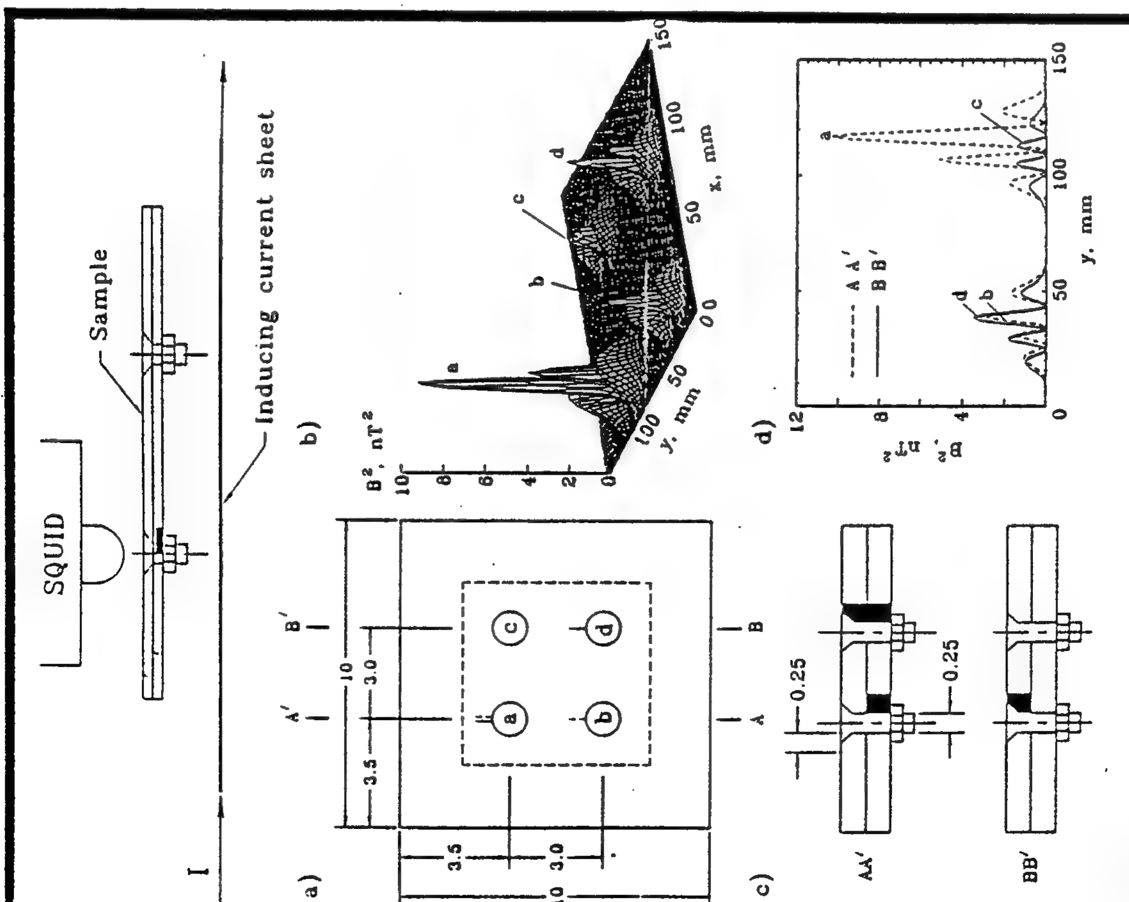

Figure 2-3. EDM simulated flaws in 7075-T6 aluminum panels (see text for detailed description).

Task 3 Image Processing

- Image optimization, constraint, stabilization
- Perturbative Green's functions
- Generalized 3-D inverse

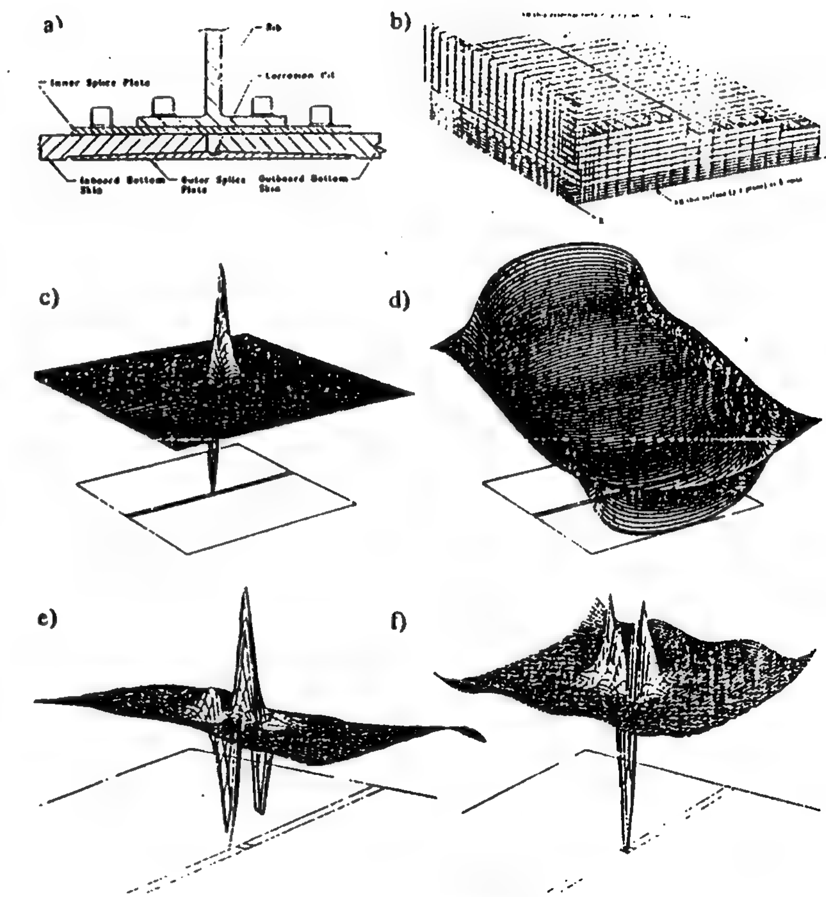

Figure 2-4. F-15 wing splice schematics and simulations (see text for description).

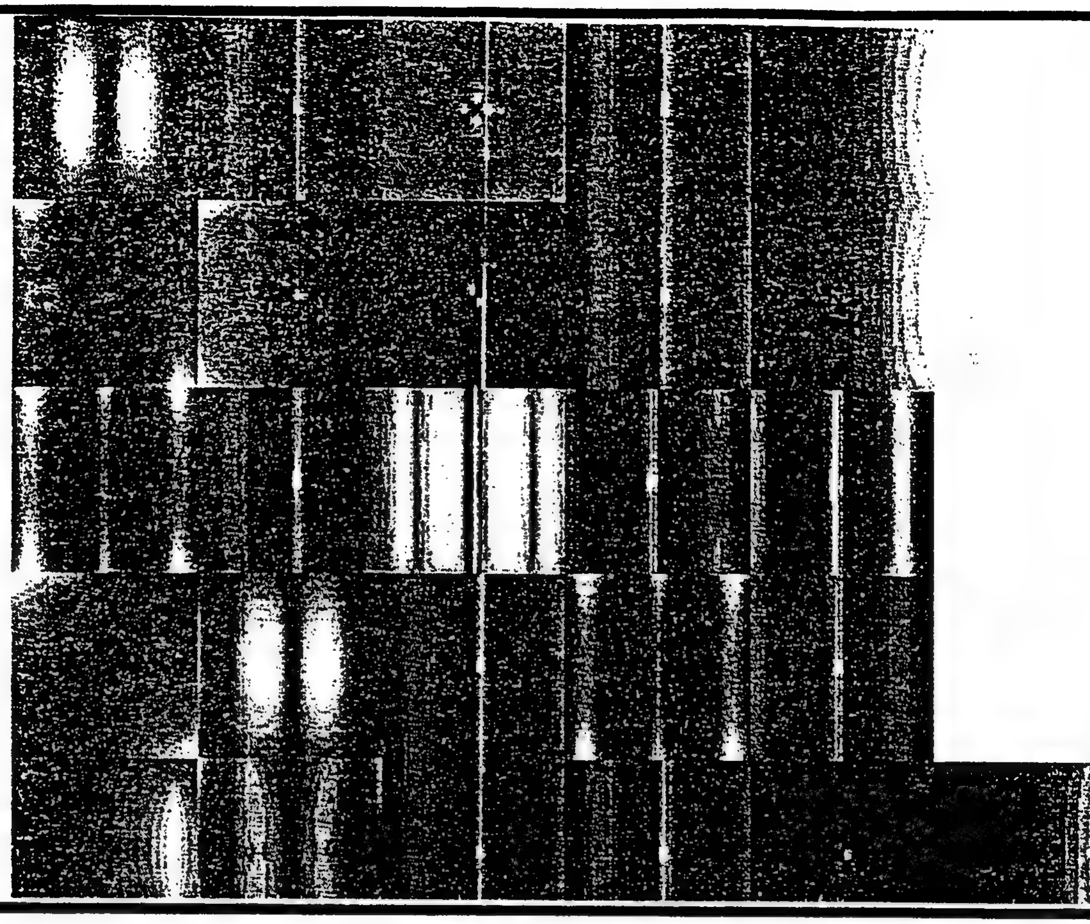

Figure 2-1. Example of image processing capability using multiple filters.

DECONVOLUTION OF DISTORTED IMAGES

Our group has been employing two basic methods for recovering current density information from magnetic field measurements. These methods have been developed at Vanderbilt and are referred to as

- Signal Enhancement
- Blind Deconvolution

Signal enhancement is a more mature technique and it has rendered useful deconvolution for recovering current density. Our groups blind deconvolution method is relatively new and is under development. It may be more promising for the task at hand.

CURRENT DENSITY RECOVERY VIA BLIND DECONVOLUTION

In the two dimensional recovery problem, the measured image (magnetic density) is assumed to be governed by

$$y(m,n) = \sum_{j=1}^{N} \sum_{k=1}^{M} g(j,k)x(m-j,n-k) + w(m,n) \qquad (1)$$

in which the point spread function $g(j,k)$ is not known. It is desired to recover the current density $x(m,n)$ from these noise contaminated magnetic density measurements. The signal processing group at Vanderbilt University is developing an algorithm for solving this two-dimensional *blind deconvolution* problem. The results shown on the next transparency have been obtained using this groups one-dimensional blind deconvolution algorithm. When the two-dimensional algorithm is finalized, significantly better image recovery performance will be obtained.

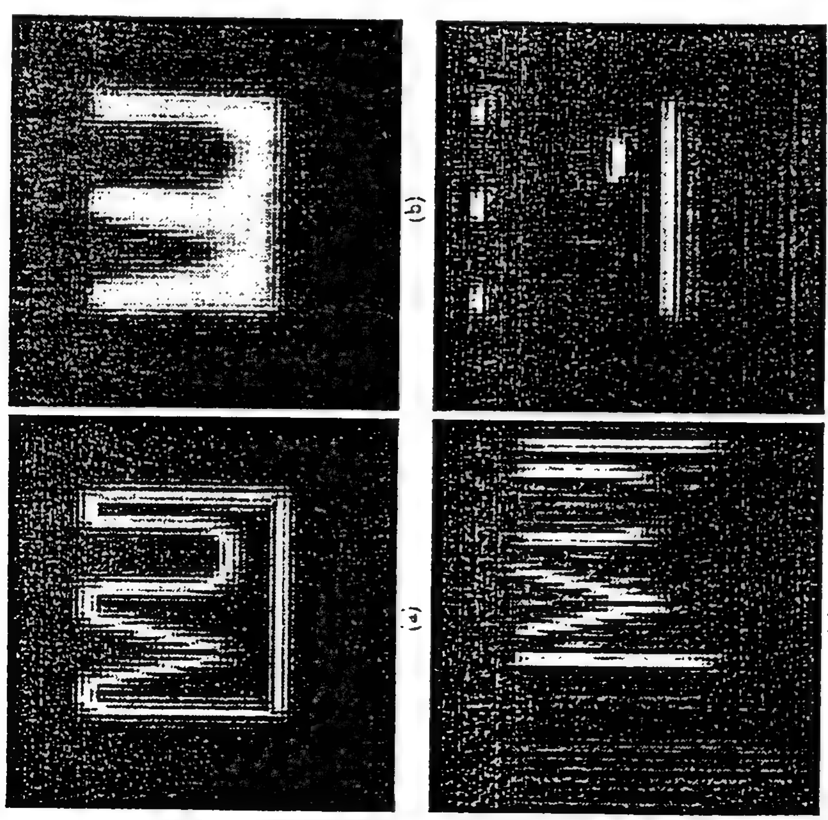

Figure 3-1. Blind deconvolution on a current carrying wire in the shape of VU; (a) Original current source density, (b) the z-component of the induced magnetic field, (c) recovered magnitude along the y-direction using blind deconvolution, (d) recovered magnitude along the x-direction using blind deconvolution.

Task 7 Evaluation of NDE Capabilities

– Reliability of detection/probability analysis

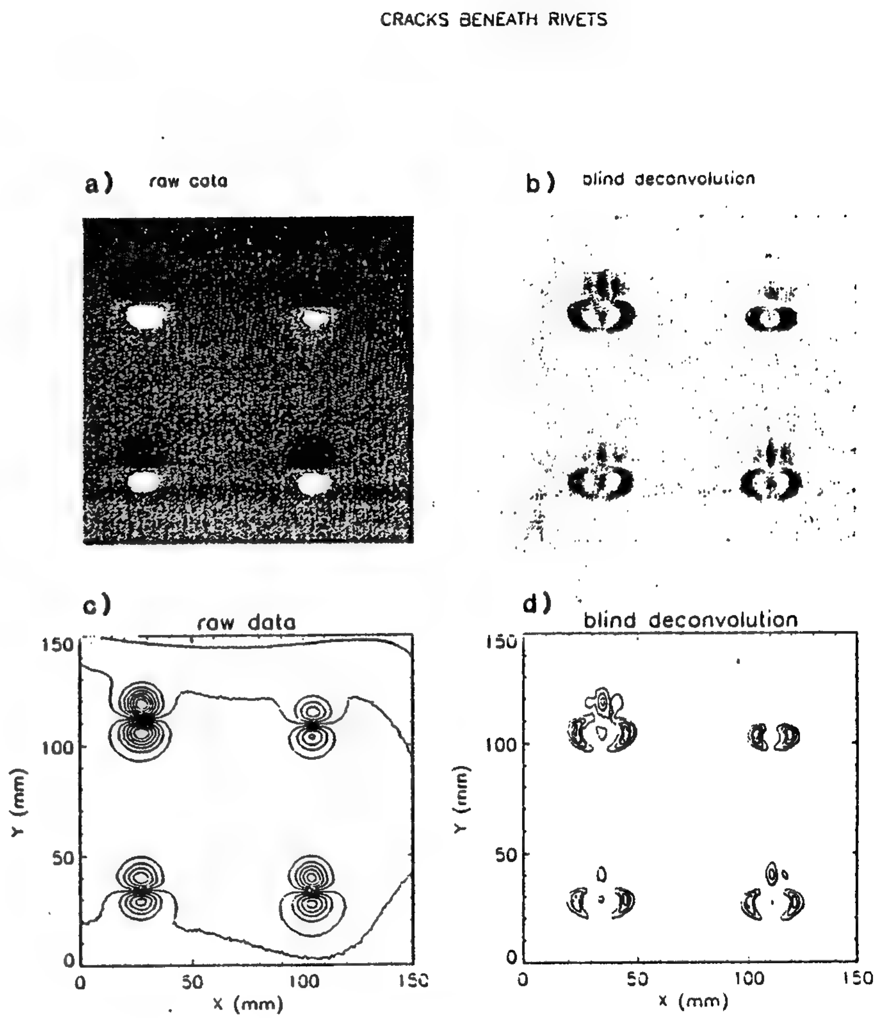

Figure 3-2. Application of blind deconvolution to magnetic image from EDM simulated flaws in panels of 7075-T6 aluminum with 0.25 inch fasteners. See Figure 2-3 for details of sample. (a) magnetic field raw data, (b) blind deconvolution yielding field source (J_y only), (c) contour plot of raw data, (d) contour plot of field source.

Task 7.1: Reliability of Detection & POD Analysis

Objective: Simulate the reliability of NDE methods based on FORM/SORM technologies

Approach: Use perturbation models of the governing physical detection processes and combine these with probabilistic models of the independent random variables

First-year Status:

- Assessed the SOA for probabilistic NDE
- Defined valid NDE POD modeling approach
- Demonstrated BEM sensitivity approach on collaborative effort
- Applied probabilistic methods to rotor cracking field problem
- Initiated engineering approach to SQUID with Tony Ewing
- Developed illustration problem for SQUID POD model

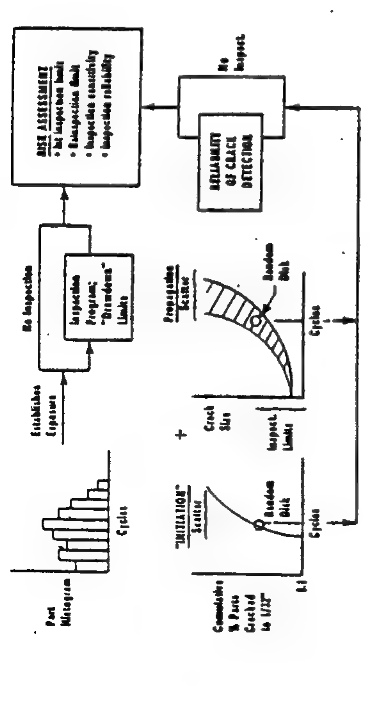

Figure 7-1. Probabilistic risk assessment logic for field cracking of gas turbine disks with POD included as one of the probabilistic issues.

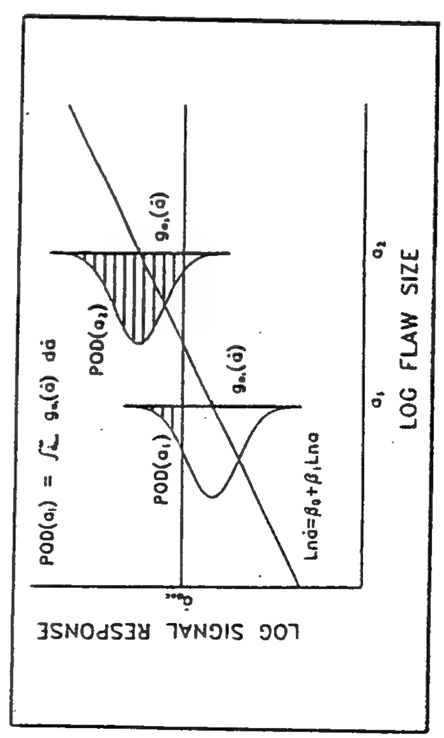

Figure 7-2. Log-Signal Response Approach to POD results in normal distribution of data at a given crack size.

Task 4 Damage Detection in Composite Materials

- Techniques for detection and characterization of matrix cracking, porosity, fiber/matrix debonding
- Real-time NDE techniques for monitoring damage evolution

Task 5 Fatigue Damage Characterization

- Preparation of flawed samples: Riveted assemblies
- Constitutive relations for cyclic deformation
- Non-linear finite element analyses of cyclically-loaded rivet holes.
- Characterization of structural changes attending fatigue: Aluminum alloy sheet with rivet holes.

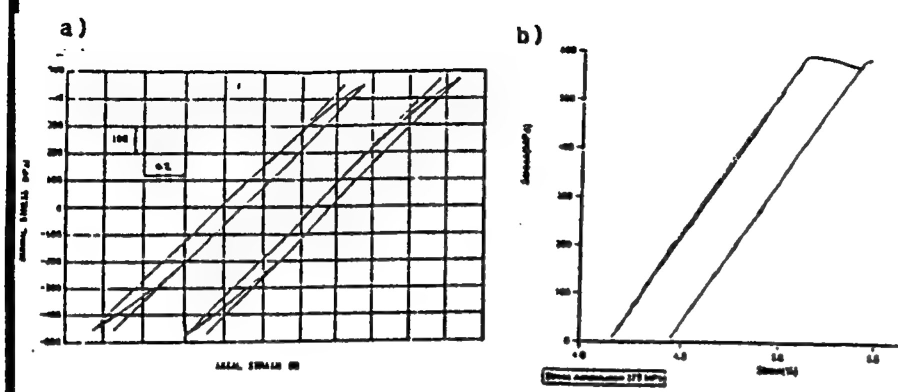

Figure 5-2. Examples of cyclic stress-strain hysteresis loops of 7075-T6 for axial, push-pull loading: (a) σ_s = 540 MPa and R = -1 after Kumar, Hahn and Rubin (A) and (b) σ_s = 275 MPa and R = 0.1, present study.

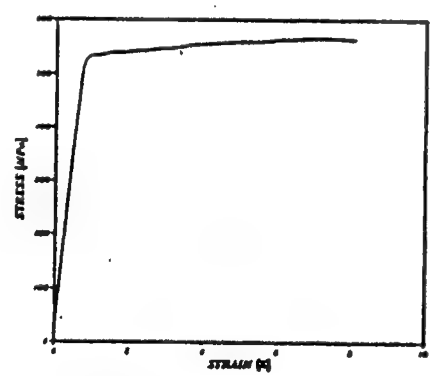

Figure 5-3. Engineering stress-strain curve of 7075-T6 sheet.

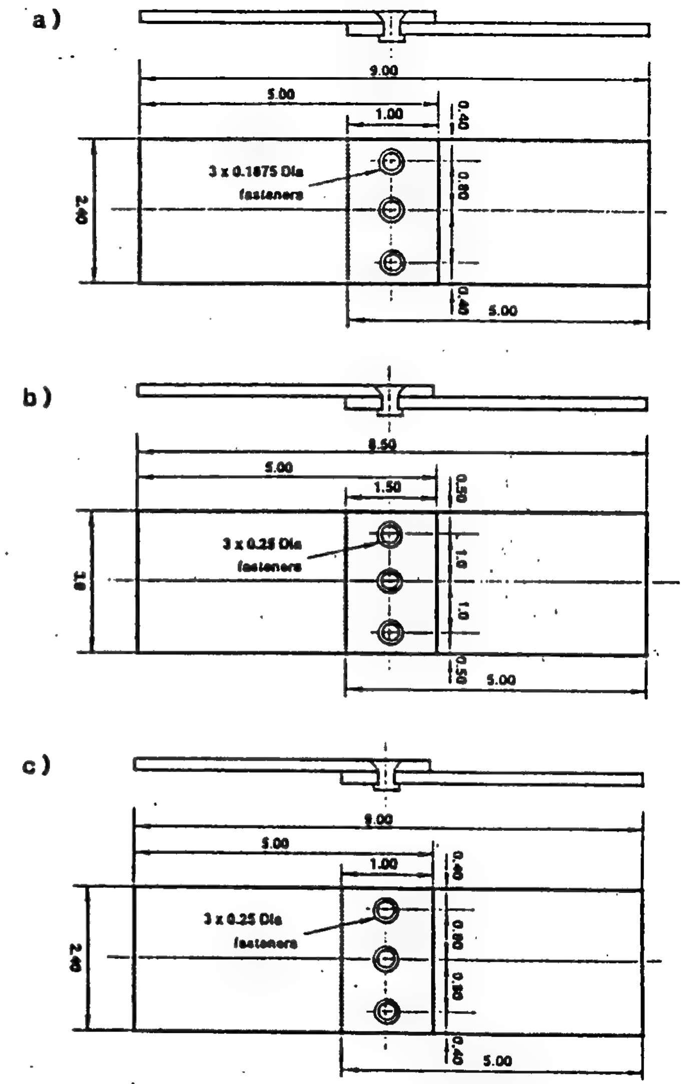

Figure 5-1. Schematics showing dimensions of aluminum lap joints: (a) thickness= 0.060 in. (b) thickness= 0.080 in. (c) thickness= 0.1 in.

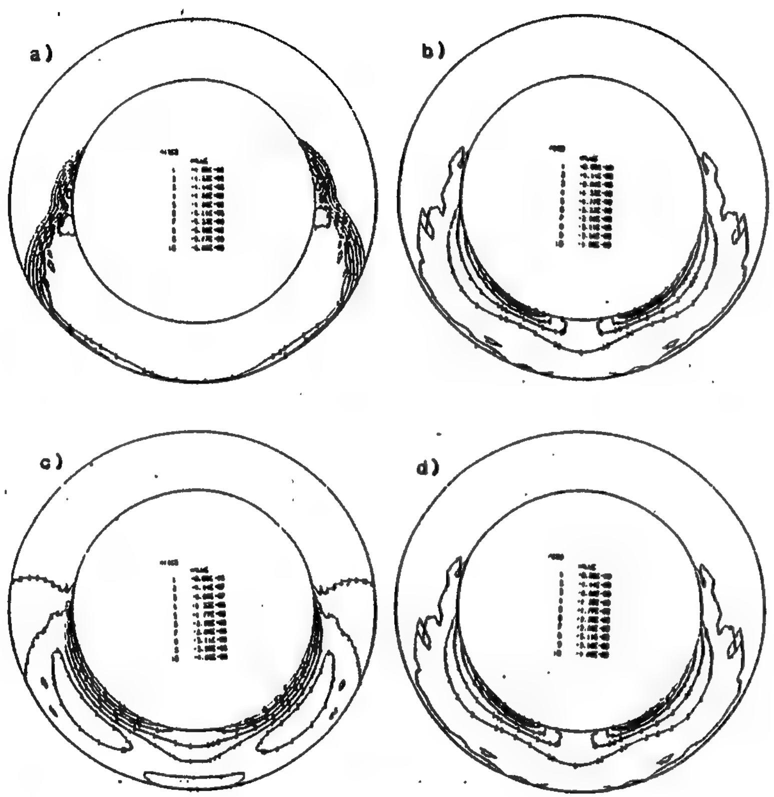

Figure 5-5. Mises stress contours and equivalent plastic strain contours obtained from 2-D in-plane finite element model for 7075-T6 sheet fastened with an aluminum pin: (a) & (b) 0% interference, coef. of friction at hole-pin interface, $\mu=0.2$, and an applied nominal stress of 125 MPa, (c) & (d) 0% interference, coef. of friction at hole-pin interface, $\mu=0.2$, after an applied nominal stress of 125 MPa and unloading to 13 MPa.

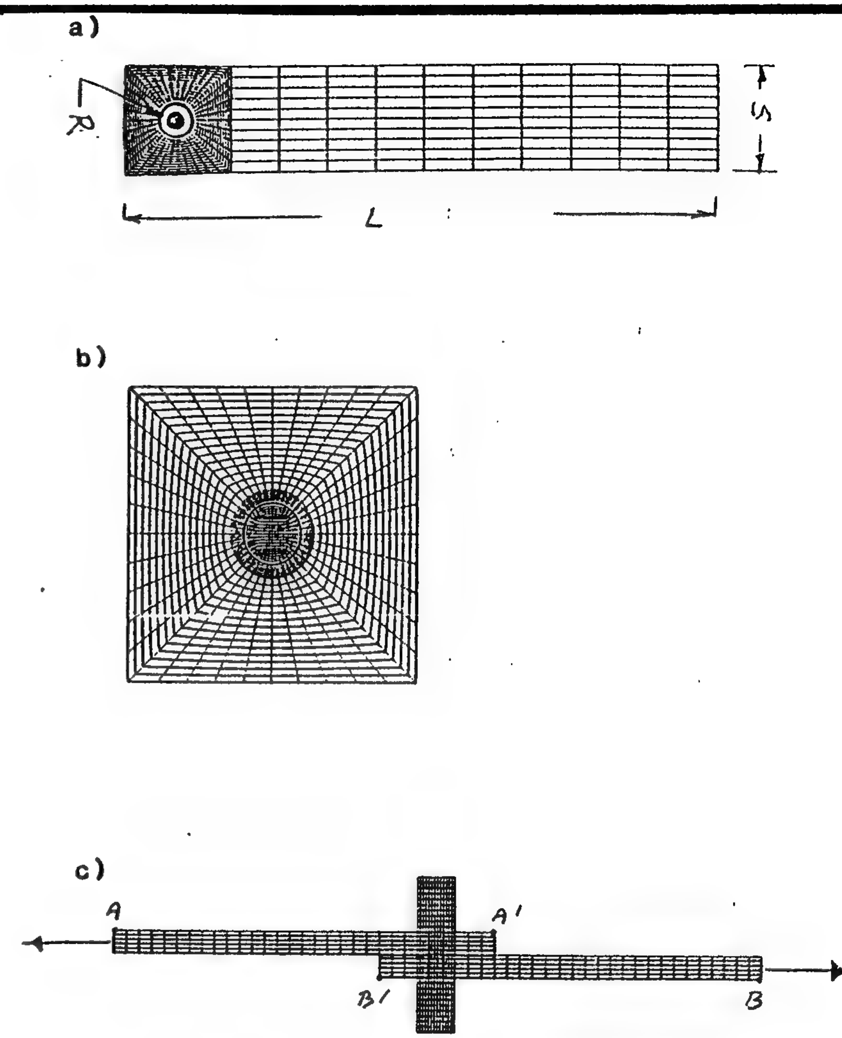

Figure 5-4. Finite element mesh for the 2-D in-plane model: (a) sheet element, and (b) detail showing pin and sheet (the dark circle identifies the location of the pin-sheet interface). The dimensions of the sheet element are: S=30.6 mm, L=168.3 mm, R=3.06 mm, and t=1.53 mm. (c) Finite element mesh of a 2-D out-of-plane model of a lap joint.

a) b)

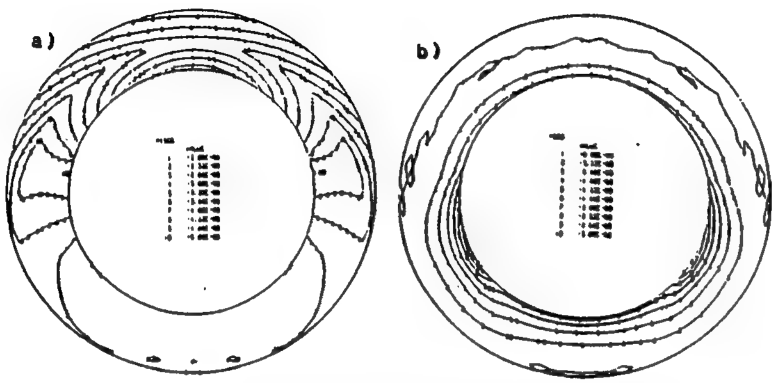

Figure 5-7. Mises stress contours and equivalent plastic strain contours obtained from 2-D in-plane finite element model for 7075-T6 sheet fastened with an aluminum pin: (a) & (b) 1% interference, coef. of friction at hole-pin interface, μ=0.2, after an applied nominal stress of 125 MPa and unloading to 13 MPa.

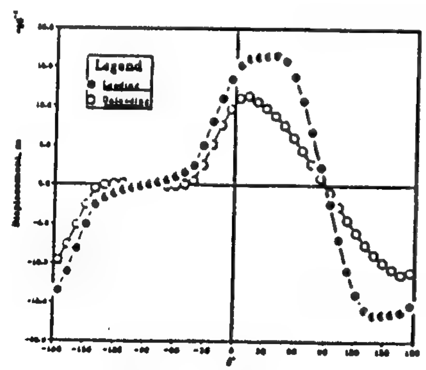

Figure 5-8. Relative tangential displacements (slip) at the pin-hole interface during loading and unloading as a function of angular position (0° and ±180° correspond with 3 o'clock and 9 o'clock, respectively).

a) b) c) d)

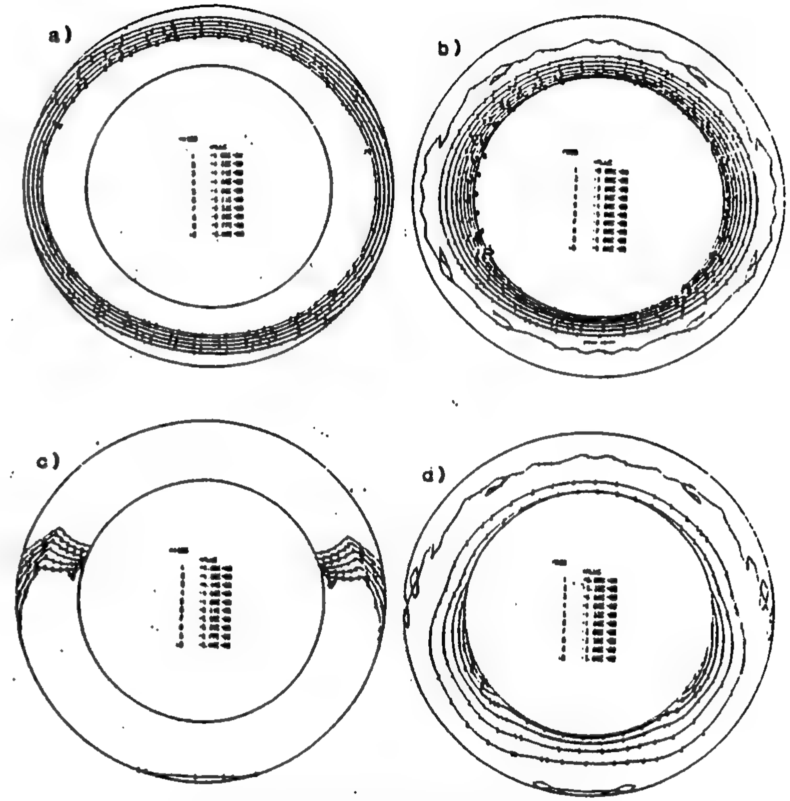

Figure 5-6. Mises stress contours and equivalent plastic strain contours obtained from 2-D in-plane finite element model for 7075-T6 sheet fastened with an aluminum pin: (a) & (b) 1% interference, coef. of friction at hole-pin interface, μ=0.2, after installing the pin. (c) & (d) 1% interference, coef. of friction at hole-pin interface, μ=0.2, after an applied nominal stress of 125 MPa.

Task 6 Corrosion

- Identification of aircraft structures and corresponding corrosion-related failure modes.
- Procedure development.
- Examination of scientific problems.
- Practical NDE detection of corrosion-related damage.

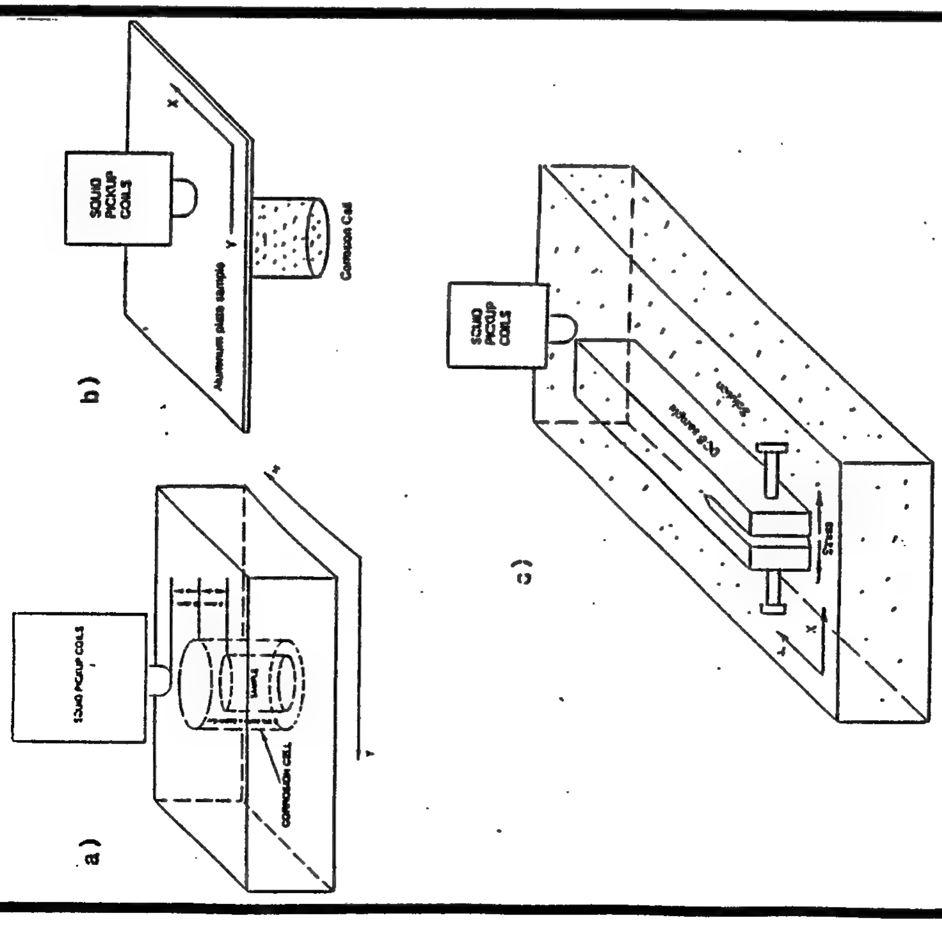

Figure 6-1. Schematics of the three active in-situ corrosion model-systems: (a) Active pitting corrosion, (b) Active uniform corrosion, and (c) Active stress corrosion cracking.

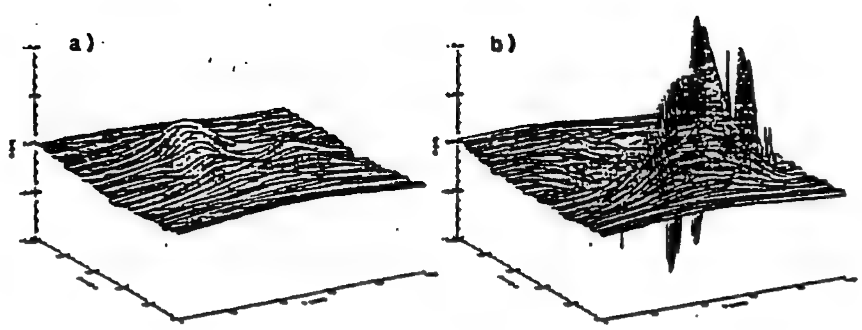

Figure 6-2. Typical magnetic field distributions on an active pitting corrosion 7075 aluminum alloy sample in a solution of 3.5% NaCl +5ppm Cu^{++}. (a) Data was obtained in the period of 25 to 43 minutes after the sample was placed in the solution, (b) in the period of 276 to 294 minutes.

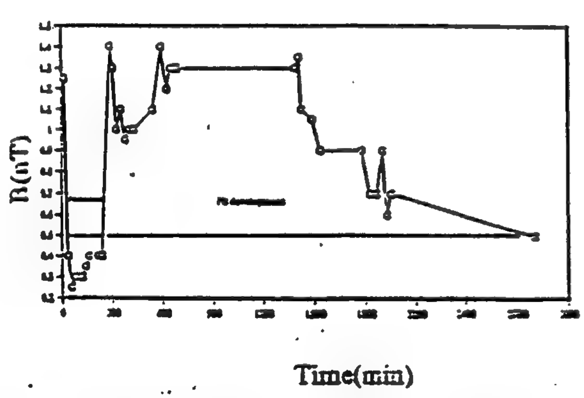

Figure 6-3. The maximum magnetic field as a function of time during pitting corrosion. The first 300 minutes represents pit initiation followed by an increase in magnetic field magnitude signifying the onset of the pit development phase.

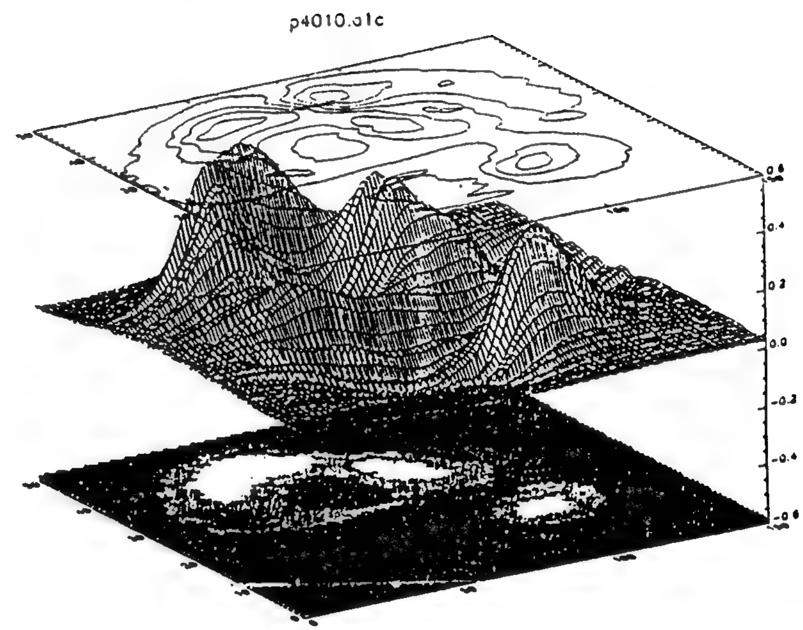

Figure 1(P4010). Typical surface magnetic field, contour map, and shaded map measured by SQUID during pitting corrosion of a 113 mm diameter circular 7075 aluminum alloy plate sample in a solution of 3.5% NaCl +10 ppm Cu^{++}. Scanning area was 151x151 mm for the whole sample. Data was obtained in the period of 1290 to 1308 minutes after the sample was placed in the solution.

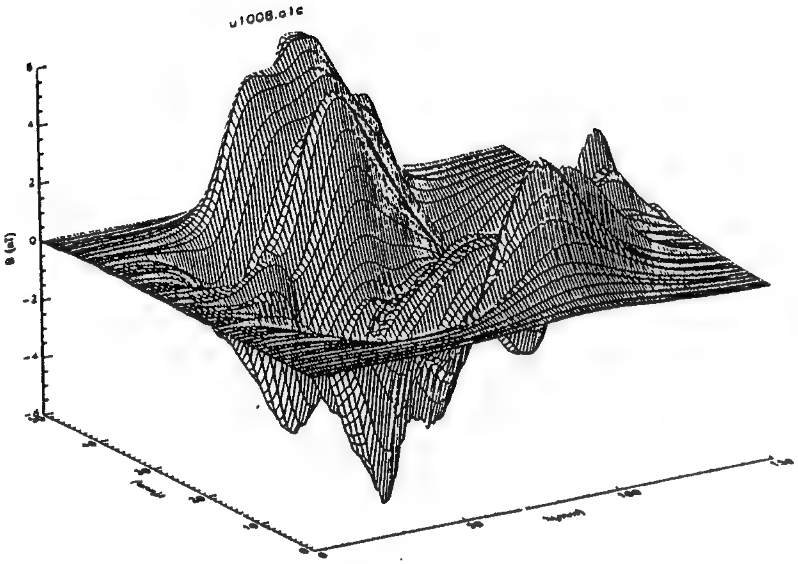

Figure 3b(u1008). Typical surface magnetic field distribution measured by SQUID during pitting corrosion of a 113 mm diameter circular 2024 aluminum alloy plate sample in a solution of 2ml HF, 3ml HNO_3, 5ml HCl, and 590ml H_2O. Scanning area was 151x151 mm for the whole sample. Data was obtained in the period of 234 to 252 minutes after the sample was placed in the solution.

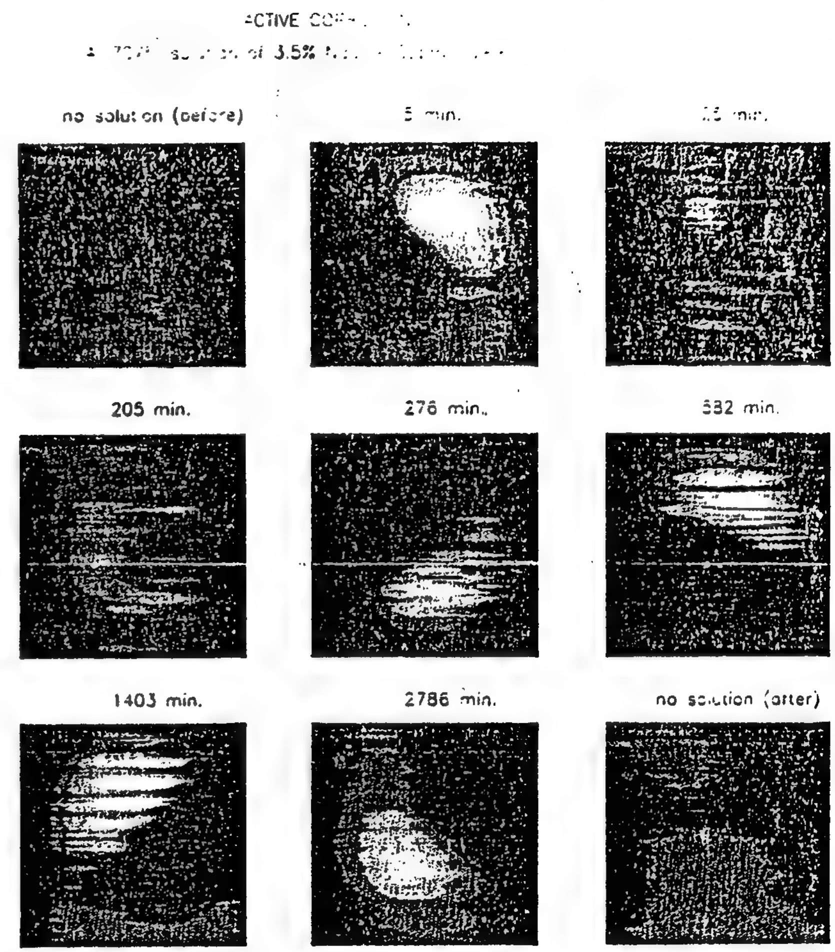

Figure 6-5. Magnetic field as a function of time during pitting corrosion of 7075 aluminum alloy sample in a solution of 3.5% NaCl + 5 ppm Cu^{++}.

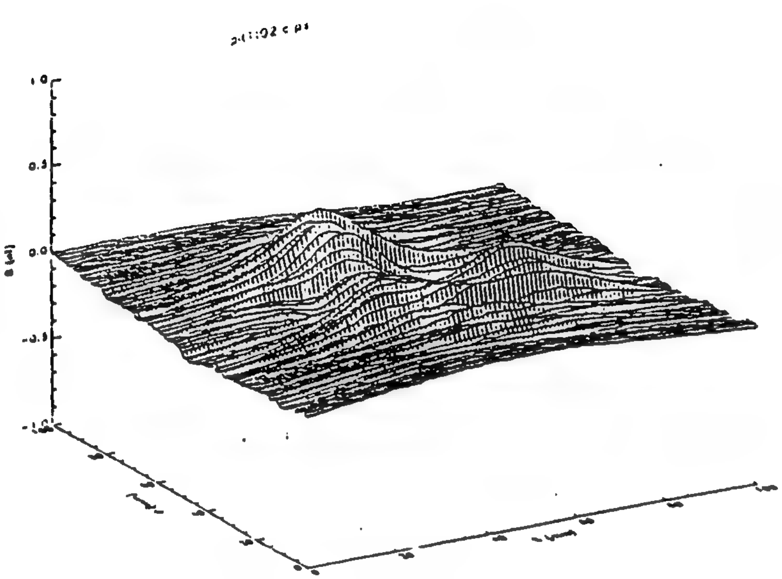

Figure 6-4. Preliminary result of magnetic field measured using the active uniform corrosion system for 2024 aluminum alloy sample which was being corroded on the bottom surface by a solution of 2ml HF, 3ml HNO_3, 5ml HCl, and 190ml H_2O. Data was obtained in the period of 15 to 40 minutes after the sample was placed in the solution.

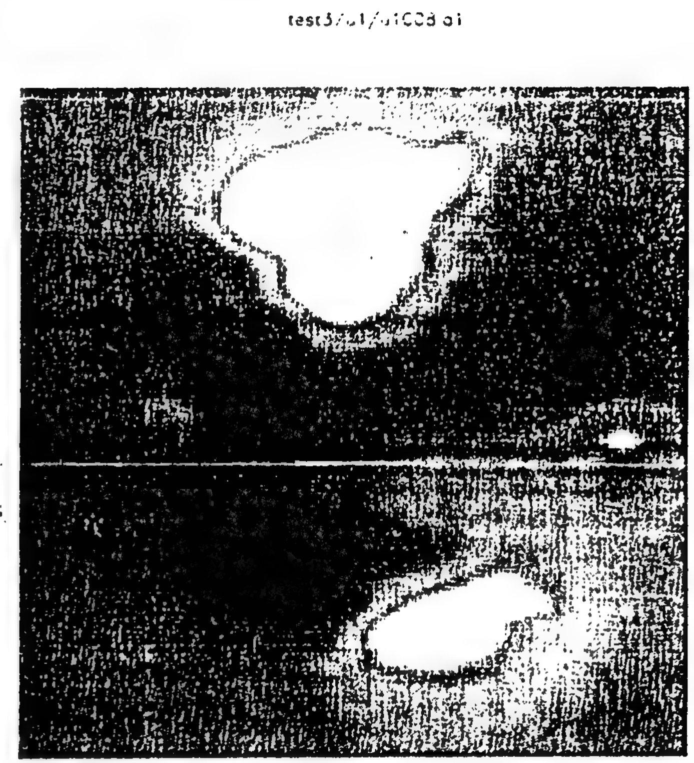

Figure 3a(u1008). Typical shaded magnetic field map measured by SQUID during pitting corrosion of a 113 mm diameter circular 2024 aluminum alloy plate sample in a solution of 2ml HF, 3ml HNO_3, 5ml HCl, and 590ml H_2O. Scanning area was 151x151 mm for the whole sample. Data was obtained in the period of 234 to 252 minutes after the sample was placed in the solution.

AGING AIRCRAFT
RESEARCH, DEVELOPMENT & TECHNOLOGY TRANSFER
AT NORTHWESTERN UNIVERSITY

RESEARCH & DEVELOPMENT ⇒ **TECHNOLOGY TRANSFER**

AFOSR / URI
NU / VU

- Damage in Composites
- Dynamic Holography
- Laser-Based Imaging
- Time-Reversal Technique
- Measurement Models

FAA / CASR
NU / ISU / WS

- Self-compensating UT
-
-
-
- X-Ray Backscattering
- Optical Speckle Interferometry
- Laser UT Equipment
- Neural Nets
- Image Processing
- Reliability-NDE connection

FAA / CASR
NU / ISU / WS

- Corrosion DC-9 Wingbox (Ultra-Imaging Inc.)
- Cracks DC-10 Spar-Cap/ Strap (Infometrics)
- X-Ray BDP Equipment
- Licensed to Laser Technology

Jan D. Achenbach
Isaac M. Daniel
Sridhar Krishnaswamy

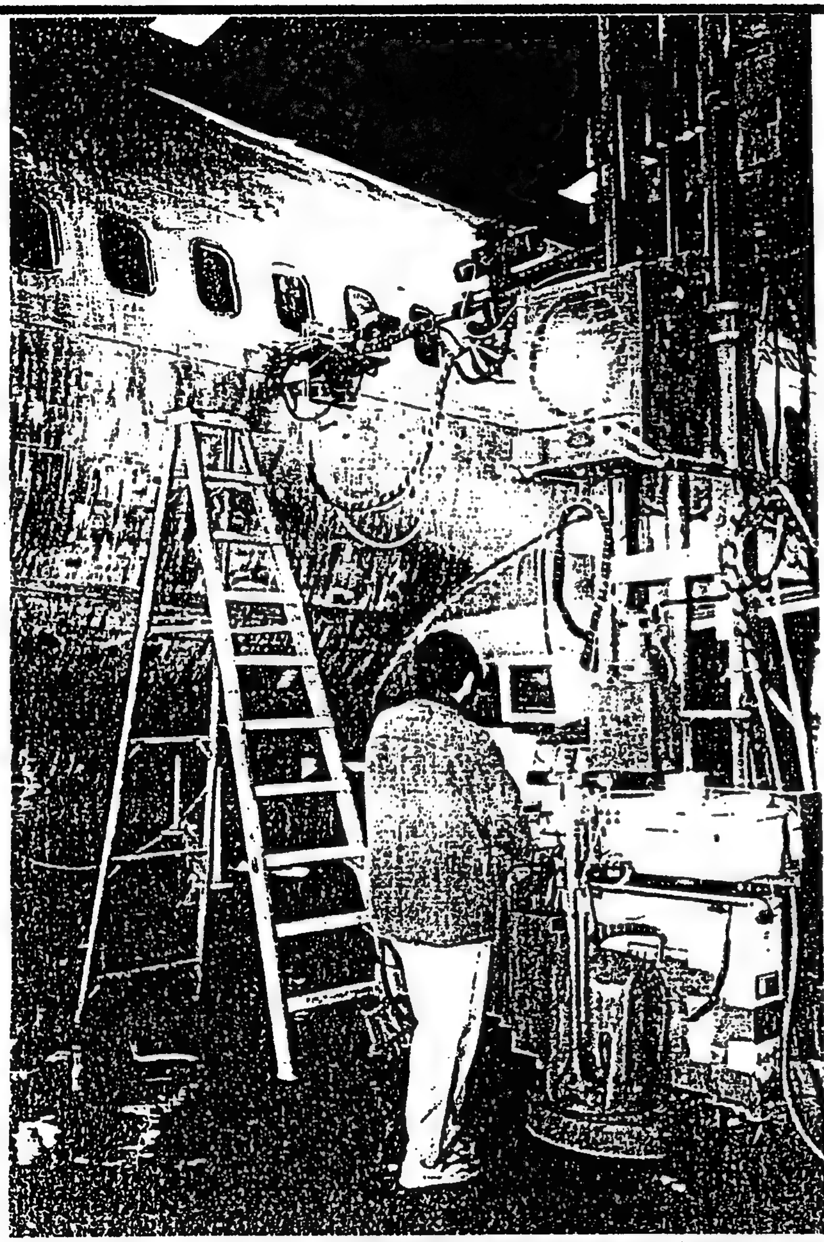

FEATURES OF COMPTON X-RAY BACKSCATTER DEPTH PROFILOMETRY

- Gives a cross-sectional view of aircraft sheet metal joints.
- Allows measurement and identification of sub-surface layers.
- 1/1000 inch measurement accuracy.
- Generates very little ambient x-radiation.
- No evacuations--Does not interfere with most hangar activity.
- Self-propelled. Scaffolding and stands are not needed.
- Data are digital files -- easily stored and transmitted via Internet.

S25LU836.300

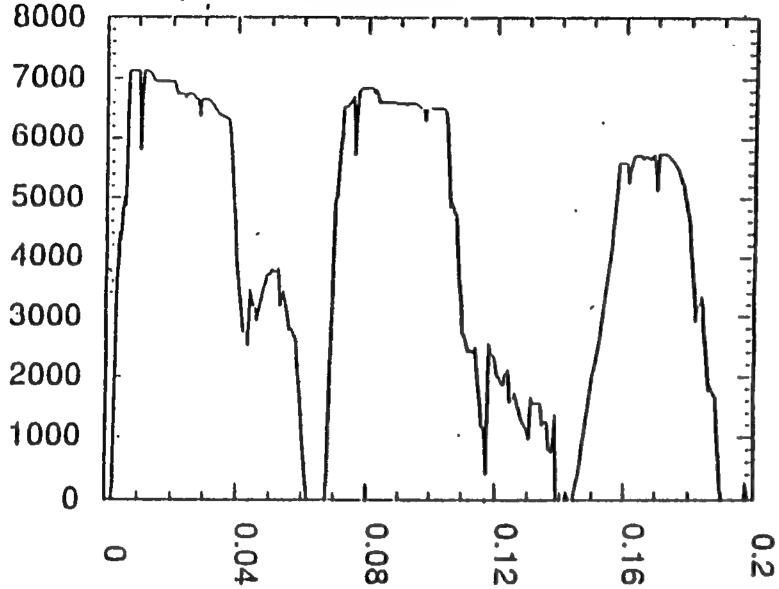

This is a scan through a lap joint, along the middle row of rivets. Large air gaps and much loose material suggest the presence of corrosion. The front layer of skin measured 0.0375". Beneath this was a layer of possibly skrim cloth or a polymer. This layer was probably disbonded to the first layer of skin with a gap of about 0.0010". The thickness of the low density possibly skrim cloth layer measured 0.0175" Beyond it was a large air gap 0.0097" wide. The second skin layer begins after the gap and measured 0.0403". Its rear surface looks rough. Again there is a low density layer disbonded layer. The thickness of this low density layer measured 0.0175" Its comparatively low density to that of other low-density layers along with its apparent looseness and large thickness suggests that it may be an aggregate of corrosion product, paint and other matter. Between this and the stringer is another air gap which measured 0.0138" The stringer, which measured 0.0355" is evidently tilted with respect to the outer surface. Its back surface may also be roughened but with less certainty than is the case for the back of the second skin.

Depth Profiling Apparatus

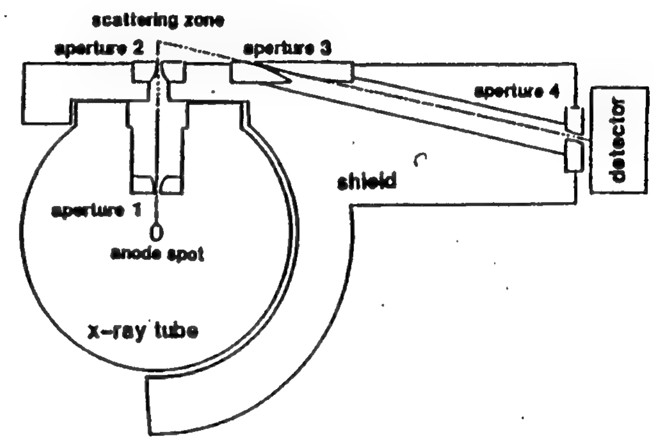

The depth profiling camera consists of four sets of apertures. The first two sets form the beam into a pencil with a narrow rectangular cross-section. The second two sets select a limited thickness region from which backscattered photons reach the detector. The intersection of the incident and backscattered beam paths form a scattering zone or focal region. Sweeping this region through the material to be examined allows visualization of the electron density of the material along the path. In depth profiling, the path is normal to the surface and the result is similar to drilling and examining a core section taken at that point.

The scattering zone is nearly Gaussian in the depth direction with a "standard deviation" size parameter of 0.0013 inches.
Limiting (10% MTF) resolution is 10 lp/mm.

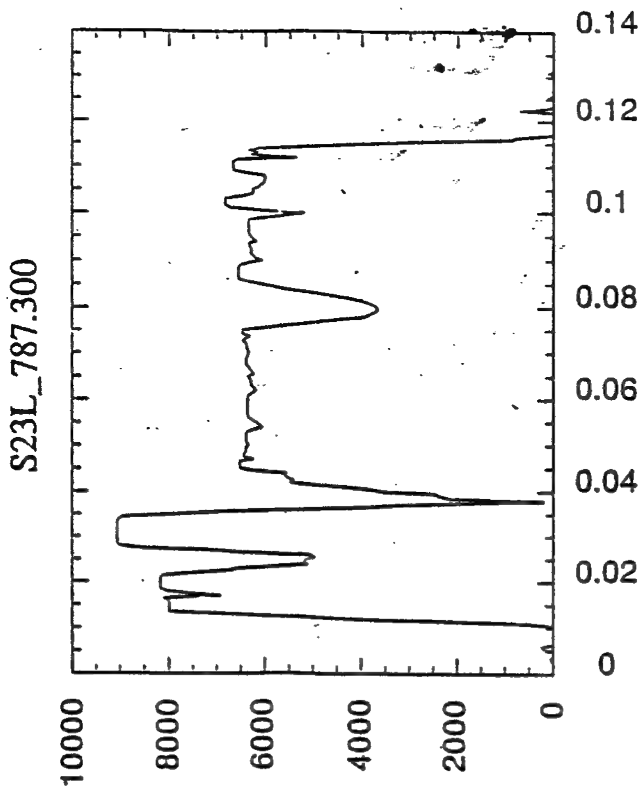

This is a scan made through a boron-epoxy patch in the center. The patch measured 0.0245" thick and appears to be composed of two layers. of boron fiber. The boron fiber has a significantly higher scattering cross-section than does aluminum. The outer layer of patch measured 0.013" while the second layer measured 0.0105". Between the two layers is a low-density region of only about 0.001" thick. This could be filled with resin or could be a disbond. Beneath the patch is what appears to be a disbond with a gap width of 0.0035" There appears to be some warpage as the planes of the patch and that of the aluminum skin are not parallel at the interface. Beneath the patch is a layer of aluminum 0.038" thick resin bonded to a layer 0.0343"thick. The thickness of the glue joint is about 0.003" Since the interfaces at the joint are not fully-resolved, there may be some ambiguity as to their exact location.

FULL-FIELD OPTICAL TECHNIQUES

ESPI, SHEAROGRAPHY, HOLOGRAPHY

ADVANTAGES
- LARGE AREA INSPECTION
- RAPID TESTING

DISADVANTAGES
- NOISE PRONE

APPLICATIONS (LTI)
- Diffusion-bonded Titanium Aircraft Structures
- Space Shuttle Component Inspection
- Shearography NDT of B1-B Engine Inlet, Wing Skins and Spars
- Concorde Elevon Inspection
- Beech Aircraft NDT of metal-metal bonds, aluminum honeycomb etc.

GOAL: To develop dynamic holographic NDE system which will be
- Noise insensitive
- analog (faster and less expensive than ESPI / Shearography)
- high-resolution

FAA - CENTER FOR AVIATION SYSTEMS RELIABILITY

DISBOND DETECTION USING ASPM-ESPI / ACOUSTIC STRESSING

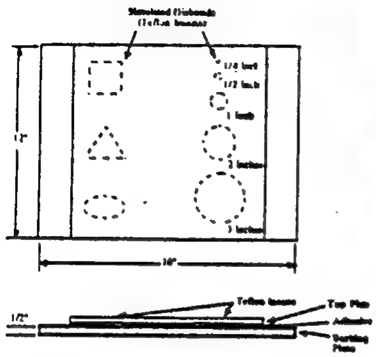

SPECIMEN GEOMETRY

CONVENTIONAL ESPI

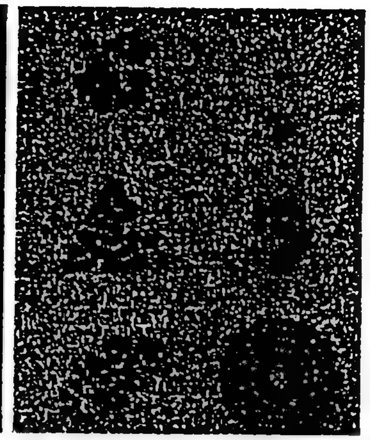

ASPM-ESPI

·Note that in the conventional technique some of the disbonds are not detected due to ambient noise.

PHOTOREFRACTIVE CRYSTALS ARE NON-LINEAR MATERIALS IN WHICH THE PROPAGATION OF AN OPTICAL BEAM MODIFIES THE INDEX OF REFRACTION VIA THE LINEAR ELECTRO-OPTIC EFFECT.

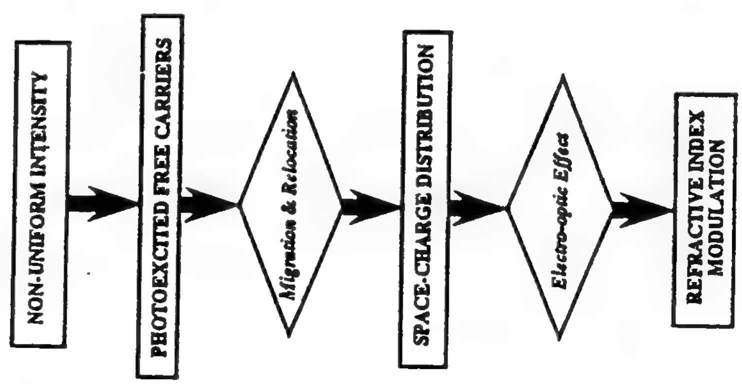

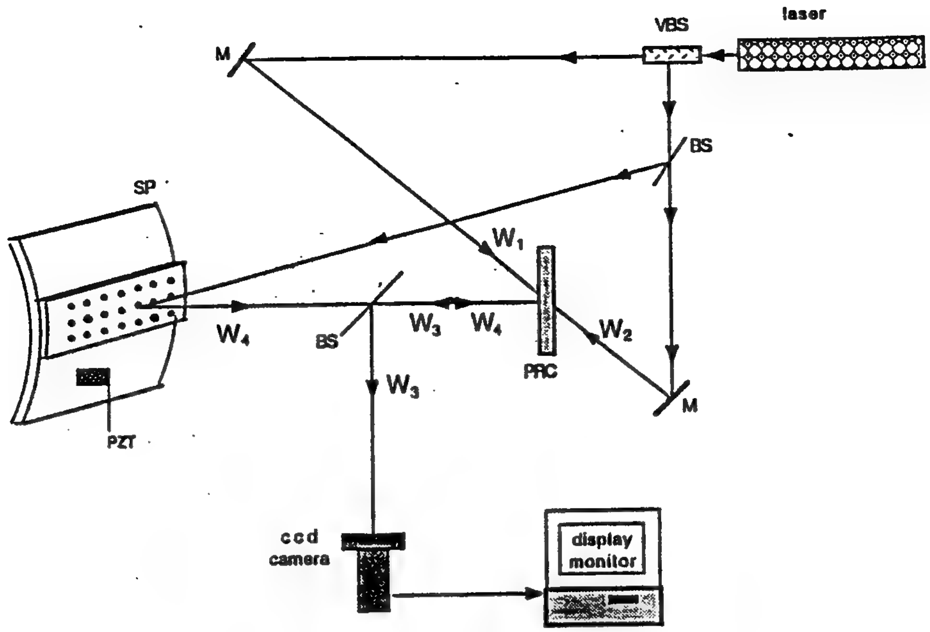

Four-wave mixing

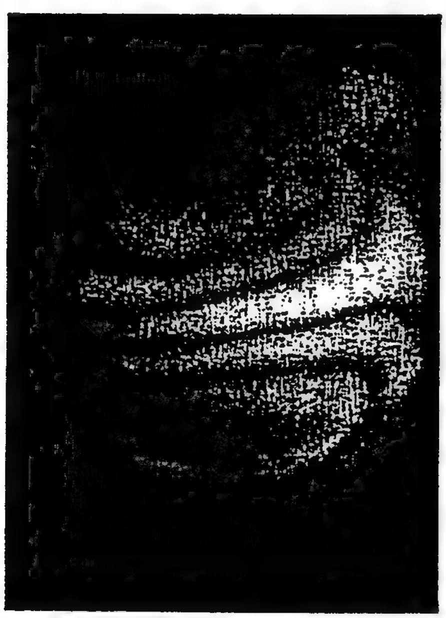

Piezoelectric membrane vibrating at 1 kHz

Two-wave mixing

Piezoelectric membrane vibrating at 9.2 kHz

ADVANCED INSTRUMENTATION AND MEASUREMENTS FOR EARLY
NDE OF DAMAGE / DEFECTS IN AGING AIRCRAFT
AFOSR-URI / NORTHWESTERN UNIVERSITY

TASK 4: DAMAGE DETECTION IN COMPOSITE MATERIALS

TASK LEADER: I.M. DANIEL

OBJECTIVES: THE OBJECTIVE OF THE PROPOSED TASK IS TO DEVELOP AND APPLY NONDESTRUCTIVE EVALUATION METHODS FOR DAMAGE DETECTION AND DAMAGE EVOLUTION IN COMPOSITE MATERIALS FOR THE PURPOSE OF DEVELOPING DAMAGE ACCUMULATION AND LIFE PREDICTION MODELS.

DELIVERABLES: TECHNIQUES FOR DETECTION AND CHARACTERIZATION OF MATRIX CRACKING, POROSITY, DELAMINATION AND FIBER/MATRIX DEBONDING IN COMPOSITE MATERIALS; REAL-TIME NDE TECHNIQUES FOR MONITORING DAMAGE EVOLUTION.

ULltrasonic Characterization of Matrix Cracking in Crossply Laminates

Material:	IM7/3501-6 carbon/epoxy.
Layup:	$[0/90_2]_s$ and $[0/90_4]_s$ crossply laminates.
Loading:	Monotonic uniaxial tension.
Measurements:	Stress-strain behavior. X-radiographs for crack density. Ultrasonic backscattered energy, wavespeeds, and attenuation. Monitoring of Acoustic Emission (AE)
Results:	Correlate ultrasonic and AE measurements with matrix cracks and degradation of material properties.

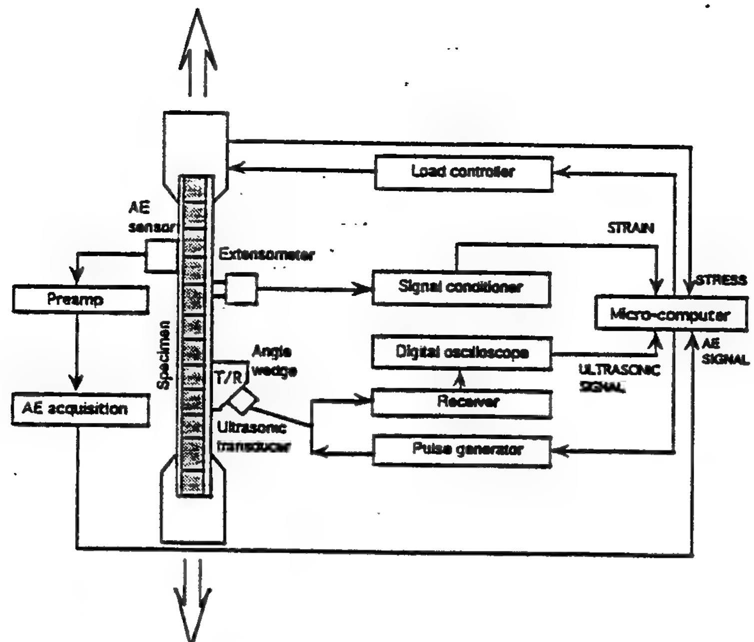

Fig. 1. Schematic diagram of system used for real-time monitoring of damage development in composite materials.

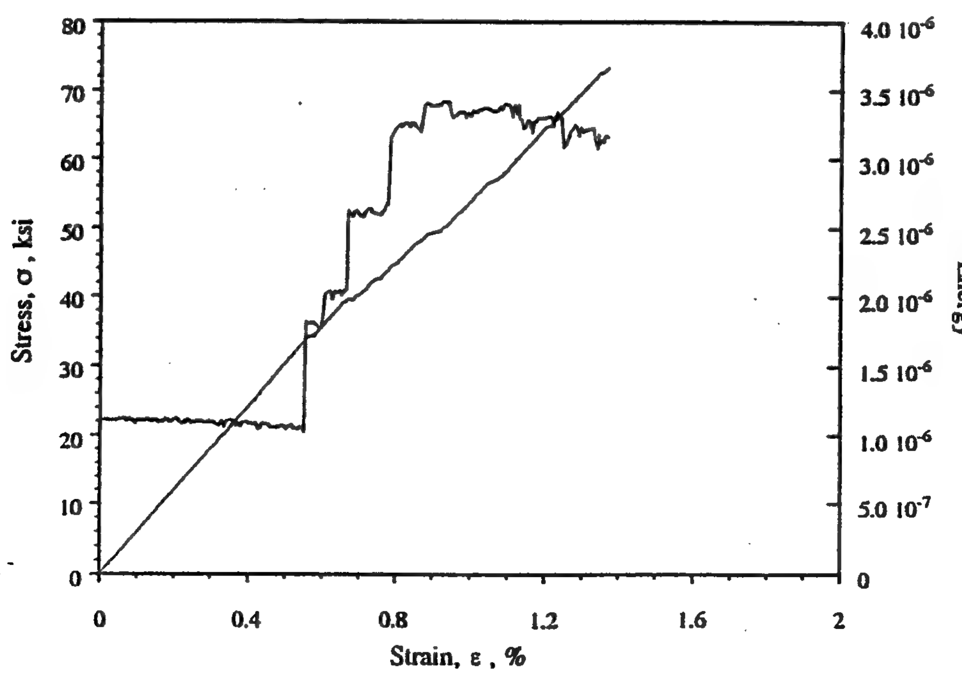

Stress-strain curve and ultrasonic back scattered energy as a function of applied strain.

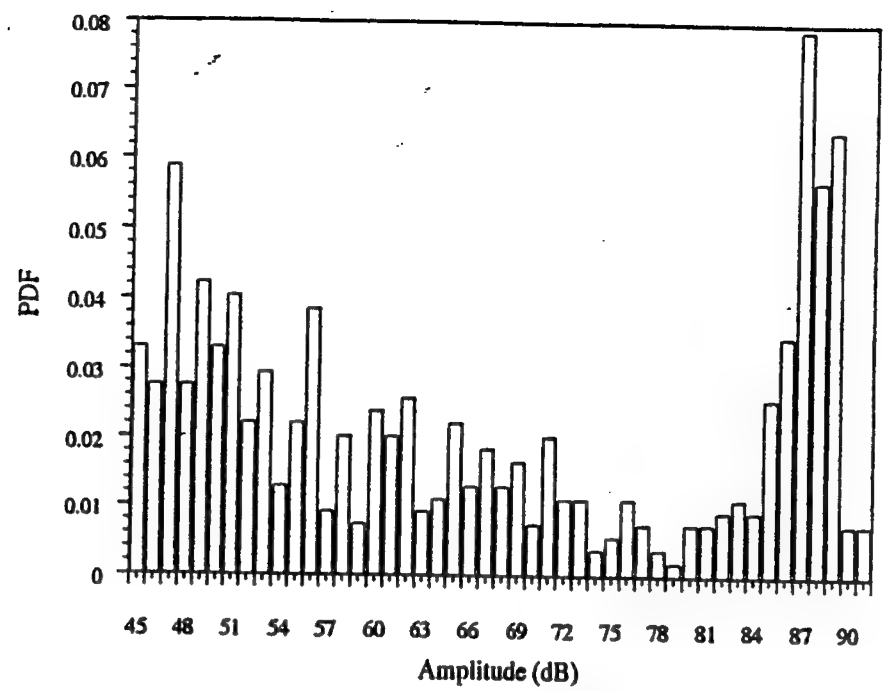

Histogram of AE events as a function of amplitude.

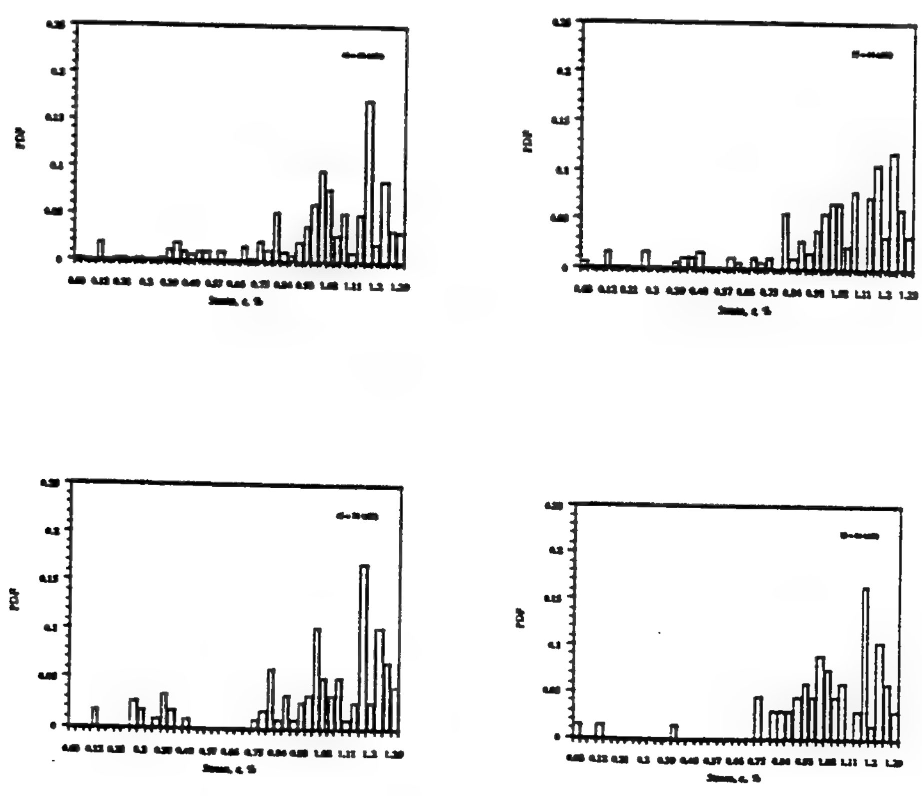

Fig. 4. Histograms of AE events for various amplitude ranges as a function of applied strain.

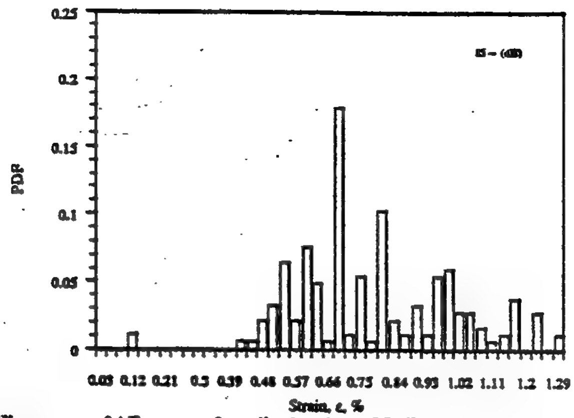

Fig. 5. Histograms of AE events of amplitudes above 85 dB as a function of applied strain.

Conclusions

- Ultrasonic backscattered energy is constant in the linear region of the stress-strain curve.
- Backscattered energy increases sharply in the matrix cracking region up to the crack saturation point.
- At the crack saturation point, the backscattered energy is stabilized or starts decreasing whereas the stress-strain behaves linearly.
- Matrix cracking produces primarily high amplitude (greater than 85 dB) AE signals.
- Low amplitude signals in large numbers are noticed in the last part of the stress-strain curve possibly associated with the failure mechanisms or internal friction.

LASER-BASED ULTRASONICS FOR QNDE

Schematic:

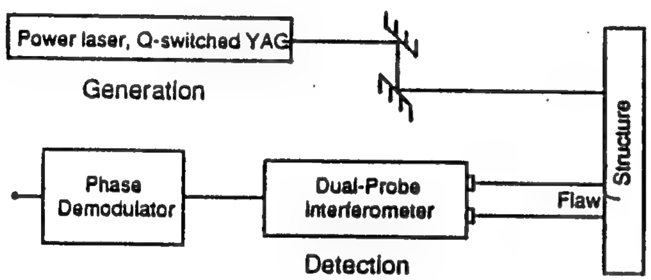

Applications Implemented:

- Characterization of Surface Roughness
- Evaluate Fatigue Damage
- Determine Material Anisotropy
- Measure Thin Film Elastic Constants
- Detect Cracks in Fuselage Panel
- Fiber Guided Remote Crack Detection

LASER-BASED ULTRASONIC INSPECTION

Principal Investigator: J. D. Achenbach

Research Associate: Jin Huang

OBJECTIVES

To exploit the advantages of laser-based ultrasonics for NDE of aircraft structures and engine components:

- Non Contact
- Point Generation and Detection
- Curved Surface Applicability
- Absolute Displacement Calibration
- Both Broad Band and Narrow Band Signal Generation
- Wide Frequency-Band Measurements
- Easy Scanning
- Remote Application by Use of Fiber Optics

The technique uses a laser to excite ultrasound and a single or dual-probe laser interferometer for the measurement of ultrasonic signals.

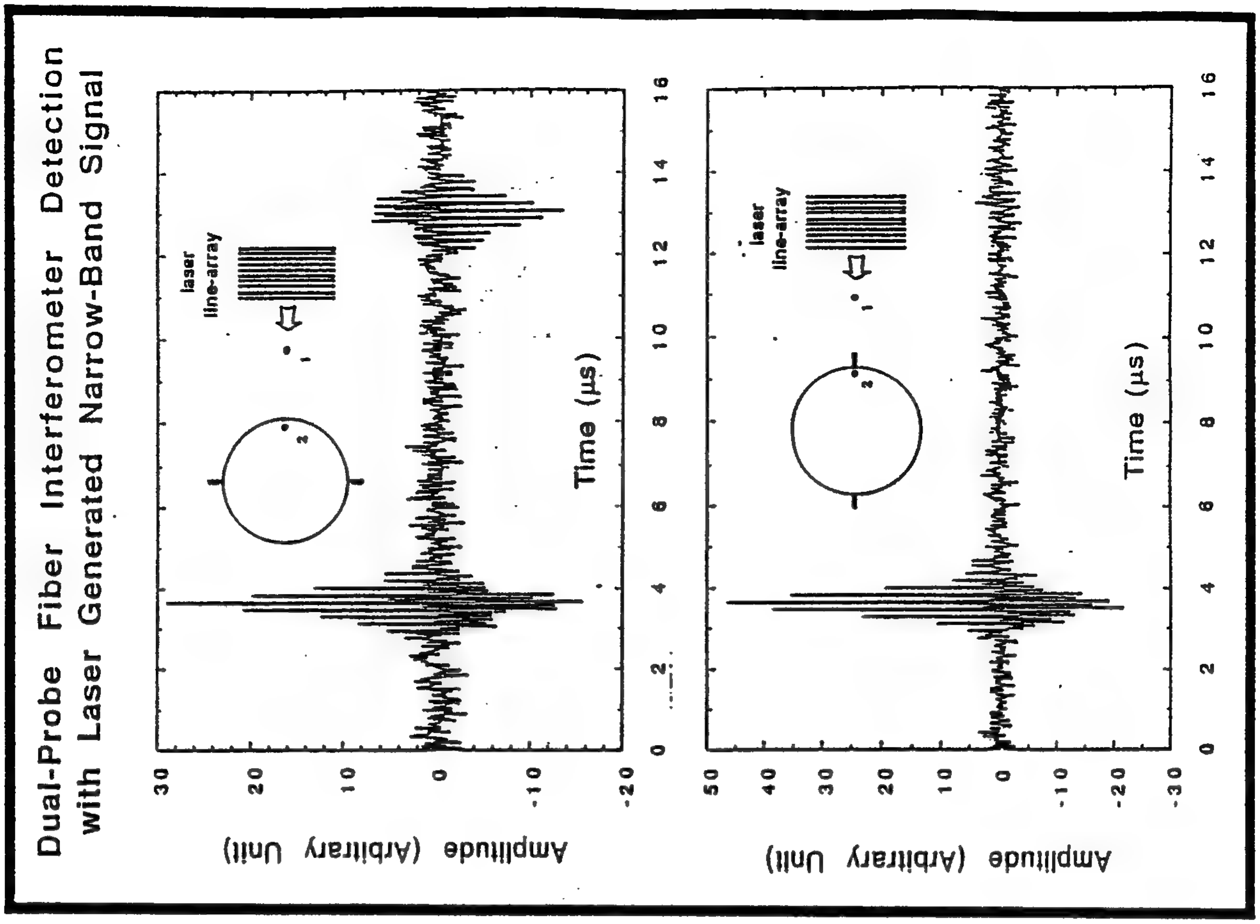

Dual-Probe Fiber Interferometer Detection
with Laser Generated Narrow-Band Signal
laser
line-array
Amplitude (Arbitrary Unit)
Time (µs)
30
20
10
0
-10
-20
50
40
30
20
10
0
-10
-20
-30
0
2
4
6
8
10
12
14
16

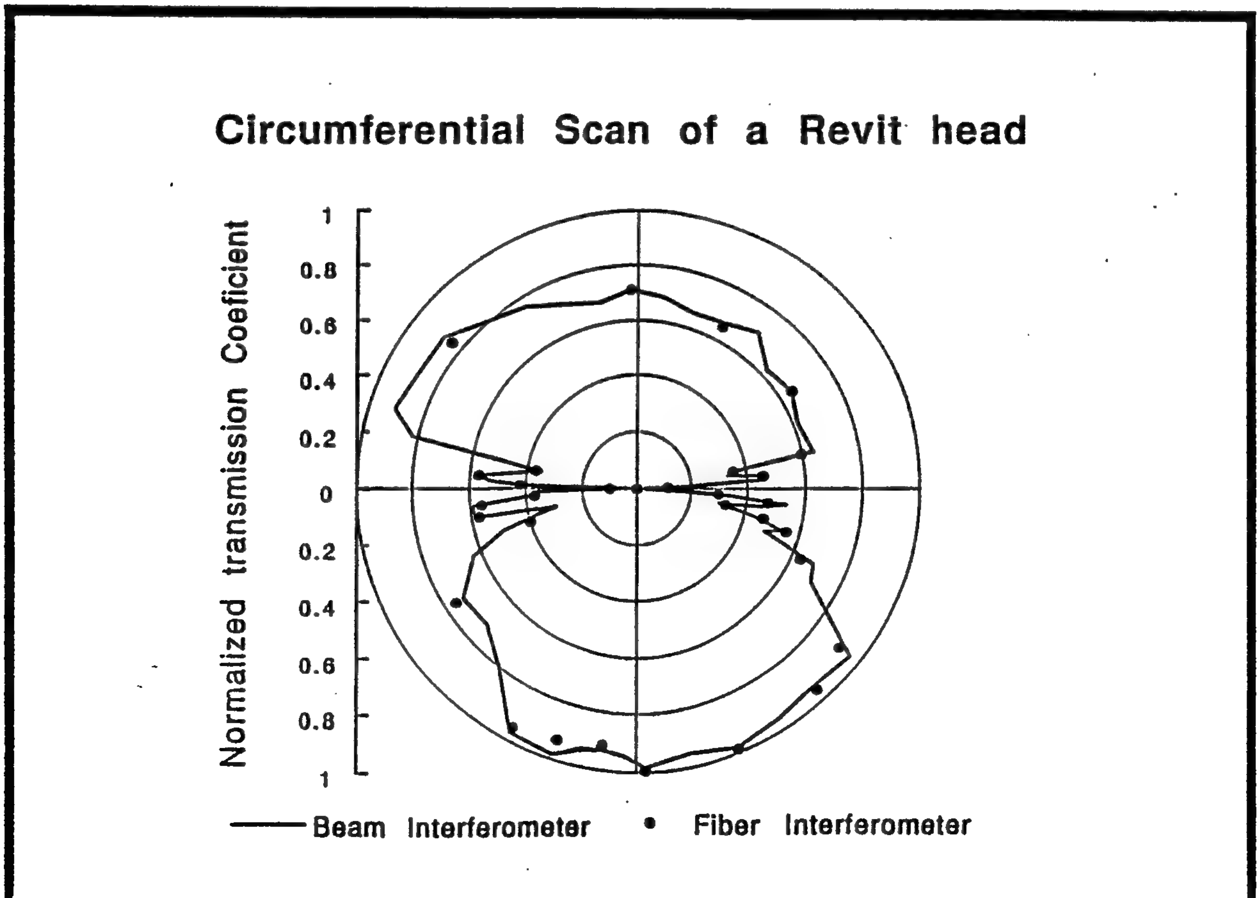

Circumferential Scan of a Revit head
Normalized transmission Coeficient
1
0.8
0.6
0.4
0.2
0
0.2
0.4
0.6
0.8
1
Beam Interferometer
Fiber Interferometer

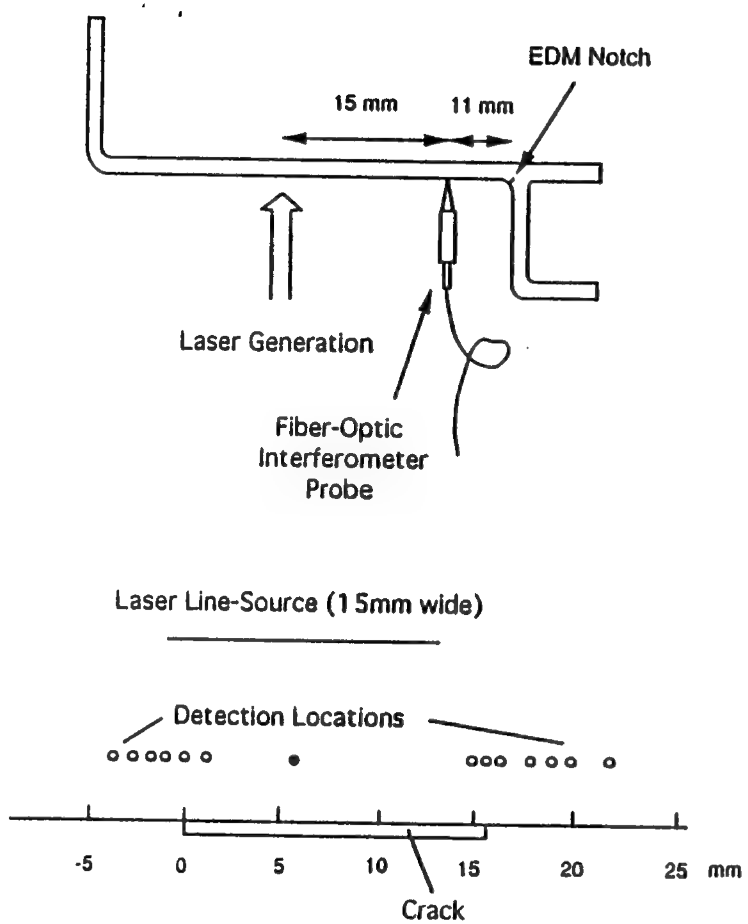
EDM Notch
15 mm
11 mm
Laser Generation
Fiber-Optic
Interferometer
Probe
Laser Line-Source (1 5mm wide)
Detection Locations
-5
0
5
10
15
20
25
mm
Crack

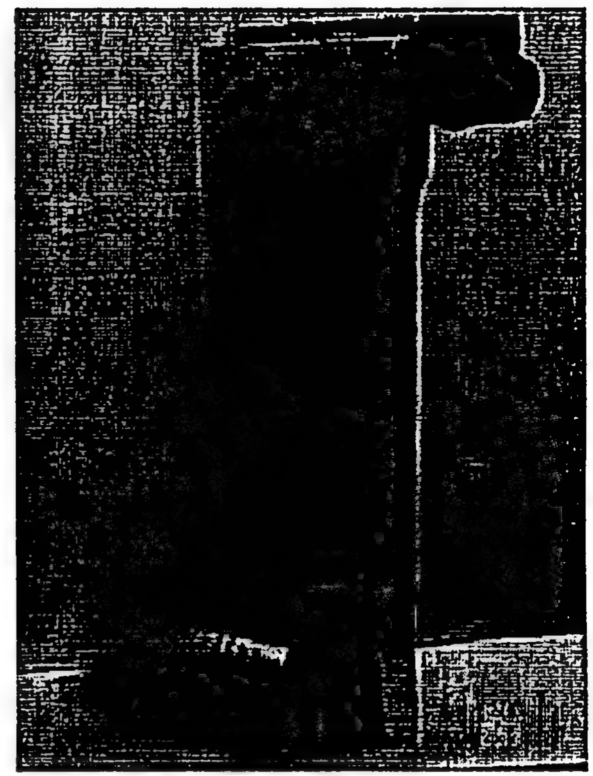

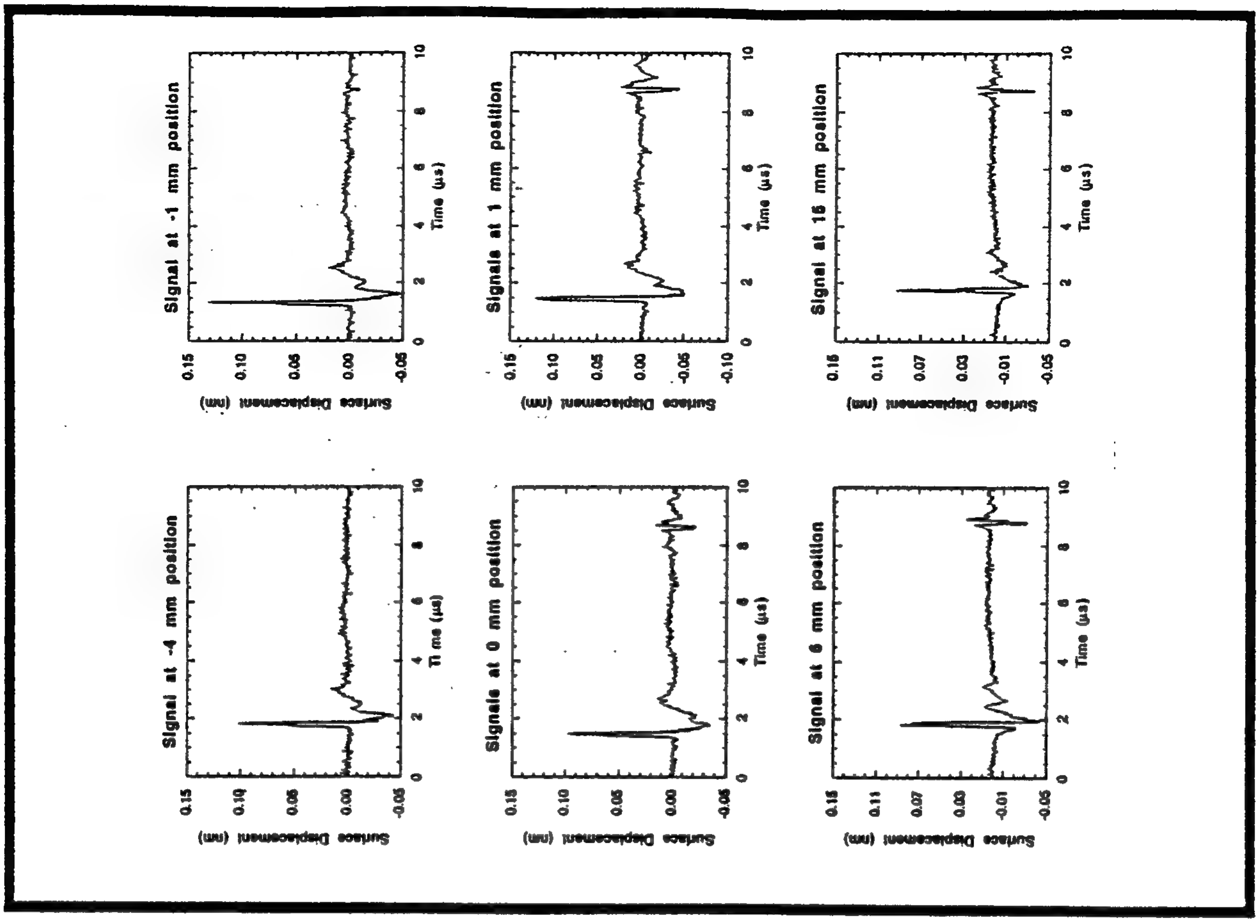
Signal at -1 mm position
Signals at 1 mm position
Signal at 15 mm position
Signal at -4 mm position
Signals at 0 mm position
Signal at 6 mm position
Time (μs)
Surface Displacement (nm)

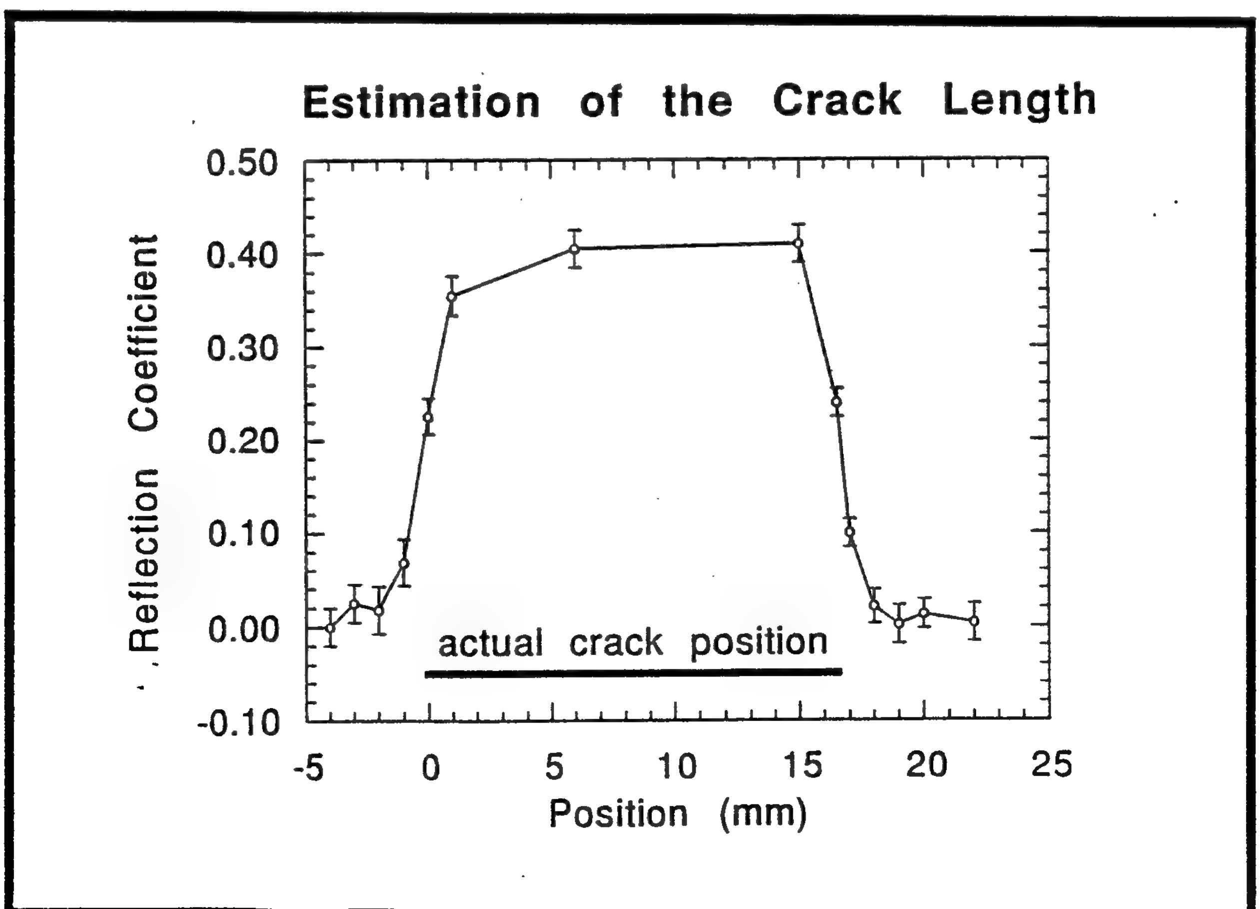
Estimation of the Crack Length
Reflection Coefficient
Position (mm)
actual crack position

TIME REVERSAL ARRAY

Detection and characterization of small flaws

Conventional focussed transducer :

The lateral position of the defect must be determined by scanning.

Fixed focal length of transducer limits the possibility of depth focussing on the defect

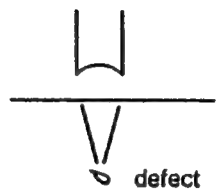

The <u>time-reversal array</u> is a technique for "<u>self-focussing</u>" by the defect.

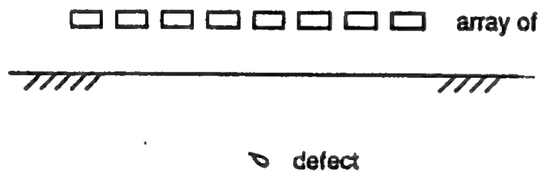

Step 1: Fire all transducers simultaneously. Generate an essentially plane pulse incident on the defect

Step 2: Defect generates a scattered wave.

Step 3: Transducers receive scattered wave with phase differences related to their positions.

Step 4: Received signals are stored, amplified and re-emitted with same phase differences but in inverse order of reception, i.e. last received signal is emitted first.

<u>Result</u> : a signal which is <u>focussed on the defect</u>

Step 5: Defect scatters self-focussed wave.

Step 6: Scattered signals are received by transducers and processed in usual manner for detection and classification.

SUMMARY OF MODALITIES

1. Laser-beam-in, Laser-beam interferometer out

2. Transducer-in, Laser-beam interferometer out

3. Laser-in, Fiberized interferometer out

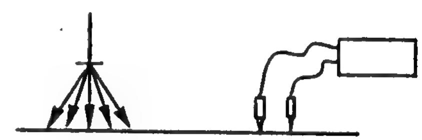

4. Transducer-in, Fiberized interferometer out

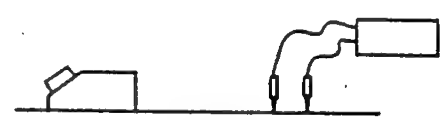

5. Laser-fiberized-in, Fiberized interferometer out

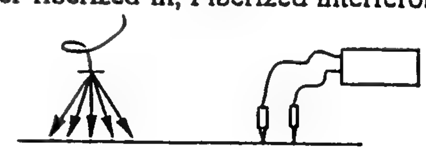

Option 4 Most Robust & Low Cost

Adaptive Time-Delay Technique

- Advantages
  - Compensates for Material Variations
  - Automatic Focusing on Largest Scatterer
  - Adaptive Focusing with Standard Hardware
- Procedure
  - Measure Reflected Signal from Scatterer
  - Calculate Time Delays with Cross-Correlation Algorithm
  - Reverse Time Delays and Excite Array Transducer

Adaptive Time-Delay Test Configuration

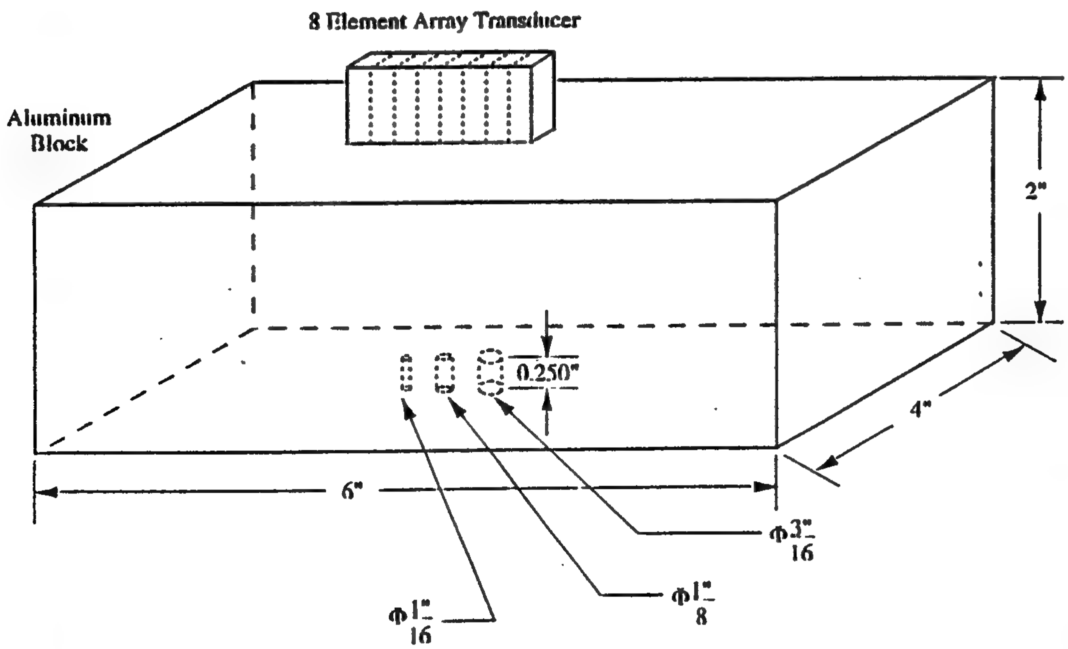

MEASUREMENT MODELS FOR QUANTITATIVE ULTRASONICS

PURPOSE: TO PREDICT FROM FIRST PRINCIPLES THE MEASUREMENT SYSTEM'S RESPONSE TO SPECIFIED ANOMALIES IN A GIVEN MATERIAL OR STRUCTURE

(CRACKS, VOIDS, DISTRIBUTED DAMAGE, CORROSION, ETC.)

REQUIRES CALCULATION OF :
- GENERATION
- PROPAGATION
- REFLECTION
- TRANSMISSION
- SCATTERING
- RECEPTION

OF ULTRASOUND

BENEFITS :

1. DESIGN AND OPTIMIZATION OF EFFICIENT TESTING CONFIGURATIONS
2. INTERPRETATION OF DATA
3. DETERMINE POD (PROBABILITY OF DETECTION)
4. IDENTIFY CHARACTERISTIC FEATURES, INVERSE PROBLEM
5. DEVELOP TRAINING SET FOR NEURAL NETWORK AND/OR KNOWLEDGE BASE FOR EXPERT SYSTEM

Reflected Signal
Unfocused

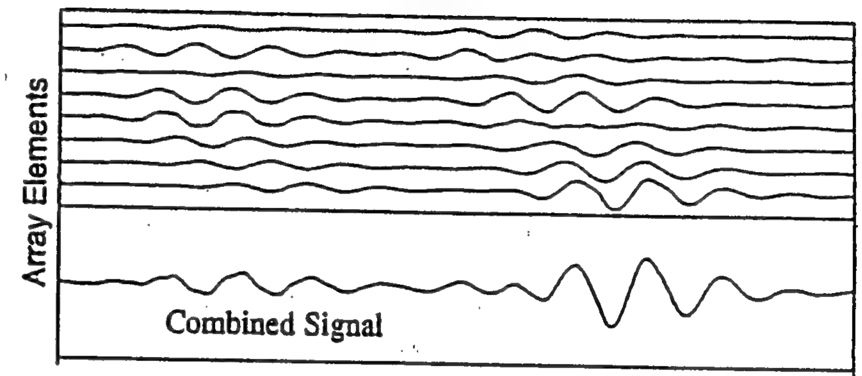

Reflected Signal
Focused

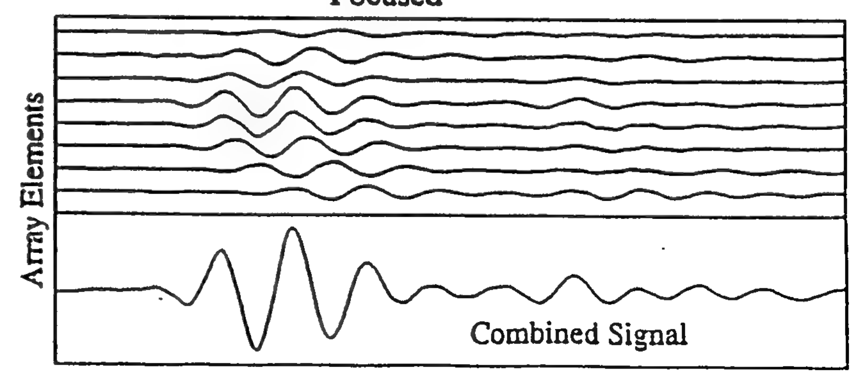

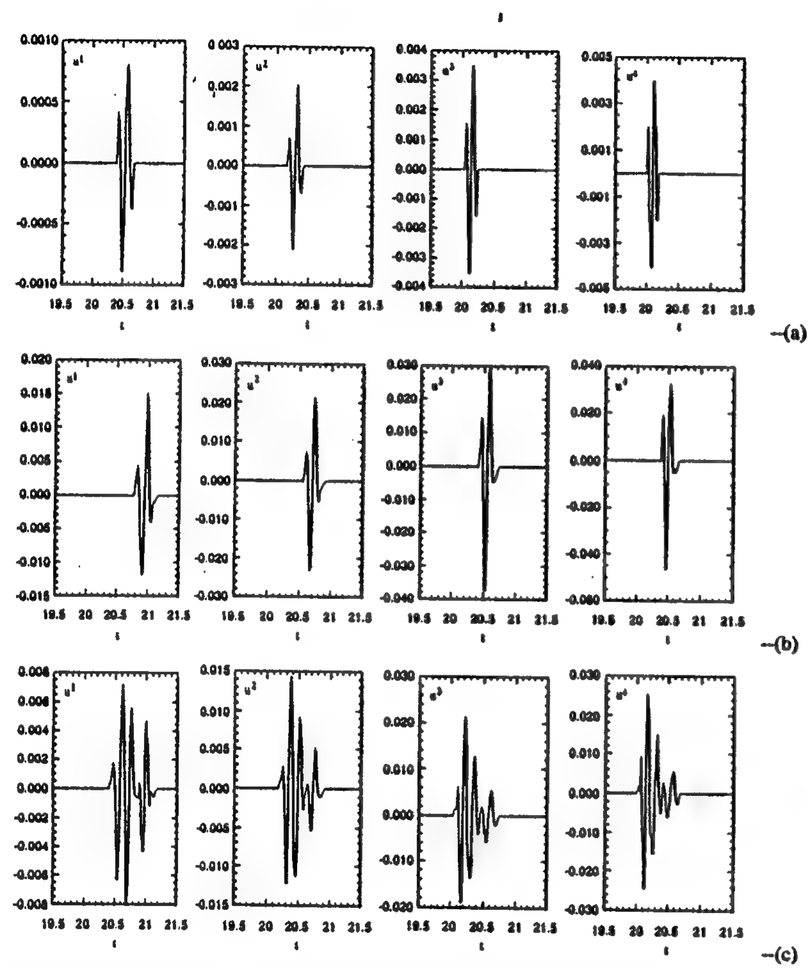

Fig. 3: (a) Reflected signal at transducers 1,2,3 and 4 when only transducer 4 is fired; (b) Reflected signals when transducers are fired with time delay; (c) Reflected signals when all transducers are fired simultaneously.

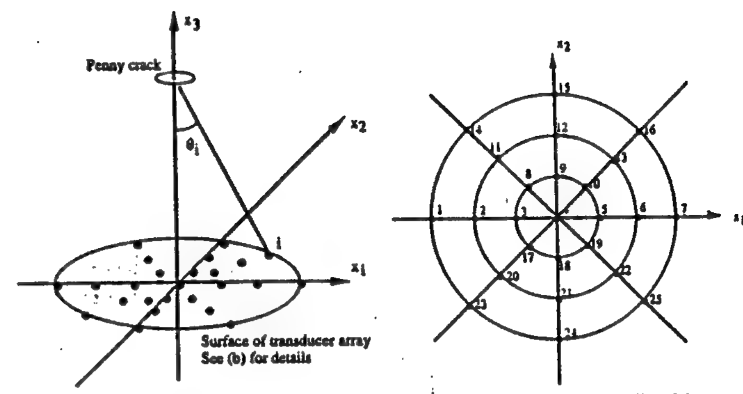

Fig.1: (a) Array of transducers and a penny-shaped crack; (b) Details of the array.

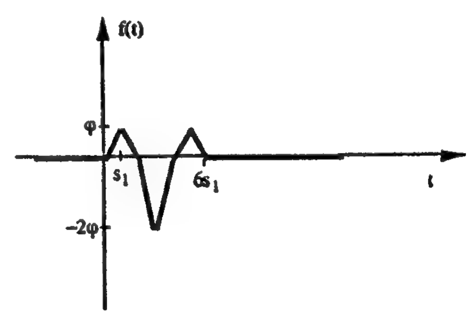

Fig. 2: Incident pulse

Philosophy

- Basic research to develop new instrumentation and to improve existing devices
- Fundamental studies on damage mechanisms
- Advanced measurement techniques
- Mathematical models
- Quantitative comparison of techniques
- Evaluation of capabilities and limitations
- Technology transfer

Quantitative NDE for Detection and Characterization of Hidden Corrosion

J. C. Moulder, J. H. Rose, and J. N. Gray

Center for NDE
Iowa State University
Ames, IA 50011

This work was supported in part by the AFOSR under Grant No. F49620-93-1-0439DEF.

Overview of Research Program

Task 1: Pulsed eddy-current detection of hidden corrosion in transport aircraft.

- Theory -- James H. Rose
- Experiment -- John C. Moulder

Task 2: X-ray energy-resolved backscatter technique for complex geometry in high performance aircraft

- Joseph N. Gray
- Terrence C. Jensen

X-ray Corrosion Detection and Characterization

- Sample Preparation and Characterization
- Backscatter Modeling
- Energy-Dispersive X-ray Backscatter Camera

Pulsed Eddy-Current Technique for Characterizing Hidden Corrosion

TOP PLATE THINNED

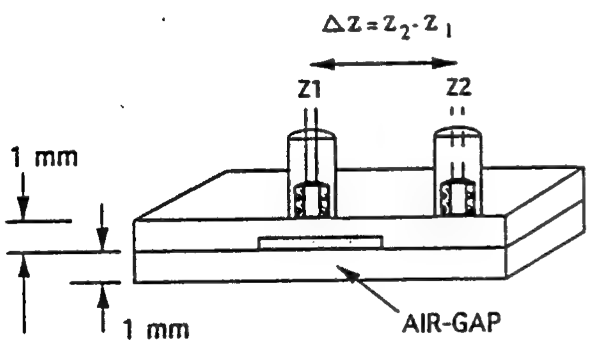

BOTTOM PLATE THINNED

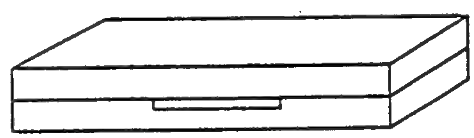

BOTH PLATES THINNED

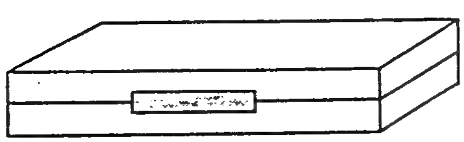

BOTTOM SURFACE THINNED

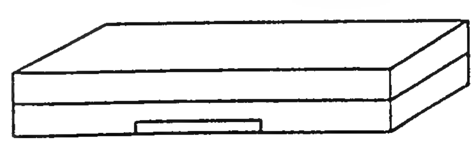

Dimensions of Drive Coil

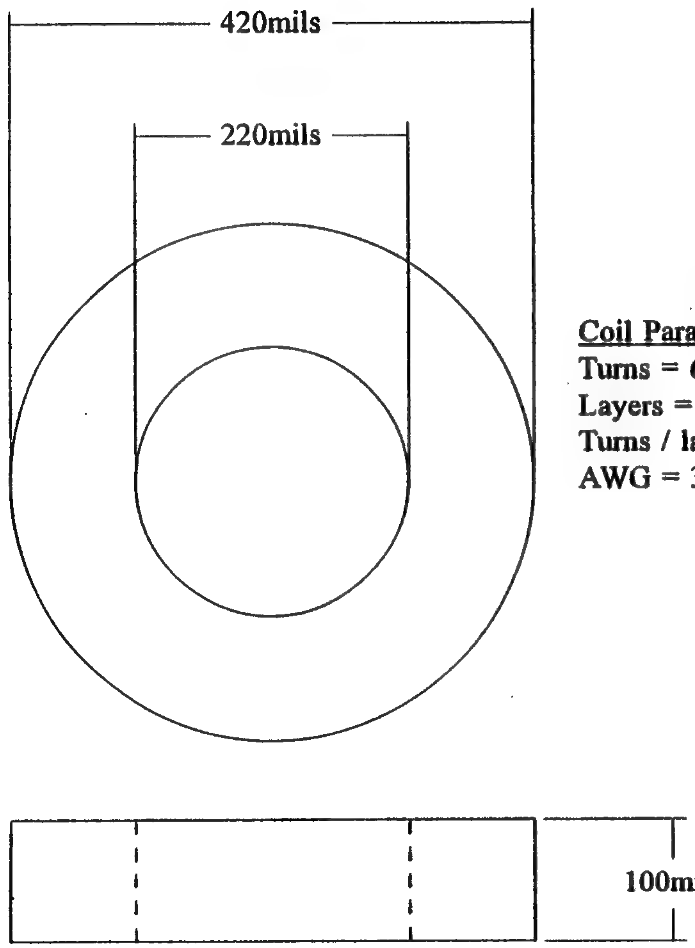

Coil Parameters
Turns = 638
Layers = 29
Turns / layer = 22
AWG = 39

Block Diagram of 16-Bit High Speed Pulsed Eddy Current Apparatus

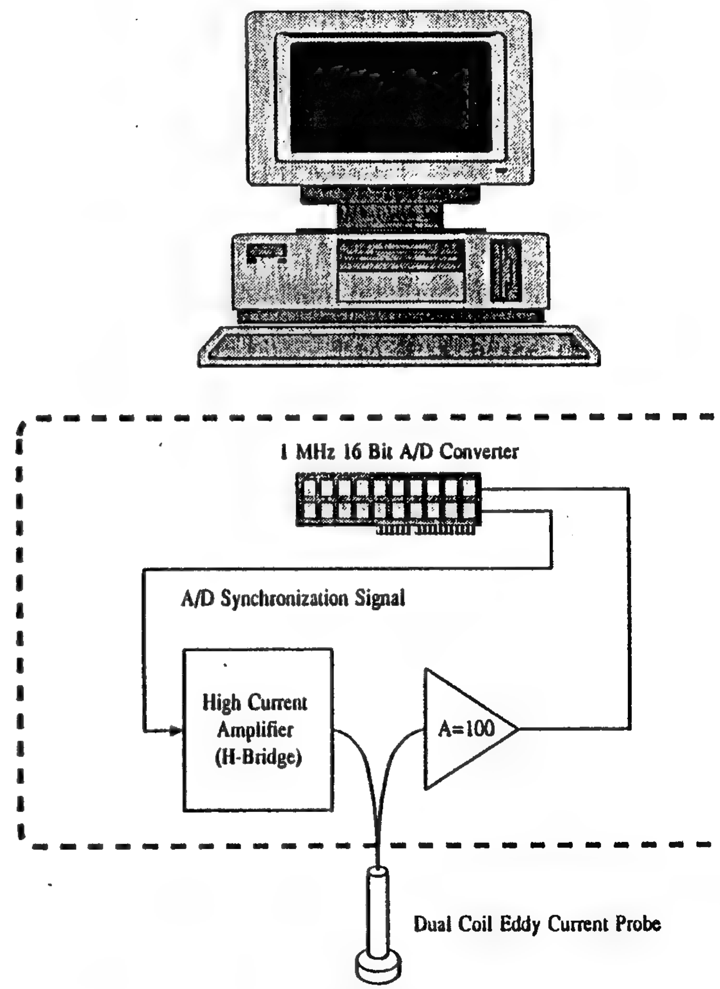

Example of Screen Image from Pulsed Eddy Current Instrument

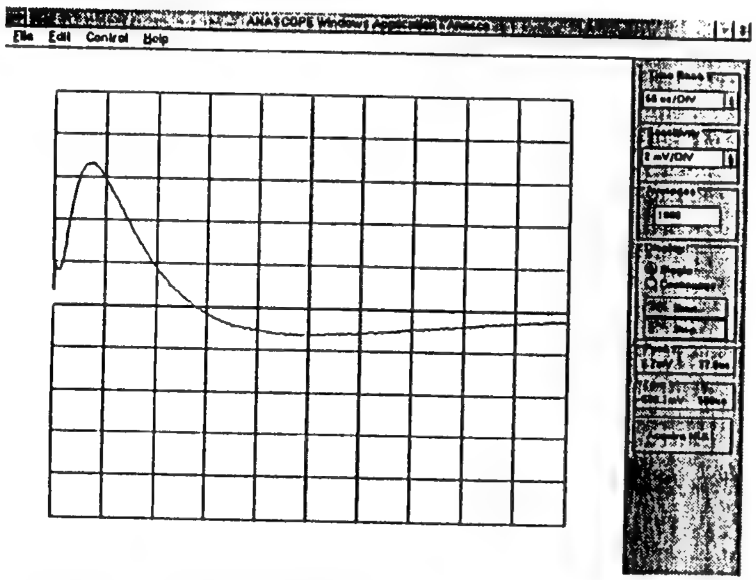

This captured computer screen shows a typical pulsed eddy current signal for 10% loss of metal in the bottom layer of a lap joint. The specimen consists of two 1-mm thick plates of 2024 aluminum, with a 0.1 mm flat bottomed hole machined in the bottom plate.

Dimensions of Receiver Coil

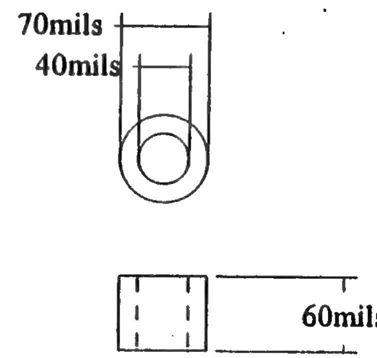

Coil Parameters
Turns = 60
Layers = 4
Turns / layer = 15
AWG = 39

Calculated Pulsed Eddy Current Signals Corrosion in Top Layer

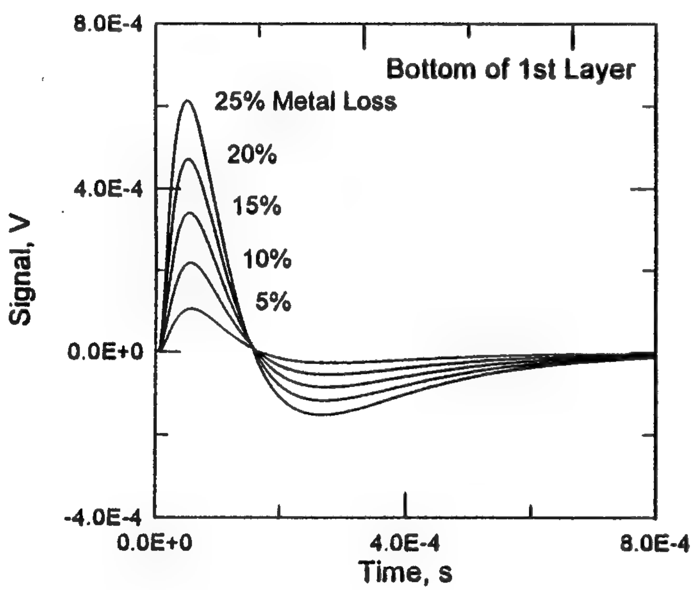

THEORETICAL CURRENT-VOLTAGE RESPONSE

Current, I, Response to Step-Function Voltage, V

$V(t) = V_o\, u(t)$ where $u(t) = 0$ for $t < 0$ and 1 for $t > 0$.

$$I(t) = \int_0^{\infty} dt'\, Y(t-t')V(t')$$

Here, Y(t) Denotes the Time-Domain Transform of Admittance

Solution Method:

- Maxwell's Equations
- Use Coulomb Gauge
- Neglect Displacement Current
- Solve in Frequency Domain
- Numerical FFT to Time-Domain

$$\Delta\vec{A}(\mathbf{r},t) = \mu_o\sigma(z)\frac{\partial\vec{A}(\mathbf{r},t)}{\partial t} + \mu_o\vec{J}_{ext}(\mathbf{r},t)$$

Solution for Piecewise Layered System -- Cheng, Dodd and Deeds

- Use Translational Symmetry - Reduce to a Set of ODE's
- Obtain Voltage and Impedance as Quadrature over ODE Solutions

Infer Frequency Domain Admittance as $Y(\omega) = 1/Z(\omega)$.

Finally, $$I(t) = \frac{V_o}{2\pi}\int_{-\infty}^{\infty} d\omega e^{-i\omega t}\frac{Y(\omega)}{i\omega}$$

Calculated Pulsed Eddy Current Signals

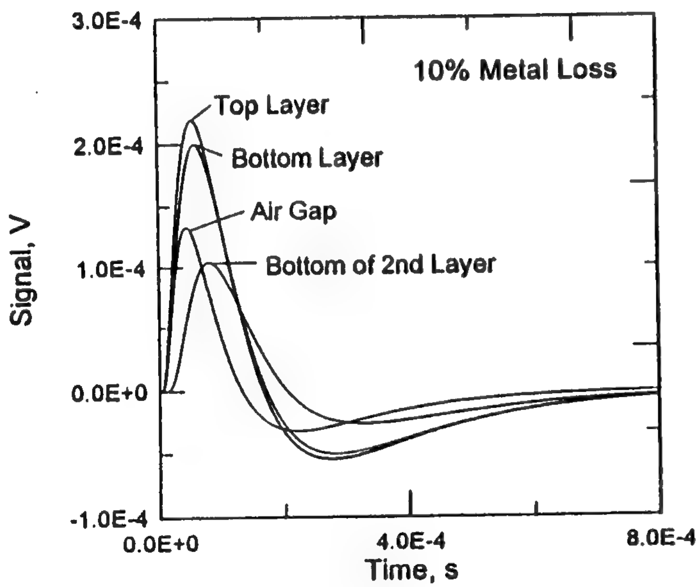

Calculated Pulsed Eddy Current Signals Corrosion in Bottom Layer

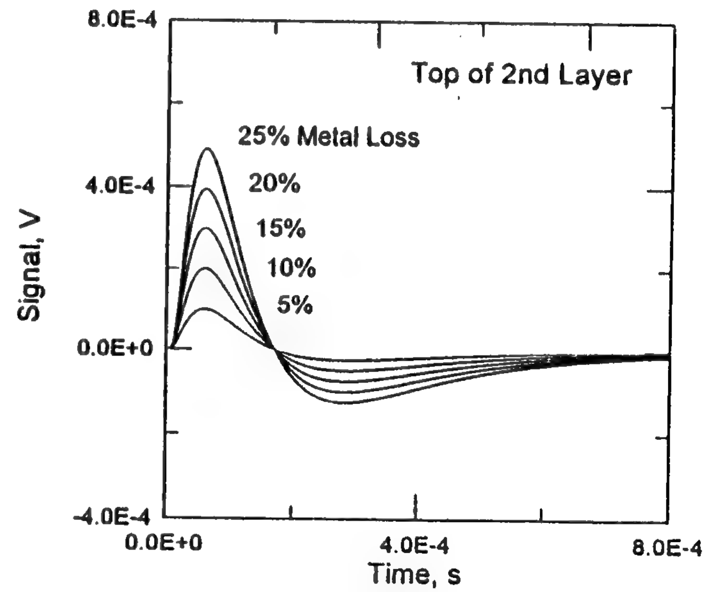

Pulsed Eddy Current Theory and Experiment

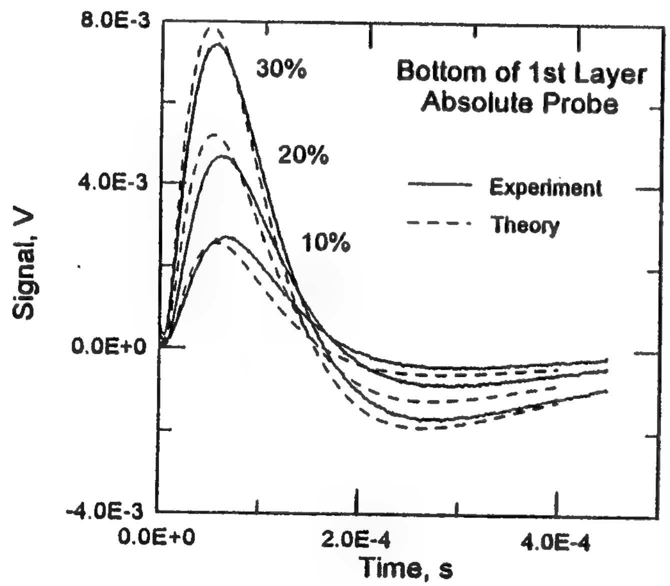

FREQUENCY-DOMAIN IMPEDANCE RESPONSE DUE TO PITTING

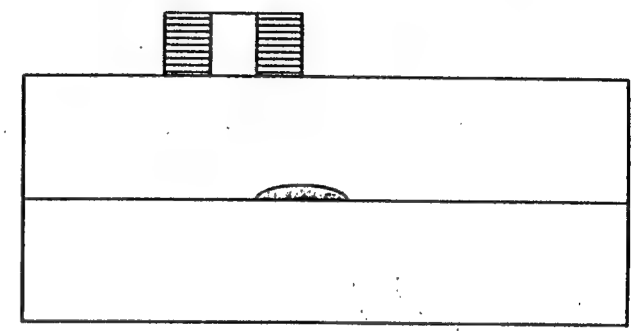

Use Auld's Reciprocity-Based Formalism to Find Change in Impedance Due to the Pit

$$\delta Z(\omega) = \frac{\sigma}{I^2} \int_{Flaw} d^3y \mathbf{E}(\omega, y) \cdot \mathbf{E}_o(\omega, y)$$

Here, E is the Electric Field with the Flaw Present
E_0 is the Electric Field with the Flaw Absent

Born Approximation (Exploratory)

Replace E by E_0.

$$\delta Z_B(\omega) = \frac{\sigma}{I^2} \int_{Flaw} d^3y \mathbf{E}_o(\omega, y) \cdot \mathbf{E}_o(\omega, y)$$

The Electric Field in the Absence of Flaw is Available from the Solution Method of Cheng, Dodd and Deeds

Calculational Method has been Completed.

Comparison with Experiment Anticipated in the Near Future.

Pulsed Eddy Current Theory and Experiment

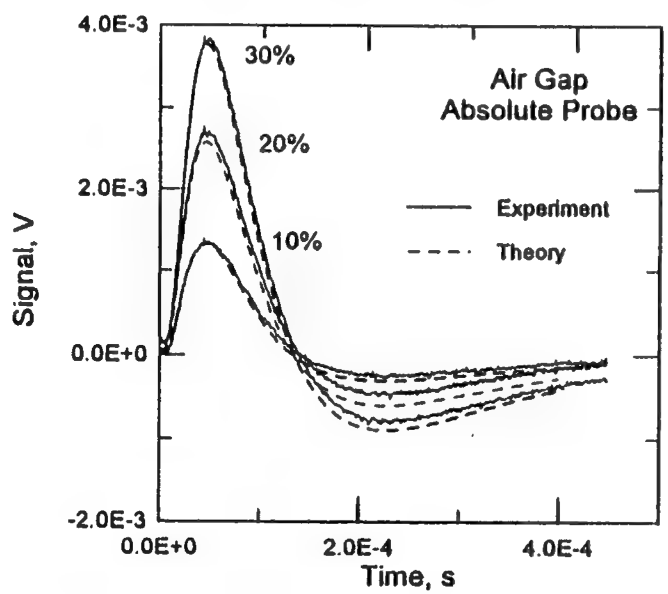

Pulsed Eddy Current Theory and Experiment

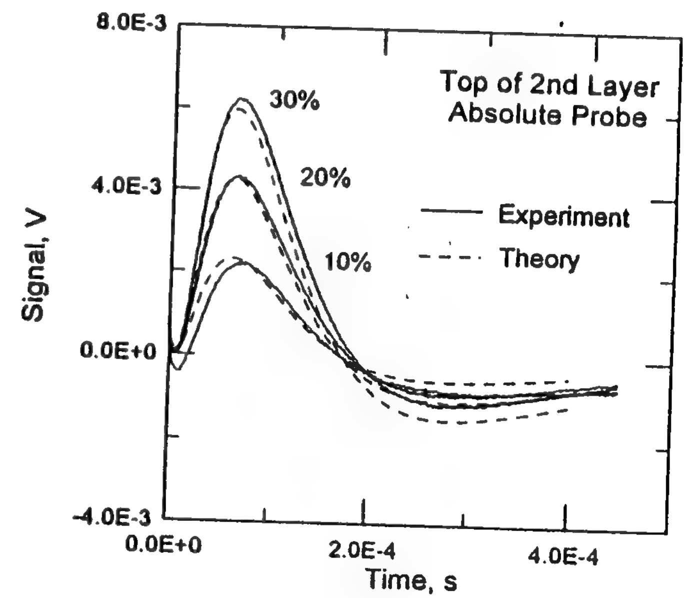

Plate Separation Compared to Simulated Corrosion (4 mils)

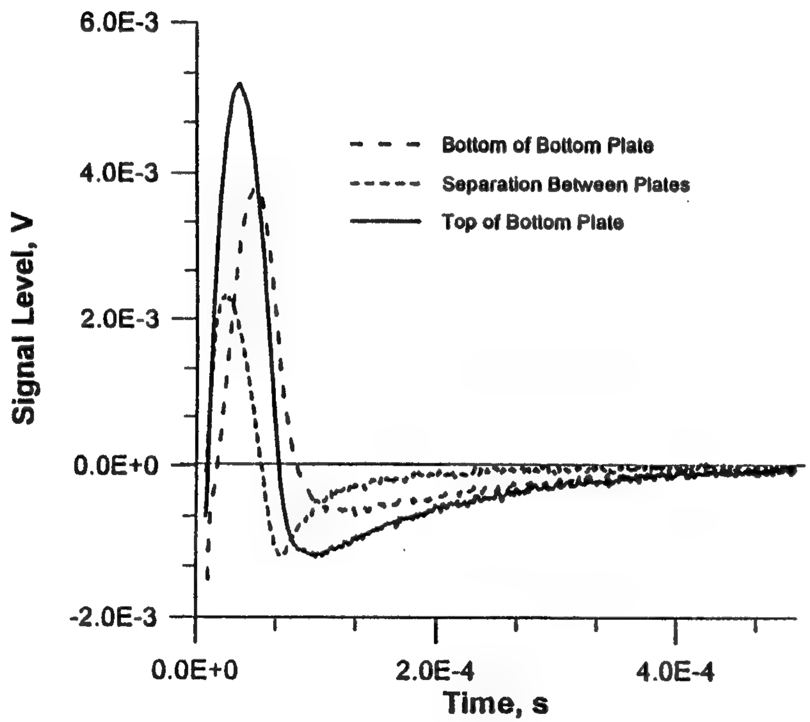

Penetration of Pulsed Eddy Currents through Multiple Layers

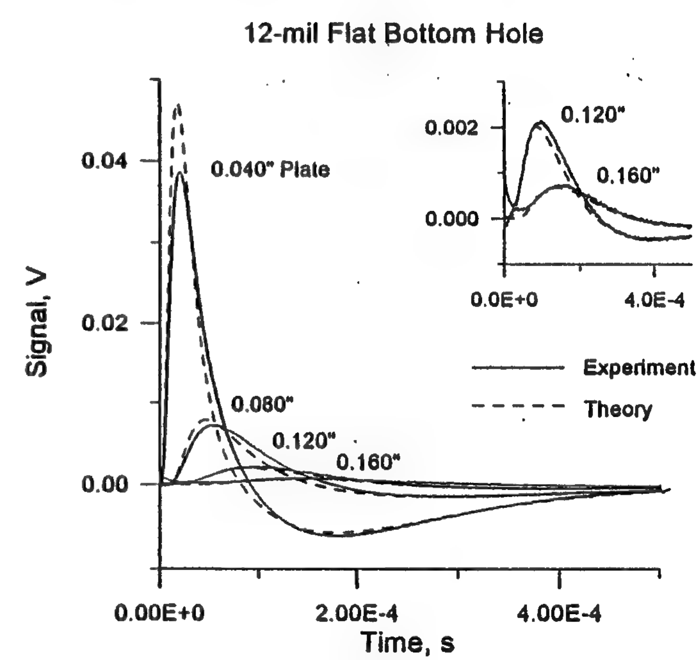

Summary

<u>Where are we?</u>

Demonstrated ability of pulsed eddy current to detect corrosion in aircraft panels (Boeing training specimens)

Demonstrated sensitivity to
- Corrosion in bottom plate
- Corrosion in top plate
- Separation of plates

Developed simple, relatively inexpensive prototype pulsed eddy current instrument (FAA funding)

Developed quantitative understanding and modeling tools for pulsed eddy current

Developed methodology to produce controlled test samples using in-house environmental corrosion chamber

Developed energy-dispersive x-ray backscatter model

Fabricated x-ray backscatter camera

Calculated Pulsed Eddy Current Signals

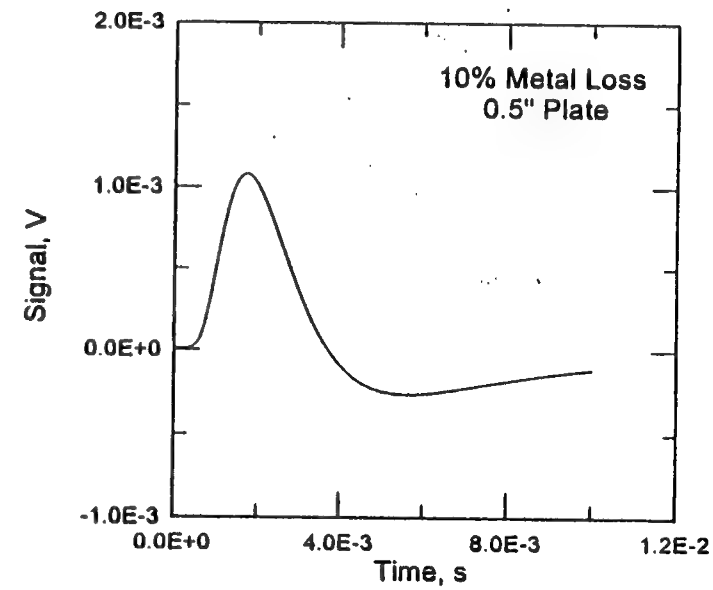

Directions in Year 2

Develop quantitative pulsed eddy current estimates for loss of metal in lap joints

Compare quantitative modeling and experiment for samples produced in corrosion chamber

Compare model and experiment for aircraft panels

Continue development of energy-dispersive x-ray backscatter camera and backscatter models

Nondestructive & Noncontact Evaluation of Corrosion and Fatigue of Aging Aircrafts by Laser Speckle and Moire

by

F.P. Chiang
Dept. of Mechanical Engineering
Lab. for Exp. Mech. Research
State University of New York
at Stony Brook
Stony Brook, NY 11794-2300
Tel: (516)632-8311
Fax: (516)632-8720

Optical NDE Techniques Used

1. ESPI (Electronic Speckle Pattern Interferometry)

2. LSS (Laser Speckle Sensor)

3. Speckle Correlation Method (Laser or White Light)

4. Moire and Projected Grating Methods with and without Phase shifting

Schematic of NDE of Aircraft Corrosion by Optical Methods

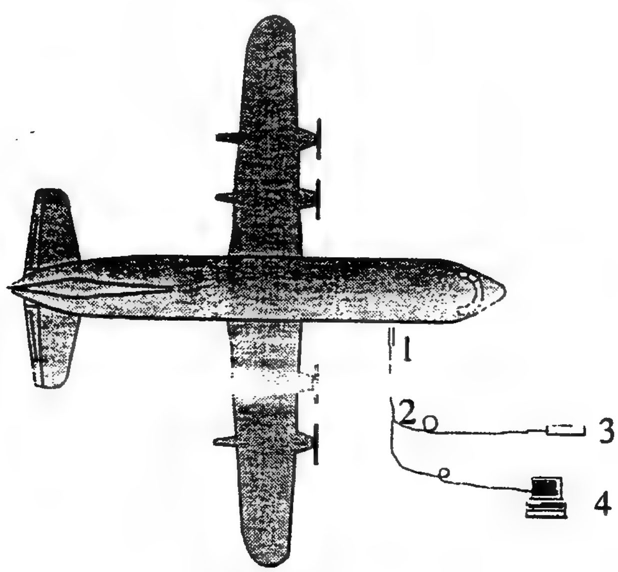

1. Robot arm with CCD camera and light source

2. Optical fiber and signal cable

3. Laser or white light 4. Image processing system

NDE by M... P... ... Grating Method: Resolution ... mm (with phase shifting).

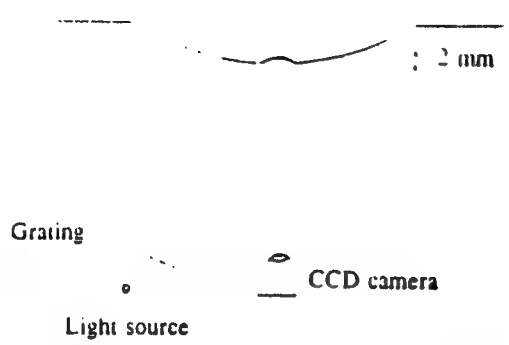

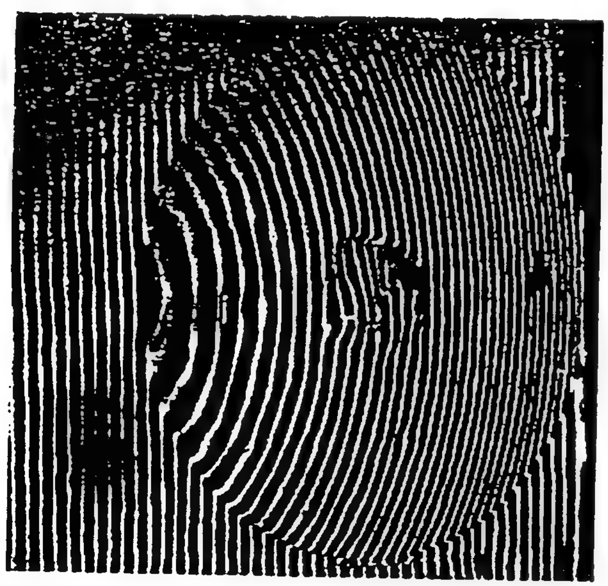

Projecttion Grating with Phase Shifting

In general, an interferometry fringe pattern can be expressed as:

$$I(x, Y) = I_0[1 + r \cos\phi(x,y)]$$

Where I(x, y) is the intensity of the interferogram, I_0 is the average intensity, r is a factor representing fringe contrast, and $\phi(x, y)$ is the phase difference, which in our case can be translated into surface height distribution.

When a phase shift is introduced into the original projected grating, the fringe pattern is also shifted the same amount. If three frames of intensity data are recorded with the phase shift of $2\pi/3$ between recordings, we have:

$$\phi = \arctan[(\sqrt{3} * (I_2 - I_1) / (2 * I_0 - I_1 - I_2))]$$

Ii (i=0,1,2) are three fringe image intensities with relative phase 0, $2\pi/3$, $4\pi/3$.

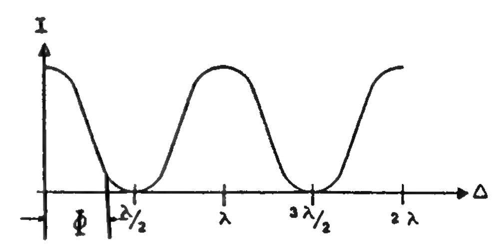

NDE by Moire (Projection Grating Method). Resolution: 1 mm.
Simulated filiform corrosion

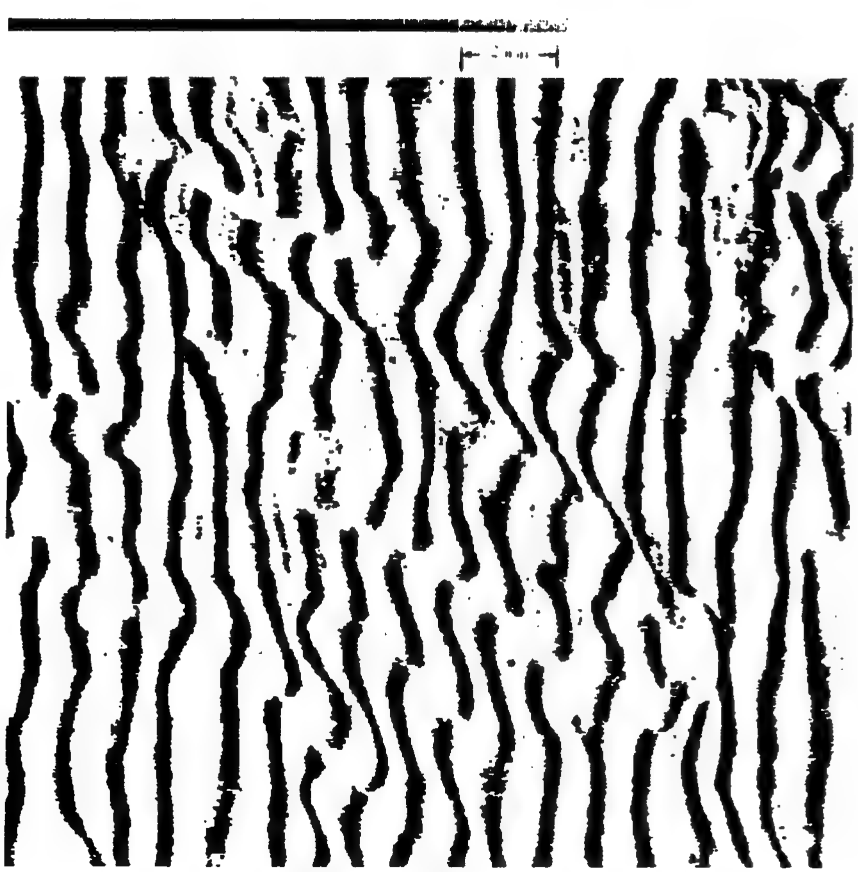

NDE by Moire (Projection Grating Method). Resolution: 1 mm.
Simulated pitting corrosion

contrast from 0 to 255

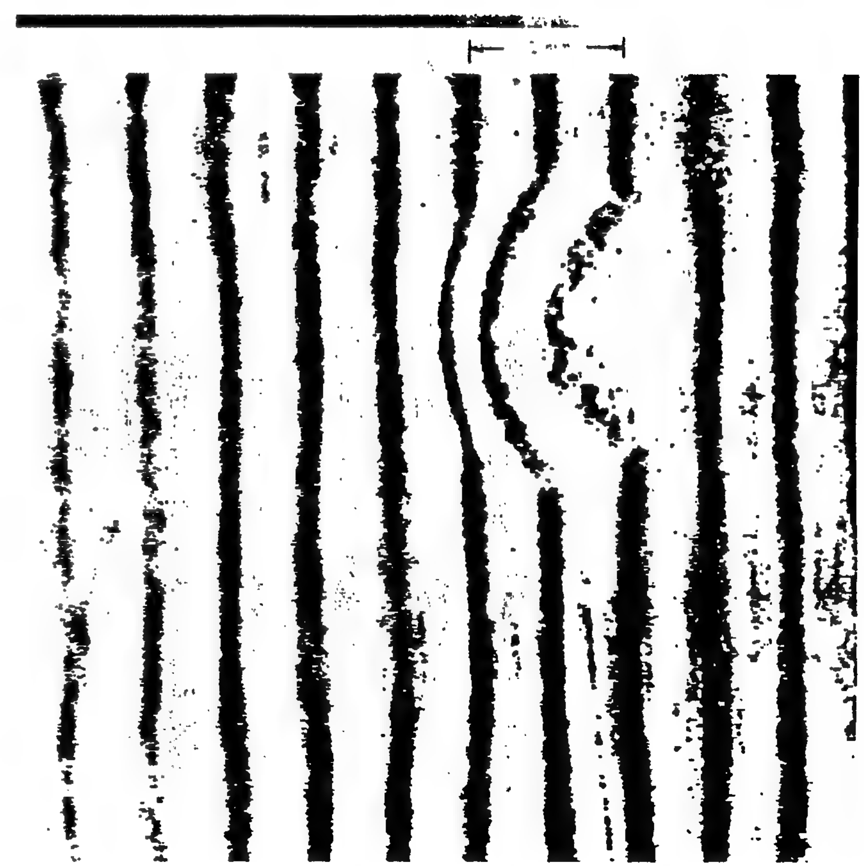

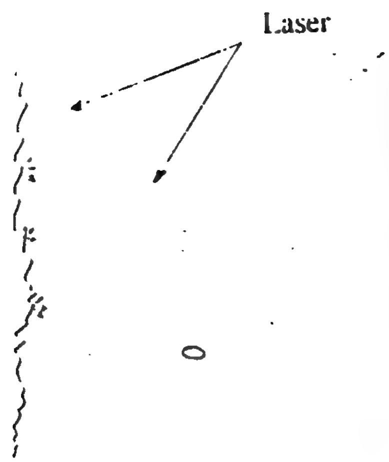

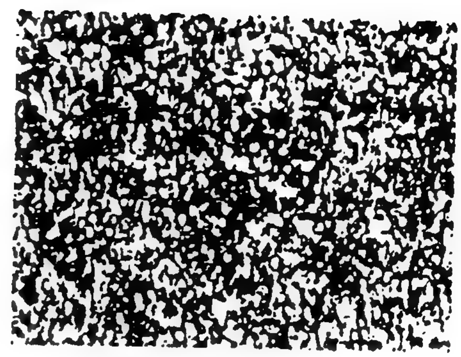

Laser Speckle Pattern

Principle of ESPI

Let $U1=u1*\exp(i\psi 1)$ and $U2=u2*\exp(i\psi 2)$ be the complex amplitudes of these wavefronts where u1, u2 and $\psi 1$, $\psi 2$ correspond respectively to the randomly varying amplitude and phase of the individual image plane speckles. The intensity of a given point in the image plane will be G1 where

$$G1 = I1 + I2 + 2\sqrt{I1I2}*\cos\Psi$$

and

$$I1 = U1U1^*$$
$$I2 = U2U2^*$$
$$\Psi = \psi 1 - \psi 2$$

when the object displaces, the intensity will change to G2 where

$$G2 = I1 + I2 + 2\sqrt{I1I2}\cos(\Psi + \Delta\phi)$$

$\Delta\phi$ is the resultant phase change.

By substraction of G1 and G2 ESPI fringe patterns are obtained:

$$G = G1 - G2 = 2\sqrt{I1I2}[\cos\Psi - \cos(\Psi + \Delta\phi)]$$
$$= 4\sqrt{I1I2}\sin(\Psi + 1/2\ \Delta\phi)\sin(1/2\ \Delta\phi)$$

Before being displayed on the monitor, G is rectified. The brightness at a given point in the monitor image is

$$B = 4K[I1I2\sin^2(\Psi + 1/2\ \Delta\phi)\sin^2(1/2\Delta\phi)]^{1/2}$$

where K is a constant.

If the brightness B is averaged along a line of constant $\Delta\phi$, we see that it varies between maximum and minimum values B_{max} and B_{min} given by

$$B_{max} = 2K\sqrt{I1I2},\ \Delta\phi = (2n + 1)\pi,\ n=0,1,2...$$
$$B_{min} = 0,\ \Delta\phi = 2n\pi,\ n=0,1,2...$$

Configuration for Electronic Speckle Pattern Interferometry
(out-plane displacement measurement)

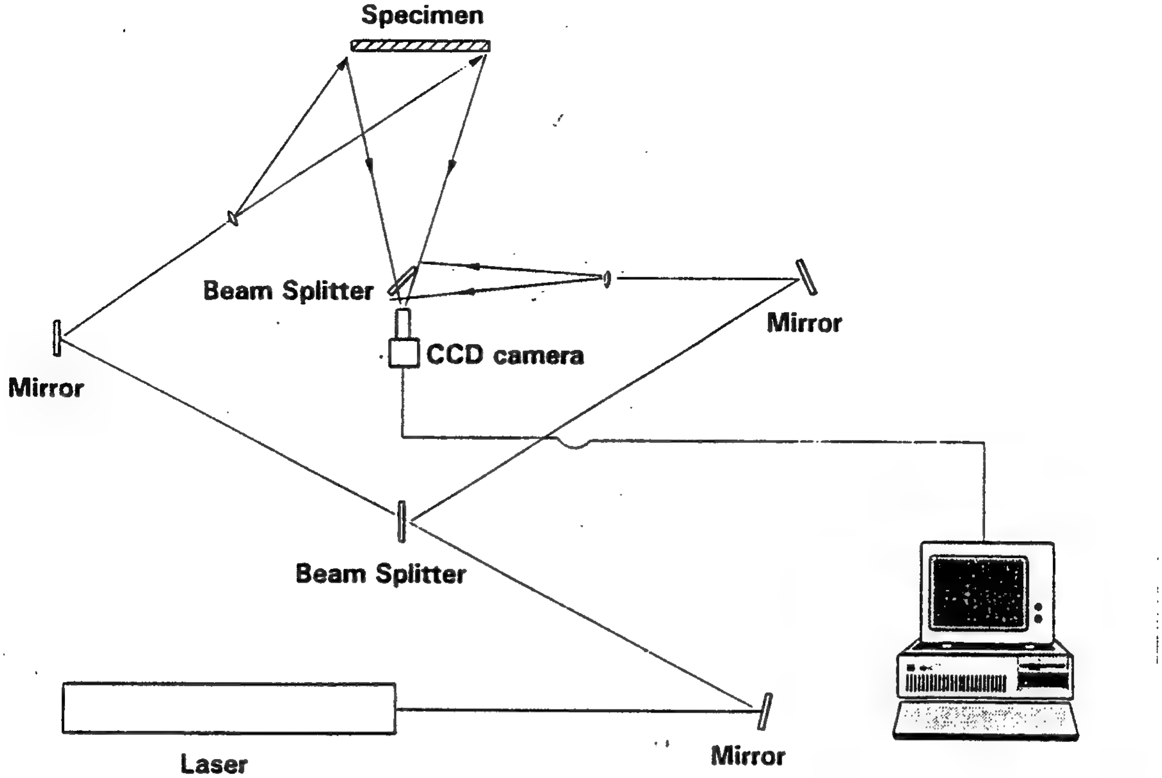

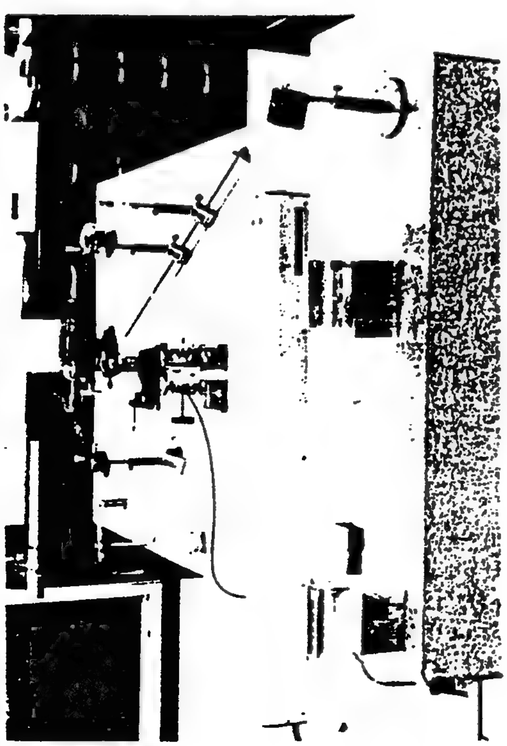

Optical Setup for ESPI

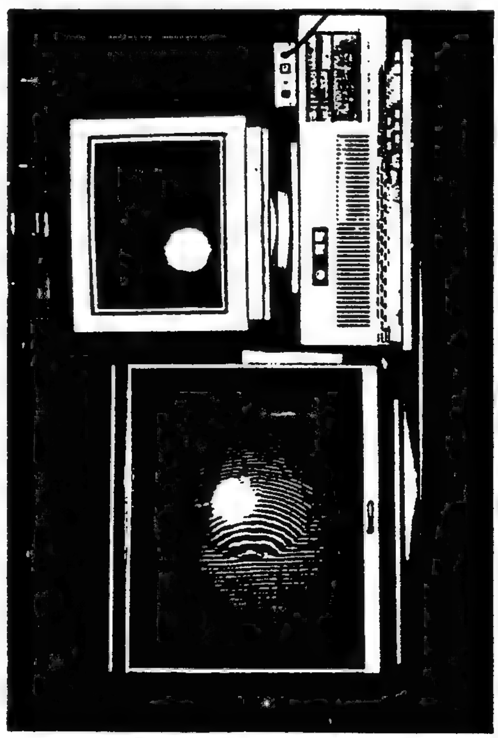

Image Processing System

Configuration for Electronic Speckle Pattern Interferometry
(in-plane displacement measurement)

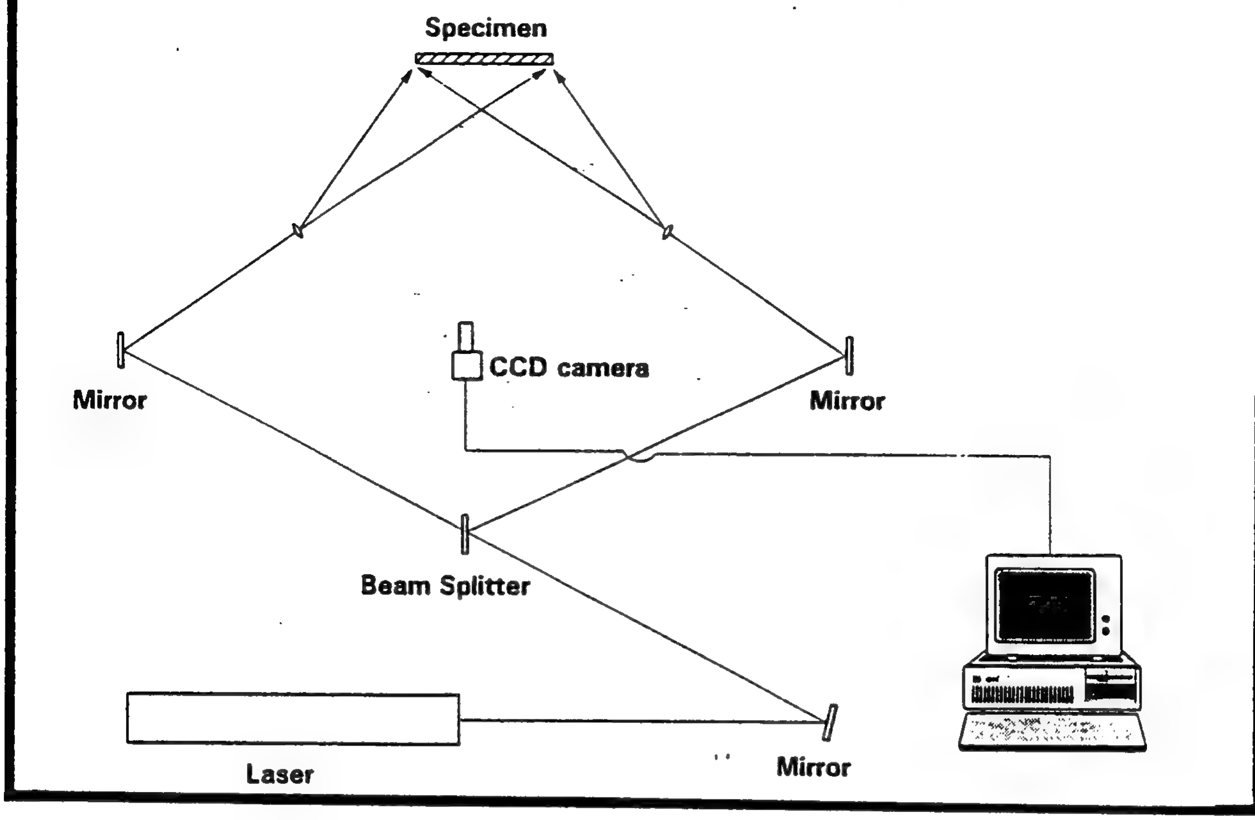

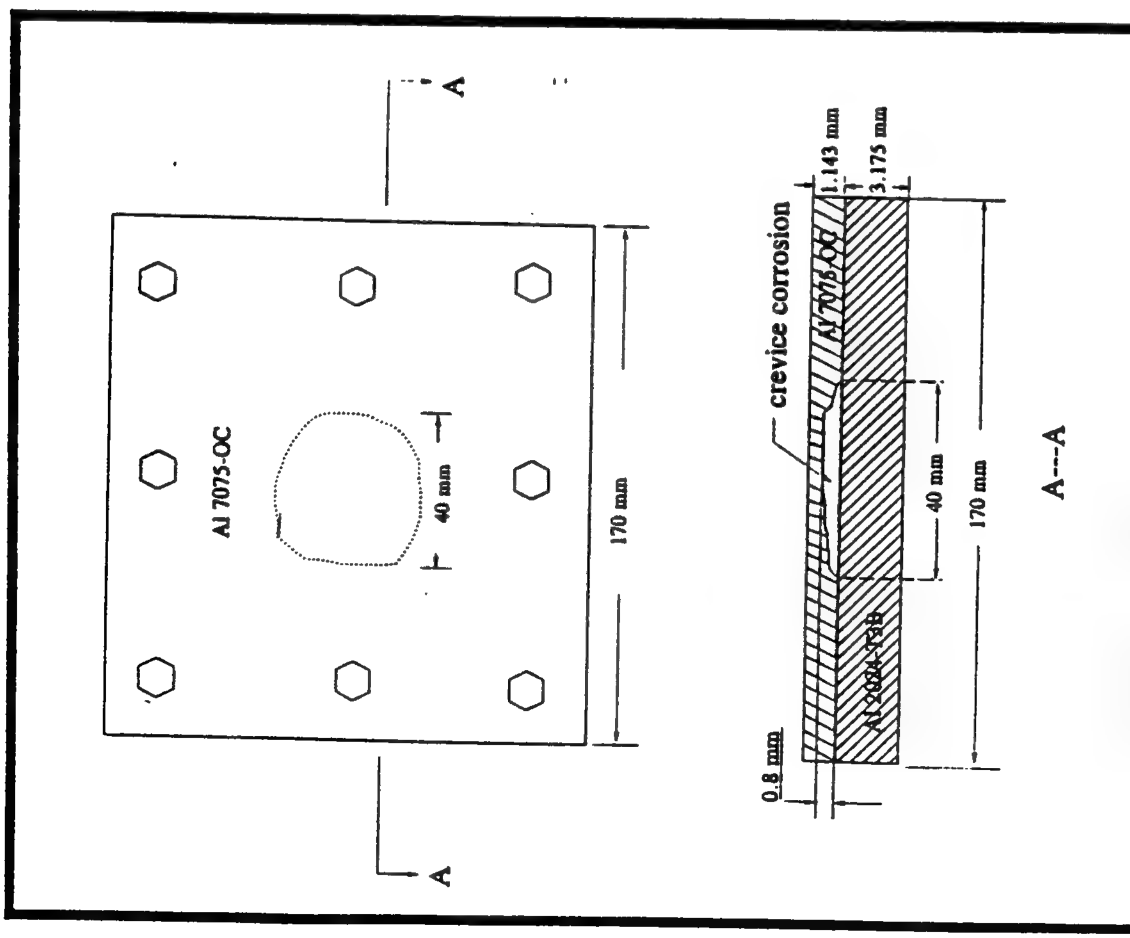

Schematic for specimen I with crevice corrosion

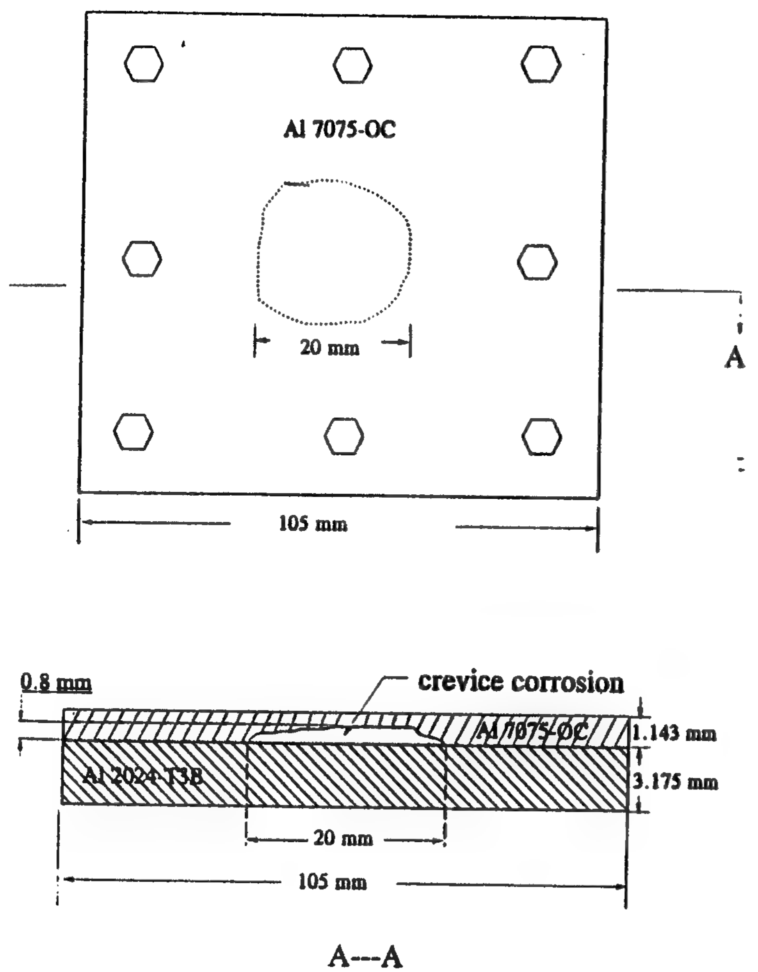

Schematic for specimen II with crevice corrosion

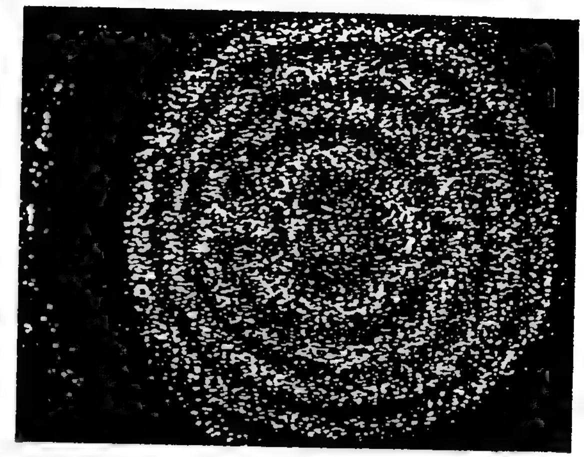

Fringe pattern of ESPI (with vacuum loading) clearly reveals the existence of crevice corrosion. Fringe Eq. : W = N * λ/2 , here W: out-plane displacement; N: fringe order; λ : laser wave length 0.6 μ.

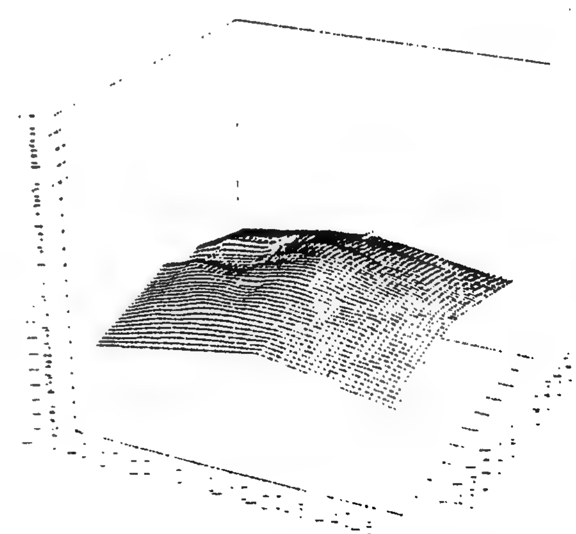

3D view of the out-plane deformation field

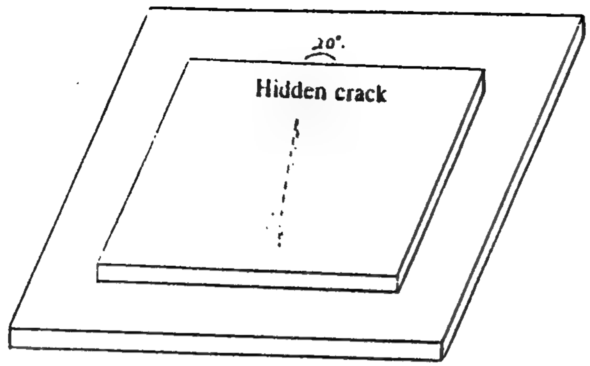

Schematic of the specimen with a hidden crack

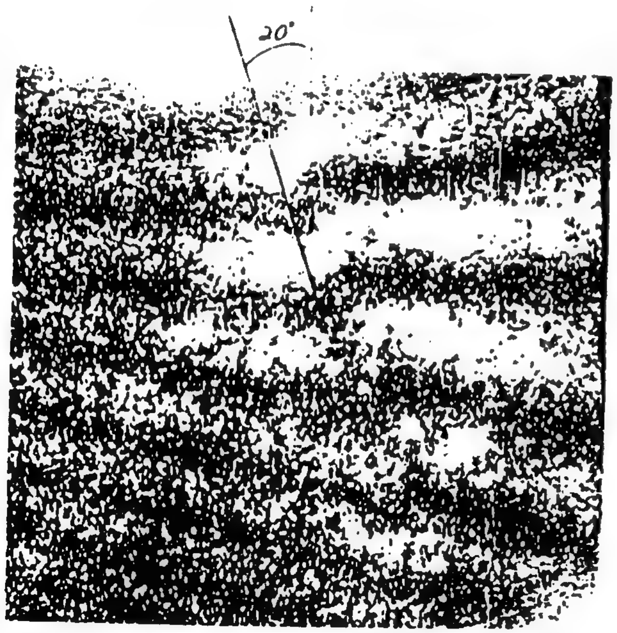

NDE by ESPI (in-plane deformation). Hidden defects are revealed as sudden slope change of fringes upon small temperature variation of the structure.

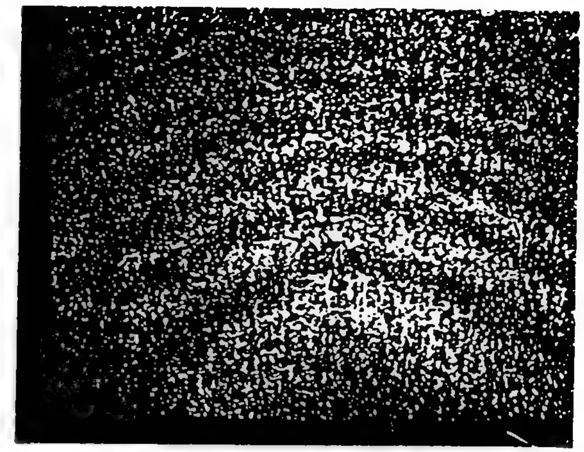

(a) without crevice corrosion

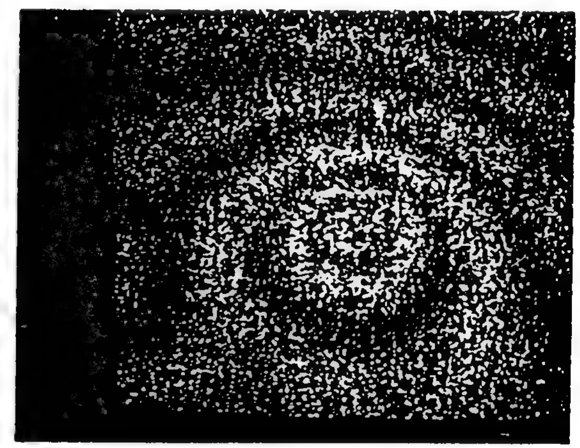

(b) with crevice corrosion

NDE by ESPI for specimen II (with thermal loading).
Each fringe represents out-plane deformation of $\lambda/2 = 0.3\ \mu m$.

NDE by ESPI

. Resolution of ESPI
Out-plane or in -plane displacement: 0.3μ

. Heat-loading by air gun

Power:1250 w/2
Heating duration: 1 ~ 3 sec
Temperature rising ΔT: 2 ~ 4 °c

. Vacuum loading : 0 ~ 25 in Hg

NDE by Correlation Method

. Cross-correlation is used to detect surface defects caused by corrosion and fatigue. The defects are revealed by significant change of correlation coefficient defined by

$$C(x=0,\ y=0) = \frac{\sum_{i=1}^{n}\sum_{j=1}^{m} f_{x+i,y+j}\, g_{i,j}}{\sqrt{\sum_{i=1}^{n}\sum_{j=1}^{m} f_{x+i,y+j}^{2} \sum_{i=1}^{n}\sum_{j=1}^{m} g_{i,j}^{2}}}$$

where: f, g are the images for calculation.

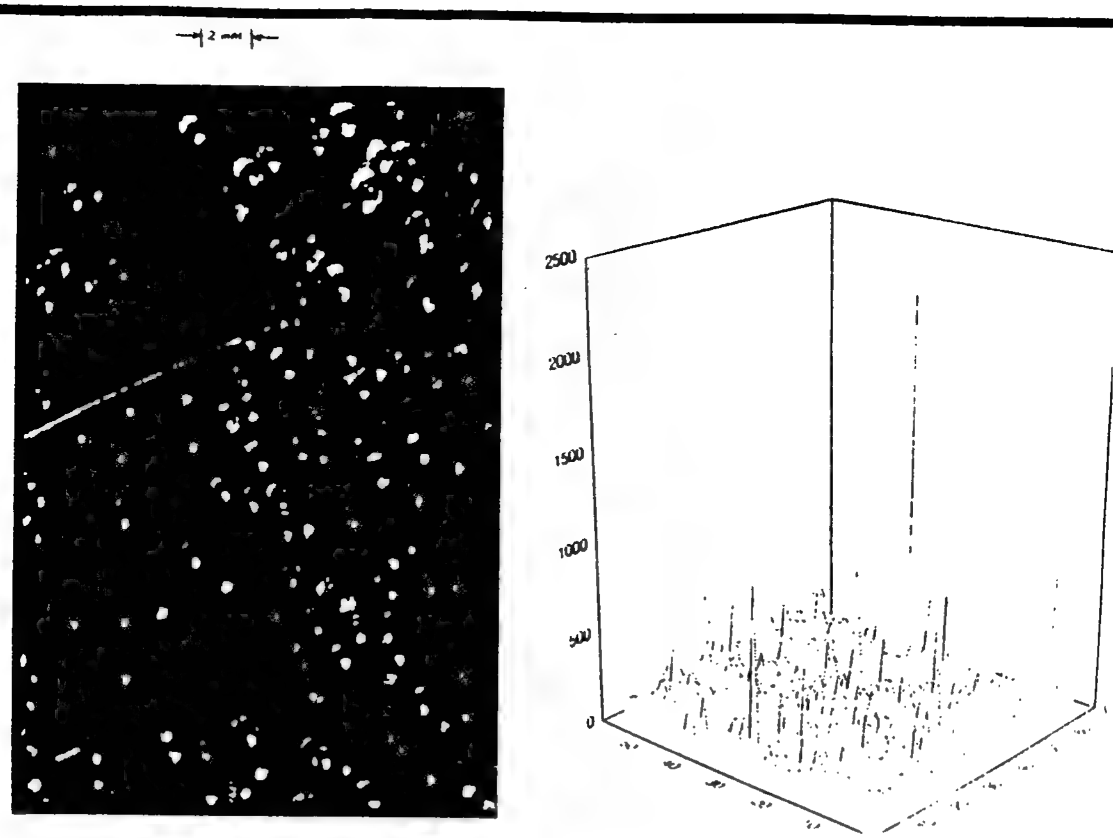

NDE by Correlation Method. Simulated pitting corrosion

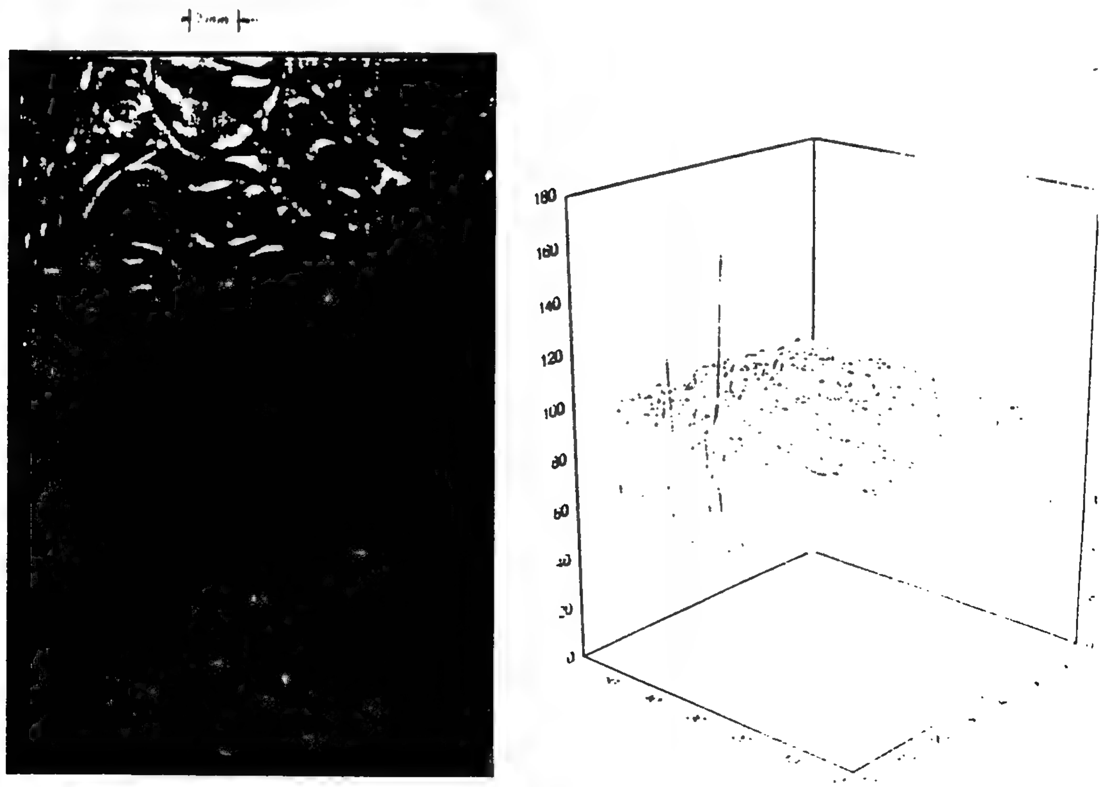

NDE by Correlation Method. Simulated filiform corrosion

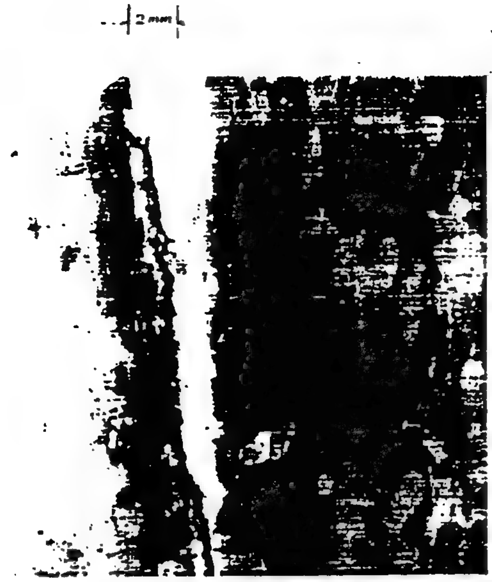

Aluminum specimen with a existing crack

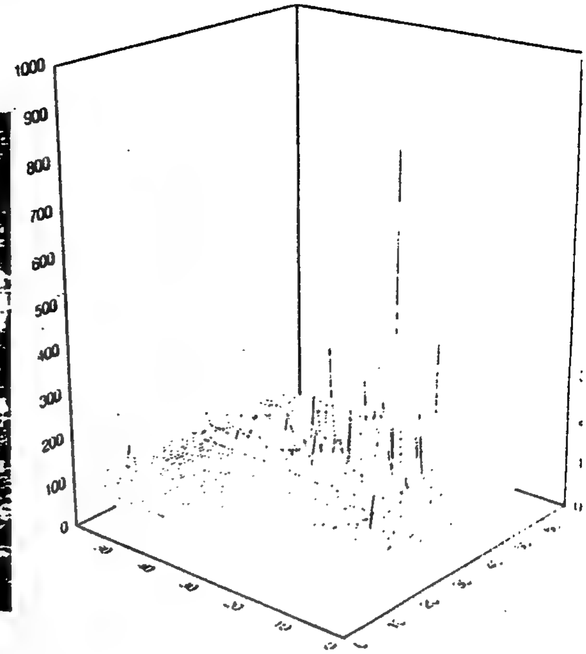

NDE by Correlation Method. Stress cracking.

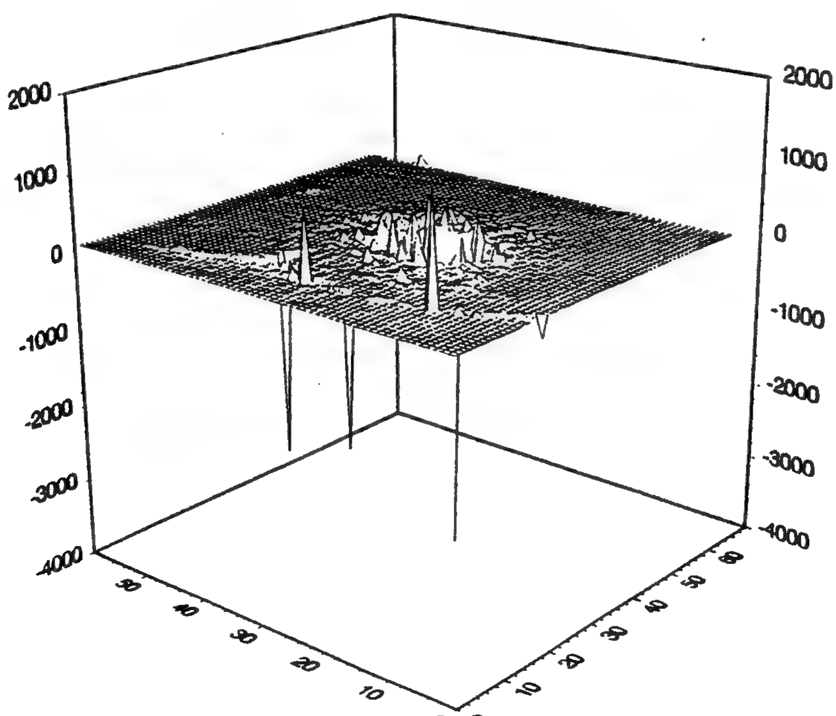

NDE of crevice corrosion by Correlation Method (with laser illumination and vacuum loading). The cross-correlation of the two speckle fields before and after vacuum loading is calculated. The crevice corrosion (specimen I) is revealed by the drastic change of correlation coefficient

Resolution of Correlation NDE

. Pit : size ~ 0.3mm. depth ~ 0.1 mm.
. Observation area: 64mm by 60mm.
. Distance between specimen and CCD camera: > 2 m.
. If the observation area is as big as 1m by 1m, we can distinguish a cluster of pits in an area as small as 5mm by 5 mm.

Proposed Approach for Quantitative NDE of Crevice Corrosion Cavity

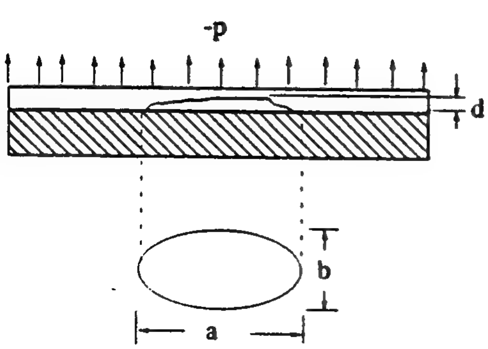

1. Use correlation method to determine the projected 2-D dimension a & b
2. Use ESPI to determine the out-of-plane deformation under slight negative pressure
3. Assuming the cavity be ellipsoidal in shape, determine the cavity height using numerical calculation.

CORROSION EFFECT ON FATIGUE LIFE OF Al7075-T6

CORROSION

PITTING CORROSION
INTERGRANULAR CORROSION
CRACKING
FILIFORM CORROSION
EXFOLIATION CORROSION

SURFACE ROUGHNESS CHANGE

REDUCED FATIGUE LIFE

Surface Roughness Measurement

- **Mechanical Profilometer**
- **Laser Speckle Sensor (LSS)**

Parameters Used in LSS Calculation

The auto-correlation coefficient of a digitized image $g(i,j)$ is defined as

$$C_a(\tau,\nu) = \frac{\sum_{i=1}^{i=M}\sum_{j=1}^{j=N} g(i,j) \times g(i+\tau, j+\nu)}{\sum_{i=1}^{i=M}\sum_{j=1}^{j=N} g^2(i,j)} \qquad (1)$$

where $g(i,j)$ is the discrete intensity level at point (i,j) of image g. M and N are total discrete points in X and Y directions ($M = 238, N = 192$). $\tau = T$, $\nu = V$ are defined as lag lengths along i, j directions respectively, when $C_a = 1/e$.

The cross-correlation coefficient of two arbitrary images $g(i,j)$ and $f(i,j)$ is defined as

$$\mathbf{C}_{gf} = \frac{\sum_{i=1}^{i=M}\sum_{j=1}^{j=N} g(i,j) \times f(i,j)}{\sqrt{[\sum_{i=1}^{i=M}\sum_{j=1}^{j=N} g^2(i,j) \times f^2(i,j)]^{1/2}}} \qquad (2)$$

where $g(i,j)$, $f(i,j)$ are the discrete intensity levels at point (i,j) of image g and f, respectively.

Specimen Geometry

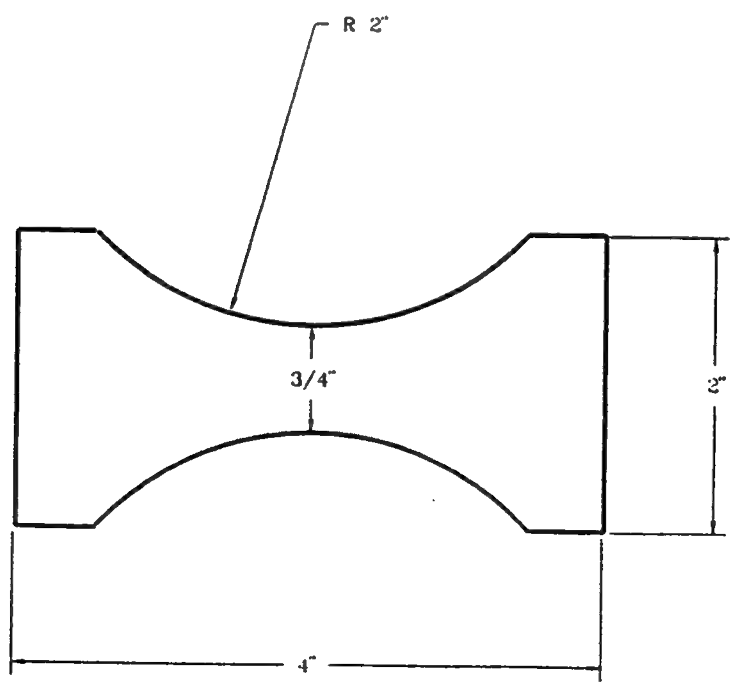

Optical Arragement of LSS

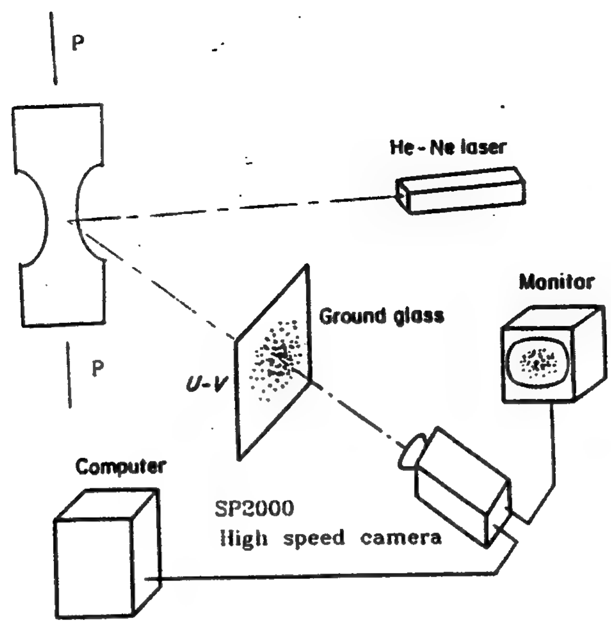

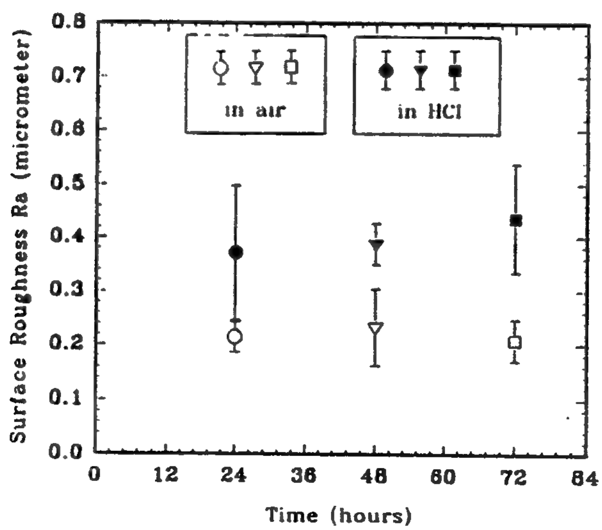

Fig.1 Surface roughness changes as measured by mechanical profilometer of Al7075-T6 specimen in 4 Mol HCl solution.

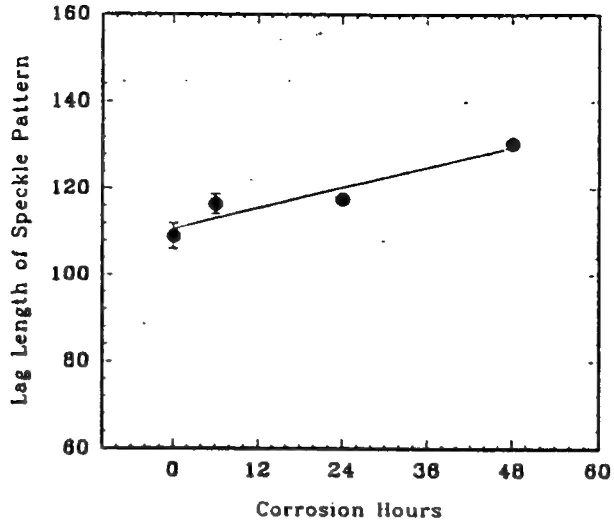

Fig.2 Roughness change characterized by auto-correlation lag length of Al7075-T6 specimens immersed in 4 Mol HCl solution.

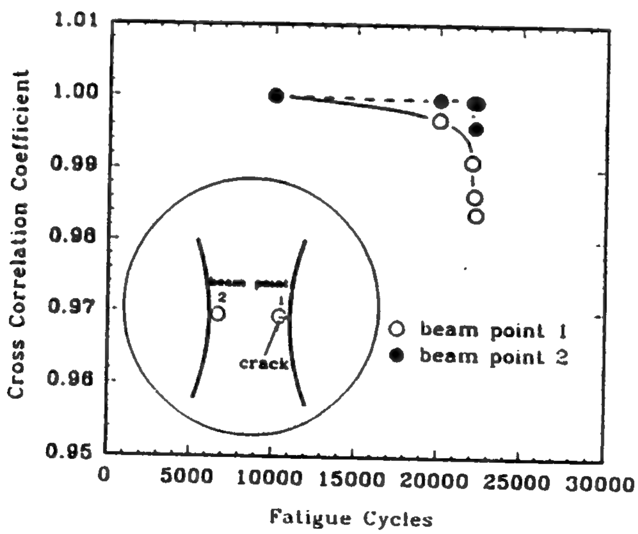

Fig 3. Fatigue life determination by speckle cross-correlation. The sample (Al7075-T6) was corroded for 48 hours in 4 Mol HCl solution and fatigued under maximum stress σ=300 MPa with stress ratio R=0.2.

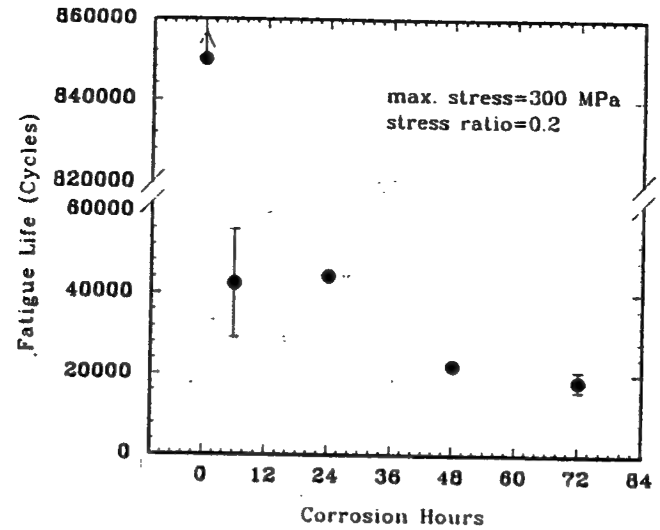

Fig.4 Fatigue life of Al7075-T6 as a function of corrosion hours in 4 Mol HCl solution. The virgin sample remain unbroken at 850,000 cycles under the same loading condition.

Strain Field Surrounding & Propagating Fatigue Crack as Mapped by Moire

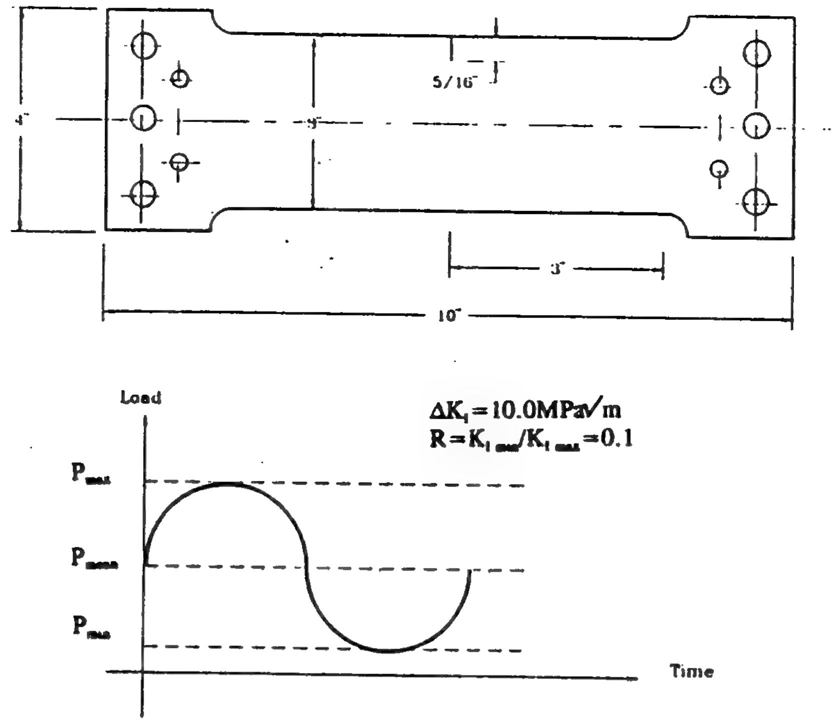

Fig.1 Fatigue specimen and the loading condition.

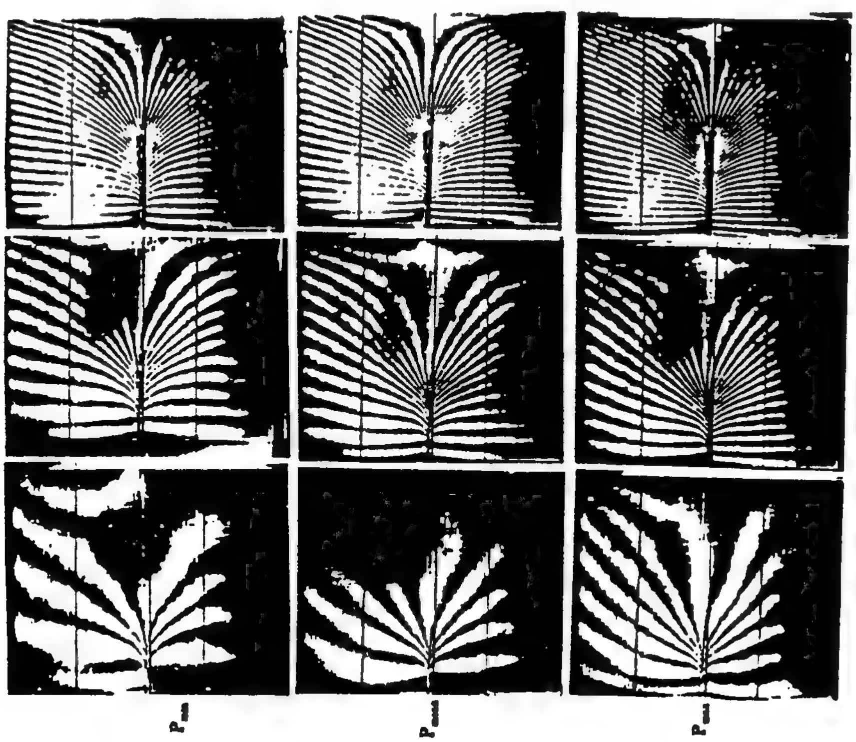

Fig.2 Moire patterns at different fatigue cycles.

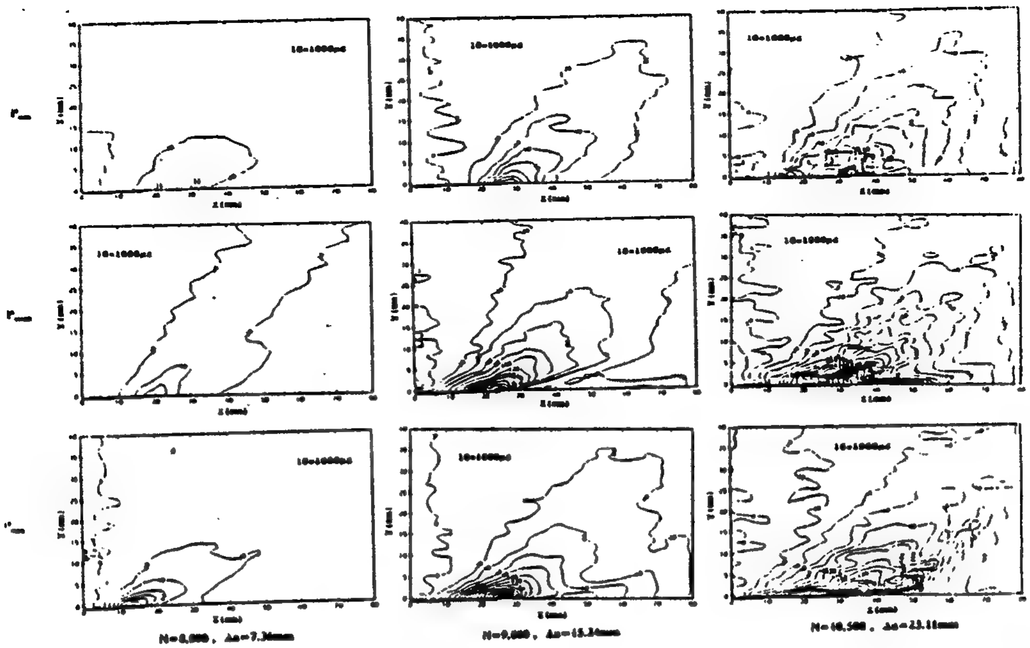

Fig.3 Strain contours ($\Delta\varepsilon_{yy}$) around crack tip at different fatigue cycles.

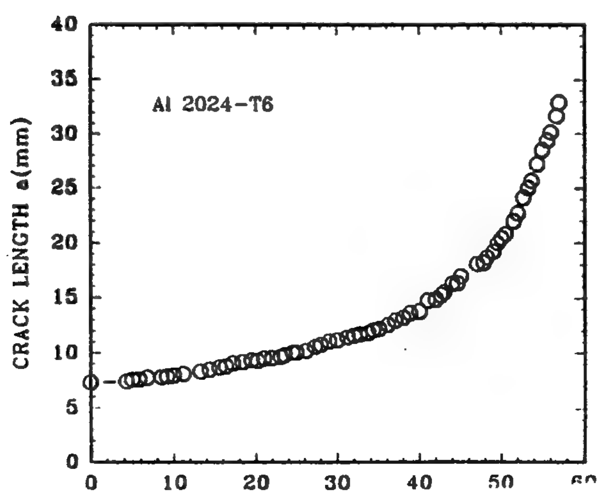

The Effect of Tensile Strain on Cumulative Fatigue Damage in Aluminum Sheet[1]

[1] Accepted for presentation at the symposia of *aging and life prediction of materials and structures*, Twelfth U.S. National congress of Applied Mechanics, Seattle, Washington, June, 1994.

- Cyclic loading produces a random roughening of the surface.
- The cross correlation technique is sensitive to surface roughness change.
- The initial static strain affect the fatigue damage acumulation and fatigue life.

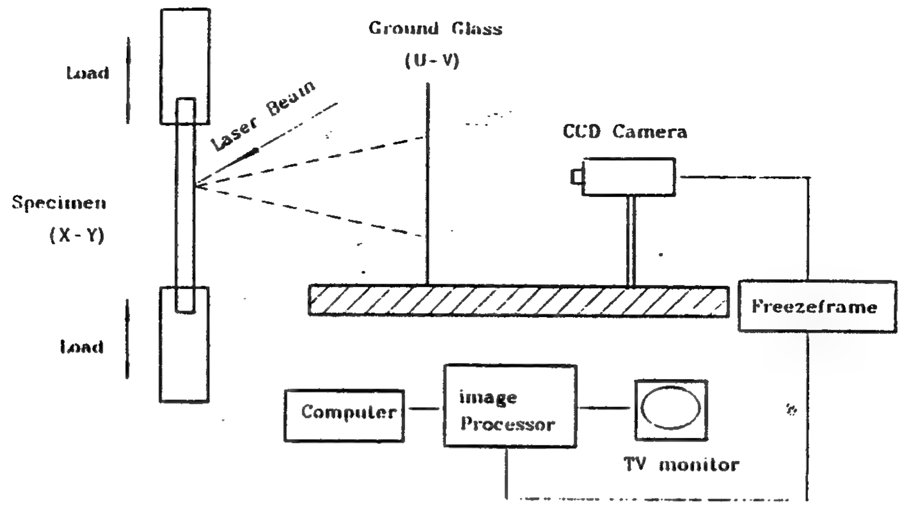

Fig.1 Experimental set-up to monitor fatigue roughness by laser speckle sensor (LSS).

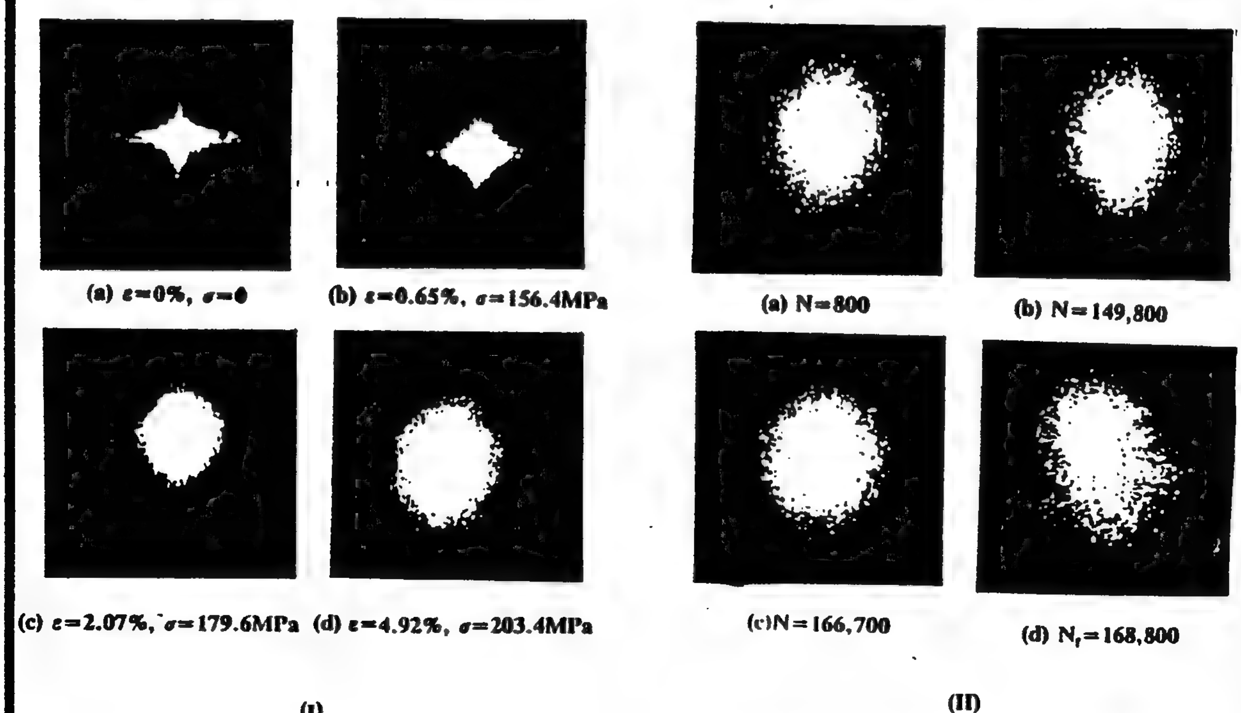

Fig.2 Successive speckle patterns (I) at different static deformation levels and (II) at different fatigue cycle of specimen.

Parameter Used in LSS Calculation

The cross-correlation coefficient of two arbitrary images $g(i,j)$ and $f(i,j)$ is defined as

$$\mathbf{C}_{gf} = \frac{\sum_{i=1}^{i=M}\sum_{j=1}^{j=N} g(i,j) \times f(i,j)}{\sqrt{[\sum_{i=1}^{i=M}\sum_{j=1}^{j=N} g^2(i,j) \times f^2(i,j)]^{1/2}}} \qquad (1)$$

where $g(i,j)$, $f(i,j)$ are the discrete intensity levels at point (i,j) of image g and f, respectively. M and N are total discrete points in X and Y directions ($M = 238, N = 192$).

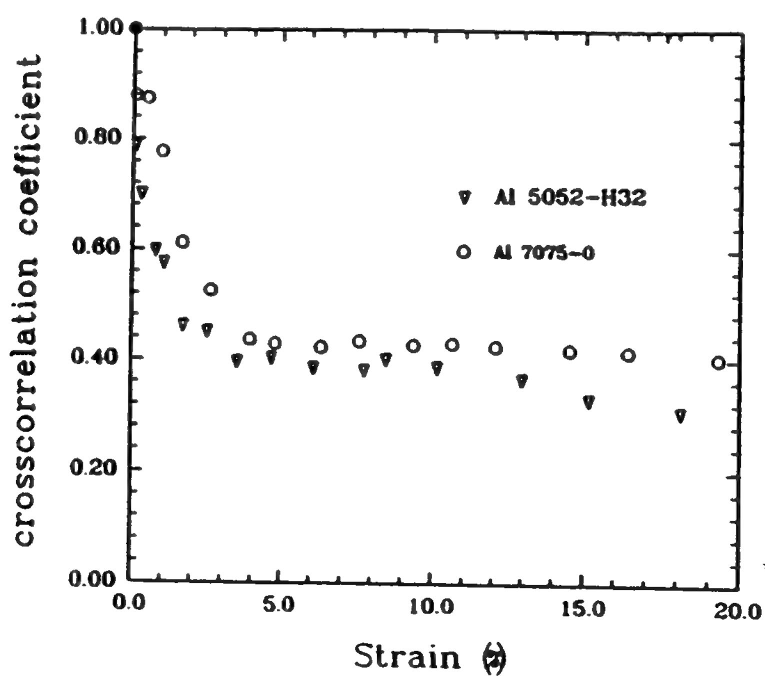

Fig.3 Cross-correlation coefficient in terms of static strain for Al5052-H32 and Al7075-O tensile specimens.

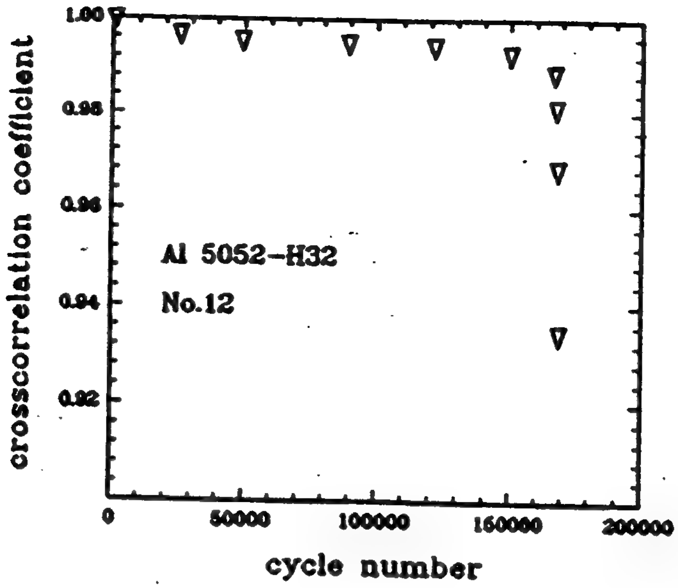

Fig.4 The relation between the cross-correlation coefficient and cycle number for a typical specimen.

A new damage criterion:

$$(\frac{\epsilon}{\epsilon_f})^\beta + \frac{\Delta\epsilon}{CN_f^\alpha} = 1 \qquad (1)$$

where, ϵ is static strain

ϵ_f is fracture ductility

$\Delta\epsilon$ is cyclic strain range

N_f is cycles to failure

α, β, *and* C are material constants

$$\Downarrow$$

Modified Coffin-Manson formula:

$$\Delta\bar{\epsilon} = CN_f^\alpha \qquad (2)$$

where

$$\Delta\bar{\epsilon} = \frac{1}{1-(\frac{\epsilon}{\epsilon_f})^\beta}\Delta\epsilon = \kappa\Delta\epsilon \qquad (3)$$

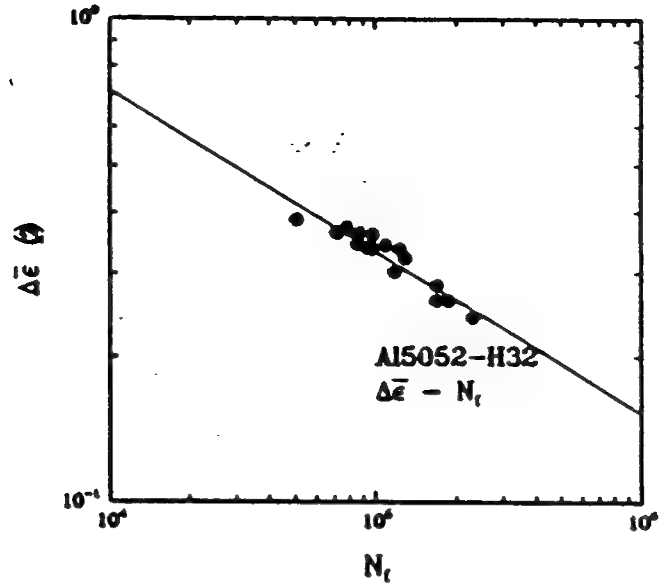

Fig.5 The generalized strain range $\Delta\bar{\varepsilon}$ as function of cycles to failure N_f.

CONCLUSIONS

1. Surface roughness change is non-linear with respect to the number of fatigue cycles in terms of cross correlation coefficient. The change is caused by fatigue damage accumulation.

2. The static strain influences fatigue life throug surface roughening and microdamage in the materials. The effect is noticeable but limited. A new damage model is introduced to incorporate the effect of static strain into the Coffin-Manson relation.

corrosion type / method	crevice	pitting	filiform	cracking
Laser Speckle (ESPI)	yes	no	no	yes
Moire (Projection Grating)	no/yes	yes	yes	no/yes
Correlation	yes	yes	yes	yes (surface crack)

Thermal Wave Imaging for NDE of Hidden Corrosion in Aircraft Components

R.L. THOMAS, L.D. FAVRO, AND P.K. KUO
WAYNE STATE UNIVERSITY
AFOSR URIP-FY93 Grant No. F49620-93-1-0428

WORKSHOP ON AGING AIRCRAFT RESEARCH
17-19 May 1994
Oklahoma City (Tinker AFB), Oklahoma

TECHNIQUE:
PULSE-ECHO THERMAL WAVE IMAGING

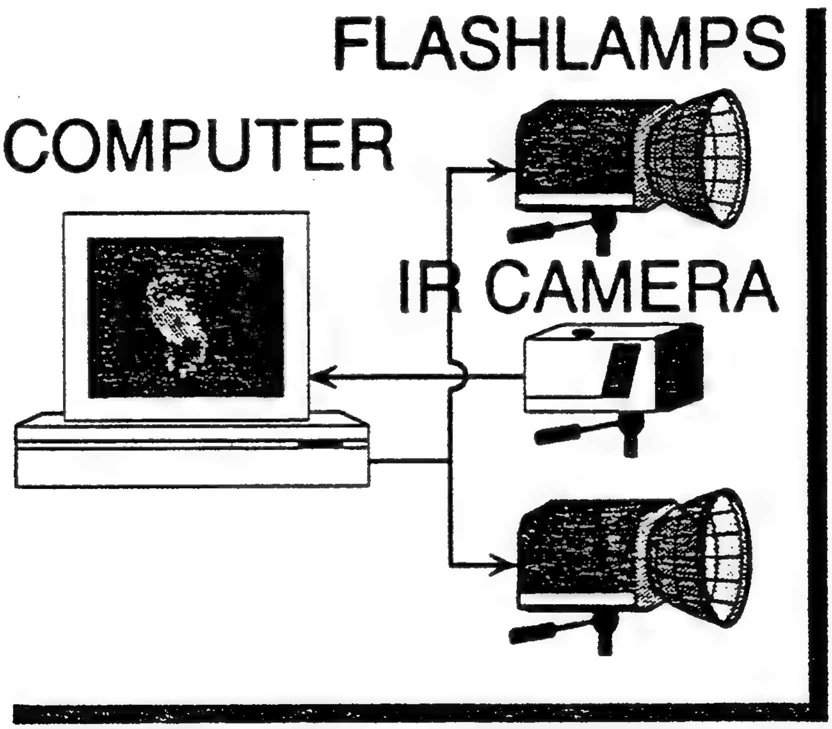

CONCEPT:
- Flash lamps pulse-heat the aircraft surface
- IR camera monitors the surface temperature following the heat pulse
- Computer and fast image processor extracts the thermal wave echo image

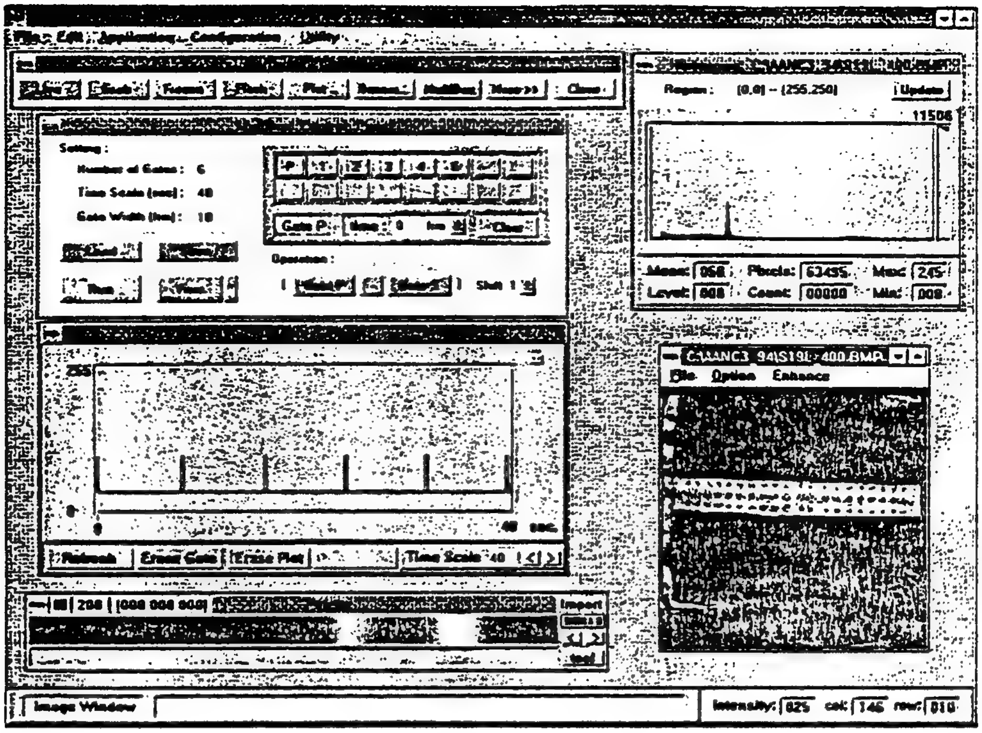

Related WSU Project:

THERMAL WAVE IMAGING OF ADHESIVE BONDS

Sponsored by the FAA-Center for Aviation Systems Reliability, operated by Iowa State University and supported by the Federal Aviation Administration Technical Center in Atlantic City, New Jersey, under Grant Number 93-G-018.

What is a thermal wave?

Thermal diffusion equation:

$$\nabla^2 T = \frac{1}{\alpha}\frac{\partial T}{\partial t} \quad \text{where} \quad \alpha = \frac{\kappa}{\rho c}$$

κ = thermal conductivity
ρ = mass density
c = specific heat

Try a plane wave solution, $T = T_0 e^{i(qx - \omega t)}$

which yields $q^2 = i\frac{\omega}{\alpha}$ or $q = (1+i)\sqrt{\frac{\omega}{2\alpha}}$

The real part of the wave is then given by

$$T = T_0\, e^{-x/\mu} \cos\left(\frac{2\pi x}{\lambda} - \omega t\right)$$

with $\mu = \sqrt{\frac{2\alpha}{\omega}}$ and $\lambda = 2\pi\mu$

the wave velocity is then $v = \frac{\omega\lambda}{2\pi} = \sqrt{2\alpha\omega}$

Earliest reference: Ångstrom, Ann. Physik, 114 (1861)

OUTLINE

- Brief introduction to thermal waves and the experimental method for thermal wave imaging.
- Background from recent FAA/CASR results:
  Hangar experience, Albuquerque FAA/AANC
- Participation in the test at OC/ALC for NDE of lapsplices and wing fastener corrosion, KC-135 (from the perspective of FAA/CASR, not as a vendor)
- Short-time scale thermal wave reflection: Theory and Experiment - significant effects due to
  1) The lateral size of the corrosion or disbond
  2) The kind of material at the aluminum boundary (e.g. air; corrosion products; or adhesive)
- Composite Structures (Boron-epoxy patches, Honeycomb structures, graphite-fiber-reinforced polymers)
- Technology transfer issues

Travelling Wave: $v = \sqrt{2\alpha\omega}$

Heavily Damped Wave: $\mu = \sqrt{2\alpha/\omega}$

Peak Time: $t_{peak} = \dfrac{x^2}{2\alpha}$

Peak Temperature: $T_{peak} = \dfrac{c}{\sqrt{2\pi e}}\,\dfrac{1}{x}$

Consider the Fourier components of the heat pulse in these experiments:

- The high frequency components propagate with high speeds, but are heavily damped;
- The low frequency components have less damping, but propagate very slowly

Net result: Intermediate frequency components dominate the behavior, and the pulse broadens dramatically as it propagates

FAA Center for Aviation Systems Reliability (CASR)

THERMAL WAVE IMAGES OF ALUMINUM SKINS WITH ADHESIVE BONDLINE SPECIMEN #4

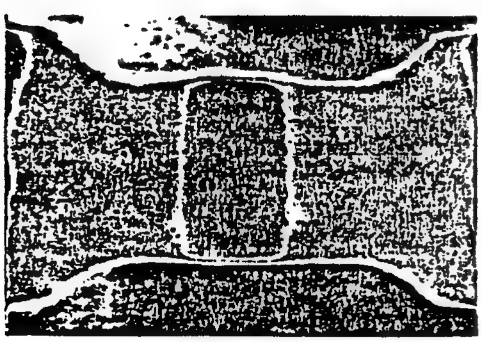

Before

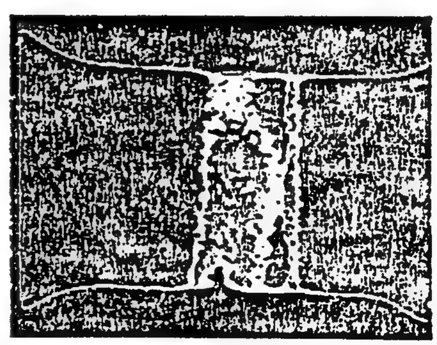

After Fatigue Test

FAA/CASR

THERMAL WAVE IMAGING

AT THE AANC NDI VALIDATION CENTER

ALBUQUERQUE, NM

MARCH 14-18, 1994

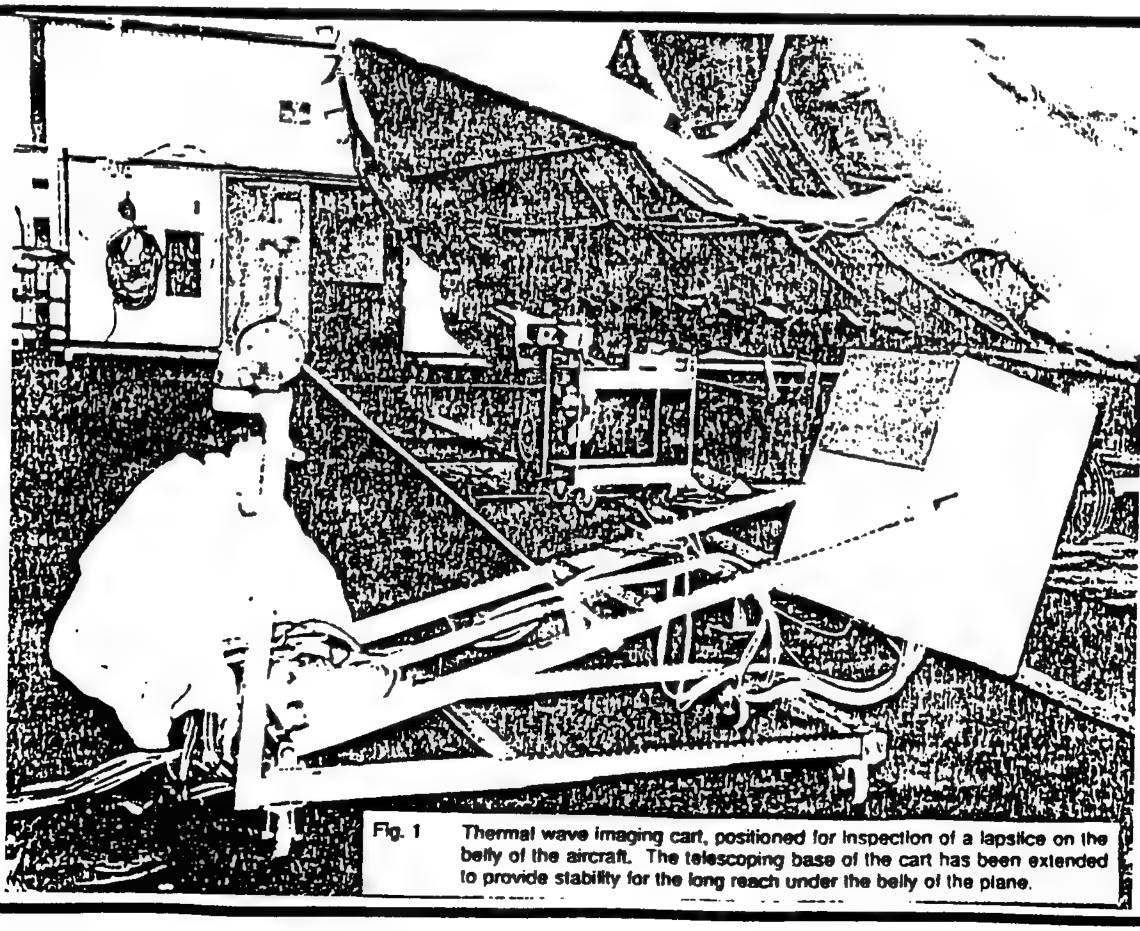

Fig. 1 Thermal wave imaging cart, positioned for inspection of a lapslice on the belly of the aircraft. The telescoping base of the cart has been extended to provide stability for the long reach under the belly of the plane.

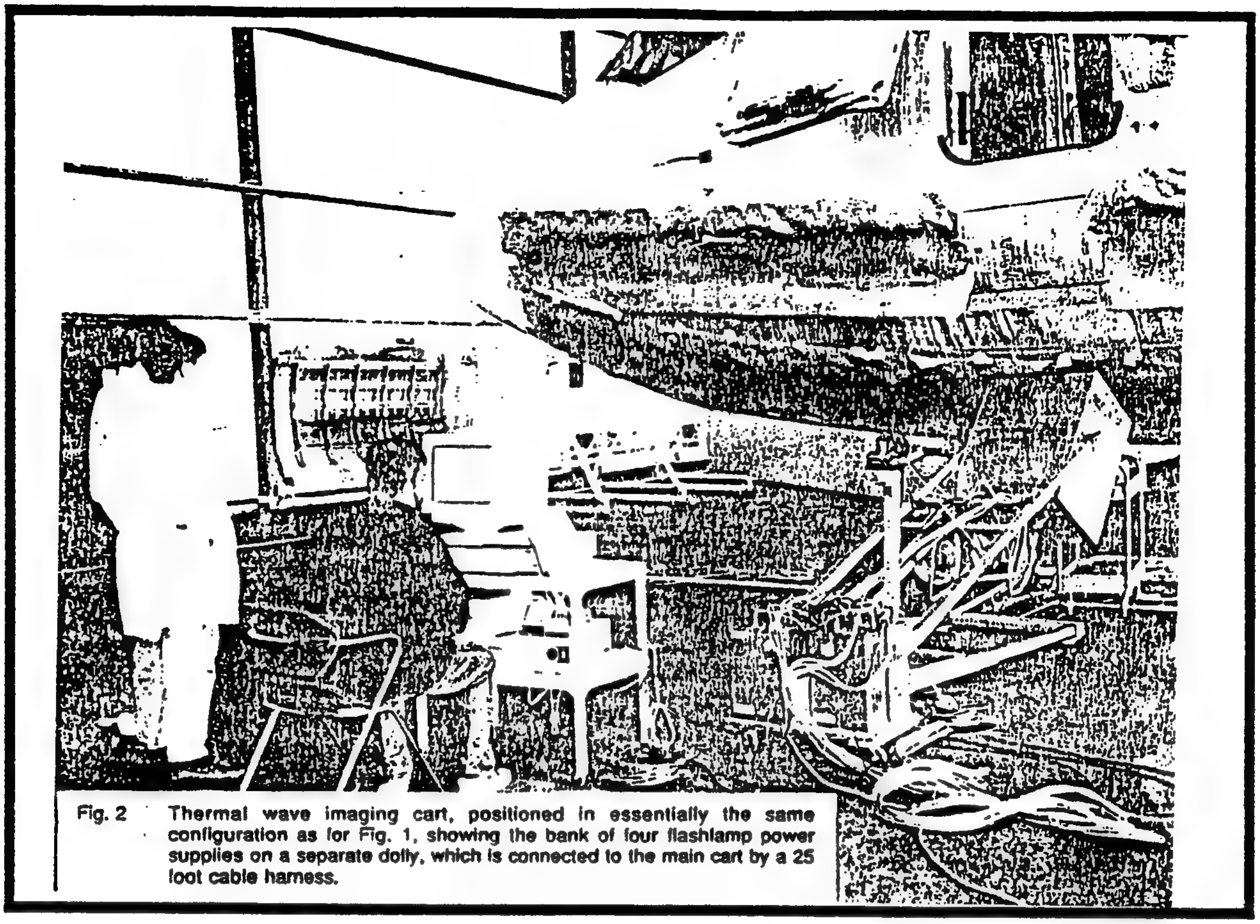

Fig. 2 Thermal wave imaging cart, positioned in essentially the same configuration as for Fig. 1, showing the bank of four flashlamp power supplies on a separate dolly, which is connected to the main cart by a 25 foot cable harness.

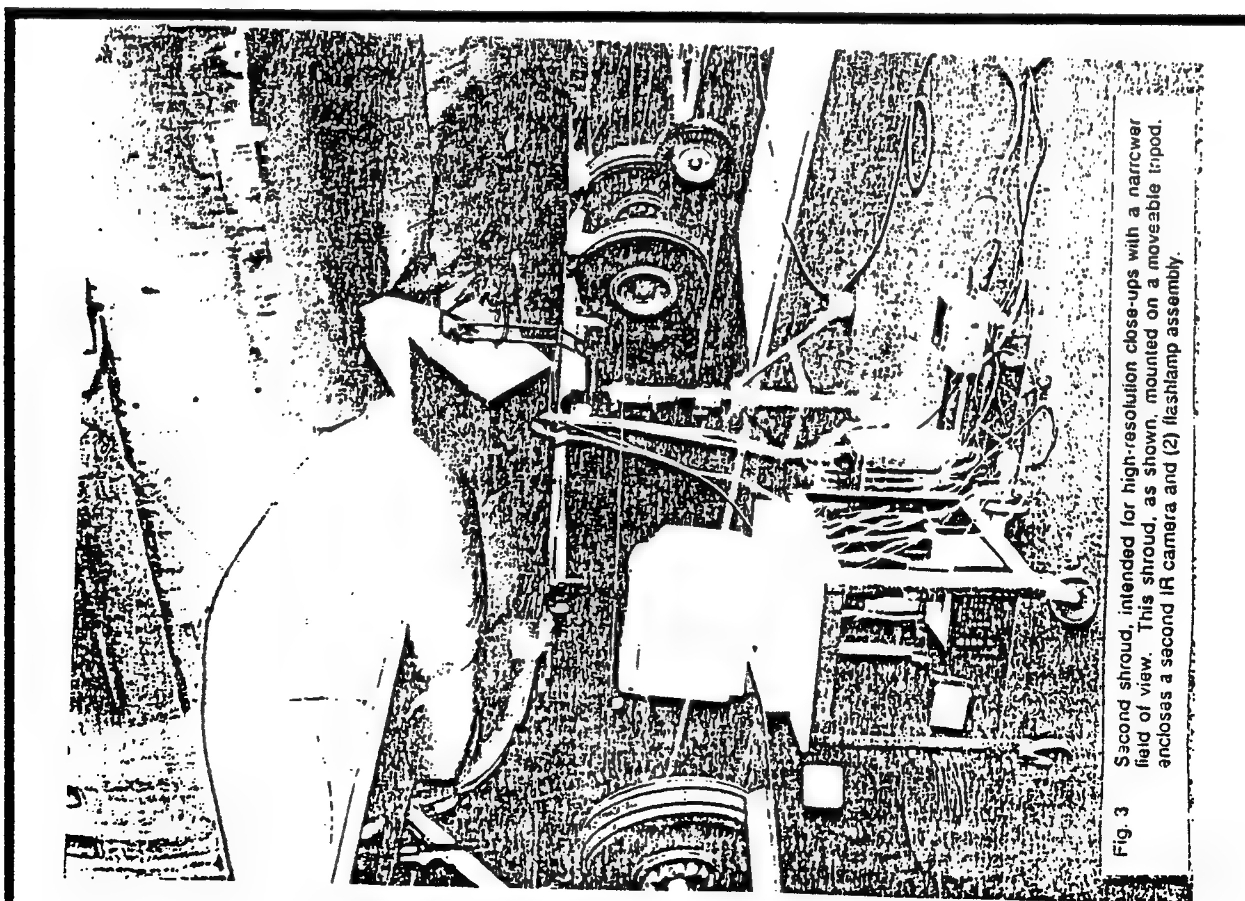

Fig. 3 Second shroud, intended for high-resolution close-ups with a narrower field of view. This shroud, as shown, mounted on a moveable tripod, encloses a second IR camera and (2) flashlamp assembly.

chemically induced corrosion regions of various geometrical shapes and sizes, and representing various percentages of material removal ranging upwards from 2%. In nearly every such laboratory test, thermal wave imaging was successful in detecting the corrosion, and in most cases could detect it even from the opposite skin (uncorroded), through the bond layer joining the two skins. Several regions of 3%, 4%, and 6% corrosion were successfully imaged in our laboratory. A typical image is shown in Fig. 4. Usually, in addition to the corrosion, thermal wave imaging also detected (unintended) adhesive bond defects as well. The success on these controlled laboratory test panel imaging experiments suggested that a field test experiment on an actual aircraft would be a logical next step, and would also provide a useful trial of the portability of our prototype instrumentation.

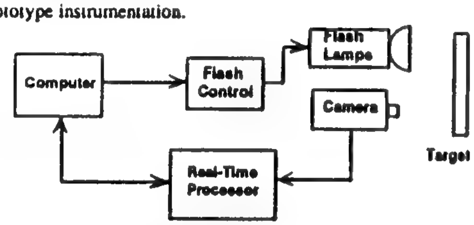

Fig. 3. Block diagram of the Box-car Imaging System.

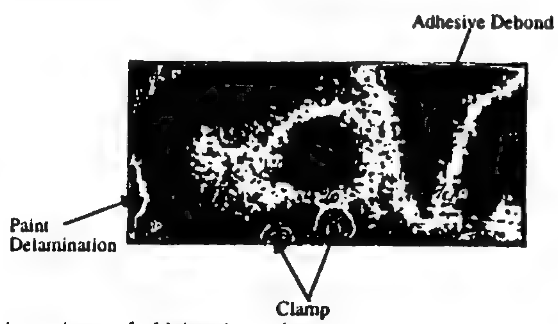

Fig. 4 Thermal wave image of a fabricated corrosion test specimen.

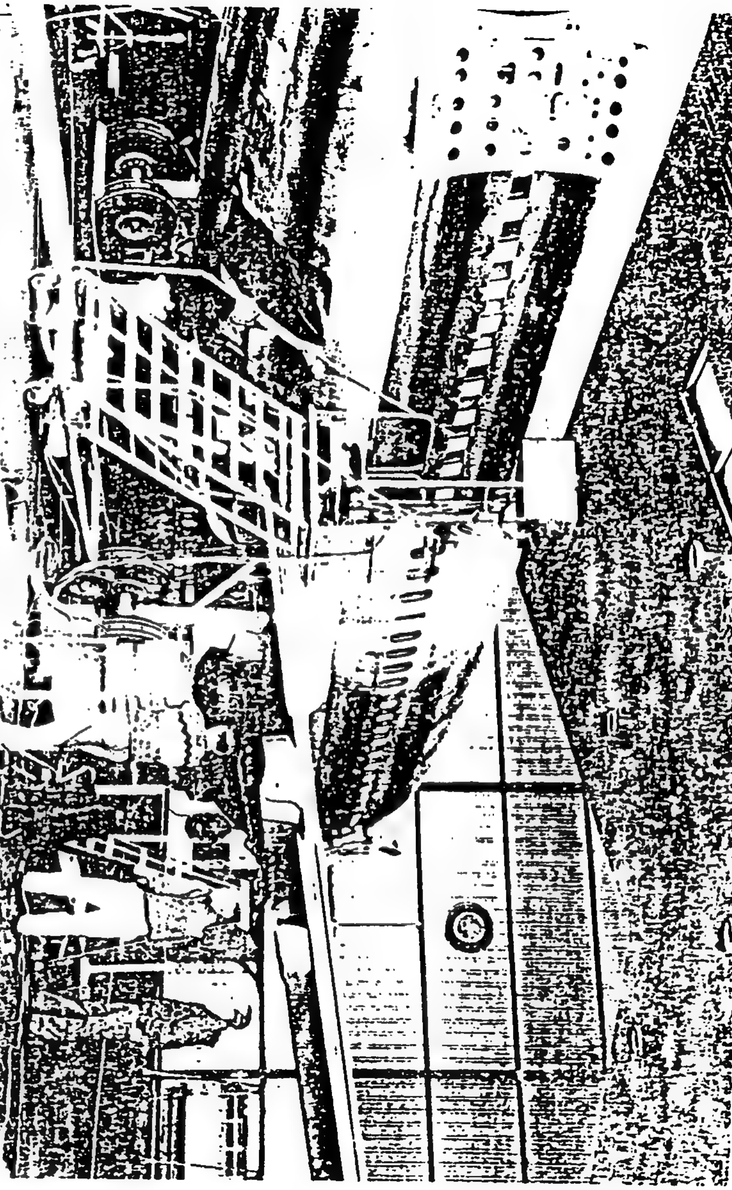

Fig. 4 Thermal wave imaging cart, deployed on the stair lift prior to positioning the shroud against the plane for imaging lapsplice 10R. Notice that the telescoping base of the cart has been collapsed so that it fits easily on the platform of the stair lift and that the power supplies, computer, etc. remain on the floor with the cable harness connecting them to the shroud.

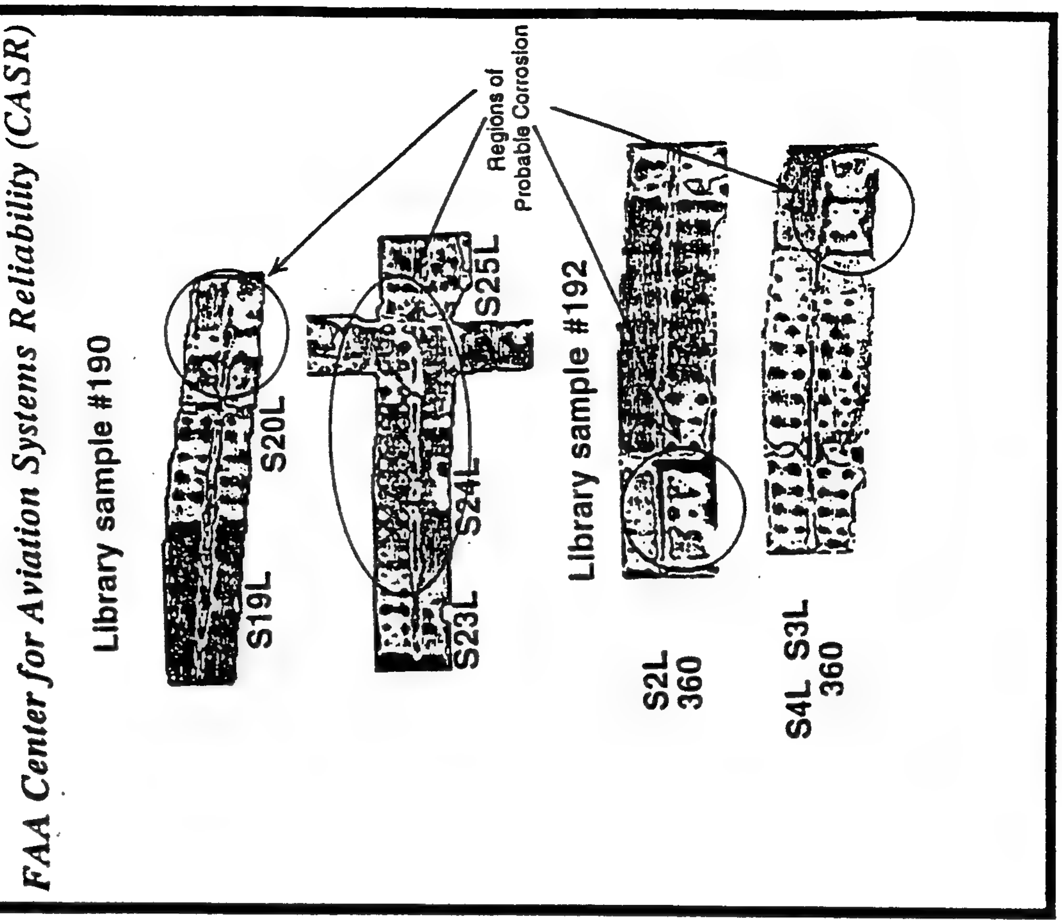

FAA Center for Aviation Systems Reliability (CASR)

THICKNESS CALIBRATION STRIP

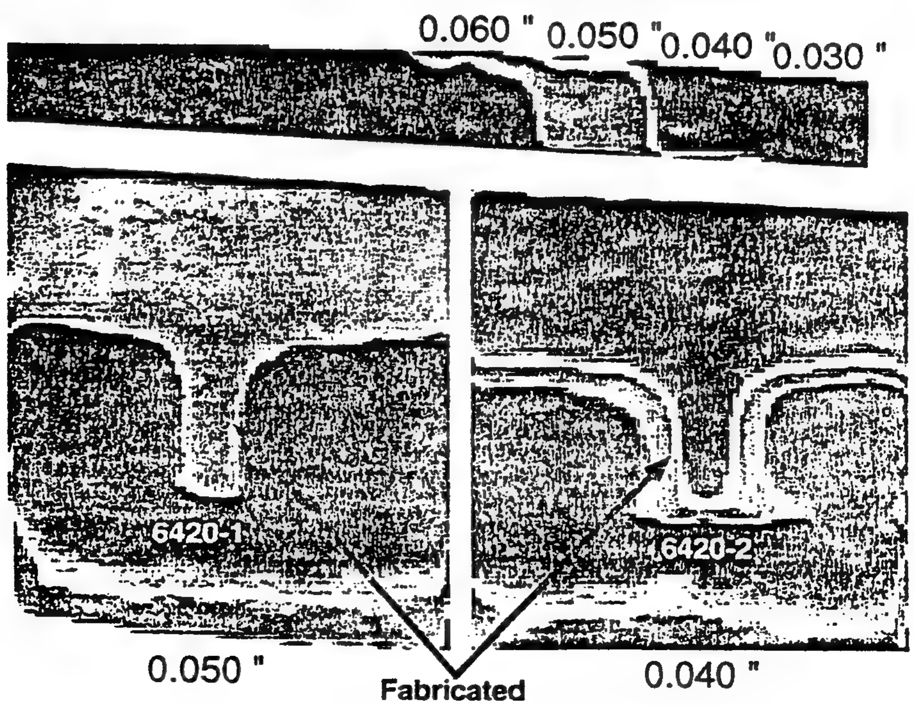

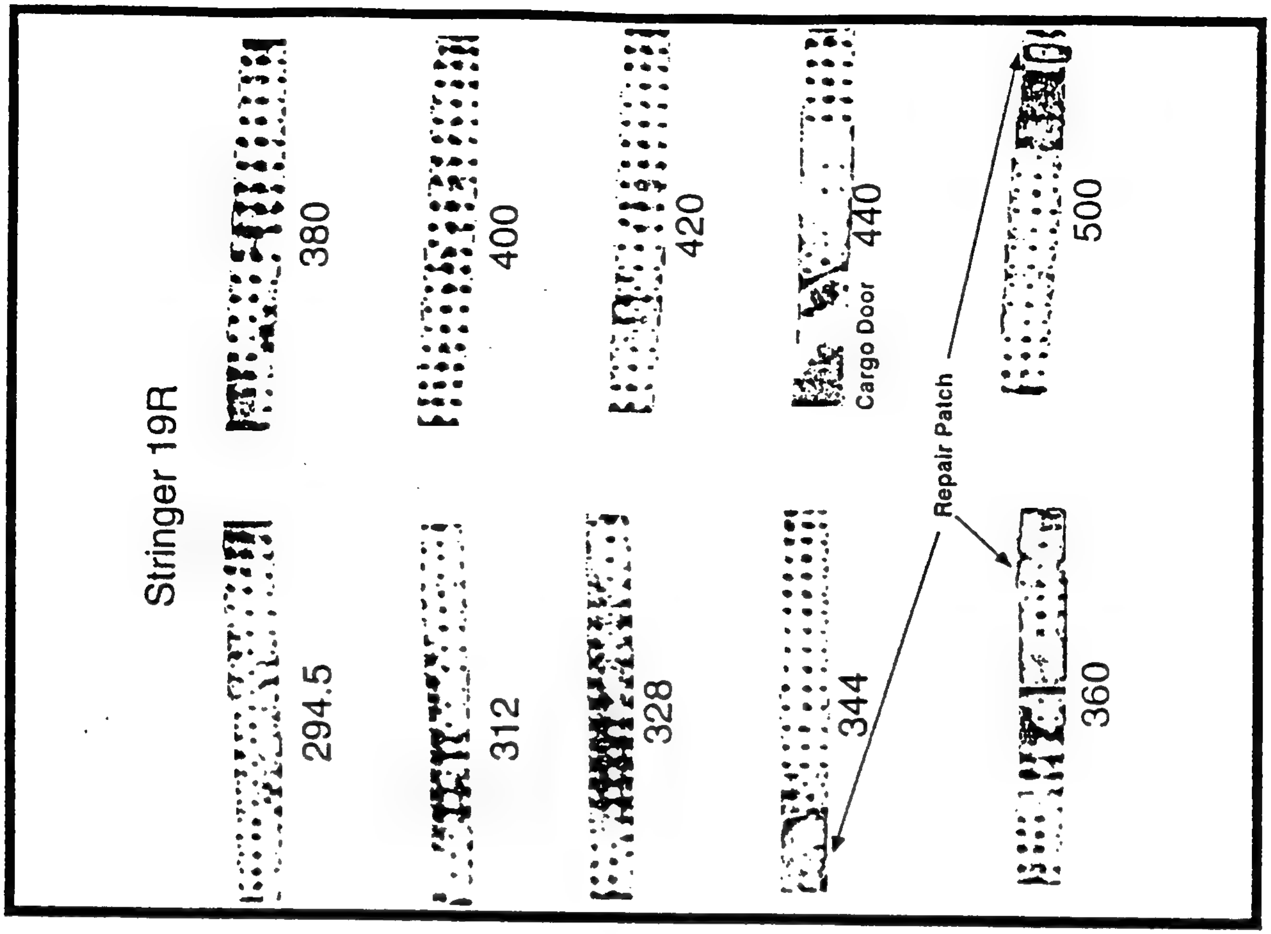

FAA/CASR

THERMAL WAVE IMAGING

MINI-FIELD DEMO

TINKER AFB

MAY 11-13, 1993

FAA Center for Aviation Systems Reliability (CASR)

BOTTOM SECTION OF INSPECTION AREA

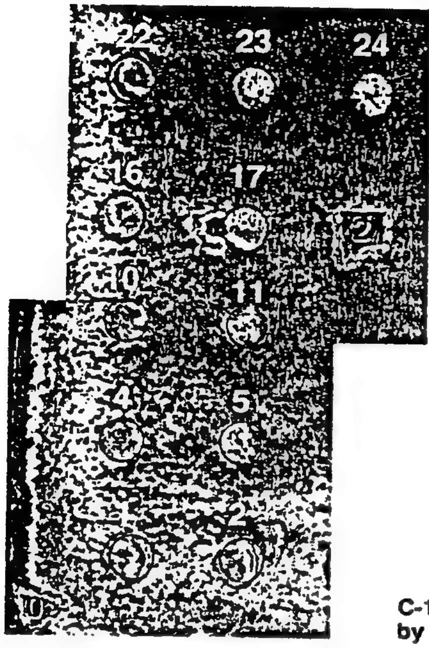

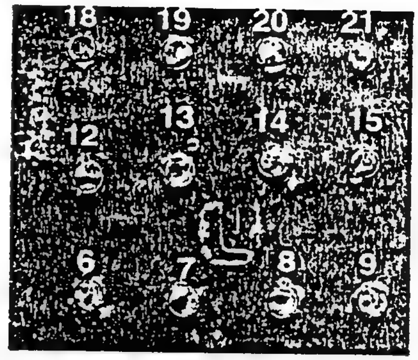

C-135 Wing Fastener Corrosion Inspection
by Thermal Wave Imaging at Tinker AFB:

Aircraft # 2671
May 13, 1993

Thermal Wave Image of a region of
wing-fastener corrosion on a C-135 Aircraft
(Imaged at Tinker AFB, Oklahoma City, May 13, 1993)

BOTTOM SECTION OF INSPECTION AREA

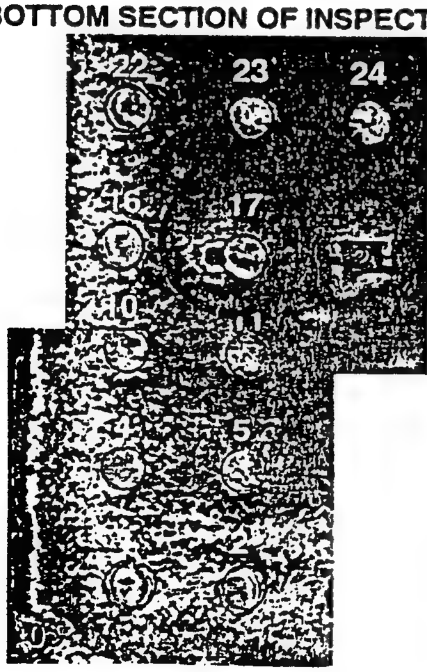

ENLARGEMENT OF REGION
SURROUNDING FASTENER # 17

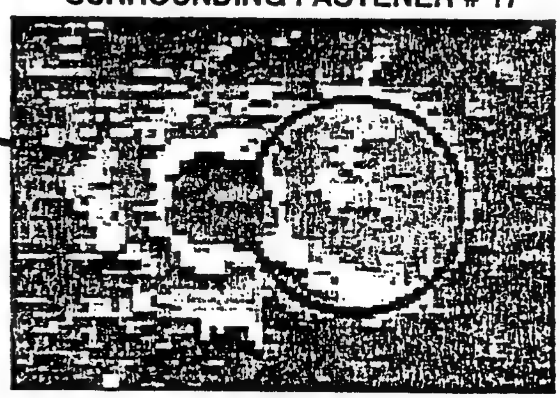

OPTICAL IMAGE OF FASTENER 17
(left side cross section)

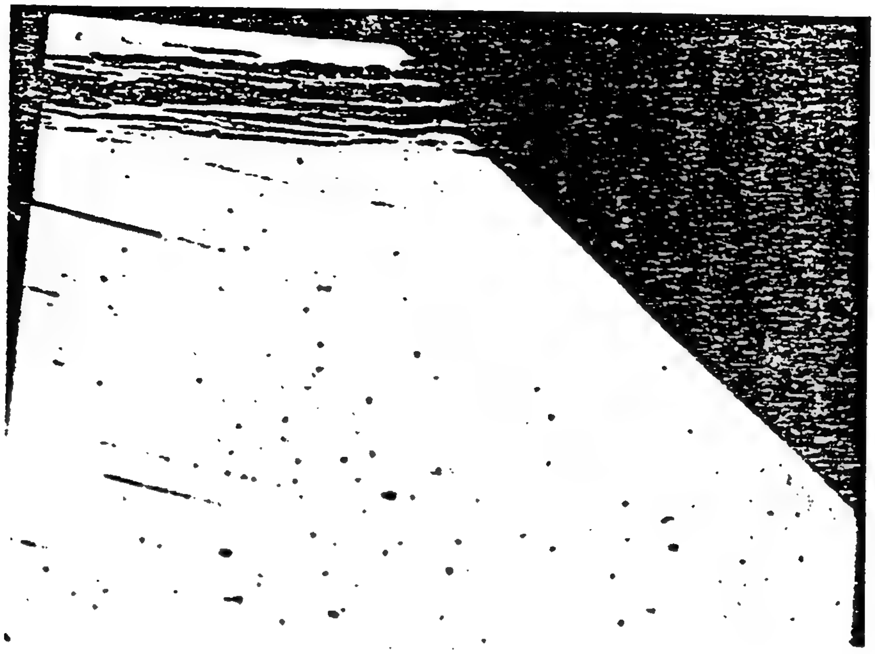

FAA Center for Aviation Systems Reliability (CASR)

MIDDLE SECTION OF INSPECTION AREA

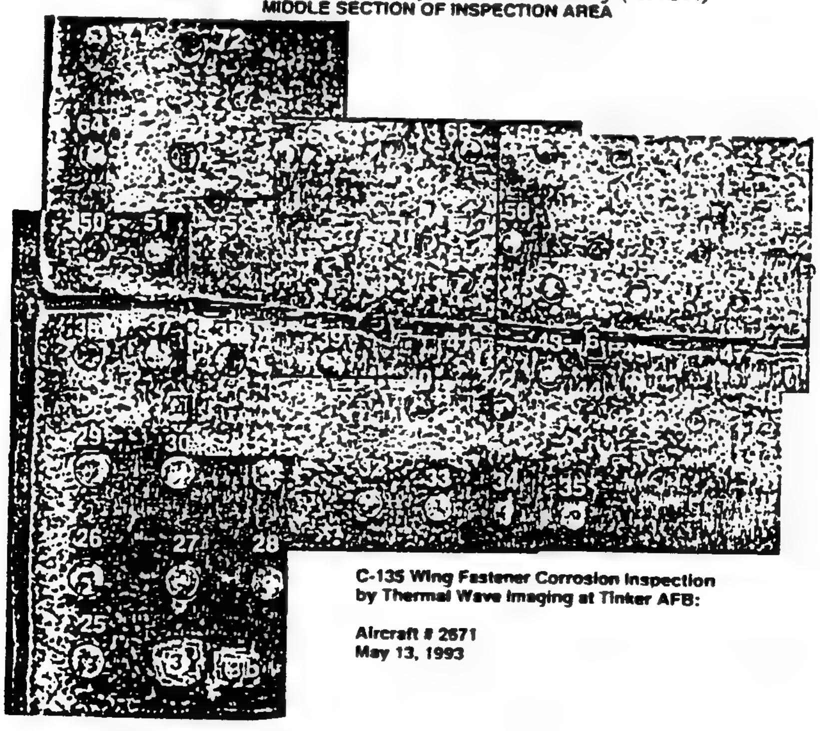

C-135 Wing Fastener Corrosion Inspection
by Thermal Wave Imaging at Tinker AFB:

Aircraft # 2671
May 13, 1993

THERMAL WAVE IMAGE OF FASTENER 76
(top down view)

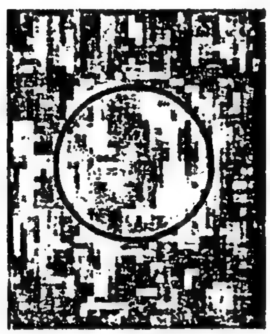

FAA Center for Aviation Systems Reliability (CASR)
TOP SECTION OF INSPECTION AREA

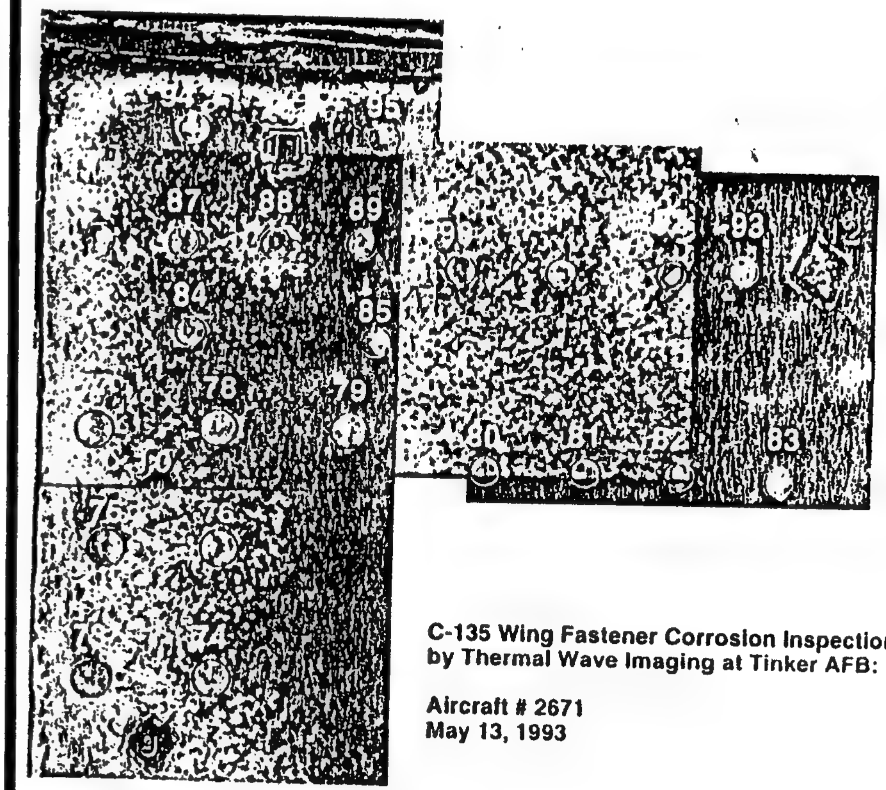

C-135 Wing Fastener Corrosion Inspection
by Thermal Wave Imaging at Tinker AFB:

Aircraft # 2671
May 13, 1993

OPTICAL IMAGE OF COUNTERSINK 76
(top down view)

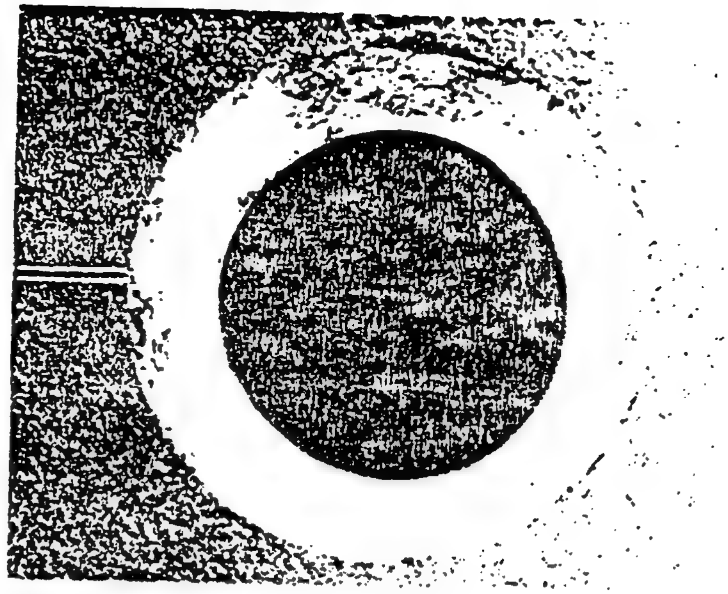

FAA Center for Aviation Systems Reliability (CASR)

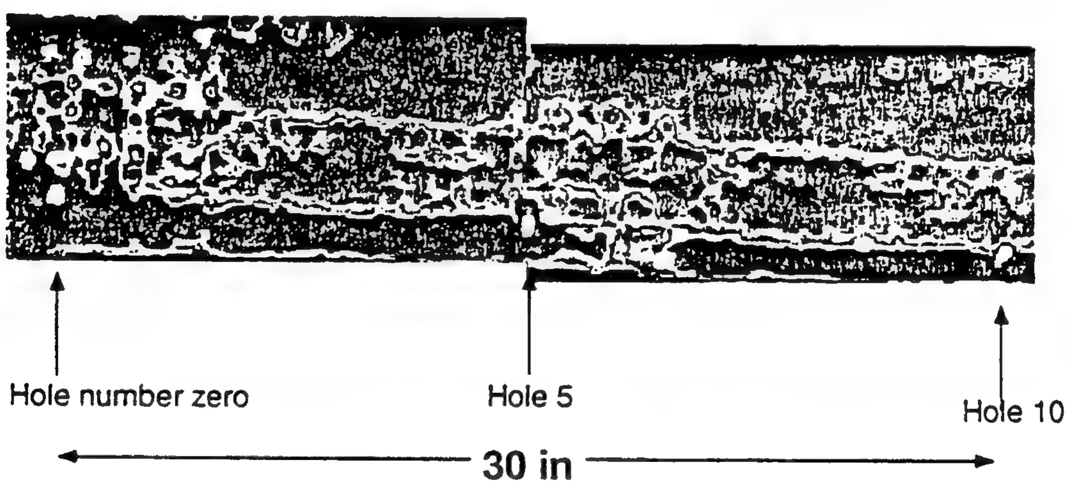

Test Area 1; Gate = 15 Frames

Stringer 18; Frame station 1070 - 1100

[Scale = 1:4]

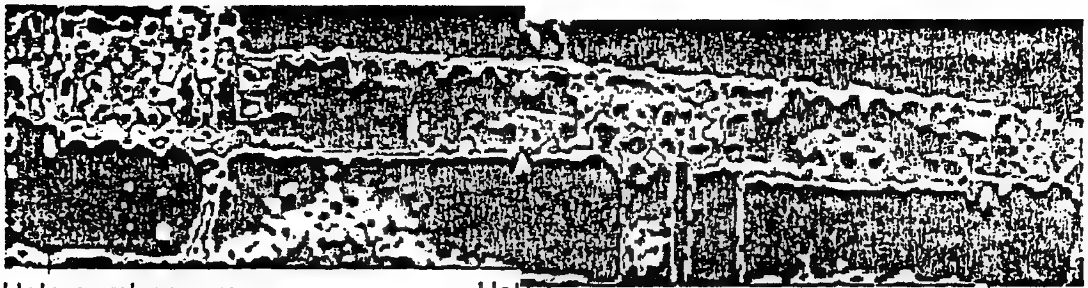

Test Area 5; Gate = 10 Frames

Stringer 18; Frame station 1020 - 1050

[Scale = 1:4]

SHORT-TIME-SCALE

THERMAL WAVE REFLECTION:

THEORY & EXPERIMENT

Motivation:

- To look for quantitative measurement of outer skin thickness.
- To study the effects of lateral defect size and boundary conditions.

$$T(r,t) - T_o(r,t) = -\frac{1}{2\pi(\pi\alpha t)^{1/2}} \frac{\partial}{\partial \ell} \int_{-\infty}^{\infty} dx' \int_{-\infty}^{\infty} dy' \frac{\exp\left[-\frac{\left\{\left[(x-x')^2+(y-y')^2+\ell^2\right]^{1/2}+\ell\right\}^2}{4\alpha t}\right]}{\left[(x-x')^2+(y-y')^2+\ell^2\right]^{1/2}} f(x',y')$$

$$T - T_o = \frac{1}{2x}\left(\frac{1}{\pi\alpha_1\alpha_2\alpha_3 t}\right)^{1/2} \iint_{-\infty}^{\infty} dx'dy' \sum_{m=1}^{\infty} \frac{A^m}{R_m}\frac{1}{\alpha_3^{1/2}} \left[\frac{\partial}{\partial z}\exp\left\{-\frac{\left[R_m+(z^2/\alpha_3)^{1/2}\right]^2}{4t}\right\}\right]_{z=\ell} f(x',y')$$

$$R_m = \left[\frac{(x-x')^2}{\alpha_1} + \frac{(y-y')^2}{\alpha_2} + \frac{(2m+1)^2\ell^2}{\alpha_3}\right]^{1/2}$$

Reflection Coefficient: $A = \frac{1-e}{1+e}$, where $e = \sqrt{\frac{(\kappa\rho c)_2}{(\kappa\rho c)_1}}$

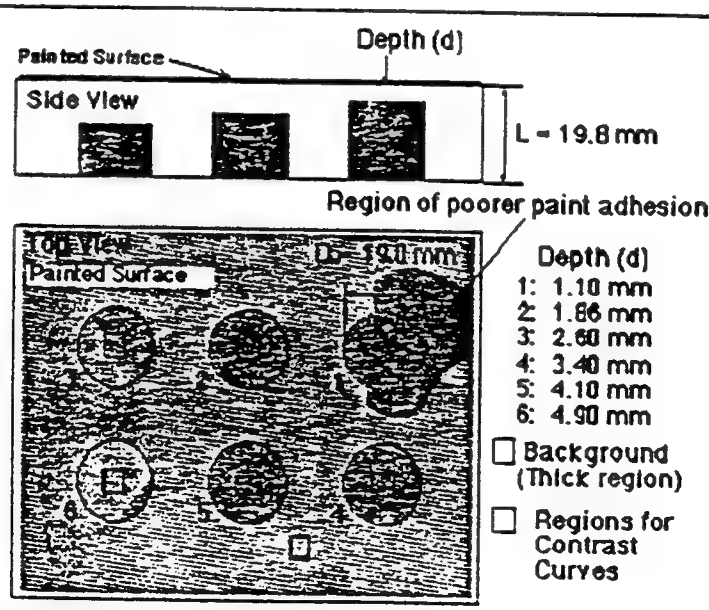

Contrast Curves: Background (T vs. t) subtracted from the (T vs. t) for the regions 1 - 6

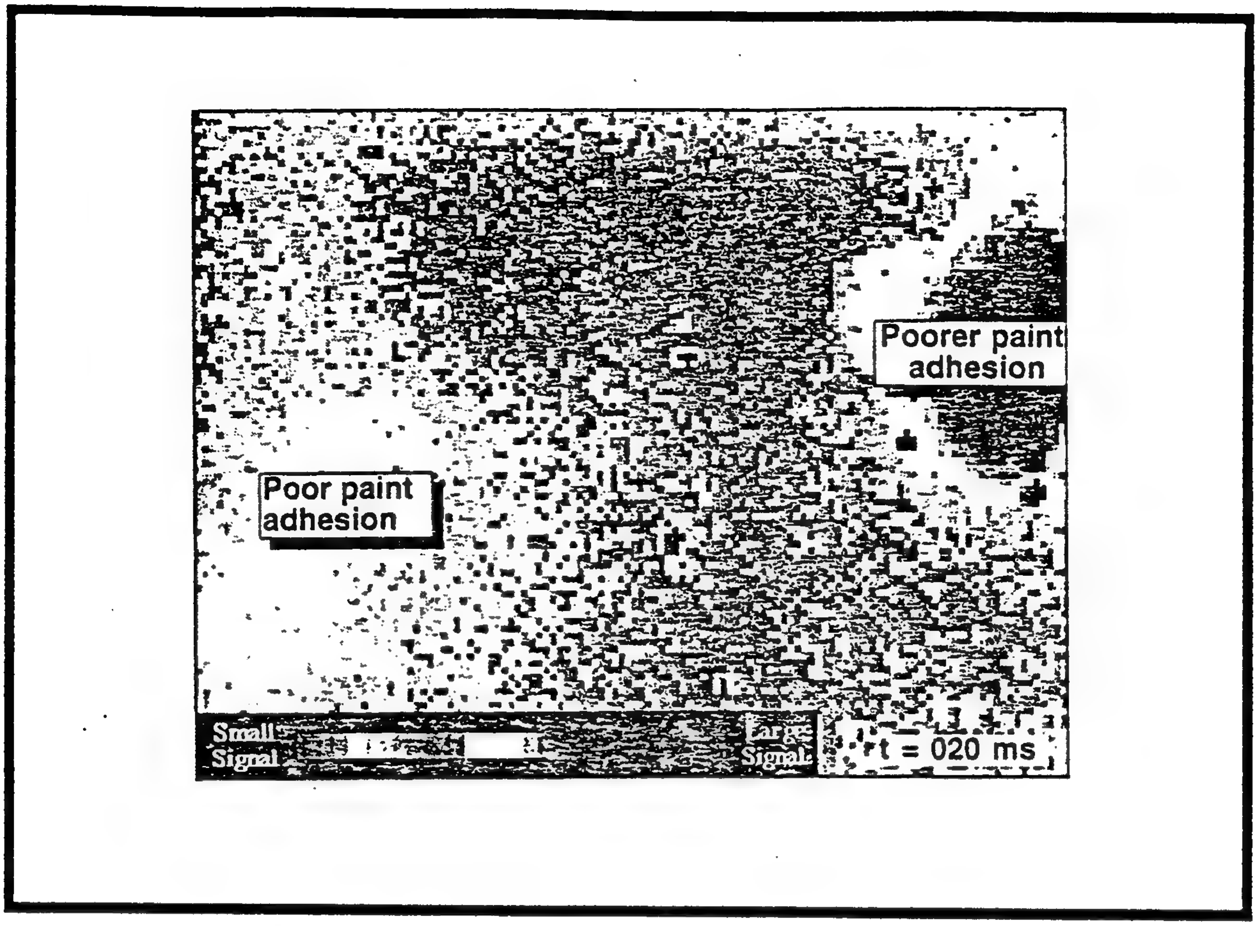
Poorer paint adhesion
Poor paint adhesion
Small Signal
Large Signal
t = 020 ms

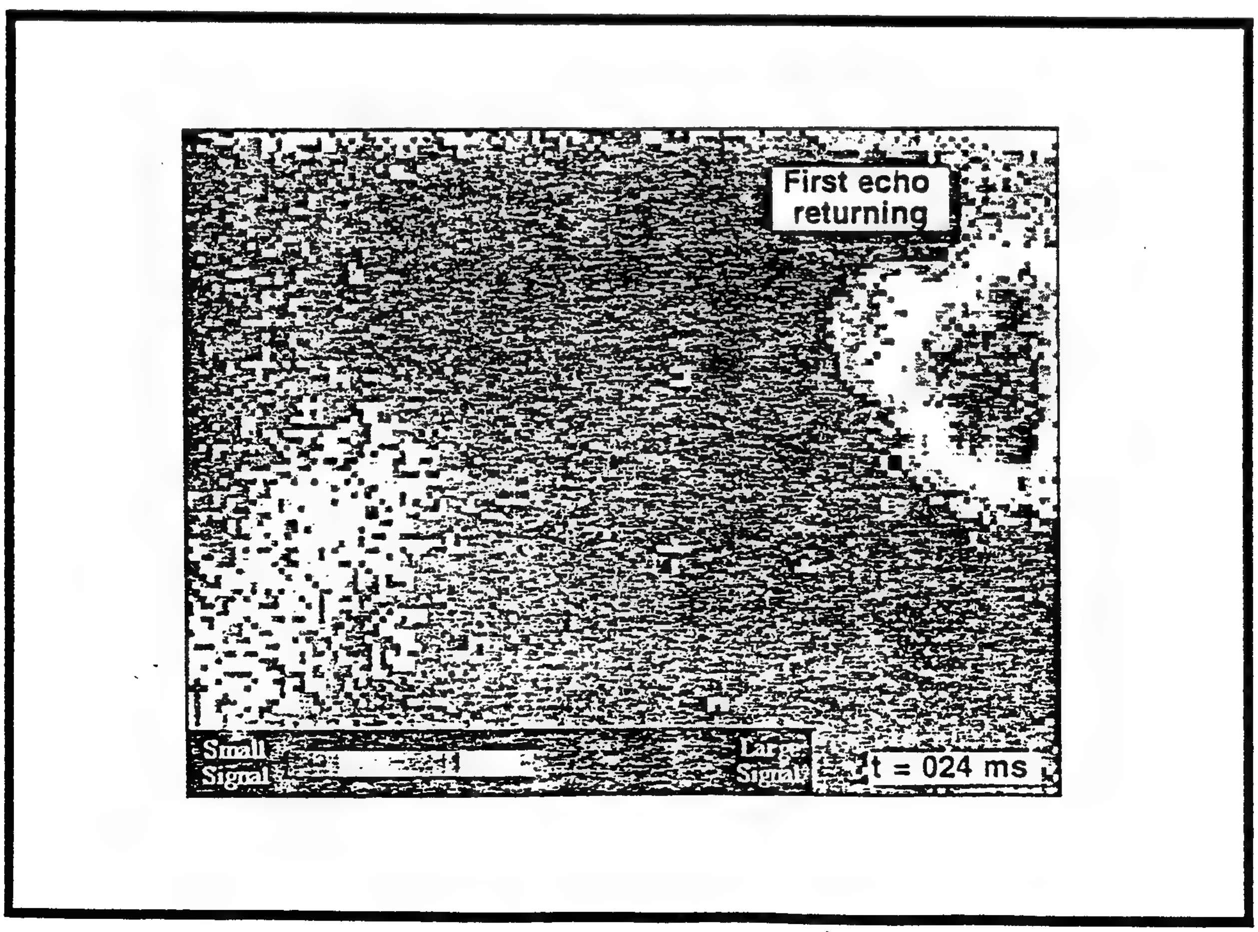
First echo returning
Small Signal
Large Signal
t = 024 ms

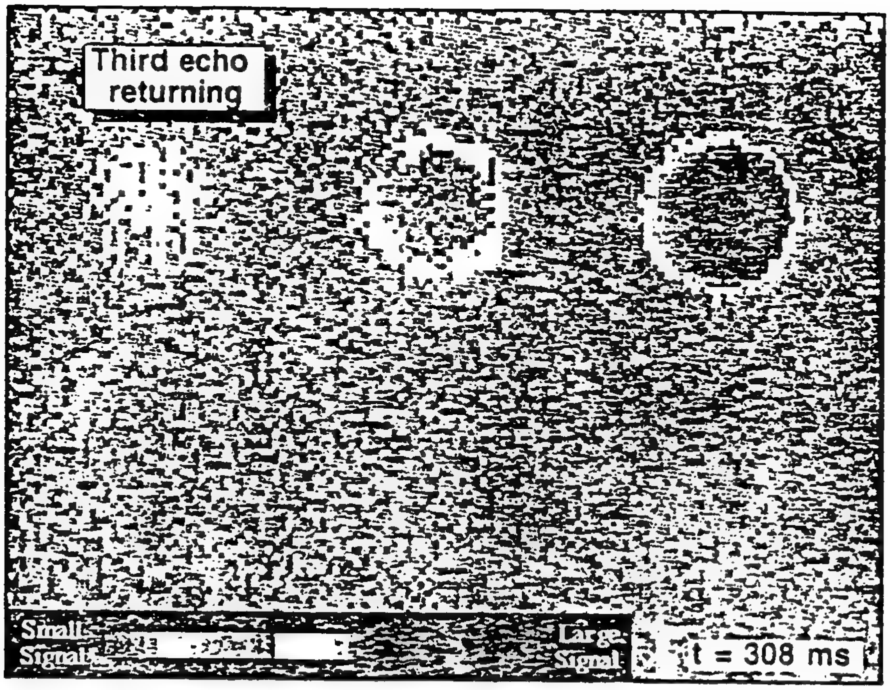
Third echo returning
Small Signal
Large Signal
t = 308 ms

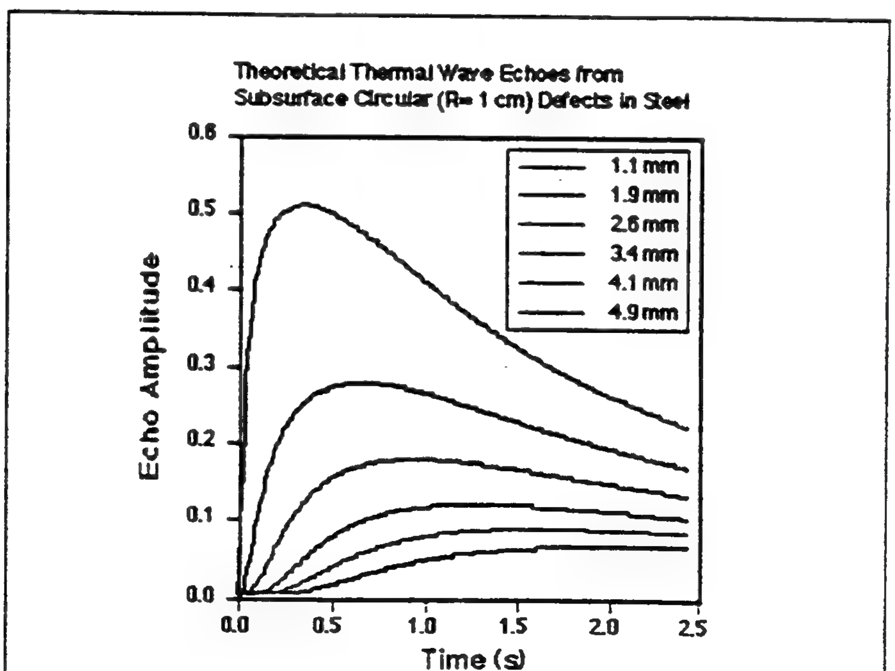
Theoretical Thermal Wave Echoes from Subsurface Circular (R= 1 cm) Defects in Steel
Echo Amplitude
Time (s)
1.1 mm
1.9 mm
2.6 mm
3.4 mm
4.1 mm
4.9 mm
0.0
0.1
0.2
0.3
0.4
0.5
0.6
0.0
0.5
1.0
1.5
2.0
2.5

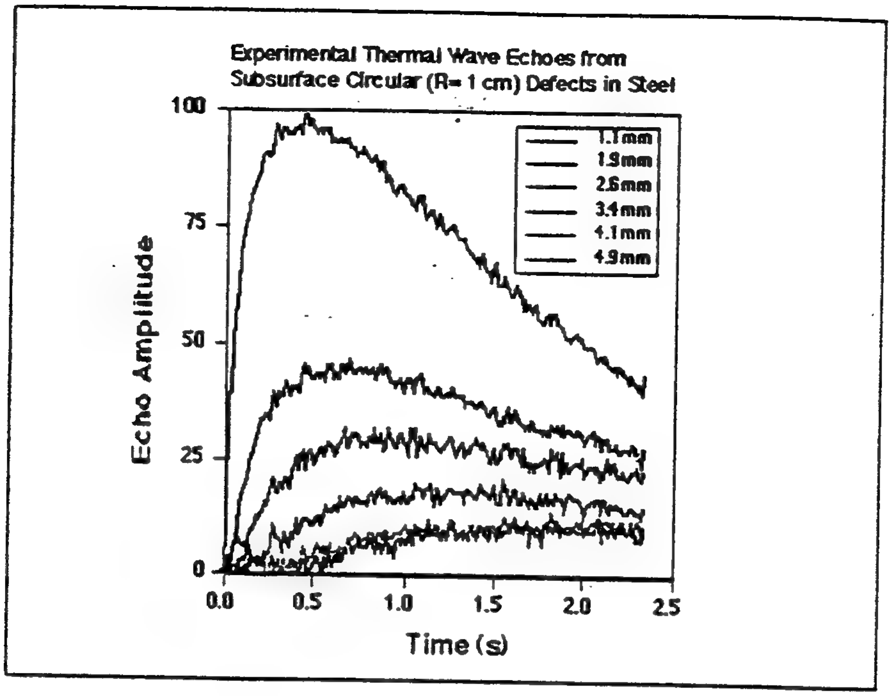

Experimental Thermal Wave Echoes from
Subsurface Circular (R= 1 cm) Defects in Steel
Echo Amplitude
Time (s)
1.1mm
1.9mm
2.6mm
3.4mm
4.1mm
4.9mm
0
25
50
75
100
0.0
0.5
1.0
1.5
2.0
2.5

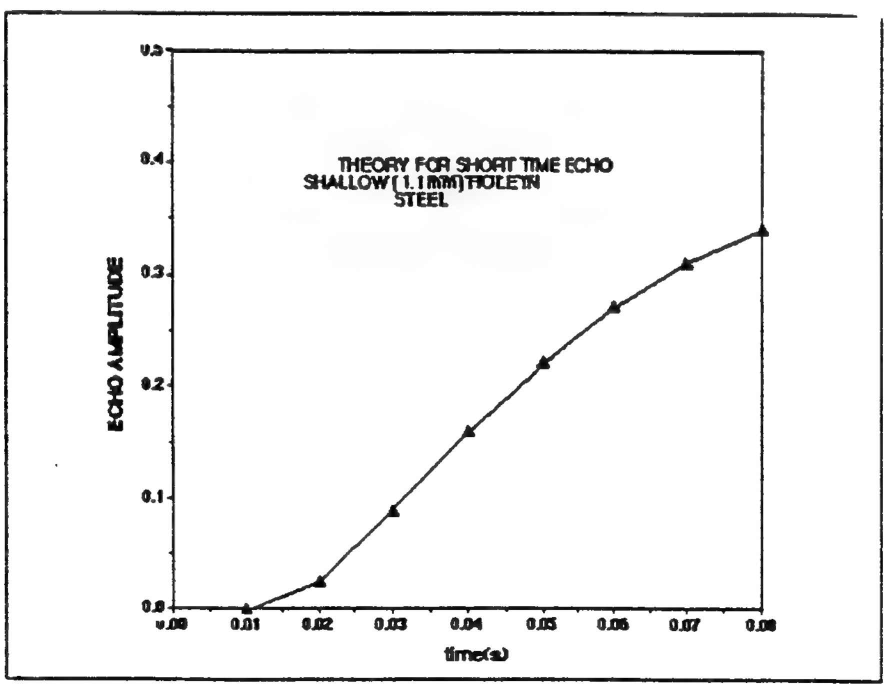

THEORY FOR SHORT TIME ECHO
SHALLOW (1.1MM) HOLE IN
STEEL
ECHO AMPLITUDE
time(s)
0.0
0.1
0.2
0.3
0.4
0.01
0.02
0.03
0.04
0.05
0.06
0.07
0.08

CONCLUSIONS FROM THE 6-HOLE RESULTS

- Thermal wave scattering theory works pretty well.
- Reflections from the bottom surface of metal skins begin on fast time scales (~ 40 ms for steel, faster for aluminum).
- The reflection signals peak at times which are predictable, and which scale as the square of the thickness of the metal to the defect, for this set of defects of radius = 1 cm.

WHAT HAPPENS FOR DEFECTS OF DIFFERENT RADII AT THE SAME DEPTH?

Repeat the previous experiment for a different type of flat-bottomed hole specimen.

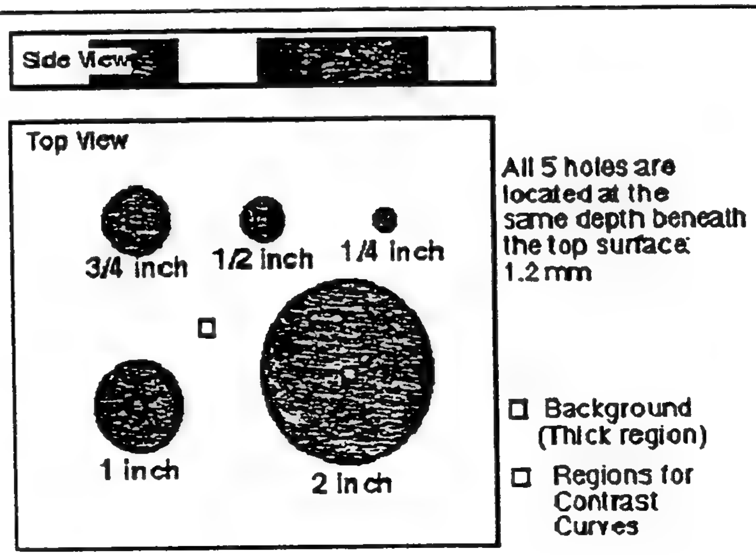

Contrast Curves: Background (T vs. t) subtracted from the (T vs. t) for the regions 1 - 5

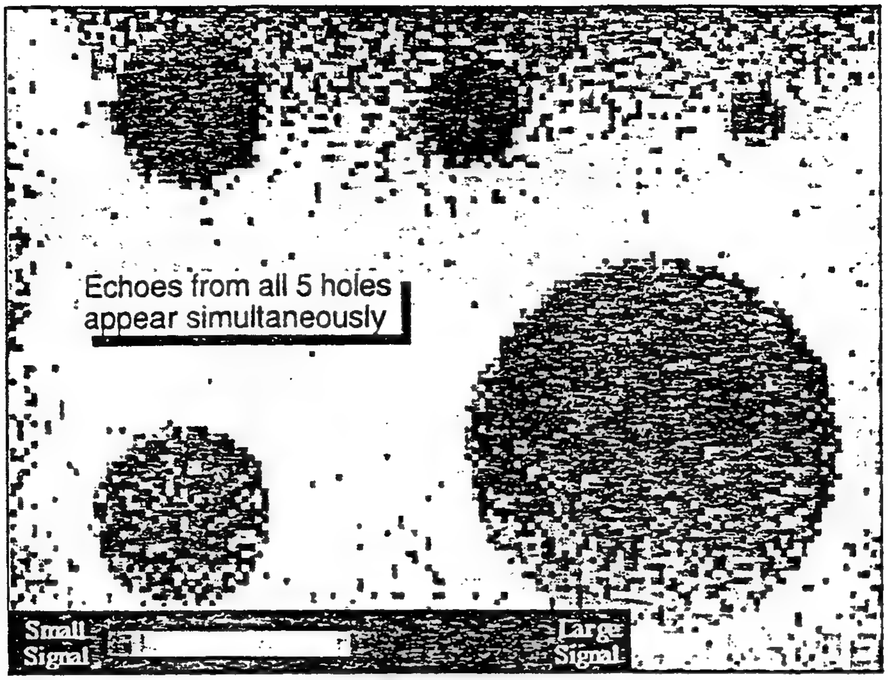
Echoes from all 5 holes appear simultaneously
Small Signal
Large Signal

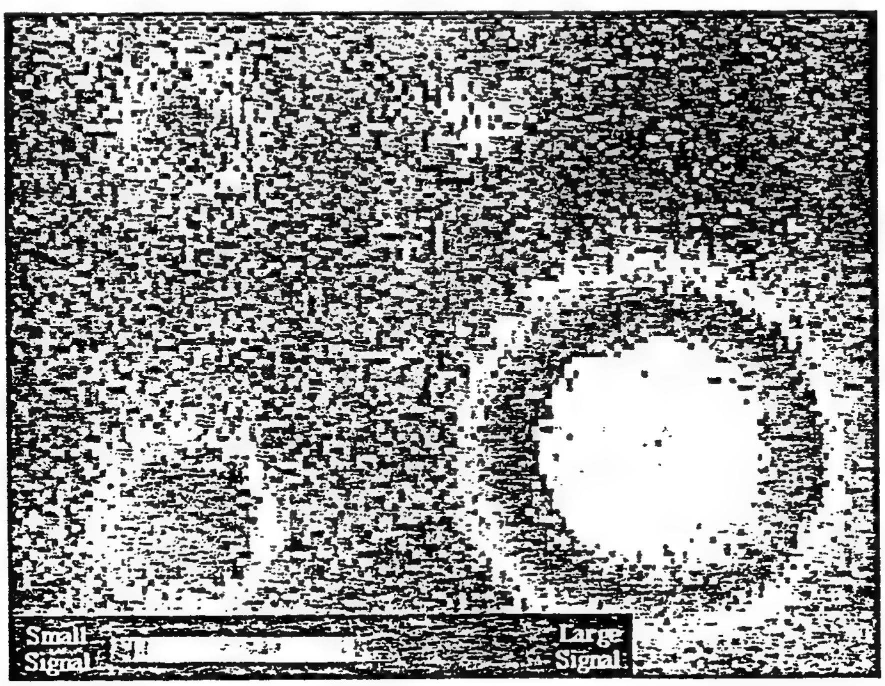
Small Signal
Large Signal

FAA Center for Aviation Systems Reliability (CASR)

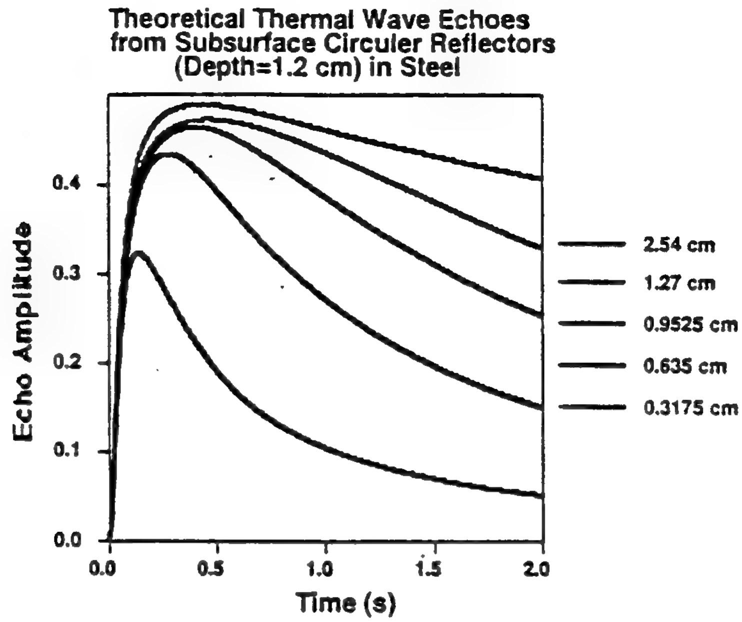

FAA Center for Aviation Systems Reliability (CASR)

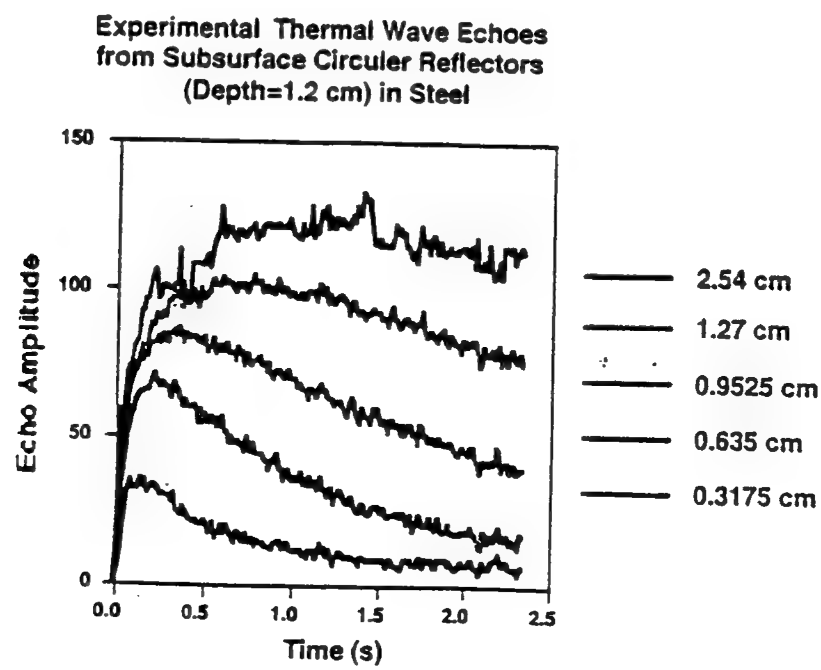

SHORT-TIME BEHAVIOR: THEORY

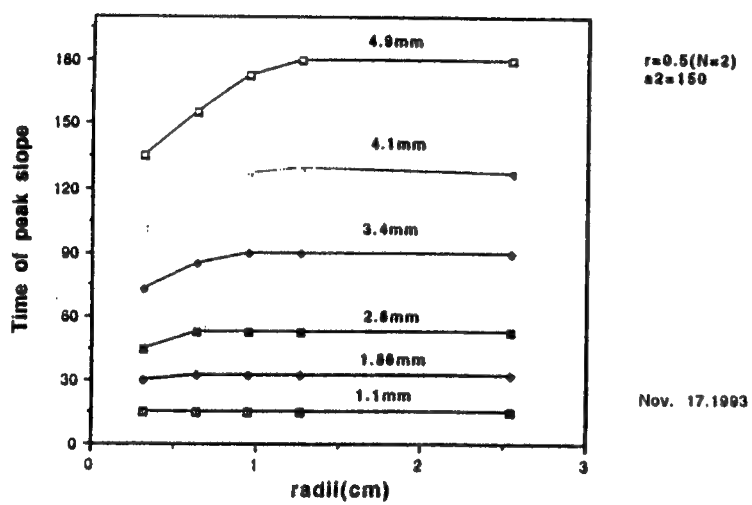

Computed <u>times</u> at which the short-time increase in $(T - T_0)$ has its maximum <u>slope</u> for the 6 flat-bottomed holes at different depths in steel. *Note that these times are independent of hole radius for large ratio of radius-to-depth.*

CONCLUSIONS FROM THE 5-HOLE RESULTS

- Thermal wave scattering theory <u>still</u> works pretty well. The larger diameter defects produce correspondingly larger effects from multiple thermal wave reflection between the boundaries at the defect and the top surface
- Only the short time behavior, corresponding to the first information back from the subsurface boundary, is unaffected by multiple reflections, and therefore independent of the radius of the defect.

COULD THE PEAK SLOPE OF THE SHORT-TIME BEHAVIOR BE USED TO DETERMINE THICKNESS? (i.e., Could it be used as a quantitative first layer corrosion measurement?

- Must be shown to be independent of radius of the defect, and also to be independent of the boundary conditions at the first layer boundary.
- Theory (following slides) predict that the answers to both questions is yes, provided that the aspect ratio (ratio of the radius of the defect to its depth) is sufficiently large , e.g. ≥ 3 or so.

SHORT-TIME BEHAVIOR: THEORY

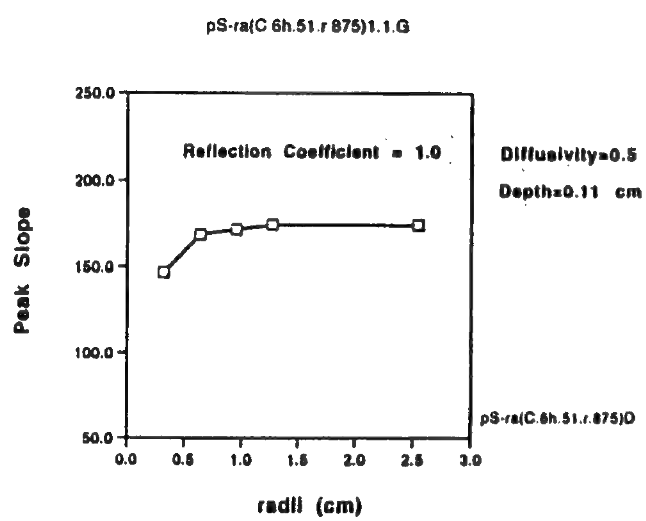

Computed <u>value</u> of the maximum <u>slope</u> of $(T - T_0)$ vs. time as a function of the lateral size of the hole for a 1.1 mm deep flat-bottomed hole. *Note that this curve verifies that the magnitude of the slope is independent of the size of the defect.*

SHORT-TIME BEHAVIOR: THEORY

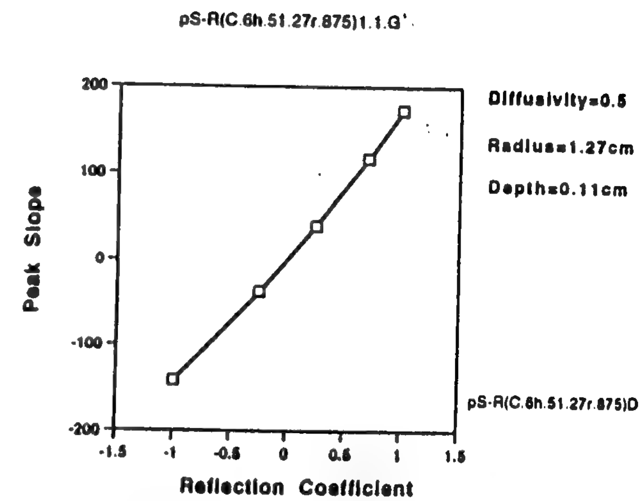

Computed <u>values</u> of the maximum <u>slope</u> of $(T - T_0)$ vs. time as a function of the thermal wave reflection coefficient for a 1.1 mm deep flat-bottomed holes. *Note that this curve can be used to determine the reflection coefficient, provided the magnitude of the slope is independent of the size of the defect.*

COMPOSITE STRUCTURES:

- Boron-Epoxy Patches
- Honeycomb Structures
- Graphite-Fiber-Reinforced Polymers

FAA Center for Aviation Systems Reliability (CASR)

Boron-Epoxy Patches

737

Foster-Miller
Test Panel

DC-9

FAA Center for Aviation Systems Reliability (CASR)

Boron-Epoxy Patch Adhesively Bonded to Aluminum (Flat Bottom Holes in Al Plate)

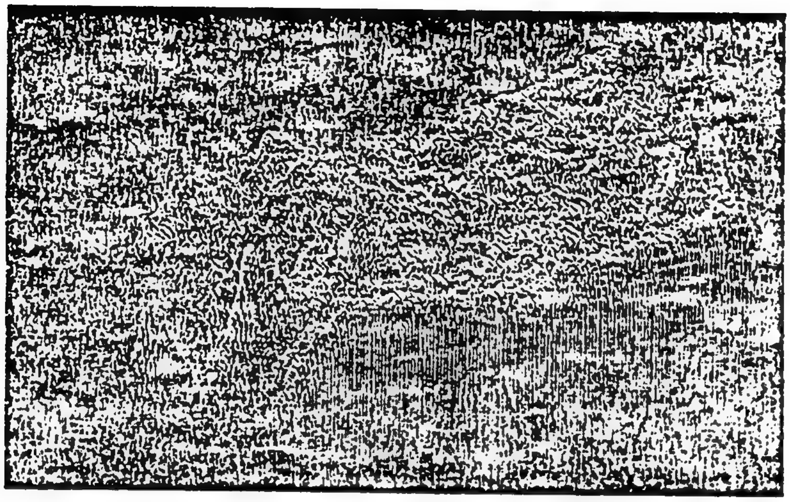

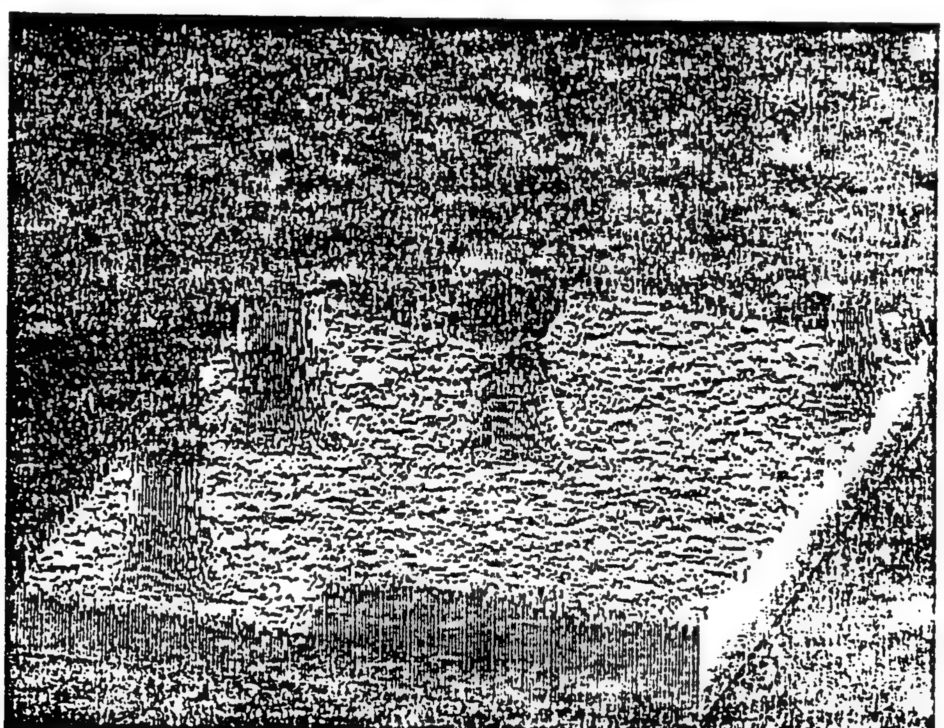

Step 3   Step4 (thickest)

Thermal Wave Image of Impact Damage on a Glass Epoxy Composite by a 2g stone at Normal Angle of Incidence

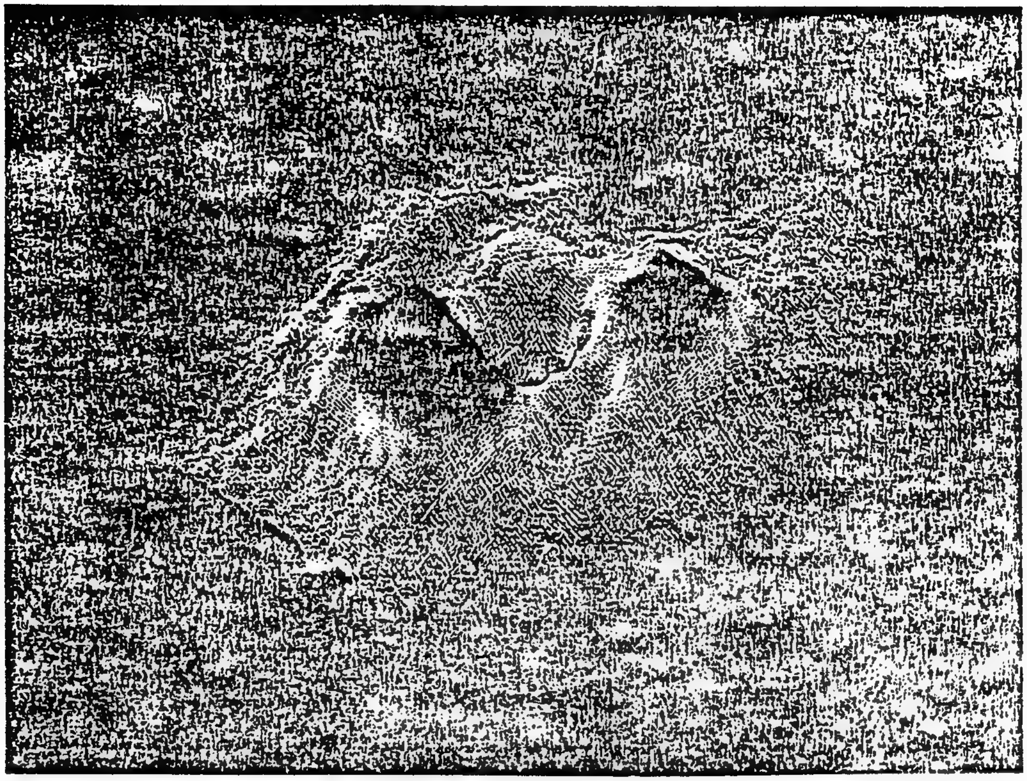

Thermal Wave Image of Boeing 747 Fixed Trailing Edge Panel (Honey Comb)

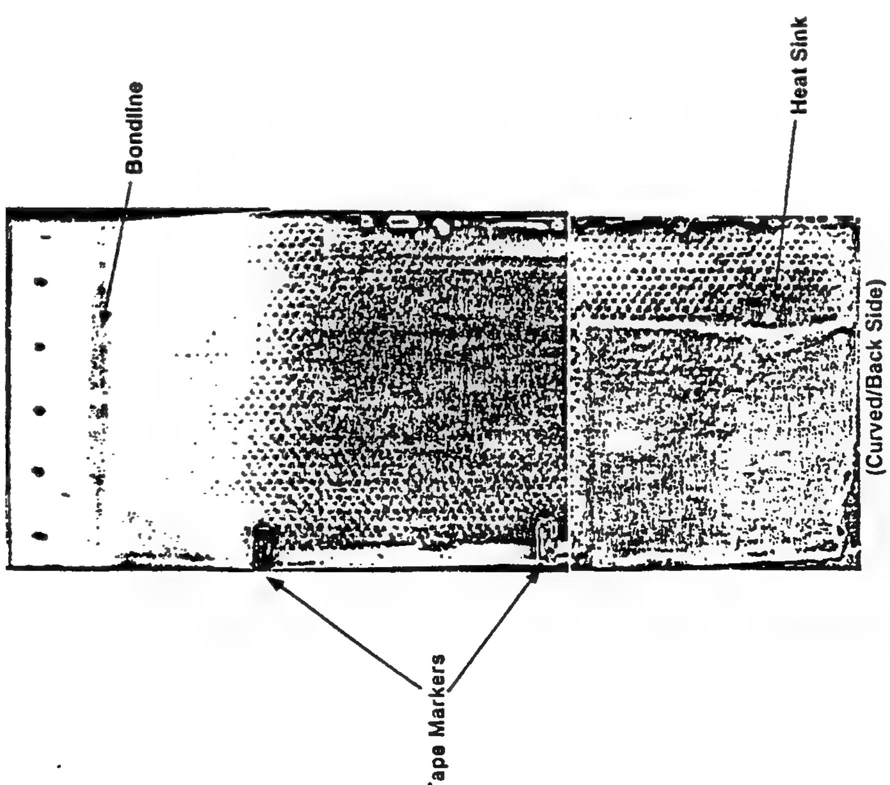

Thermal Wave Image of Boeing 747 Fixed Trailing Edge Panel
(Honey Comb)

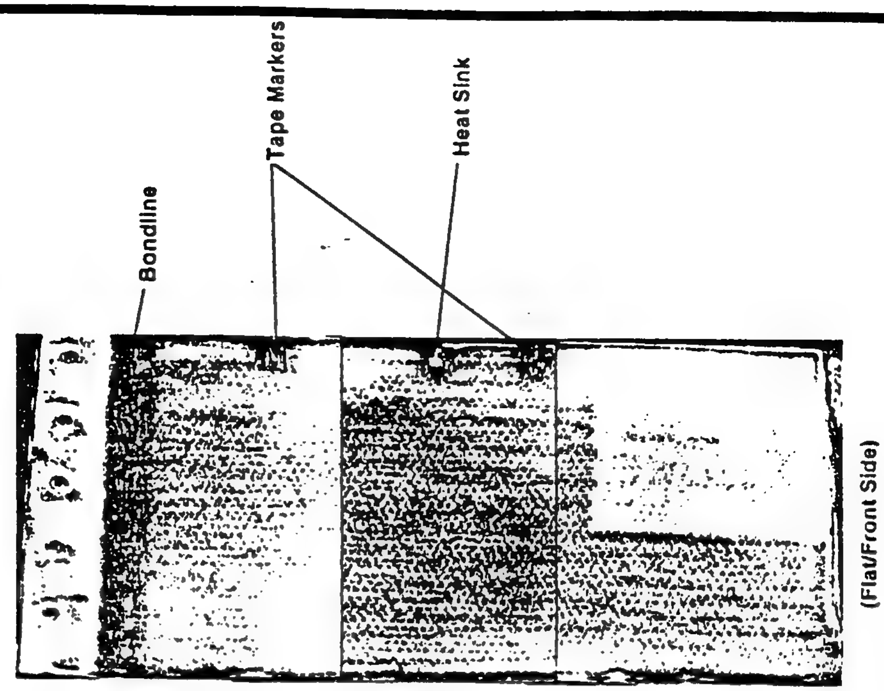

Thermal Wave Image of Composite Aircraft Assembly

Front Side / Upper Half
Wide Angle Lens / Short Gate Time (167 ms)

Front Side / Upper Half
Wide Angle Lens / Long Gate Time (1 s)

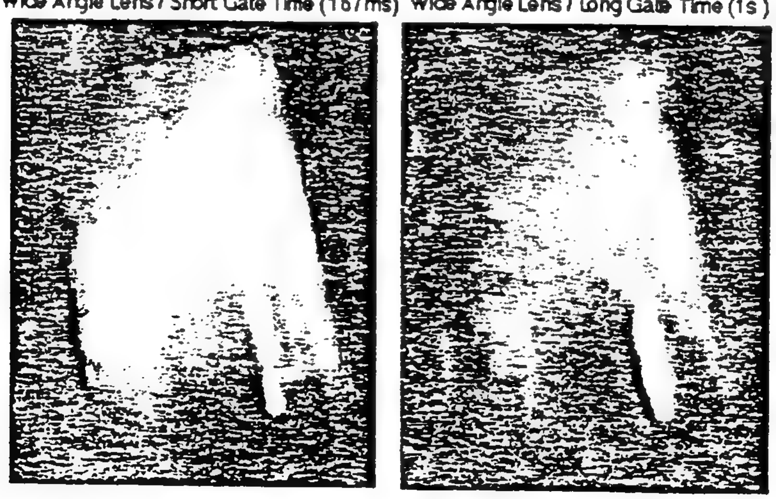

THERMAL WAVE IMAGE OF A COMPOSITE AIRCRAFT PART

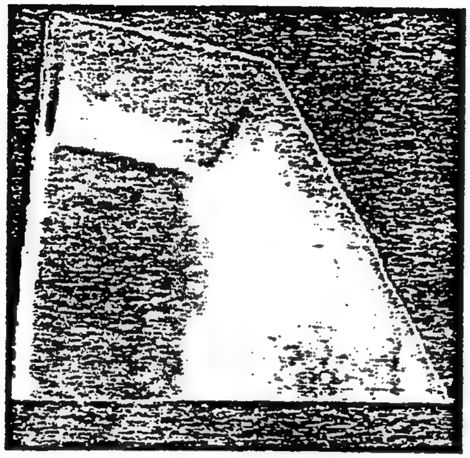

FAA Center for Aviation Systems Reliability (CASR)

THERMAL WAVE IMAGE OF A COMPOSITE AIRCRAFT PART WITH A SUBSURFACE DEFECT

Pulse-Echo Thermal Wave Imaging for Nondestructive Evaluation of Advanced Composite Structures

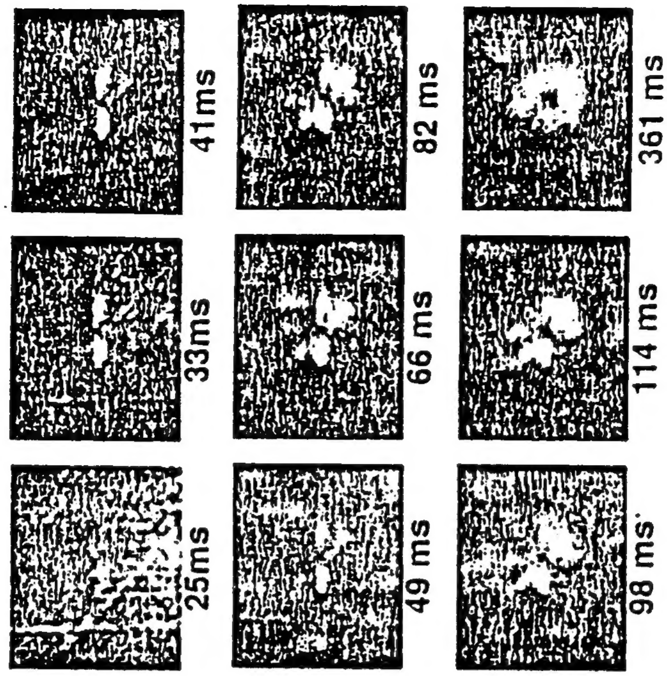

Thermal wave image of sequentially deeper interply delamination damage caused by impact loading in a graphite fiber reinforced polymer composite material.

DUAL RESIN BONDED PANEL

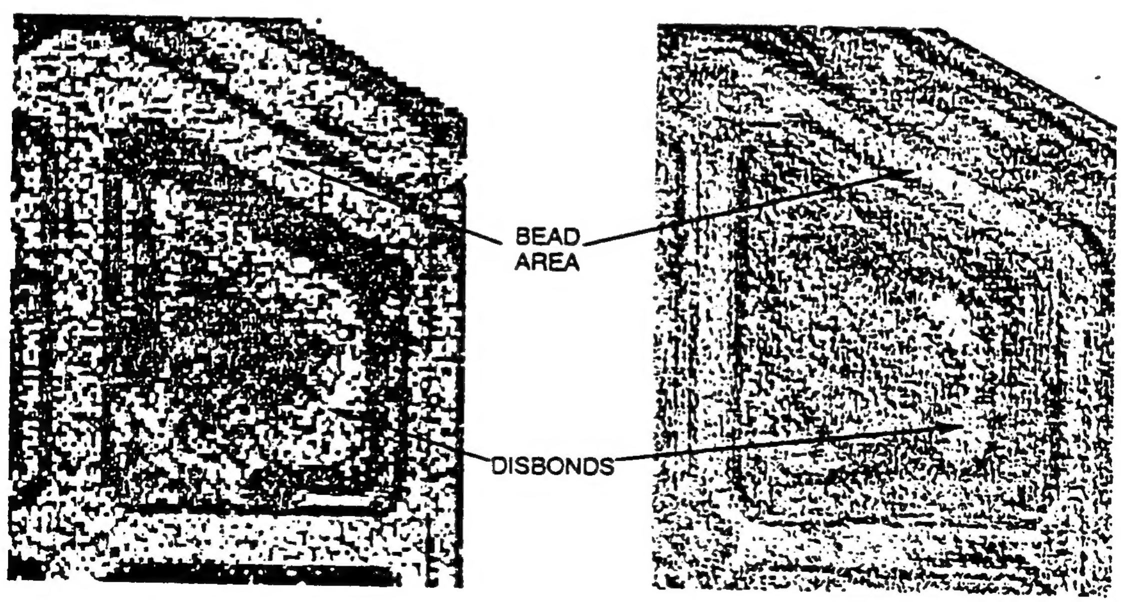

ULTRASONIC

THERMAL WAVE

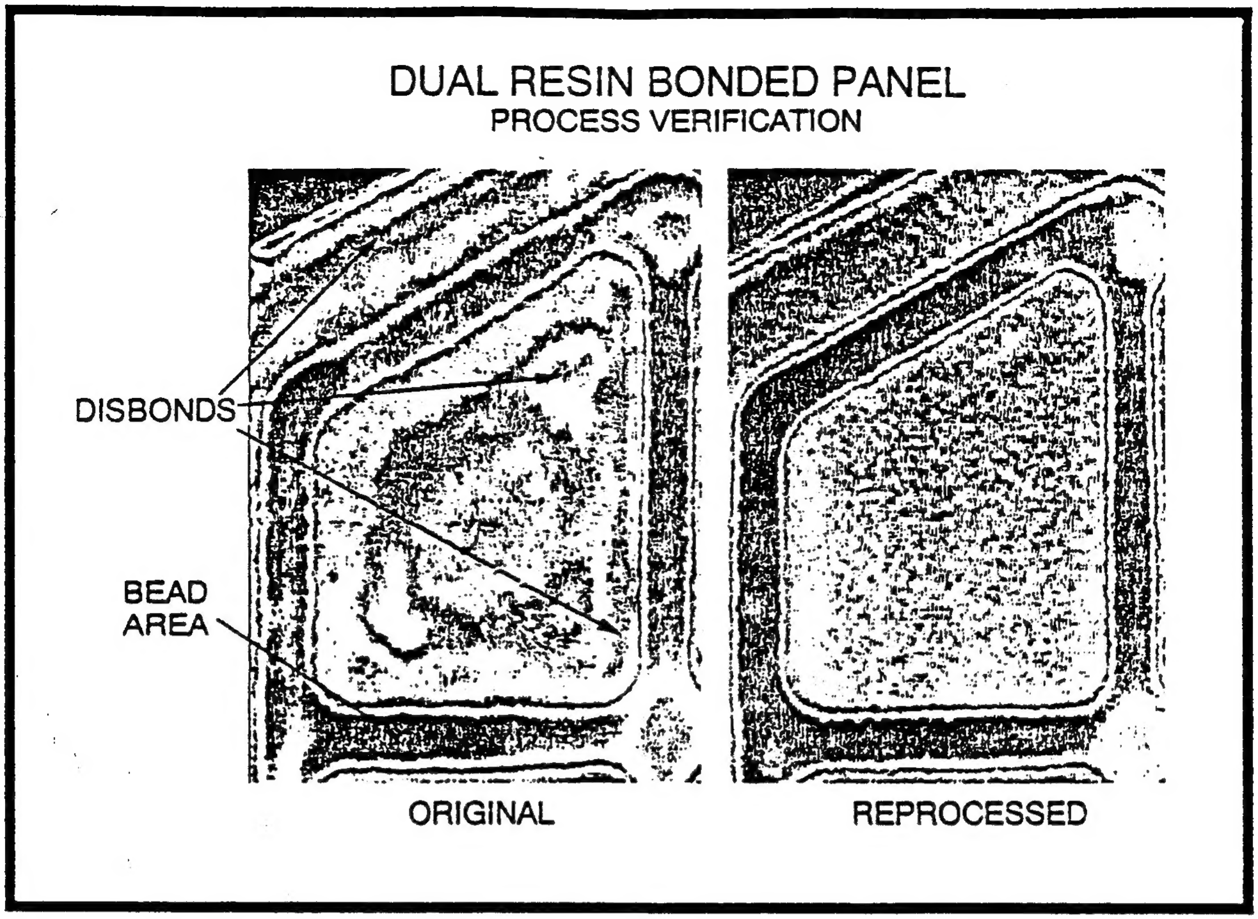
DUAL RESIN BONDED PANEL
PROCESS VERIFICATION
DISBONDS
BEAD AREA
ORIGINAL
REPROCESSED

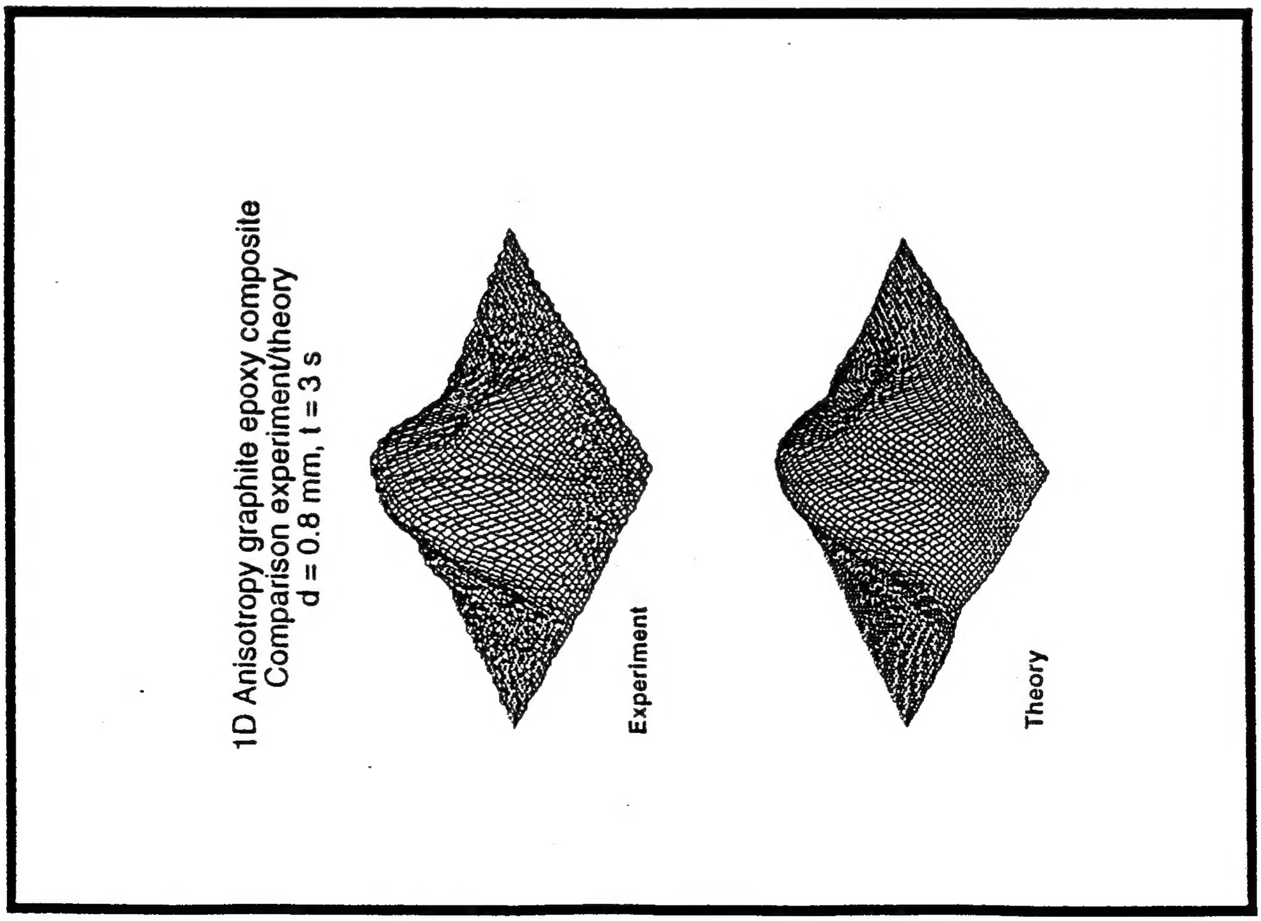
1D Anisotropy graphite epoxy composite
Comparison experiment/theory
d = 0.8 mm, t = 3 s
Experiment
Theory

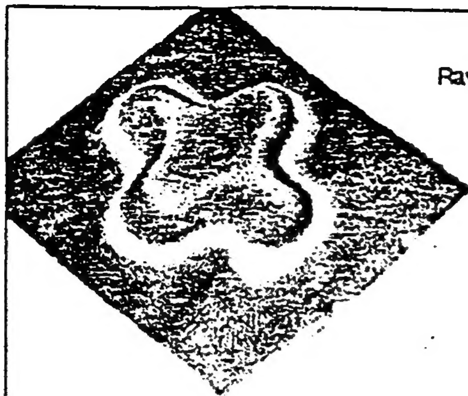

Raw Thermal wave image of a cross-shaped defect in an anisotropic composite

Result of the application of an inverse scattering algorithm to the image shown

THERMAL WAVE IMAGING

TECHNOLOGY DEVELOPMENT & TRANSFER

- Flash lamps, shroud, cart.
- Hardware (board-level pipeline image processing on a 486 PC) .
- Software (dedicated to real-time thermal wave imaging) .
- Commercial availability (WSU-licensed to Thermal Wave Imaging, Inc.)

EchoTherm™

Infrared thermal wave imaging for IBM-PC compatible computers. For real-time nondestructive evaluation of subsurface defects in metals, composites, ceramics, polymers, and plastics.

This thermal wave image of a graphite epoxy laminate, impacted from the front, shows the impact damage on the rear surface, oriented in the ply direction.

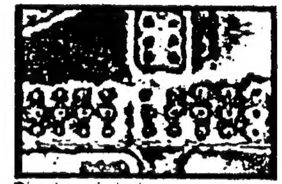

The red areas in this image of an aircraft lap seam indicate the more intense reflection of thermal waves associated with corrosion.

Acquisition and processing PC plug-in

- *Real-time pipeline processor.*
- *8-bit digitizer at 30 Hz frame rate.*
- *Compatible with standard AT bus.*
- *Controls flash or step heat sources.*
- *Programmable gain and offset.*
- *Accepts RS-170 video sources.*
- *Live VGA video display.*

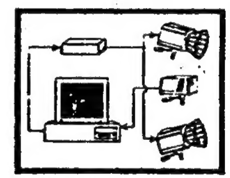

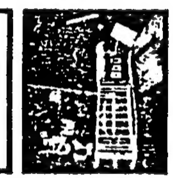

EchoTherm uses flashlamps to heat the sample and an IR camera to detect time-dependent temperature changes due to thermal wave echoes from subsurface defects. Systems can be configured for a wide range of NDE applications.

Control, processing, and display software

- *Temperature and echo amplitude plots.*
- *Variable capture gate widths and delays.*
- *Image scaling and contrast enhancement.*
- *Region-of-interest or full field processing.*
- *Operates under Microsoft Windows 3.1.*
- *User definable pseudocolor palettes.*
- *Image annotation and archiving.*
- *Histogram and image statistics.*
- *Standard PC graphics format.*

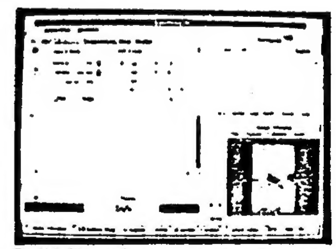

The EchoTherm software combines thermal wave image acquisition, processing and annotation in an easy-to-use Windows compatible user interface.

FUTURE WORK

- Experimental testing to compare with theoretical predictions: Short-time peak slope time; value of the peak slope for holes of different depths and with different boundary conditions.
- Implementation of the method on corrosion test specimens.
- Implementation of the method on aircraft panels.